



11th German Pharm-Tox Summit 2026

Published online: 12 March 2026

© The Author(s), under exclusive licence to Springer-Verlag GmbH Germany, part of Springer Nature 2026

Abstracts of the

92. Jahrestagung der Deutsche Gesellschaft für Experimentelle und Klinische Pharmakologie und Toxikologie (DGPT) in Zusammenarbeit mit der AGAH, APHAR, NVT

17 – 20 March 2026 | Düsseldorf, Germany

This supplement was not sponsored by outside commercial interests. It was funded entirely by the publisher.

01

Characterization of in vitro models to determine the pre-systemic metabolism of the human intestine following oral administration
 P. Lundquist¹, M. Cylan¹, R. Hammar¹, A. C. C. Lopes², M. E. Sellin¹, H. S. Hammer Wagner³, O. Poetz^{2,4}, P. Artursson¹

¹Uppsala University, Department of Pharmacy, Uppsala, Sweden

²Uppsala University, Department of Medical Biochemistry and Microbiology, Uppsala, Sweden

³Signatope GmbH, Reutlingen, Germany

⁴NMI Natural and Medical Sciences Institute, Reutlingen, Germany

In the EU-funded project RISK-HUNT3R, the primary objective is to study human exposure to chemicals and drugs through the lung, skin, and intestine. The project is focused on developing new approach methodologies (NAM) that more accurately reflect human absorption barriers. These models are designed to provide data for predictive toxicokinetic models of human exposure. Specifically, the assessment of oral exposure involves evaluating the permeability of a compound across intestinal epithelial cells, which gives an estimate of absorption after oral administration. However, to improve accuracy, it is necessary to also measure the fraction of a compound metabolized by enterocytes, the cells of the small intestinal epithelium.

A common tool used for measuring permeability is the Caco-2 cell model, but it has a limitation in that it lacks major metabolizing enzymes present in human intestines. To address this, primary human jejunal enterocytes were isolated, which retain the full spectrum of metabolizing enzyme activities. These enterocytes are obtained from human jejunal mucosa samples collected from patients at Uppsala University Hospital. The enterocytes are isolated using a gentle, enzyme-free method, and the team is also cultivating small intestinal 3D organoids (enterocytes derived from human jejunal stem cells) for more detailed permeability and metabolism analysis.

The enterocyte isolation process yields highly viable cells, with more than 90% viability, although 25–35% of the cells express caspase-8, indicating early apoptosis. Proteomic analysis of these enterocytes reveals the presence of important ADME (Absorption, Distribution, Metabolism, and Excretion)-relevant enzymes. These include cytochrome P450 enzymes and several phase II enzymes. Additionally, the team is working on developing 3D enteroid models. In functional tests, the expression levels of ADME proteins in these enteroids are often similar to those found in tissue and enterocytes.

Overall, the findings suggest that the enteroids express many ADME enzymes at levels similar to those in vivo, which makes them promising models for studying intestinal metabolism. The isolation of enterocytes and the cultivation of enteroids are reproducible, and the ADME protein expression in these models is more reflective of human mucosa tissue than traditional Caco-2 cell cultures. These advances provide a more accurate in vitro approach for studying oral drug absorption and metabolism.

02

Next Generation Risk Assessment: Implementation and Mechanistic Insights of NAMs for Toxicokinetics and Toxicodynamics Characterization with case study examples

A. Schepky¹, D. Lange¹, J. Ebmeyer¹, M. Böttcher¹, S. Voss¹, J. Kuehn¹, A. Najjar¹

¹Beiersdorf AG, Global Toxicology, Hamburg, Germany

Next Generation Risk Assessment (NGRA) is an exposure-led and hypothesis-driven approach that integrates non-animal data derived new approach methodologies (NAMs). The availability of Toxicokinetics (TK) and Toxicodynamics (TD) data significantly enhances confidence in risk assessment decisions by providing reliable estimates of internal exposure and potential modes of action (MoAs). Several case studies were performed to guide the implementations of NAMs and NGRA. For the iTTC approach, the role of metabolism and PBPK modeling will be shown. The hypothesis formulation for an *ab initio* approach included here bottom-up PBPK modeling to estimate the PK profile following relevant exposure scenario of a formulation containing 0.5% Benzyl salicylate (BSal). The ADME parameters for the modeling were in vitro/in silico generated: in vitro skin penetration, major metabolite identification, skin and liver metabolism, and renal clearance. Toxicogenomics and Pharmacological Profiling were used for Point of Departure (PoD) finding. The implementation of iTTC and *ab initio* approaches, that are considered to evaluate the safety of certain ingredients e.g., UV-filters and Benzyl salicylate. Internal exposure can be determined through methods such as PBPK modeling or clinical studies, and then compared to an iTTC limit of 1 µM. That will be shown with known UV filters which fit all under this iTTC limit of 1 µM. In the *ab initio* example the total dermal penetration of BSal was up to 9.1% of the applied dose. BSal is metabolized in fresh skin to Salicylic Acid (SA), benzyl alcohol, benzoic acid and hippuric acid. Benzyl metabolites do not reach high concentrations. The deterministic PBPK model resulted in SA concentrations approx. 90 times higher compared to BSal, an approximate estimation of the total plasma concentrations of the most BSal/SA were at C_{max} 1/93.2 nM. Thus, SA is considered as the most relevant metabolite for the safety assessment. Therefore, toxicodynamics assays were performed with SA to derive the *in vitro* point of departure (PoD). The derived PoD was used for the quantification risk assessment together with the SA internal exposure assessment. Probabilistic PBPK model was used to estimate plasma concentration distribution.

Conclusion: The case studies demonstrate the protectiveness and the applicability of various approaches in NGRA to ensure human safety, aligning with the first principle of 3Rs "replacement".

03

Disruption of Early Human Neurodevelopment by Mitochondria-Targeting Fungicides

L. Dittmann¹, L. M. Stark¹, E. Fritsche^{2,3,4}, J. Tigges¹, K. Koch^{1,4}

¹Leibniz Research Institute for Environmental Medicine (IUF), Environmental Toxicants and the Brain, Düsseldorf, Germany

²Swiss Centre for Applied Human Toxicology (SCAHT), Basel, Switzerland

³University of Basel, Department of Pharmaceutical Sciences, Basel, Switzerland

⁴DNTOX GmbH, Düsseldorf, Germany

The increasing use of pesticides in agriculture raises concerns about their persistence and potential toxicity in humans and other non-target organisms. Fungicides such as succinate dehydrogenase inhibitors (SDHIs) and strobilurins (STR) target mitochondrial complexes II and III, disrupting oxidative phosphorylation and cellular energy metabolism. Since mitochondria are essential for all cells, including developing neurons and glia, disruptions may affect key neurodevelopmental processes (KNDPs) in the developing brain. Indeed, epidemiological and experimental studies link perinatal pesticide exposure to neurodevelopmental disorders, highlighting the need for predictive, mechanism-based chemical testing beyond resource-intensive *in vivo* methods. The Developmental Neurotoxicity In Vitro Battery (DNT-IVB) is a compilation of new approach methodologies (NAMs) that model KNDPs *in vitro*, providing a human-relevant alternative to DNT *in vivo* studies.

As part of the DNT IVB, the human Neurosphere Assay assesses KNDPs such as proliferation, migration, neurite outgrowth, and differentiation into neurons and oligodendrocytes using human neural progenitor cell (hNPC) neurospheres. In this study, we assessed the effects of three SDHIs (bixafen, fluopyram, fluxapyroxad) and one STR (pyraclostrobin) within the Neurosphere Assay, both as single compounds and exposure-relevant mixtures that remain in active use (mixture A, bixafen/fluopyram 1:1; mixture B, fluxapyroxad/pyraclostrobin 1:2). Despite their shared proposed mitochondria-related mode of action (MoA), we observed chemical-specific effects on KNDPs *in vitro*. While the proliferation of hNPCs was negatively affected by bixafen, pyraclostrobin, and mixture B, their differentiation into neurons and oligodendrocytes was disturbed by all tested fungicides and mixtures, with neurons being the most sensitive cell type overall. Complex III inhibitor pyraclostrobin was the most potent fungicide across all KNDPs, with increased potency within mixture B compared to single exposure. Alarming, pyraclostrobin impaired neurogenesis at concentrations in range of the EFSA-established acceptable daily intake (ADI).

Here, we provide novel insights into how mitochondria-targeting fungicides can disrupt human neurodevelopment. Our data demonstrate the utility of the Neurosphere Assay for testing exposure-relevant pesticide mixtures while underscoring the potential risk of mitochondria-targeting fungicides for the developing brain.

05

Optimized EPI-X4 derivatives as potent CXCR4 inhibitors in colorectal cancer models

A. Haase¹, J. Münch², M. Harms², R. A. Benndorf¹

¹Ruhr University Bochum, Institute of Pharmacology and Toxicology, Bochum, Germany

²Ulm University Medical Center, Institute of Molecular Virology, Ulm, Germany

The chemokine receptor CXCR4 is highly overexpressed in a wide range of tumor entities, including breast, lung, pancreatic, hematological, and colorectal cancers, where it correlates with aggressive tumor behavior, enhanced metastatic potential, and poor prognosis. Upon binding to its ligand CXCL12, CXCR4 activates key downstream signaling pathways that promote cell migration, survival, proliferation, and angiogenesis, making it a promising therapeutic target. However, currently available CXCR4 antagonists such as AMD3100 display limited pharmacokinetics and tolerability, highlighting the need for novel inhibitors.

The endogenous CXCR4 antagonist EPI-X4 and its optimized derivatives (JM#21, JM#198, JM#285) exhibit high receptor specificity, improved stability, and potent antagonistic activity (Harms *et al.*, 2024). Here, we evaluated optimized EPI-X4 derivatives in the colorectal cancer (CRC) cell lines DLD1 and HT29 using a range of *in vitro* assays, including cell viability, proliferation and apoptosis. In addition, first *in vivo* experiments were performed in the chicken chorioallantoic membrane (CAM) model, an established 3R-compliant assay that enables rapid assessment of tumor growth, angiogenesis, and metastatic behavior.

Treatment with optimized derivatives led to a reduction in cell viability and proliferation, accompanied by increased apoptotic rates. In the CAM assay, which utilizes the highly vascularized chorioallantoic membrane of fertilized chicken eggs to model tumor growth and metastasis, we observed a pronounced decrease in tumor size and strongly diminished metastatic spread. These effects exceeded those observed with AMD3100, indicating the advantage of molecular optimization.

Our results demonstrate that EPI-X4 derivatives represent highly effective CXCR4 inhibitors in CRC models, combining improved stability with potent anti-tumorigenic activity. These findings highlight the translational potential of optimized EPI-X4 peptides as innovative therapeutic candidates for targeting CXCR4-driven tumor progression and metastasis in colorectal cancer.

References: 1. Harms, M.; Haase, A. *et al.* Fatty acid conjugated EPI-X4 derivatives with increased activity and in vivo stability. *Journal of Controlled Release* 373, 583–598 (2024). 10.1016/j.jconrel.2024.07.049

06

FRET-based Prostanoid receptor conformation-sensors reveal arachidonic acid as a partial agonist at the human EP1 and TP receptorM. Ulrich¹, M. Kurz², M. Bünemann¹¹Marburg University, Institut für Pharmakologie und Klinische Pharmazie, Marburg, Germany

Prostanoid receptors are class A G protein-coupled receptors (GPCRs) that are activated by arachidonic acid (AA) metabolites known as prostaglandins. This receptor family comprises nine distinct subtypes, including the prostaglandin E receptors (EP1–EP4) and the thromboxane receptor (TP). Prostaglandin E2 (PGE2) is the endogenous ligand for EP1, whereas thromboxane A2 serves as the physiological agonist for the TP receptor. Because thromboxane A2 is highly unstable its synthetic analogue U46619 is commonly used as a TP receptor agonist. Both receptors are critically involved in various physiological and pathological processes, including inflammation, smooth muscle contraction and platelet aggregation.

We constructed Fluorescence Resonance Energy Transfer (FRET) based conformation sensors of the human EP1 and TP receptor to further investigate the pharmacology and dynamics of these important prostanoid receptors. Stable HEK293 cell lines expressing the respective sensors were established and analysed by FRET measurements using an inverted fluorescence microscope. Furthermore, FRET measurements of multiple cells carrying the constructs, were performed at a plate reader.

The FRET conformation sensors based on the human EP1 and TP receptors showed a concentration dependent decrease in emission ratios upon stimulation with different agonists. We observed a decent signal to noise ratio for the EP1 and we were able to measure concentration response curves in multi-cell FRET recordings. The EP1 and TP receptor was activated by a number of substances besides PGE2 and U46619, which reflects the wt receptor properties. Arachidonic acid (AA) has previously been shown to activate the DP2 receptor. In this study, AA was additionally identified as a partial agonist at the EP1 and TP receptors, exhibiting EC50 values approximately three orders of magnitude higher than those of their endogenous ligands. Subsequent downstream analyses, including BRET-based G protein activation assays, confirmed that arachidonic acid (AA) can activate both the EP1 and TP receptors.

Arachidonic acid (AA), a central lipid mediator and precursor of prostaglandins and thromboxanes, was found to directly activate not only the DP2 receptor but also the EP1 and TP receptors. This suggests an additional receptor-mediated pathway through which AA may modulate cellular signalling, although its physiological relevance remains to be clarified.

07

Functional Diversity of Gβγ Dimers in Modulating constitutive and GPCR-Promoted G Protein ActivationS. J. Bonn Garcia¹, A. Langolf¹, D. Hilger¹, H. Schihada¹¹Marburg University, Institut für Pharmazeutische Chemie, Marburg, Germany

Heterotrimeric G proteins are composed of multiple combinations of α-, β-, and γ-subunits. While most of the 21 known Gα-subunits have been extensively characterized, the functional diversity of the Gβγ dimer remains poorly understood. These dimers are formed from 5 β- and 12 γ-subunits, giving rise to 60 possible combinations with potentially distinct signaling properties. We hypothesize that distinct βγ dimers modulate the activation kinetics of G proteins by regulating the spontaneous rate of nucleotide exchange on the Gα-subunit, thereby contributing to heterotrimer-specific basal signaling properties.

To test this, we employed BRET-based biosensors to monitor the GTPγS-induced dissociation of GDPβS-loaded G protein heterotrimers. For this purpose, we optimized the G-CASE biosensor with a split fluorescent protein that reconstitutes exclusively upon formation of a defined βγ dimer, allowing us to selectively investigate individual subunit combinations. Using this system, we quantified G protein dissociation rates for 12 different Gα-subunits in combination with 48 Gβ1-4/Gγ1-5, 7-13 dimers. Our data reveal an α-dependent modulatory effect of both β- and γ-subunits on heterotrimer activation kinetics.

Building on these findings, we extended our analysis to receptor-promoted activation. To do this, we examined a set of prototypical GPCRs, each selectively coupling to one of the four Gα families: the bradykinin B2 receptor (G12/13), β2-adrenergic receptor (Gs/o1f), muscarinic M1 receptor (Gq/11), and μ-opioid receptor (Gi/o). Across all families, we find that βγ dimers also modulate the rate of receptor-dependent G protein activation. These results demonstrate that βγ-dependent regulation is not limited to basal G protein activity but also extends to receptor-catalyzed activation, suggesting that specific βγ compositions can shape G protein signaling outputs.

Taken together, our findings highlight the regulatory role of Gβγ dimers in controlling G protein activation and lay the groundwork for exploring their potential contribution to altered signaling dynamics in human disease.

08

Inactivation of HDAC2 counter regulates action potential alterations in CREM-IbΔC-X transgenic mice, a model of atrial fibrillationM. Gleske¹, L. B. Tardio¹, J. P. Reinhardt¹, M. D. Seidl¹, C. Apicella³, M. Stoll³, F. U. Müller¹, J. S. Schulte¹¹Universität Münster, Institut für Pharmakologie und Toxikologie, Münster, Germany²University Medical Centre of Münster, Klinik für Kardiologie II: Rhythmologie,

Münster, Germany

³Universität Münster, Centrum für Medizinische Genetik, Münster, Germany

Objective: Atrial fibrillation (AF) is the most common cardiac arrhythmia, associated with extensive atrial remodeling. Mice with cardiomyocyte (CM)-specific expression of the cAMP-dependent transcription factor CREM-IbΔC-X (TG), a model of AF, exhibit heterogeneous, depolarized resting membrane potentials (RMP) and prolonged action potentials (APs) in atrial CMs (ACMs). The pan class I HDAC inhibitor valproate decreased prolonged AP duration (APD), reversed atrial remodeling and delayed onset of AF in TG mice. Here, we investigated if genetic inactivation of the class I isoform HDAC2 (KO) is sufficient to reverse proarrhythmic AP alterations in TG mice using fluorescence microscopy.

Methods: Isolated ACMs from 6-8 weeks old mice were loaded with the membrane potential dye FluoVoltTM to record action potentials via fluorescence microscopy. Fluorescence intensity at 470 nm was recorded with an IonOptix Myocyte Calcium and Contractility System. Atrial tissue homogenates were analysed by RNAseq and western blots.

Results: Baseline fluorescence depended mainly on corresponding changes in ACM size. Baseline fluorescence was increased by 100% in TG vs CTR ACMs (animal/ACM n=7-11/68-93) but reduced by 35% in TGxKO vs TG (n=11/93-103). The amplitude of an AP decreases, if the RMP rises. In TG vs CTR ACMs, the relative AP amplitude was significantly reduced by 37%, but restored in TGxKO vs CTR ACMs. APD₅₀ and APD₇₀ were prolonged by 50% and 35% in TG vs CTR. HDAC2 inactivation in TGxKO led to a significant reduction in APD₅₀ and APD₇₀ by 27% and 24% vs TG. HDAC2 inactivation alone had no effect on APDs (KO vs CTR). RNAseq (n=10/genotype) revealed a multitude of deregulated ion channel-encoding genes in TG vs CTR. HDAC2 inactivation in TGxKO led to an increased expression of *Kcnk3*, *Kcne1*, *Kcnd3*, *Kcnj5* and *Kcnj11* vs TG, encoding K⁺ channel subunits that stabilize repolarisation or the RMP. Moreover, NCX1 protein levels were increased in TG vs CTR, which has been shown to prolong APs. Again, this increase was counter regulated in TGxKO vs TG atria.

Conclusion: Genetic inactivation of HDAC2 normalizes the proarrhythmic AP alterations in CREM-IbΔC-X transgenic mice by limiting the deregulation of NCX1 and K⁺ subunits, which control AP repolarization and RMP stability. Consequently, the inhibition of HDAC2 emerges as a promising strategy for restoring electrophysiological properties in patients with atrial fibrillation.

Supported by the DFG and Deutsche Herzstiftung

09

Acute inhibition of lipolysis after MI using a murine adipocyte specific inhibitory DREADD model attenuates inflammation and improves cardiac systolic functionL. Wang¹, H. Zabir¹, S. Gorreßen¹, D. Semmler¹, S. Lehr², J. W. Fischer¹, K. Bottermann¹¹Institut für Pharmakologie, Düsseldorf, Germany²Institut für Klinische Biochemie und Pathobiochemie, Düsseldorf, Germany

Myocardial infarction (MI) triggers catecholamine-driven lipolysis in peripheral adipose tissue, elevating circulating free fatty acids which may exacerbate cardiac injury. In this study, we achieved spatio-temporal inhibition of lipolysis using an inducible, adipocyte-specific inhibitory DREADD mouse model to improve cardiac function after cardiac ischemia/reperfusion (I/R).

DREADD expression was induced in 10-week-old male mice by 5-day intraperitoneal injections of 4-OH-tamoxifen. DREADD was activated by DREADD agonist 21 (CP21) administration immediately before and after 60' experimentally induced ischemia. This successfully inhibited peripheral lipolysis, as shown by significantly reduced circulating NEFA levels at 30' I/R in DREADD mice. NEFAs are known to induce insulin resistance, accordingly, circulating insulin levels were decreased in DREADD mice at 30' I/R revealed by multiplex analysis. NEFAs are also suggested to suppress PKA activity in cardiomyocytes. In line with reduced circulating NEFA and insulin levels, western blot analysis revealed increased PKA activity in both remote and ischemic areas of the heart. Additionally, the PKA downstream target phospholamban (PLN) is involved in cardiac contractility and had an increased phosphorylation at serine 16 in the remote zone. Improved remote contractile performance was thereby considered the main contributor to enhanced cardiac systolic function at 7d I/R, as evidenced by increased EF, FAC and SV.

As NEFAs also influence transcription factors, spatial transcriptomic analysis was used to identify niche-specific transcriptional regulations at 30' I/R. This revealed a suppressed inflammatory signature in the remote zone of DREADD mice, with inhibition of pro-inflammatory pathways identified by Ingenuity Pathway Analysis (Qiagen). Upstream regulator analysis indicated suppressed IL-1B, TNF, IFNG, STAT3 and NFκB, consistent with findings from scRNA sequencing at 24h I/R, which further indicates a stress-adapted phenotype of neutrophils, promoted M2 polarization through activated IL-4 and IL-13 signaling and inhibited macrophage classical activation signaling.

Taken together, acute inhibition of peripheral lipolysis during and shortly after MI reduces circulating NEFAs and insulin, enhances cardiac PKA signaling and contractile function, and attenuates remote-zone inflammation. This transient intervention is sufficient to improve cardiac systolic function at later time points following reperfusion.

10

A Prodomain-Derived ADAM10 Inhibitor Selectively Reduces Post-Infarction Inflammation and Preserves Cardiac Function

E. Klapproth¹, J. Marks¹, S. Grell¹, P. Diaba-Nuhoho¹, C. Prince², K. Lorenz², P. Saftig², A. El-Armouche³

¹Institute of pharmacology and toxicology, Faculty of Medicine Carl Gustav Carus, Technische Universität Dresden, Dresden, Germany

²Verra Therapeutics, Lansing, NY, United States

³Institute of Pharmacology and Toxicology, Julius-Maximilians-University Würzburg, Würzburg, Germany

⁴Christian-Albrechts-University Kiel, Biochemical Institute, Kiel, Germany

Background: ADAM10 is a central sheddase controlling inflammatory and regenerative signaling by cleaving substrates such as CX3CL1, IL-6R, and Notch ligands. After myocardial infarction (MI), excessive ADAM10 activity amplifies leukocyte recruitment, cytokine release, and maladaptive cardiac remodeling. Despite its therapeutic relevance, selective inhibition of ADAM10 remains challenging, as existing metalloprotease inhibitors lack specificity and cause systemic side effects. This study aimed to develop a prodomain-derived ADAM10 inhibitor with improved pharmacokinetic stability and to evaluate its therapeutic efficacy and safety after MI.

Methods: Using AlphaFold3-based structural modeling, we identified the ADAM10 prodomain as a selective inhibitory scaffold and engineered a stabilized peptide variant (VTH144) optimized for enhanced binding, resistance to proteolysis, and superior pharmacokinetics compared to the wild-type (WT) prodomain. Enzymatic selectivity was confirmed via FRET-based assays across ADAMs and MMPs. Mice subjected to left anterior descending (LAD) artery ligation were treated with VTH144 for 72 h post-MI, and cardiac function, scar size, and inflammation were analyzed by echocardiography, histology, and immunohistochemistry. Systemic safety was assessed in cardiac, hepatic, renal, and pulmonary tissues of naïve mice.

Results: VTH144 selectively inhibited ADAM10 without affecting other metalloproteases. Compared to the WT prodomain, VTH144 displayed markedly improved plasma stability and sustained inhibitory activity in vivo. Treatment during the first 72 h after MI preserved left ventricular function, reduced scar size, and significantly lowered neutrophil infiltration and IL-1 β -driven inflammation. Mechanistically, ADAM10 inhibition limited CX3CL1 shedding and CX3CR1-dependent leukocyte recruitment. No structural or biochemical toxicity was detected in major organs.

Conclusion: The prodomain-derived peptide VTH144 constitutes a novel and selective ADAM10 inhibitor with superior pharmacokinetic properties that effectively mitigates post-infarction inflammation and preserves cardiac performance without systemic toxicity. These findings highlight protease-selective inhibition as a promising strategy to restore inflammatory balance and improve cardiac recovery after MI.

11

Novel inhibitors and combination therapies targeting the Serum Response Factor (SRF) cofactor Myocardin Related Transcription Factor A (MRTF-A)

S. Muehlisch¹, D. Chalvatzis¹, L. Rupprecht¹, M. Heinrich¹, L. Lochschmidt¹, M. J. Franz², P. Wenisch¹, T. Gudermann², V. Chubanov²

¹Friedrich-Alexander University of Erlangen-Nuremberg, Department of Chemistry and Pharmacy, Erlangen, Germany

²Ludwig Maximilian University of Munich, Walther-Straub Institute of Pharmacology and Toxicology, Munich, Germany

Myocardin-related transcription factor A (MRTF-A) is a coactivator of the transcription factor serum response factor (SRF) that promotes the expression of genes

involved in cell proliferation, migration and differentiation and triggers hepatocellular carcinoma (HCC) progression. We recently demonstrated that the

negative gating modulator NS8593 of the transient receptor potential cation channel TRPM7 inhibits MRTF-A by promoting its nuclear export.

We generated derivatives of NS8593 which are more potent in inhibiting SRF transcriptional activity. Upon administration of the improved

NS8593 analogues, the expression of the MRTF/SRF target genes such as Myoferlin and Tetraspanin 5 (TSAN5) was significantly reduced in HCC cells and xenografts, resulting in senescence induction and proliferation arrest.

Our studies highlight the potential of novel MRTF-A inhibitors to combat HCC growth and drug resistance.

12

First Insights into the Pharmacological Potential and Mechanisms of Action of the Natural Compound Xenocoumacin 2

C. Lam¹, T. Denk², A. Steinbach³, N. Bach³, S. A. Sieber³, R. Beckmann², H. B. Bode², R. Fürst¹, S. Zahler¹

¹Ludwig Maximilian University of Munich, Pharmaceutical Biology, Munich, Germany

²Ludwig Maximilian University of Munich, Gene Center and Department of Biochemistry, Munich, Germany

³Technical University of Munich, Chair of Organic Chemistry II, Munich, Germany

⁴Max-Planck-Institute for Terrestrial Microbiology, Natural Products in Organismic Interactions, Munich, Germany

Xenocoumacins have initially been identified as antibiotic metabolites produced by the bacterium *Xenorhabdus nematophila*. Among these, xenocoumacin 2 (Xcn2) emerged as a particularly promising bioactive compound due to its pronounced anti-inflammatory [1] and anti-ulcer activities [2] in vitro and in vivo. However, its molecular mode of action still remains poorly understood.

In this study, we aimed to elucidate the pharmacological potential of Xcn2 in an oncological context and gain insights into its cellular mode of action. A comprehensive panel of in vitro assays was performed, including analyses of proliferation, migration, apoptosis, mitochondrial function, and proteome-wide alterations.

Xcn2 strongly inhibited the proliferation of HeLa cells with an IC50 of 90 nM. Early responses included a marked inhibition of protein biosynthesis, as supported by cryo-electron microscopy, which revealed Xcn2 binding to vacant 80S ribosomes. At later time points, Xcn2 inhibited both directed and undirected migration starting at concentrations of 100 nM and induced apoptosis from 1 μ M onwards. Notably, while cellular ATP production decreased over time, the mitochondrial membrane potential remained unaffected by Xcn2, suggesting that mitochondrial integrity is preserved. Proteomic profiling revealed that Xcn2 triggered a marked downregulation of proteins associated with translation and the extracellular matrix. In addition, a subset of stress-related proteins, most notably c-JUN, was upregulated. This was independently validated by qPCR-based gene expression analysis, which confirmed a rapid and robust induction of c-JUN as early as 15 min after Xcn2 treatment, rising more than 100-fold within 2 hours. Such an immediate transcriptional response indicates the activation of ribotoxic stress signaling pathways and constitutes a primary cellular reaction to Xcn2 exposure.

Taken together, our findings identify Xcn2 as a potent inhibitor of HeLa cell proliferation and migration. Beyond ribosomal inhibition, the remarkably early induction of c-JUN suggests a primary engagement of stress response signaling, which may underlie the observed downstream cellular effects. However, further research will be necessary to validate these observations and fully elucidate the underlying mode of action.

1. Erkoc, P., et al., Biomedicine & Pharmacotherapy, 2021. **140**.
2. McInerney, B.V., et al., Journal of Natural Products, 1991. **54**: p. 785-95.

13

Pantoprazole metabolic ratios for CYP2C19 phenotyping in patients under pantoprazole treatment

J. P. Müller¹, S. Yamoune¹, V. N. Belov², B. Miller¹, M. Hasoumi¹, J. Wozniak¹, J. Tupiec¹, T. Laurentius^{3,4}, L. C. Bollheimer³, J. C. Stingl^{1,5}, K. S. Just¹

¹University Hospital RWTH Aachen, Institute of Clinical Pharmacology, Aachen, Germany

²Max Planck Institute for Multidisciplinary Sciences (MPI-NAT), Department of NanoBiophotonics, Göttingen, Germany

³University Hospital RWTH Aachen, Department of Geriatric Medicine, Aachen, Germany

⁴Carl von Ossietzky University Oldenburg, Department of Geriatrics, Oldenburg, Germany

⁵Heidelberg University Hospital, Department of Clinical Pharmacology and Pharmacoepidemiology, Heidelberg, Germany

Question: CYP2C19 activity may be influenced by factors such as genetics, drug-drug interactions or inflammation. CYP2C19 phenotyping may approve therapy safety and efficacy. Previously, we demonstrated a strong correlation between the metabolic ratios (MR) of the validated phenotyping metric 5-hydroxyomeprazole/omeprazole and 4-desmethylpantoprazole-sulfate/pantoprazole in a single-dose pharmacokinetic study in cross-over design. The correlation was best with single plasma samples 4 - 8 hours after pantoprazole intake (spearman $\rho \geq 0.8$), suggesting accurate CYP2C19 phenotyping during this timeframe. Currently, no reliable CYP2C19 biomarker is available. As a surrogate method, pantoprazole may be used from the already prescribed medication to phenotype CYP2C19 due to stable pharmacokinetics during repeated dosing. Our aim was to test the MR 4-desmethylpantoprazole-sulfate/pantoprazole as a novel CYP2C19 phenotyping method in a real-world setting with patients on daily pantoprazole treatment and during multiple dosing.

Methods: In this pilot study, we reanalyzed plasma samples from a cohort of geriatric, multi-medicated patients under pantoprazole treatment (NCT05247814). Patients were genotyped for CYP2C19 *2, *3, and *17 using TaqMan assays. Due to the lack of an exact documentation of the time of pantoprazole intake, inclusion criteria were oral pantoprazole intake once daily in the morning and a documented blood sampling at or after 10 a.m. Plasma concentrations of pantoprazole and its metabolite 4-desmethylpantoprazole-sulfate were quantified by LC-MS/MS in a single plasma sample per patient.

Results: In total, n=14 patients were included with a mean age of 81 years and a mean intake of 15 drugs. CYP2C19 genotyping resulted in the identification of 2 poor (PM), 2 intermediate (IM), 6 normal (NM), 1 rapid (RM) and 3 ultrarapid metabolizers (UM). Of the 14 patients included, 13 patients had detectable plasma levels of pantoprazole or 4-desmethylpantoprazole-sulfate. By using pantoprazole MR we demonstrate a significant discrimination between genotype-predicted CYP2C19 PM and non-PM patients (p=0.026).

Conclusions: Pantoprazole MR may be used as a CYP2C19 phenotyping method in patients under pantoprazole treatment. Further studies are needed to

test the predictive ability of pantoprazole MR during multiple dosing. Exact information on the timing of drug intake and plasma sampling are likely to further improve phenotyping accuracy.

14

FAIR-Oriented Evaluation of PBPK Models under the OECD Assessment Framework within an NGRA Context: A Case Study on PFAS

D. Deepika^{1,2}, K. Bharti¹, S. Sharma¹, S. Kumar^{1,2}, V. Kumar^{1,2}

¹Pere Virgili Health Research Institute (IISPV), Universitat Rovira i Virgili, Department of Chemical Engineering, Tarragona, Spain

²Bundesinstitut für Risikobewertung (BfR), Department of Pesticide Safety, Berlin, Germany

Physiologically based Pharmacokinetic (PBPK) models play a crucial role in quantitative chemical risk assessment by providing a mechanistic link between external exposures and internal tissue concentrations. To ensure confidence in PBPK models used for regulatory decision-making, the OECD issued a guidance document in 2021 outlining principles for model characterization, evaluation, and reporting. Despite its publication, practical adoption in chemical toxicology has remained limited. This study evaluated PBPK models for per- and polyfluoroalkyl substances (PFASs) following the OECD guidance to assess their validity and regulatory credibility. Among 28 published PFAS PBK models identified, 11 were systematically reviewed using an online evaluation framework developed from the OECD criteria, encompassing documentation quality and model validity dimensions such as biological plausibility, parameter reliability, uncertainty analysis, and predictive performance. The evaluation revealed significant variability in reporting transparency and biological representation, particularly regarding inclusion of diverse population groups, enterohepatic circulation, and mechanistic compartments. Moreover, most models focused on a limited subset of PFAS compounds, underscoring the need for broader chemical coverage via data-driven read-across strategies. To facilitate harmonization, we developed an open-access R Shiny template implementing the OECD evaluation framework (https://app.shiny.insilicohub.org/Evaluation_PBPK/) [1]. This open access application supports model developers and regulators in applying consistent criteria and enhances reproducibility and FAIR model practices. Overall, this case study represents the first structured assessment of PFAS PBPK models under OECD guidance, providing insights for improving PBPK model transparency, reproducibility, and acceptance for regulatory applications.

[1] Deepika D, Bharti K, Sharma S, Kumar S, Husøy T, Wojewodzic MW, Komproová K, Ratier A, Westerhout J, Gastellu T, Moriceau MA, Majid S, Hoondert R, Kruisselbrink J, Engel J, Noorlander A, Vogs C, Kumar V, Evaluation of PBK models using the OECD assessment framework taking PFAS as case study, *Comp Toxicology*, Vol 36, 2025, 100381, 10.1016/j.comtox.2025.100381.

15

Echinacea purpurea pressed juice: Bidirectional interactions with the human gut microbiota

M. E. Grafakou¹, E. M. Pferschy-Wenzig¹, O. Kelber², C. Moissl-Eichinger³, R. Bauer²

¹Institute of Pharmaceutical Sciences, Department of Pharmacognosy, Graz, Austria

²Phyto & Biotics Tech Platform, Phytomedicines Supply and Development Center, Bayer Consumer Health, Steigerwald Arzneimittelwerk GmbH, Darmstadt, Germany

³Medical University of Graz, Diagnostic and Research Institute of Hygiene, Microbiology and Environmental Medicine, Graz, Austria

Question: The role of the bidirectional interactions of the gut microbiome gain increasingly attention. This applies especially for herbal medicinal products. To understand the influence of these interactions on the action of a medicinal product used in common cold, *Echinacea purpurea* pressed juice, was studied in a model of the human gut microbiota.

Methods: Dried *Echinacea purpurea* pressed juice was subjected to *in vitro* upper intestinal tract digestion [1], followed by *ex vivo* incubation using microbiota derived from fecal samples of ten healthy human donors [2]. Metabolites were characterized by UHPLC-HRMS, the composition of the gut microbiota by 16S rRNA gene sequencing and differential abundance analysis.

Results: We identified caffeic acid derivatives, organic acids and alkamides in the initial dried pressed juice and determined a fructofuranoside content of 9% (calc. as fructose). The overall chemical profile was highly impacted by the gastric phase, but the enhanced levels returned to basal levels or slightly decreased in the intestinal phase of upper intestinal tract digestion. Upon fermentation with human fecal samples, the annotated compounds underwent intensive biotransformation, producing metabolites like caffeic acid, 3,4-dihydroxyphenylpropionic acid, and cinnamic acid, which are known from *in vitro* and *in vivo* studies to possess immunomodulatory properties. 16S rRNA gene sequencing and differential abundance analysis revealed significant modulation of gut microbial taxa, including few, such as *Prevotellaceae* and *Erysipelotrichaceae*, which are associated with immunity and inflammation. Incubation with *E. purpurea* pressed juice also led to significant stimulation of SCFA production and reduction of proteolytic fermentation, while mild donor-dependent immunomodulatory effects were observed in a Caco-2/THP1 co-culture *in vitro* model.

Conclusions: Provided that they also happen *in vivo*, these bidirectional interactions between *E. purpurea* constituents and gut microbiota might contribute to the extract's overall pharmacological effects.

References:

- [1] Brodkorb A, Egger L, Alminger M et al. INFOGEST static *in vitro* simulation of gastrointestinal food digestion. *Nat Protoc* 2019; 14, 991–1014.
- [2] Pérez-Burillo S, Molino S, Navajas-Porras B, et al. An *in vitro* batch fermentation protocol for studying the contribution of food to gut microbiota composition and functionality. *Nat Protoc* 2021; 16, 3186–3209.

16

Slick potassium channels limit TRPM3-mediated activation of sensory neurons

P. Engel¹, F. Zhou¹, B. T. T. Tran¹, A. Schmidt¹, R. Lu¹

¹Goethe University Frankfurt, Institute of Pharmacology and Clinical Pharmacy, Frankfurt a. M., Germany

Objectives: The sodium-dependent potassium channel Slick (KNa1.2, Kcnt2) is expressed throughout the nervous system where it is important for the generation of sodium-activated potassium currents and for maintaining neuronal excitability. Using different mouse models of pain in Slick knockout mice, we found that Slick modulates heat sensation. However, the mechanism by which Slick modulates heat sensation is poorly understood.

Materials & Methods: The tissue distribution of Slick was investigated using immunohistochemistry, *in situ* hybridization and RT-qPCR. The nociceptive behavior of mice lacking Slick globally (Slick^{-/-}), conditionally in sensory neurons expressing Nav1.8 (SNS-Slick^{-/-}), and conditionally in the dorsal horn of the spinal cord (Lbx-Slick^{-/-}) was assessed. Calcium imaging and patch-clamp recordings were performed using primary dorsal root ganglion neurons.

Results: In Slick^{-/-} and SNS-Slick^{-/-} mice, but not in Lbx-Slick^{-/-} mice, the latency to express any nociceptive behavior was reduced in the hot plate and tail immersion tests. *In situ* hybridization experiments revealed Slick was highly co-expressed with the essential heat sensor, transient receptor potential (TRP) melastatin (TRPM) 3, but not with TRP vanilloid 1, TRP ankyrin 1, or TRPM2 in sensory neurons. Notably, SNS-Slick^{-/-} mice exhibited increased nociceptive behaviors following the intraplantar injection of the TRPM3 activator pregnenolone sulfate. Patch-clamp recordings detected increased sodium-dependent outward potassium current (IK) after TRPM3 activation in sensory neurons, which showed no prominent IK after the replacement of NaCl with choline chloride.

Conclusion: Our findings indicate that Slick limits TRPM3-mediated activation of sensory neurons, thereby inhibiting noxious heat sensing.

17

Hypothalamic TRH-Neurons in the Energy Metabolism of Mice

A. Chandrasekar¹, L. Kleindienst¹, A. Constantinescu¹, M. Schwaninger¹, H. Müller-Fielitz¹

¹University of Lübeck, Institute of Experimental and Clinical Pharmacology and Toxicology, Lübeck, Germany

Thyrotropin-releasing hormone (TRH) neurons are distributed across several brain regions involved in metabolic regulation, yet their specific roles remain incompletely understood. This thesis examines the function of TRH-expressing neurons in energy metabolism by selectively activating them within three hypothalamic nuclei—the paraventricular nucleus (PVN), dorsomedial hypothalamus (DMH), and medial preoptic area (MPA)—using chemogenetic tools and inactivation with tetanus toxin. Metabolic effects of TRH-neuron activation were assessed under conditions of food restriction and leptin co-administration and cold tolerance tests.

Despite sharing a common neurochemical phenotype, TRH-neuron populations in these nuclei exhibited distinct metabolic functions. Activation in all three regions increased food intake and energy expenditure, while only PVN and DMH activation elevated core body temperature and BAT temperature. The rise in energy expenditure persisted during fasting, indicating food-independent effects. Activation of TRH neurons in the PVN and MPA during fasting induced a torpor-like state specifically in females. Inactivation of the TRH-neurons in the MPA influence dramatically the body weight and cold tolerance. Leptin co-administration revealed nucleus-specific modulation, suggesting differential integration of peripheral metabolic cues. Notably, only activation of PVN TRH-neurons increased circulating thyroid hormone levels, demonstrating that TRH-neurons in the DMH and MPA affect metabolism independently of the hypothalamic-pituitary-thyroid (HPT) axis.

Together, these findings show that distinct TRH-neuron subpopulations differentially integrate hormonal, neuronal, and environmental signals to regulate energy balance. Understanding these nucleus-specific mechanisms enhances our knowledge of neural circuits governing energy homeostasis and may inform new strategies to address metabolic and endocrine disorders.

18

Vioprolide A elicits anti-inflammatory actions in leukocytes most likely by impeding intracellular cytokine trafficking

N. Frey¹, R. Müller^{2,3}, M. Völkl¹, R. Fürst¹

¹Ludwig Maximilian University of Munich, Pharmaceutical Biology, Department of Pharmacy - Center for Drug Research, Munich, Germany

²Helmholtz Institute for Pharmaceutical Research Saarland (HIPS), Helmholtz Centre for Infection Research (HZI), Department of Microbial Natural Products (MINS), Saarbrücken, Germany

³Saarland University, Department of Pharmacy, Saarbrücken, Germany

Vioprolide A (VioA), a secondary metabolite of the myxobacterium *Cystobacter violaceus*, has been intensively studied for its anti-cancer and anti-angiogenic properties¹. Very recently, VioA has been linked to anti-inflammatory actions in endothelial cells by interacting with NOP14 – an underexplored component of the small ribosome processome and hence a key factor for protein biosynthesis². In addition to endothelial cells, a plethora of immune cells regulate both the induction and resolution of inflammation. Therefore, this study aims to further unravel the effects of VioA on inflammatory processes in human immune cells.

VioA treatment of primary lymphocytes, primary monocytes, and monocytic THP-1 cells disrupted the interaction between endothelial cells and leukocytes already at a low concentration of 10 nM. In line, the surface expression of several crucial adhesion proteins (e. g. VLA-4) was lowered, especially on the surface of primary monocytes. Intriguingly, typical macrophage functions, including phagocytosis and efferocytosis, remained unaltered, highlighting a certain selectivity of the VioA treatment on different leukocytes. Furthermore, VioA treatment of primary monocytes significantly lowered the amount of pro-inflammatory cytokines secreted into the cell culture medium, with IL-6 and IL-8 being most prominently affected. Interestingly, gene and intracellular protein expression of these cytokines remained unaltered. This implies that VioA, while still impeding protein biosynthesis in primary monocytes, might additionally affect other cellular functions, such as intracellular cytokine trafficking. In this context, analysis of transcriptomics data revealed a striking downregulation of genes involved in secretion pathways, further corroborating this hypothesis.

Taken together, this study has demonstrated the ability of VioA to impair key immune cell functions as it reduced cell adhesion of leukocytes to the endothelium and cytokine secretion in human leukocytes. These findings highlight the potential of VioA to not only inhibit protein biosynthesis but also to modulate other essential mechanisms like intracellular cytokine trafficking and secretion. Ongoing research, including proteomic analyses, aim to further elucidate the underlying mode of action and to identify further potential novel target proteins.

1. Burgers, L.D., et al. (2022). *Biomed Pharmacother* 152, 113174.
2. Burgers, L.D., et al. (2021). *Biomed Pharmacother* 144, 112255.

19

Leupyrins Inhibit Oxidative Phosphorylation via ATP Synthase Suppression and Attenuate Pro-inflammatory Responses in Macrophages

J. E. Weber¹, A. B. Mahmoud², B. Diesel¹, R. Müller¹, A. K. Kierner¹

¹Saarland University, Department of Pharmacy, Pharmaceutical Biology. Center for Gender-Specific Biology and Medicine (CGBM). PharmaScienceHub (PSH), Saarbrücken, Germany

²Saarland University, Helmholtz Centre for Infection Research, Helmholtz Institute for Pharmaceutical Research Saarland (HIPS). PharmaScienceHub (PSH), Saarbrücken, Germany

Leupyrins represent a structurally unique family of secondary metabolites derived from *Sorangium cellulosum*. Their nonsymmetric macrodialide scaffold incorporates an unusually substituted γ -butyrolactone alongside pyrrole and oxazoline rings, reflecting a remarkable biosynthesis. They exhibit potent antifungal, antiproliferative, and anti-HIV activities *in vitro*, and have been reported to inhibit nucleic acid and protein synthesis, while showing only moderate cellular toxicity. This, together with their structural optimization potential, makes them interesting candidates for drug development among natural products. Although human leukocyte elastase has been proposed as a molecular target for leupyrins, the mechanisms driving their diverse bioactivities remain unresolved. Aim of this study was to investigate possible immunomodulatory properties of leupyrins, and to identify potential molecular targets.

Human and murine monocytes and macrophages (M ϕ s) were utilised to evaluate potential immunomodulatory effects of leupyrins, employing RT-qPCR, and reporter cell assays. To provide insights into mitochondrial function and metabolic activity, Seahorse[®] analysis and a MitoCheck[®] Complex V Activity assay were performed. Cellular viability was monitored across a range of treatment conditions, and *in vivo* tolerability was evaluated in zebrafish larvae.

Treatment with leupyrin B1, B2, or D resulted in anti-inflammatory effects in RAW-Blue[™] and THP1-Blue[™] NF- κ B cells and reduced gene expression of pro-inflammatory cytokines. Seahorse[®] analysis revealed a suppression of oxidative phosphorylation (OXPHOS) accompanied by increased extracellular acidification rate (ECAR) consistent with a compensatory upregulation of glycolysis, comparable to the effects of the ATP synthase inhibitor oligomycin. The measurement of the direct effect of leupyrins on complex V showed their strong inhibitory activity. Besides, no substantial cytotoxicity was detected under the conditions tested. Complementary metabolomic profiling and structure-based binding studies are ongoing to clarify the ATP synthase as molecular target.

Leupyrins influence the metabolic cell activity as functional inhibitors of mitochondrial ATP synthase, in addition to exhibiting immunomodulatory properties. These findings confirm leupyrins as a promising class of new drug candidates, demonstrating potent pharmacological effects that warrant further investigation to elucidate their molecular targets.

20

Investigations into the mechanism of Cdc2-like kinase inhibitors in Wnt/ β -catenin pathway suppression

J. Hammer¹, T. Zech¹, S. Thieme², R. Fürst¹

¹Ludwig Maximilian University of Munich, Pharmacy, Munich, Germany

²Ludwig Maximilian University of Munich, Gene Center - Laboratory for Functional Genome Analysis, Munich, Germany

Aberrant Wnt/ β -catenin signaling is implicated in various pathological processes, including neurodegenerative diseases, chronic inflammation, and above all, cancer. Accordingly, Wnt/ β -catenin is regarded as a promising therapeutic target system. However, no anti-cancer drug has yet been approved that specifically targets this pathway.

In this context, Cdc2-like kinases (CLKs), which are members of the CMGC kinase family, have recently gained attention. These kinases are known for regulating pre-mRNA splicing, as they phosphorylate serine/arginine-rich splicing factors. Interestingly, CLK inhibitors have been shown to potentially inhibit Wnt/ β -catenin signaling and are currently being evaluated in clinical trials as potential treatment for cancer and inflammatory diseases. However, the mechanism underlying this inhibition remains unknown. To address this issue, we are investigating cirtuvivint, a pan-CLK inhibitor.

Cirtuvivint strongly reduced the proliferation of HeLa cells (crystal violet staining) and induced their apoptosis (hypodiploidic DNA). Crucially, we showed that cirtuvivint inhibits Wnt/ β -catenin signaling in a dual-luciferase assay. Surprisingly, nuclear translocation of β -catenin was unaffected by CLK inhibition, as shown both microscopically and via western blot analysis of nuclear fractions. These results indicate that cirtuvivint acts downstream in the pathway.

Given that CLK inhibition promotes alternative splicing, we performed long-read RNA sequencing. Notably, AMD1, a key enzyme in polyamine biosynthesis, exhibited pronounced exon skipping upon cirtuvivint treatment. AMD1 activity has been linked to the expression of TCF7L2, a critical transcription factor in Wnt signaling. Moreover, we also observed reduced TCF7L2 expression after cirtuvivint treatment.

In summary, our findings demonstrate that cirtuvivint exerts strong anti-cancer effects and inhibits canonical Wnt signaling downstream of β -catenin nuclear translocation. Moreover, we showed that AMD1 splicing is altered, while TCF7L2 mRNA expression is downregulated, both representing potential mechanisms contributing to Wnt signaling inhibition. Currently, we are investigating the link between these observations using inducible overexpression and miRNA-mediated knockdown of AMD1, with the goal of improving our understanding of the Wnt/ β -Catenin signaling pathway.

22

Role for R-loops and DNA replication stress in Mycotoxin genotoxicity

T. Hofmann¹

¹Institute of Toxicology at the University Medical Center Mainz, Mainz, Germany

Food-borne Mycotoxins, such as Aflatoxins, pose major medical problems since they can contaminate food and accumulate in the nutrient chain. In particular in children, Aflatoxin incorporation is linked to acute toxicity and Aflatoxicosis, which is characterized by liver damage and inflammation, while chronic exposure fosters liver carcinogenesis. Although it is well established that Aflatoxins, such as the highly potent Aflatoxin B1 (AFB1), are metabolically activated and cause the formation mutagenic DNA base adducts, the molecular mechanisms by which AFB1 activates the DNA damage response (DDR) and mediate cytotoxicity still remains incompletely understood.

Here we analysed the molecular events and DNA signalling pathways underlying mycotoxin genotoxicity in human liver cells. Our results indicate that AFB1 exposure triggers activation of the DNA replication stress response characterized by checkpoint kinase ATR activation, RPA phosphorylation, increased stalled replication forks and a slowdown of replication speed. In addition, we found that ATR activation mediated by AFB1 triggers activation of the DNA damage-responsive kinase HIPK2 at DNA double-strand breaks. Activated HIPK2 stimulates cell death through phosphorylation-mediated activation of the tumour suppressor p53, which triggers the transcription of pro-apoptotic and pro-ferroptotic target genes. Mechanistically, we found that AFB1 stimulates the formation of specific RNA-DNA hybrids termed R-loops, which can result in DNA lesions and activate the DDR by causing transcription-replication conflicts.

Collectively, our results suggest an unforeseen role for R-loops and DNA replication stress as basal mechanism in AFB1 hepatotoxicity by activating a detrimental ATR-HIPK2-p53 signalling axis leading to liver cell death. Our data also suggests the short-term treatment with ATR inhibitors as potential antidotes to treat AFB-induced acute liver toxicity and Aflatoxicosis.

23

Host KDEL Receptors Are Required for Full Toxicity of EHEC Subtilase Cytotoxin Subunit A

L. König¹, V. Hunszinger², C. Arnold¹, N. Hundertmark¹, J. Fellendorf³, H. Schmidt⁴, K. Sparrer⁴, H. Barth¹, P. Papatheodorou¹

¹Institut für Experimentelle und Klinische Pharmakologie, Toxikologie und

Naturheilkunde/ Universitätsklinikum Ulm, Ulm, Germany

²Institut für Molekulare Virologie/ Universitätsklinikum Ulm, Ulm, Germany

³Institut für Lebensmittelwissenschaft und Biotechnologie/ Universität Hohenheim, Hohenheim, Germany

⁴German Center for Neurodegenerative Diseases (DZNE), Ulm, Germany

Shiga toxin-producing *E. coli* (STEC) are zoonotic pathogens which can cause severe disease in humans by virulence factors such as Shiga toxin and Subtilase cytotoxin (SubAB). SubAB, an AB-type toxin, binds host cell sialoglycans for cell entry via its binding (B) component SubB and delivers the enzymatically active (A) component SubA to the endoplasmic reticulum (ER). In the ER, SubA cleaves the ER chaperone GRP78, thereby triggering ER stress, activation of the unfolded protein response (UPR), and eventually apoptosis.

We recently showed that SubA is cytotoxic by itself without SubB (Sessler et al. 2021). However, the underlying mechanisms of cellular internalization of SubA remained unclear. Here, we performed a genome-wide CRISPR/Cas knockout screen in HeLa cells to identify host factors contributing to the toxicity of SubA. From this screen host KDEL receptors (KDELRL1/2) emerged as required for full SubA-mediated cytotoxicity. In their cellular function, KDEL receptors return escaped ER proteins from the Golgi by recognizing their C-terminal Lys-Asp-Glu-Leu (KDEL) motif. Knockout of KDELRL1 or KDELRL2 in HeLa cells significantly delayed SubA-induced morphological changes, cleavage of GRP78 and inhibition of protein synthesis.

Our study revealed that KDELRL1 and KDELRL2 play key roles in the uptake and/or mode-of-action of SubA, providing a basis for deeper investigation into their molecular mechanisms and for advancing anti-toxin therapeutic strategies.

Recommended literature:
Sessler, Katharina et al. "The enzyme subunit SubA of Shiga toxin-producing *E. coli* strains demonstrates comparable intracellular transport and cytotoxic activity as the holotoxin SubAB in HeLa and HCT116 cells in vitro." *Archives of toxicology* vol. 95,3 (2021): 975-983. doi:10.1007/s00204-020-02965-2

24

Aetokthonotoxin uncouples oxidative phosphorylation due to protonophore activity

V. Rebhahn¹, M. Saoud², M. Winterhalter³, F. Schanbacher¹, M. Jobst⁴, R. Ruiz⁵, A. Sonntag¹, J. Kollatz¹, R. Sprengel¹, S. Donovan⁶, G. Del Favero⁴, R. Rennert², T. Niedermeyer¹

¹Free University of Berlin, Berlin, Germany

²Leibniz Institute of Plant Biochemistry, Halle (Saale), Germany

³Universität Hamburg, Constructor University Bremen, Hamburg, Germany

⁴Universität Wien, Vienna, Austria

⁵Pion Inc., Forest Row, United Kingdom

⁶retired, Willow Grove, PA, United States

Wildlife in the south-eastern United States suffer from vacuolar myelinopathy. This disease comprises severe neurological impairment with disruption of myelin sheaths in the white matter and is eventually lethal. We recently determined aetokthonotoxin (AETX) as the causative agent. AETX is a unique natural product synthesized by the epiphytic freshwater cyanobacterium *A. hydrillicola*, and transmitted via the food chain [1]. With the aetiology of the disease being unravelled, we now focused on the mode of action of AETX in mammalian cells and bacteria. Integrating metabolomic profiling, fluorescence microscopy, and assays targeting oxygen consumption, ATP production, membrane potential, and conductance demonstrate that the primary mechanism of AETX is the uncoupling of the oxidative phosphorylation. For the first time, biological activity of AETX was characterized beyond cytotoxicity assays with the aim to elucidate its mode of action. We have found that AETX uncouples the oxidative phosphorylation in mitochondria by acting as a protonophore.

References: [1] Breinlinger et al. 10.1126/science.aax9050 (2021).

25

Toxic friends? Co-exposure to selected genotoxicants in human liver cell culture models

A. M. Dilger¹, M. Sängler¹, N. Herzog², J. H. Küpper², A. Mangerich¹

¹University of Potsdam, Potsdam, Germany

²Brandenburg University of Technology Cottbus-Senftenberg, Senftenberg, Germany

Humans are continuously exposed to numerous dietary xenobiotics, and the concept of the "human exposome" research aims to take such real-life complexities of potential adverse health outcomes. For instance, combined substance effects may critically influence processes such as aging and carcinogenesis. In both cases, genotoxic compounds are of particular importance, as DNA damage represents a central mechanism in their etiology. Consequently, a deeper understanding into the combined effects of nutritionally relevant genotoxicants can provide valuable support for future toxicological risk assessments.

To investigate potential toxicological outcomes and mechanisms of combined toxicant exposure, this project focuses on three nutritionally relevant genotoxicants: ethanol (EtOH), benzo[a]pyrene (B[a]P), and acrylamide (ACR). These compounds have been associated with an increased cancer risk and are classified by the IARC as class I or class II carcinogens. Notably, little is known about the mixture and combined adverse effects of these compounds.

Each of these substances relies on hepatic metabolism to form toxic metabolites (acetaldehyde, BPDE and glycidamide), yet studying these mechanisms in *in-vitro* systems is challenging as hepatic cells typically lose metabolic capacity in culture. To overcome this, genetically modified HepG2 cell lines overexpressing, e.g., CYP2E1, and matching control cells were generated. Additionally, immortalized human hepatocytes (IHH cells) are employed. This set of cell lines provides a valuable tool for studying metabolic aspects, while supporting reproducibility and higher throughput in analyses of potential mechanistic interactions between compounds of interest.

Based on single substance exposure studies, binary mixture matrices have been developed and tested in a comparative manner for EtOH and B[a]P, as well as ACR and B[a]P, revealing synergistic and additive effects of combined exposure, respectively. Differential responses were observed between control and CYP2E1 overexpressing HepG2 cells. Also, mRNA and protein expression of relevant enzymes upon single substance exposure was verified. Further objectives of this

study, both ongoing and planned, are to characterize and compare other hepatic cellular models and to investigate mechanistic aspects. Therefore, endpoints of interest involve DNA damage response, cellular stress response and defence mechanisms, as well as senescence under single and combined exposure schemes.

26

Combined effects of steatosis- and phospholipidosis-inducing compounds on lipid and xenobiotic metabolism in human liver cells

N. Wewer¹, J. Jablinski¹, H. Sprenger¹, A. Braeuning¹, D. Lichtenstein¹

¹German Federal Institute for Risk Assessment (BfR), Berlin, Germany

Introduction + Question: The incidence of obesity and related disorders is rising worldwide. In addition to genetic factors and lifestyle, metabolism disrupting chemicals (MDCs) are suspected to contribute to the progression of these diseases. As the liver is involved in lipid metabolism, MDCs may affect related pathways which can lead to adverse effects, such as steatosis (STD), an accumulation of triglycerides, or phospholipidosis (PLD), an accumulation of phospholipids. So far, investigations mainly focused on single MDC treatment which is far from real life scenarios with exposure of many chemicals at the same time. Therefore, we investigated combinational effects of a PLD- and STD-inducer mixture on hepatic lipid metabolism.

Methods + Results: Differentiated HepaRG cells were used as a human hepatocyte model, as HepaRG cells preserved various liver-specific functions and are capable of regulating metabolic pathways at levels very similar to primary human hepatocytes. To assess potential mixture effects, cells were exposed to a defined combination of a STD inducer and a PLD inducer, followed by analysis of cell viability and lipid accumulation. The investigated mixture resulted in increased cytotoxicity and PLD induction, as well as reduced STD induction. Analysis of these findings with different mathematical models revealed that observed mixture effects deviate from dose additivity. Investigations of the mixture on the inhibition of CYP enzyme expression and activity revealed synergistic effects, indicating toxicokinetic interaction of the mixture. Observed effects on lipid metabolism will be further investigated on a mechanistic level, and transcriptome analysis will be performed to improve understanding of PLD induction and possible overlap with STD induction.

Conclusions: In conclusion, the presented study revealed synergistic and antagonistic effects of the chosen mixture on different lipid endpoints, as well as synergistic inhibition on xenobiotic metabolism. These findings highlight the importance of mixture investigation, especially for mixtures of substances with different adverse outcomes.

27

Characterisation of the toxicity of hexahydrocannabinol, cannabidiol and their mixtures

B. Bauer¹, L. Waggmann², S. Jenabi¹, V. Berens¹, L. Bofinger¹, A. Hoffmann¹, M. Meyer¹, H. Hintzsche¹

¹University of Bonn, Food Safety, Bonn, Germany

²Saarland University, Experimental and Clinical Toxicology and Pharmacology, Homburg, Germany

Due to recent legislative changes in many countries, consumption of cannabinoids is on the rise worldwide. Consequently, their hazard characterisation is gaining importance. Hexahydrocannabinol (HHC) is a newly emerging semi-synthetic cannabinoid that has been used as a recreational drug for only a few years. Apart from its narcotic properties, data on the toxic effects of HHC remain scarce. HHC is often sprayed onto hemp buds that contain cannabidiol (CBD), making the assessment of combined HHC/CBD toxicity particularly relevant. Therefore, the aim of this study was to evaluate the toxic properties of HHC, CBD, and their mixtures.

To this end, cytotoxicity and genotoxicity were investigated in V79 fibroblasts and CYP-overexpressing HepG2 cells, while organ-specific toxicity was evaluated in transgenic *fabp10:GFP* zebrafish larvae. Cytotoxicity in cannabinoid-treated cells was drastically reduced when a metabolic system like rat liver S9 or CYP 2D6 was present, compared to treated cells without S9 or without CYP 2D6 expression. This metabolic detoxification was especially profound after treatment with CBD. Genotoxic effects were only detected after 24 h treatment with HHC and CBD but not with the mixture of HHC/CBD in the micronucleus test. Comet assay results were completely negative.

In zebrafish larvae, hepatotoxicity after cannabinoid treatment was shown by decreased liver size and increased expression of the reporter gene *fatty acid binding protein 10*. Correspondingly, histopathological findings revealed swelling of hepatocytes and vacuolation, as indicative for steatosis. Additionally, cardiotoxic effects, comprising bradycardia, cardiac arrest and pericardial edema, were observed after treatment with the cannabinoids. These effects were accompanied by blood cell accumulation in the cardiac ventricle and flattening of the epicardium. Exposure to a mixture of CBD/HHC resulted in a pronounced antagonism that was observed across several endpoints, including mortality and cardiotoxicity. Bioanalysis of internal concentrations will complement current findings to unravel potential toxicokinetic mechanisms responsible for the observed mixture effects.

These data will strengthen the regulatory assessment for the consumption of HHC and CBD as individual substances and in combination.

28

Next generation risk assessment: An integrated transcriptomic, phenotypic profiling and IVIVE approach for plant protection product mixture effects
 Y. Museng^{1,2}, I. Cuciu¹, V. Kumar^{1,3}, D. Deepika^{1,3}, S. Liu¹, V. Fetz¹, M. Wedler¹, A. S. Aßmann¹, M. Oelgeschläger¹, P. Marx-Stölting¹, T. Tralau¹, D. Bloch¹
¹Bundesinstitut für Risikobewertung (BfR), Berlin, Germany
²University of Potsdam, Department of Food Chemistry, Potsdam, Germany
³Univeritat Rovira i Virgili, Dep. of Chemical Engineering (DEQ), Tarragona, Spain

The pursuit of eliminating animal testing in human health risk assessment has driven a transformative shift towards next-generation risk assessment (NGRA) across multiple sectors and regulatory bodies. NGRA is a human-relevant, exposure-led, hypothesis-driven risk assessment approach that employs new approach methodologies (NAMs). Currently, plant protection product (PPP) risk assessment relies on evaluating individual substances based on animal testing. This innovative framework enables a comprehensive assessment of whole mixtures, overcoming the limitations of traditional compound-based PPP risk assessment, which often overlooks interactions that may increase toxicity. This study aims to evaluate the feasibility of a NGRA approach that integrates systems toxicology-based NAMs, including cell painting and transcriptomics with toxicokinetic models, to determine PPP-based human equivalent doses (HED) and threshold values corresponding to *in vitro* concentration-response data. Notably, toxicological threshold values were derived from cell painting data, and transcriptomics analysis using two concentrations was included as an additional component to further investigate mechanisms associated with steatosis. To this end, transcriptomics analysis and *in vitro* phenotypic profiling using the cell painting plus (CPP) method were performed on a PPP containing two metabolically interacting active substances. This study investigated the effect of individual active substances, PPP-equivalent mixture, and the PPP on HepaRG cells at the transcriptomic level and on HepG2 cells through phenotypic profiling. Transcriptomics data were analyzed to identify the affected biological pathways and benchmark concentrations (BMCs) were derived from CPP data. *In vitro-in vivo* extrapolation (IVIVE) was performed using the htk package, with relevant parameters and model assumptions for the PPP, to estimate HEDs and toxicological threshold values. Although the BMCs of individual substances exceeded those of the PPP, the affected cellular organelles remained consistent across all scenarios. The predicted PPP-based toxicological threshold value was below the acceptable operator exposure level (AOEL). This study indicates that risk assessment based solely on active substances may not sufficiently capture complex interactions within PPPs. These findings underscore the importance of integrating NAMs to provide valuable insights into PPP interactions for regulatory purposes and advance NGRA.

29

A Shiny-based framework for aggregating repeated-dose toxicology and organ-specific findings: A case study across eighteen alpha-chloroacetamide herbicides
 D. Gasthaus¹, N. Kraft¹, J. Korus¹, J. Tigges¹, A. Dönmez^{1,2}, K. Koch^{1,2}, M. Frericks³

¹Leibniz Research Institute for Environmental Medicine (IUF), Düsseldorf, Germany

²DNTOX GmbH, Düsseldorf, Germany

³BASF SE, Ludwigshafen, Germany

Regulatory dossiers contain extensive but dispersed toxicity information. We developed an application that aggregates study-level histopathology data and harmonized metadata from repeated-dose rat and dog studies. The app incorporates four standardized templates: study-design metadata, histopathology findings, chemical identifiers, and historical-control baselines for simulation. It enables reproducible visualization (user-defined seed/template) via class or substance filters, organ-agnostic and specific heatmaps (legend: finding/no finding/no data), and dot plots displaying all doses and the no observed adverse effect Level (NOAEL) (mg/kg bw/day). Lowest observed adverse effect level (LOAEL) findings are shown as text when units are not comparable (e.g., ppm). The app supports data aggregation across studies and compounds. To explore biological correlations or map data to adverse outcome pathways.

We present a case study investigating the role of hepatic enzyme induction in correlation to anti-androgenicity. Molecular initiating event information was derived from ToxCast and CoMPARA (AR agonism/antagonism, AUC_{0.1}), AR binding from CoMPARA, and cytochrome P450 enzyme (CYP) surrogate data for hepatic enzyme induction from ToxCasts (CYP1A1/3A4/2B6). *In vivo* repeated dose data for 18 α -chloroacetamide herbicides were extracted from regulatory documents and transferred to in standard templates. Ten substances yielded evaluable data (89 studies), eight had none. Across the 89 studies, organs coverage was 52.8% for testis (47/89), 41.6% for epididymis (37/89), 43.8% for prostate (39/89), and 36.0% for seminal vesicles (32/89). Author-designated treatment-related findings were reported for testis (n=6), epididymis (n=1), and prostate (n=4), but none for seminal vesicles. Treatment-related findings occurred in long-term rat, dog 90-day, and dog 1–2-year studies, but not short-term studies (rat 28/90-day or dog 28-day).

The application consolidates repeated-dose and long-term data in a transparent, reproducible framework that highlights coverage and data gaps, enabling class- and substance-level comparisons while preserving authors' treatment-related/adverse designations flags. Limitations include reliance on author classifications, variable historical organ coverage (notably seminal vesicles), and heterogeneous LOAEL units (text-only). The combination of AOPs with data visualization across studies will allow for an in-depth WoE evaluation across compounds.

30

Physiologically-based toxicokinetic model of the transfer of branched and linear perfluoroalkyl acids in dairy goats
 L. Przygoda¹, H. Just¹, S. Lerch², J. L. Moenning¹, J. Kowalczyk¹, J. Numata¹, R. Pieper¹

¹German Federal Institute for Risk Assessment (BfR), Food and Feed Safety in the Food Chain, Berlin, Germany

²Agroscope, Poiseux, Switzerland

Introduction Perfluoroalkyl acids (PFAAs) are a subgroup of per- and polyfluoroalkyl substances (PFAS) that are extremely persistent and linked to adverse health effects in humans and animals. The European Union has set maximum levels for four PFAAs in foods of animal origin to limit dietary exposure. Predicting PFAA accumulation kinetics in livestock is therefore crucial for assessing their transfer into food products. This study aims to develop a physiologically based toxicokinetic (PBTK) model for branched (br-) and linear (n-) PFAAs in dairy goats. The model covers several perfluorocarboxylates and perfluorosulfonates with chain lengths from 4 to 13 carbons and quantifies their distribution across tissues and excretory routes.

Materials and methods The dynamic compartmental model represents twelve physiological compartments (blood plasma, liver, kidney, spleen, stomachs, intestines, mammary gland, heart, brain, muscles, lungs, and rest) and three excretion pathways (urine, feces, milk). It was parameterized using literature data and results from an in-house *in vivo* feeding study, in which eight goats received PFAS-contaminated hay for eight weeks followed by a twelve-week depuration phase. PFAA concentrations were measured in serum, milk, and excreta over time, and in body tissues at slaughter (end of depuration). Key parameters were optimized to minimize prediction error, and model uncertainty was quantified using jackknife and Monte Carlo analyses. The model, implemented in Python (v3.14), applies an analytical matrix solution enabling efficient computation.

Results and discussion Preliminary results show that the model achieved high predictive performance across 17 PFAAs ($R^2 = 0.96$; mean absolute error [MAE] = 0.18) with 86% confidence interval coverage, indicating robust uncertainty characterization. Predicted mean residence times ranged from 23.3 h (half-life = 0.7 days) for branched perfluorotridecanesulfonic acid (br-PFTrDS) to 427.9 h (half-life = 12.4 days) for non-branched perfluorooctanesulfonic acid (n-PFOS), reflecting the influence of molecular structure on the kinetics of different PFAAs.

Conclusion and implications This model enables the simulation of accumulation and depuration under various exposure scenarios. It may support quantitative risk assessment by predicting transfer into edible tissues and milk and can address questions related to animal health by estimating internal exposure in livestock.

31

Quantitative *in vitro-in vivo* relationship of hepatotoxic concentrations: A case study for food-relevant compounds in the rat

L. Gründler¹, J. G. Hengstler¹, W. Albrecht¹

¹IfAdo, Toxicology, Dortmund, Germany

Question:

How closely are toxic concentrations *in vitro* related to toxic concentrations *in vivo*?

Humans are exposed to a broad variety of substances through food and drinking water, including natural constituents, additives and contaminants. Potential toxicity – for example hepatotoxicity – of these compounds is a significant hazard to public health. The evaluation of human toxicity for the large number of relevant compounds poses a challenge for regulatory toxicology. A high-throughput screening system would therefore be desirable. For the development of such a test system a quantitative comparison of the derived toxic *in vitro* concentrations such as the EC10 to toxic *in vivo* concentrations after administration of known toxic dosages is necessary.

Methods:

As proof-of concept a substance set of 40 food relevant compounds with conventionally derived lowest observed adverse effect levels (LOAEL) for hepatotoxicity was tested with an *in vitro* test battery comprising cytotoxicity and lipid accumulation assays in the rat hepatoma cell lines H4IIE and Zajdela as well as cultured primary rat hepatocytes. In addition, physiologically based pharmacokinetic models were established for all compounds and utilized to obtain *in vivo* concentrations after oral application of the compounds at the LOAEL. To evaluate the *in vitro-in vivo* relationship a quality criterion (Toxicity Iso-concentration Index (TII)) was introduced. A TII of 1 hereby indicates a 100% agreement of all *in vitro* and *in vivo* concentrations.

Results:

The best agreement of the *in vitro* and *in vivo* concentrations was observed with the EC10 for cytotoxicity in H4IIE cells and the peak plasma concentrations in the portal vein. In detail a TII of 0.85 was obtained and 75% of the compounds were within a 10- fold deviation range.

Conclusion:

In conclusion, we demonstrated a correlation between the lowest *in vitro* toxic concentrations and blood concentrations at the LOAEL, but the range of uncertainty is relatively large.

Reference: Gründler L. In vitro – in vivo extrapolation of hepatotoxicity for food-relevant compounds in the rat. Dortmund: TU Dortmund University. Thesis, 2025.

32**Untangling the Toxicities of Ethanol and Its Metabolite Acetaldehyde in the 3R-compliant Model Organism *C. elegans***

A. S. Wohlenberg¹, D. S. Krause¹, N. Ende¹, P. Lölsberg¹, M. M. Nicolai¹, A. Mangerich¹

¹Institute of Nutritional Science, Potsdam University, Nutritional Toxicology, Golm, Germany

Ethanol, classified as a Group 1 human carcinogen (IARC), is associated with over 200 diseases and contributes to ~3 million deaths worldwide annually. According to the WHO, there is no safe level of alcohol consumption.

Ethanol toxicity involves multiple, interrelated mechanisms, including direct cytotoxicity, alterations of energy and xenobiotic metabolism, oxidative stress, and formation of acetaldehyde, a genotoxic, DNA-reactive metabolite. While the carcinogenic potential of ethanol is well established, the precise genotoxic mechanisms and specific contribution of acetaldehyde remain incompletely understood. Beyond carcinogenesis, ethanol exposure has been linked to age-related disorders such as neurodegeneration and accelerated ageing. Thus, ethanol and acetaldehyde serve as model compounds to study gerontotoxic mechanisms, i.e., addressing the question how toxic exposures influence ageing.

The nematode *C. elegans* combines the simplicity of in vitro systems with the biological complexity of a metabolically active multicellular organism. With conserved DNA repair pathways, genetic tractability, short lifespan, and absence of somatic tumours, *C. elegans* is well suited for investigating ethanol- and acetaldehyde-induced geno- and gerontotoxicity.

We established exposure protocols for these volatile compounds in *C. elegans*, ensuring reproducible conditions and minimising bacterial metabolism. L4-stage worms were exposed for 1–3 h, and survival assessed 24 h later. Both substances induced time- and dose-dependent toxicity, with acetaldehyde ~16× more potent than ethanol. Toxicokinetic analyses indicated ethanol uptake, and a distinct sublethal "altered phenotype" was identified, characterised by reduced size and/or increased transparency.

Strain-specific sensitivities were investigated in worms lacking genes involved in ethanol metabolism, DNA repair and NAD metabolism, providing initial mechanistic insights that warrant further investigation. Reproductive toxicity studies demonstrated dose-specific effects. Lifespan analyses will complete the life-cycle toxicity profiles.

Future studies aim to systematically elucidate the differential toxicities of ethanol and acetaldehyde, from organismal to molecular levels. This work advances the mechanistic understanding of alcohol-related geno- and gerontotoxicity and further establishes *C. elegans* as a 3R-compliant model for studying volatile substances, supporting the concept of evidence-based toxicology.

33**In vitro and in vivo bioactivation of alkylfurans to reactive α,β -unsaturated dicarbonyls**

C. Burger¹, R. Dekant¹, J. Buchholz¹, L. Willi¹, L. Geisenfelder¹, A. Mally¹

¹Julius Maximilian University of Würzburg, Department of Toxicology, Würzburg, Germany

Heat-treatment of food can give rise to furan, a hepatotoxin and rodent liver carcinogen, and furan derivatives. Of these, alkyl-substituted furans, including 2-methylfuran (2-MF), 2-ethylfuran (2-EF) and 2-pentylfuran (2-PF) are considered to be of most concern, as CYP450-mediated oxidation of the double bond and subsequent ring opening of the furan moiety may give rise to alkyl-substituted dicarbonyls similar to the reactive furan metabolite cis-2-butene-1,4-dial. Considering the lack of data on alkylfuran biotransformation and toxicity, and the possibility that differences in alkyl-chain length may affect the rate of bioactivation to reactive dialdehydes, the aim of the present study was to investigate the biotransformation of alkylfurans with different chain lengths in vitro using rat and human microsomes and HepaRG cells, as well as in rats in vivo. Reactive metabolite formation was characterized through quantitative analysis of glutathione (GSH)- and N-acetyllysine (NAcLys)-adducts derived from ring opened alkylfuran metabolites using LC-MS/MS. Similar to furan, GSH- and NAcLys-adducts were detected in liver microsomes incubated with 2-MF, 2-EF, and 2-PF in the presence of GSH and NAcLys, confirming bioactivation of these alkylfurans to reactive α,β -unsaturated dicarbonyls. Quantitative analysis of adduct formation in liver microsomes showed overall lower rates of alkylfuran bioactivation compared to furan (Furan > 2-MF >> 2-EF > 2-PF), with consistently higher formation rates in rat vs. human microsomes. Similarly, lower rates of bioactivation of alkylfurans as compared to furan were observed in HepaRG cells treated with (alkyl)furans for 24h, further supporting the influence of the side-chain on the extent of bioactivation. In F344 rats, a single dose of 1 mg/kg bw of 2-MF, 2-EF, or 2-PF resulted in significantly lower 24-hour urinary GSH adduct excretion as compared to furan, with a clear decrease with increasing side-chain length (Furan >> 2-MF > 2-EF > 2-PF). Taken together, our data demonstrate that metabolic ring opening giving rise to a reactive intermediate occurs at lower rates

with alkyl-substituted furans compared to furan, suggesting that alkylfurans may have a lower toxic potential. Furthermore, species differences observed in liver microsomes indicate that humans may be less susceptible to (alkyl)furan toxicity than rodents.

This work was supported by Nestlé Research and the Deutsche Forschungsgemeinschaft (DFG) - 517627564.

34**Telmisartan improves hyperlipidemia-induced cognitive and cerebral/microvascular dysfunction**

L. Hernandez Torres¹, H. Napieczynska², Y. Chakko^{3,4}, F. Spiecker¹, I. Stölting¹, Ü. Özoran¹, O. Müller^{1,5}, R. Aherrahrou^{3,4}, Z. Aherrahrou⁴, H. Hille⁵, M. Schwaninger¹, R. Dechend⁶, W. Raasch¹

¹University of Lübeck, Institute of Experimental and Clinical Pharmacology and Toxicology, Lübeck, Germany

²MDC in the Helmholtz Society, Experimental and Clinical Research Center (ECRC), Berlin, Germany

³University of Lübeck, Lübeck, Germany

⁴University of Lübeck, Institute for Cardiogenetics, Lübeck, Germany

⁵University Hospital Schleswig-Holstein (UKSH), Campus Kiel, Department of Internal Medicine V, Kiel, Germany

⁶Max-Delbrück Center for Molecular Medicine, Preclinical Research Center (PRC), Berlin, Germany

Objective: Using the PCSK9^{DY} approach, we demonstrated in mice that hyperlipidemia impairs cognition and hippocampal blood flow (HBF), both of which are consolidated by telmisartan (TEL). We furthermore suggested that regulation of pericytes contributes to the favorable TEL-effects regarding HBF and memory consolidation.

Methods: To elucidate the mechanisms, we conducted μ CT examinations in brains of mice that received AAV-PCSK9DY injections (2×10¹¹ VG) or AAV and were fed with either Western diet (WD) or chow. Mice were treated with TEL (8 mg/kg) or vehicle. RNAseq analyses and further immunohistological analyses were performed on 20 μ m-thick frozen sections.

Results: μ CT examinations showed rarefaction of the smallest cerebral capillaries with a diameter of less than 10 μ m and normalization by TEL treatment. RNA-seq analyses in mouse hippocampi confirm the results from behavioral studies in the Barnes maze test at the gene regulatory level in KEGG analyses, that cognition is impaired in hyperlipidemic mice but normalized by TEL. The comparative evaluation of gene expression in the hippocampus between chow+VEH- versus PCSK9^{DY}/WD+VEH-treated mice revealed a striking dysregulation of ApoE and Ace. This became apparent after comparing the results from this study with the top 100 regulated human genes in the GenCard database (<https://www.genecards.org>) by searching, using the search terms "hyperlipidemia", "cerebral small vessel disease" or "Alzheimer's disease". Further immunohistological analyses of the IgG/Col IV ratio suggested that the blood-brain barrier (BBB) was disrupted in the hyperlipidemic mice, but that it was normalized again by TEL. This assumption was confirmed by additional MMP9 and CD68 staining and by the determination of CD206 as a marker for perivascular macrophage infiltration. Although we found no evidence of increased hippocampal gene expression of MMP9 in the PCSK9^{DY}/WD+VEH-treated mice in the RNAseq analyses, we did find downregulation in miR-370 and miR-133a. Both microRNAs suppress the formation of MMP9. This explains why MMP9 was elevated in the immunohistological studies, but we did not find any regulation on gene expression level.

Conclusions: We conclude that cognitive impairments in hyperlipidemic mice manifest in altered hippocampal gene expression associated with Alzheimer's disease, in a BBB break down and in a rarefaction of small vessels in the hippocampus, and that all these impairments improved under TEL treatment.

35**Inhibition of the dual-leucine zipper kinase or its conditional gene ablation protect beta-cells from prediabetic signals**

J. Duque Escobar¹, M. Dethlefs¹, K. A. Köster¹, S. Schröder¹, E. Oetjen¹

¹University Medical Center Hamburg-Eppendorf, Hamburg, Germany

Diabetes mellitus (DM) is one of the most increasing diseases worldwide and associated with several cardio- and cerebrovascular diseases. Besides peripheral insulin resistance, loss of beta-cell function and mass lead to type 2 DM (T2DM). Our previous studies in a beta-cell line suggested that activation of the dual leucine zipper kinase (DLK; MAP3K12) by prediabetic signals contributes to the pathogenesis of T2DM. Hence, the role of DLK in beta-cell apoptosis and in glucose homeostasis under prediabetic conditions was studied in isolated murine islets of Langerhans and in transgenic mice.

Treatment of isolated islets with a high glucose/high palmitate concentration to mimic glucolipotoxic conditions induced the phosphorylation of the DLK downstream kinase JNK. Additional treatment with the small molecule DLK inhibitor GNE-3511 attenuated JNK phosphorylation. In line, in islets from mice with a beta-cell selective *Dlk* – deletion (beta-DLK^{-/-}), the prediabetic cytokine TNF α did not induce JNK phosphorylation, and islets from these mice were protected against high glucose caused beta-cell apoptosis. Beta-DLK^{-/-} and their control mice were fed a Western Diet (WD) (21.2% fat, 33.2% sucrose) for 20 weeks. All mice gained more weight under WD than under normal diet (ND). In histological analysis, the islets of beta-DLK^{-/-} and of RIP-Cre mice showed increased cell proliferation, measured as Ki67 positive cells, and islet area under WD. After 20 weeks of WD, only beta-DLK^{-/-} mice exhibited no diet-dependent increase in HbA1c. Under WD, blood glucose levels were elevated in RIP-Cre and in DLK^{fl/fl} mice, but not in beta-DLK^{-/-} mice. In line, insulin serum levels after WD

were higher in beta-DLK/-mice than in RIP-Cre or DLK^{fl/fl} mice; the insulin/glucose ratio was significantly increased in beta-DLK/- compared to RIP-Cre- and DLK^{fl/fl} mice, respectively. Furthermore, treatment of isolated islets from db/db – mice, a well-known mouse diabetes model, with GNE-3511 reduced beta-cell apoptosis. These data show that deletion of *Dlk* in beta-cells or inhibition of DLK preserve beta-cell mass despite a prediabetic setting. Thus, inhibition of DLK presents a promising and novel drug target in antidiabetic therapy.

36

BK channels regulate Ca²⁺ signaling pathways in brown adipocytes to promote diet-induced obesity

D. Spaehn¹, E. Binder¹, K. Serafimov², S. Bolz³, C. Kabagema-Bilan¹, S. Fromknecht¹, H. Bischoff⁴, V. Leiss⁵, M. Hoene⁶, A. Birkenfeld⁷, A. Peter⁸, C. Weigert^{9,10}, M. Ueffing³, M. Laemmerhofer², L. Matt¹, R. Lukowski¹

¹University of Tübingen, Institute of Pharmacy, Department of Experimental Pharmacology, Tübingen, Germany

²University of Tübingen, Institute of Pharmacy, Department of Pharmaceutical (Bio-)analysis, Tübingen, Germany

³University of Tübingen, Institute for Ophthalmic Research, Department for Ophthalmology, Tübingen, Germany

⁴Medical University of Graz, Department of Internal Medicine, Molecular Biology and Biochemistry, and Division of Oncology, Graz, Austria

⁵University of Tübingen, Institute for Experimental and Clinical Pharmacology and Pharmacogenomics, Department of Pharmacology, Experimental Therapy and Toxicology, Tübingen, Germany

⁶University Hospital Tübingen, Institute for Clinical Chemistry and Pathobiochemistry, Department for Diagnostic Laboratory Medicine, Tübingen, Germany

⁷University of Tübingen, Institute for Diabetes Research and Metabolic Diseases of the Helmholtz Center Munich, Tübingen, Germany

Question

Obesity and its comorbidities pose a growing global health burden. Genome-wide association studies linked expression of voltage- and Ca²⁺-activated K⁺ channels of big conductance (BK) to morbid obesity¹. Consistently, global or adipocyte-specific BK knockout mice are protected from diet-induced obesity and exhibit enhanced browning of adipose tissue². Here, we investigate BK's function in brown adipocytes (BA) and its impact on systemic metabolism during diet-induced obesity and at the cellular level.

Methods

To investigate BK's role in BA, we subjected brown adipose tissue (BAT)-specific conditional knock-out mice (cKO) and corresponding controls (CTR) to 18 weeks of high-fat diet (HFD). We evaluated their metabolic status through body composition, plasma lipid profiling, adipose tissue histology and mitochondrial ultrastructure, food intake, glucose tolerance, energy expenditure, body temperature and activity. Additionally, we analyzed BK function *in vitro* using pharmacological inhibition with paxilline (Pax) during live-cell imaging of primary murine BA and a metabolomics approach.

Results

Despite comparable food intake, cKO accumulated markedly less body fat during HFD than CTR. This likely results from elevated energy expenditure due to increased body temperature. Although diabetic status was similar between genotypes, cKO exhibited a distinct, predominantly anti-inflammatory plasma lipid profile. In murine BK-KO BA, glucose uptake, glycolysis, lipolysis, and mitochondrial activity were strongly enhanced to possibly compensate for reduced intracellular ATP levels. Regarding BK's role in ion homeostasis, adrenergically induced K⁺ efflux was highly sensitive to Pax. Furthermore, Pax significantly enhanced nifedipine-sensitive L-type Ca²⁺ channel-mediated Ca²⁺ influx upon adrenergic stimulation. Consistent with this, BK-KO BA displayed amplified adrenergic Ca²⁺-dynamics. Together with low ATP levels, this likely activates AMP-activated protein kinase (AMPK) through a Ca²⁺ - calmodulin - Ca²⁺/calmodulin-dependent protein kinase kinase II (CaMKKII) signaling pathway to promote a markedly more catabolic phenotype in BK-KO BA compared to wild-type cells.

Conclusion

Selective ablation of BK in BA strongly increased metabolism, which likely contributes to DIO resistance. Future studies will clarify the translational potential of BAT-specific BK channels in the human system.

References

1. Jiao et al., 2011
2. Illison et al., 2016

37

Inter-individual variability in drug response: estimating the potential impact of pharmacogenetics in Norway and among the Norwegian Sami population

H. Bruckmüller^{1,2}, K. A. Abuzed², J. Sadallah², K. Svendsen²

¹University Hospital Schleswig-Holstein (UKSH), Campus Kiel, Institute of Experimental and Clinical Pharmacology, Kiel, Germany

²UIT The Arctic University of Norway, Department of Pharmacy, Tromsø, Norway

Inter-individual variability in drug response is a well-documented phenomena in patient treatment. The consideration of pharmacogenetics (PGx) is increasingly recognized as one strategy to optimize treatment outcome and reduce adverse drug effects. Despite the availability of international PGx guidelines as from the Clinical Pharmacogenetics Implementation Consortium (CPIC) or the Dutch Pharmacogenetics Working Group (DPWG), the implementation of PGx into clinical practice remains limited. Furthermore, the impact of PGx on population level including minority groups has been explored only in a few studies.

This study aimed to identify the type of prescribed actionable PGx drugs, the number of users per PGx drug and estimate the proportion of individuals who could potentially benefit from PGx-guided treatment. This analysis focused on the entire Norwegian population and on the northern Norwegian region as proxy for the Norwegian Sami population, a recognized minority.

Data on actionable PGx drugs were extracted from the Norwegian drug prescription registry (NorPD) for the entire Norwegian population aged ≤ 18 years in 2018 and 2019. The potential number of users who might benefit from PGx testing was estimated using actionable genotypes or phenotype frequencies from literature.

In 2019, 72.9% of the entire Norwegian population received at least one prescribed drug and 50% of these individuals were prescribed at least one PGx drug corresponding to 36.4% of the entire Norwegian population. Actionable PGx drugs accounted for 16.7% of all prescribed medications in Norway. In total, 100 drug-gene interactions (DGIs) involving 80 unique drugs were identified. The estimated frequency of actionable genotypes or phenotypes among PGx drug users ranged from 5% to 40% depending on the drug. Lipid lowering agents, antidepressants and opioids were the most frequently administered drugs with actionable DGIs. The usage of PGx drugs in the Sami population was quite similar to the rest of the Norwegian population.

This study highlights the relatively high prevalence of DGIs in primary care across Norway including the potentially genetically diverse Sami population. This finding emphasizes the critical need to address the lack of diversity in PGx research. Targeting this gap is crucial to ensure equitable clinical translation of PGx findings and to provide a fair access to personalized medical treatment for all individuals, irrespective of their ethnic or genetic background.

38

AI reliably assesses undergraduate prescribing skills and provides comprehensive feedback

S. Trescher¹, M. Stadler², T. Gudermann¹, J. Schredelseker¹

¹Ludwig-Maximilians-University Munich, Walther-Straub-Institute of Pharmacology and Toxicology, Munich, Germany

²LMU Munich, University Hospital, Institute of Medical Education, Munich, Germany

"Creation and implementation of a treatment plan based on the principles of evidence-based medicine and clinical decision-making" is a core entrusted professional activity (EPA) in the national competency-based catalog of learning objectives (NKLm). While rational prescribing is a complex process involving higher-order cognitive skills, summarized as pharmacological reasoning, clinical pharmacology education often focuses on the presentation of factual knowledge. Though numerous teaching formats exist to foster diagnostic reasoning, transferring these approaches to pharmacological reasoning is challenging. In diagnostic reasoning cognitive processes and clinical decision-making converges towards a well-defined goal - the single correct diagnosis, while in pharmacological reasoning several therapeutic options may be equally appropriate, yet errors in the reasoning process itself, like overlooking a contraindication, can have drastic consequences. This "journey is the destination" nature of pharmacological reasoning poses specific challenges for assessment, particularly in large-enrollment or self-directed learning settings, where individual assessment and feedback from instructors or peers are not feasible. To address this, we evaluated the potential of large language models (LLMs) to assess and provide feedback on medical students' pharmacological reasoning. We developed a structured, case-independent input format based on the six-step model of the WHO Guide to Good Prescribing. For clinical paper cases students submitted their diagnosis, a concise description of standard care and patient-specific adaptations, a prescription and medication plan, and finally documentation of patient information and monitoring. Submissions were analyzed by an LLM prompted to generate structured feedback. The LLM-generated feedback was comprehensive and presented in a multidimensional evaluation structure. For every step a detailed evaluation of reasoning activities was given, structured into positive aspects, suggestions for enhancement, and further additions. Errors such as incorrect dosing or incompletely filled prescriptions were consistently identified and corrected based on national clinical guidelines. In summary, we created a flexible tool that can be applied to any clinical case and integrated into various teaching formats. Our findings indicate that LLMs can reliably assess the reasoning skills of undergraduate medical students and provide meaningful feedback.

39

Synthesis and biological effects in vitro of titanium dioxide fibers of different length, diameter, and shape

N. Rosenkranz¹, K. Kostka², D. G. Weber¹, G. Johnen¹, A. Winter², A. Brik¹, K. Loza², K. Szafranski¹, N. Bialas², T. Brünig¹, J. Krabbe¹, M. Epple², G. Westphal¹

¹Ruhr University Bochum, Institute for Prevention and Occupational Medicine of the German Social Accident Insurance, Bochum, Germany

²University of Duisburg-Essen, Inorganic Chemistry, Essen, Germany

Background: Inhalation of biopersistent fibers, in particular asbestos fibers, can lead to strong chronic inflammatory effects, fibrosis, and cancer. Fiber shape, size, and stiffness determine these biological effects. However, it is not known

exactly which fiber length, diameter, or aspect ratio determines the threshold for the devastating pathology compared to granular particles.

Methods: Different titanium dioxide fibers with defined diameter and shape were synthesized. Fiber characterization and uptake was studied by scanning electron microscopy and confocal laser scanning microscopy. Biological effects including cell toxicity, mRNA expression, and the induction of chemotaxis were investigated in rat NR8383 cells.

Results: Titanium dioxide fibers were prepared by different synthesis routes, resulting in fiber populations with defined lengths around 15 μm and 25 μm , with a maximum length of up to 28 μm . Aspect ratios of 1:8 up to 1:70 were achieved. For comparison, natural crocidolite asbestos fibers and the straight needle like Multiwalled Carbon Nanotube NM-401 (MWCNT NM-401) were studied. The titanium fibers were internalized very effectively by the cells but caused comparatively low toxicity and only weak particle-induced chemotaxis. Crocidolite asbestos and the MWCNT NM-401 caused massive membrane damage apparent by electron microscopy, in contrast to the titanium dioxide fibers, which evoked barely visible damage. This can be explained by the sharp fiber ends of the asbestos fibers and the MWCNT NM-401, in contrast to the blunt ends of the titanium fibers.

Conclusion: In our in vitro model, macrophages incorporated titanium dioxide up to 28 μm length, but the biological effects remained weak. Comparison with crocidolite asbestos fibers and the MWCNT NM-401 supports the hypothesis that the needle-shaped character of the fiber ends contributes significantly to the inflammatory effects, while the average fiber thickness has less effect in our model.

40 Role of TRPV4 in human bronchial epithelial cell differentiation after application of Cigarette Smoke Extract (CSE)

J. Müller¹, P. Alt¹, M. Kieffmann¹, T. Gudermann¹, A. Dietrich¹

¹Ludwig Maximilian University of Munich, Walther-Straub-Institute, Munich, Germany

1. Introduction/Question

Cigarette smoke exposure is one of the main causes for the development of Chronic Obstructive Pulmonary Disease (COPD), characterized by a remodeled airway epithelium [1]. TRPV4 is expressed in ciliated cells and modulates ciliary beat frequency in the mice [2]. Single cell sequencing data revealed expression of TRPV4 mRNA in human basal cells (www.copdcellatlas.com), which differentiate to a pseudostratified epithelium. Therefore, TRPV4 might play an important role in the development and functionality of a healthy epithelium.

2. Methods

Primary human bronchial epithelial cells (HBECs) were differentiated in an Air-Liquid-Interface (ALI) model. Cigarette Smoke Extract (CSE) was used for chronic basolateral treatment. Differentiation pattern was investigated by immunofluorescence (IF-) staining and confocal microscopy. Subcellular localization of TRPV4 was examined by IF- staining and fractionation assays. Protein expression was analyzed via Western Blotting. Real time fluorescence imaging of HBECs was performed for ratiometric (Fura-2 AM) cytosolic Ca^{2+} signaling.

3. Results

While non-treated HBECs differentiated into a pseudostratified epithelium with a seamless basal cell layer, ciliated, club and goblet cells, CSE-exposed HBECs showed less ciliated, club and goblet cells and a perforated basal cell layer. Compared to untreated cells, IF- staining against TRPV4 revealed an altered localization. Subcellular fractionation assays revealed not only less membrane expression of TRPV4 but also less TRPV4 in the cytosol. Lack of TRPV4 located at the membrane was confirmed by Ca^{2+} -imaging experiments, showing a decrease of Ca^{2+} influx upon TRPV4 activation. Additionally, Protein kinase C and casein kinase substrate in neurons protein 3 (PACSLN3), responsible for membrane expression of TRPV4, was also found to be significantly downregulated on protein level upon CSE treatment.

4. Discussion/Outlook

Primary HBECs differentiated under CSE exposure with reduced numbers of ciliated, club and goblet cells and a changed subcellular localization of TRPV4 channels. Decreasing levels of PACSLN3 protein point to a defective membrane trafficking of TRPV4, which has to be further investigated

References:

[1] Schamberger, A et al., Sci Rep 5, 8163 (2015). <https://doi.org/10.1038/srep08163>.

[2] Lorenzo et al., Proc Natl Acad Sci U S A. 2008 Aug 26;105(34):12611-6.

doi: 10.1073/pnas.0803970105. Epub 2008 Aug 21. PMID: 18719094; PMCID: PMC2527959.

41

Building a ToxAtlas for Carbon-Based Nanomaterials: Single-Cell RNA Sequencing Maps Early Cellular Circuits Driving Pulmonary Inflammation

Q. Lei¹, O. Huzain², C. Barro², L. Han², H. Schiller², T. Stoeger², C. Voss^{1,2}

¹Hannover Medical School (MHH), Clinic for Cardiac, Thoracic, Transplantation and Vascular Surgery, Leibniz Research Laboratories for Biotechnology and Artificial Organs (LEBAO), Hannover 30625, Germany; Biomedical Research in Endstage and Obstructive Lung Disease Hannover (BREATH), Hannover, Germany

²Institute of Lung Health and Immunity (LHI), Comprehensive Pneumology Center (CPC), Helmholtz Center Munich; Member of the German Center for Lung Research (DZL), Neuherberg, Germany

³Institute of Experimental Pneumology, LMU University Hospital, Ludwig-Maximilians University; Research Unit for Precision Regenerative Medicine, Helmholtz Center Munich; Comprehensive Pneumology Center Munich, Neuherberg, Germany

Question

Understanding how specific physicochemical properties of nanomaterials trigger acute lung inflammation is essential for designing applicable in vitro assays. For low-solubility carbon-based nanomaterials (CBN), however, the molecular events that initiate pulmonary inflammation remain poorly defined. Our study aimed to resolve early, cell-type specific responses that drive neutrophilic inflammation after exposure to distinct CBN.

Methods

Mouse lungs were analyzed 12 h after intratracheal instillation of spherical carbon nanoparticles (CNP), tangled double-walled carbon nanotubes (DWCNT), rigid multi-walled carbon nanotubes (MWCNT), or lipopolydisaccharide (LPS) as a positive control. Doses were selected to induce comparable, moderate neutrophilia. Single-cell RNA sequencing identified 41 transcriptionally distinct cell states, enabling mapping of material-specific initiation pathways at single-cell resolution. Predicted activation patterns were evaluated for in vitro reproducibility, and a public webtool (ToxAtlas) was established to visualize CBN-specific gene responses for assay development.

Results

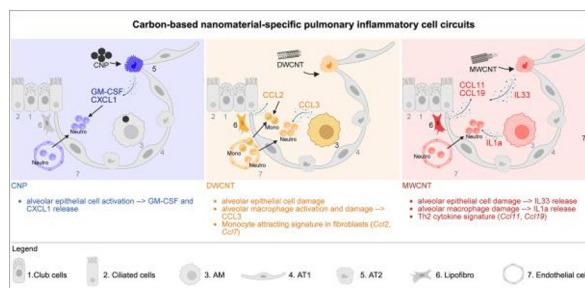
Although chemically related, the tested CBNs triggered inflammation through distinct modes of action. CNP exposure induced neutrophilia predominantly through alveolar epithelial activation, characterized by Cxcl1 and Csf2 expression, without clear evidence of epithelial injury or macrophage activation. By contrast, both CNT types caused epithelial and macrophage injury with alarmin release. MWCNT exposure was dominated by IL-1 α and IL-33 signaling, whereas DWCNT induced epithelial damage accompanied by pro-inflammatory macrophage activation and fibroblast-derived monocyte attractants (Ccl2, Ccl7). Single-cell circuit analysis revealed early fibroblast activation—especially in lipofibroblasts adjacent to type 2 epithelial cells—as a central amplifier of inflammatory signaling.

Conclusions

This work uncovers material-specific epithelial and mesenchymal initiation mechanisms underlying acute CBN-induced inflammation. The data highlight that early fibroblast responses contribute to pulmonary defense and may prime chronic inflammation, particularly relevant to MWCNT exposure. The integrated single-cell dataset and ToxAtlas resource support the design of cell-based assays for next-generation nanomaterial safety testing and may guide safer material engineering.

Reference: Voss et al. 2025 ACS Nano. <https://doi.org/10.1021/acsnano.5c12054>

Fig. 1



42

Comparative characterization of astrocytes from primary and iPSC-derived neural progenitors for in vitro developmental neurotoxicity (DNT) assessment

E. Zühr¹, A. S. Cheruvil Lilikumar¹, L. Petersilie², L. A. Neu², C. Rose², E. Fritsche^{1,3,4,5}, K. Koch^{1,3}

¹Leibniz Research Institute for Environmental Medicine (IUF), Environmental Toxicants and the Brain, Düsseldorf, Germany

²Heinrich Heine University Düsseldorf, Institute of Neurobiology, Düsseldorf, Germany

³DNTOX GmbH, Düsseldorf, Germany

⁴Swiss Centre for Applied Human Toxicology (SCAHT), Basel, Switzerland

⁵University of Basel, Department of Pharmaceutical Sciences, Basel, Switzerland

Current in vivo test guidelines for developmental neurotoxicity (DNT) are resource-intensive, ethically challenging, and limited by inherent scientific uncertainties. To advance toward a more efficient and predictive risk assessment, a DNT in vitro battery (DNT-IVB) based on human-relevant key neurodevelopmental processes was established. Gap analyses revealed that glial cells remain underrepresented, emphasizing the need for complementary assays capturing astrocyte-mediated toxicity. Here, we developed a human astrocyte maturation (hAM) assay to evaluate the potential added value of integrating astrocyte-related endpoints into the DNT-IVB framework.

The hAM assay builds upon the DNT-IVB Neurosphere Assay based on human fetal neural progenitor cells (hNPCs). As an alternative and scalable source for astrocyte differentiation, hiPSC-derived NPCs (hiNPCs) were generated via dual SMAD inhibition for comparison. Astrocyte differentiation from NPCs was promoted with BMP2 and CNTF and astrocytic identity was confirmed based on the expression of key astrocyte markers (e.g. AQP4, GFAP) after 5 days. Transcriptome profiling revealed converging differentiation trajectories in hNPC- and hiNPC-derived astrocytes, with principal component analysis indicating comparable transcriptional reprogramming and robust lineage commitment.

Functional characterization demonstrated inflammatory competence of both astrocyte models, as TNF α stimulation induced a concentration-dependent ICAM1 upregulation. Transcriptomic profiling further confirmed cytokine responsiveness, with distinct expression patterns according to the applied stimulus (TNF α , IFN γ). Functional maturation was supported by calcium imaging, revealing spontaneous as well as glutamate-evoked signaling activity. Following comprehensive assay characterization, alterations in astrocyte differentiation, morphology, and inflammatory activation were defined as quantitative endpoints for assessing astrocyte-mediated toxicity.

Both astrocyte models displayed high phenotypic and transcriptomic similarity to in vivo counterparts and can be cryopreserved for downstream applications such as defined co-cultures. Proof of concept testing with a set of DNT-relevant environmental compounds demonstrated the assay's ability to discriminate between known human DNT-positive and negative substances. Future testing with a broader compound set will further evaluate the assay's predictive capacity and potential contribution to the DNT-IVB.

43

DNA damage plays a critical role in cisplatin-induced neurotoxicity in *C. elegans*

J. Krautstrunk¹, A. K. Weishaupt², J. Bornhorst², G. Fritz¹

¹Heinrich Heine University Düsseldorf, Institute of Toxicology, Düsseldorf, Germany

²University of Wuppertal, Food Chemistry with focus on Toxicology, Wuppertal, Germany

Background

Cisplatin (CisPt), an FDA-approved chemotherapeutic drug, induces apoptosis in proliferating cells. It exerts this effect by forming DNA intra- and interstrand crosslinks, thereby disrupting normal transcription and replication. This is especially detrimental to highly proliferative cells (like malignant tumour cells). However, in platinum-based chemotherapy patients often suffer from adverse side effects predominantly affecting sensory neurons, despite their non-proliferative nature.

Method

Here, we used a loss of function mutant in the nucleotide excision repair (NER) gene *ercc-1* of the 3R-compliant model organism *Caenorhabditis elegans* to analyse the role of unrepaired, CisPt-induced DNA crosslinks on evoking neurotoxicity in sensory neurons. To this end, we examined CisPt-induced sensory dysfunction in wildtype and *ercc-1* mutant animals through a chemotaxis assay that quantifies neuronally mediated attraction to diacetyl. Furthermore, we also analysed neurotransmitter levels using mass spectrometry and gene expression analysis using RNA Seq.

Result

The *ercc-1* mutant animals displayed heightened sensitivity to CisPt-induced sensory dysfunction in the chemotaxis assay at concentrations that caused only moderate effects in wildtype animals. Notably, the observed sensory deficits appeared to be mostly independent of cell death in chemosensory AWA neurons. Neurotransmitter levels of GABA were reduced in CisPt-treated animals while showing only moderate effects on dopamine, serotonin and acetylcholine levels. Moreover, GABA substitution ameliorated the neurotoxic effects in *ercc-1* mutant animals in the chemotaxis assay. To explore the mechanism behind the increased CisPt sensitivity of *ercc-1* mutant animals, we performed RNA sequencing. The results revealed differences in transcription with 425 genes being significantly dysregulated in CisPt-treated *ercc-1* mutant animals.

Conclusion

Summarizing, we conclude that DNA-damage plays a role in the pathophysiology of neuronal dysfunction following CisPt-treatment.

44

Advancing Next-Generation Neurotoxicity Testing with human 3D-BrainSpheres - One platform for different exposure scenarios across developmental stages

I. Scharkin¹, S. Canesi², K. Bartmann^{1,3}, U. Hübenthal¹, F. Bendt³, N. Pierchala¹, J. Dobner¹, A. Dönmez^{1,3}, C. Recordati², A. Rossi¹, K. Koch^{1,3}, E. Fritzsche^{1,3,4,5}

¹Leibniz Research Institute for Environmental Medicine (IUF), Düsseldorf, Germany

²Università degli Studi di Milano, Dipartimento di Medicina Veterinaria, Milano, Italy

³DNTOX GmbH, Düsseldorf, Germany

⁴University of Basel, Department of Pharmaceutical Sciences, Basel, Switzerland

⁵Swiss Centre for Applied Human Toxicology (SCAHT), Basel, Switzerland

Current neurotoxicity assessment of chemicals relies on rodent in vivo OECD guideline studies, which are costly, low-throughput, and ethically challenging with limited human relevance due to inter-species differences. As no single in vitro assay can fully capture the complexity of neural network formation and function, a comprehensive set of assays is needed to systematically address relevant modes of action (MoAs) associated with adult neurotoxicity (ANT). Despite this need, a standardized in vitro battery for ANT (ANT IVB) is lacking. To address this gap, we developed the human multi-neurotransmitter receptor (hMNR) assay using human induced pluripotent stem cell (hiPSC)-derived 3D neuron-glia BrainSpheres. This model covers multiple neurotransmission-associated MoAs and substantially contributes to the development of an ANT IVB.

BrainSpheres are generated by neural induction of hiPSCs using dual SMAD inhibition, followed by three weeks of 3D differentiation and four weeks of 2D network maturation on microelectrode arrays (MEAs). Matured neuron-glia networks express markers for GABAergic, glutamatergic, dopaminergic, serotonergic and cholinergic neurons, respective neurotransmitter receptors, and functionally respond to modulators of the different neurotransmission modalities.

The classical hMNR assay detects acute neurotoxic effects, including altered firing, bursting, and network synchrony following 15-minute chemical exposure, and differentiates compound-specific effects on neurotransmission modalities through spike sorting. Beyond acute exposure, the system supports (sub)chronic exposure studies, allowing the investigation of progressive or reversible network dysfunction. BrainSpheres provide a platform that enables modeling of diverse human-relevant exposure scenarios within a single test system, ranging from early network formation to mature network function. Ongoing refinements include in-depth functional and transcriptomic characterization of the test system, development of robust data evaluation strategies and further exploration of applicability domains using model compounds and environmental chemicals.

BrainSpheres offer a human-relevant, ethical, and efficient alternative to animal-based neurotoxicity testing. By investigating key neurotoxicity-associated MoAs, it provides mechanistic understanding, supports chemical screening and prioritization, and drives ANT IVB development in line with next generation risk assessment (NGRA) strategies.

45

Leukocytic ADAM10 and ADAM17 modulate disease severity and systemic outcome in bacterial and viral pneumonia

A. Aljohmani¹, M. Witzernath², O. Schilling³, R. Bals⁴, D. Yildiz¹

¹Saarland University, Molecular Pharmacology, Homburg, Germany

²Charité - Universitätsmedizin Berlin, Department of Infectious Diseases, Respiratory Medicine and Critical Care, Berlin, Germany

³University of Freiburg, Institute for Surgical Pathology, Medical Center, Freiburg, Germany

⁴Saarland University, Department for Internal Medicine V – Pulmonology, Allergology, Intensive Care Medicine, Homburg, Germany

Background

Pneumonia caused by viral or bacterial pathogens, such as SARS-CoV-2 and *Pseudomonas aeruginosa*, can progress to life-threatening disease in which dysregulated protease activity is implicated. We investigated how the metalloproteinases ADAM10 and ADAM17 expressed by leukocytes, and their presentation on circulating exosomes, shape local lung inflammation and systemic sequelae.

Methods

We integrated analyses of samples from patients with SARS-CoV-2 or bacterial pneumonia with mechanistic in vitro and in silico assays, together with a preclinical pneumonia model using conditional knockout mice lacking ADAM10 or ADAM17 in leukocytes. Exosomal activities of both proteases were quantified and linked to functional consequences for endothelial barrier integrity and cardiomyocyte physiology.

Results

Both bacterial pneumonia and COVID-19 were associated with a severity-dependent increase in exosomal ADAM10 and ADAM17 activity. Secretome and functional analyses of patient-derived exosomes showed disruption of endothelial barrier function and altered cardiomyocyte signaling, indicating a potential conduit for systemic injury. In silico deconvolution of human and murine blood datasets identified leukocytes as a major source of protease-active exosomes during pneumonia. Within the lung, ADAM10 drove an exaggerated pro-inflammatory program characterized by M1-like macrophage polarization, increased reactive

oxygen species, heightened cytokine release, and perturbed tissue homeostasis, including effects on leukocyte survival, phagocytosis, and bacterial killing, culminating in tissue damage and edema. In contrast, ADAM17 tempered early inflammation and promoted a more anti-infective, ROS-balanced state. Together, these data support opposing immunomodulatory roles for the two proteases at the site of infection, with exosomal export providing a mechanism for distal effects.

Conclusion

Leukocytic ADAM10 and ADAM17, actively displayed on circulating exosomes, emerge as central regulators of host responses in viral and bacterial pneumonia. By amplifying or restraining local inflammation and propagating injury signals systemically, these proteases present translational opportunities as biomarkers of disease severity and as therapeutic targets. Prospective preclinical and clinical studies should evaluate ADAM10/ADAM17 activity, particularly on exosomes, for diagnostic, prognostic, and interventional applications aimed at improving outcomes in severe pneumonia.

46

Investigating the role of $G\alpha_2$ and $G\alpha_3$ in cerebral ischemia reperfusion injury

R. Kushwaha^{1,2}, S. Schwegmann¹, B. Weigelin², S. Beer-Hammer¹

¹University of Tübingen, Institute of Experimental and Clinical Pharmacology and Toxicology, Department of Pharmacology and Experimental Therapy, Tübingen, Germany

²University Hospital Tübingen, Werner Siemens Imaging Center, Department for Preclinical Imaging and Radiopharmacy, Tübingen, Germany

Ischemic stroke causes brain injury not only through oxygen deprivation but also via reperfusion injury, during which excessive neutrophil infiltration drives secondary inflammation. While $G\alpha_2$ and $G\alpha_3$ signaling pathways are known to protect myocardial tissue from reperfusion injury, their roles in post-stroke neuroinflammation remain unclear.

We combined in vitro chemotaxis and migration assays and ex vivo light-sheet microscopy of intact brains to dissect if $G\alpha_2$ and $G\alpha_3$ influence neutrophil behavior during cerebral ischemia-reperfusion. Loss of $G\alpha_2$ in neutrophils impaired their directional migration towards fMLP and CXCL2 gradients in 3D collagen, without affecting overall speed or distance travelled, indicating a specific defect in guided chemotaxis.

To connect these mechanistic findings to stroke pathology, we implemented a transient middle cerebral artery occlusion (MCAO) model and established a tissue-clearing and multiplexed light-sheet microscopy pipeline. Using a five-antibody panel, we achieved single-cell resolution to map whole-brain neutrophil infiltration. Three-dimensional reconstructions revealed that neutrophil accumulation peaked 24 hours after reperfusion and declined thereafter, with distinct hemispheric patterns and minimal infiltration immediately post-reperfusion. Ischemic and reperfused regions were delineated using CD31, revealing microglia-covered vessels but sparse neutrophil infiltration immediately after reperfusion.

Together, our results demonstrate that $G\alpha_2$ regulates neutrophil chemotaxis towards fMLP and CXCL2 in 3D collagen matrices without altering overall motility. The new clearing and imaging workflow provides a robust platform to track immune cell dynamics in cerebral ischemia-reperfusion, offering insights into how targeting Gai signaling could modulate post-stroke inflammation.

47

Pseudo-worsening of kidney function due to oral antitumor therapeutics – a real-world data analysis of the AMBORA cohort

M. L. Sponfeldner¹, P. Dürr^{1,2,3,4}, P. Lensker^{1,2,3,4}, K. Gessner^{1,3,4}, L. Cuba^{1,2,3,4,5}, R. Fietkau^{6,3,4}, M. F. Neurath^{3,4,7}, B. Wullich^{3,4,8}, M. Pave^{3,4,7}, C. Berking^{3,4,9}, M. W. Beckmann^{3,4,10}, A. Mackensen^{3,4,11}, F. Dörje^{2,3,4,12}, M. F. Fromm^{1,3,4,12}

¹Friedrich-Alexander University of Erlangen-Nuremberg, Institute of Experimental and Clinical Pharmacology and Toxicology, Erlangen, Germany

²Erlangen University Hospital and Friedrich-Alexander-Universität Erlangen-Nürnberg, Pharmacy Department, Erlangen, Germany

³Comprehensive Cancer Center Erlangen-EMN, Universitätsklinikum Erlangen, Erlangen, Germany

⁴Bavarian Center for Cancer Research, Erlangen, Germany

⁵Clinic Floridsdorf, Vienna Healthcare Group., Pharmacy Department, Vienna, Austria

⁶Uniklinikum Erlangen and Friedrich-Alexander-Universität Erlangen-Nürnberg, Department of Radiation Oncology, Erlangen, Germany

⁷Uniklinikum Erlangen and Friedrich-Alexander-Universität Erlangen-Nürnberg, Department of Medicine 1, Gastroenterology, Pneumology and Endocrinology, Erlangen, Germany

⁸Uniklinikum Erlangen and Friedrich-Alexander-Universität Erlangen-Nürnberg, Department of Urology and Pediatric Urology, Erlangen, Germany

⁹Uniklinikum Erlangen and Friedrich-Alexander-Universität Erlangen-Nürnberg, Department of Dermatology, Erlangen, Germany

¹⁰Uniklinikum Erlangen and Friedrich-Alexander-Universität Erlangen-Nürnberg, Department of Obstetrics and Gynecology, Erlangen, Germany

¹¹Uniklinikum Erlangen and Friedrich-Alexander-Universität Erlangen-Nürnberg, Department of Internal Medicine 5, Hematology and Oncology, Erlangen, Germany

¹²Friedrich-Alexander University of Erlangen-Nuremberg, FAU NeW - Research Center New Bioactive Compounds, Erlangen, Germany

Question

Kidney function is commonly estimated by calculation of glomerular filtration rate (eGFR) based on serum creatinine concentrations (SCR). In addition to glomerular filtration, creatinine is actively secreted into the proximal tubules by various transport proteins such as OCT2 and MATE1/2-K. Multiple oral antitumor therapeutics (OAT) inhibit renal creatinine secretion leading to a decrease in eGFR without altering kidney function, i.e., causing pseudo-worsening of kidney function. Non-recognition of this effect in clinical practice can lead to dose reductions, unnecessary interruptions or discontinuations of OAT. The aim of our study was the evaluation of incidence and extent of OAT-induced pseudo-worsening of renal function in a clinical real-world setting within the AMBORA cohort.

Methods

A retrospective cohort study using real-world data from the AMBORA cohort was performed. Cancer patients with a broad spectrum of tumor entities newly treated with OAT were assessed for eligibility. eGFR values were compared between baseline, i.e., prior to OAT initiation and within 30 days of treatment. OAT were separated into the groups unlikely causing and likely causing / proven pseudo-worsening of kidney function. In addition, the extent of cystatin C measurements as alternative method for assessing kidney function was evaluated.

Results

A total of 695 patients were assessed for eligibility. Of these, 34.2% (n=238/695) were included, who had received 38 different OAT likely causing / proven to cause pseudo-worsening of kidney function. In these patients, eGFR decreased significantly (-6.8 ml/min, p<0.001). In 17.2% of the 238 patients, eGFR decreased by ≥ 20 ml/min. The largest mean decreases in eGFR were observed in patients receiving niraparib (-27.8 ml/min \pm 18.9 ml/min), abemaciclib (-20.6 ml/min \pm 11.3 ml/min), and ribociclib (-20.5 ml/min \pm 15.8 ml/min). Cystatin C measurements were not performed in 95.8% of the patients. 67 patients receiving OAT unlikely causing pseudo-worsening of kidney function showed no significant change in eGFR.

Conclusions

In clinical routine, a considerable number of oral antitumor therapeutics cause decreases in serum creatinine-based estimated glomerular filtration rate. Low usage of alternative methods for assessing kidney function (e.g. cystatin C) indicates that further education of oncologists on oral antitumor therapeutic-induced pseudo-worsening of kidney function is necessary to improve medication safety.

48

A pan-cancer multi-pharmacogenomics analysis reveals extensive tumor-driven modifications affecting pharmacogene expression with possible impact on drug response

R. Tremmel^{1,2}, S. Pirmann³, E. Schäffeler^{1,2,4}, H. Glimm^{5,6,7}, S. Fröhling^{5,7,8,9}, D. Hübschmann^{3,7,9,10,11}, M. Schwab^{1,2,4,12}

¹Bosch Health Campus, Dr. Margarete Fischer-Bosch Institute of Clinical Pharmacology, Stuttgart, Germany

²University of Tübingen, Tübingen, Germany

³National Center for Tumor Diseases (NCT) Heidelberg and German Cancer Research Center (DKFZ), Computational Oncology Group, Molecular Precision Oncology Program, Heidelberg, Germany

⁴University of Tübingen, Cluster of Excellence iFIT (EXC 2180) "Image-Guided and Functionally Instructed Tumor Therapies", Tübingen, Germany

⁵German Cancer Research Center (DKFZ), Division of Translational Medical Oncology, Heidelberg, Germany

⁶Translational Medical Oncology, National Center for Tumor Diseases Dresden (NCT/UCC), Technical University Dresden and Helmholtz-Zentrum Dresden, Dresden, Germany

⁷German Cancer Consortium (DKTK), Core Center Heidelberg, Heidelberg, Germany

⁸National Center for Tumor Diseases (NCT) Heidelberg and German Cancer Research Center (DKFZ), Heidelberg, Germany

⁹Heidelberg University, Institute of Human Genetics, Heidelberg, Germany

¹⁰German Cancer Research Center (DKFZ), Innovation and Service Unit for Bioinformatics and Precision Medicine, Heidelberg, Germany

¹¹Pattern Recognition and Digital Medicine Group, Heidelberg Institute for Stem cell Technology and Experimental Medicine (HI-STEM), Heidelberg, Germany

¹²University of Tübingen, Departments of Clinical Pharmacology, and of Pharmacy and Biochemistry, Tübingen, Germany

Objective Inter-individual variation in drug efficacy and safety is significantly influenced by pharmacogenetics (PGx). Genetic variants of phase I/II drug-metabolizing enzymes and transporters, such as the *CYP*, *UGT*, and *ABC* gene families, are key determinants of their expression and activity. Today, PGx guidelines integrate this evidence to support personalized recommendations for drug selection and dosing. This is especially important in cancer therapy, where variants in genes like *DPYD* can markedly affect the metabolism and toxicity of fluoropyrimidines. However, this is based on the germline. The impact of the somatic genome on extrahepatic, intra-tumoral drug metabolism and its potential consequences for drug response has not yet been systematically investigated across cancer types. To address this, we aimed to assess the pan-cancer landscape of PGx alterations and analyze their influence on tumor expression, using data from the multi-institutional DKFZ/NCT/DKTK MASTER cohort of rare and refractory cancers.

Methods We analyzed short-read whole-genome sequencing data from tumors across 21 entity baskets and their matched normal controls in more than 2,500 patients. A dedicated PGx pipeline was established to extract germline and somatic genotypes and metabolizer phenotypes of 60 key pharmacogenes. In addition, DNA methylation and RNA sequencing data were analyzed. All identified genetic and epigenetic alterations were associated with expression through multivariate analyses.

Conclusion We confirmed that actionable germline PGx variants are present in the vast majority of individuals (98%). In tumors, somatic copy number alterations, rather than somatic single-nucleotide variants, together with tumor-specific epigenetic modifications, accounted for substantial genetic variability across cancer types. Pharmacogenes typically involved in hepatic metabolism exhibited pronounced tumor-specific expression, ranging from absent to ubiquitously high. Genetic and epigenetic factors collectively drive this variability, with dominant contributors varying by cancer type and pharmacogene. Finally, for oncological drugs (e.g. 5-FU, pazopanib), we showed that these findings may have clinical implications, as variable expression could influence intra-tumoral metabolism and overall drug response.

This work was supported by the Robert Bosch Stiftung and by a Twinning Grant of the DKFZ and the Robert Bosch Center for Tumor Diseases. MASTER is supported by NCT and DKTK.

49

Hybrid biomolecules for targeted pharmacological modulation of macrophages during distal lung tissue injury

J. Diehm¹, J. Borho¹, M. Frick², H. Barth¹

¹Institute of Experimental and Clinical Pharmacology, Toxicology and Pharmacology of Natural Products University of Ulm Medical Center, Ulm, Germany

²Institute of General Physiology, University of Ulm, Ulm, Germany

Acute respiratory distress syndrome (ARDS) is a common cause of respiratory failure, frequently arising in the context of a damaged alveolar-capillary barrier caused by severe trauma¹. Effective recovery from ARDS requires proper repair of the alveolar tissue. However, many ARDS survivors will later develop progressive pulmonary fibrosis, a fatal condition resulting from disrupted or inadequate repair processes during the fibroproliferative phase^{1,2}.

A key contributor to both repair and pathology are monocytes recruited to the injured lung tissue, followed by differentiation into macrophages which are involved in tissue repair^{3–5}. However, excessive monocyte recruitment and M2 macrophage polarization have been associated with fibrotic tissue remodeling and fibrosis³. Recent studies showed that the bifunctional, adenylyl cyclase domain-harboring toxin CyaA from *Bordetella pertussis* inhibits monocyte-to-macrophage differentiation and de-differentiates terminally differentiated alveolar macrophages into monocyte-like cells⁶. Upon CyaA binding to complement receptor 3 of myeloid phagocytes, the adenylyl cyclase domain (AC) is delivered into the cytosol thus converting ATP into cAMP⁷. Increased intracellular cAMP levels lead to protein kinase A activation resulting in reduced expression of differentiation factors and macrophage markers⁸.

This study focused on the development of novel recombinant fusion toxins for targeted pharmacological inhibition of monocyte differentiation and migration. Therefore, the established recombinant fusion protein C2IN_C3limE174Q was covalently crosslinked to AC based on either heterobifunctional crosslinker or engineered protein fragment SpyCatcher-SpyTag systems. The uptake of the fusion protein into primary human monocytes and macrophages was examined by fluorescence microscopy and western blotting. Upon AC delivery into macrophages, elevated intracellular cAMP as well as pCREB levels could be observed. The influence of C2IN_C3limE174Q_AC on monocytic differentiation and migration was assessed by microscopy and migration assays.

References

- 1 Matthay, M. A. et al. *Nat. Rev. Dis. Primer* 5, 1–22 (2019)
- 2 Huppert, L. A. et al. *Semin. Respir. Crit. Care Med.* 40, 31–39 (2019)
- 3 Ta, W. et al. *Immunity* 44 (2016)
- 4 Huang, X. et al. *Mediators Inflamm.* 2018, 1264913 (2018)
- 5 Kim, S. Y. et al. *Immunol. Cell Biol.* 97, 258–267 (2019)
- 6 Ahmad, J. N. et al. *mBio* 10 e01743-19 (2019)
- 7 Osicka, R. et al. *eLife* 4, e10766 (2015)

50

GenomeTox: Advancing Human Mutagenicity Testing through Whole Genome Sequencing and AI-Based Prediction

B. Scherer^{1,2}, L. Kulaeva^{1,2}, M. Ayllon Gavilan¹, M. van Roosmalen^{1,2}, E. Westerink^{1,2}, R. Hagelaar^{1,2}, R. van Bostel^{1,2}

¹Prinses Máxima Centrum for pediatric oncology, Utrecht, Netherlands

²Oncoode Institute, Utrecht, Netherlands

Accurate prediction of the mutagenic potential of compounds intended for human use remains a major bottleneck in pharmaceutical development. Regulatory-dictated genotoxicity assays still rely on decades-old methods with limited sensitivity, high inter-assay variability and poor predictivity for human mutagenicity. The standard assessment is therefore composed of a complementary battery of *in vitro* assays that determine alterations of specific genomic loci on the one hand and chromosomal alterations on the other hand. Hence, the current pipeline of genotoxicity assays is fragmented and resourceful, while yielding only a binary result without revealing underlying molecular mechanisms.

To address these limitations, we developed the GenomeTox assay, a whole genome sequencing (WGS)-based approach that detects all types of mutational events in a single assay at nucleotide-resolution. We employ primary cord blood-derived hematopoietic stem and progenitor cells, providing a sensitive and human relevant system with extraordinarily low mutational background. The GenomeTox assay reliably distinguishes known human mutagens from non-mutagens and captures single-nucleotide variants, copy number alterations and structural lesions across the genome. The high resolution allows sensitive detection of mutagenicity and additionally offers detailed mechanistic insights.

Complementing this experimental approach, we developed a machine learning-based *in silico* model that integrates chemical structure and experimentally determined mutagenicity. Independent validation using the GenomeTox assay confirmed the reliable classification of compounds with known mutagenic or non-mutagenic potential.

Together, these approaches provide an integrated framework for next-generation mutagenicity assessment that combines the scalability of computational modeling and sensitivity and resolution of whole genome analysis. This framework enhances human relevance, mechanistic understanding and efficiency in early drug discovery and development.

51

Cell type-specific epigenetic dysregulation following acute and chronic arsenite exposure in human BEAS-2B and HepG2 cells

S. Stöber¹, T. Lupp¹, S. Gunesch¹, F. Fischer¹, P. Schumacher¹, A. Hartwig¹

¹Karlsruhe Institute of Technology (KIT), Lebensmittelchemie und Toxikologie, Karlsruhe, Germany

Inorganic arsenic compounds are widespread environmental contaminants classified as human carcinogens. Chronic exposure occurs mainly through contaminated drinking water, particularly in South and East Asia. Arsenic-induced carcinogenesis involves multiple, yet not fully understood mechanisms, including oxidative stress, impaired DNA repair, and epigenetic alterations in DNA methylation, identified as key contributors to its toxicity.

This study investigated the effects of acute and chronic sodium arsenite exposure on global DNA methylation and gene expression in two human cell models, epithelial lung (BEAS-2B) and liver (HepG2) cells. Particular attention was given to the cumulative effects of low but prolonged exposures reflecting environmentally and occupationally relevant conditions.

Cytotoxicity analyses showed that BEAS-2B cells were markedly more sensitive to arsenite than HepG2 cells under both acute and chronic exposure. Despite higher intracellular but comparable nuclear arsenic levels in HepG2 cells, this suggests efficient metabolic detoxification and tightly regulated nuclear arsenic uptake. Furthermore, BEAS-2B cells exhibited a pronounced G2/M arrest, while this effect in HepG2 cells occurred only at substantially higher concentrations.

Gene expression profiling revealed a dose- and time-dependent induction of stress- and DNA damage-related genes. BEAS-2B cells showed repression of *TET1/2*, whereas HepG2 cells exhibited induction of *DNMT1/3B* following chronic exposure, indicating disruption of epigenetic homeostasis. Distinct effects on global DNA methylation were already evident after chronic exposure to sub- and micromolar arsenite concentrations. BEAS-2B cells displayed pronounced hypomethylation and DNMT inhibition despite stable DNMT1 protein levels, whereas HepG2 cells showed increased DNMT activity and DNMT1 expression with moderate hypomethylation, likely due to arsenite-induced SAM depletion.

In conclusion, arsenite induces complex, dose- and cell type-specific epigenetic dysregulation leading to transcriptional alterations. Even low chronic exposures elicit significant changes in DNA methylation, highlighting arsenite as a potent epigenetic disruptor.

52

Targeting therapy-induced senescence in glioblastoma: an effective tool to combat recurrences?

J. Sallbach¹, M. Woods¹, C. Schwarzenbach¹, B. Rasenberger¹, M. Christmann¹, M. T. Tomicic¹

¹University Medical Center Mainz, Department of Toxicology, Mainz, Germany

For decades, the first-line treatment of glioblastoma (GB) patients combines radiotherapy with the monoalkylating compound temozolomide (TMZ). While second-line treatment of recurrences via the topoisomerase I inhibitor irinotecan (IT) can delay surgery for recurrence, overall patient survival remains poor (approximately 12 months after diagnosis). Previously, we showed TMZ mostly induces senescence in p53/p21-proficient GB lines and combinatory treatment with senolytics can trigger cell death. We now sought to investigate whether IT triggers senescence in the same genetic background. Furthermore, we evaluated if adjuvant senolytic therapy could be beneficial for GB patients by targeting therapy-induced senescence.

Alike to TMZ, we observed IT predominantly induced senescence in p53/p21-proficient and cell death in p53/p21-deficient GB lines. Here, p21 induction was essential for IT-mediated senescence while p14, p16 and PTEN were not. Combination of IT and a cIAP1/2 inhibitor decreased senescence and elevated cell death. Potentially recurrence-forming clones (R-clones), which lost sensitivity to TMZ, exhibited a strong basal p21 expression which was not further inducible by TMZ. In contrast, IT was still able to induce p21 and senescence in the R-clones. This observation could explain the delay of the necessary surgery for recurrence of patients having received IT after relapse, compared to patients

receiving continuously TMZ. RNA analyses of patients' primary tumors and correspondent recurrences revealed different expression profiles that may be traced down to the origin of the recurrence (due to senescence escape or avoidance). Here, a strong upregulation of *CDKN1A* (encoding p21) was seen in most recurrences which showed no increased expression of factors related to the senescence-associated secretory phenotype (SASP), indicating these recurrences stem from cells resistant to senescence induction.

Next, we subcutaneously implanted glioma tumor cells in immunodeficient mice to build xenografts *in vivo*. The mice were intraperitoneally treated with either TMZ or TMZ combined with anti-apoptotic drugs targeting cIAP1/2 and Bcl-2/Bcl-xL to analyze impact on tumor growth. Additionally, we are currently testing whether IT has similar effects in this model. The experiments are ongoing and may underscore our *in vitro* results, highlighting treatment of GB recurrences by combining TMZ or IT with agents inhibiting senescent cell anti-apoptotic pathways (SCAPs).

53

Chemically induced cell deformation as source of genotoxic damage?

M. Jobst¹, F. Crudo¹, D. Marko¹, C. Gerner², G. Del Favero¹

¹University of Vienna, Food Chemistry and Toxicology, Vienna, Austria

²University of Vienna, Analytical Chemistry, Vienna, Austria

Bladder cells are constantly exposed to chemical and physical stressors. This includes a complex mixture of xenobiotics excreted in urine [1], as well as mechanical cues stemming from the filling-voiding of the organ. As a drawback of this remarkable adaptive capacity, bladder cancers develop in aggressive phenotypes. To delve deeper into the molecular mechanism granting this plasticity, T24 bladder cancer cells were studied in relation to chemical modulation of autophagy: here reorganization of intracellular organelles seemed more predictive of the "mechanical phenotype" (i.e. response to shear stress and migration) rather than the activation of inhibition of the cascade [2-3]. Further elaborating these aspects, we described how autophagy inhibitors wortmannin and bafilomycin affected non-cytoskeletal organelles like mitochondria and the endoplasmic reticulum. Importantly, redistribution in the intracellular compartments mirrored variations of the intracellular stiffness measured as Young's modulus via Atomic Force Microscopy [4-5]. Short-term exposure to bafilomycin triggered an increase of the mitochondrial clustering the perinuclear region (4 h, BAF1 0.1, 1, and 10 nM) associated to an increase of subcellular stiffness and nuclear deformation. Alteration of the nuclear shape was accompanied by genotoxic damage measured via comet assay and γH2AX signals [5]. These opened the question if naturally occurring contaminants could share a similar mechanism of action, possibly predisposing bladder cells to genetic instability and reduced biomechanical compliance. Pursuing this hypothesis, the fungal secondary metabolite enniatin B1 (like bafilomycin a potassium ionophore) was applied to T24 bladder cancer cells (0.1-1.5 μM). As previously described for bafilomycin, incubation with the mycotoxin was accompanied by mitochondrial rearrangement toward the perinuclear compartment coherent to a parallel increase of the γH2AX signal, as suggestive for DNA damage. Overall, these findings support the existence of mechanisms of genotoxic damage linked to deformation of the intracellular compartment which may represent previously overlooked contributors in bladder carcinogenesis.

[1] Jobst et al., 2025, 10.1016/j.ecoenv.2025.118649; [2] Jobst et al., 2023 DOI: 10.1007/s00204-022-03375-2 [3] Del Favero et al., 2021 DOI: 10.3389/fphar.2021.647350; [4] Gruber-Jobst et al., 2023, 10.1186/s12964-023-01295-x [5] Jobst et al., 2025, 10.1016/j.isci.2025.112955

54

Application of hiPSC-derived renal models for nephrotoxicity testing

G. Carta¹, A. Wilmes¹

¹Vrije Universiteit Amsterdam, Chemistry and Pharmaceutical Sciences, Amsterdam, Netherlands

New Approach Methodologies (NAMs), including advanced human-based *in vitro* models, are being developed and evaluated for toxicity testing. The kidney is one of the most frequently affected organs to toxic compounds. This is partly due to its high exposure to xenobiotics and its role in excretion. Human-based renal *in vitro* models are hence an important tool in toxicity testing. We have developed two protocols to drive human induced pluripotent stem cell (iPSC) into proximal tubular-like cells (PTL)¹ and into podocyte-like cells (PODL)². PTL show expression of characteristic renal markers, including megalin, tight junction formation (ZO3) and barrier integrity and functional transport of P-glycoprotein, organic cation transport and megalin-facilitated endocytosis. PODL show expression of the podocytes specific markers synaptopodin and WT1.

PTL and PODL have been challenged with various compounds in TempO-Seq transcriptomics studies, including cyclosporine A, doxorubicin, flutamide, nafidrofuryl, rofecoxib and tamoxifen. Upon 24 h treatment cytotoxicity was determined with the resazurin assay, mitochondrial function was evaluated by means of oxygen consumption rate (OCR) using the Seahorse bioanalyzer, and glycolytic activity was monitored by measurement of lactate production.

PODL were most sensitive to doxorubicin treatment and showed activation of stress response pathways, including p53 activation in the low nM range, whereas PTL were highly sensitive to cyclosporine A, flutamide and nafidrofuryl, showing activation of the Nrf2 oxidative stress response pathway and the Unfolded Protein Response.

Currently, we are further developing the PTL model in organ-on-a-chip systems in combination with iPSC-derived endothelial cells to evaluate whether microfluidics can further improve on transport capacity of the model.

This project received funding from Stiftung Pro Care Switzerland.

References:

1. Meijer, T., Naderlinger, E., Jennings, P. & Wilmes, A. Differentiation and Subculturing of Renal Proximal Tubular-like Cells Derived from Human iPSC. *Curr. Protoc.* **3**, e850 (2023).
2. Murphy, C., Naderlinger, E., Mater, A., Kluin, R. J. C. & Wilmes, A. Comparison of human recombinant protein coatings and fibroblast-ECM to Matrigel for induced pluripotent stem cell culture and renal podocyte differentiation. *ALTEX* (2022) doi:10.14573/altex.2112204.

55

Next-generation safety assessment in the CHIASMA project: Modeling neurotoxicity with human *in vitro* NAMs

R. R. Chowdhury¹, I. Scharkin^{1,2}, K. Koch^{1,2}, E. Fritsche^{1,2,3,4,5}

¹Leibniz Research Institute for Environmental Medicine (IUF), Düsseldorf, Germany

²DNTOX GmbH, Düsseldorf, Germany

³Heinrich Heine University Düsseldorf, Düsseldorf, Germany

⁴Swiss Centre for Applied Human Toxicology (SCAHT), Basel, Switzerland

⁵University of Basel, Department of Pharmaceutical Sciences, Basel, Switzerland

The Horizon Europe-funded CHIASMA project aims to develop and integrate mechanistically informed NAMs within regulatory frameworks for human and environmental safety assessments. The NAMs will be applied in three case-studies, including per- and polyfluoroalkyl substances (PFAS), (nano-) pesticides and 2D materials for energy applications.

Focussing on developmental neurotoxicity (DNT), we utilize the mechanistically validated Neurosphere Assay, which is part of the DNT *in vitro* battery (DNT IVB). This DNT IVB comprises of a set of DNT NAMs modeling eight key neurodevelopmental processes (KNDPs) developed under the guidance of the EFSA, US EPA and the OECD. Within the human Neurosphere Assay, we evaluate chemical effects on human neural progenitor cell proliferation, radial glia migration, neuronal migration and differentiation, neurite outgrowth, and oligodendrocyte migration and differentiation, KNDPs whose disruption is linked to neurodevelopmental disorders.

To identify chemicals causing adult neurotoxicity (ANT) or neurodegeneration, we apply hiPSC-derived 3D neuron-glia BrainSpheres (BS) forming functional neural networks on microelectrode arrays (MEAs). Exposure of matured networks after 4 weeks of network development enables evaluation of acute and subacute chemical effects on distinct neurotransmission modalities (e.g., glutamatergic, GABAergic, dopaminergic, serotonergic, and cholinergic). In addition, BS-derived networks are used to study Parkinson's disease (PD)-related pathophysiology. Exposure during adulthood (one-hit) is modelled through chronic exposure of matured networks to case-study chemicals and PD model compounds (e.g., rotenone, paraquat, MPP+). Further, the impact of developmental chemical exposure on the prevalence of PD later in life is modelled using a two-hit exposure paradigm, combining developmental exposure to case-study chemicals during BS differentiation with subsequent chronic exposure of matured networks to PD model compounds. Experimental readouts include dopaminergic transmission, immunostaining and transcriptomic profiling to identify PD-related neurodegenerative signatures.

In conclusion, our DNT and ANT NAMs will form a key contribution to the CHIASMA framework. By enhancing mechanistic understanding and human relevance, CHIASMA will strengthen confidence in NAM-based toxicity testing and support the transition toward regulatory application in human and environmental safety assessment.

56

Primary Thyroid Follicles from Pigs as a New Approach Methodology to Improve *in vitro* Testing Strategies for Thyroid Hormone System Disruptors

L. Dahmen¹, S. Arnold¹, G. Mahlis², D. Hilgert³, M. H. E. Lajine⁴, J. Wiest¹, B. Kleuser², F. Schumacher², M. Oelgeschlager¹, K. Renko¹

¹German Federal Institute for Risk Assessment (BfR), German Centre for the Protection of Laboratory Animals, Berlin, Germany

²Landkreis Potsdam-Mittelmark, Fachdienst Veterinärwesen und Lebensmittelüberwachung, Bad Belzig, Germany

³Free University of Berlin, Institute of Pharmacy, Berlin, Germany

⁴University of Potsdam, Institute of Biochemistry and Biology, Potsdam, Germany

Currently, the regulation of thyroid hormone system disruptors (THSDs) primarily relies on animal testing. However, ethical concerns and scientific limitations underscore the growing need for new approach methodologies (NAMs) that can fully capture thyroid function *in vitro*. Existing models often lack the complexity necessary to accurately replicate thyroid hormone (TH) biosynthesis. Thyroid follicle (TF) models represent a promising alternative, offering a physiologically more relevant system that closely mimics the native thyroid's structure and function. In this study, we present a functional *in vitro* TF model for hazard identification. The TFs are derived from pig thyroid glands, which are sourced as a by-product of conventional meat production, thus addressing tissue availability issues while avoiding the use of laboratory animals. Blood levels of THs, as well as thyroid-specific enzyme activities were measured for each donor animal to establish reference values for the pig THS, providing a basis for cross-species comparisons. The cultured TFs demonstrated responsiveness to key physiological stimuli, like thyroid-stimulating hormone and iodide supply, as evidenced by both hormone production and gene expression patterns. Known TH biosynthesis inhibitors, such as methimazole (MMI), propylthiouracil, and sodium perchlorate, successfully reduced hormone production in this model, verifying its sensitivity and qualifying the test system for further use. We applied acceptance criteria for

each TF culture, including sufficient TH production and appropriate inhibition by MMI, to ensure reliable performance and responsiveness in substance testing. Further, an optimization step demonstrated that adjusting iodide and TSH concentrations could broaden the effective range and determines quality measures of the assay. A strategic testing approach was then developed to screen chemicals for their potential to interfere with in vitro TH production, using a library of more than 500 compounds. A high-throughput sodium iodide symporter inhibition assay was employed to identify candidate disruptors. Alongside a literature-derived set of chemicals, the compounds were tested for their effects on TH synthesis within the TF model. The newly introduced TF model shows considerable promise in enhancing the predictive capability of in vitro testing for THSDs, potentially offering a more ethical and accurate complementary testing strategy to reduce traditional animal testing.

57

Comparative Transcriptomic Analysis of Hepatic Cell Culture Models for Next Generation Risk Assessment: Evaluation of 2D and 3D In Vitro Systems Using RNA-Seq and Benchmark Modeling

P. Demuth¹, M. Riede², F. Gröschl³, M. Eichenlaub², E. Fabian¹, R. Landsiedel^{1,4}

¹BASF SE, Experimental Toxicology and Ecology, Ludwigshafen, Germany

²BASF SE, White Biotechnology Research, Ludwigshafen, Germany

³BASF SE, Computational Biology, Ludwigshafen, Germany

⁴Free University of Berlin, Pharmakologie und Toxikologie, Berlin, Germany

Next generation risk assessment (NGRA) leverages new approach methods (NAMs) to facilitate animal-free safety evaluations. Transcriptome analysis via next generation sequencing (NGS) has emerged as a robust approach, enabling early detection of molecular changes induced by chemical exposure. The liver, as a frequent target organ in systemic toxicity, is commonly surrogated using various in vitro hepatic cell systems. This study aimed to evaluate and compare the suitability of three hepatic cell culture models — 2D HepG2, 2D and 3D (spheroid) HepaRG—for transcriptomic analysis within the NGRA framework. Two reference compounds, Paracetamol (PCM) (CAS-Nr.: 103-90-2) and Wyeth-14,643 (WYT) (CAS-Nr.: 50892-23-4), were selected to assess the models' ability to recapitulate in vivo effects quantitatively and qualitatively.

Cells were exposed for 48 hours to non-cytotoxic concentrations of the test compounds, established via prior cytotoxicity screening. Transcriptomic changes were assessed using total RNA sequencing (RNA-Seq), followed by differential expression analysis (DEA) and benchmark concentration (BMC) modeling. Quantitative extrapolation of transcriptomic points of departure (iPODs) was performed using a physiologically based toxicokinetic (PBTK) model of the rat, and results were compared to no observed adverse effect levels (NOAEL) from in vivo rat feed studies.

HepaRG 2D cells exhibited the highest number of differentially expressed genes (DEGs) and the strongest transcriptional response for both PCM and WYT. Quantitative extrapolation of iPODs demonstrated higher predictive accuracy for HepaRG models compared to HepG2. The extrapolated iPODs for WYT (6.4 mg/kg bw) and PCM (74.6 mg/kg bw) correlated with the corresponding NOAELs from rat studies (3 mg/kg bw, 100 mg/kg bw), supporting the utility of 2D HepaRG model for a transcriptomics-based approach in NGRA. The 3D HepaRG model was limited by lower RNA concentration and quality leading to higher technical variability.

The HepaRG 2D cell culture model is identified as the most suitable for high-throughput NGRA applications, balancing biological relevance, data quality, and practicability. While 3D cultures may offer future advantages in mimicking in vivo physiology, our results support the use of the 2D HepaRG model for routine risk assessment. This study underscores the importance of a robust transcriptomic workflow and appropriate in vitro models for reliable, animal-free safety evaluation.

58

In-depth Substrate Characterization using a CRISPR/Cas9-derived Knockout Platform for ABC Transporters

A. Kasten¹, J. T. Loeffler-Kapezov¹, S. K. Neeß¹, S. P. Gorantla³, H. Metten¹, E. Puris⁴, M. Gynther², J. Kulartz¹, I. Vater⁵, N. von Bubnoff⁶, S. Oswald¹, M. Schwab^{2,8}, I. Cascorbi¹, M. Kaehler¹

¹University Hospital Schleswig-Holstein (UKSH), Institute of Experimental and Clinical Pharmacology, Kiel, Germany

²Bosch Health Campus, Dr. Margarete Fischer-Bosch Institute of Clinical Pharmacology, Stuttgart, Germany

³University Hospital Schleswig-Holstein (UKSH), Department of Hematology and Oncology, Lübeck, Germany

⁴University of Eastern Finland, A.I. Virtanen Institute for Molecular Sciences, Kuopio, Finland

⁵University of Eastern Finland, School of Pharmacy, Kuopio, Finland

⁶University Hospital Schleswig-Holstein (UKSH), Institute of Human Genetics, Kiel, Germany

⁷Rostock University Medical Center, Institute of Pharmacology and Toxicology, Rostock, Germany

⁸University of Tübingen, Departments of Clinical Pharmacology and of Biochemistry and Pharmacy, Tübingen, Germany

QUESTION: Detailed insights into the function and specificity of ATP-binding cassette (ABC) transporters are crucial for both drug bioavailability and approval. Knockout models offer new chances for comprehensive transport studies circumventing the limitations of conventional inhibitor-based approaches, e.g. dose-dependence or overlapping substrate spectra. Using our previously established ABC transporter knockout platform, we aimed to gain a deeper understanding of the transporter spectra of six putatively specific substrates.

METHODS: Single and double knockouts for *ABCB1*, *ABCG2*, *ABCC1* and *ABCC2* were generated in Caco-2 cells using CRISPR/Cas9-genome editing. Bidirectional transport studies followed by LC-MS/MS were performed for digoxin, sulfasalazine, cyclophosphamide, valsartan, loperamide and rosuvastatin. For rescue experiments, plasmids encoding *ABCG2* and *ABCC1* were retrovirally transduced in the respective single knockout cells. Transporter levels were analyzed by immunoblotting, targeted proteomics and genome-wide gene expression assays.

RESULTS: Digoxin transport was shown to be specific for *ABCB1* being only significantly reduced in the *ABCB1* single and *ABCB1/ABCG2* double knockout (both: $p < 0.001$). For all other substrates the efflux was mediated by multiple transporters: Although rosuvastatin is regarded as *ABCG2*-specific, its efflux was not only decreased in the *ABCG2* single knockout ($p < 0.001$), but was also further diminished in the *ABCB1/ABCG2* double knockout (-36.2% , $p < 0.001$) and by the *ABCB1* inhibitor cyclosporin A (-35.5% , $p < 0.001$). *ABCC1* and *ABCG2* protein levels could be successfully restored, as demonstrated by immunoblotting and an increased transport capacity for the fluorescent dyes Fluo-3 and BODIPY-prazosin ($+40\%$, $p = 0.03$). Genome-wide expression data showed a slight compensatory upregulation of other transporters in single knockout cells, e.g. *ABCB1* in the *ABCG2* (3.7-fold) and *ABCG2* in the *ABCB1* single knockout (2.8-fold).

CONCLUSION: Our ABC transporter knockout platform is a new powerful tool for precise transport studies: Despite the high affinity of some drugs (e.g. digoxin for *ABCB1*), our data indicate that most substrates lack transporter specificity. For instance, rosuvastatin is not only transported by *ABCG2*, but also by *ABCB1*. Beyond the characterization of transporter spectra, this knockout platform holds the potential for many more applications, such as analyzing the impact of pharmacogenetic variants.

59

Elucidating the substrate spectrum of the orphan transporter OATP5A1

E. Kohlmann¹, N. Schmid¹, A. Gessner¹, M. F. Fromm¹, J. König¹

¹Friedrich-Alexander University of Erlangen-Nuremberg, Erlangen, Germany

Introduction: OATP5A1 (*SLCO5A1*) belongs to the organic anion transporting polypeptide (OATP, *SLCO/SLC21*) transporter family and represents a so far orphan transport protein. Based on human expression data, OATP5A1 is ubiquitously expressed in the human body, with a pronounced expression in brain, heart, skeletal muscle, and various cancerous tissues. As a member of an important drug transporter family, OATP5A1 could have relevance for drug disposition or as a drug target. To date, no substrates of OATP5A1 have been characterised.

Methods: Using stably transfected human embryonic kidney (HEK) cells recombinantly overexpressing OATP5A1 (HEK-OATP5A1) and the respective control cells (HEK-VC), the subcellular localisation of OATP5A1 was evaluated by immunofluorescence analysis. Candidate OATP5A1 substrates were identified through untargeted metabolomics after incubation with human plasma and by assessing the uptake of selected known substrates of other OATP family members. Km values for OATP5A1-mediated substrate uptake were determined.

Results: OATP5A1 was localised in the plasma membrane of HEK-OATP5A1 cells. Untargeted metabolomics analysis revealed a significantly higher intracellular accumulation of thiamine in HEK-OATP5A1 compared to HEK-VC cells. Transport assays using thiamine and the known substrates of other OATP family members estrone-3-sulfate and tyrosine showed higher compound uptake into HEK-OATP5A1 compared to HEK-VC cells ($p < 0.01$). The apparent Km values were $15.6 \pm 6.0 \mu\text{M}$, $102.2 \pm 50.9 \mu\text{M}$, and $169.9 \pm 85.3 \mu\text{M}$ for thiamine, estrone-3-sulfate, and tyrosine uptake, respectively.

Conclusions: Untargeted metabolomics analysis and transport studies using known substrates of other OATP family members enabled the deorphanisation of OATP5A1. Thiamine, estrone-3-sulfate, and tyrosine are newly identified OATP5A1 substrates. Therefore, OATP5A1 is involved in the uptake of vitamins, hormone conjugates, and amino acids into non-cancerous and cancerous cells.

60

TRPML channels in lung emphysema and fibrosis

C. Grimm¹

¹University of Munich LMU and University of Oxford, Pharmacology, Munich, Germany

Research on endolysosomal ion channels and transporters has gained considerable momentum in recent years, as new technologies are now available to investigate the function and physiology of these important intracellular membrane proteins in more detail. For example, endolysosomal patch-clamp electrophysiological techniques, intracellular sensors for endolysosomal Ca^{2+} and pH measurements or new animal models have been developed. Using these new techniques, it has been discovered that endolysosomal cation channels such as TRPML channels or two-pore channels (TPCs) play important physiological and pathophysiological roles in a variety of organs and that defects or alterations in their function are associated with lysosomal storage diseases and neurodegenerative diseases, infectious diseases, immune cell dysfunction, lung, liver and heart diseases as well as cancer (e.g. melanoma). Thanks to significant advances also in the availability of pharmacological tools for these endolysosomal membrane proteins, accompanied by numerous cryo-EM structures research in this area is progressing rapidly. We aim to present recent and current (unpublished) findings on the physiological and pathophysiological role of TRPML channels with a particular focus on lung disease.

This work was supported, in part, by funding of the German Research Foundation (SFB/TRR152 P04, SFB1328 A21, GRK2338 P08, DFG GR4315/2-2, DFG GR4315/6-1 and DFG GR4315/7-1).

Selected publications: • Spix B et al. & Grimm C#: Lung emphysema and impaired macrophage elastase clearance in mucolin 3 deficient mice. *Nature Commun* 13(1):318, 2022. • Chen C-C et al. & Grimm C#: Patch clamp technique to characterize ion channels in individual intact endolysosomes. *Nature Protoc* 12:1639–1658, 2017.

61

A rapid untargeted metabolomics approach for the detection of CYP2E1-mediated metabolites in a genetically engineered Hep-G2 cell line

Y. Schermer¹, S. Stegmüller¹, J. H. Küpper², E. Richling¹

¹University of Kaiserslautern-Landau (RPTU), Chemistry, Kaiserslautern, Germany

²Brandenburg University of Technology Cottbus-Senftenberg, Molecular Cell Technology, Senftenberg, Germany

Cytochrome P450 (CYP) 2E1 is among the highest expressed CYPs in the human liver and catalyzes the oxidation of a variety of low molecular weight compounds.^[1,2] Due to its ability to activate a large number of xenobiotics to form cytotoxic or carcinogenic metabolites, it is of great toxicological interest.^[3] Although several *in vitro* systems exist for the investigation of CYP2E1-mediated metabolites, they are often expensive and/or highly artificial, and, as in the case of animal-derived primary hepatocytes may also pose ethical concerns. On the other hand, wild type Hep-G2 cells (Hep-G2-wt) which are a popular model for *in vitro* toxicological and pharmacological studies usually do not show any CYP2E1 activity.^[4] To overcome these problems, Carlsson *et al.* recently presented a genetically engineered Hep-G2 cell line (Hep-G2-2E1) with a considerable CYP2E1 expression, that was able to metabolically activate several nitrosamine compounds in a CYP2E1-dependent manner.^[5]

In this work, we developed a mass spectrometry-based untargeted metabolomics workflow for the detection of potential xenobiotics-derived metabolites formed in Hep-G2-2E1 cells. Untargeted metabolomics aims to semi-quantify as many metabolites as possible in a biological sample. This allows for a comprehensive analysis of metabolites without deep *a priori* knowledge or lengthy method development making the approach rapid and highly versatile. As a proof of principle, Hep-G2-2E1 cells were treated with a panel of established CYP2E1 substrates and their metabolite profile was compared to that of Hep-G2-wt. Furthermore, a data analysis pipeline was established which allowed for a fast annotation of potential metabolites generated by CYP2E1. The presented method is fast and inexpensive, since Hep-G2 cells can practically be expanded indefinitely, and will therefore greatly accelerate the elucidation of potential metabolites generated by CYP2E1 *in vitro*.

This work was supported by the German Research Foundation (DFG) [grant number INST 248/338-1 FUGG; project number 460221948].

[1] F. J. Gonzalez, *Drug Metab. Dispos.* **2007**, *35*, 1–8.

[2] J. Chen *et al.*, *Drug Metab. Rev.* **2019**, *51*, 178–195.

[3] J. L. Raucy, *Toxicology* **1995**, *105*, 217–224.

[4] L. A. Stanley, C. R. Wolf, *Drug Metab. Rev.* **2022**, *54*, 46–62.

[5] M. J. Carlsson *et al.*, *Chem. Res. Toxicol.* **2025**, *38*, 1134–1146.

62

Effects of BPDE treatment in iPSCs and Neuronal cells differentiated from healthy and CSB-patient derived iPSCs

A. Lofrano¹, W. Wruck¹, N. Graffmann¹, J. Adjaye^{1,2}

¹University Hospital Düsseldorf, Heinrich Heine University Düsseldorf, Institute for Stem Cell Research and Regenerative, Düsseldorf, Germany

²University College London, EGA Institute for Women's Health, Zayed Centre for Research into Rare Diseases in Children (ZCR), London, United Kingdom

Maintenance of genome integrity is essential for correct human development, particularly during pluripotent stages when rapid proliferation and intense transcription increase susceptibility to DNA damage. Environmental genotoxins such as benzo[a]pyrene (BaP) and its reactive metabolite benzo[a]pyrene diol epoxide (BPDE) form bulky DNA adducts that interfere with replication and transcription, posing significant risks to embryonic genome stability. To examine how defects in DNA repair influence these effects, we assessed human induced pluripotent stem cells (iPSCs) carrying pathogenic ERCC6 mutations, which cause Cockayne syndrome B (CSB), a severe neurodevelopmental disorder marked by growth failure, premature aging, and multisystemic degeneration. Exposure of CSB-deficient patient derived iPSCs to BPDE revealed impaired proliferation, persistent DNA damage accumulation and defective checkpoint activation compared with the control line. Although pluripotency remained largely preserved, altered SOX2/p-SMAD1/5 signaling and early lineage priming were observed in CSB-patient derived iPSCs, indicating that unrepaired DNA damage can perturb developmental-associated signaling pathways. Transcriptomic profiling showed broad suppression of DNA repair and cell-cycle pathways in CSB-deficient iPSCs, accompanied by activation of p53-, TNF α -, and MAPK/JNK-mediated stress responses. Interestingly, while control iPSCs exhibited a robust DNA damage response to BPDE, this resilience decreased during differentiation. Neuronal progenitor cells (NPCs) derived from healthy donors and exposed to BPDE for 24 hours showed dysregulation of neuronal development and impaired neuronal induction pathways. Our findings demonstrate that CSB is essential for coupling DNA repair and transcriptional recovery in pluripotent cells. BPDE exposure destabilizes the developing genome in the absence of CSB, leading to pronounced pathological effects. However, CSB does not fully protect against BPDE toxicity once cells exit the pluripotent state, as differentiation is accompanied by reduced genomic resilience. Consequently, BPDE exposure impacts neuronal development and induction, emphasizing the importance of

investigating BPDE-induced genotoxicity during neuronal development and considering genetic susceptibility in developmental toxicology and environmental health risk assessment.

63

Carbonyl reductase 3 drives oxidative stress and apoptosis in epidermal keratinocytes under chemical and physical stress

E. Hartung¹, C. F. A. Vogel², A. Rossi¹, S. Grether-Beck¹, J. Krutmann¹, T. Haarmann-Stemmann¹

¹Leibniz Research Institute for Environmental Medicine (IUF), Düsseldorf, Germany

²University of California, Center for Health and the Environment & Department of Environmental Toxicology, Davis, CA, United States

Carbonyl reductases (CBRs) are NADPH-dependent oxidoreductases that catalyze the reduction of a wide range of carbonyl compounds to their corresponding alcohols. The human genome encodes the two monomeric CBR isoforms 1 and 3, which share high amino acid sequence homology but differ in their substrate spectrum. While CBR1 has been extensively studied, the current knowledge of CBR3 remains largely limited to its involvement in the reduction of anthracyclines. As CBR3 is highly expressed in epithelial cells of the skin and oral cavity, and we have previously observed its upregulation in human HaCaT keratinocytes exposed to the polycyclic aromatic hydrocarbon (PAH) benzo[a]pyrene (BaP), we here characterized the regulation and function of CBR3 in human keratinocytes exposed to environmental stressors. We found that treatment of keratinocytes with BaP and benzo[k]fluoranthene increased CBR3 expression via a non-canonical aryl hydrocarbon receptor (AHR) signaling pathway, involving the sequential activation of epidermal growth factor receptor and NRF2. PAHs are generated during incomplete combustion of organic material and thus are often bound to the surface of airborne particulate matter (PM). Hence, we next asked if CBR3 is also inducible by real-world PM. In fact, treatment of HaCaT cells with PAH-rich traffic-related PM resulted in an AHR-dependent upregulation of CBR3. Importantly, a repetitive topical application of PAH-rich diesel exhaust particles, confirmed an induction of CBR3 in human *ex vivo* skin. To elucidate CBR3 function, we next generated CBR3-mutated HaCaT cells using CRISPR/Cas9 technology. Treatment of HaCaT cells with BaP resulted in the formation of superoxide anions, which clearly was CBR3-dependent. In addition, CBR3-deficiency largely protected the keratinocytes against apoptosis induced by BaP-4,5-quinone, pointing to a critical role of CBR3 in PAH-related redox-cycling. Strikingly, CBR3 was also upregulated in UVA-irradiated keratinocytes in an NRF2-dependent manner, and CBR3-deficiency protected against UVA-induced apoptosis. Since the latter is driven by the excitation of endogenous photosensitizers and subsequent formation of oxidative stress, we hypothesize that CBR3 catalyzes the redox-cycling of endogenous photosensitizers. Our data identify CBR3 as a driver of oxidative stress and apoptosis induced by PAH and UVA exposure that might contribute to environmentally-induced skin damage and the development of associated diseases.

64

Trace Copper elicits severe Iron Toxicity targeting mitochondrial Iron-Sulfur cluster enzymes

J. Sailer¹, J. Gottal², L. Kaub^{3,4}, A. T. Jauch¹, J. Engler¹, C. Eberhagen⁵, C. von Törne^{5,6}, S. Engelhardt⁷, P. Knolle⁸, A. DiSpirito⁹, M. Vujic Spasic¹⁰, H. Zischka^{2,5}

¹Technical University of Munich, Institute of Toxicology and Environmental Hygiene, TUM School of Medicine and Health, Munich, Germany

²Technical University of Munich, Department of Computer Science, TUM School of Computation, Information and Technology, Garching, Germany

³Ludwig Maximilian University of Munich, Dept. Of Earth and Environmental Sciences, Munich, Germany

⁴Ludwig Maximilian University of Munich, Dept. Of Anatomy II, Faculty of Medicine, Munich, Germany

⁵Heimholtz Center Munich, German Research Center for Environmental Health GmbH, Institute of Molecular Toxicology and Pharmacology, Neuherberg, Germany

⁶Heimholtz Center Munich, German Research Center for Environmental Health GmbH, Research Unit Protein Science, Munich, Germany

⁷Technical University of Munich, Institute of Pharmacology and Toxicology, Munich, Germany

⁸Technical University of Munich, Institute of Molecular Immunology and Experimental Oncology, University Hospital rechts der Isar, TUM School of Medicine and Health, Munich, Germany

⁹Iowa State University, Roy J. Carver Department of Biochemistry, Biophysics and Molecular Biology, Ames, IA, United States

¹⁰Ulm University, Institute of Comparative Molecular Endocrinology, Ulm, Germany

Methods

Hfe knockout mice (1,2) were examined to characterize hepatic iron loading and adaptive responses to iron excess. Hemochromatosis Huh7 hepatocytes (3) were used to study both iron accumulation and defense mechanisms, including ferritin and ferroportin regulation, as well as mitochondrial bioenergetics, oxidative stress, proteotoxicity, and iron-sulfur cluster enzyme activity. Trace copper supplementation and chelation, along with inhibition of cell death pathways, were employed to explore the effect of copper under iron loading.

Results

In *Hfe* knockout mice, hepatic iron overload activated compensatory mechanisms affecting iron storage and export. In hepatocytes, iron treatment induced similar adaptive responses via ferritin upregulation and ferroportin expression, preventing overt toxicity and limiting ROS formation. However, the addition of low, non-toxic copper dramatically sensitized cells to iron, triggering proteotoxic stress, iron-sulfur enzyme inactivation, and severe mitochondrial dysfunction. These effects were independent of Fenton chemistry and could be fully prevented by high-affinity copper chelation but not by inhibition of typical cell death pathways.

Conclusion

Copper critically amplifies cellular vulnerability to otherwise compensated iron overload via non-ROS-mediated mechanisms. These findings identify copper as a key factor converting adaptive iron handling into mitochondrial and proteotoxic injury, underscoring the importance of copper monitoring in hepatic iron overload conditions.

(1) Herrmann, T., et al., *Iron overload in adult Hfe-deficient mice independent of changes in the steady-state expression of the duodenal iron transporters DMT1 and Ireg1/ferroportin*. Journal of Molecular Medicine, 2004. **82**(1): p. 39-48.

(2) Vujčić Spasić, M., et al., *Hfe Acts in Hepatocytes to Prevent Hemochromatosis*. Cell Metabolism, 2008. 7(2): p. 173-178.

(3) Vecchi, C., G. Montosi, and A. Pietrangelo, *Huh-7: a human "hemochromatotic" cell line*. Hepatology, 2010. 51(2): p. 654-9.

Animal experimentation research

P001

Low-dose environmental dioxin exposure reveals sex-dependent microbial glycan changes

D. Reicher¹, S. Janssen², A. Rossi¹, C. Esser¹

¹Leibniz Research Institute for Environmental Medicine (IUF), Düsseldorf, Germany

²Justus Liebig University Gießen, Gießen, Germany

2,3,7,8-Tetrachlorodibenzo-p-dioxin (TCDD) is a persistent environmental contaminant that affects liver and gut microbiota at high doses. Here, we examined whether chronic low-dose TCDD exposure induces gut dysbiosis and whether effects differ between sexes. Male and female C57BL/6 mice received an initial oral dose of 1 µg TCDD/kg body weight followed by biweekly maintenance doses for 12 weeks; controls received DMSO/corn oil.

Body weight, liver-to-body weight ratio, and intestinal barrier gene expression remained unchanged across groups. 16S rRNA sequencing showed a general increase in α -diversity over time but no TCDD-related differences. β -Diversity analyses revealed compositional differences between sexes and across time points, though statistical significance was limited by sample size.

Using our flow cytometry-based microbiota profiling tool, FlowSoFine™, we detected distinct microbial signatures in TCDD-treated females. Lectin-based glycan staining of cecal bacteria revealed significant changes in concanavalin A, soybean agglutinin, and Dolichos biflorus agglutinin binding, indicating altered microbial glycosylation in females only. Fluorescence-activated cell sorting and subsequent 16S sequencing showed increased Lachnospiraceae and decreased Lactobacillaceae, CAG-508, and Oscillospiraceae in TCDD-treated female samples.

Our findings suggest that chronic low-dose TCDD exposure modifies gut microbial glycosylation patterns in a sex-specific manner. Monitoring bacterial glycosylation may reveal subtle xenobiotic effects on host–microbe interactions beyond conventional sequencing approaches.

P002

From Antiviral Defense to Immunomodulation – Animal Experiments as a Key to the Therapeutic Use of Interferons

D. Yildiz¹

¹Saarland University, Homburg, Germany

The discovery and therapeutic application of interferons (IFNs) represent a paradigmatic example of the indispensable role of animal research in advancing medical innovation. Early experiments (1950s/1960s) in mice and rats demonstrated that interferons inhibit viral replication and induce expression of antiviral proteins such as Mx and PKR. Mouse knockout models later clarified the signaling cascades of the JAK-STAT pathway, defining the molecular mechanisms of interferon action. Studies in non-human primates provided critical pharmacokinetic and toxicological data, paving the way for safe human administration. Of particular importance were investigations using experimental autoimmune encephalomyelitis (EAE), a murine model of multiple sclerosis, which revealed the immunomodulatory effects of IFN- β on T-cell differentiation and cytokine regulation. These results directly supported the development of interferon- β as the first disease-modifying therapy for multiple sclerosis. The development of interferon-based therapies (e.g. Hepatitis B/C, MS, chronic granulomatosis) exemplifies how animal research has been fundamental to understanding complex immune mechanisms and translating them into breakthrough pharmacotherapies. Despite ongoing ethical debates, such research remains vital for uncovering disease pathophysiology and ensuring the safe and effective development of future treatments.

P003

Bridging the gap: Animal evidence explaining *in vitro*–*in vivo* mismatch in serious infections

A. Aljohmani¹, A. Abdelwahed¹, D. Yildiz¹

¹Saarland University, Molecular Pharmacology, Homburg, Germany

Across pathogens and antibiotic classes, *in vitro* activity often fails to predict *in vivo* efficacy, a gap that becomes evident in whole-organism studies and is confirmed in clinical practice. Extended-spectrum beta-lactamase producing Enterobacteriales provide a primary example. Minimum inhibitory concentration testing may label piperacillin–tazobactam or cefepime as susceptible, yet high bacterial burden, enzyme kinetics, and site-specific pharmacology yield poorer outcomes than meropenem. Convergent evidence from other settings shows a similar pattern and clarifies its mechanisms. Daptomycin appears potent *in vitro*, yet pulmonary surfactant neutralises the drug and clinical failure follows in primary pneumonia. Polymyxins can appear active against carbapenem-resistant Klebsiella, yet heteroresistant subpopulations expand during therapy and diminish effectiveness. Among Gram-positive infections, the ceftazolin inoculum effect in methicillin-susceptible *Staphylococcus aureus* can erode efficacy when the bacterial load is high.

These observations do not indict MIC methodology; they expose a structural gap between simplified assays and the biology of infection. Key determinants include the inoculum and its dynamics, tissue penetration and local drug distribution, protein binding that limits free-drug exposure, the immune context that modulates bacterial clearance, and adaptive or heteroresistant subpopulations selected during treatment. Animal models remain the practical bridge, integrating burden, distribution, binding, immunity, and adaptation within an intact organism that mirrors clinical exposure. In ESBL pneumonia models, piperacillin–tazobactam

fails at high inoculum while meropenem succeeds, aligning with patient-level outcomes and informing practice. Related organism-level insights elucidate the surfactant effect on daptomycin and the clinical impact of polymyxin heteroresistance, reinforcing the need to evaluate promising *in vitro* signals within physiologically relevant systems.

P004

SMAFIRA: deep machine learning to assist researchers in finding alternatives to animal testing

B. Bert¹, K. Gulich¹, M. Lara Neves¹, D. Butzke¹

¹German Federal Institute for Risk Assessment (BfR), German Centre for the Protection of Laboratory Animals (Bf3R) and Experimental Toxicology, Berlin, Germany

Before conducting an animal experiment, researchers have to consider all 3R methods to replace, reduce and refine the use of animals. An essential part of the application for approval is scientifically substantiated evidence that the planned animal experiment cannot be replaced by an alternative method. Such information retrieval entails a time-consuming screening of databases that mirror the current state of knowledge in experimental biomedicine.

Here, we introduce SMAFIRA, an open access online tool to facilitate a 3R-relevant information retrieval that employs state-of-the-art language models from the field of deep learning. The tool is based on PubMed's similar articles to a reference document that best describes the intended research purpose. These similar articles are re-ranked according to their relevance. SMAFIRA assigns these articles to various categories such as *in vivo*, organs, primary cells, immortal cell lines, invertebrates, humans, and *in silico*. Thereby, SMAFIRA alleviates the search for alternative methods in PubMed. It fills in a significant gap in the collection of available 3R-relevant tools and AI based literature search queries.

The tool is freely available at <https://smafira.bf3r.de>.

P005

Refining Preclinical Research: Spheroid Cultures from Novel Transporter Mouse Models as a 3R-Compliant Alternative to *In Vivo* Experiments

J. Dressler^{1,2}, C. Kölz^{1,3,4}, S. Beer-Hammer^{2,5}, M. Schwab^{1,3,4,6}, A. T. Nies^{1,3}

¹Bosch Health Campus, Dr. Margarete Fischer-Bosch Institute of Clinical Pharmacology, Stuttgart, Germany

²University of Tübingen, Tübingen, Germany

³University of Tübingen, Cluster of Excellence iFIT (EXC 2180) "Image-Guided and Functionally Instructed Tumor Therapies", Tübingen, Germany

⁴University of Tübingen, Department of Clinical Pharmacology, Tübingen, Germany

⁵University of Tübingen, Department of Pharmacology, Experimental Therapy and Toxicology, Tübingen, Germany

⁶University of Tübingen, Department of Pharmacy and Biochemistry, Tübingen, Germany

Organic anion transporters 2 and 7 (OAT2/SLC22A7; OAT7/SLC22A9) are members of the solute carrier 22 family mediating organic anion transport across the sinusoidal hepatocyte membrane. Several endogenous and drug substrates have been identified for OAT2, including cGMP, uric acid, uric acid and 5-FU. For OAT7 only few substrates are known so far, specifically estrone-3-sulfate and pravastatin (reviewed in Nies et al., Pharmacol Ther 2022). However, physiological and pharmacological roles of both transporters remain insufficiently understood.

This project aimed to establish an animal-sparing workflow for generating 3D spheroids from ex-vivo isolated primary mouse hepatocytes using newly created, well-characterized global *mOat2* knockout and hepatocyte-specific *hOAT7* knockin mice. Spheroids serve as an advanced model for mechanistic liver studies bridging the gap between 2D hepatocyte cultures and *in vivo* experiments.

Ex-vivo liver perfusion of mouse liver was used to isolate viable primary hepatocytes for establishing 3D spheroid cultures, that were characterized at mRNA and protein levels. Spheroid viability was assessed with a bioluminescence assay. Uptake of radiolabeled prototypic substrates cGMP and estrone-3-sulfate into spheroids was measured to assess OAT2 and OAT7 function, respectively.

Ex-vivo perfusion of *mOat2* knockout and *hOAT7* knockin mice as well as control mice yielded viable hepatocytes forming stable 3D spheroids, which could be maintained for 4 weeks with preserved viability, hepatocyte-specific morphology and transporter expression. Knockout of *mOat2* and knockin of *hOAT7* could be confirmed on RNA and protein level over the culture period. As expected, uptake of cGMP was significantly reduced in spheroids isolated from *mOat2* knockout mice and uptake of estrone-3-sulfate was increased in *hOAT7* knockin spheroids, confirming their utility for studying transporter pharmacology. Additional substrates are currently under investigation.

In conclusion, the ex-vivo isolated hepatocyte spheroid cultures derived from our novel OAT2 and OAT7 mouse models provide valuable tools for mechanistic investigation of hepatic organic anion transporters under physiologically relevant conditions prior to *in vivo* pharmacokinetic studies. The use of ex-vivo isolated hepatocytes and the long-term stability and functionality of the spheroids substantially reduce animal use and stress, supporting the 3R principles and promoting animal welfare in preclinical research.

P006

A GLP-1R-Centric Mechanism Underlies the Insulinotropic Actions of a GLP-1R/GIPR/GCGR Triagonist

P. C. F. Schreier¹, P. Beyerle¹, S. Boulassel¹, A. Cebrian Serrano^{2,3}, T. D. Müller^{1,2,3}, I. Boekhoff¹, T. Gudermann^{1,4}, N. Khajavi¹

¹LMU Munich, Walther Straub Institute of Pharmacology and Toxicology Faculty of Medicine, Munich, Germany

²Helmholtz Munich, Institute of Diabetes and Obesity, Munich, Germany

³German Center for Diabetes Research (DZD), Neuherberg, Germany

⁴German Center for Lung Research, Germany

Rationally designed unimolecular GLP-1R/GIPR/GCGR triagonists targeting glucagon-like peptide-1 (GLP-1), glucose-dependent insulinotropic polypeptide (GIP), and glucagon (GCG) receptors represent a promising new therapy for improving glycemic control in both humans and mice. Nevertheless, the precise mechanisms by which this multi-agonist enhances β -cell function and insulin secretion remain unclear. In this study, we investigated the effects of the GLP-1R/GIPR/GCGR triagonist IUB447 on insulin secretion in murine pancreatic islets. Islets were isolated from wild-type, *Gipr*^{-/-}, *Gcgr*^{-/-}, and *Glp-1r/Gipr* double knockout mice, and insulin release in response to mono- and multi-agonist stimulation was assessed. The triagonist potentiated glucose-stimulated insulin secretion (GSIS) more effectively than combined mono-agonists in wild-type islets. This effect was maintained in the absence of either *Gipr* or *Gcgr* but was abolished in *Glp-1r/Gipr* double knockout islets or upon inhibition of the GLP-1 receptor with exendin-3 (9-39) in wild-type islets. Our results clearly demonstrate that the triagonist fails to enhance insulin secretion in the absence of functional GLP-1R activity. Accumulating evidence suggests that GLP-1R activates both Gq and Gas signaling pathways, whereas GIPR and GCGR primarily couple to Gas. Under diabetic conditions, persistent β -cell depolarization shifts GLP-1R signaling toward Gq dominance, preserving its insulinotropic effect. The results from our study demonstrated that inhibition of Gq signaling and its downstream effector TRPM5 prevents the triagonist-mediated enhancement of GSIS. Consistently, high-fat-fed *Trpm5*^{-/-} mice showed no improvement in glycemic control following triagonist administration. These findings indicate that the insulinotropic effect of the triagonist is largely mediated through GLP-1R and downstream Gq/TRPM5 signaling. Our results provide mechanistic insight into the GLP-1-centric activity of multi-receptor agonists and underscore the therapeutic potential of selectively targeting the Gq/TRPM5 signaling pathway as a novel strategy for mitigating T2D pathophysiology.

Biogenic Toxins

P007

Okadaic acid affects xenobiotic metabolism *in vitro* and *in vivo*

S. Hessel-Pras¹, L. T. D. Wuerger¹, H. Sprenger¹, A. Braeuning¹

¹German Federal Institute for Risk Assessment (BfR), Berlin, Germany

Okadaic acid (OA), a potent marine biotoxin produced by dinoflagellates, has been associated with various toxicological effects, including liver toxicity and disruption of xenobiotic metabolism. *In vitro* studies have shown that exposure to OA significantly downregulates cytochrome P450 (CYP) enzymes and transport proteins in human HepaRG liver cells, impairing hepatic metabolic homeostasis. These effects were observed at non-cytotoxic concentrations, suggesting that OA interferes with the expression and function of key components involved in drug metabolism and detoxification processes. Investigating the molecular mechanisms behind OA-induced CYP inhibition revealed that OA activates NF- κ B signaling, leading to the release of proinflammatory cytokines such as interleukin-6 (IL-6) and tumor necrosis factor- α (TNF- α). These cytokines activate the JAK/STAT pathway, resulting in the downregulation of CYP enzymes.

To validate these *in vitro* findings and elucidate the systemic implications of OA-induced CYP inhibition, an *in vivo* study was conducted. Male C57BL/6 mice were administered 100 μ g of OA intraperitoneally per kg of body weight. After 48 hours, the mice were sacrificed, and their liver RNA was isolated for RNA sequencing. Differentially expressed genes were identified and compared to *in vitro* HepaRG RNA sequencing data. Our comparative analysis will focus on whether the OA-induced CYP inhibition observed *in vitro* is also relevant *in vivo*. These findings could highlight the potential for OA to disrupt drug metabolism in the liver.

Together, our studies will improve the understanding of the toxicological effects of OA, especially its impact on hepatic xenobiotic metabolism. Combining *in vitro* and *in vivo* approaches provides a more comprehensive view of the molecular mechanisms underlying OA-induced toxicity, emphasizing the need to consider these effects in risk assessments and regulatory frameworks.

P008

Clostridioides difficile toxins TcdA and TcdB are inhibited by an antimicrobial peptide derived from human β 2-microglobulin

S. Lietz¹, K. Lindner¹, V. Vogel², B. Spellerberg², H. Barth¹

¹Institute of Experimental and Clinical Pharmacology, Toxicology and Pharmacology of Natural Products, Ulm University Medical Center, Ulm, Germany

²Institute of Medical Microbiology and Hygiene, Ulm University Medical Center, Ulm, Germany

Clostridioides (C.) difficile is a nosocomial pathogen of the human gut and responsible for gastrointestinal infections. Depending on the strain, *C. difficile* produces up to three AB-type protein toxins, including Toxin A (TcdA), Toxin B (TcdB), and CDT. As main virulence factors of *C. difficile*, these toxins are the causative agents of the symptoms after infection that include diarrhea or more life-threatening conditions. The large, single-chain proteins TcdA and TcdB are part of the clostridial glucosylating toxin family and consist of multiple domains. The toxins can enter target cells via binding to specific cell surface receptors and subsequent receptor-mediated endocytosis. Upon acidification of endosomes, the insertion and pore formation of the toxins into the endosomal membrane is

triggered. This enables the delivery of the toxic subunit, i.e. the enzymatically active glucosyltransferase domain (GTD), into the cytosol through the pore. In the cytosol, GTD glucosylates small GTPases of the Rho and/or Ras family which results in collapse of the actin cytoskeleton and cell death (1).

To identify novel peptide-based inhibitors of TcdA and TcdB, we tested four antimicrobial peptides derived from human β 2-microglobulin (β 2-MG) (2). Here, we showed that the β 2-MG D6 peptide is a potent inhibitor for TcdA, TcdB, and the medically relevant combination of both toxins in HeLa cells, Vero cells, and the physiologically more relevant human colon carcinoma cell line CaCo-2. In addition, the β 2-MG D6 peptide inhibits growth of *C. difficile* bacteria. In Vero cells treated with β 2-MG D6 and TcdB, the TcdB-mediated glucosylation of its substrate protein Rac1 is reduced, as demonstrated by Western blotting, while β 2-MG D6 had no direct effect on GTD enzyme activity *in vitro*. β 2-MG D6 peptide inhibits intoxication of cells most likely via formation of aggregates with TcdB in solution, which trap the toxin. These results form a basis for therapeutic strategies based on endogenous proteins and peptides as anti-toxin strategies for future treatment of *C. difficile*-associated diseases.

1. Papatheodorou P, Minton NP, Aktories K, Barth H. An Updated View on the Cellular Uptake and Mode-of-Action of Clostridioides difficile Toxins. *Adv Exp Med Biol*. 2024;1435:219-247. doi:10.1007/978-3-031-42108-2_11
2. Holch A, Bauer R, Olari LR, et al. Respiratory β 2-Microglobulin exerts pH dependent antimicrobial activity. *Virulence*. 2020;11(11):1402-1414. doi:10.1080/21505594.2020.1831367

P009

Flow cytometry-based characterization of cell surface binding of large clostridial glucosyltransferases

Y. Wu¹, H. Tatge¹, R. Gerhard¹

¹Hannover Medical School (MHH), Toxicology, Hanover, Germany

Clostridioides difficile infection (CDI) remains the most prevalent nosocomial infection worldwide. The major virulence factors responsible for CDI are two toxins, TcdA and TcdB, which are glucosyltransferases and enter target cells via receptor-mediated endocytosis. Both toxins contain a combined repetitive oligopeptide (CROP) domain, which - at least for TcdA - has been described to function as carbohydrate-binding region. To gain a deeper understanding of the cell-binding mechanism, we generated recombinant full-length toxins carrying a C-terminal His- and TwinStrep-Tag, along with isolated domains, particularly focusing on the CROP domain.

We employed a flow cytometry assay (FAC) to examine the direct binding of the recombinant toxins to primarily HT-29 cells by using DY-488 labeled StrepTactin. A distinct difference in binding behavior was observed between the recombinant TcdA VPI10463 (reference) strain and the hypervirulent TcdA R20291 strain. Specifically, the binding of the recombinant TcdA R20291 strain to HT-29 cells was markedly reduced compared to that of the recombinant TcdA from reference strain VPI10463. The isolated CROP domains from both strains exhibited similar binding characteristics. This observation was confirmed by substituting the CROP domain of the VPI10463 strain with that of the R20291 strain, which altered both the binding behavior and the cellular uptake of TcdA VPI10463. In competition assays we proved that the CROP domains from both strains bind to cell surface via GalII carbohydrate structure (Gal α 1,3-Gal β 1,4-GlcNAc).

We conclude that carbohydrate-independent binding differs in TcdA from reference and hypervirulent strains. Since CROP domains from both strains exhibit similar binding, differences in binding of full length toxin is presumably based on conformational alterations.

P010

Increase in Rab7/SQSTM/LC3B positive autophagic vesicles is due to lysosomal dysfunction induced by large clostridial glucosyltransferases

A. Langejürgen¹, E. Oyson¹, R. Gerhard¹

¹Hannover Medical School (MHH), Institute of Toxicology, Hanover, Germany

Besides inactivation of Rho and Ras GTPases large clostridial glucosyltransferases affect endolysosomal trafficking resulting in decreased lysosome function. As representatively shown for *C. difficile* TcdB, reduced lysosomal function is accompanied with reduced cathepsin D, resulting in slowed down degradation of toxin which is in favor of a more efficient toxin translocation and autophagy. Toxin-induced lysosomal dysfunction is accompanied by an increase in autophagic vesicles. To investigate this, we analyzed marker proteins SQSTM, LC3B and Rab7 after treatment of cells in immunoblot and immunofluorescence microscopy. Since Rab7 is also involved in transport and fusion of late endosomes and lysosomes, we put focus on the activity state of Rab7.

We found that all marker (SQSTM, LC3B and Rab7) were increased in HEp-2 cells after 24 h of treatment with TcdB. LC3B was an early and the most prominent surrogate for TcdB-induced effect. Specifically Rab7, which also regulates transport of late endosomes, was examined to evaluate its possible inactivation as reason for downstream lysosomal dysfunction. Rab7 increased in abundance as was also observed for the other autophagic marker LC3B and SQSTM. The toxin-induced effect was mimicked by bafilomycin A1, an inhibitor of endosomal acidification, indication disturbance of endosomal ion homeostasis as reason for lysosome dysfunction. We performed pull down assays to estimate activity state of Rab7 by using the GST-fusion protein of the RILP GTPase binding domain. The Rab interacting lysosomal protein (RILP) was first validated regarding specificity for active, GTP-bound Rab7. Interestingly, in accordance with

increased abundance of Rab7 the amount of active Rab7 (Rab7GTP) also increased. It is assumed that lysosomal dysfunction either triggers compensatory upregulation of regulatory proteins or leads to accumulation of autophagic vesicles due to reduced degradation. To further understand the role of Rab7 we applied the specific inhibitor CID 1067700. Inhibition of Rab7 neither affected lysosomal and autophagic marker cathepsin D and LC3B, respectively, nor altered the TcdB-induced effect.

In summary, TcdB interferes with endolysosomal trafficking and processing. Reduced lysosome activity affects autophagic processes resulting in increase in abundance and activity of related marker proteins. Thus, altered activity state of Rab7 is rather a consequence than the cause for toxin-induced lysosomal dysfunction.

P011

Discovery of endogenous toxin-inhibiting compounds in human blood

S. Kistermann¹, S. Heber¹, H. Barth¹

¹Institute of Experimental and Clinical Pharmacology, Toxicology and Pharmacology of Natural Products, Ulm, Germany

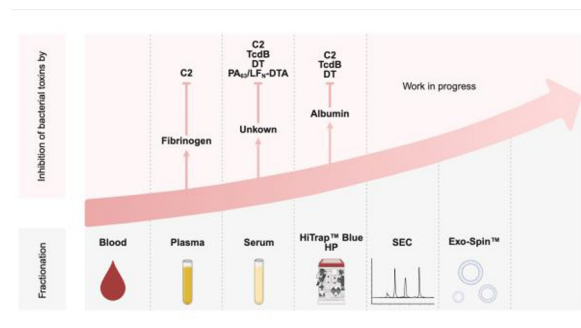
Bacterial AB-type protein toxins are key virulence factors of various diseases in humans and animals such as diphtheria, pertussis, botulism or anthrax and relevant in bioterrorism scenarios as well as in trauma-related clinical settings [1], [2]. As exotoxins, they are secreted by bacteria and can cause toxic effects independently of the producing microorganism. They contain a binding (B) domain that mediates receptor recognition and cellular uptake, and an enzymatically active (A) domain that modifies a toxin specific intracellular target [3]. Here, we systematically search for endogenous toxin inhibiting compounds with potential therapeutic properties and to elucidate their role within the innate immunity (figure 1).

We discovered that fibrinogen, representing an abundant plasma protein in the human blood specifically inhibited *Clostridium botulinum* C2 toxin (C2). Next, we observed that human serum protects HeLa cells from intoxication with various bacterial protein toxins (C2, *Clostridioides difficile* toxin B (TcdB), *Corynebacterium diphtheriae* diphtheria toxin (DT) or combinations of toxins including *Bacillus anthracis* components (PA63) and fusion toxins (LFN-DTA)). Our data showed a robust inhibition of all tested toxins using a morphology-based intoxication assay. Subsequent analysis focused on the identification of the inhibitory compounds present in human serum to narrow down the possible factors contributing to the observed effect. Therefore, serum samples were fractionated via HiTrap™ Blue HP columns, size exclusion chromatography (SEC) and Exo-spin™ columns. Preliminary data showed an almost comparable inhibitory capacity of the flowthrough serum from HiTrap™ Blue HP columns and a delayed intoxication of C2, TcdB and DT with the eluted fraction mainly containing human serum albumin. Moreover, the flowthrough from the HiTrap™ Blue HP column was fractionated via SEC and Exo-spin™ columns. Although not all analyses have been completed, preliminary results showed that none of the SEC-derived protein fractions inhibited any of the tested toxins.

Figure 1: Schematic illustration of our approach to identify endogenous toxin-inhibiting compounds in human blood. Created in BioRender.com.

- [1] H. Barth et al. (2004), *Microbiol. Mol. Biol. Rev.*
- [2] H. Barth et al. (2024) *Naunyn. Schmiedeberg's Arch. Pharmacol.*
- [3] R. Benz et al. (2017). *Uptake and Trafficking of Protein Toxins*

Fig. 1



P012

Xenorhabdus nematophilus TcA: Generation of a novel targeted toxin?

S. Richter¹, H. Gröttrup¹, G. Schmidt¹

¹University of Freiburg, Institute of Experimental and Clinical Pharmacology and Toxicology, Freiburg, Germany

Xenorhabdus and *Photorhabdus* species produce syringe-like toxin complexes (TCs) (Meusch *et al.* 2014, Gatsogiannis *et al.* 2016, Martin *et al.* 2023). TCs are high-molecular-mass tripartite ABC-type holotoxins, consisting of three subunits, namely TcA, TcB and TcC. Importantly, the A-subunit (TcA) mediates receptor binding on target membranes, while TcB and TcC assemble into a cocoon-like

complex that encapsulates the enzymatic component located at the C-terminus of TcC. TcC assemblies into a homo-pentameric complex, forming a large (~1.4 MDa) structure that features a central syringe-like channel through which the toxic protein is delivered into the host (Njenga Ng'ang'a *et al.* 2019). While *Photorhabdus* TCAs are capable of binding to both insect and mammalian cells, *Xenorhabdus* TCAs have been reported to bind exclusively to insect cells (Sheets *et al.* 2011). We are engineering a targeted TcA toxin by modifying its binding specificity. To achieve this, we inserted a HER2-specific affibody into the TcA component of *Xenorhabdus nematophilus*. The HER2 affibody targets the human epidermal growth factor receptor 2 (HER2), which is overexpressed in certain breast and ovarian cancers. We then combined the engineered *Xenorhabdus* TcA with the toxic TcCB component from *Photorhabdus luminescens* to evaluate the functionality of our hybrid construct in both mammalian and insect cells.

Cancer pharmacology

P013

Generation of colorectal cancer cell lines for functional and pharmacological analysis of PIK3CA-mutated colorectal cancer

C. B. Langen¹, R. A. Benndorf

¹Ruhr University Bochum, Institute of Pharmacology and Toxicology, Bochum, Germany

Introduction: In 2020, there were approximately 493,200 new cancer cases in Germany, with colorectal cancer (CRC) being the second most common cancer in women and the third most common in men. The development of malignant tumors is closely linked to mutations in oncogenes and tumor suppressor genes, including frequent mutations in *PIK3CA*. Mutations in this gene, encoding the catalytic subunit of phosphoinositol-3-kinase (PI3K), are found in 10-20% of CRC cases. These mutations, particularly the hotspot variants E542K, E545K, and H1047R, lead to hyperactivation of the downstream PI3K/Akt signaling pathway, which contributes to cancer development and progression by increasing cell proliferation and reducing apoptosis. Stable cell line models with a defined genetic background are crucial for the precise investigation of the pathophysiological consequences of these mutations.

Methods: We generated PIK3CA-mutated CRC cell lines based on DLD1 and HT-29 genetic backgrounds. In a first step, we generated and validated endogenous PIK3CA knockout cell lines using CRISPR-Cas9 technology. Subsequently, we reexpressed PIK3CA wild-type or the three most common hotspot mutation variants (E542K, E545K, H1047R) using lentiviral gene transfer. Control cell lines were generated by transducing DLD-1 and HT-29 with a lentiviral non-target-sgRNA CRISPR-Cas9 vector or, in the case of PIK3CA reexpression cell lines, with an empty lentiviral vector to account for the general effects of the lentivirus or sgRNA itself and to serve as negative controls for genetic manipulation (reexpression of PIK3CA). Successful knockout and reexpression of PIK3CA was confirmed by Western blot analyses. Additionally, luciferase was integrated into all cell lines as a reporter for future *in vivo* experiments.

Results & Conclusion: In our view, the generated cell lines provide a valuable tool for analyzing the functional consequences of *PIK3CA* mutations. They can be used in 2D and 3D *in vitro* assays as well as in *in vivo* experiments such as the chick embryo chorioallantoic membrane assay. The integrated luciferase allows for imaging and monitoring in small animal models like mice and rats. Taken together, we believe that these cell lines will contribute significantly to gaining new insights into the pharmacological characteristics of PIK3CA-mutated CRC entities.

P014

P014
Improvement of medication safety in patients with (neuro)endocrine malignancies initiating oral antitumor treatment: characterization of medication errors

M. Simon^{1,2,3,4}, P. Dürr^{1,2,3,4}, L. Cuba^{1,2,3,4,5}, T. Bergmann^{3,4,6}, F. Dörje^{2,3,4,7}, M. F. Fromm^{1,3,4,7}, M. Pavel^{3,4,6}, K. Gessner^{1,3,4}

¹Friedrich-Alexander University of Erlangen-Nuremberg, Institute of Experimental

and Clinical Pharmacology and Toxicology, Erlangen, Germany

²Universitätsklinikum Erlangen, Pharmacy Department, Erlangen, Germany

³Comprehensive Cancer Center Erlangen-EMN, Universitätsklinikum Erlangen, Erlangen, Germany

⁴Bavarian Center for Cancer Research, Erlangen, Germany

⁵Clinic Florisdorf, Vienna Healthcare Group, Pharmacy Department, Vienna, Austria

⁶Universitätsklinikum Erlangen, Department of Internal Medicine 1, Erlangen, Germany

⁷Friedrich-Alexander University of Erlangen-Nuremberg, FAU NeW - Research Center New Bioactive Compounds, Erlangen, Germany

Background: In recent years, the importance of oral antitumor therapies (OAT) has considerably grown, including in treatment of relatively rare (neuro)endocrine tumors (N[ET]). Although oral therapy is more compatible with patients' everyday lives than intravenous application, it carries considerable risks such as drug-drug/food-interactions and non-adherence. Medication safety is endangered by complex and often off-label regimens, side effect management, and multimodal systemic therapy. Types and frequencies of medication errors occurring at initiation of OAT in patients with N[ET] have not been studied so far.

Methods: This analysis comprised 69 patients, with 22 patients from the randomized AMBORA trial¹ (medication safety with oral antitumor therapy) and 47 patients from the AMBORA Competence and Consultation Center². As part of the structured AMBORA program, patients underwent a pharmaceutical/pharmacological counselling session at OAT initiation. This session contained e.g., information regarding their new medication, and advice on side effects. Medication errors were categorised employing validated classification systems [e.g., regarding cause (PCNE) and severity (NCC-MERP)].

Result: The most prevalent malignancy was pancreatic NET (26%). The majority (51%) of all patients received everolimus, followed by cabozantinib, temozolomide/capecitabine and lenvatinib. A total of 88 medication errors were identified, corresponding to 1.3 errors per patient. Of these, 49% were related to the OAT. 30% of the medication errors were caused by the patients. The most common cause of OAT-related medication errors was "no drug in spite of indication" (e.g., due to missing prophylaxis). In 40% of patients, who initiated treatment with everolimus, the mucositis prophylaxis solution was not administered.

Conclusion: Similar to patients with other types of tumors, patients with (neuro)endocrine malignancies experience a relatively high number of medication errors when starting their oral antitumor therapy. This should be taken into account in pharmaceutical/pharmacological support in order to contribute to improved medication safety through interprofessional collaboration.

¹Dürr P et al. J Clin Oncol 39:1983–1994, 2021

²Cuba L et al. JCO OP 20:1219–1230, 2024

P015

The Role Of Cell-Adhesion-Signalling In Therapy Resistance Of Chronic Myeloid Leukemia

P. Ahlf¹, S. P. Gorantla², L. Tiedemann¹, N. von Bubnoff², I. Cascorbi¹, M. Kaehler¹

¹University Hospital Schleswig-Holstein (UKSH), Campus Kiel, Institute of Experimental and Clinical Pharmacology, Kiel, Germany

²University Hospital Schleswig-Holstein (UKSH), Campus Lübeck, Department of Hematology and Oncology, Lübeck, Germany

Question: The discovery of tyrosine kinase inhibitors targeting the BCR::ABL1 kinase has substantially improved the survival rate of chronic myeloid leukaemia (CML) patients to 80–90%. However, a limitation in the treatment is the development of resistance. Beyond BCR::ABL1-mutations, cell adhesion signalling and ECM interactions present potential drivers of TKI resistance. Previous studies implicate deregulation of cell adhesion protein, such as fibronectin 1, in TKI resistance, suggesting adhesion signalling as an additional resistance mechanism. Therefore, the aim of the study was to identify further adhesion molecules affecting TKI resistance with focus on the cell surface molecules SPARC, involved in ECM synthesis, and LTBP1, regulating TGF- β availability in the ECM. Moreover, a stromal-leukemic cell system was established to assess cell–cell interactions.

Methods: Using an in vitro-TKI resistance K-562 cell model (2 μ M imatinib/0.1 μ M nilotinib), genome-wide gene expression was analysed to identify deregulated genes in resistance. Protein and pathway analyses were performed by immunoblotting; gene expression by RT-qPCR. Resistant cells were transfected with an LTBP1-directed siRNA or a SPARC-encoding plasmid with subsequent analysis of TKI sensitivity under imatinib treatment measuring cell number, proliferation and metabolic activity. In co-culture, the stromal H5-5 and leukemic K-562 cell interaction was analysed via immunofluorescence, MACS and cell counting.

Results: SPARC mRNA levels were significantly downregulated in imatinib- and nilotinib-resistance, whereas LTBP1 was not recurrently deregulated. In K-562 resistant cells, siRNA-mediated LTBP1 knockdown had a significant negative effect only on metabolic activity (-21.2%, $p = 0.007$). In contrast, overexpression of SPARC decreased metabolic activity and in addition, cell number (-30.4%, $p = 0.009$) and proliferation rate (-30.8%, $p = 0.03$) were reduced. Regarding cell–cell interaction, TKI-resistant cells demonstrated a direct interaction with stromal cells in contrast to sensitive cells.

Conclusions: Our data indicate that LTBP1 has no major impact on TKI-resistant cells, while restoration of SPARC increased TKI sensitivity in vitro. Since SPARC affects TKI sensitivity it may act synergistically with fibronectin. This, along with the altered binding of resistant cells, supports the findings that cell adhesion signalling contributes to mechanisms of TKI resistance.

P016

The BELCANTO protocol and preliminary results: a randomized, placebo-controlled phase II trial assessing the effect of cannabinoid extracts on the well-being of patients undergoing palliative oncological treatment

J. Domschikowski¹, R. Böhm², T. Herdegen³, A. Letsch⁴, M. Rostock⁵, A. F. Hamm⁶, D. Steinmann⁷, R. El Shafie⁸, S. Dickhut⁹, A. Hartmann¹⁰, J. Dunst², C. Schmalz²

¹St. Franziskus Hospital, Klinik für Strahlentherapie, Flensburg, Germany

²University Hospital Schleswig-Holstein (UKSH), Klinik für Strahlentherapie, Kiel, Germany

³University Hospital Schleswig-Holstein (UKSH), Institute of Experimental and Clinical Pharmacology, Kiel, Germany

⁴University Hospital Schleswig-Holstein (UKSH), Klinik für Innere Medizin II, Kiel, Germany

⁵Universitätsklinikum Hamburg-Eppendorf, II. Medizinische Klinik Onkologisches Zentrum & Hubertus Wald Tumorzentrum Universitäres Cancer Center Hamburg (UCCH), Hamburg, Germany

⁶University Hospital Schleswig-Holstein (UKSH), Klinik für Hämatologie und Onkologie, Lübeck, Germany

⁷Hannover Medical School (MHH), Klinik für Strahlentherapie und Spezielle Onkologie, Hanover, Germany

⁸Universitätsmedizin Göttingen, Klinik für Strahlentherapie und Radioonkologie, Göttingen, Germany

⁹Pharma Consulting, Aachen, Germany

¹⁰SocraMetrics GmbH, Erfurt, Germany

Background

The therapeutic promise of medical cannabinoids (CAM) for patients in Germany is impeded by reservations from the medical community and health insurers, in part due to limited knowledge and perceived excessive costs, but mainly due to a lack of randomized controlled trials (RCT). Despite positive indications from experiential medicine and case studies, the scarcity of evidence-based studies hinders widespread acceptance. In palliative oncology care, the evidence on CAM is conflicting, as there are both positive and negative surveys on CAM effects in pain management.

Methods

"Befindlichkeitsverbesserung unter Cannabinoid-Extrakten bei palliativ-Onkologischen Patienten" (BELCANTO) is a multicenter, placebo-controlled RCT. 170 patients will be randomized 1:1 to placebo or the investigational medicinal product (IMP), an oily solution of 1:1 Δ^9 -tetrahydrocannabinol (THC) and cannabidiol (CBD). After randomization, the IMP will be administered according to a Patient-reported Outcome (PRO)- and adverse event-triggered dosing protocol. The maximal dosage is 24 mg per day. The visits will be performed 12 days, 4 weeks and 8 weeks after start of IMP. The primary endpoint is the between-group difference in change from baseline in the physical and psychological symptom burden assessed with the Edmonton Symptom Assessment System Total Symptom Distress Score (ESAS TSDS) on day 12 \pm 2. Results will be reported according to the Consolidated Standards of Reporting Trials (CONSORT) guidelines. Secondary endpoints among others are: change in daily dose of morphine equivalent, distress, sleep quality, adverse events and quality of life (assessed with the European Organization for Research and Treatment of Cancer Quality of Life Questionnaire, EORTC QLQ). Clinical Trials ID: NCT06097533

Results

As of 2025-10-01, 70 patients were enrolled, and blinded, pooled analyses were conducted. ESAS TSDS decreased statistically significantly and clinically relevantly (\geq MCID ESAS TSDS of 5.7 points) over time (Fig 1). Important improvements were observed in the domain pain (Fig 2). Formal testing of the primary between-group endpoint will follow unblinding/database lock.

Discussion

Early blinded pooled data indicate clinically meaningful improvements. This is the first RCT with CAM in Germany investigating the unexplored potential of CAM therapy in palliative cancer care, aiming to contribute to evidence-based medicine by addressing gaps and identifying therapeutic goals.

Fig. 1

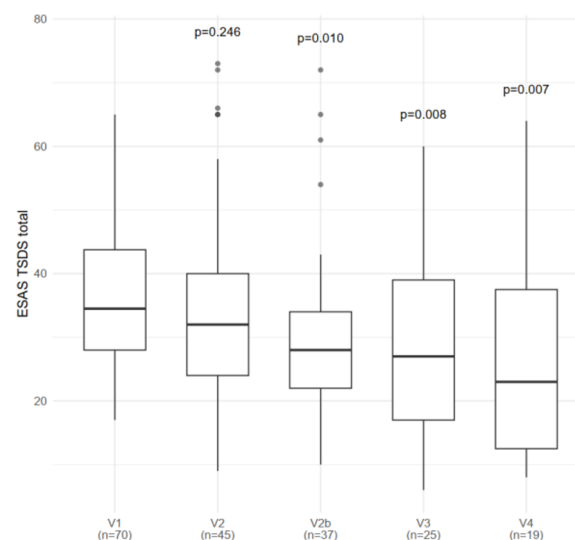
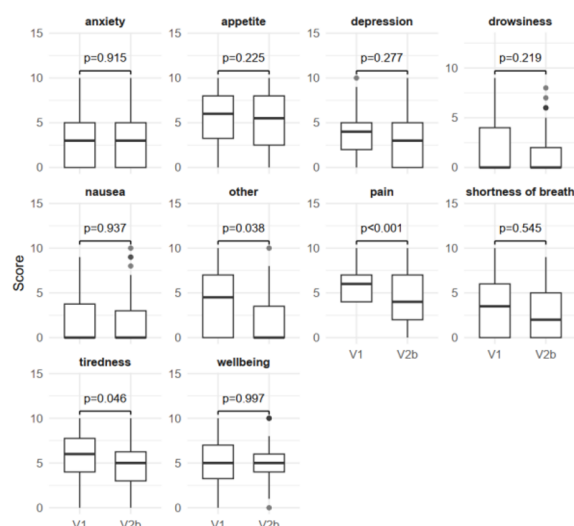


Fig. 2



P017

Differential regulation of sphingosine-1-phosphate metabolism under 2D and 3D culture conditions in colorectal cancer cells

M. C. Müller¹, C. Baume¹, U. Meyer¹, B. H. Rauch¹

¹Carl von Ossietzky University Oldenburg, Pharmacology and Toxicology, Oldenburg, Germany

Introduction

Colorectal cancer (CRC) remains a major cause of cancer-related morbidity and mortality, underscoring the need for improved therapies and diagnostics. Three-dimensional (3D) cell culture models more accurately mimic *in vivo* tumour behaviour than traditional two-dimensional (2D) systems, allowing the targeted study of factors such as sphingosine-1-phosphate (S1P). Investigating S1P signalling may reveal novel or more effective therapeutic targets and strategies for CRC treatment.

Objective

3D cell systems have shown divergent results compared to 2D cultures across various experimental settings. The aim of this study was to investigate whether similar differences occur in sphingolipid metabolism and to expand current knowledge on the signaling functions of S1P in colorectal cancer.

Materials and Methods

HCT116 cells were cultured simultaneously under 2D and 3D culture conditions. 3D cultures were established using forced floating cultivation in agarose-coated 96-well plates. Levels of S1P and sphingosine were quantified by HPLC-MS analysis, and gene expression changes at the mRNA level were assessed using qRT-PCR.

Results

Analysis of the S1P and sphingosine levels in 2D and 3D cell cultures under comparable experimental conditions showed variations in the lipid composition of cells cultured under these two culture types. When comparing the lipid levels of cell pellets prepared from these two culture types, the lipid levels of S1P and its sphingosine precursor differed significantly. The levels of S1P (d18:1) were significantly increased in cells cultured under 3D conditions compared to cells grown in 2D cultures. A similar effect could be observed for the S1P precursor sphingosine (d18:1) in the cell pellets. The associated analysis of expression patterns of S1P associated receptors and enzymes show an initially opposite effect, where the expression of the receptors for S1P (S1PR1 - S1PR5) is increased in 2D cultures compared to 3D cultures. S1P-associated enzymes (SPHK1, SPHK2, SGPL1) are also differentially regulated and also show elevated levels in 2D cultures compared to 3D cultures.

Conclusion

Increased S1P levels in 3D cultured cells are accompanied by downregulated expression of S1P-associated receptors and enzymes. These findings emphasize that 3D culture systems yield significantly different outcomes from 2D cultures when examining S1P metabolism and may contribute to a deeper understanding of S1P's role in cancer progression.

Ion channels and membrane transporters

P018

Generation of an ABC-Transporter Blood-Brain-Barrier Model using CRISPR/Cas9 Genome Editing

J. Kulartz¹, N. Denker¹, L. Muehe¹, A. Kasten¹, S. Petralia², G. Fricker², I. Cascorbi¹, M. Kaehler¹

¹University Hospital Schleswig-Holstein (UKSH), Experimental and Clinical Pharmacology, Kiel, Germany

²Heidelberg University, Institute for Pharmacy and Molecular Biotechnology, Heidelberg, Germany

Introduction: Separating plasma and brain compartments, the blood-brain barrier (BBB) restricts potentially harmful substances from entering the brain through endothelial cells connected by tight junction proteins. Thereby, luminal expression of ABC transporters such as *ABCB1*, *ABCG2* and *ABCCs* mediates the elimination of various compounds back into the plasma. To investigate the role of transporters for substance permeability the application of transporter inhibitors is well established. However, these inhibitors often lack specificity and/or inhibition is dose-dependent. To overcome these limitations, we aimed to generate an ABC transporter knockout model in human cerebral microvascular endothelial cells in order to determine substance permeability more specifically through the BBB.

Methods: The endothelial cell line hCMEC/D3 was used as an endothelial cell BBB model. ABC transporter expression was measured using RT-qPCR and immunoblotting. Knockouts for *ABCB1*, *ABCC1* and *ABCG2* were generated by CRISPR/Cas9 genome editing. Successful homozygous knockouts were validated by Sanger sequencing and immunoblotting. Functional transport analysis was performed using the fluorescent dyes rhodamine-123 for *ABCB1* and Fluo-3 AM for *ABCC1*, as well as doxorubicin. Monolayer integrity was evaluated using FITC-dextran 4 kDa.

Results: *ABCB1* showed the highest expression of the tested ABC transporters in hCMEC/D3 cells followed by *ABCC1* and *ABCG2*. We successfully established single and double knockouts of *ABCB1* and *ABCC1* in hCMEC/D3 cells by CRISPR/Cas9 genome editing. The hCMEC/D3 knockout cells exhibited a combination of deletions and insertions in the *ABCB1* gene for the single knockout. The *ABCC1*-/- showed a 1 bp-insertion, thereby forming a frameshift mutation. The *ABCB1/ABCC1*-/- was generated by deleting 61 bp of the *ABCC1* gene in the *ABCB1*-/- cells. All hCMEC/D3 knockout cells lost the respective protein level in the membrane fraction and total protein lysates as detected by immunoblotting.

Conclusion: We successfully generated an ABC transporter knockout model of the BBB based on the hCMEC/D3 cell line, which could be used to determine more precisely ABC transporter function in the BBB. This platform could be also used as model to further evaluate drug invasion into the brain or ABC transporter-dependent substance clearance through the BBB.

P019

Sulfur Mustard Induces Hyperpermeability and Process of Cadherine-switching: In Vitro Analysis of Pulmonary Epithelial and Endothelial Damage

M. Kern¹, J. Meyer¹, S. Rothmiller¹, D. Steinritz¹, K. Lutterberg¹

¹Bundeswehr Institute of Pharmacology and Toxicology, Munich, Germany

Question

Sulfur mustard (SM), an alkylating chemical warfare agent, mainly induces skin blisters. The inhalation of the agent can, however, cause major pulmonary issues, which can lead to death. Previous studies have shown that SM poisoning leads to increased hyperpermeability of the endothelial/epithelial barrier. This results in the secretion of fibrin-rich exudates into the alveoli and in the formation of pseudomembranes, which can cause suffocation. Cadherins, a part of adherens junctions, are a potential cause of the induced hyperpermeability. The internalisation of vascular endothelial cadherins (VE-cadherins) and translocation of neural cadherins (N-cadherins) are believed to play a promising role. In this study, we investigated the role of SM on pulmonary hyperpermeability caused by a change of cadherins, a so called "cadherin switch" / "cadherin shedding".

Methods

We identified two endothelial cell lines (ISO-HAS+HUVEC) and one epithelial cell line (H441) to examine an alveolar model. ISO-HAS and H441 are established in a co-culture method that mimics alveoli. With HUVEC, a primary endothelial cell line, we investigated reactions on oxidative stress (ROS) due to SM. A XTT cell proliferation assay was performed to determine the 50% lethal concentration (LC₅₀). The cells were then treated with the respective dose of SM for 2 hours. Western Blot analysis was then used to evaluate the expression of VE-cadherin protein before and after SM exposure. Immunocytochemistry (ICC) was used to display the localisation and the quantity of VE- and N-cadherin as well as the cadherin switch.

Results

LC₅₀ Values of the XTT assay resulted in 318µM SM for ISO-HAS, 501µM SM for H441 and 407µM SM for HUVEC. Western blot analysis showed a decrease in VE-cadherin (130kDa) for ISO-HAS and HUVEC cells after sulfur mustard exposure and indicated fission products (35kDa) of the VE-cadherin and therefore revealed cadherin shedding. The ICC indicated that there is a decrease in the

amount of VE-cadherins expressed whereas N-cadherin appeared on the cell surface.

Conclusion

In our Study we can show that SM has an impact on cell-cell-connections as ROS and it can be supposed that the cadherin switch and shedding are a reason for hyperpermeability after SM-inhalation. This is a promising approach for possible therapeutics, since no therapy is known yet. Here further investigations are needed to get a better understanding of the cadherin-switch to find suitable inhibitors.

P020

Triagonist Amplifies Glucose-Stimulated Cytosolic Ca²⁺ Signaling
P. C. F. Schreier¹, S. Boulassel¹, P. Beyerle¹, I. Boekhoff¹, T. Müller^{1,2,3}, T. Gudermann^{1,4}, N. Khajavi¹

¹Ludwig-Maximilians-University Munich, Walther-Straub-Institute of Pharmacology and Toxicology, Munich, Germany

²Helmholtz Center Munich, Institute of Diabetes and Obesity, Neuherberg, Germany

³German Center for Diabetes Research (DZD), Neuherberg, Germany

⁴German Center for Lung Research, Munich, Germany

Question: Current research in obesity and diabetes emphasizes multi-target therapies that simultaneously address several dysregulated metabolic pathways. A major breakthrough has been the development of a *triagonist*, designed to activate GLP-1R, GIPR, and GqR in a balanced manner. This strategy has shown greater efficacy than single-agonist treatments and is now in phase 2 clinical trials, although its precise molecular mechanisms remain unclear.

Methods: Isolated wild-type mouse islets were used for glucose-stimulated insulin secretion (GSIS) and confocal Ca²⁺ imaging. GSIS was assessed after 1 h incubation at low (2.8 mmol/L) or high (20 mmol/L) glucose with or without triagonist or monoagonists, and insulin was quantified by ELISA. For Ca²⁺ imaging, Fluo-4 AM-loaded islets were imaged using confocal microscopy. Changes in intracellular Ca²⁺ were recorded in response to glucose elevation and pharmacological treatments, and oscillation parameters were analyzed.

Results: We demonstrated that triagonist enhances GSIS more strongly than monoagonists. Next, we investigated whether this effect involves altered Ca²⁺ dynamics in murine pancreatic β -cells in isolated islets. At low glucose (2.8 mmol/L), [Ca²⁺]_i remained stable, while high glucose (20 mmol/L) induced transient peaks and oscillations. Although the initial Ca²⁺ peak was comparable across treatments, the triagonist maintained elevated [Ca²⁺]_i and significantly increased oscillation amplitude during the plateau phase, with only modest effects on oscillation frequency. Specific inactivation of TRPM5 with the blocker TPPO reduced glucose-induced Ca²⁺ peaks and attenuated sustained Ca²⁺ elevation under triagonist treatment. Notably, triagonist had no effect on [Ca²⁺]_i in the absence of extracellular Ca²⁺. Ca²⁺ release after SERCA inhibition confirmed ER Ca²⁺ availability, excluding ER stores as the source of triagonist-induced Ca²⁺ signaling.

Conclusion: Triagonist amplifies glucose-evoked Ca²⁺ dynamics in pancreatic β -cells via extracellular Ca²⁺-dependent mechanisms, providing novel insight into its superior insulinotropic action and highlighting its therapeutic potential as a multi-receptor agonist in type 2 diabetes.

P021

Regulation of α -Cell Mass, Glucagon Production, and Secretion via TRPM7 Kinase in Mice

S. Boulassel¹, P. C. F. Schreier¹, A. Beck², H. Choi¹, A. M. Melyshi¹, P. Reinach³, M. Duraj¹, M. Vinogradov¹, B. Suleimen¹, J. Berger¹, K. Jacob¹, A. Breit¹, S. Zierler⁴, I. Boekhoff¹, T. Gudermann^{1,5}, N. Khajavi¹

¹Ludwig-Maximilians-University Munich, Walther-Straub-Institute of Pharmacology and Toxicology, Munich, Germany

²Institute of Experimental and Clinical Pharmacology and Toxicology, Saarland University, Homburg, Germany

³Wenzhou Medical University, Ophthalmology Department, Wenzhou, China

⁴Johannes Kepler University Linz, Institute of Pharmacology, Linz, Austria

⁵German Center for Lung Research, Munich, Germany

Objectives: Mammalian target of rapamycin (mTOR) plays a central role in controlling pancreatic α -cell function by influencing α -cell mass and the production and secretion of glucagon, a key hormone in glucose homeostasis. It has been shown that the transient receptor potential cation channel subfamily M member 7 (TRPM7) regulates mTOR signaling in various cell types. TRPM7 is a ubiquitously expressed bifunctional membrane protein that combines a divalent cation-selective channel with a protein kinase moiety. In recent work, we described the importance of TRPM7 kinase in murine pancreatic β -cell function and regulation of glucose metabolism. In light of the pivotal role of mTOR on α -cell function, we now aimed to study the role of TRPM7 in α -cell biology and investigate its potential interaction with the mTOR signaling pathway.

Materials and methods: Pancreatic islets were isolated from TRPM7 kinase-dead (*Trpm7^{RR}*) and WT mice in C57BL/6J background. Functional analyses included Bio-Plex assays, RNA sequencing, glucagon ELISA, qRT-PCR, Western blotting, immunocytochemistry, and patch-clamp recordings. α TC1c9 cells were used as a murine α -cell model. NS8593, a small synthetic compound, was used as a potent TRPM7 inhibitor.

Results: WT islets treated with TRPM7 inhibitor, NS8593, and *Trpm7^{RR}* islets showed reduced mTOR signaling. *Ex vivo* studies revealed that *Trpm7^{RR}* islets exhibit reduced glucagon secretion upon hypoglycemia or amino acid stimulation compared to WT islets. Plasma glucagon was reduced in *Trpm7^{RR}* mice. Additionally, glucagon content was diminished in *Trpm7^{RR}* islets as well as in WT islets treated with NS8593. These reductions were associated with downregulation of key transcriptional regulators of glucagon biosynthesis, including *Gcg*, *Mafb* and *Foxa2*. Morphological analysis revealed reduced proliferation and increased apoptosis of α -cells in *Trpm7^{RR}* islets, as well as following pharmacological inhibition of TRPM7 in both WT islets and α TC1c9 cells *in vitro*.

Conclusion: Collectively, our findings demonstrate that the kinase domain of TRPM7 plays a role in regulating α -cell function and glucagon secretion via mTOR signaling pathway. Loss of TRPM7 kinase function impairs mTOR signaling, leading to reduced α -cell mass and glucagon secretion and biosynthesis. Our findings identify the TRPM7 kinase/mTOR axis as a critical regulator of α -cell function in mice.

P022

TRPV2 Expression and Function in Polarized Alveolar Macrophages

M. Kieffmann¹, T. Gudermann¹, A. Dietrich¹

¹Ludwig Maximilian University of Munich, Walther Straub Institut of Pharmacology and Toxicology, Munich, Germany

Introduction

Tissue-resident alveolar macrophages (AMs) are essential players in innate immunity and in maintaining lung homeostasis (1). The transient receptor potential vanilloid 2 (TRPV2) protein forms a non-selective, Ca²⁺-permeable ion channel that is expressed in AMs (2). Impaired TRPV2-mediated phagocytic function in AMs renders the lung more susceptible to cigarette smoke-induced alveolar space enlargement (3). AMs can be polarized by specific stimuli into a pro-inflammatory M1 or an anti-inflammatory M2 phenotype (1). However, the expression and functional role of TRPV2 in polarized AMs remain poorly understood.

Methods

Primary murine AMs from wild-type (WT) and TRPV2^{-/-} mice, as well as the AM cell line MH-S, were cultured in RPMI-1640 medium supplemented with 10% fetal bovine serum and 1% penicillin-streptomycin under standard conditions (37°C, 5% CO₂). To induce polarization, AMs were stimulated with interferon- γ (50 ng/ml) and lipopolysaccharide (50 ng/ml) for M1 polarization, or with interleukin-4 (20 ng/ml) for M2 polarization. TRPV2 expression was analyzed using qRT-PCR and Western blotting. Live-cell fluorescence microscopy with the ratiometric dye fura-2 AM was employed to assess TRPV2-mediated Ca²⁺ influx in polarized AMs.

Results

In both primary AMs and the MH-S cell line, stimulation with interferon- γ /lipopolysaccharide induced an M1 phenotype characterized by upregulation of CD86 and SOCS3, whereas interleukin-4 treatment induced an M2 phenotype with increased expression of arginase-1 and CD206. Compared to unpolarized (M0) AMs, TRPV2 mRNA expression did not significantly differ in M1 or M2 AMs. However, TRPV2 protein expression was reduced in M1 cells and remained unchanged in M2 cells relative to M0 AMs. Upon TRPV2 activation, M1-polarized AMs exhibited the highest Ca²⁺ influx, followed by M2 AMs, while M0 AMs showed the lowest response.

Conclusions

Our findings indicate that TRPV2 protein expression is decreased in M1-polarized AMs compared to M0 and M2 cells. Interestingly, despite the reduced total protein level, M1 AMs displayed a stronger TRPV2-mediated intracellular Ca²⁺ influx. This suggests enhanced TRPV2 trafficking to the plasma membrane upon M1 polarization, implying a potential role for TRPV2 in M1 macrophage-specific mechanisms.

References

(1) Aegerter H. et al., *Immunity*, 2022; 55:1564–1580. (2) Link T.M. et al., *Nat Immunol*, 2010; 11:232–239. (3) Masubuchi H. et al., *BMC Pulm Med*, 2019; 19:70.

P023

Mitochondrial K_{Ca}3.1 channels in pancreatic β -cells: Evidence for regulatory significance by mitochondria-targeting channel blockers

L. Beuke¹, C. Kick¹, E. Bulik¹, B. Wünsch¹, A. Schwab², M. Düfer¹

¹University of Münster, Pharmaceutical and Medicinal Chemistry, Münster, Germany

²University of Münster, Faculty of Medicine, Münster, Germany

The existence of intermediate conductance Ca²⁺-activated potassium channels (K_{Ca}3.1) in the mitochondria of pancreatic β -cells has not yet been confirmed. Mitochondrial K_{Ca}3.1 channels could alter ion gradients depending on mitochondrial Ca²⁺ concentration and thereby influence mitochondrial function. As β -cell function crucially depends on mitochondrial energy supply, this study aims

to identify those channels and to determine their relevance in the context of β -cell physiology and pathology in type 2 diabetes mellitus (T2DM).

Functional effects of the $K_{Ca}3.1$ inhibitor senicapoc and two novel, mitochondria-targeted derivatives (WMS98-02 with permanent triphenylphosphonium (TPP) conjugation; WMS98-03 with hydrolysable TPP ester) were evaluated on $\Delta\psi_m$ in primary mouse islet cells (C57BL/6N mice), either acutely or after 18 hours of preincubation. Mitochondrial fractions of MIN6 cells were analysed by Western Blot to test for the expression of $K_{Ca}3.1$ channels. For WST-1 cell viability assays and MitoSOX-based measurement of mitochondrial ROS, MIN6 cells were treated with the compounds for 3 hours.

$K_{Ca}3.1$ channel protein was detected in mitochondrial fractions of MIN6 cells. In primary islet cells, senicapoc did not alter $\Delta\psi_m$ either acutely or after an 18-hour culture period even at a high concentration of 30 μ M. By contrast, 1.5 μ M WMS98-02 caused acute depolarisation and seems to be toxic after 18 hours, visible in a greatly reduced cell number, whereas 1.5 μ M WMS98-03 induced depolarization without any morphological signs of cellular damage. Consistent with the negative influence of WMS98-02 on β -cell number, this compound significantly reduced the cell viability of MIN6 cells and increased mitochondrial ROS within 3 hours, while WMS98-03 did not alter both parameters. Of note, senicapoc decreased mitochondrial ROS thereby further illustrating the difference between targeting plasma membrane or mito $K_{Ca}3.1$ channels.

These findings indicate the presence of mito $K_{Ca}3.1$ channels in pancreatic β -cells and demonstrate that mitochondria-targeted senicapoc derivatives modulate $\Delta\psi_m$, cell viability, and mitochondrial ROS. The distinct properties of the novel compounds illustrate, that subtle structural modifications alter mitochondrial effects, from acute toxicity to sustained but non-lethal depolarization. Our results provide a basis for further studies exploring mito $K_{Ca}3.1$ channels as regulators of β -cell homeostasis and their relevance in the context of T2DM.

P024

Organelle Ca²⁺ Regulator 2 (OCA2) critically controls primary hemostasis by regulating Ca²⁺ release from NAADP-mediated Ca²⁺ stores
V. Throm¹, R. Ottenheim¹, J. E. Camacho-Londoño¹, U. Schulte², D. Jašlan³, C. Grimm³, K. Krauel⁴, D. Dürschmied⁴, M. Freichel¹

¹Heidelberg University Hospital, Pharmakologisches Institut, Heidelberg, Germany

²University of Freiburg, Institute of Physiology, Freiburg, Germany

³Ludwig Maximilian University of Munich, Walther-Straub-Institut für Pharmakologie und Toxikologie, Munich, Germany

⁴Universitätsklinikum Mannheim, Department of Angiology, Haemostaseology and Medical Center Mannheim, Mannheim, Germany

Platelets are small, anucleate cells essential for hemostasis. Upon activation, they remodel morphologically and secrete mediators that promote further platelet recruitment. This process is tightly regulated by cytosolic Ca²⁺ signaling. Ca²⁺ is mobilized from the dense tubular system and acidic organelles such as lysosomes [1]. Activation of PAR-4 and GPVI receptors generates NAADP, a second messenger mediating Ca²⁺ release from acidic stores [2]. Full activation involves exocytosis of dense granules (ATP, ADP, Ca²⁺), α -granules (P-selectin, PF4), and lysosomes (proteases, Ca²⁺). Platelets thereby drive both physiological hemostasis and pathological thrombosis, underlying conditions such as myocardial infarction and stroke [2].

We identified the membrane protein OCA1 (Organelle Ca²⁺ Regulator 1), encoded by *Tmem63a*, in acinar cells, where it regulates Ca²⁺ release from endo-lysosomes and secretory granules. Microscopic analysis of acinar cells and organelle proteomics reveal OCA1 within lysosomes and granules during endo-/exocytosis. Acting as a gatekeeper for NAADP-mediated Ca²⁺ release through Two-Pore Channels (TPCs), OCA1-/- leads to loss of Ca²⁺ release from secretory granules and causes uncontrolled enzyme secretion, resulting in pancreatitis [3,4].

In this study, we investigated the role of OCA2, another protein of the same family, in platelet primary hemostasis and thrombosis formation by determining the activation pathway of OCA2, as it has previously been detected in the platelet proteome [5]. Mice with platelet-specific deletion of OCA2 (OCA2^{pl}-KO) exhibited significantly reduced bleeding times along with more rapid thrombus formation, suggesting increased platelet sensitivity towards external stimuli. These findings are in line with our *in vitro* studies, showing full platelet aggregation upon stimulation of the GPVI receptor of ~80% in OCA2^{pl}-KO compared to no aggregation in control cells. Furthermore, we investigate how OCA2 regulates NAADP-mediated Ca²⁺ release from endo-lysosomal via TPCs in thrombocytes. We are currently investigating ATP and P-Selectin release from dense and α -granules in OCA2^{pl}-KO vs. WT platelets to determine whether the heightened reactivity observed in the KO can be attributed to differences in granule secretion.

1.Feng, M., et al. Circ Res, 2020

2.Coxon, C.H., et al. Biochem J, 2012

3.Tsilovskyy V., Ottenheim, R., et al. J Clin Invest, 2024

4.Freichel, M., Cell Calcium, 2024

5.Zeiler, M., Mol Cell Proteomics. 2014

P025

Opposite role of Cavβ3 and Cavβ2 in the regulation glucose homeostasis
H. Salah¹, S. Mannebach Götz², C. Richter¹, C. Zhao¹, B. Wardas², A. Beck², F. Schmitz², V. Flockerzi², A. Belkacem¹

¹Heidelberg University, Pharmakologisches Institut, Heidelberg, Germany

²Universität des Saarlandes, Homburg, Germany

High voltage-gated Cav channels are composed of the ion-conducting Cav α 1 pore and the auxiliary Cav α 2 δ and Cav β subunits. Our group previously demonstrated that Cav β 2 and Cav β 3 proteins are present in mouse pancreatic islets and that glucose clearance is accelerated in global Cav β 3 KO (Cav β 3global KO-1) mice. To determine whether this phenotype is specific to pancreatic β -cells and Cav β 3, we pursued three independent approaches. (i) We used insulin-secreting rat β -cells (INS-1) lacking Cav β 3 (CRISPR/Cas9) and isolated primary mouse β -cells to test whether Cav β 3 regulates β -cell function in a cell-autonomous manner. (ii) From mice with a conditional Cav β 3 allele, we generated a new global Cav β 3 KO (Cav β 3global KO-2) and a β -cell-specific Cav β 3 KO (Cav β 3 β -cell KO). (iii) To compare Cav β 2 and Cav β 3 functions, we used extra-cardiomyocyte Cav β 2 KO mice (Cav β 2global KO) and created β -cell-specific Cav β 2 KO mice (Cav β 2 β -cell KO). Glucose tolerance tests were performed on Cav β 3 β -cell KO, Cav β 2 β -cell KO, and litter-matched control mice. Similar to Cav β 3global KO-1, both Cav β 3global KO-2 and Cav β 3 β -cell KO mice exhibited enhanced glucose clearance, whereas Cav β 2global KO and Cav β 2 β -cell KO mice showed impaired glucose tolerance. In Cav β 3 KO mice, plasma insulin levels, glucose-stimulated insulin secretion, total insulin content, insulin mRNA, and insulin granule numbers were significantly increased, while insulin sensitivity and islet morphology remained unchanged, indicating a specific role of Cav β 3 in insulin expression. Cav β 3 deletion did not alter K⁺-induced Ca²⁺ influx or Cav current density. Cytosolic Ca²⁺ levels were stable at low glucose and rose with high glucose, showing a peak and plateau with regular oscillations; these oscillations were markedly reduced by Cav β 3. Carbachol-induced, IP3-dependent Ca²⁺ release was also diminished in the presence of Cav β 3, without changes in intracellular Ca²⁺ stores. Cav β 2 deletion impaired first-phase glucose-induced insulin secretion and reduced K⁺-evoked Ca²⁺ influx, Cav current density, and Ca²⁺-oscillation frequency. Deletion of Cav β 3 or Cav β 2 in pancreatic β -cells revealed opposing roles: Cav β 2 is essential for Cav channel activity, whereas Cav β 3 reduces β -cell sensitivity to low IP3 levels. Future studies will examine the distinct functions of Cav β 3 (vs Cav β 2) in insulin transcription and β -cell survival in diabetic mouse models.

P026

Caco-2 Cell Metabolism and Transporter-Mediated Efflux of Solanidine
Phase II Metabolites and Variability in Solanidine Absorption

P. Koczera¹, J. P. Müller¹, K. S. Just¹

¹Uniklinik RWTH Aachen, Institute of Clinical Pharmacology, Aachen, Germany

Question

Solanidine is a steroidal alkaloid naturally found in potatoes. While extensive amounts of solanidine and its derivatives are toxic, it gained recent popularity in clinical pharmacology research due to its substantial metabolism by CYP2D6. Metabolic ratios of solanidine and its CYP2D6-derived metabolites are promising biomarkers for CYP2D6 activity in humans [1]. Although, solanidine is abundant in western diet and has a long half-life, variable consumption and absorption from dietary intake may influence its predictability for CYP2D6 activity. Recently, a study demonstrated directed transport of solanidine phase II metabolites from Caco-2 cells suggesting active efflux by transport proteins in the gut wall [2]. Aim of this project was to study the metabolic activity of Caco-2 cells to form solanidine phase II metabolites and to identify transport proteins potentially responsible for their active efflux.

Methods

Caco-2 cells were cultivated as a monolayer and incubated with solanidine. Transport assays were performed and medium supernatants as well as cell lysates were analysed via LC-MS/MS to identify solanidine, solanidine-sulfate and -glucuronide. By using specific transporter inhibitors verapamil (for p-glycoprotein (p-gp)), fumitremogin C (breast cancer resistance protein (BCRP)), and MK-571, (multidrug-resistance associated protein (MRP)), we aimed to identify the responsible transport proteins.

Results

Phase II metabolites solanidine-sulfate and solanidine-glucuronide were identified in cell lysates and medium supernatants after incubation with solanidine. By using selective inhibitors for P-gp, BCRP and MRP, we demonstrate decreased solanidine-sulfate and -glucuronide levels in surrounding medium, suggesting involvement in efflux.

Conclusions

Our results confirm the ability of Caco-2 cells to metabolize solanidine to its phase II metabolites solanidine-sulfate and -glucuronide. We conclude active transport of phase 2 metabolites by natively expressed transporters p-gp, BCRP and MRP. In vivo activity changes of these transporters may lead to variable absorption of dietary solanidine.

[1] Müller et al., 2023. Nutrimeric Validation of Solanidine as Dietary-Derived CYP2D6 Activity Marker In Vivo. Clin Pharmacol Ther, 115, pp. 309 – 317

[2] Keuter et al. 2024. Structural Impact of Steroidal Glycoalkaloids: Barrier Integrity, Permeability, Metabolism, and Uptake in Intestinal Cells. *Mo Nutr Food Res*, 68, e2300639

Cardiac pharmacology

P027

Adipokine Expression in Perivascular Adipose Tissue Differs Between Atherosclerosis-Prone and -Resistant Arteries in Patients Undergoing Coronary Artery Bypass Surgery - The Role of Chemerin

N. Xia¹, J. Lee¹, L. Hartmann¹, K. Buschmann², N. Kastner¹, G. Reifenberg¹, L. Wojnowski¹, H. Treede², H. Li¹

¹University Medical Center Mainz, Department of Pharmacology, Mainz, Germany

²University Medical Center Mainz, Department of Heart Surgery, Mainz, Germany

Background: Approximately 70% of individuals over 70 years develop coronary artery disease (CAD), and most patients undergoing elective coronary artery bypass grafting (CABG) are overweight or obese. Previous work in adipocyte-specific eNOS knockout mice demonstrated that perivascular adipose tissue (PVAT)-derived chemerin promotes vascular inflammation and remodeling in obesity. While the aorta and coronary arteries are prone to atherosclerosis, the internal mammary artery (IMA) remains relatively resistant and is considered the gold-standard graft for CABG. This study investigated whether adipokine expression, particularly chemerin, differs between PVAT surrounding atherosclerosis-prone and -resistant vessels in patients with advanced CAD.

Methods: Samples of serum, vascular tissue (aorta and IMA), and corresponding PVAT (aortic PVAT [C-PVAT] and IMA-PVAT) were collected from 60 patients undergoing elective CABG. Body composition was assessed by bioimpedance, including BMI, waist circumference, fat and muscle mass percentage, and visceral fat index. Serum chemerin was measured by ELISA. Gene expression of adipokines, inflammatory, fibrotic, oxidative stress markers, and eNOS was analyzed by quantitative PCR. Fibrosis was assessed histologically using Masson's trichrome staining.

Results: The cohort exhibited a mean BMI of 29 kg/m², consistent with overweight or obesity. Serum chemerin was positively associated with C-reactive protein and body fat percentage and negatively correlated with muscle mass. Aortic tissue showed greater fibrosis and fibrotic gene expression than IMA. Similarly, aortic PVAT displayed higher fibrosis and upregulation of fibrotic, inflammatory, and oxidative stress genes compared with IMA-PVAT. While adiponectin and leptin expression were similar between sites, chemerin expression was markedly higher in aortic PVAT.

Conclusions: Systemic chemerin is linked to adiposity and systemic inflammation. Elevated chemerin expression in PVAT surrounding atherosclerosis-prone vessels suggests a potential role of PVAT-derived chemerin in promoting local vascular inflammation and atherogenesis in obesity-related cardiovascular disease.

P028

Knockout of proteoglycan versican attenuates adverse cardiac remodeling after myocardial infarction

L. Gebert¹, D. J. Gorski¹, S. Gorresen¹, A. Petz¹, T. Lautwein², M. Piroth¹, T. Hube¹, H. Pfeifle¹, K. Köhrer², T. N. Wight³, K. Bottermann¹, J. W. Fischer¹

¹University Hospital Düsseldorf, Heinrich Heine University Düsseldorf, Institute for Pharmacology, Düsseldorf, Germany

²Heinrich Heine University Düsseldorf, Biologisch-Medizinisches Forschungszentrum (BMFZ), Düsseldorf, Germany

³Benaroya Research Institute, Seattle, WA, United States

Versican as a large multifunctional chondroitin sulfate proteoglycan is expressed in several cell types involved in healing of acute myocardial infarcts (AMI), especially fibroblasts and immune cells. Its specific binding to hyaluronan (HA) molecules makes versican a modulator of HA-rich extracellular matrix (ECM). In addition, fibrotic responses in various organs including the heart after AMI, are known to be associated with pathologically elevated unfolded protein response (UPR) signaling in response to endoplasmic reticulum (ER) stress.

We investigated the role of versican in cardiac ischemia/reperfusion (I/R) injury using ubiquitous and fibroblast-specific (*Tcf21*) conditional knockout (KO) mice subjected to 45 minutes of closed-chest I/R to induce AMI. Cardiac function was assessed by echocardiography. Cardiac cell composition and gene expression were analyzed via single cell sequencing followed by in vitro analysis of UPR signaling in primary isolated cardiac fibroblasts.

Versican gene expression is elevated early in hearts after AMI (6h) and stays upregulated in the infarct zone for up to 3 weeks. Single-cell RNA sequencing shows that versican is expressed mainly by cardiac fibroblasts and that genes associated to ER stress are downregulated in versican KO fibroblasts. Indeed, ubiquitous conditional KO of versican leads to an improved systolic pump function shown by improved ejection fraction (EF) and limited end-systolic volume (ESV). Mechanistically fibroblasts from KO mice as well as fibroblasts with knockdown (KD) of versican using siRNA exhibit reduced ER stress, which is reflected by the downregulation of UPR target genes (e.g. *Hspa5*, *Manf* and *Crel2*), a mechanism known to limit fibrotic remodeling.

Consistently, fibroblast-specific KO of versican also suggests signs of reduced cardiac fibrosis after myocardial infarction as evidenced by improved EF, limitation of ventricular dilation and reduced isovolumic relaxation time (IVRT). Scar size 3

weeks after AMI is significantly smaller in fibroblast-specific versican KO hearts compared to control.

In conclusion, both global and fibroblast-specific knockout of versican confer a protective phenotype after AMI by reducing adverse cardiac remodeling caused by diminished ER stress in versican KO fibroblasts. Our findings show that versican is a key regulator of fibroblast-driven fibrosis after AMI and reveal a mechanistic link between ECM remodeling and UPR signaling in the injured heart.

P029

Inhibition of late sodium current as a therapy for alcoholic cardiomyopathy

M. Baier^{1,2}, S. Schildt², T. Krammer², L. Neufeld², E. Korn², D. Lukas², S. Graber², L. S. Maier², S. Neef², S. Lebek², J. Mustroph^{1,2}

¹University of Regensburg, Department of Pharmacology, Regensburg, Germany

²University Hospital Regensburg, Internal Medicine II, Regensburg, Germany

Background: Chronic alcohol consumption is a leading cause of acquired cardiomyopathy. However, no targeted pharmacological therapy exists to prevent or reverse ethanol-induced cardiac dysfunction. We investigated in human and murine cardiomyocytes whether inhibition of the late sodium current (late I_{Na}) by ranolazine confers cardioprotection in acute and chronic models of ethanol exposure.

Methods and Results: In isolated human failing ventricular cardiomyocytes, acute ethanol exposure markedly increased late I_{Na}, leading to cytosolic Na⁺ overload, sarcoplasmic reticulum (SR) Ca²⁺ depletion, and reduced cellular contractility. Ranolazine fully prevented these alterations, normalizing Na⁺ and Ca²⁺ homeostasis and contractile performance. Similar protection was observed in human failing ventricular trabeculae, where ranolazine preserved developed tension during acute ethanol challenge.

To determine long-term efficacy, mice were exposed to ethanol in drinking water for 10 weeks, inducing alcoholic cardiomyopathy with a significant reduction in ejection fraction (40.6±1.3% vs. 52.9±1.9% upon vehicle, p<0.0001) and enhanced late I_{Na} (-48.7±3.7 vs. -22.5±6.2 A/F*ms upon vehicle, p=0.0003). Chronic co-treatment with ranolazine completely prevented the decline in left ventricular function (48.5±1.4%, p=0.02 vs. EtOH), abrogated late I_{Na} enhancement (-20.1±3.4 A/F*ms, p=0.0001 vs. EtOH), and normalized Ca²⁺ spark frequency (EtOH: 1.74±0.15 1/100 μm⁻¹ s⁻¹ vs. EtOH+Ran: 0.93±0.09 1/100 μm⁻¹ s⁻¹, p=0.0002), indicating restored SR Ca²⁺ stability. Importantly, ranolazine also exerted therapeutic effects when initiated after onset of contractile dysfunction (week 8), significantly improving ejection fraction within two weeks (week 10: 55.0±1.9% vs. week 8: 43.7±1.6%, p=0.006) and reversing ionic dysregulation.

Mechanistically, ethanol induced CaMKII-dependent phosphorylation of Na_v1.5 at serine 571 (S571), which was abolished by ranolazine. In S571A knock-in mice lacking this phosphorylation site, ethanol failed to enhance late I_{Na} or cause contractile dysfunction, mimicking the protective effect of ranolazine.

Conclusion: Ranolazine prevents and reverses ethanol-induced cardiomyopathy by inhibiting late I_{Na} and thereby preserving Na⁺/Ca²⁺ homeostasis and SR Ca²⁺ stability. These findings identify late I_{Na} inhibition as a promising pharmacological strategy for both prevention and treatment of alcoholic cardiomyopathy.

P030

Receptor of Hyaluronan-Mediated Motility (RHAMM) benefits cardiac fibrotic remodelling after cardiac ischemia and reperfusion through a pre-activated cardiac fibroblast phenotype

M. Schwingen¹, A. Petz¹, D. J. Gorski¹, S. Gorresen¹, T. Lautwein¹, J. W. Fischer¹, K. Bottermann¹

¹Institute for Pharmacology - UKD/HHU, Düsseldorf, Germany

During cardiac ischemia and reperfusion (I/R) the synthesis of hyaluronic acid (HA) is crucial for post-infarct healing, by providing an environment for cells involved in the remodelling process as immune cells and fibroblasts (Petz et al. *Circ Res* 2019). HA also acts as signalling molecule via its receptors CD44 and receptor of hyaluronan-mediated motility Rhamm (*Hmmr*). The role of HA-signalling via Rhamm in cardiac healing after I/R and its influence on murine cardiac fibroblasts (MCF) is largely unknown.

Transgenic mice, either overexpressing *Hmmr* (*Hmmr* – OE) or with a deletion of *Hmmr* (*Hmmr* – KO) were compared to littermate wildtype controls (WT) after 45 minutes cardiac ischemia followed by reperfusion for up to 3 weeks. *Hmmr* – OE mice developed smaller scars, while *Hmmr* – KO mice exhibited enlarged scars at 3 weeks. Concomitantly, cardiac function was impaired in *Hmmr* – KO mice. Spatial transcriptomics (ST) and single-cell RNA sequencing (scRNA-seq) analysis were used to investigate gene expression in different niches and cell clusters in WT and *Hmmr* – OE mice at 72 h and 7 d post I/R. Using ST 12 genetically specific niches within the heart after 7d I/R were identified, from which scar and borderzone (BZ) exhibited the highest number of differentially expressed genes (DEGs). Overrepresentation analysis revealed an upregulated response to wounding and regulation of inflammatory response in the scar as well as increased leukocyte migration and chemotaxis in the BZ, pointing to a faster remodelling process in *Hmmr* – OE. scRNA-seq identified 18 different cell clusters, from which the fibroblast cluster showed the highest number of DEGs. While resting MCF exhibited a higher expression of periostin (POSTN), indicating a more activated phenotype, activated MCF showed a downregulation in several fibrillar collagens. Additionally, *Rhamm* – OE MCF had an accelerated transition through pseudotime. To further investigate this fibroblast phenotype, the migration, proliferation and activation of MCF from *Hmmr* – OE mice were investigated *in vitro*. *Hmmr* – OE MCF showed increased migration and proliferation and upregulation of AKT on protein level compared to WT.

Our data suggest that the *Rhamm* signalling alter the dynamics of fibroblast activation. *Hmmr* – OE MCF show a pre-activated phenotype, indicating that they can reach a more differentiated state (matrifibrocyte) earlier than WT MCF, thereby improving healing after cardiac I/R.

Funding: DFG, CRC1116, Project S01 and A08 to JF

P031

Impact of white adipose tissue derived lipolytic products on the activation of isolated murine cardiac fibroblasts

R. Kretschmer¹, E. Maruyama¹, J. W. Fischer¹, K. Bottermann¹

¹Institute for Pharmacology, Düsseldorf, Germany

Lipolytic products, such as non-esterified free fatty acids (NEFAs), are released from white adipose tissue (WAT) during myocardial infarction (MI) in a catecholamine-dependent manner. Besides lipids, WAT secretes various adipokines and cytokines that influence the myocardium in health and disease. Cardiac fibroblasts are essential for post-MI healing and represent a promising therapeutic target. While increased NEFA levels are considered detrimental for ischemic heart injury, the impact of WAT-derived lipolytic products on CF activation however is mainly unknown.

In this study, we investigated the effects of lipolytic products derived from different WAT depots *ex vivo* on the *in vitro* activation of murine cardiac fibroblasts (mCFs). Subcutaneous inguinal (IWAT) and visceral gonadal WAT (gWAT) were isolated from C57BL/6J mice to generate conditioned medium (conM). WAT explants were incubated for two hours with either PBS (control) or the β 3-adrenoceptor agonist CL316,245 (CL) to induce lipolysis. UV/VIS spectrometry revealed a significantly higher NEFA release in agonist-treated tissue. Consistently, Western blot analysis of iWAT and gWAT showed increased phosphorylation of hormone-sensitive lipase (HSL) at Ser563 after CL treatment, indicating a lipolytic activation and release of lipolytic products into the medium.

The resulting conM was used to treat primary mCFs isolated by retrograde heart perfusion with collagenase. After 24 h starvation, mCFs were stimulated for 24 h with PBS (negative control), TGF β (positive control), or conM. qPCR analysis showed that TGF β markedly upregulated all analyzed activation markers, whereas CL-conM treatment increased only *Acta2* expression in both iWAT- and gWAT-derived media.

Our findings indicate that WAT-derived lipolytic products modulate mCF activation marker expression and may promote fibroblast-to-myofibroblast transition. Since no correlation between the concentration of NEFAs in CM and *Acta2* expression level could be observed, this pro-fibrotic effect of conM on mCF might be due to other WAT derived factors, such as adipokines or cytokines.

P032

Global CD44 deficiency reduces blood pressure in mice

S. M. Jülicher¹, S. Samson¹, J. W. Fischer¹, T. Suvorava¹

¹University Hospital Düsseldorf, Heinrich Heine University Düsseldorf, Institute of Pharmacology, Düsseldorf, Germany

CD44 is a multifunctional transmembrane and hyaluronan (HA) binding glycoprotein implicated in cell adhesion, migration, and tumor progression. However, its importance for normal vascular homeostasis remains largely unexplored. We hypothesized an interconnection between CD44, HA and nitric oxide (NO) signaling pathways and studied the role of CD44 in maintaining of endothelial function and blood pressure. To accomplish this, mice with global CD44 knockout (CD44-KO) and C57BL/6J wild-types (WT) were examined.

Measurement of systolic blood pressure (sBP) and heart rate (HR) by non-invasive tail-cuff plethysmography revealed no difference in HR but a significant 10 mmHg reduction of sBP in CD44-KO mice compared with WT. While acute deficiency on CD44 induced by i.p. injection of CD44-antibody lead to the impairment of flow-mediated dilation (FMD), global CD44-KO mice displayed a normal iliac artery response to increased blood flow. Endothelial function measured *ex vivo* by relaxation of aortic rings to cumulative concentrations of acetylcholine did not differ between genotypes. Similarly, WT and CD44-KO mice exhibited comparable contractile responses to phenylephrine and similar sensitivity to exogenous NO, and in both genotypes inhibition of NO-synthase (NOS) equally enhanced these responses. These findings indicate preserved endothelial function and arterial reactivity in chronic global CD44 deficiency. Quantitative PCR and Western blot analyses confirmed the absence of CD44 and showed similar expression of endothelial NOS (eNOS), HA synthases 1-3, versican, and hyaluronan-mediated motility receptor genes in aortas from CD44-KO and WT. While total eNOS protein levels remained unaltered, basal phosphorylation at Ser1177 was increased in CD44-deficient aortas, decreased in the heart, and stayed unchanged in skeletal muscle, suggesting organ-specific heterogeneity. Basal Thr495 eNOS phosphorylation was similar in skeletal muscle of both genotypes and undetectable in aortic and cardiac tissues.

Taken together, these data suggest that CD44 may contribute to blood pressure homeostasis. While the impairment of FMD in acute CD44 deficiency points to CD44 as a potential mechanosensor, its chronic absence appears to trigger compensatory mechanisms. Further studies are needed to confirm the observed reduction in blood pressure using telemetry and to elucidate the molecular mechanisms responsible for this effect in CD44 deficiency.

P033

The role of focal adhesion kinase in 2D and 3D homo and heterocellular cardiac tissues

S. Qasem^{1,2}, B. Berečić^{1,2}, G. M. Dittrich^{1,2}, S. Lutz^{1,2}

¹University Medical Center Göttingen, Pharmacology and Toxicology, Göttingen, Germany

²German Center for Cardiovascular Research (DZHK), Partner Site Lower Saxony, Göttingen, Germany

Background and objective

Focal adhesion kinase (FAK) has been widely studied in various diseases, particularly cancer. Recently, FAK has been identified as a key mediator of fibrosis, and its inhibition has emerged as a promising therapeutic strategy. Many FAK inhibitors have been developed but have shown limited efficacy in oncology, leading to the development of FAK proteolysis targeting chimera (PROTACs) targeting kinase-dependent and -independent functions.

This study aims to elucidate FAK's role in 3D homo- and heterocellular cardiac tissues focusing on its role in cardiac fibrosis.

Methods

A series of functional analyses were conducted in 2D human cardiac fibroblast (hCF) culture and in 3D engineered connective tissues (hCF and collagen I; ECT) and engineered heart muscle (hCF, inducible pluripotent stem cell-derived cardiomyocytes (CM) and collagen I; EHM) with FAK inhibitor VS-4718 and its corresponding PROTAC GSK215. We evaluated FAK expression and phosphorylation, fibrosis-associated gene expression, cell proliferation, cell cycle, and contractile performance of the engineered tissues.

Results

In 2D, GSK215 abolished FAK expression and phosphorylation, whereas VS-4718 inhibited only FAK phosphorylation. Both compounds reduced the fibrosis marker connective tissue growth factor (CTGF), in the presence and absence of the pro-fibrotic TGF- β 1. All effects were concentration dependent, with the PROTAC significantly more potent than the inhibitor. Both GSK215 and VS-4718 reduced hCF proliferation. However, GSK215 had no detectable effect on the proportion of cells in different cell cycle phases. In contrast, VS-4718 induced a concentration-dependent increase in the proportion of cells in the G2/M phase. In ECT, GSK215 efficiently inhibited pole deflection with and without TGF- β 1, whereas VS-4718 had no effect. In EHM, VS-4718 dramatically impaired force generation and isometric force, whereas GSK215 did not affect these parameters.

Conclusion

The effects of FAK targeting molecules varied between 2D and 3D cardiac models. In 2D, the data suggest that GSK215 is more potent than VS-4718. In 3D, GSK215 reduced pole deflection in ECT, while VS-4718 had no effect. Conversely, VS-4718 impaired contractile force in EHM, while GSK215 did not affect force generation. Additional 2D and 3D experiments are needed to further elucidate the underlying mechanisms. 3D models are essential for deeper understanding of FAK's role in fibroblast mechanobiology.

P034

Fluphenazine inhibits Dopamine D₁ receptors in cardiac preparations of transgenic mice

W. Nenoff¹, J. Neumann¹, B. Hofmann², U. Gergs¹

¹Martin Luther University Halle-Wittenberg, Institute for Pharmacology and Toxicology, Halle (Saale), Germany

²Mid-German Heart Center, University Hospital Halle, Department of Cardiac Surgery, Halle (Saale), Germany

Fluphenazine (4-[3-(2-trifluoromethylphenothiazine-10-yl)propyl]-1-piperazineethanol) belongs to the class of phenothiazine antipsychotics and was introduced in the 1960s as a neuroleptic (antipsychotic) drug and in the 1970s it was listed by the World Health Organization as an essential drug. It is established that fluphenazine binds and inhibits dopamine D₁ receptors *in vitro*. Here, the hypothesis was tested that fluphenazine blocks D₁ receptors in the mammalian heart. To this end, a transgenic mouse model with cardiac specific overexpression of the human dopamine D₁ receptor in the heart (D₁-TG) was utilized [1]. For the control experiments, wild-type (WT) mice were used. Moreover, the effects of fluphenazine were compared with the effects of aripiprazole, an atypical antipsychotic. The force of contraction was measured in isolated, electrically stimulated (1 Hz) preparations of mouse left atria (LA) in Tyrode's solution (37°C). The same setup was then employed to analyze isolated human right atrial preparations from patients undergoing bypass surgery for comparison. In the presence of 10 μ M propranolol, cumulatively applied dopamine increased the force of contraction in LA from D₁-TG but not in LA from WT controls ($p < 0.05$, $n = 5-7$). Preincubation of the D₁-TG LA with 10 μ M fluphenazine shifted the concentration-response curve of dopamine dextrally by about two orders of magnitude ($p < 0.05$, $n = 5-7$). In contrast, 10 μ M aripiprazole, acting preferentially on dopamine D₂ receptors, failed to alter the force of contraction in LA from D₁-TG. The administration of 10 μ M fluphenazine or aripiprazole alone had no effect on the force of contraction in LA from D₁-TG or WT. Furthermore, in human atrial preparations, fluphenazine, but not aripiprazole, attenuated the increase in force of contraction mediated by fenoldopam, a selective dopamine D₁ receptor agonist ($n = 3$). In summary, the data suggest that fluphenazine can antagonize dopamine D₁ receptors in the transgenic mouse heart and, more importantly, in the human heart. This may explain cardiac side effects of fluphenazine.

[1] Abella LMR et al. Naunyn Schmiedeberg's Arch Pharmacol. 2024;397(7):4939-4959. doi: 10.1007/s00210-023-02901-y

P035**Inotropic effects of the dual incretin-based agonist survodutide in human atria**F. Lehnert¹, J. Neumann¹, B. Hofmann², U. Gergs¹¹Martin Luther University Halle-Wittenberg, Institute for Pharmacology and Toxicology, Halle (Saale), Germany²Mid-German Heart Center, University Hospital Halle, Department of Cardiac Surgery, Halle (Saale), Germany

Survodutide (BI 456906) belongs to the novel class of dual incretin-based agonists, which can activate both glucagon receptors (GCGR) and glucagon-like peptide-1 receptors (GLP-1R). The stimulation of both receptors leads to the activation of adenylyl cyclases, followed by an increase in cyclic adenosine monophosphate. In the present study, the hypothesis was tested that survodutide, like the GLP-1R agonist semaglutide, increases force of contraction (FOC) in human right atrial preparations (HAP) via GCGR and/or GLP-1R. Additionally, the effect on the sinus node was examined in spontaneously beating mouse right atria. The force of contraction was measured in isolated, electrically stimulated (1 Hz) preparations of HAP from adult patients undergoing open-heart surgery due to severe coronary heart disease in Tyrode's solution (37°C). Spontaneously beating right atrial preparations (RA) from adult wild-type mice were isolated and analyzed using the same experimental setup as for human preparations, but without stimulation. It was noted that survodutide, starting at 3 nM, raised FOC in HAP in a concentration- and time-dependent manner (n=3). In the additional presence of the phosphodiesterase (PDE) III inhibitor cilostamide, survodutide was more potent and effective to raise FOC (n=3-4). Moreover, the positive inotropic effect of survodutide could be reduced by the GCGR antagonist adomeglivan (10 µM) and by the GLP-1R antagonist exendin (100 nM). 100 nM survodutide shortened the time of relaxation in HAP. Survodutide was less effective and less potent than isoprenaline in increasing the FOC in HAP. In spontaneously beating mouse right atrial preparations, survodutide exerted positive chronotropic effects (p<0.05, n=4), which were antagonized by the GCGR antagonist adomeglivan (10 µM). From these data, it is suggested that survodutide affects the beating rate via GCGR in mouse RA and increases the FOC via GLP-1R and GCGR in HAP. It is reasonable to hypothesize that, in the human heart, the heart rate could be elevated by both the GCGR and the GLP-1R.

P036**Protein phosphatase 2A-induced cardiac hypertrophy is attenuated by an inhibitory protein**R. Schwarz¹, K. Hadova², J. Klimas², J. Neumann¹, U. Gergs¹¹Martin Luther University Halle-Wittenberg, Institute for Pharmacology and Toxicology, Halle (Saale), Germany²Faculty of Pharmacy, Comenius University, Department of Pharmacology and Toxicology, Bratislava, Slovakia

We had previously demonstrated that the cardiac overexpression of the catalytic subunit of protein phosphatase 2A in transgenic mice (PP2A-TG) resulted in cardiac hypertrophy, as evidenced by an increase in the relative heart weight (heart weight divided by body weight) [1]. Furthermore, other studies have demonstrated that the PP2A activity is elevated in human heart failure. Consequently, it is of clinical significance to ascertain whether the augmentation in PP2A-induced relative heart weight can be averted. To this end, a new transgenic mouse model was generated with cardiac overexpression of the inhibitor 2 of PP2A, known as SET (SET-TG), which functions to regulate the activity of PP2A. After the crossbreeding of PP2A-TG with SET-TG to get double transgenic PP2A-TG x SET-TG (DT) mice, the heart weight was monitored, and cardiac function was analyzed by echocardiography. The expression levels of the endogenous and transgenic genes were measured via detection of the corresponding messenger ribonucleotide acids (mRNA) by quantitative PCR. While the cardiac expression of endogenous SET and PP2A mRNAs was comparable in all genotypes, the expression of PP2A was enhanced in PP2A-TG and DT. The expression of exogenous SET mRNA was enhanced in SET-TG and DT. In the PP2A-TG, an elevated relative heart weight (p<0.05) was observed when compared to the wild-type (WT) and the SET-TG. A notable observation was the unaltered heart weight in the DT mice, in comparison to both WT and SET-TG. Consequently, it was normalized compared to PP2A-TG (p<0.05). Furthermore, the left ventricular function, assessed by echocardiography, exhibited a similar pattern for e.g. ejection fraction, ventricular diameters, and ventricular wall thickness (p<0.05). These findings suggest that PP2A can indeed induce cardiac hypertrophy, and that this hypertrophy can be prevented by reducing the activity of PP2A. Consequently, PP2A might be a druggable target in the context of human heart failure.

[1] Gergs et al. J Biol Chem. 2004;279(39):40827-34. doi: 10.1074/jbc.M405770200

P037**Phospholamban phosphorylation site S10 modulates PKA-dependent phosphorylation at S16**J. te Vrugt¹, J. Schmitt², M. Krüger², F. Funk¹¹Universitätsklinikum der Heinrich-Heine-Universität Düsseldorf, Institut für Pharmakologie, Düsseldorf, Germany²Universitätsklinikum der Heinrich-Heine-Universität Düsseldorf, Institut für Herz- und Kreislaufphysiologie, Düsseldorf, Germany**Introduction:**

Phospholamban (PLN) is a key regulator of the cardiac calcium ATPase SERCA2a and plays an essential role in regulating the contractility of the heart muscle. Its function is modulated via several phosphorylation sites. Serine 16 (S16) has been characterized as the main functionally relevant site. The significance of the phosphorylation site serine 10 (S10) remains to be elucidated.

Objectives:

Investigation of the influence of S10 modification on protein kinase A (PKA)-dependent phosphorylation of the main regulatory site, S16.

Methods:

PLN phosphorylation was analyzed by Western blot using phospho-specific antibodies as well as Phos-tag™ gels to unravel the stoichiometry of different phospho-species. For mechanistic studies, PLN mutants with a phosphomimetic (glutamate, S10E) and an inactivating (alanine, S10A) amino acid substitution at S10 as well as a PLN wild-type (PLN-wt) construct were generated and expressed in HEK293 cells. Phosphorylation at S16 in HEK293 was analyzed either under basal conditions or after PKA activation with forskolin.

Results:

Western blot analyses of PLN phosphorylation in mouse heart tissue using phospho-specific antibodies revealed phosphorylation of all three phosphorylation sites (S10, S16 and T17). Analyses of the phosphorylation stoichiometry using Phos-tag™ suggested that certain PLN phosphorylation states may be mutually exclusive.

To gain mechanistic insights that explain these findings, S10E, S10A and PLN-wt were expressed in HEK293. Both Western blots with an antibody specific for phosphorylation at S10 and Phos-tag™ analyses confirmed S10E as a suitable model for constitutive phosphorylation of PLN at S10. Under basal conditions, the S10E mutant showed significantly reduced PKA-dependent phosphorylation at S16 (41±15% of PLN-wt, N=5-6, p<0.01), whereas S16 phosphorylation of the S10A mutant did not significantly differ from PLN-wt. After PKA activation with forskolin, S16 phosphorylation of S10E and S10A was indistinguishable from PLN-wt already at sub-maximum stimulation. The effects of S10E on PKA-dependent phosphorylation were observed both for PLN monomers and pentamers.

Conclusions:

The data suggest an interaction between PLN phosphorylation sites S10 and S16 that reduces PKA-dependent phosphorylation. Phosphorylation at S10 may therefore act as a mechanism to modify how basal PKA activity is translated into SERCA2a regulation.

P038**The direct PDE2 stimulation with 5,6-DM-cBIMP as a novel antiarrhythmic therapeutic strategy in heart failure**N. Kaiser¹, L. Hellmann¹, K. Rose¹, M. Gröner¹, E. Cachorro¹, A. El-Armouche¹, S. Kämmerer¹¹TU Dresden University of Technology, Institut für Pharmakologie und Toxikologie, Dresden, Germany**Introduction:**

Patients with heart failure (HF) have an increased risk of fatal arrhythmias and sudden cardiac death. In particular, the chronic activation of the sympathetic nervous system as a compensatory response to reduced cardiac function, promote arrhythmia development via β -adrenergic cAMP signaling in cardiomyocytes (CM). As a result, intracellular Ca^{2+} homeostasis is disturbed, leading to pro-arrhythmic Ca^{2+} fluxes. In HF, the phosphodiesterase 2 (PDE2) is upregulated and might mitigate these pro-arrhythmic triggers by cAMP degradation. Mice with cardiac-specific PDE2 overexpression developed less arrhythmia under β -adrenergic stress and after myocardial infarction. Here, we aim to investigate potential anti-arrhythmogenic effects of direct PDE2 activation via 5,6-DM-cBIMP (cBIMP) mic with HF.

Materials and Methods:

HF was induced in control mice (PDE2-WT) and mice with CM-specific PDE2 knockout (PDE2-KO) using a 60% high-fat diet (HFD) and the NO-synthase inhibitor L-NAME (0.5 g/L) for 5 weeks. Cardiac function was evaluated by echocardiography. In isolated ventricular CM, pro-arrhythmic triggers, like spontaneous action potentials (sAP), Ca^{2+} influx via the L-type Ca^{2+} current (I_{CaL}), spontaneous Ca^{2+} -waves (SCWs) and Ca^{2+} -sparks (CaSp) were quantified using patch-clamp and Ca^{2+} -imaging techniques, while single-cell contraction was assessed by sarcomere shortening.

Results:

After 5 weeks, the metabolic and hemodynamic stress under via HFD and L-NAME resulted in elevated body weight, increased mean arterial pressure, and diastolic dysfunction, as indicated by an increased E/E' , in both PDE2-WT and PDE2-KO animals. Interestingly, PDE2-KO showed reduced systolic function and more arrhythmia compared to PDE2-WT. In isolated CM from diseased PDE2-WT, β -adrenergic stimulation with isoprenaline markedly enhanced the number of pro-arrhythmic sAP, SCWs and CaSp as well as I_{CaL} amplitude. Importantly, all of these arrhythmogenic Ca^{2+} -signals were markedly reduced under cBIMP via cAMP hydrolysis. This antiarrhythmic effect was abolished by the specific PDE2

inhibitor BAY 60-7550, and was absent in CM of diseased PDE2-KO. cBIMP did not affect cellular contraction amplitudes in CM of PDE2-WT with HF.

Conclusion:

The direct activation of PDE2 via cBIMP lowered cAMP levels and markedly reduced arrhythmogenic calcium triggers, without impairing single-cell contractility in isolated CM from mice with HF serving for a new antiarrhythmic strategy.

P039

Atglstatin-treatment of diet-induced obesity mice after cardiac I/R alters adipose tissue biology but does not influence cardiac function

P. Hebar¹, H. Zabir¹, D. Semmler¹, S. Gorreßen¹, S. Lehr², J. W. Fischer¹, K. Bottermann¹

¹University Hospital Düsseldorf, Heinrich Heine University Düsseldorf, Institute of Pharmacology, Düsseldorf, Germany

²German Diabetes Center (DDZ), Düsseldorf, Germany

Obesity is a major risk factor for cardiovascular diseases, including myocardial infarction (MI). The function of white adipose tissue (WAT) is severely impaired in obese individuals. MI acutely stimulates WAT lipolysis but also chronically affects its metabolic and secretory functions.

This study utilised the ATGL-inhibitor Atglstatin to characterise the impact of chronic WAT dysfunction following ischaemia/reperfusion (I/R) injury in obese C57BL/6J male mice. Analysis of the morphology, structure, and function of cardiac tissue, subcutaneous (iWAT) and visceral (gWAT) WAT and blood was performed. Cardiac I/R was induced using a two-step closed-chest model after 9-week high-fat/high-sucrose diet. The administration of Atglstatin started 24 hours after I/R. Tissues were harvested at 24 hours, 7 days, and 28 days after I/R.

Surprisingly, obesity prevented acute lipolytic stimulation in response to I/R as diet-induced obese (DIO)-mice did not exhibit increase in NEFA levels compared to sham-operated mice after 60 minutes ischemia and 30 minutes reperfusion. However, iWAT from ischaemic DIO-mice compared to sham DIO-mice, showed smaller adipocytes, an upregulation of ATGL gene expression and a downregulation of leptin and galectin-3 (macrophage marker), indicating a more chronic effect of cardiac I/R on WAT in obesity.

Treatment with Atglstatin led to a significant decrease in body weight 28 days after I/R, lower tissue weight and smaller adipocytes in iWAT, but not in gWAT. Interestingly, ischemia per se and even more Atglstatin-treatment reduced circulating leptin levels, while vice versa ghrelin levels were increased, indicating enhanced appetite. A similar regulation of leptin expression could be observed in gWAT. Furthermore, Atglstatin-treatment reduced circulating resistin levels, pointing to reduced inflammation, which was supported by reduced galectin 3-expression in ischemia- and Atglstatin-groups compared to sham/vehicle, also in gWAT.

Despite strong changes in WAT and circulating adipokines, cardiac function, and scar size of the Atglstatin-fed animals showed no significant differences compared to the vehicle-group.

After I/R, acute lipolytic activation is blunted in obese mice. However, following Atglstatin treatment, which normalised body weight, reduced inflammation and leptin expression in adipose tissue and blood serum, cardiac function remained unaffected after I/R.

Funding: Else Kröner Fresenius Stiftung grant to KB.

P040

The role of phospholamban pentamer formation in cardiac adaptation to myocardial infarction

M. Krotov¹, F. Funk¹, S. Gorreßen¹, M. Krüger², J. Schmitt¹

¹Institute of Pharmacology, Düsseldorf, Germany

²Institute of Cardiovascular Physiology, Düsseldorf, Germany

Introduction: The sarco/endoplasmic reticulum (SR) Ca²⁺ ATPase (SERCA2a) and its inhibitor phospholamban (PLN) regulate the intracellular redistribution of Ca²⁺ in cardiomyocytes and thus contraction and relaxation. Previously, we have shown that the formation of PLN pentamers critically affects PKA-dependent PLN phosphorylation at serine 16 (pPLN-S16) and, consequently, SERCA2a activity. Hypertensive mouse hearts that lacked PLN in total or the ability to form PLN pentamers demonstrated impaired hemodynamics, reduced adrenergic responsiveness, adverse myocardial remodeling, and reduced survival, indicating the relevance of PLN pentamers in myocardial stress adaptation (PMID: 36869774).

Objective: To evaluate the role of PLN and PLN pentamers in cardiac adaptation to myocardial infarction (MI).

Material and Methods: PLN knockout (KO) and wild-type (wt) mice were compared with strain-matched transgenic mice with (TgPLN) and without (TgAFA) the ability to form PLN pentamers. MI was induced *in vivo* by transient coronary artery occlusion for 60 min. Ca²⁺ kinetics (using Fura-2) and sarcomere length were measured in paced cardiomyocytes of the non-ischemic remote myocardium (RM). Mice underwent echocardiography before surgery and before sacrifice.

Expression and phosphorylation of Ca²⁺ regulatory proteins were determined by western blot.

Results:

24 hours after MI, the speed of cytosolic Ca²⁺ elimination was indistinguishable between wt, TgPLN and TgAFA mouse hearts in the RM, but more than doubled in KO compared to each of the other groups, both at baseline and after stimulation with 10⁻⁷ M isoproterenol (p<0.0001 for all comparisons). Cytosolic Ca²⁺ increase was only moderately faster in KO (p<0.05) and the height of the Ca²⁺ transients was unchanged. Importantly, TgPLN and TgAFA did not differ in any of these parameters, and only TgPLN responded well to isoproterenol (p<0.01). While pPLN-S16 is generally decreased in mouse hearts 24 hours after MI, it was 2.7-fold higher in the ischemic zone of TgAFA compared to TgPLN (p<0.001), indicating PLN inactivation. However, pPLN-S16 and expression of SERCA2a and SR Ca²⁺ release channels were unchanged between groups in the RM.

Conclusion:

PLN-deficiency counteracts suppressed cardiomyocyte Ca²⁺ cycling in the RM 24 hours post MI. In contrast to basal conditions, PLN pentamerization did not affect PLN-S16 phosphorylation nor cardiomyocyte calcium cycling in the RM.

P041

Guduchi Sattva, a Tinospora cardifolia based ayurvedic preparation causes thromboprophylaxis by inhibiting thrombin

A. G. Potnuri¹, L. Allakonda², A. Dharamvir Singh¹

¹All India Institute of Medical Sciences, Department of Pharmacology, New Delhi, India

²Regional Ayurveda Research Institute, Department of Pharmacology, Gwalior, India

Question: Direct thrombin inhibition is indicated for thrombo-prophylaxis in various cardiovascular and cerebrovascular conditions. It is advantageous by virtue of faster onset, quick reversal, lower bleeding events and fewer drug interactions. Classical ayurvedic texts indicates the Guduchi Sattva (GS) for cardiovascular conditions. As its role in thromboprophylaxis is largely unknown the current study aims to understand the effect of GS on coagulation profile and thromboprophylaxis and to understand the mechanism behind.

Methods: SD rats were orally administered with 200mg/kg of GS, once daily for a period of seven days. Post Treatment, PT, aPTT, Platelet Count, Bleeding Time and Capillary Clotting time were measured. Similarly, carotid artery thrombus was induced by FeCl₃ and the Carotid weight and Lumen occlusion were estimated. Further serum thrombin activity and thrombin induced fibrinogen polymerization assay were performed. Molecular docking studies were performed between Human Thrombin (4UFD. Resolution: 1.43 Å) and (+)-Magnoflorine (Pubchem ID: 73337).

Results: Treatment with GS delayed haemostasis by increased PT (1.5-fold), aPTT (1.5-fold), BT (2.98-fold) and CCT (3.1-fold) with unaltered PLT count (p=0.866). Similarly, there was a lesser Lumen occlusion and 2.1-fold smaller thrombus observed with treatment indicating significant thrombo-prophylaxis. Gu.Sat caused 2.2-fold scale down in Plasma thrombin activity and caused dose dependent decrease in thrombin induced fibrinogen polymerization indicating that it inhibits thrombin. Molecular docking studies revealed that (+)-Magnoflorine had a higher binding affinity (-4.5) with hydrogen bonding with critical residues such as Gly-219, CYS 220, ALA-190 and GLY-216 of the catalytic site.

Conclusion: GS inhibits thrombin and there by delays haemostasis with reduced lumen occlusion and thrombus weight making it a complimentary alternative for thrombo-prophylaxis in cerebro and cardiovascular conditions. Molecular docking studies revealed that the major phytoconstituent (+)-Magnoflorine interact with critical residues in the catalytic site of thrombin.

Figure Legends:

Fig 1: Effect of GS on coagulation profile and thrombus morphology

Fig 2: Effect of GS on thrombin activity and interaction between Human Thrombin and (+)-Magnoflorine

References:

1. <https://doi.org/10.1111/j.1538-7836.2010.04084.x>
2. <https://doi.org/10.4103/0974-8520.190697>
3. <https://DOI: 10.1038/srep44040>

Fig. 1

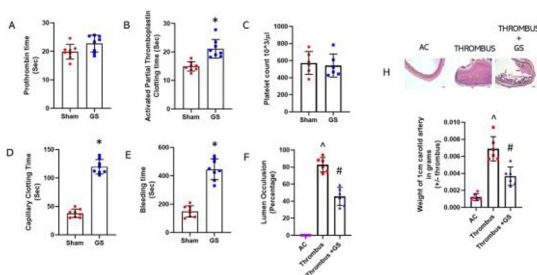
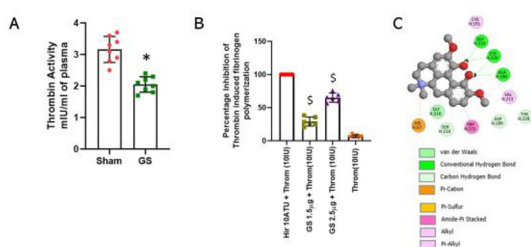


Fig. 2



P042

Development of a fluorescence-based *in vitro* assay for the measurement of SERCA2a activity in microsomal preparations

P. Gohla¹, J. Schmitt¹, F. Funk¹

¹Universitätsklinikum der Heinrich-Heine-Universität Düsseldorf, Institut für Pharmakologie, Düsseldorf, Germany

Introduction: SERCA2a is a key protein of cardiomyocyte calcium cycling, as it eliminates cytosolic calcium during diastole, thereby initiating cardiomyocyte relaxation. SERCA2a dysfunction can directly cause heart failure and down-regulation of SERCA2a is regularly observed in failing hearts. Currently available assays to measure SERCA2a activity either use radioactively labelled substrates or lack specificity in complex samples.

Objective: Our aim was to develop a non-radioactive fluorescence-based method for measuring ATP- and calcium-dependent SERCA2a activity.

Methods: Microsomes enriched for sarcoplasmic reticulum were isolated from mouse cardiac tissue by differential centrifugation. Different isolation methods were evaluated for SERCA2a enrichment and phospholamban phosphorylation by western blot. The fluorescent calcium indicator Calcium Green-5N (CaG5N, $K_d = 14 \mu\text{M}$, Ex 506 nm / Em 532 nm) was used to quantitatively monitor the rate of calcium uptake into microsomes pre-loaded with oxalate. Concentrations of free calcium in the assay system were measured using a calcium-selective electrode. SERCA2a activity was determined as the difference in calcium transport rates $\pm 1 \mu\text{M}$ thapsigargin. Genetically engineered mouse lines with known differences in SERCA2a activity were used to evaluate the suitability of the method.

Results: Different microsomal preparation protocols showed variable SERCA2a enrichment and phospholamban phosphorylation states. The measurements consistently showed calcium- and ATP-dependent activity that could be blocked by thapsigargin. Importantly, the concentrations of free calcium measured using a calcium-selective electrode differed drastically from the nominal calcium concentrations. These differences were attributed to calcium precipitated by residual oxalate of pre-loaded microsomes, an underrecognized problem that may affect every oxalate-dependent assay method. At calcium concentrations below K_m , SERCA2a activity was significantly increased in mice deficient for phospholamban or phospholamban pentamers. In contrast, these differences were abolished at calcium concentrations that exceeded V_{max} .

Conclusion: Here, we present a non-radioactive fluorescence-based method for measuring calcium- and ATP-dependent SERCA2a activity in microsomal fractions of heart tissue. Furthermore, the data demonstrate the need to measure free calcium ion concentrations directly using ion-selective electrodes in oxalate-based assays.

P043

Repurposing mesna (Uromitexan®) for cardiometabolic protection

H. Marte¹, C. Mann¹, C. van Alst¹, M. Otten¹, D. Dobrev¹, F. Bruns¹, A. Fender¹

¹University Hospital Essen, Institute of Pharmacology, Essen, Germany

Objective: Obesity-associated lipoperoxidation generates reactive aldehydes like 4-hydroxy-2-nonenal (4-HNE) and acrolein, which modify proteins critical for metabolic regulation in the heart. Mesna is an acrolein scavenger in clinical use to prevent acute urothelial injury during alkylating chemotherapy. We examined whether mesna can also protect against cardiometabolic stress. **Methods:** Human primary cardiac fibroblasts (hCF) and mouse atrial cardiomyocytes (HL-1 cells) were exposed to high glucose/palmitate (HG/P) for 48h; mesna was added after 24h. Plasma and atrial myocardium from obese and lean patients undergoing cardiac surgery were incubated *ex vivo* with mesna or PBS vehicle. C57BL6/J mice were fed a Western diet (WD) or chow for 10 weeks. Mesna or vehicle were applied *i.p.* from week 8, or *ex vivo* to myocardial biopsies and plasma. Regulators and products of cell injury, oxidative stress and metabolism were quantified by qPCR, immunoblotting, ELISA; mouse blood was profiled using the IDEXX blood chemistry analyzer. **Results:** HG/P increased the formation of reactive aldehydes and advanced oxidation protein products (AOPP) in hCF and HL-1 cells, induced cell injury and modified key proteins regulating cellular metabolism and redox control. The effects of mesna on these parameters were highly variable depending on cell-type and donor, but mesna consistently lowered AOPP formation, normalized superoxide dismutase 2 expression and restored AMPKa phosphorylation, thus activity. Myocardium and plasma from obese patients and WD-fed mice contained more 4-HNE and acrolein than samples from lean controls. These reactive aldehydes were decreased by mesna *ex vivo*. Mesna applied *in vivo* over 2 weeks did not significantly modify WD-induced increases in body or organ (adipose tissue, heart, spleen, liver) weights, but did reduce plasma glucose. No significant differences were noted between the groups in terms of blood cell counts and parameters, except for a modest reduction in reticulocytes in WD-fed mice supplemented with mesna. **Conclusion:** Our data suggest that mesna can acutely lower aldehyde burden and indices of cardiometabolic stress. Ongoing *in vivo* studies will verify whether mesna is a suitable repurposing candidate for cardiometabolic protection.

P044

Contractile effects of myosin modulators versus beta-adrenergic agonist isoprenaline in engineered human myocardium

G. M. Dittich¹, W. H. Zimmermann¹

¹University Medical Center Göttingen, Pharmacology and Toxicology, Göttingen, Germany

New Approach Methodologies (NAMs), such as engineered human myocardium (EHM), evolve as important tools for the assessment of wanted and unwanted drug effects. EHM are produced from induced pluripotent stem cell (iPSC)-derived cardiomyocytes and stromal cells in a collagen hydrogel. Culture in multi-well platforms (myrPlate) allows for longitudinal, non-destructive functional assessments (myrImager) of contractility.

Here, we investigated the effects of myosin modulators omecamtiv mecarbide (OM) and mavacamten (MV) as well as the beta-adrenoceptor agonist isoprenaline (ISO) on EHM contractility at 3 concentrations (0.1, 1, 10 μM) over 1 hour using video-optic myrImager recordings. EHM were cultured and maintained in serum-free culture medium at isotropically submaximal effective Ca^{2+} concentrations (1.8 mM). Spontaneous beating frequency showed concentration dependent increase in OM (+46%/+70%/+78%) and ISO (+52%/+132%/+200%) at 0.1/1/10 μM concentrations (n=16 per group). Spontaneous beating amplitude did not show apparent change in OM treated EHM up to 1 μM but decreased at the highest test concentration of 10 μM (-70%). Isoprenaline led to an acute increase of beating amplitude measured within 1 minute after exposure at 1 μM and 10 μM concentrations (+9%/+15%). MV treated EHM showed an increased spontaneous beating frequency (+36%/+68% at 0.1 μM /1 μM) and decreased beating amplitude (-15%/-86%) at 0.1/1 μM with a complete loss of spontaneous contractility at 10 μM after 30 minutes exposure. After exposure to the maximum drug concentration of 10 μM , all EHM were cultured in standard medium for 24 hours and beating recovery was measured. While OM and ISO treated EHM showed normal contractility after 24 hours, MV exposed EHM did not recover spontaneous contractility.

Our data demonstrate robust time- and concentration dependent response of EHM in response to OM, ISO or MV. OM and MV demonstrated therapeutically unwanted depression of contractility at $\geq 1/10 \mu\text{M}$, respectively, which was irreversible in MV treated EHM, pointing to narrow therapeutic window and toxicity in the latter. The provided example demonstrates the use of longitudinal EHM cultures in safety assessments of contractility modulators.

P045

Regulation of spatially heterogeneous gene expression in diseased cells and tissues

D. Papenheim¹, S. Wirth¹, L. Jurida¹, M. Kracht¹

¹Justus Liebig University Gießen, Rudolf-Buchheim-Institut für Pharmakologie, Gießen, Germany

Question

In both homeostatic and pathological conditions cells of identical origin can acquire distinct functional cell states. These cell states depend, at least in part, on tissue location and contribute to quantitative and qualitative changes of cell responses in diverse tissues. A prominent example are cells in diseased tissues which exhibit a very heterogeneous mRNA expression; however, the understanding of the mechanisms behind this phenomenon as well as its functional relevance are unclear. We analyzed two different disease models at single cell level regarding the heterogeneity of gene expression patterns. These two models

encompass whole heart tissues from rats with progressive right ventricular failure (RHF) and human lung adenocarcinoma (LUAD) tissues.

Methods and Results

Gene expression was systematically assessed by smRNA-FISH to identify cells with high co-expression of constitutive and disease-associated genes and their spatial organization. The results indicate that chronic RHF caused by pulmonary artery banding results in the activation of distinct subpopulations of cardiomyocytes and fibroblasts, which are scattered throughout the heart. These subpopulations often seem to be located in close vicinity to each other, suggesting the existence of unique and novel cardiac niches in RHF. Likewise, human LUAD tissues from patients with high serum levels of the tumor marker glycodein (> 10 ng/mL) exhibited areas in which glycodein mRNA expression was strongly increased. Additionally, the mRNA levels of different NF- κ B pathway components and NF- κ B target genes, both of which mark areas of inflammatory cell activation, were differentially regulated across LUAD tissue sections. Comparative analysis of the mRNA expression of glycodein with that of NF- κ B components revealed patterns of colocalisation and as well as separate areas of gene expression.

Conclusion

In conclusion, in two unrelated disease models, relevant to right heart failure or lung cancer, respectively, we identified patterns of heterogenous gene expression representing different cell states. These initial results support the hypothesis of the existence of specialized tissue niches and for a basis for further exploring the role of such niches as key drivers of the disease phenotypes.

P046

Multi-omic profiling reveals cardiac microenvironments and cellular diversity in iPSC-derived cardiac bioengineered heart muscle organoids
J. Wang¹, A. Sikandar¹, A. Nedunchezian¹, I. Ullah¹, L. Priesmeier¹, T. Meyer¹, B. Berečić¹, W. H. Zimmermann¹, O. Bergmann¹
¹Georg August University of Göttingen, Göttingen, Germany

Question:

Human induced pluripotent stem cell (iPSC)-derived bioengineered heart muscle (BHM) organoids hold great promise as platforms for therapeutic evaluation and drug screening. However, their application has been limited by undefined cellular composition and variable functionality. This study aims to systematically characterize the differentiation trajectory, cellular architecture, and functional maturity of BHM organoids.

Methods:

We integrated temporal bulk RNA sequencing with high-resolution spatial transcriptomic analyses to map the developmental and structural features of BHM organoids. Functional assays were performed to assess contractile activity. Preliminary hypoxia experiments were conducted to evaluate the organoids' potential in modeling cardiac pathology.

Results:

Integrated transcriptomic analyses revealed that BHM organoids develop a heart-like structure, with distinct spatial organization of cardiomyocytes, fibroblasts, endothelial cells, epicardial cells, and other supporting cell types. Functional assays demonstrated that the organoids possess robust and rhythmic contractile activity, indicative of physiological relevance. Spatial transcriptomics further mapped the organized arrangement of various cell types within in vivo-like microenvironments. Hypoxia experiments underscored the suitability of BHM organoids for studies of cardiac mechanisms and drug testing.

Conclusions:

Our findings establish iPSC-derived BHM organoids as a versatile and functionally competent platform for evaluating therapeutic interventions, modeling cardiac pathology, and studying interactions among diverse cardiac cell types under perturbation.

P047

Role and regulation of the Raf kinase inhibitor protein under ischemic conditions

C. Schanbacher^{1,2}, K. Lorenz^{1,2}

¹Julius Maximilian University of Würzburg, Institute of Pharmacology and Toxicology, Würzburg, Germany

²Leibniz-Institut für Analytische Wissenschaften - ISAS - e.V., Dortmund, Germany

Introduction and aim: The Raf kinase inhibitor protein (RKIP) was found to protect from the development of pressure overload-induced heart failure. Upregulation of RKIP under these conditions suggests that this might be a protective endogenous feedback mechanism of the heart. However, we could also show that RKIP protein levels are reduced under ischemic conditions, i.e. in patients with ischemic cardiomyopathy, in mice after induction of myocardial infarction (MI) and in cardiomyocytes using an ischemic buffer. Thus, the aim of

this study was to investigate if RKIP overexpression may also be able to prevent heart failure under ischemic conditions and to analyze the mechanisms leading to reduced RKIP levels.

Methods and results: To study the effects of RKIP overexpression in ischemia, we induced MI by ligation of the left anterior descending coronary artery in mice with cardiac specific overexpression of RKIP (RKIP-tg) and wild-type controls. As observed in pressure overload induced heart failure, RKIP-tg mice showed an improved cardiac function assessed by echocardiography and survival after MI compared to control mice underscoring the protective role of RKIP in the heart. To identify the mechanisms responsible for RKIP reduction in response to ischemia, cardiomyocytes were treated with an ischemic buffer and different inhibitors of protein degradation mechanisms, e.g. 3-methyladenine for autophagy or clasto-lactacytin β -lactone for the ubiquitin proteasome system (UPS), and RKIP protein levels were analyzed by western blot. These experiments revealed autophagy and the UPS as central mechanisms for the downregulation of RKIP under ischemic conditions. In addition, we searched for modifications in RKIP, that make RKIP more susceptible to degradation. Using purified proteins and autoradiography, we could identify that the 90 kDa-ribosomal S6-kinase (RSK) is able to phosphorylate RKIP. In cardiomyocytes, inhibition of RSK also reduced ischemia-induced RKIP degradation.

Conclusion: RKIP is differentially regulated under different stimuli as for example ischemia or pressure-overload. Our study further shows that overexpression of RKIP improves the outcome in various disease models. The herein gained insights in regulatory mechanisms of RKIP may help to define new therapeutic targeting strategies in heart failure.

P048

Cell Migration Inducing Protein (CEMIP) mitigates adverse cardiac remodeling post I/R by controlling cardiac fibroblast activation

R. Schneckmann¹, V. Darakchieva¹, M. Balan², T. Hube¹, A. Zardkhoui¹, K. Bottermann¹, S. Gorresen¹, J. W. Fischer¹

¹Heinrich Heine University Düsseldorf, Institute for Pharmacology, Düsseldorf, Germany

²Heinrich Heine University Düsseldorf, Core Unit Bioinformatics (CUBI), Düsseldorf, Germany

Question: Fibroblast activation is a critical determinant for scar formation after myocardial infarction (MI). However, chronic myofibroblast survival and activity can result in adverse cardiac remodeling characterized by the excessive deposition of extracellular matrix (ECM) in the heart. CEMIP (Cell Migration Inducing Protein) is a hyaluronidase which is highly expressed in cardiac fibroblasts. This study aims to unveil CEMIPs function in the healing and remodeling process post MI using a mouse model of cardiac ischemia/reperfusion (I/R) injury.

Methods: 12 week (w) old C57BL/6J mice were used to determine Cemip expression in left ventricles after cardiac I/R injury in a closed chest model. Six to 8w-old CAGG Cre-ERTM^{+/+} Cemip^{lox/lox} and littermate control mice (WT) were injected with tamoxifen to induce global Cemip deletion (Cemip-KO) followed by induction of I/R. Flow cytometric cell sorting was used for KO validation. Echocardiography was used to examine cardiac function. Gomori trichrome and Picrosirius red staining were performed to assess scar size and collagen deposition, respectively. Periostin deposition and myofibroblast abundance were analyzed at 21 days post I/R. Flow cytometry was used to analyze cardiac cell composition and apoptosis. Proliferation was assessed via Ki67 immunofluorescence stainings in cardiac sections. Single cell RNA sequencing (scRNAseq) was used to elucidate effects of CEMIP deletion on the fibroblast and immune cell phenotype.

Results: Cemip mRNA expression was significantly upregulated in left ventricles peaking at 72 hours post I/R. While ejection fraction was decreased, end diastolic and end systolic volumes were significantly increased in Cemip-KO mice. Moreover, Cemip-KO hearts exhibited increased scar size, ECM deposition and chronic myofibroblast abundance in the scar. Mechanistically, scRNA seq revealed a pro-fibrotic gene signature, regulation of integrin-mediated ECM adhesion and TGF β -pathway activity in Cemip-KO (myo)fibroblasts. Furthermore, a critical role for CEMIP in the macrophage-fibroblast-crosstalk is suggested by the results of scRNA seq.

Conclusions: Our data suggest that CEMIP contributes to post-infarct healing by regulating cardiac fibroblast survival in the post-infarct environment while limiting excessive activation and fibroblast to myofibroblast-transition during scar formation. Thus, CEMIP may be considered as a novel target in post MI healing.

P049

Cell Migration Inducing Protein (Cemip) is regulator of fibroblast-to-myofibroblast transition

V. Darakchieva¹

¹Heinrich-Heine-University, University Hospital Düsseldorf, Institute for Pharmacology, Düsseldorf, Germany

Introduction

Fibroblast plasticity is a key determinant of cardiac remodeling and healing after myocardial infarction (MI). Following MI, cardiac fibroblasts (cFs) undergo a phenotypic transition into activated myofibroblasts critical for wound healing and scar formation. Persistent activation, however, promotes cardiac fibrosis through excessive extracellular matrix (ECM) deposition leading to impaired cardiac function. In this context, Cell Migration Inducing Protein (CEMIP) may represent a

potential key player given its high expression in cFs and involvement in hyaluronan depolymerization.

Objectives

Recently, we have demonstrated that *Cemip* deletion contributes to cardiac dysfunction following ischemia/reperfusion injury in mice. In this study, we aim to investigate CEMIP's influence on the phenotypic transition of cFs as well as the underlying mechanisms using silencing (si)RNA mediated *Cemip* knockdown *ex vivo*.

Materials and methods

cFs from 12–16 weeks old C57BL/6J mice were isolated and transfected with siRNA targeting *Cemip*. Morphological changes as well as activation marker expression were analyzed. Fibroblast proliferation was assessed by flow cytometric analysis using BrdU labeling as validated by Ki67 cell staining. Functional assays were performed to evaluate cell migration as well as cell contraction and morphology in a 3D collagen matrix. Focal adhesion formation was examined via Vinculin immunostaining while integrin gene expression was analyzed by qPCR.

Results

Cemip-KO promoted myofibroblast transition and inhibited fibroblast proliferation. In a 3D matrix, the cells exhibited hypercontractility and an increased formation of dendritic-like network extensions. In correlation with the distinct morphology visualized in 2D and 3D, we detected reduced *Stathmin 1* expression in the absence of *Cemip* suggesting altered microtubule dynamics. Consistent with the myofibroblast-like and "dendritic phenotype", increased vinculin expression was revealed indicating enhanced focal adhesion formation.

Conclusions

Our results suggest that CEMIP is a critical regulator of fibroblast-to-myofibroblast transition. Alterations in the cF phenotype were not only demonstrated in the classical 2D model, but also observed in 3D, supporting a role of CEMIP for cell-ECM interactions in tissues *in vivo*. Our findings highlight CEMIP's potential as a target molecule for cardiac fibroblast activation and ECM remodeling in the context of scar formation post MI.

P050

Analysis of the Efficacy and Safety of SGLT2 inhibitors (SGLTi) in diabetes mellitus and heart failure: analysis of real-world data (THIN) from the UK
N. Heß^{1,2}, S. A. Gómez Ochoa^{1,2,3}, C. Eteve-Pitsaer⁴, R. T. Levinson^{2,3}, M. Freichel^{1,2}

¹Heidelberg University, Institute of Pharmacology, Heidelberg, Germany

²German Center for Cardiovascular Research (DZHK), Heidelberg, Germany

³Heidelberg University Hospital, Department of Internal Medicine II, Heidelberg, Germany

⁴Cegedim Health Data, Boulogne-Billancourt, France

Sodium-glucose co-transporter-2 (SGLT2) inhibitors have demonstrated strong cardioprotective and renoprotective effects in multiple large-scale randomized controlled trials (RCTs) among patients with type 2 diabetes mellitus (T2DM) and/or heart failure. However, their long-term effectiveness in routine clinical practice remains insufficiently understood. We conducted a retrospective study using "The Health Improvement Network" (THIN), a large standardised European database network of longitudinal primary care electronic health records. We extracted data from 2003–2020 from the UK. Adult patients (≥ 20 years) with T2DM with complete data were classified as SGLT2 inhibitor initiators ($n=11287$) or non-initiators ($n=110935$). After applying exclusion criteria (including pregnancy, pre-existing cardiovascular disease (CVD), and malignant tumors before T2DM, among others, we conducted 1:3 propensity score matching exactly on sex, and matching on age at T2DM in 5-year bands, year of T2D in 2-year bands, insulin, metformin, beta-blockers, ACE inhibitors and angiotensin receptor blockers. Within the matched population ($n=11287$ initiators, $n=45148$ non-initiators) a time-to-event analysis was performed using a time-varying Cox proportional hazard model assessing the effect of SGLT2 initiation on outcomes in matched strata. Individuals were censored at the date of their last record, or January 1, 2020. The primary outcomes were all-cause mortality (documented by codes indicating death, autopsy, or postmortem preparation) and incidence of a composite CVD endpoint consisting of stroke, myocardial infarction, and heart failure. SGLT2 inhibitor initiation was associated with significantly lower risk of all-cause mortality (HR [95% CI]=0.52 [0.40, 0.67], $p=1.04e-06$). There was no statistically significant association of SGLT2 with the CVD endpoint (HR [95% CI]=0.89 [0.70, 1.15], $p=0.37$), although after adjusting for year of diabetes, the association became significant (HR [95% CI]=0.71 [0.55, 0.92], $p=0.01$). These findings provide real-world evidence of the long-term benefit of SGLT2 inhibitors in patients with T2DM and support their wider integration into routine diabetes care. While we were unable to detect the known cardioprotective effects in initial models, we propose this is due to the heterogeneity of real-world data, as further adjustment, even after matching, allowed us to see an effect. A replication analysis using a German dataset is currently underway.

P051

Towards improved human in vitro models: Advanced maturation of human induced pluripotent stem cell-derived cardiomyocytes for drug testing
M. Schubert¹, W. Li¹, X. Luo¹, M. Hasse¹, A. Strano¹, O. Gamm¹, S. Arun¹, K. Guan¹

¹TU Dresden University of Technology, Institute of Pharmacology and Toxicology, Dresden, Germany

Human induced pluripotent stem cell-derived cardiomyocytes (iPSC-CMs) provide an unlimited source of patient-specific human CMs for disease modeling and drug testing. However, their immature phenotype remains a major limitation, as it alters responses to pathophysiological stimuli or cardioactive drugs compared with adult CMs.

In this study, we established an approach to enhance iPSC-CM maturation by integrating fatty acid-supplemented maturation medium (MM) with nanopatterning (NP) and electrostimulation (ES). Using this model, we investigated the effect of maturation on drug response of iPSC-CMs (Li et al. 2025).

We compared iPSC-CMs cultured in widely used B27 medium (B27) with those matured in MM, MM+NP, and MM+NP+ES. Progressive maturation, most pronounced in iPSC-CMs under MM+NP+ES, was evidenced by increased cell volume, cardiac troponin T expression, and polyploidy, as well as enhanced connexin 43 membrane localization. Action potential (AP) measurements revealed gradual improvement of electrophysiological properties with MM, NP, and ES, including a lower resting membrane potential, faster AP upstroke velocity, and increased AP amplitude. A "notch-and-dome" AP morphology, characteristic of adult CMs, was observed in 43% of iPSC-CMs matured under MM+NP+ES but not in other groups. Transient outward potassium (I_{to}), sodium (I_{Na}), and hERG (I_{Kr}) currents were markedly increased, while L-type calcium current (I_{Ca-L}) was reduced in iPSC-CMs under MM+NP+ES. Consistently, expression of genes contributing to I_{Na} (SCN5A adult/fetal isoform ratio, SCN1B), I_{to} (e.g. KCNA7, KCND2) and I_{Kr} (KCNH2) was upregulated, whereas levels of those involved in I_{Ca-L} (e.g. CACNA1C, CACNA1D) were downregulated under MM+NP+ES. Multi-electrode array measurements revealed an enhanced chronotropic response to β -adrenergic stimulation and hERG blocker (E-4031)-induced prolongation of field potential duration in iPSC-CMs matured in MM, MM+NP, and MM+NP+ES compared with B27. Interestingly, verapamil caused beating arrest, indicative of potential cardiotoxicity, in less mature iPSC-CMs (B27, MM, MM+NP) but not cells matured under MM+NP+ES.

Our findings demonstrate that integrating MM, NP, and ES promotes advanced iPSC-CM maturation and profoundly affects their pharmacological responses, suggesting that enhanced maturation may improve the predictive value of iPSC-CMs in drug screening.

Reference

Li, W. et al. *Nat. Commun.* **2025**;16(1):2785.

P052

Targeting ERK Dimerization to Prevent Cardiac Hypertrophy in a Noonan Syndrome Mouse Model

M. Hedtstück¹, C. Peddinghaus¹, C. Schanbacher², K. Lorenz^{1,2}

¹ISAS-Dortmund, Cardiovascular Pharmacology, Bochum, Germany

²Julius Maximilian University of Würzburg, Institute of Pharmacology and Toxicology, Würzburg, Germany

Noonan Syndrome (NoS) is a rare genetic disorder caused by mutations in the Raf/MEK/ERK1/2 pathway, which plays a central role in cellular growth and differentiation. It is characterized amongst others by short stature, craniofacial anomalies, and congenital heart defects, which are associated with heart failure and death. Inhibition of this cascade by MEK-inhibitors showed beneficial effects, but their long-term use is limited by cardiotoxicity and resistance development.

To overcome these limitations, we investigated the therapeutic potential of EDI, a peptide inhibitor that selectively blocks ERK1/2 dimerization. ERK dimerization has been linked to pathological nuclear signaling by phosphorylation at threonine 188, a modification that enhances maladaptive nuclear signaling and drives cardiac hypertrophy. EDI prevents this specific phosphorylation while preserving the cytosolic anti-apoptotic functions of ERK1/2.

To investigate the therapeutic potential of EDI in NoS, we used knock-in mice expressing the NoS-associated Raf mutant L613V (RafL613V) and induced chronic left ventricular pressure overload by transverse aortic constriction (TAC). Mice were treated with an adeno-associated virus serotype 9 mediated gene transfer of EDI (AAV9-EDI) two weeks prior to TAC, allowing targeted cardiac-specific expression of EDI. We also used a transgenic model with ubiquitous EDI expression to study systemic effects. In addition to these experiments, both approaches were tested in long-term survival groups without TAC to evaluate the broader impact of EDI under baseline conditions. Echocardiography and histological analyses revealed that AAV9-EDI treatment reduced TAC-induced hypertrophic cardiomyopathy in both wild-type and RafL613V mice. Left ventricular wall thickness and systolic function of the heart almost normalized in AAV9-EDI treated RafL613V and WT mice, while diastolic function significantly improved compared to controls. Organ weight measurements and Western blot analyses further confirmed reduced cardiac hypertrophy and suppressed nuclear ERK1/2 signaling in EDI-treated groups.

These results suggest that selective inhibition of nuclear ERK1/2 signaling is a promising targeting strategy to treat pathological cardiac hypertrophy in NoS.

However, further studies are needed to assess EDI's safety and efficacy in NoS. Further studies are ongoing to expand the sample size, evaluate long-term survival, and analyze ERK1/2 signaling in more detail.

P053

Raman spectroscopy in combination with AP-MALDI MSI for cardiac tissue analyses of a Fabry disease mouse model

J. Dierks¹, E. Brockmann², T. Bocklitz^{1,3}, P. Arias-Loza⁴, P. Nordbeck⁴, K. Lorenz^{1,5}, S. Heiles², E. Tolstik¹

¹Leibniz-Institut für Analytische Wissenschaften - ISAS - e.V., Translational Research, Dortmund, Germany

²Leibniz-Institut für Analytische Wissenschaften - ISAS - e.V., Lipidomics, Dortmund, Germany

³Friedrich Schiller University Jena and Abbe Center of Photonics (ACP), Institute of Physical Chemistry, Jena, Germany

⁴University Hospital Würzburg, Medical Clinic and Polyclinic, Würzburg, Germany

⁵Julius Maximilian University of Würzburg, Institute of Pharmacology and Toxicology, Würzburg, Germany

Here, we combined Raman micro-spectroscopy (2 µm pixel size) with atmospheric-pressure MALDI mass spectrometry imaging (AP-MALDI MSI, 5 µm pixel size) as a label-free approaches to investigate the chemical composition of biological tissue at cellular resolution [1, 2].

The study was conducted using a Fabry disease (FD) mouse model. FD is a lysosomal storage disorder caused by deficient α -galactosidase A (α -Gal A) activity, leading to the accumulation of globotriaosylceramides (Gb3) that results in a progressive cardiac dysfunction. Using Raman imaging, we identified distinct spectral features corresponding to nucleic acids, proteins, collagen, and lipids, enabling contextualization of structural and biochemical alterations across three genotypes. The GLAWT mice served as controls, the GLAKO mice, lacking α -Gal A, modeled early/asymptomatic FD with moderate Gb3 accumulation, and the G3Stg/GLAKO mice, combining GLAKO with human Gb3 synthase overexpression, modeled symptomatic FD [3,4,5].

We designed an automated co-localization algorithm that precisely aligned Raman and MSI data from the same tissue section, enabling multimodal overlays at micrometre resolution [6]. The combined analysis resolved heterogeneous Gb3 accumulation and revealed distinct lipid species in cardiac tissue of G3Stg/GLAKO compared to GLAKO and wild-type controls.

With the help of the Raman - AP-MALDI MSI data integration, we demonstrated the potential of hyperspectral multimodal imaging to elucidate the molecular distribution of FD-affected heart tissue. The approach not only enhances our understanding of disease-associated lipid heterogeneity but will also support the generation of pathomechanistic insights in further disease processes.

References:

- [1] Tolstik et al. Trends Biotechnol. 42(2), 2024
- [2] Luh et al. Anal. Chem. 96 (16) 2024
- [3] Ohshima et al. Proc Natl Acad Sci USA, 94(6), 1997
- [4] Taguchi et al. Biochem J. 456(3), 2013
- [5] Pieroni et al. J. Am. Coll. Cardiol. 77 (7), 2021
- [6] Bocklitz et al. Anal Bioanal Chem. 407, 2015

Computational Toxicology

P054

Read-Across Prediction of the toxicity of Active Ingredients and Residues in Plant Protection Products using Metabolic Similarity

S. Enoch¹, Z. Hasarova¹, M. Cronin¹, K. Bridgwood², S. Rao³, M. Frenicks⁴

¹Liverpool John Moores University, Liverpool, United Kingdom

²Syngenta, Bracknell, United Kingdom

³Gowan Company, Yuma, AZ, United States

⁴BASF SE, Limburgerhof, Germany

Crop protection products are used for prevention of crop infestation by disease and pests. The active ingredient and its residues must not cause direct or indirect pernicious impact on human health, particularly relating to genotoxicity. Unadopted European Food Safety Authority (EFSA) guidance proposes a workflow to estimate the genotoxic potential of residues of the active ingredient. This guidance suggests predicting genotoxicity of substances without sufficient available data by read-across. A key aspect to identify analogues for read-across is metabolic similarity, although its definition is very difficult.

Datasets have been compiled consisting of active ingredients and their residues for several pesticide chemical classes and their residues. These datasets consist of structural information and corresponding ADME and toxicity study results. Importantly, some chemicals in these datasets have an incomplete set of toxicity data – enabling data-gaps to be filled via read-across. These data have been

extracted from the EFSA Draft Assessment Report/Renewal Assessment Reports (DARs/RARs). The information in these DAR/RAR documents was used to define *in-silico* profiling schemes.

Read-across case studies were undertaken. These case studies developed initial groupings based on the defined metabolic transformations within the profiling scheme, followed by subsequent *in silico* definition of the domain of the category. In addition, these case studies also demonstrated how this information could be used to increase confidence in the read-across predictions.

This work has demonstrated how a combination of metabolic similarity, chemistry profiling and physical-chemistry properties can be used to predict the toxicity of pesticide residues via read-across. The method presented represents a robust and repeatable approach to such read-across predictions, with the potential to reduce unnecessary testing.

The research presented in this project is funded by CropLife Europe.

P055

Advancing risk assessment with TXG-MAPr: Toxicogenomic profiling of neonicotinoids and azoles in rat liver and kidney

I. Suciu¹, S. Kießig¹, V. Raolji¹, R. Puts¹, A. Kadic¹, H. Sprenger², D. Lichtenstein², G. Callegaro³, B. van de Water³, A. Braeuning², P. Marx-Stötinger¹

¹Bundesinstitut für Risikobewertung (BfR), Pesticides Safety, Berlin, Germany

²Bundesinstitut für Risikobewertung (BfR), Chemical and Product Safety, Berlin, Germany

³University of Leiden, Leiden Academic Centre for Drug Research (LACDR), Leiden, Netherlands

In modern toxicology, new approach methodologies (NAMs) are being developed and validated to complement - and eventually replace - animal testing, which remains the gold standard for regulatory risk assessment. Among these NAMs, toxicogenomics (TGx) offers rich insights into a compound's mode of action. However, its integration into risk assessment frameworks has lagged behind that of *in vitro* and *in silico* methods, primarily due to challenges in standardization and data interpretation - critical factors for regulatory acceptance.

The rat liver and kidney TXG-MAPr are two user-friendly bioinformatics NAMs that apply gene co-expression network analysis to map transcriptomic data onto organ-relevant biological response modules. Trained on a broad set of toxicants, the MAPrs enable both qualitative and quantitative interpretation of transcriptomic changes, providing a standardized approach for risk assessment.

In this study, we performed targeted RNA sequencing (TempO-Seq) on archived liver and kidney tissues from 28-day repeat-dose toxicity studies in rats, conducted with neonicotinoids (thiacloprid, clothianidine) and azoles (tebuconazole, imazalil). Gene expression data were analyzed using the R-Omics Data Analysis Framework (R-ODAF), and the resulting statistical outputs - further evaluated with the TXG-MAPr tools. Each compound was tested at five dose levels to enable dose-response modeling and the determination of transcriptomics-based points of departure (PoDs).

To assess variability in the data generation and processing steps prior to TXG-MAPr analysis, we compared rat liver data from negative control samples obtained by RNA-Seq and TempO-Seq. Furthermore, we included independent isolates of different chunks from the same control tissue samples for comparison. In a future phase of the project, *in vitro* data will be generated using primary human hepatocytes (PHH) and human renal proximal tubule epithelial cells (RPTEC), exposed to the four compounds at seven different subtoxic concentrations. These data will be integrated with physiologically-based pharmacokinetic (PBPK) modeling to facilitate *in vitro-in vivo* comparisons. Finally, this case study will contribute to the development of a Transcriptomics Interpretation Framework (TIF) in collaboration with EFSA, as well as EMA, ECHA, and OECD stakeholders, advancing the regulatory acceptance of TGx-based approaches.

P056

Agent-Driven knowledge system for Adverse Outcome Pathway (AOP) development in Chemical Risk Assessment

S. Kumar^{1,2}, S. Sharma², D. Deepika^{1,2}, V. Kumar^{1,2}

¹Bundesinstitut für Risikobewertung (BfR), Berlin, Germany

²IISPV, Hospital Universitari Sant Joan de Reus, Tarragona, Spain

The Adverse Outcome Pathway (AOP) framework has emerged as a key paradigm in chemical risk assessment, providing mechanistic linkages between molecular initiating events and adverse outcomes across different levels of biological organization. However, traditional AOP development remains resource-intensive, often requiring years of manual curation and expert coordination and extensive literature review. A significant portion of AOP development efforts is spent on curating knowledge from multiple sources and evaluating the relevance of collected evidence supporting specific biological hypotheses. Recent advances in agent-driven systems that integrate large language models (LLMs) with diverse knowledge sources provide transformative opportunities to automate AOP hypothesis curation while maintaining human oversight for refinement and validation.

Our agent-based system employs a multi-agent architecture to orchestrate complex knowledge extraction tasks. The system leverages specialized agents for literature mining, utilizing the in-house developed S2CIE system to perform real-time queries across large knowledge bases such as PubMed. Additional curated datasources, such as AOP-Wiki, Comparative Toxicogenomics Database

(CTD), KEGG, Reactome, Gene Ontology, STRING-DB, PubChem, and ToxCast, are seamlessly integrated to provide comprehensive biological context. Following a ReAct (Reasoning and Acting) architecture, the environment provides specialized tools enabling agents to perform targeted actions, store intermediate reasoning steps in a structured memory, and systematically derive hypotheses to address gaps in existing AOPs (refinement) or develop new AOPs. Researchers serve as top-level orchestrators in this human-in-the-loop framework, guiding workflows and providing critical feedback to ensure scientific rigor and domain relevance.

This innovative approach not only supports toxicologists and regulatory scientists by streamlining evidence synthesis but also democratizes access for non-experts while significantly accelerating AOP development timelines. By automating labor-intensive curation tasks while preserving human expertise for oversight and interpretation, our system addresses a critical bottleneck in next-generation risk assessment methodologies.

Disease models, drug development

P058

A defined low-fermentative diet induces robust and uniform immune responses in rodent models of autoinflammatory disease

J. Gotthardt¹, M. Martorelli¹, M. Dengler¹, K. Eisel¹, K. Sauter¹, M. Burnet¹
¹Synovo, Pharmacology, QM, Tübingen, Germany

Introduction

Robust, reliable *in vivo* models are essential in preclinical drug development. However, even gold standard models can suffer from high variation and non-responders, necessitating larger group sizes.

In the past decades, the effect of dietary fiber on gut microbial health and diversity has been established. Diet, particularly fiber intake, plays a key role in immune balance via gut microbial metabolites like short-chain fatty acids (SCFAs). In turn, a low-fiber (LF) diet, and a resulting lack of SCFAs, is a risk factor for developing metabolic syndrome and chronic-inflammatory diseases like colitis and rheumatoid arthritis.

We hypothesized that diet influences *in vivo* models of inflammatory disease, with LF diets enhancing autoimmune responses. To test this, we compared high-fiber chow with a LF diet in two models of autoimmune disease: collagen-induced arthritis, CIA and experimental autoimmune encephalomyelitis, EAE.

Methods

We compared the effects of normal chow (high-fiber) vs. a LF, low-fermentative diet ("AIN93M") on arthritis pathology in DBA1/J mice (CIA *model*) and CNS pathology in C57BL/6 mice (EAE *model*). Mice received AIN93M diet for 14 days before induction or normal chow throughout.

Results

EAE:

The AIN93M diet increased incidence of symptoms to 100 % (vs. 75 % for high-fibre chow), with corresponding changes in CNS histology and inflammatory markers, but improved uniformity and without increased severity or burden.

CIA:

AIN93M diet increased arthritis incidence to 100% (vs. 67 %, normal chow) and led to earlier onset, slightly higher scores and paw swelling, and elevated serum AST/ALT ratios, suggesting higher peripheral inflammation, despite similar body weights and lower liver weights.

Conclusion

Our goal was to achieve consistent disease responses with low deviation, higher statistical power, comparability with other laboratories and clinical translatability. In both models, a low-fermentative diet significantly increased uniformity of disease induction and signs. This means a LF diet can be used to obtain robust, uniform immune responses, reducing non-responder rates, allowing the use of fewer animals, and thus fulfilling the Refine and Reduce parts of the "3R" principle. AIN93M is a defined diet which will reduce variation between laboratories. Our findings also suggest a fundamental role of dietary fiber in development and progression of autoimmune disease that may be relevant to translation of preclinical data to the clinical setting.

P059

Plant-based production of functional cytokines and antibodies as an alternative to mammalian expression systems

L. Koehler¹, E. Klapproth¹, A. El-Armouche¹, A. Lippert¹, N. Weser¹, K. Fester², C. Drewniak², J. Messerschmidt², T. Nagel³, M. Beckmann¹

¹TU Dresden University of Technology, Institute for Pharmacology and Toxicology, Dresden, Germany

²Hochschule Zittau/Görlitz University of Applied Sciences, Pharmaceutical Biotechnology, Zittau/ Görlitz, Germany

³Nagel Ingenieurbau GmbH, Schwarze Pumpe, Germany

⁴TU Dresden University of Technology, Chair of Energy Process Engineering, Dresden, Germany

Question: Cell and immunotherapies represent one of the fastest-growing fields in modern medicine, yet their success critically depends on the reliable supply of functional proteins such as interleukins and therapeutic antibodies. These key reagents are still produced mainly in energy-intensive mammalian or bacterial systems, creating costly, CO₂-heavy and globally dependent supply chains. Plant-based expression systems are emerging as efficient and sustainable platforms for recombinant protein production. Especially *Nicotiana benthamiana* has proven suitable for the transient expression of biopharmaceuticals. Interleukins including IL-7, and IL-15 are of special interest, as they are already used in CAR-T and NK cell therapy to support cell expansion and are currently produced in microbial systems such as *E. coli*. Transferring their production into plants offers the potential to reduce costs, and provide more sustainable alternatives.

Methods: In this project, using the GreenGate cloning system, constructs encoding selected interleukins and antibody e.g. anti-PSCA (Prostate stem cell antigen) modules were implemented in plant expression vectors. The vectors were introduced into *Agrobacterium tumefaciens*, which were later used to infiltrate *N. benthamiana* plants. Six days post-infiltration, leaf tissue was harvested and processed into lysates. Protein expression was analyzed via Western blot confirming successful transient expression of the recombinant proteins.

Results and Conclusion: The results provide a technical foundation for further development and scale-up of plant-based pharmaceutical production. In the context of an interdisciplinary collaboration with process engineers and mechanical engineers, this approach will be optimized for larger-scale, decentralized applications in the more rural area of Saxony. Ultimately, integrating molecular plant biotechnology with engineering solutions could enable more cost-efficient manufacturing pipelines for biopharmaceuticals while contributing to circular production strategies and resource efficiency.

P060

Induction of Metabolic Dysfunction-Associated Fatty Liver Disease by Western-style diet? A feasibility study in cynomolgus monkey

S. Kanzler¹, D. Smieja¹, L. Mecklenburg¹

¹Labcorp Early Development Services GmbH, Münster, Germany

Metabolic Dysfunction-Associated Fatty Liver Disease (MAFLD) is a leading cause of obesity, type 2 diabetes mellitus, metabolic syndrome, cardiovascular diseases, chronic kidney disease, extrahepatic malignancies, cognitive disorders, and polycystic ovarian syndrome. Prevention and treatment of MAFLD are still challenging and existing animal models have not proven to be particularly useful. We aimed to demonstrate feasibility of MAFLD induction in non-human primates by adaptation of feeding regimen only in compliance with the 3R principle. We have selected 12 cynomolgus monkeys with an obese body condition and fed them either a western style high caloric diet over 6 months or the standard diet as a control. Animals were euthanized after 13 or 26 weeks and liver was investigated for signs of early MAFLD. Some of the animals developed early signs of MAFLD after 26 weeks of treatment indicating feasibility to induce early stages of MAFLD. This animal model could be useful in detecting new biomarkers for patients that are at risk to develop MAFLD and it could assist in identifying new pharmacological targets to prevent progression of MAFLD before manifestation of disease with potential poor outcome.

P061

Functional recovery after chronic spinal cord injury by hyper-interleukin-6 and CLP290 treatment

M. Leibinger¹, I. Moskaliov¹, P. Gobrecht¹, L. Hechler¹, D. Fischer¹

¹University of Cologne, Pharmacology, Cologne, Germany

Question

In the adult mammalian central nervous system (CNS), axonal regeneration after injury is extremely limited, resulting in severe and often permanent functional deficits. Overcoming this regenerative failure remains a major challenge in neuroscience and regenerative pharmacology. Our previous studies demonstrated that cortical delivery of the designer cytokine **hyper-interleukin-6 (hIL-6)** activates intrinsic growth programs in corticospinal neurons and promotes transneuronal signaling, leading to regeneration of descending serotonergic tracts and partial functional recovery after complete spinal cord injury. The present study investigated whether **AAV2-hIL-6** can promote recovery even in the **chronic injury stage**, and whether this effect can be enhanced by **pharmacological reactivation of dormant spinal interneurons** using the small molecule **CLP290**.

Methods

AAV2-hIL-6 was injected into the primary motor cortex of mice at chronic stages after complete spinal cord transection. In a subset of animals, CLP290 was administered to increase excitability of spinal interneurons and promote neuronal plasticity. Anatomical regeneration was analyzed in the spinal cord and also in the **optic nerve model**, as well as in **primary adult PNS and CNS neuron cultures**.

Functional recovery was evaluated by behavioral tests, while axonal regeneration and connectivity were assessed by anatomical tracing and histology.

Results

Delayed cortical hIL-6 delivery promoted significant functional recovery even in the chronic injury phase. Although **hindlimb stepping** wasn't reestablished initially, it could be **reactivated by combinatorial treatment with CLP290**. However, early CLP290 administration interfered with axonal regeneration, indicating that **timing is critical** for optimal benefit.

Conclusions

hIL-6 retains its regenerative and **functional potential even after chronic spinal cord injury**. Subsequent pharmacological reactivation of dormant spinal interneurons using CLP290 further improves recovery once regeneration is established. These findings highlight the translational potential of **combined gene- and pharmacotherapy** to restore function after severe and chronic CNS injury.

P062

The role of HAS2 in bone marrow niche alterations in the development and progression of type 2 diabetes

M. Döring¹, K. Heller¹, V. Niemann¹, O. Steinhoff¹, T. Seher¹, L. Lahu¹, B. Levkau², J. W. Fischer³, A. Reichert⁴, U. Flögel⁵, M. Grandoch¹

¹Institute for Translational Pharmacology Düsseldorf, Medical Faculty, University Hospital and Heinrich Heine University Düsseldorf, Düsseldorf, Germany

²Institute for Molecular Medicine III, Düsseldorf, Germany

³Institute for Pharmacology Düsseldorf, Medical Faculty, University Clinics and Heinrich Heine University Düsseldorf, Germany, Düsseldorf, Germany

⁴Medical Faculty and University Hospital Düsseldorf, Heinrich Heine University, Institute of Biochemistry and Molecular Biology I, Düsseldorf, Germany

⁵University Clinics and Heinrich Heine University Düsseldorf, Germany, Experimental Cardiovascular Imaging, Institute for Molecular Cardiology, Medical Faculty, Düsseldorf, Germany

Bone Marrow Adipose Tissue (BMAT) is a dynamic and metabolically active component of the BM niche, involved in energy homeostasis and bone metabolism. Conditions such as obesity and type 2 diabetes (T2D) are associated with increased BMAT accumulation and metabolic dysfunction¹. Hyaluronan (HA), a key extracellular matrix component, regulates adipose tissue (AT) function. In T2D, excessive HA deposition in white AT promotes inflammation², while in brown AT, inhibition of HA stimulates activation³. However, HA's role in BMAT remains unexplored. Aim of the study was to analyze the HA-rich matrix and its impact on BMAT metabolism in a murine model of diet-induced obesity and insulin resistance.

Indeed, HA is expressed in the BM niche, with HAS2 as the predominant isoenzyme. During adipogenic differentiation of primary BM adipocytes (BMAd) from male C57BL/6J mice, *Has2* expression and HA secretion increased in parallel. Furthermore, BMAd of *Has2*^{-/-} mice exhibited significantly reduced lipid accumulation compared to controls.

To investigate the effects of HAS2 more specifically, *Has2*^{-/-} mice were fed a diabetogenic diet (DD) for 9 weeks. BM lipid content was assessed, and mesenchymal stem cells (MSCs) were analyzed using flow cytometry. Metabolic activity was measured with Seahorse analyzer, and gene expression was evaluated by RNA sequencing and quantitative PCR. Feeding DD impaired lipid accumulation in the BM of *Has2*^{-/-} mice, while no changes were observed in WAT or BAT, possibly due to differences in the microenvironment or matrix composition. Additionally, MSC numbers remained unchanged. Reduced metabolic activity and increased glucose consumption indicated a shift towards glycolysis. Importantly, glucose-6-phosphate dehydrogenase (G6PDH) activity was significantly decreased in *Has2*^{-/-} BMAd, pointing to impaired pentose phosphate pathway function and reduced capacity for *de novo* lipogenesis. Mechanistically, reduced CD44 surface expression in *Has2*^{-/-} BMAd and impaired adipogenesis upon CD44 blockade support a role of HA–CD44–G6PDH signaling in BMAT metabolism.

In conclusion, our findings show that HA is expressed in BMAT, with HAS2 as predominant isoenzyme. Deletion of HAS2 compromises adipocyte differentiation by shifting metabolism towards glycolysis and impairing *de novo* lipogenesis, resulting in reduced lipid accumulation.

1. Guimaraes GC et al. Osteoporos Int. 2024
2. Jiang D et al. Physiol Rev. 2011
3. Grandoch M et al. Nat Metab. 2019

P063

Characterization of Myotonic Dystrophy type 1 (DM1) disease modifiers in patient-derived DM1 cell lines

M. Kucharak¹, L. Theisen¹, U. Brüggeheimer¹, M. Quanz², V. Brizi³, M. Noble¹, D. Mateju¹, F. Wunder¹

¹Bayer AG, Drug Discovery Sciences, Wuppertal, Germany

²Bayer AG, Research & Early Development, Wuppertal, Germany

³Axxam SpA, Cell Biology, Milano, Italy

Myotonic dystrophy type I (DM1) is an autosomal dominant, monogenic neuromuscular disease and is the most common form of adult-onset muscular dystrophy. DM1 is caused by the expansion of CTG repeats in the 3'-untranslated

region (UTR) of the gene encoding dystrophin myotonia protein kinase (DMPK), resulting in 37–4000 repeats in DM1 patients compared to 5–37 repeats in healthy individuals. This RNA gain-of-function leads to the sequestration of the regulatory splicing factor muscleblind-like splicing regulator 1 (MBNL1) into nuclear aggregates known as nuclear foci.

Here we report the establishment, miniaturization and optimization of a combined FISH-IF phenotypic assay using patient-derived DM1 immortalized myoblasts (Institut de Myologie, Paris, France) useful for the characterization of putative DM1 disease modifiers. Using combined FISH-IF assay, nuclear MBNL1-CUG foci co-localization and the inhibition of foci formation after treatment with selected compounds can be detected. Measurements were performed on 384-well microtiter plates. Antisense oligonucleotides (ASOs) with different nucleotide chemistry were used as positive controls and showed the expected effect on the dissolution of nuclear foci. In addition, several candidate small molecule therapeutics were also tested. Various HDAC inhibitors, proposed to increase MBNL1 protein levels, reduced the number of co-localized MBNL1-CUG foci in a concentration-dependent manner. In contrast, most other DM1 drug candidates did not significantly reduce the number of nuclear foci.

One mechanism underlying DM1 disease symptoms is the sequestration of MBNL1 into nuclear aggregates, which interferes with the MBNL1-regulated alternative splicing of certain pre-mRNAs. Therefore, we used exon-specific RT-qPCR to determine mis-splicing correction of several DM1-relevant genes (e.g. ATP2A1, MBNL1, INSR) after drug treatment. We were able to detect mis-splicing correction on treatment with positive control ASOs as well as various HDAC inhibitors to varying degrees.

The miniaturized phenotypic DM1 assay described here is well-suited for the identification and characterization of novel DM1 disease modulators.

P064

Compound screening identifies DMBQ as a novel inhibitor of NLRP3-dependent pyroptosis

C. Mäder¹, R. Baumann¹, S. Gaul¹, S. Fikenzer¹, M. Schaefer², H. Kalwa², U. Laufs¹, A. Kogel¹

¹University of Leipzig Medical Center, Klinik und Poliklinik für Kardiologie, Leipzig, Germany

²Universität Leipzig, Rudolf-Boehm-Institut für Pharmakologie und Toxikologie, Leipzig, Germany

The inflammatory cell death pyroptosis has emerged as a significant contributor to various forms of sterile inflammation, such as atherosclerosis, myocardial ischemia-reperfusion injury, and diabetes. It is mediated by inflammasomes and results in the release of pro-inflammatory cytokines, such as IL-1 β .

Currently, no selective inflammasome inhibitors are available for human use. Therefore, we aimed to identify and validate novel inhibitors through compound screening.

Medium-throughput screening of 6,280 drugs and drug-like compounds was performed using propidium iodide fluorescence as a pyroptosis readout. The quinone compound 2,6-Dimethoxybenzoquinone (DMBQ) was identified as a promising candidate among the 22 "hits". THP-1 cells primed with 1 μ g ml⁻¹ LPS 3h prior to the addition of 5 μ g ml⁻¹ nigericin for 1h were used to examine DMBQs inhibitory properties on NLRP3-mediated pyroptosis.

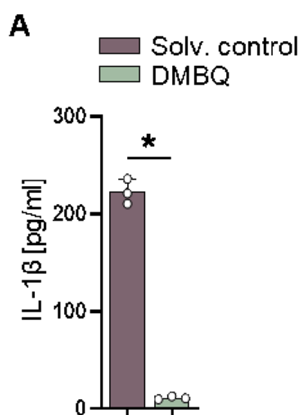
The results demonstrated a significant reduction in cell death at a concentration of 10 μ M DMBQ accompanied by a substantial decrease in IL-1 β secretion (222.6 pg ml⁻¹ vs. 11.19 pg ml⁻¹, p < 0.05, Figure 1A) without affecting cell viability assessed via WST-assay at given concentration. In addition, DMBQ significantly reduced the intracellular formation of inflammasome specks by 83.4% (vs. solvent control, p<0.05) and the cleavage of the pore-forming protein Gasdermin D compared to the solvent control (ratio of Gasdermin D full-length:cleaved 66.58 vs. 5.71) in LPS- and nigericin-treated THP-1 cells. The addition of DMBQ to LPS-treated THP-1 macrophages did not alter the NF- κ B pathway, as analysed by I κ B α phosphorylation and p65 nuclear translocation.

In conclusion, DMBQ is a novel inhibitor of NLRP3-mediated pyroptosis that interferes with inflammasome assembly and potently reduces IL-1 β release.

Figure 1:

A: IL-1 β concentration in the supernatant of THP1 cells that were primed with LPS, followed by the addition of nigericin. The cells were treated with either 10 μ M DMBQ or a solvent control prior to priming with LPS. Data are presented as mean + SD. The data were analysed using a Student's t-test. *p<0.05.

Fig. 1



P065

Alantolactone prevents double-stranded DNA induced inflammasome activation in human immune cells

C. Mäder¹, R. Baumann¹, S. Gaul¹, M. Schaefer², H. Kalwa², U. Laufs¹, A. Kogel¹

¹University of Leipzig Medical Center, Klinik und Poliklinik für Kardiologie, Leipzig, Germany

²Universität Leipzig, Rudolf-Boehm-Institut für Pharmakologie und Toxikologie, Leipzig, Germany

Introduction: The AIM2 inflammasome, a cytosolic detector of double-stranded DNA (dsDNA), is essential for innate immunity and is associated with cardiovascular diseases. The discovery of specific inflammasome inhibitors could lead to new therapeutic approaches.

Methods: Inflammasome modulation was assessed by observing changes in propidium iodide fluorescence following inflammasome activation in over 6,000 drugs from the Spectrum and Selleckchem Bioactive compound libraries, leading to the identification of alantolactone as a candidate compound. THP-1 cells were primed overnight with 100 ng/ml lipopolysaccharide (LPS), treated with 100 nM alantolactone or DMSO, and transfected with 1 µg/ml polydA:dT using Lipofectamine 2000 for 4 h. The WST-1 assay was used to evaluate cell viability, and IL-1β levels were measured using ELISA. NF-κB activity was determined by performing immunoblotting. AIM2 binding was examined using the DARTS assay and co-immunoprecipitation.

Results: Alantolactone at 100 nM significantly decreased IL-1β release in THP-1 cells stimulated with nigericin (276.9 vs. 48.7 pg/ml, $p < 0.05$) and double-stranded DNA (polydA:dT) (69.8 vs. 16.5 pg/ml). The suppression of polydA:dT-induced IL-1β release by alantolactone peaked at 1 µM compared to that by the solvent control (58.2 vs. 4.8 pg/ml, $p < 0.05$). At this concentration, alantolactone did not affect cell viability, as shown by the WST-1 assay. Western blot analysis showed that IκBα phosphorylation was not altered after 100 nM alantolactone treatment. Mechanistically, alantolactone did not directly interact with AIM2, as shown by the DARTS assay and Co-Immunoprecipitation of AIM2 and ASC. In ex vivo studies, interleukin release in PBMCs was reduced without toxicity at the tested concentrations (-76.1 %, $p < 0.05$, Fig. 1).

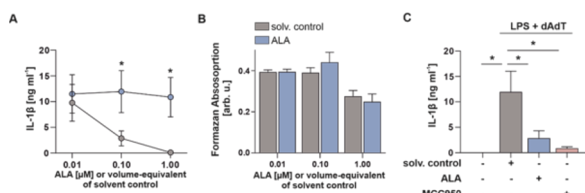
Conclusion: Alantolactone suppresses inflammasome activity triggered by double-stranded DNA in THP-1 cells and peripheral blood mononuclear cells, operating independently of NF-κB.

Figure 1: A: Concentration-response curve of LPS and polydA:dT transfected PBMCs depicting IL-1β release.

B: Cell viability was analysed using the WST-1 assay.

C: IL-1β concentration in the supernatant of LPS-primed polydA:dT-transfected PBMCs. Cells were treated with 100 nM alantolactone, 10 µM MCC950, or solvent control prior to LPS-priming. Data are presented as mean + SD. Data were analysed using the Student's t-test. * $p < 0.05$.

Fig. 1



P066

PKC inhibition by ruboxistaurin to counteract cardiomyocyte calcium dysregulation and contractile dysfunction in the remote myocardium early after ischemia/reperfusion injury

M. Müller¹, F. Engel¹, S. Gorreßen¹, F. Funk¹, M. Krüger², J. Schmitt¹

¹Institute of Pharmacology, Düsseldorf, Germany

²Institute of Cardiovascular Physiology, Düsseldorf, Germany

Introduction: Ischemia/reperfusion injury (I/R) of the heart impairs contractile function both in the infarct zone and the non-infarcted remote myocardium (RM). Using a mouse model, we previously showed that impaired cardiomyocyte Ca²⁺ cycling due to reduced activity of the sarco-/endoplasmic reticulum (SR) Ca²⁺ ATPase 2a (SERCA2a) contributes to RM dysfunction in the early phase, 24 hours after I/R. The underlying causes involve increased phosphatase activity leading to dephosphorylation and thereby activation of the SERCA2a inhibitor phospholamban (PLN). Furthermore, the activity of protein kinase C (PKC) was found increased in the RM (PMID: 29674140).

Objective: We tested the hypothesis that pharmacological PKC inhibition by ruboxistaurin (RBX) would normalize cardiomyocyte Ca²⁺ cycling and contractile function of the RM by deactivating protein phosphatases via inhibitor-I, thereby increasing PLN phosphorylation and SERCA2a activity.

Materials and methods: Cardiac function was assessed by echocardiography of 10 to 12-week-old C57BL/6 mice. Cardiomyocytes were isolated from the RM 24 hours after application of RBX by oral gavage and induction of I/R (1 h ischemia, closed-chest model). Ca²⁺ cycling and sarcomere function were measured in electrically paced cells using Fura-2 and camera-based tracking of sarcomere lengths. Protein expression and phosphorylation were analysed by western blot.

Results: The PKC inhibitor RBX (10⁻⁶ M) enhanced cardiomyocyte Ca²⁺ cycling when directly added to isolated mouse cardiomyocytes within 10 minutes. SR Ca²⁺ release was increased by 13.7±2.9% and the rate of SR Ca²⁺ uptake, indicating SERCA2a activity, by 59.4±14.5% ($p < 0.005$). Sarcomere contraction and relaxation were also enhanced ($p < 0.05$).

In vivo, RBX increased the phosphorylation state of PLN within 24 hours after oral application in a dose-dependent manner. Based on these data, 40 µg/g RBX were administered to mice that subsequently were subjected to I/R. Echocardiography before and 24 hours after the intervention showed a trend reduction of I/R-induced left ventricular dysfunction by RBX (n=13) compared to vehicle-treated mice (n=11). Ca²⁺ cycling and sarcomere function of cardiomyocytes isolated from the RM were not significantly different between groups.

Conclusion: The data demonstrate that cardiomyocyte Ca²⁺ cycling and sarcomere function can be enhanced by the PKC inhibitor RBX, but not in the RM early after I/R by an oral dose of 40 µg/g.

P067

Locus-specific isolation of gene-regulatory complexes in inflammation

G. Schneider¹, J. Meier-Sölch¹, M. Kracht¹

¹Justus Liebig University Gießen, Rudolf-Buchheim Institute of Pharmacology, Gießen, Germany

Inflammation is a complex and tightly regulated response to cellular damage or infection. Defects in the multitude of genes that govern the onset and resolution of inflammation are a major contributing factor in the development of various human diseases. This highlights the importance of improving our understanding of the underlying genetic regulatory components. One of the earliest and most important mediators of inflammation is the pro-inflammatory cytokine IL-1α/β, which induces the expression of a broad spectrum of inflammatory genes via the canonical NF-κB signalling pathway. Previous work of the Kracht group has identified an IL-1α-regulated genomic enhancer upstream of the *CXCL8/IL8* gene in the chemokine gene cluster localized on Chr.4. This enhancer appears to play a direct role in the regulation of not only *IL8*, but also further inflammatory genes in cis or trans, leading to the hypothesis that the transcription of multiple IL-1α-inducible genes is coordinated within the nucleus by locus-specific genomic hubs. In this project, lenti-virally transduced stable HeLa cervical carcinoma cell lines were created and will be used to characterise the proteins and their post-translational modifications, involved in the hierarchical organisation of co-regulated cytokine-responsive genes. These cell lines express a fusion protein of the biotin ligase miniTurbo (mTb) with a catalytically inactive Cas9 variant (dCas9), as well as small guide RNAs (sgRNAs) targeting the dCas9-mTb to individual genomic loci of the ten most strongly regulated IL-1α target genes. Within these loci the dCas9-mTb facilitates the biotinylation of nearby proteins. Cell lines were characterized by Western blotting and RT-qPCR, confirming the expression of the dCas9-mTb fusion protein and an intact IL-1 response. The expression and correct targeting of the sgRNAs was confirmed by ChIP-qPCR. In addition, a protein isolation protocol for nuclear extracts by streptavidin-affinity purification has been established successfully. In the next phase of the project, the characterized cell lines will be used for the purification of chromatin fractions by sucrose density centrifugation, followed by the isolation of locus-specific biotinylated proteins, and identification by LC-MS/MS. In conclusion, this newly established approach will help to identify locus-specific protein interactomes to resolve molecular mechanisms and higher order structures that define the IL-1α induced gene response.

P068**Role of glucocorticoids in inhibiting bradykinin-induced PGI₂ generation in human dermal microvascular endothelial cells (HMECs)**C. Aközbe¹, G. Kojda¹¹University Hospital Düsseldorf, Heinrich Heine University Düsseldorf, Institute of Pharmacology, Düsseldorf, Germany

Introduction: Non-allergic angioedema, which can occur as a side effect of ACE inhibitor therapy, is caused by increased bradykinin release. Activation of B₂ receptors by bradykinin stimulates prostaglandin production and enhances vascular permeability and tissue swelling, which can become life-threatening if the upper airways are affected. Glucocorticoids reduce prostaglandin production but have not been systematically studied in non-allergic angioedema and are generally considered ineffective.

Objectives: The aim of the study was to evaluate the role of glucocorticoids in inhibiting bradykinin-induced PGI₂ generation in human dermal microvascular endothelial cells (HMEC).

Methods: HMECs from male and female donors were cultured and analysed separately to control for sex-specific differences in prostacyclin signalling. Cells were treated for three hours with 10 µM or 100 µM dexamethasone or vehicle control, washed, and stimulated for ten minutes with 10 µM bradykinin or phosphate-buffered saline (PBS). Cell culture supernatants were collected and immediately frozen at -80°C for later analysis. The generation of 6-keto-PGF_{1α}, a stable metabolite of prostacyclin (PGI₂), was quantified as an indirect indicator of PGI₂ production using a competitive ELISA which accuracy was validated by Liquid chromatography with tandem mass spectrometry (LC-MS/MS).

Key Results: Preincubation with dexamethasone (180 min) inhibited the release of 6-keto-PGF_{1α} induced by bradykinin in a concentration-dependent manner (n = 12; male = 6, female = 6). Stimulation with 10 µM bradykinin without prior dexamethasone treatment, significantly increased 6-keto-PGF_{1α} release compared to the unstimulated control group ****p<0.0001. Pretreatment with 10 µM dexamethasone resulted in a moderate reduction, that did not reach statistical significance (ns). In contrast, pretreatment with 100 µM dexamethasone led to a significant decrease of 6-keto-PGF_{1α} release (####p < 0.0001), also compared to 10µM dexamethasone. Furthermore, dexamethasone had no effect after a preincubation of 20 min.

Conclusion: These findings are consistent with previous in vivo observations from Miles assay, suggesting a genomic mechanism that appears to be sex-independent.

P069**Specific activation of angiotensin receptor type II increases bradykinin-induced skin extravasation in mice, potentially mimicking sartan-induced angioedema**C. Aközbe¹, V. Thao-Vi Dao^{1,2}, E. Fahimi¹, M. Bisha¹, T. Kurz³, F. K. Hansen⁴, T. Suvorava¹, G. Kojda¹¹University Hospital Düsseldorf, Heinrich Heine University Düsseldorf, Institute of Pharmacology, Düsseldorf, Germany²Hanau Hospital, Clinic for Pediatrics and Adolescent Medicine, Hanau, Germany³Heinrich Heine University Düsseldorf, Institute of Pharmaceutical and Medicinal Chemistry, Düsseldorf, Germany⁴University of Bonn, Department of Pharmaceutical and Cell Biological Chemistry, Bonn, Germany

Introduction: While non-allergic angio-oedema induced by ACE inhibitors and sacubitril are caused by over-activation of bradykinin receptor type 2 (B₂), the pathophysiology of sartan-induced angio-oedema is still poorly understood. As angiotensin II receptor (AT₁) type 1 blockers increase the circulating concentration angiotensin II, enhanced activation of AT₂ by angiotensin II may occur.

Objectives: The aim of this study was to investigate whether AT₂ activation inhibits ACE activity and attenuates bradykinin metabolism.

Methods: Increased plasma angiotensin II by telmisartan was measured at a dose that reduced systolic blood pressure by 20 mmHg. The AT₂ agonist compound 21 (C21) was synthesized. Its purity was proven by HPLC and its biological activity by vasorelaxation of aortic rings of FVB/N and C57BL/6J mice which was absent in rings of AT₂-ly mice. Blood pressure was not changed by C21.

Key Results: In Miles assays in C57BL/6J, but not in AT₂-ly-C57, C21 potentiated dermal extravasation induced by bradykinin, while extravasation by the ACE resistant B₂ agonist labradilim remained unchanged. Furthermore, pre-treatment of human endothelial cells with C21 strongly reduced ACE activity in cell homogenates in an AT₂ dependent manner suggesting a cellular loss of ACE. Correspondingly, there was an increase in supernatant ACE protein in mouse lung tissue incubated with C21. In mice treated with C21, ACE activity in plasma increased, while ACE protein in lung tissue was reduced, also suggesting a loss of membrane-bound ACE.

Conclusion: These data suggest that increased ACE-dependent bradykinin-induced dermal extravasation due to AT₂ activation may underlie sartan-induced non-allergic angioedema.

P070**Muscle lim protein and parthenolide synergistically accelerate functional recovery upon peripheral nerve injury**P. Gobrecht¹, J. Gebel², D. Fischer^{1,2}¹Universitätsklinikum Köln, Institut für Pharmakologie, Cologne, Germany²Universitätsklinikum Köln, Cologne, Germany

Introduction: Peripheral neurons can regenerate damaged axons but restoring lost functions may be im-possible if distances to overcome are too long. Therefore, strategies that accelerate axonal growth are of substantial clinical interest but not yet available in the clinic. In the CNS, muscle lim protein (MLP) overexpression promotes axon regeneration of retinal ganglion cells by acting as an actin cross-linker in the growth cone. Another approach to accelerate axon regeneration is to reduce microtubule detyrosination in axonal growth cones by parthenolide. This drug increases microtubule dynamics and promotes axon elongation.

Methods/Results: Here, we show that unlike in adult rats, mice lack endogenous MLP expression in sensory neurons, making them ideal for studying its role in peripheral nerve regeneration. Neuronal MLP overexpression in cultured sensory neurons from adult mice markedly accelerates axon extension. These effects are synergistically enhanced by additional parthenolide treatment. In vivo, intrathecal application of AAV1-MLP effectively transduces sensory and motor neurons projecting in the sciatic nerve. This treatment markedly speeds up functional motor and sensory recovery upon sciatic nerve crush. As in culture, additional systemic application of parthenolide further shortens the recovery time.

Conclusion: Thus, gene therapeutic MLP overexpression might be a suitable approach to facilitate nerve repair, particularly in combination with other pharmacological approaches, such as parthenolide.

P071**A 3D Microphysiological Model for Drug Testing in Clear Cell Renal Cell Carcinoma**J. Matsch¹, H. Heinrich¹, L. Vogt¹, S. Lohse¹, S. Rausch², S. Winter¹, J. Bedke³, I. Tsau¹, E. Nössner⁴, M. Schwab^{5,1}, E. Schäffeler¹¹Bosch Health Campus, Dr. Margarete Fischer-Bosch Institute of Clinical Pharmacology, Stuttgart, Germany²University Hospital Tübingen, Department of Urology, Tübingen, Germany³Eva Mayr-Stihl Cancer Center, Klinikum Stuttgart, Department of Urology & Transplantation Surgery, Stuttgart, Germany⁴Heimholtz Center Munich, Immunoanalytics-Tissue Control of Immunocytes, Munich, Germany⁵University of Tübingen, Departments of Clinical Pharmacology, Pharmacy and Biochemistry, Tübingen, Germany

Question: Clear cell renal cell carcinoma (ccRCC) is the most common and aggressive subtype of kidney cancer, associated with poor outcomes in patients with metastatic disease. Its tumor microenvironment (TME) is highly complex, involving interactions between tumor, immune, and endothelial cells as well as stromal components that influence tumor progression and therapy response. To better reproduce these processes and enable physiologically relevant drug testing, we aimed to establish a 3D microphysiological ccRCC model that incorporates key features of the TME and allows assessment of crosstalk among tumor, immune, and vascular cells.

Methods: A three-dimensional microphysiological ccRCC model was established using the OrganoPlate® from MIMETAS to recreate physiological gradients and multicellular communication absent in conventional 2D cultures. The system comprises a perfusable vascular channel, extracellular matrix (ECM), tumor cells, angiogenic factors, and T lymphocytes. Human umbilical vein endothelial cells (HUVECs), ccRCC A498 cells, and TCR53 T cells (expressing an HLA-A2–restricted, tumor-specific TCR) were co-cultured under dynamic perfusion.

Results: A stable and perfusable endothelial barrier was established in the OrganoPlate® system. After seven days, HUVECs formed a continuous monolayer with a tight barrier phenotype and no leakage between compartments. Under angiogenic stimulation, endothelial cells extended sprouts into the adjacent ECM, confirming their functional responsiveness within the 3D environment. A498 cells seeded in the lower perfusion channel adhered to the ECM interface, proliferated, and formed confluent, viable layers. T cells migrated into the ECM only in the presence of an endothelial layer, indicating that endothelial–immune interactions were required for transendothelial migration. In co-culture with HUVECs and A498 cells, TCR53 T cells extravasated through the endothelial barrier, migrated within the ECM, and bound to HLA-A2–positive tumor cells, demonstrating specific immune–tumor interactions in the 3D microenvironment.

Conclusions: We established a microphysiological 3D ccRCC model that allows assessment of endothelial barrier function, immune cell infiltration, and tumor–immune crosstalk. This model enables more comprehensive analysis of drug responses and metastatic processes, increasing its physiological and translational relevance.

Supported by DFG-funded RTG2816 and Robert Bosch Stiftung.

072
Revisiting the Relationship Between Measured Creatinine Clearance and Measured Glomerular Filtration Rate Using Marker Substances: A Systematic Review
W. Yang¹, M. Taubert¹, U. Fuhr¹
¹University of Cologne, Department I of Pharmacology, Center for Pharmacology, Cologne, Germany

Question:

How much does measured creatinine clearance (CrCL) overestimate glomerular filtration rate (GFR), given the wide variability in reported creatinine secretion?

Methods:

A PubMed search identified studies reporting raw CrCL and GFR values. Population characteristics, measurement methods, and other relevant data were summarized, and raw data were extracted and grouped for exploratory analysis (Table 1). Empirical functions (e.g., linear, power, and secretion saturation) to describe the CrCL-GFR relationship were fitted to each group's data and assessed by the corrected Akaike Information Criterion (AICc) and goodness-of-fit (GoF) plots. To evaluate the predictive performance of the final functions, Lin's concordance correlation coefficient (CCC), bias, variance, and root mean square error (RMSE) were calculated. Mean observed CrCL/GFR ratios across GFR ranges were also summarized.

Results:

A total of 118 studies provided raw data, allocated to 16 (partially overlapping) groups. Power functions were most suitable to describe the CrCL-GFR relationship, showing the lowest AICc values and acceptable GoF plots in almost all groups (median Lin's CCC: 0.716). However, CrCL reflected the variance in GFR only to a limited extent (median *Pseudo-R*²: 0.541), while prediction variability remains relatively large (median variance: 566.2) and the median RMSE was 23.8 mL/min/[1.73m²]. Although the power functions captured the general trends reasonably well, substantial inter-individual variability remained, suggesting that incorporating covariates may further improve the description of individual CrCL-GFR relationship. Regression lines (Figure 1) and observed mean CrCL/GFR ratios (Table 1) showed the ratio decreased with increasing GFR, with higher variability at lower GFR. CrCL approximated GFR in healthy subjects (CrCL overestimated GFR by <20% at GFR 90–149 mL/min/[1.73m²]) and non-renal disease subjects (by <15% at GFR 45–89 and 3% at 90–119 mL/min/[1.73m²]). Ratios <1 for GFR exceeding 90 mL/min/[1.73m²] may be related to creatinine re-absorption. Within the same population, groups with simultaneous measurement of CrCL and GFR generally yielded higher ratios than those measuring CrCL for 24 h, which may reflect circadian fluctuations in creatinine kinetics or errors in urine collection.

Conclusions:

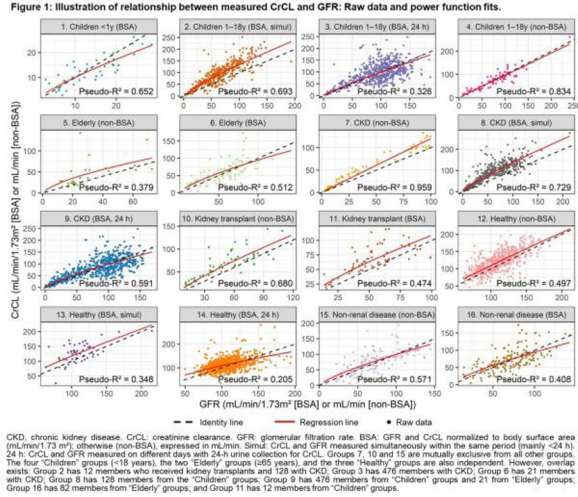
Measured CrCL is not a precise predictor for GFR. The extent to which CrCL overestimates GFR increases as renal function declines.

Fig. 1

Table 1. Observed mean CrCL/GFR ratios classified by population and GFR.										
Population	No. Study/ Data	GFR: <15	GFR: 15–29	GFR: 30–44	GFR: 45–59	GFR: 60–89	GFR: 90–119	GFR: 120–149	GFR: 150–200	
1. Children <1y (BSA)	2/44	1.16 ± 0.63 (n=24)	0.86 ± 0.16 (n=20)	/	/	/	/	/	/	/
2. Children 1–18y (BSA, simultaneous)	8/365	1.66 ± 0.62 (n=19)	1.68 ± 0.56 (n=41)	1.70 ± 0.82 (n=44)	1.48 ± 0.43 (n=68)	1.39 ± 0.37 (n=110)	1.43 ± 0.27 (n=57)	1.28 ± 0.33 (n=25)	0.76 (n=1)	/
3. Children 1–18y (BSA, 24 h)	6/590	1.39 ± 0.58 (n=21)	1.53 ± 1.26 (n=25)	1.17 ± 0.37 (n=29)	1.32 ± 0.35 (n=32)	1.23 ± 0.50 (n=137)	1.03 ± 0.37 (n=208)	0.90 ± 0.27 (n=119)	0.74 ± 0.20 (n=19)	/
4. Children 1–18y (non-BSA)	4/76	1.42 ± 0.24 (n=3)	1.42 ± 0.54 (n=7)	0.92 ± 0.12 (n=7)	0.91 ± 0.21 (n=7)	1.02 ± 0.21 (n=23)	0.94 ± 0.20 (n=19)	0.91 ± 0.17 (n=8)	0.96 (n=1)	/
5. Elderly (BSA)	3/30	1.95 ± 0.45 (n=6)	1.61 ± 1.29 (n=14)	1.70 ± 0.73 (n=9)	1.02 (n=5)	1.14 ± 0.47 (n=4)	/	/	/	/
6. Elderly (non-BSA)	3/103	1.82 ± 0.30 (n=9)	1.41 ± 0.74 (n=13)	1.24 ± 0.51 (n=15)	0.98 ± 0.37 (n=21)	1.09 ± 0.39 (n=39)	0.81 ± 0.09 (n=5)	1.00 (n=1)	/	/
7. CKD (BSA, simultaneous)	2/86	1.39 ± 0.27 (n=37)	1.67 ± 0.24 (n=11)	1.40 ± 0.15 (n=10)	1.43 ± 0.13 (n=3)	1.16 ± 0.12 (n=14)	1.18 ± 0.14 (n=11)	/	/	/
8. CKD (BSA, 24 h)	7/435	2.24 ± 1.51 (n=61)	1.82 ± 0.78 (n=57)	1.88 ± 0.76 (n=49)	1.85 ± 0.57 (n=67)	1.50 ± 0.30 (n=103)	1.30 ± 0.28 (n=77)	1.23 ± 0.31 (n=19)	1.24 (n=1)	/
9. CKD (non-BSA)	7/670	1.78 ± 1.49 (n=1)	1.48 ± 0.59 (n=60)	1.25 ± 0.40 (n=57)	1.22 ± 0.32 (n=53)	1.17 ± 0.46 (n=125)	0.99 ± 0.34 (n=195)	0.89 ± 0.28 (n=99)	0.83 ± 0.12 (n=12)	/
10. Kidney transplant (non-BSA)	2/66	1.94 ± 0.38 (n=7)	1.59 ± 0.21 (n=9)	1.57 ± 0.57 (n=12)	1.43 ± 0.21 (n=12)	1.16 ± 0.28 (n=19)	1.07 ± 0.25 (n=7)	/	/	/
11. Kidney transplant (BSA)	4/70	3.00 (n=1)	1.39 ± 0.12 (n=8)	1.47 ± 0.33 (n=18)	1.42 ± 0.32 (n=17)	1.18 ± 0.29 (n=23)	0.79 ± 0.13 (n=3)	/	/	/
12. Healthy (non-BSA)	8/550	/	/	/	/	1.19 ± 0.25 (n=135)	1.09 ± 0.17 (n=247)	1.04 ± 0.18 (n=149)	1.04 ± 0.12 (n=27)	/
13. Healthy (BSA, simultaneous)	4/52	/	/	/	/	1.29 ± 0.54 (n=8)	1.20 ± 0.24 (n=30)	1.07 ± 0.16 (n=12)	1.18 (n=1)	/
14. Healthy (BSA, 24 h)	6/726	/	/	/	/	1.89 (n=1)	1.24 ± 0.27 (n=144)	1.07 ± 0.21 (n=399)	0.92 ± 0.28 (n=32)	/
15. Non-renal disease (non-BSA)	3/168	1.19 ± 0.34 (n=3)	1.22 ± 0.62 (n=13)	1.16 ± 0.61 (n=24)	1.10 ± 0.32 (n=23)	1.12 ± 0.42 (n=52)	1.03 ± 0.27 (n=38)	0.87 ± 0.11 (n=15)	/	/
16. Non-renal disease (BSA)	5/167	2.08 (n=1)	1.51 ± 0.88 (n=9)	1.22 ± 0.56 (n=19)	1.08 ± 0.43 (n=27)	1.03 ± 0.35 (n=72)	0.90 ± 0.27 (n=37)	0.98 ± 0.12 (n=3)	/	/

Values are presented as mean ratios ± SD. n denotes the number of data points. CKD, chronic kidney disease. CrCL, creatinine clearance. GFR, glomerular filtration rate. BSA, GFR and CrCL normalized to body surface area (mL/min/1.73 m²); otherwise (non-BSA), expressed in mL/min. Simul, CrCL and GFR measured simultaneously within the same period (mainly <24 h). 24 h, CrCL and GFR measured on different days with 24-h urine collection for CrCL.

Fig. 2



P073
Rapid Evaluation of Affinity Protein Libraries via Bacterial Surface Display and Biolayer Interferometry
T. Müller¹, L. Hofacker¹, L. Arndt¹, G. Schmidt¹
¹University of Freiburg, Institute of Experimental and Clinical Pharmacology and Toxicology, Freiburg, Germany

Affibodies are small, robust protein scaffolds that can be engineered to bind a wide range of targets, making them valuable tools for research and diagnostic applications [1, 2]. Although bacterial surface display is an established method for screening scaffold-peptide libraries, quantifying the enrichment of target-binding variants remains challenging [3].

Here, we present a workflow that integrates bacterial surface display with biolayer interferometry (BLI) to monitor affibody library selections against diverse target proteins. Affibody variants are displayed on the surface of *Escherichia coli* via fusion to the AIDA-I autotransporter [4, 5]. Following solid-phase selection, enrichment is quantitatively assessed using BLI in combination with protease-based shedding of the displayed affibodies. Individual clones can then be analyzed directly using the same display construct to determine their binding kinetics, without the need for subcloning.

This BLI-assisted screening strategy improves the efficiency and precision of affibody library evaluation, providing a robust and scalable platform for the identification of high-affinity binders.

Freyd FY, Kim KT. Affibody molecules as engineered protein drugs. *Exp Mol Med*. 2017;49:e306. <https://doi.org/10.1038/emmm.2017.35>

Müller T, Gieß S, Maier F, Hofacker L, Stenger L, Parker L, Grosse R, Schmidt G. Injection of affibodies by a self-organizing bacterial syringe to interfere with intracellular signaling. *Toxins*. 2025;17(9):448. <https://doi.org/10.3390/toxins17090448>

Löfblom J. Bacterial display in combinatorial protein engineering. *Biotechnol J*. 2011;6:1115–1129. <https://doi.org/10.1002/biot.201100129>

Parks L, Ek M, Ståhl S, Löfblom J. Investigation of an AIDA-I-based expression system for display of various affinity proteins on *Escherichia coli*. *Biochem Biophys Res Commun*. 2024;696:149534. <https://doi.org/10.1016/j.bbrc.2024.149534>

Jarmander J, Gustavsson M, Do TH, Hägglund P, Löfblom J. A dual tag system for facilitated detection of surface-expressed proteins in *Escherichia coli*. *Microb Cell Fact*. 2012;11:118. <https://doi.org/10.1186/1475-2859-11-118>

P074
Marshmallow root extract: Physical effects - a precondition of its pharmacological effects
Q. Kelber¹, J. Seibelf²
¹Phyto & Biotics Tech Platform, Phytomedicines Supply and Development Center, Bayer Consumer Health, Steigerwald Arzneimittelwerk GmbH, Darmstadt, Germany
²Bayer Vital GmbH, Medical Affairs Consumer Health, Leverkusen, Germany

Question: The use of the aqueous extract of marshmallow root for respiratory symptoms has been described for the first time by Pliny the Elder [1], prominent victim of the outbreak of Mt. Vesuvius in 79 AD. STW 42 (Phytohustil®), a cough syrup based on this extract, has characterized analytically [2,3], as well as their anti-inflammatory effects [4–6], but still, their physical effects [7] are key for their fast and strong action in irritative cough [8]. To characterize these, physical

parameters were studied in comparison to 5 other liquid cough preparations available in the German market.

Methods: STW 42 and the other liquid cough preparations (coded 1–5) were studied by rotational viscosimetry and regarding their retention on a mucosal surface (EpiOral resp. ex vivo) after labelling with [^{14}C]-galactose and repeated rinsing, mimicking the effect of swallowing saliva on the pharyngeal mucosa.

Results: The viscosity of the preparations tested was in a range of 482–26 mPas, ranking in order of decreasing viscosity STW 42 > 2 > 1 > 3 > 4. The order of retention was (in decreasing order) STW 42 > 4 > 1 > 5 > 2 > 3 (Fig. 1). Comparison of the viscosity values with epithelial retention data indicated that viscosity alone did not account for the retention on epithelial tissues.

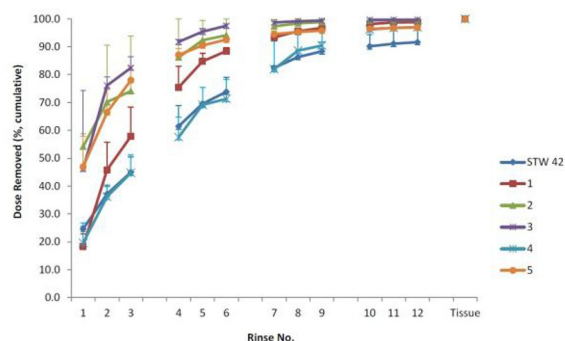
Conclusions: The results confirm the unique physical properties of marshmallow cough syrup, which are a precondition of its local pharmacological effects, and so underline its usefulness in irritative cough already described by Pliny the Elder and confirmed since then by a huge body of evidence.

Acknowledgements: Many thanks to Marcus Frieler and Konstanze Bedal for fruitful discussions.

References:

- Möller J, Kelber, O, Nieber K. Zeitschrift für Phytotherapie 2019; 40 (S01): S23–S24
- Sendker J, Böker I, Lengers I et al. J Nat Prod 2017; 80: 290–297
- Sendker, J.; Böker, I.; Fink, C. et al. Zeitschrift für Phytotherapie 2015; 36: V23.
- Bonaterre, G.A.; Bronischewski, K.; Hunold, P. et al. Front Pharmacol. 2020; 11: 290.
- Bonaterre GA, Schmitt J, Schneider K et al. Front Pharmacol 2022; 13: 948248
- Deters A, Zippel J, Heilenbrand N et al. Ethnopharmacol 2010; 127: 62–69.
- European Medicines Agency: Amsterdam. 2016, https://www.ema.europa.eu/en/documents/herbal-summary/marshmallow-root-summary-public_en.pdf [Accessed August 15, 2023].
- Fink C, Schmidt M, Kraft K. Complement Med Res 2018; 25: 299–305

Fig. 1



P075

Apically accessible intestinal organoids composed of stroma and macrophages - A model to test ingested chemical substances

J. Heuberger^{1,2}, L. Liu², L. Geisler², J. Beranek¹, P. Seidler², R. Dreyer³, S. Kunz⁴, M. Oelgeschläger¹, F. Heymann², M. Sigal²

¹German Federal Institute for Risk Assessment (BfR), Department German Centre for the Protection of Laboratory Animals and Experimental Toxicology, Berlin, Germany

²Charité – Universitätsmedizin Berlin, Department of Hepatology and Gastroenterology, Berlin, Germany

³German Federal Institute for Risk Assessment (BfR), Unit Viruses in Food, Berlin, Germany

⁴MDC in the Helmholtz Society, Electron Microscopy Core Facility, Berlin, Germany

The development of intestinal organoid cultures emerged as a potential replacement for animal experiments. However, the current state of organoid cultures is characterized by limitations in their capacity to accurately replicate in vivo conditions, attributed to the inaccessibility of the apical surface and the absence of stromal and immune cells. To overcome these constraints, we have developed a novel self-maintaining intestinal apical-out organoid (AOO) system that can be enriched by bone marrow-derived macrophages. AOOs consist of a stromal cell core covered by an epithelial layer and possess a constant apically accessible surface. At early stage, the epithelia exhibit regenerative properties and while covering the core the epithelia mature and are finally composed of proliferative precursors, stem cells and terminally differentiated secretory and absorptive cells. The AOOs exhibit a cellular turnover and allow a constant culture for several weeks. Containing macrophages form inter-epithelial dendrites to sample environmental particles, migrate and accumulate beneath the epithelial sheet. Macrophages respond to external stimuli and epithelial barrier disruption although with varying intensity compared to pure and 2D cultured macrophages. This model underscores the utility of AOOs in analyzing tissue and immune cell responses to ingested and apically acting biological or chemical agents.

Endocrine pharmacology

P076

Urinary steroid conjugate concentrations in patients with adrenocortical carcinoma and adenoma: clinical validation of novel biomarkers

E. North¹, A. Gessner^{1,2}, M. Kroiss^{3,4}, M. Kurlbaum^{3,5}, M. Fassnacht^{3,5}, M. F. Fromm^{1,2}, N. Bartels¹

¹Friedrich-Alexander University of Erlangen-Nuremberg, Institute of Experimental and Clinical Pharmacology and Toxicology, Erlangen, Germany

²Friedrich-Alexander University of Erlangen-Nuremberg, FAU NeW - Research Center New Bioactive Compounds, Erlangen, Germany

³University Hospital Würzburg, Department of Internal Medicine I, Division of Endocrinology and Diabetes, Würzburg, Germany

⁴University Hospital Munich, Department of Internal Medicine IV, Munich, Germany

⁵University Hospital Würzburg, Central Laboratory, Core Unit Clinical Mass Spectrometry, Würzburg, Germany

Questions: Metabolic conjugates of steroids have been proposed as promising biomarker candidates for the crucial, clinically challenging differential diagnosis of rare, aggressive adrenocortical carcinoma (ACC) and highly prevalent, benign adrenocortical adenoma (ACA). In this work, extensive data on concentrations of various steroid conjugates in 24h-urine of patients with ACC and ACA was acquired with the purpose of clinically validating respective compounds as reliable biomarkers for ACC.

Materials and Methods: A targeted, validated LC-MS/MS method was used for the sensitive quantification of 22 intact steroid sulfates, disulfates and glucuronides in more than 300 24h-urine samples of patients with ACC or ACA. Analysis was performed according to FDA guidelines. The patients were part of the European Network for the Study of Adrenal Tumours (ENSAT) registry.

Results: Approximately every fifth patient in the study cohort was previously diagnosed with ACC based on histology. Median analyte concentrations of multiple compounds were significantly higher in urine of patients with ACC than in urine of patients with ACA. Furthermore, a considerably higher interindividual variability of analyte concentrations was observed in the ACC group compared to the ACA group.

Conclusion: The urinary profile of steroid conjugates displays significant differences between patients with ACC and ACA. Based on these findings, clinical validation of steroid conjugates as biomarkers for the differential diagnosis of ACC versus ACA could result in notable progress in this area of medical research. Data analysis of a training-test model is currently ongoing. Such reliable biomarkers could refine diagnosis regarding time and effort for patients and medical staff, enabling early pharmacological and surgical treatment and thereby improving the poor prognosis of ACC.

P077

Phase 1, first-in-human trial to evaluate the safety, tolerability, and pharmacokinetics of ascending single oral doses of octreotide / LipOra peptide in healthy volunteers

M. Bergamini¹, M. Sauter¹, P. Uhl¹, C. Bay¹, A. Meid¹, N. Struß¹, J. Burhenne¹, D. Czock¹, A. Blank¹, W. E. Haefeli¹

¹Heidelberg University Hospital, Internal Medicine IX – Department of Clinical Pharmacology and Pharmacoeconomics, Heidelberg, Germany

Introduction: Octreotide (OTT)/LipOra, a new oral (po) formulation of OTT, consists of the active ingredient OTT and the novel functional excipient LipOra. The latter is an arginine-rich cyclic cell-penetrating peptide/phospholipid conjugate without pharmacological activity, which is intended to enhance intestinal peptide absorption. Preclinical studies in Beagle dogs showed a 417 % increase of OTT bioavailability (F) with LipOra, yielding an absolute F of 7,1 %.

Objectives: To evaluate the safety and tolerability of OTT / LipOra, to determine the optimal dose of both substances for reaching the largest AUC_{0-∞} of po OTT, to describe the pharmacokinetics (PK) of OTT and LipOra, and to compare the relative po OTT F of a given dose formulated with and without LipOra peptide as related to 0.1 mg subcutaneous (sc) OTT.

Methods: In a first-in-human, PK-guided adaptive trial in healthy volunteers (EU CT-Nr. 2024-514225-30-00), LipOra dose escalation (10, 20, 50, and 100 mg) with a low, fixed OTT po dose of 3 mg was performed in small explorative cohorts of 3 participants each (Phase A). Then, a confirmatory 3-period cross-over proof-of-concept cohort [Comparative Cohort 1 (CC1)] followed, in which 8 participants received 0.1 mg sc OTT and 3 mg oral OTT with and without 100 mg LipOra. Last, the OTT dose was escalated according to a PK-guided algorithm for achieving therapeutic OTT plasma concentrations. A 3-period cross-over cohort of 16 participants [Comparative Cohort 2 (CC2)] was then exposed to 0.1 mg sc OTT and 20 mg po OTT with and without 100 mg LipOra.

Results: The 100 mg po LipOra dose reached the largest OTT AUC_{0-∞} in Phase A, but interindividual variability was high. In CC1, 100 mg LipOra increased average OTT AUC_{0-∞} from 0.602 h*ng/mL to 0.907 h*ng/mL, C_{max} from 0.144 ng/mL to 0.246 ng/mL, and relative F from 0.16 % to 0.26 % (p = 0.36). In CC2, 100 mg LipOra increased OTT AUC_{0-∞} from 8.52 h*ng/mL to 10.7 h*ng/mL, C_{max} from 2.05 ng/mL to 2.54 ng/mL, and relative F from 0.31 % to 0.39 % (p = 0.33). Sixty-six adverse events (AE) occurred, of which 43 were considered related. All AEs were Grade 1, except one unrelated Grade 2 AE. There were no serious AEs.

Conclusions: OTT / LipOra was safe and well tolerated. The increase of po OTT F with LipOra was smaller than expected and not statistically significant in CC1 and CC2.

Carcinogenesis

P078

Does 5G FR2 cause genomic instability in human skin? An *in vitro* study in primary skin cells

M. A. Diuani¹, M. Engelke¹, S. Chatterjee¹, M. L. Winkler¹, C. Bär¹, C. Ziemann¹, A. Bitsch¹

¹Fraunhofer Institute for Toxicology and Experimental Medicine (ITEM), Hanover, Germany

The fifth generation of mobile phone technology (5G New Radio [NR]) was rolled out in 2020 to meet the ever-increasing demand for stable and fast internet connection. A major change to 5G NR in comparison to 1G to 4G, which uses the frequency range 1 (FR1; <6 GHz) is the utilization of the frequency range 2 (FR2) in millimeter wavelength (24.25–52.6 GHz). Currently, data on potential adversity of 5G FR2 are limited, whereas FR1 has been studied extensively in the last 30 years. Therefore, European Union Horizon Europe-funded project SEAWave aimed to investigate effects of 5G FR2 exposure on human health, focused on skin cancer induction, as 5G FR2 has low penetration depth in human tissue. Here, we investigated whether intermittent exposure to 27.5 GHz 5G FR2 (10/5 min on/off) can cause genomic instability in three *in vitro* primary human skin cell models, i.e., adult and juvenile keratinocytes (NHEK-c and NHEK-fc, respectively) and adult melanocytes (NHEM). Micronucleus induction (MN), telomere length measurement and DNA methylation landscape served as adversity endpoints. Cells were exposed in a blinded manner to 3 different power densities (sham, 3.33 W/m² and 10 W/m²) for 4 or 24 h, before subjected to peptide-nucleic acid fluorescence in-situ hybridization (PNA-FISH) with DNA counter-staining (MN and telomere analysis) or DNA epigenetic array analysis. Samples were decoded after end of analysis. After 4 and 24 h exposure, 5G FR2 did not induce any MN formation, as cells maintained basal frequency of 0.2% and 0.6% MN in 2000 cells for the NHEKs and NHEM, respectively. When analyzing telomere number and length, a slight decrease in telomere number was detected in NHEK-fc only, after 24 h of exposure to 10 W/m². Exposure of 5G FR2 also did not change the cell type-specific DNA methylation landscape in all skin cell models tested. In conclusion, the findings are in line with our previous observations that 5G FR2 exposure did not induce DNA strand breaks in comet assay and mediated no (NHEK-c and NHEM) or small changes (NHEK-fc) in gene expression [1,2]. The experiments on human skin cells thus indicate that 5G FR2 does not cause genomic instability under the conditions used. As a further endpoint the microRNA landscape will be analyzed after exposure of all three skin cell models to 5G FR2.

References:

1. Diuani M., et. al. (2025), doi: <https://doi.org/10.1007/s00210-025-03881-x>
2. Diuani M., et. al. (2025), doi: <https://doi.org/10.1016/j.toxtlet.2025.07.318>

P079

Targeting Senescence – the key to overcome glioblastoma recurrences?

J. Sallbach¹, M. Woods¹, B. Rasenberger¹, M. Christmann¹, M. T. Tomicic¹

¹University Medical Center Mainz, Department of Toxicology, Mainz, Germany

Glioblastoma (GB) remains one of the most aggressive and fatal cancers of the central nervous system. Standard of care (Stupp-protocol) is radio-chemotherapy consisting of concomitant and adjuvant administration of the monoalkylating agent temozolomide (TMZ). However, relapses are inevitable and patients have a mean survival of approx. one year. The topoisomerase I inhibitor irinotecan (IT) is alternatively used as a second-line treatment for recurrences. In this study we examined the extent and conditions under which IT induces senescence in GB cells and how this could be exploited for recurrent GB therapy [1].

A panel of GB cell lines differing in p53, p21, p14, p16 and PTEN status was analyzed, where only cells with functional p53/p21 axis (e.g. LN229 and A172 cells) induced senescence upon IT. Here, IT exposure led to an increase in senescence-associated beta-galactosidase activity, senescence-associated secretory phenotype (SASP) and senescent cell anti-apoptotic pathways (SCAPs). Interference with p53 activity or reduction of p21 levels in this system completely abrogated senescence induction. When targeting SCAPs by a cIAP1/2 inhibitor, IT-induced senescence was markedly reduced and cell death elevated. p14, p16 and PTEN were not essential for induction of senescence. In p53/p21-deficient lines, IT induced predominantly cell death. In potentially recurrence-forming clones (R-clones), showing elevated p21 levels, as compared to parental LN229 cells, TMZ failed to further induce p21. Conversely, IT exposure effectively raised p21 levels, leading to a pronounced senescence induction and cell death. Distinct response patterns were observed on mRNA level in paired samples from primary and recurrent GB from the same patient. These differences may explain longer progression-free survival, observed in patients who received IT after recurrence emergence rather than continuation of TMZ therapy. Furthermore, these expression profiles may indicate the source of recurrence lying in either senescence escape or avoidance, showing the potential of adjuvant senolytic therapy.

Overall, we found p21 plays a pivotal role in inducing and sustaining senescence upon IT which cannot be substituted by PTEN, p14 or p16. Our results also indicate that the interaction between senescence induction by IT and SCAP inhibition could be a promising therapeutic approach for recurrent GB.

[1] Sallbach J, et al (2024) *Biomed Pharmacother*, 181:117634 doi:10.1016/j.biopha.2024.117634

P083

Threshold concentrations for BPDE-induced cell death are characterized by altered DNA damage signaling and associated with unrepaired double-strand breaks

M. Christmann¹, A. Schmidt¹, M. T. Tomicic¹

¹University Medical Center Mainz, Department of Toxicology, Mainz, Germany

Benzo(a)pyrene (B[a]P), a widespread environmental carcinogen, arises in the course of incomplete combustion. It can be found in tobacco smoke, exhaust fumes and at barbecues. B[a]P is metabolized in the liver to its activated form benzo(a)pyrene-9,10-diol-7,8-epoxide (BPDE). Traditionally, genotoxic carcinogens are thought to exhibit no thresholds, however, cellular defense mechanisms like DNA repair and apoptosis can neutralize low levels of genotoxic stress implying different *Points of Departure* (PoDs) for different cellular endpoints. Here we analyzed whether PoDs for distinct cellular processes induced by BPDE are observed at the same or different level of DNA damage and whether these PoDs correlate with activation of different DNA damage signaling routes. Our data indicate a PoD with a LOAEL (lowest observed effect level) between 0.1 and 0.25 µM for DNA strand break formation, DDR activation, induction of cell death and cellular senescence. A switch from cellular senescence to cell death occurred at a dose of 1 µM and was accompanied by accumulation of DNA strand breaks and was mediated by a switch from the ATR-CHK1-p53Ser15 signaling axis to the ATM-CHK2-p53Ser46 axis of the DDR. Importantly, BPDE-induced mutagenicity was observed only up to a concentration of 0.25 µM including low BPDE concentration that failed to trigger the DDR and concomitant cellular consequences. These results suggest that low BPDE concentrations, which are unable to activate the DDR and DNA damage signaling, are more harmful than DDR-activating concentrations.

P084

Comparative Tissue Selectivity of N-Nitrosamines and Related Nitroso Structures in Rodent Bioassays

J. Irwan¹, A. Londenberg¹, A. Bassan², K. Cross³, S. Greco², S. E. Escher¹

¹Fraunhofer Institute for Toxicology and Experimental Medicine (ITEM), Hanover, Germany

²Innovatune Srl, Padova, Italy

³Instem, Columbus, OH, United States

The presence of N-nitrosamines (NAs) in human medicinal products raises significant concern given their potential carcinogenicity. The MUTAMIND SC05 project investigates the main target organs of NAs observed in existing carcinogenicity studies in animals to inform the study design of future toxicology studies.

Carcinogenicity data were collated from the Carcinogenic Potency Database (CPDB) and supplemented with curated studies from Fraunhofer RepDose® and ECHA CHEM databases, resulting in a project database of 1567 compound and 4638 studies. These studies provide TD50 values, which were complemented with data extracted from the Lhasa CPDB. The current project dataset comprises 86 NAs, 3 N-Nitrosamine Drug-Substance Related Impurities (NDSRIs) derived from active pharmaceutical ingredients (API), as well as a comparative set of 107 primary and 77 secondary aromatic amines. Aromatic amines were included because, like NAs, they require metabolic activation to produce carcinogenic effects, providing a mechanistic reference group for comparison. Relevant data, e.g. tumor sites and organ/tissues, were harmonized. Significant differences of the NA targets/incidence to the other compound groups were determined using Fisher's exact test.

The most frequently observed target organs per chemical group are presented, accounting for the impact of study design differences such as route of exposure, species and treatment duration. Sensitivity differences of target organs are shown, using the current TD50 values.

The results of this analysis point to distinct tissue selectivity of tumor formation by NAs and NDSRIs and will aid in the selection of tissue for sampling and analytical endpoints in *in vivo* mutagenicity studies of NAs for future toxicological evaluations.

P085

Decisive steps in Benzo[a]pyrene-induced cellular senescence

G. Nagel¹, M. Christmann¹

¹Institute of Toxicology, University Medical Center, Johannes Gutenberg University, Mainz, Germany

The polycyclic aromatic hydrocarbon benzo[a]pyrene (B[a]P) is an environmental carcinogen, which arises from incomplete combustion of organic materials. This process is relevant during food preparation or smoking of tobacco as well as in industry or road traffic. Metabolic activation of B[a]P by cytochrome P450 (CYP) 1A1, or to a lesser extent by CYP1A2, leads to bulky adducts at DNA, which could cause DNA double-strand breaks (DSB).

Here we show via various methods that the subtoxic concentration of 1 µM B[a]P induces senescence in metabolic competent MCF-7 cells. Furthermore, 24 hours after B[a]P exposure we found both, phospho-p53 (Ser15) and p21 to be induced. In immunofluorescence experiments at the timepoint of 120 hours we observed a co-localization of γH2AX foci with foci of 53BP1, indicating DSB. This supports a model in which low concentrations of B[a]P, when metabolized to benzo[a]pyrene diol epoxide (BPDE), induce replication-dependent DSB that remain largely unrepaired. No evidence was found for a significant occurrence of DSB at the

telomeres. The resulting DNA damage response could initiate cellular senescence via the p53/p21 signalling pathway. Since p21 was still strongly expressed 120 hours after exposure, this cell cycle regulator could also be involved in maintaining B[a]P-induced senescence.

Striking epigenetic changes were observed in B[a]P-exposed MCF-7 cells. Thus, H3K27m3, which is associated with facultative heterochromatin and acts as a transcriptional repressor, was induced 120 hours post exposure. Another repressive marker, H3K9me2, revealed changes in the staining pattern following treatment with B[a]P. These findings might indicate an epigenetic reprogramming of the cells, probably to downregulate unnecessary processes during B[a]P-induced cellular senescence.

P086

N-nitroso-hydrochlorothiazide: Evaluation of its genotoxic potential *in vitro* in mammalian cell models

M. A. Djuric¹, M. L. Winkler¹, M. Engelke¹, C. Ziemann¹

¹Fraunhofer Institute for Toxicology and Experimental Medicine (ITEM), Genetic Toxicology, Hanover, Germany

Nitrosamine drug-substance related impurities (NDSRIs) are currently treated as cohort of concern compounds, due their potential mutagenicity. N-nitrosohydrochlorothiazide (NHCTZ) represents an NDSRI, derived from hydrochlorothiazide (HCTZ), a thiazide-type anti-hypertensive drug with high prescription rates. Mutagenicity of NHCTZ was previously shown in Ames tests, but most likely based on formaldehyde, as degradation product. As NHCTZ-induced formation of nuclear buds was evident in primary human hepatocytes in the EMA-funded MUTAMIND project without DNA-strand break induction, genotoxicity of NHCTZ was subsequently evaluated *in vitro*, in different mammalian cell models, i.e., human hepatoblastoma HepG2 cells, L-929 mouse fibroblasts, and V79 Chinese hamster lung fibroblasts). Both alkaline comet assays \pm S9-mix, quantification of nuclear bud and micronucleus formation (combined with PNA-FISH), and a hypoxanthine-guanine phosphoribosyltransferase (HPRT)-test were performed to cover the endpoints clastogenicity, aneugenicity, and mutagenicity. In both HepG2 cells (4 h; \pm S9-mix) and L-929 cells (4 h; -S9-mix) incubated with 0.5–5 mM NHCTZ, comet assays were consistently negative but nuclear buds were significantly increased in HepG2 cells at 5 mM. Subsequently, micronucleus tests without S9-mix (4 h incubation + 44 h recovery) and reduced concentrations were done to enable sufficient cell proliferation, as cytotoxicity was evident in L-929 cells at 5 mM NHCTZ. L-929 cells treated with 0.125–2 mM NHCTZ for 4 h showed micronucleus formation, starting already at 0.125 mM with a fold change of 4.3, compared to negative controls. Parallel PNA-FISH indicated that detected micronuclei mostly contained both telomere and centromere signals (starting at 0.5 mM), thus indicating aneugenic mechanism of micronucleus formation. In line with these results, HepG2 cells showed about 2-fold increase in micronuclei at 0.1 and 0.25 mM NHCTZ. To finally look for mutagenicity (DNA base mutations) of NHCTZ, an HPRT-test was performed with V79 cells (0.125 and 0.25 mM NHCTZ, 4 h), but no enhanced mutation frequency was detected. In conclusion, the present results indicate that NHCTZ exhibits no clastogenic and mutagenic potential but might trigger aneugenic events with loss of chromosomes. Further tests with the parent compound of NHCTZ, i.e., HCTZ, and its degradation products, e.g., formaldehyde will now be performed to evaluate nitrosamine-specificity of the observed effects.

Drug transport/delivery and metabolism

P087

In vitro and in vivo studies on the effects of OCT/MATE inhibitors on novel potential biomarkers for OCT2/MATE-mediated renal drug-drug interactions

J. Picurová¹, F. Müller^{1,2}, J. König¹, M. F. Fromm¹, A. Gessner¹

¹Friedrich-Alexander University of Erlangen-Nuremberg, Institute of Experimental and Clinical Pharmacology and Toxicology, Erlangen, Germany

²Boehringer Ingelheim Pharma GmbH & Co. KG, Biberach an der Riß, Germany

Introduction & Objectives

Transporters are crucial for the renal elimination of drugs. Organic cation transporter 2 (OCT2) and multidrug and toxin extrusion proteins (MATE1 and MATE2-K) determine the renal excretion of metformin and other clinically important drugs. The regulatory guideline ICH M12 on drug interaction studies requires the evaluation of potential OCT2/MATE-mediated drug-drug interactions (DDI) during drug development. Endogenous biomarkers are an emerging tool to improve risk assessment for transporter-mediated DDI and to reduce the number of DDI studies in healthy volunteers. However, currently only few biomarkers are fully validated for clinical DDI risk assessment.

In a previous metabolomics study, urinary excretion of serotonin, 1-methylhistamine and 5-aminovaleic acid betaine was significantly reduced by cimetidine, a classical OCT/MATE inhibitor. All three potential biomarkers are substrates of OCT2 and MATE1. In the current study *in vitro* inhibition experiments using the three potential biomarkers as substrates with four clinically used OCT/MATE inhibitors were performed. Moreover, *in vivo* sensitivity of serotonin, 1-methylhistamine and 5-aminovaleic acid betaine to treatment with the OCT/MATE inhibitor trimethoprim was evaluated in order to provide new insights into their potential suitability as biomarkers for OCT2/MATE-mediated DDI.

Methods

IC₅₀ values for the inhibition of OCT2- and MATE1-mediated transport of serotonin, 1-methylhistamine and 5-aminovaleic acid betaine by four classical

inhibitors (trimethoprim, cimetidine, pyrimethamine and dolutegravir) were determined using cell models stably overexpressing the respective transporters with substrate quantification via scintillation counting or LC-MS. Moreover, a validated LC-MS method was used to determine the impact of trimethoprim on disposition of these biomarkers in plasma and urine samples of healthy volunteers.

Results

In vitro data revealed that trimethoprim inhibited the OCT2-mediated uptake of serotonin and 1-methylhistamine with IC₅₀ values of 67.3 μ M and 131.0 μ M, respectively. Moreover, plasma concentrations of 5-aminovaleic acid betaine were decreased by trimethoprim in healthy volunteers.

Conclusion

This study provides novel insights into the potential use of serotonin, 1-methylhistamine and 5-aminovaleic acid betaine as biomarkers in clinical studies with the objective of improving risk assessment for transporter-mediated drug-drug interactions.

P088

Rifabutin enhances intracellular rifampicin uptake in THP-1 derived M2 macrophages by P-gp inhibition

K. Hamburg^{1,2}, C. Bay¹, J. Weiß¹, J. Burhenne¹, D. Theile¹

¹Medizinische Klinik, Universitätsklinikum Heidelberg, Innere Medizin 9, Abteilung für Klinische Pharmakologie und Pharmakoepidemiologie, Heidelberg, Germany

²Heidelberg University, Graduate Academy, Heidelberg, Germany

Question:

The influence of pro-inflammatory M1 and anti-inflammatory M2 macrophages on the pathogenesis of tuberculosis is studied broadly. M2 macrophages are known to be more prominent in multidrug resistant granuloma than M1 cells [1]. Also, M2 macrophages have been shown to exhibit higher P-gp activity, potentially mediating rifampicin resistance by lowering its uptake. However, cellular rifampicin kinetics in M2 has been unknown so far. This study investigated the uptake of rifampicin in THP-1 monocytes-derived M1 and M2 macrophages. Finally, we examined if the recently identified potent P-gp inhibitor rifabutin can restore rifampicin accumulation in M2 macrophages.

Methods:

For differentiation of THP-1 monocytes to macrophages, 200 nM phorbol-12-myristate-13-acetate (PMA) was used for 3 days. After resting for 5 days, cells were polarized for 48 h either to the M1 (50 ng/mL lipopolysaccharides; 20 ng/mL interferon gamma) or the M2 subtype (interleukin-4, interleukin-13; 20 ng/mL each). Rifampicin kinetics into M1 and M2 was measured using ultra-performance liquid chromatography coupled to tandem mass spectrometry (UPLC-MS/MS). Concentration-dependent inhibition of P-gp by rifabutin was analyzed by flow cytometry (rhodamine 123 efflux) and its impact on rifampicin accumulation by UPLC-MS/MS.

Results:

High P-gp activity in M2 macrophages was associated with impaired rifampicin uptake compared to M1 macrophages. Potent P-gp inhibition was confirmed for rifabutin (EC₅₀ 0.8 μ M; 10 μ M enhancing rhodamine fluorescence 2.6-fold); but not rifampicin (10 μ M only enhancing rhodamine fluorescence 1.4-fold). Finally, combining 0.05 μ M rifampicin with rifabutin (0.01 – 10 μ M) significantly enhanced rifampicin uptake into M2 macrophages.

Conclusion:

Activity of P-gp and uptake of its substrates (e.g. rifampicin) differ between the macrophage phenotypes. Consequently, this is a potential rifampicin resistance mechanism of M2 macrophages that contributes to the poor treatment outcome of M2-enriched tuberculosis granulomas. More importantly, we here offer a solution to this problem: Adding rifabutin to rifampicin to restore rifampicin accumulation in M2 cells is a promising outlook for future drug therapy of tuberculosis patients.

References: [1] Cho, H.J., Lim, Y.J., Kim, J. et al. Different macrophage polarization between drug-susceptible and multidrug-resistant pulmonary tuberculosis. BMC Infect Dis 20, 81 (2020). <https://doi.org/10.1186/s12879-020-4802-9>

P089

Aptamer-based approaches for immunotargeting: Enhancing drug delivery by combining aptamers with pharmaceuticals

J. Stahnke¹, Y. Kerler¹, M. G. Schulze¹, M. Menger¹, F. Ramm¹

¹Fraunhofer-Institut für Zelltherapie und Immunologie (IZI-BB), Potsdam, Germany

Targeted drug delivery is an increasingly important approach in modern therapeutics, aiming to enhance treatment efficacy while minimizing off-target effects. Aptamers are short single-stranded DNA or RNA molecules that fold into

specific three-dimensional structures, allowing them to bind their targets with high affinity and specificity.

In this study, we focus on the application of aptamers targeting clinically relevant surface proteins: the interleukin-7 receptor (IL7R) which is a protein complex found on immune cells, namely T cells and B cell precursors. The IL7R is essential for the development, survival, and homeostasis of lymphocytes. Defects in the IL7R or its signaling pathway can cause severe immunodeficiencies, such as Severe Combined Immunodeficiency, due to the failure of proper T cell development. Conversely, overactive IL-7R signaling has been linked to autoimmune diseases and leukemias. Building on this knowledge, our goal is to develop IL7R-specific aptamers capable of recognizing receptor variants that carry disease-related mutations which can be used as targeted delivery vehicles, enabling the transport of therapeutic cargos, such as small molecules or receptor-modulating agents to affected cells. Another important surface protein involved in T cell function is CD4, a key marker on T-helper cells involved in immune regulation and HIV infection. CD4 was explored as a potential immunomodulatory target, enabling selective interaction with CD4⁺ T cells. CD4-specific aptamers could be conjugated to toxins to selectively eliminate CD4⁺ leukemic cells, such as those found in T-cell acute lymphoblastic leukemia or peripheral T-cell lymphomas.

Aptamer selection is performed using SELEX (Systematic Evolution of Ligands by EXponential enrichment), involving cycles of incubation, binding, and amplification to enrich high-affinity sequences. Binding affinities are evaluated using electrophoretic mobility shift assays, microscale thermophoresis, and fluorescence-linked aptamer assays. Functional validation includes fluorescence imaging and flow cytometry to assess target engagement and uptake. Aptamers combined with pharmaceuticals are tested with endosomal escape enhancers to improve uptake. These EEAs are further characterized for hemolytic and mutagenic effects.

Our results demonstrate the potential of aptamers as targeting tools with promising applications in cancer treatment, immunomodulation and other therapeutic approaches.

P090

Munronia pinnata* as an application of pharmacological properties of plant-based remedies to rely on traditional medicine for primary health care** ***S. Hapuarachchi

¹Faculty of Indigenous Medicine, University of Colombo, Ayurveda Pharmacology, pharmaceuticals and Community Medicine, Sri Jayawardanapura, Sri Lanka

Indigenous medical systems have evolved into structured frameworks for diagnosing and treating disease, with a substantial portion of the global population still relying on traditional medicine for primary health care. These systems emphasize a holistic view of health and wellness. This study aimed to explore the pharmacological potential of *Munronia pinnata* [(Wall) Theob (Meliaceae)], a widely used traditional medicinal herb in traditional medicine for primary health care systems. *Munronia pinnata* (MP) is an important traditional medicinal herb in Sri Lanka, to support its scientific application in primary health care. The powdered plant and decoctions of MP are used traditionally for various inflammatory, hepatic, and metabolic disorders. In this study, aqueous (MPA) and ethanol (MPE) extracts of MP were evaluated in vivo for anti-inflammatory, hepatoprotective, and mechanism of hypoglycaemic activity using standard experimental animal models. Based on the previously established oral hypoglycaemic effects, mechanistic studies demonstrated that both extracts significantly reduced intestinal glucose absorption and serum glucose concentrations compared to control groups (following glucose challenge). The hepatoprotective study confirmed the potential of MP extracts as therapeutic agents for hepatic disorders. Anti-inflammatory evaluation using the carrageenan-induced rat paw oedema model revealed significant inhibition of inflammation in both healthy and diabetic Wistar rats treated with MPA and MPE compared to distilled water controls. MPA also significantly reduced peritoneal phagocytic cell infiltration and nitric oxide production in peritoneal cells, indicating an immunomodulatory mechanism. These findings scientifically validate the traditional use of *Munronia pinnata* as an anti-inflammatory, hepatoprotective, and hypoglycaemic agent and support the integration of validated herbal remedies into primary health care frameworks, promoting safe and evidence-based use of traditional medicine.

Key words: Traditional medicine, *Munronia pinnata*, hypoglycaemic activity, hepatoprotective activity, anti-inflammatory activity.

References:

Hapuarachchi, S. D., Suresh, T. S., Senarath, W. T. P. S. K. A preliminary study of the oral hypoglycaemic activity of ethanolic and water extracts of *Munronia pinnata* in healthy Wistar rats. Sri Lankan Journal of Indigenous Medicine 2011a; 1(1):1-4.

P091

Blood-brain barrier permeability screening in 3D-spheroids with UPLC-MS/MS quantification

C. Bay¹, E. Mühlig^{2,3}, M. Kästing¹, J. Chu¹, G. Bajraktari-Sylejmani¹, P. Uhl^{1,2}, J. Burhenne¹, M. Sauter¹, J. Weiß¹

¹Heidelberg University Hospital, Department of Clinical Pharmacology & Pharmacoevidentiology, Heidelberg, Germany

²Heidelberg University Hospital, Department of Nuclear Medicine, Heidelberg, Germany

³Heidelberg University, Institute of Pharmacy and Molecular Biotechnology, Heidelberg, Germany

Question: The blood-brain barrier (BBB) protects and nurtures the central nervous system (CNS). However, it impedes the effective delivery of several drugs to the brain. Furthermore, for non-CNS drugs, BBB permeability represents a crucial factor in preventing serious adverse effects in the CNS. Consequently, the evaluation of BBB permeability is of paramount importance in the preclinical development of novel or repurposed therapeutic agents. We evaluated and optimized a screening-platform centering on 3D-BBB-spheroid model for the permeability assessment of drugs using ultra-performance liquid chromatography tandem mass spectrometry (UPLC-MS/MS).

Methods: Based on the protocol for 3D-BBB-spheroids (Bergmann et al., 2018), composed of primary human astrocytes, pericytes and immortalized brain capillary endothelial cells (hCMEC/D3), we developed a simple and fast setup to measure intra-spheroidal drug concentrations with UPLC-MS/MS on a single-spheroid level. The expression of BBB markers and the correct cell localization were evaluated with CellTracker™ probes and antibody staining imaged by confocal laser scanning microscopy. The paracellular integrity of the spheroids was evaluated concomitantly during each permeability experiments with a newly developed D-amino acid-based dipeptide permeability marker as an internal control.

Results: Our UPLC-MS/MS assay for 3D-BBB-spheroids enables the screening of BBB permeability in a 96-well format, offering a time- and cost-efficient approach. The subsequent evaluation of the translational relevance of this model can be achieved by correlating the *in vitro* spheroid-to-incubation-ratios with published *in vivo* brain-to-plasma-ratios. The novel permeability marker as an internal control for paracellular integrity can be simultaneously used to exclude compromised spheroids.

Conclusions: In summary, we developed an experimental setup for preclinical analysis of BBB permeability in single 3D-BBB-spheroids, measured with UPLC-MS/MS. The parallel integrity control has the potential to enhance translational significance while facilitating straightforward and expeditious drug screening.

Reference:

Bergmann S, Lawler SE, Qu Y, Fadzen CM, Wolfe JM, Regan MS, Pentelute BL, Agar NYR, Cho CF. Blood-brain-barrier organoids for investigating the permeability of CNS therapeutics. Nat Protoc. 2018 Dec;13(12):2827-2843. doi: 10.1038/s41596-018-0066-x.

P092

Fine-tuning drug efficacy and inflammation at the endosomal barrier

A. M. Wölbern¹, J. Stahnke¹, F. Flores Espinoza¹, F. Ramm¹

¹Fraunhofer-Institut für Zelltherapie und Immunologie (IZI-BB), Bioanalytik und Bioprozesse, Potsdam, Germany

The behavior of drugs in endosomal compartments has a tremendous effect on their efficacy and immunogenicity. Endosomes represent a barrier that most drugs need to overcome, and a certain degree of damage to endosomal membranes may be necessary before they can unfold their effects. However, leaky or broken endosomes can lead to the formation of active NLRP3-inflammasomes. This can lead to detrimental side effects during reoccurring treatments, such as chemo- or protein replacement therapy– or present an advantage for vaccines.

To support the release of drugs from endosomes, a diverse set of endosomal escape enhancers that can disrupt endosomal membranes has been identified. We studied nine different endosomal escape enhancers, including plant-derived saponins, lysosomotropic amines, cationic polymers and a calcium-channel antagonist with the potential to improve drug efficacy and increase or mitigate inflammation. Toxicity experiments revealed varying effects on HeLa cells even from enhancers with the same mechanism. We characterized the endosomal damage caused by different enhancers by studying galectin recruitment to endosomes and assessed the effect of enhancers on the expression of inflammatory markers (NLRP3, ASC, IL-1β), as well as the activation of the NLRP3 inflammasome. Further, we determined other side-effects, such as hemolysis, ROS production, and effects on translation. Our data demonstrate the necessity to evaluate the characteristics of endosomal escape enhancers before co-administration with drugs to fine-tune drug efficacy and inflammation.

CNS

P093

Reduced Epileptogenic Threshold in Alzheimer's Diseases: Experimental Validation and Neurochemical Interplay

A. Kaur¹, R. K. Goel¹

¹Punjabi University Patiala, Department of Pharmaceutical Sciences and Drug Research, Patiala, India

Background: Alzheimer's diseases (AD) is increasingly associated with reduced seizure threshold suggesting a bidirectional relationship with epilepsy. Emerging evidence highlight shared neurochemical alterations including excitatory and inhibitory balance a key contributors in hyperexcitability. Therefore, current study is designed to address reduced seizure threshold in the context of STZ (streptozotocin) induced Alzheimer's disease, by evaluating the susceptibility to chemo convulsions. The ultimate aim is to identify the shared neurochemical targets for management of AD

Methods: Swiss albino mice were underwent for streptozotocin ICV injections and pentyleneetetrazol (PTZ) kindling. Seizure threshold was validated by injecting PTZ(35mg/kg) in STZ mice. Following kindling behavioral parameters was done for STZ, PTZ and STZ + PTZ mice such as elevated plus maze (EPM), novel object recognition test (NORT) and radial arm maze (RAM) test. Animal were sacrificed and brain sample were collected for biochemical (GSH, TBARS, ROS and AChE) estimation and neurochemical analyzing using HPLC ECD method.

Results: Results revealed reduced onset of seizure and increased seizure severity in STZ mice as convulsive seizures observed compared to PTZ mice. Behavioural assessments indicate significant cognitive impairment in STZ + PTZ, STZ and PTZ group compared to saline treated in EPM, NOR and RAM test. Further significant reduced GSH and elevated level of TBARS, ROS, AChE indicates increased oxidative stress and cholinergic dysfunctioning. Neurochemical analysis showed increased level of glutamate, glutamine and reduced level of glycine and GABA signify imbalance of excitatory and inhibitory response in STZ + PTZ, STZ and PTZ group. Moreover, reduced level of nor-epinephrine, dopamine serotonin support impaired cognition. However, more significant results were observed in STZ + PTZ, in comparison to AD control (STZ) and epileptic control (PTZ) mice.

Conclusion: The administration of PTZ showed reduced seizure threshold in STZ induced AD mice associated with increased oxidative stress, cholinergic dysfunction, excitatory-inhibitory neurotransmitter imbalance, and reduced monoaminergic transmission. These findings suggest a potential bidirectional link between epilepsy and Alzheimer's disease pathology and shared neurochemical targets.

P094

RIPK1 inhibition reduces NEMO deletion induced vascular pathology in CSVDs

T. C. Faupel¹, J. Lampe¹, R. Strasburger¹, Ü. Özörhan¹, A. Buhmann¹, P. Ehrlich¹, M. Schwanninger¹

¹Universität zu Lübeck, Institut für Experimentelle und Klinische Pharmakologie und Toxikologie, Lübeck, Germany

Targeting receptor-interacting protein kinase (RIPK)1 could offer therapeutic potential for ameliorating microvascular pathology in *Incontinentia Pigmenti* (IP) and other cerebral small vessel diseases (CSVDs). IP is caused by mutations in the *IKBKG* gene, encoding the NF- κ B essential modulator (NEMO) protein. One-third of patients with IP show neurological symptoms including seizures and intellectual disability due to NEMO deficiency in endothelial cells causing the blood-brain barrier (BBB) to become leaky. We found that the SARS-CoV-2 main protease Mpro cleaves NEMO, providing a mechanism by which COVID-19 induces a NEMO deficiency and contributes to CSVD.

To model CSVD, we generated mice with a conditional knockout of *Ikbkg* in brain endothelial cells (*NemobekO* mice). We investigated vascular parameters by immunofluorescence staining and confocal microscopy of brain sections. Images were analyzed by Fiji macros.

NemobekO mice revealed a severe microvascular pathology. It was characterized by the formation of string vessels which are empty basement membrane tubes due to the death of brain endothelial cells, rarefaction of brain microvessels, cerebral hypoperfusion, IgG leakage in the brain parenchyma as a measure of a disrupted BBB, as well as epileptic seizures.

We hypothesized that the inhibition of RIPKs, central mediators in necroptosis, can prevent vascular pathology induced by the NEMO-deletion. Therefore, we crossed *NemobekO* mice with *Ripk3* knockout mice or animals with a kinase-dead *Ripk1* mutation (*Ripk1 D138N*). Genetic deletion of *Ripk3* delayed the onset of *NemobekO* induced vascular pathology whereas genetic *Ripk1* kinase inhibition caused a long-lasting prevention of the pathology. In addition to the genetic approaches, we treated *NemobekO* mice with the pharmacological RIPK1 inhibitor RA¹⁸⁷. This treatment strongly reduced several hallmarks of the NEMO deficiency induced vascular pathology 2 weeks post knock out induction.

Overall, this study provides new insights into the molecular mechanisms driving brain endothelial cell pathology and suggests that targeting RIPK1 offers a therapeutic potential for ameliorating endothelial cell death in IP and other CSVDs such as Alzheimer's disease, stroke, COVID-19 or aging-related vascular degeneration.

P095

Linalool Reverses Thermal Hypersensitivity in Experimental Diabetic Neuropathy via Catecholaminergic (α_2 , β_2) Signaling

Ü. Kandemir¹, C. Yazıcı², Ü. Demir Özkay², Ö. D. Can²

¹Bilecik Şeyh Edebali University, Medical Pharmacology, Bilecik, Turkey

²Anadolu University, Department of Pharmacology, Eskişehir, Turkey

Objective: Painful diabetic neuropathy (PDN) affects roughly one-third of individuals with diabetes and remains difficult to treat due to multifactorial pathophysiology. Linalool, a naturally occurring monoterpene, exhibits analgesic, anti-inflammatory, antioxidant, and neuroprotective activities. Building on our prior work showing that linalool (75–150 mg/kg, i.p.) normalizes heat-evoked sensory abnormalities in streptozotocin (STZ)-diabetic rats [1], we investigated whether catecholaminergic mechanisms underlie its anti-hyperalgesic and anti-allodynic effects.

Methods: Experimental diabetes was induced by intravenous streptozotocin (STZ, 50 mg/kg). Thermal allodynia was assessed on the warm-plate (38 °C) and

thermal hyperalgesia with the Hargreaves' method. Linalool (75 mg/kg, i.p.) was tested alone and under pharmacological interference of catecholaminergic signaling. AMPT (α -methyl-p-tyrosine; catecholamine synthesis inhibitor, 200 mg/kg, i.p.) was administered 4 h before linalool to allow acute catecholamine depletion. Yohimbine (α_2 -adrenoceptor antagonist, 2 mg/kg, i.p.) and ICI 118,551 (β_2 -adrenoceptor antagonist, 1 mg/kg, i.p.) were given 15 min before linalool. All procedures were approved by the Anadolu University Animal Experiments Local Ethics Committee.

Results: In STZ-diabetic rats, linalool significantly attenuated both thermal hyperalgesia and allodynia. Pre-treatment with AMPT, yohimbine, or ICI 118,551 abrogated linalool's anti-hyperalgesic and anti-allodynic actions on both assays, implicating catecholaminergic, particularly adrenergic, pathways. These data point to a contributory role of α_2 - and β_2 -adrenoceptors in mediating linalool's efficacy.

Conclusions: Linalool's antihyperalgesic and antiallodynic effects in PDN-like pain depend on intact catecholaminergic signaling, consistent with engagement of noradrenergic mechanisms via α_2 - and β_2 -adrenoceptors. Further work using receptor-selective tools or neurochemical assays is warranted to delineate its mechanism of action more precisely.

Keywords: Allodynia, catecholaminergic system, ICI 118,551, linalool, thermal hyperalgesia, yohimbine.

Reference

[1] Yazıcı C, Kandemir Ü, Demir Özkay Ü, Can OD. Linalool reduces thermal stimulus-induced abnormalities in the pain sensation of rats with diabetes. International Gevher Nesibe Health Sciences Conference-XI, October 10-11, 2023, Ankara, Türkiye.

P096

Identification and in vitro Evaluation of Potential Acetylcholinesterase Inhibitors for Alzheimer's Disease via Drug Repurposing Approach

B. Ciftci¹, Ş. Beydemir²

¹Bilecik Şeyh Edebali University, Vocational School of Health Services, Bilecik, Turkey

²Anadolu University, Department of Pharmacy, Eskişehir, Turkey

INTRODUCTIONAlzheimer's disease (AD) currently lacks an effective treatment capable of halting disease progression (1).Computational drug repositioning enables the reuse of existing toxicological and clinical data, providing a faster and safer discovery process (2).The aim of this study was to identify potential drug candidates for AD and verify their efficacy *in vitro*.

METHODSGene expression profiles for AD were obtained from the NCBI GEO database (GSE48350). The GEO2R tool was used to analysis identified genes up- and down-regulated in AD by selecting genes with an adjusted p-value less than or equal to 0.05, as well as genes with a log fold change (logFC) greater than or equal to 1, or less than or equal to -1.Potential candidate molecules were identified through the Connectivity Map (cMAP) platform on clue.io.Based on cMAP analysis, the following compounds were identified as candidates; dehydroisoandrosterone, moricizine, SKF-96365, KU-0063794, ouabain, proscillaridin, digoxin, WYE-354, MK-212, parabendazole and cinobufagin.The *in vitro* activity of the selected candidates was evaluated using the Ellman method through acetylcholinesterase (AChE) enzyme inhibition. IC_{50} and K_i values were calculated and tacrine was used as a positive control.

RESULTSThe IC_{50} values of the investigated compounds ranged from 31.181 nM to 113.134 nM, while the IC_{50} value for tacrine was 33.052 nM. K_i values were measured between 8.065 \pm 4.700 nM and 123.164 \pm 92.915 nM, with the K_i value for tacrine at 7.177 \pm 4.429 nM. Ouabain (Na⁺/K⁺-ATPase inhibitor) had the lowest IC_{50} value at 31.181 nM, indicating non-competitive inhibition.

CONCLUSIONSOne of the limitations of the study is that gene expression data were obtained from open access databases and the consistency of these data may vary.This study also limited its methodology by evaluating only *in vitro* AChE inhibition.Therefore, although some compounds appear to have potential for AD treatment through AChE inhibition, their clinical relevance will remain limited unless their *in vitro* AChE inhibition effects are supported by parameters such as *in vivo* bioavailability, blood-brain barrier permeability, metabolic stability and toxicity.

This study was supported by the Scientific Research Projects Coordination Unit of Anadolu University under project number TYL-2024-2572.

KEYWORDS:drug repositioning,Alzheimer's disease,AChE

REFERENCES:(1)Molecular Neurodegeneration, 2018, 13(1):64,(2)Applied Sciences, 2020, 10(15):5076

P097

Centrally-Mediated Antinociceptive Effects of Some Novel Pyrazoline Derivatives

İ. Rahat¹, D. Osmaniye², N. Turan Yücel³

¹Anadolu University, Institute of Graduate Education, Eskişehir, Turkey

²Anadolu University, Department of Pharmaceutical Chemistry, Eskişehir, Turkey

³Anadolu University, Department of Pharmacology, Eskişehir, Turkey

Pyrazoline ring is a five-membered heterocyclic structure which has been demonstrated to have various biological effects. In the present study, twelve original pyrazoline derivatives (3a–3l) were synthesized and the potential antinociceptive effects of these compounds on animals were investigated. Nuclear magnetic resonance spectroscopy (^1H -NMR and ^{13}C -NMR) method was used to elucidate their chemical structure. The motor activities of mice (Balb-c, 30–35 g) following the administration of derivatives (at a dose of 100 mg/kg, *i.p.*) were examined using the activity meter test, and the possible antinociceptive effects of the compounds were evaluated using hot plate, tail immersion and tail clip tests. The test derivatives did not induce a significant change in the motor performance of mice. The compounds coded 3i–3l increased the reaction times of the mice to thermal and mechanical painful stimuli in the hot plate and tail clip tests; indicating that the substances exerted their effects through the supraspinal and spinal pathways, respectively. Furthermore, the test compounds coded 3h, 3j, 3l showed antinociceptive activity against thermal painful stimulus in the tail immersion test, which was mediated by spinal mechanisms. These findings corroborate earlier studies suggesting the antinociceptive activity potential of compounds bearing pyrazoline ring. However, a comprehensive investigation into the underlying mechanism of centrally-mediated effects of these pyrazoline compounds is necessary to determine their potential as drug candidates.

Keywords: Antinociceptive, Hot plate test, Pyrazoline, Tail clip test, Tail immersion test

P098

Do the effects of the fixed-dose combination aspirin/paracetamol/caffeine (APC) for treating acute headache differ in males and females? Analysis of data from an observational study

J. Weiser¹, C. Gaul²

¹A. Nattermann & Cie. GmbH, Medical Affairs CHC, Frankfurt a. M., Germany

²Kopfschmerzszentrum Frankfurt GbR, Frankfurt a. M., Germany

Question: Are the treatment effects of APC different in males and females?

Methods: New analysis of data from a pharmacy-based survey [1]. Patients buying a specific brand of an APC product (250/200/50 mg or 250/250/50 mg per tablet) in community pharmacies were offered a questionnaire with questions about demographic data, pain severity, number of days with pain/impaired daily activities per month, previous experience with the product, number of tablets taken to treat the pain event, onset of analgesic effect, assessments of perceived efficacy and tolerability, willingness to recommend APC to others. Results were stratified to sex. Analysis with descriptive statistics (Mann-Whitney and contingency tests).

Results:

In total, 945 patients took APC for treating headache (including migraine); 265 (27%) were male, 688 (73%) were female.

Means with standard deviations (SD) of baseline pain intensity were 5.6 ± 1.7 in males, and 5.8 ± 1.7 in females ($p=0.19$; Fig. 1A; NRS, numeric rating scale). Males reported 4.4 ± 4.5 pain days per month, females 5.1 ± 4.9 ($p=0.015$; Fig. 1B). Days with impaired activities were 1.0 ± 2.8 , and 1.3 ± 2.7 for males and females ($p=0.009$; Fig. 1C). The number of tablets taken to treat one headache episode was similar between males and females (1 tablet: 63% and 70%; 2 tablets: 37% and 30%; $p=0.3$; Fig. 1D).

About 22% reported onset of pain relief within 15 min (about 70% within 30 min) with no relevant effect of sex ($p=0.45$; Fig. 2A). More than 95% of males and females assessed efficacy to be "very good" or "good" ($p=0.42$; Fig. 2B), with similar results for tolerability ($p=0.38$; Fig. 2C). 89% of males and 96% of females would recommend APC to others ($p=0.41$; Fig. 2D). Previous experience with the product did not affect the findings (data not shown).

Discussion and Conclusion:

APC relieves (migraine) headache pain more effectively than aspirin, paracetamol, ibuprofen and sumatriptan [2, 3, 4]. In our sample, headache burden in women was higher than in men (days with headache/impaired daily activities per month). Treatment effects of APC were comparable between men and women. Thus, APC is well suited for the treatment of acute headache irrespective of sex.

References:

- [1] Gaul et al. SpringerPlus. 2016; 5:721–729
- [2] Diener et al. Cephalalgia. 2005; 25:776–87.
- [3] Goldstein et al. Headache. 2006; 46:444–53.
- [4] Goldstein et al. Headache 2005; 45:973–82

Sponsor: A. Nattermann & Cie. GmbH

Fig. 1

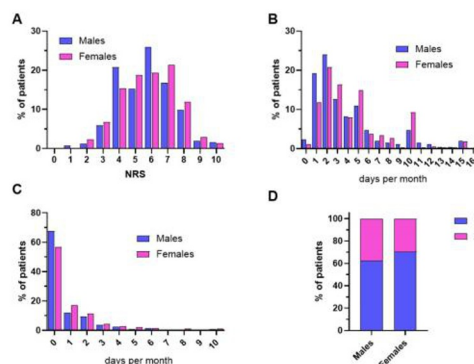


Figure 1: (A): baseline pain; (B) headache days per month; (C) days per month with headache-impaired activities; (D) numbers of tablets taken for treating the investigated headache attack. NRS: numerical rating scale; Tab: tablet.

Fig. 2

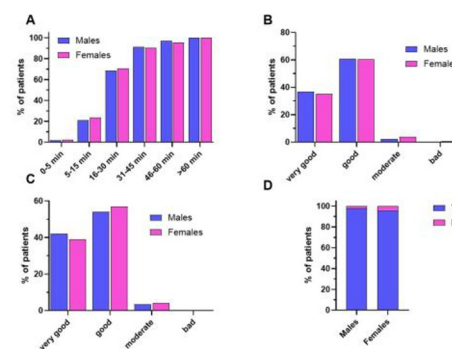


Figure 2: (A) Onset of pain relief; (B) perceived efficacy; (C) perceived tolerability; (D) willingness to recommend the branded APC product to others.

Endocrine Toxicology

P099

ThyreoSafe: Validation of In Vitro Assays Targeting Key Mechanisms of Thyroid Hormone Homeostasis

K. Stefanidis^{1,2}, S. Arnold³, D. Hilgert⁴, S. Krey⁴, B. Kleuser², T. May⁵, K. Renko³, L. Schomburg⁴, N. Hambrich¹, D. Funk-Weyer¹, R. Landsiedel^{1,2}

¹BASF SE, Experimental Toxicology and Ecology, Ludwigshafen, Germany

²Free University of Berlin, Pharmacy, Pharmacology and Toxicology, Berlin, Germany

³German Federal Institute for Risk Assessment (BfR), Berlin, Germany

⁴Charité - Universitätsmedizin Berlin, Institute of Experimental Endocrinology, Berlin, Germany

⁵Inscrenax, Brunswick, Germany

Disruption of thyroid hormone (TH) homeostasis by chemicals poses health risks, affecting brain development and metabolism. Regulatory authorities increasingly demand, mechanistically informed test strategies to identify endocrine disruptors. The ThyreoSafe project aims to establish and validate a battery of *in vitro* assays to investigate chemical effects on the TH system, with a focus on reducing and replacing animal testing. While other initiatives also aim to validate test systems for thyroid disruption, they often lack critical components such as laboratory transfer and blinded testing. These elements are essential to ensure reproducibility, reliability and regulatory confidence across different settings.

In the focus of ThyreoSafe are the sodium-iodide symporter (NIS), thyroperoxidase (TPO) and the three Deiodinase (DIO) isoforms DIO1, DIO2, and DIO3, as crucial molecular key functions contributing to TH biosynthesis and metabolism. NIS facilitates iodide uptake into the thyroid gland, TPO catalyses the synthesis of hormone precursors and the DIOs regulate TH activation and inactivation in peripheral tissues. Partially established *in vitro* assays for NIS, TPO, and DIO are being optimized and harmonized SOPs are transferred to partner laboratories to ensure robustness, reproducibility and sensitivity. This work combines EU-NETVAL and academic efforts and addresses the key regulatory endpoints prioritized by EFSA and ECHA, to facilitate regulatory acceptance. Within the project developed robust and standardized recombinant cell lines serve as test systems with the goal to make these available under FRAND conditions. For each assay, transfer of SOPs and training between partners will take place, followed by a blinded currently ongoing ring study. This approach ensures methodological consistency and collaborative validation across all endpoints.

ThyreoSafe's integrative approach includes interlaboratory validation, transferability studies, and aims to conceptualize an Integrated Approach to

Testing and Assessment (IATA). The goal is the inclusion of these assays in OECD test guidelines, enabling global regulatory acceptance and widespread adoption. By providing reliable, human-relevant toxicological data with new approach methodology, ThyreoSafe will contribute to the reliable assessment of substances affecting thyroid homeostasis and are therefore potentially endocrine-disrupting chemicals, while reducing or eliminating the need for animal studies.

P100

Physiologically-Based Quantitative System Toxicology Thyroid Hormones Modeling Platform: Species-dependent Thyroid Hormone Changes by Test Substances in Rats and Humans

S. Melching-Kollmuss¹, P. Balazki², E. Fabian³, R. Lesage², B. Riffle¹, S. Stinchcombe¹, S. Schaller², R. Landsiedel^{3,4}

¹BASF SE, Global Toxicology, Agriculture Solutions, Limburgerhof, Germany

²EsqLABs GmbH, Saterland, Germany

³BASF SE, Experimental Toxicology and Ecology, Ludwigshafen, Germany

⁴Free University of Berlin, Pharmazie, Pharmakologie und Toxikologie, Berlin, Germany

Introduction

Disruption of the thyroid hormone (TH) homeostasis by endocrine-disrupting chemicals poses a potential health concern. The extrapolation of animal data to humans is of special interest because (TH) regulation differs between species. These differences may lead to species-specific sensitivities to substances that disturb TH homeostasis, for example, through the indirect mechanism of liver enzyme induction.

Objectives

The presented project aims to develop a physiologically based kinetics (PBK) quantitative systems toxicology (QST) model for predicting TH levels following exposure to test substances in rats and humans.

Materials & Methods

The model was constructed using the Open Systems Pharmacology (OSP) Suite Version 12, integrating PBK models of thyroid-active compounds with QST modules for TH regulation and quantitative adverse outcome pathway (qAOP) modules. The modular architecture allows for the incorporation of new compounds and physiological processes. Model validation was performed using Quarto and the {esqlabsR} package.

Results and Discussion The QST modules encompass pituitary synthesis of thyroid-stimulating hormone (TSH), feedback-controlled synthesis of triiodothyronine (T3) and thyroxine (T4), species-specific plasma protein binding, and active transport and clearance of TH. The platform includes PBK models for the TH disrupting chemicals methimazole (MMI), propylthiouracil (PTU), and phenobarbital (PB), each with distinct mechanisms of action, such as inhibition of thyroperoxidase (TPO) or induction of T4-specific Glucosyltransferases (UGTs). Simulations demonstrate dose-dependent changes in T3, T4, and TSH following administration of MMI or PTU in rats, as well as effects of MMI and combined MMI+PTU treatment in humans. For PB, the model predicts a decrease in T4 levels by up to –20% (observed: –6 to –60%) and an increase in TSH by up to +70% (observed: +3 to +100%) in rats, with negligible effects in humans.

Conclusion

The developed platform identified key events of thyroid toxicity in rats, with minimal impact observed in humans. The critical key events, such as UGT induction, can be addressed by specific in vitro assays and the results of these in vitro assays can be fed into the QST model to assess the overall effect on human or rat thyroid hormone level.

P101

Cellular Deiodinase 1 and Dehalogenase 1 Activity Assays for the Identification of potential Thyroid Hormone System Disruptors

S. Arnold¹, L. Dahmen¹, D. Hilgefort², R. Sane³, K. Renko¹

¹Bundesinstitut für Risikobewertung (BfR), Berlin, Germany

²Free University of Berlin, Berlin, Germany

³Charité – Universitätsmedizin Berlin, Institute of Experimental Endocrinology, Berlin, Germany

In vitro models for the identification of potential thyroid hormone system disruptors (THSDs) usually mimic specific molecular initiating events (MIEs) of the thyroid hormone system (THS) and provide mechanistic insights into the mode of actions (MoA) of such chemicals. A range of enzymatic activity assays make use of cell lysates to assess inhibition by measuring the conversion of substrates. These approaches appear to be unbound from the context of intact cells, ignoring cellular properties, like barrier functions of membranes, metabolism, and viability.

Two established lysate-based assays are the Deiodinase 1 (DIO1) and the Dehalogenase 1 (DEHAL1) inhibition assays. DIO1 plays a crucial role in the activation of THs, e.g. by deiodinating inactive T4 to T3, whereas DEHAL1 is crucial for iodine recycling by releasing iodide from TH synthesis-products moniodotyrosine (MIT) and diiodotyrosine (DIT). Disruption of these enzymes might lead to dysregulation of the THS, potentially causing severe adverse outcomes. Therefore, the accurate identification of inhibiting chemicals is crucial to ensure human health.

In this study, we improved and developed cell-based inhibition assays for DIO1 and DEHAL1 activity and compared them to their lysate-based counterparts. We identified potent inhibitors by screening a chemical library (over 500 chemicals, tested at 20 µM) with each setup to investigate overlap and differences in performance.

Overall, cell-based assays for these MIEs provide a promising additional option to increase predictivity of in vitro testing for THSDs. Using intact cells, we are able to include general cell-toxicity as a relevant confounder, therefore adding an additional layer of information for evaluation. Extensive, comparative use of these two assay concepts (cellular vs cell-free) and comparison to in vivo data will be necessary to assess the value of the presented testing approach in hazard identification strategies for THSDs.

Receptor tyrosine kinases

P102

Beyond Hinge Motifs: The Molecular Basis of Transporter-mediated Kinase Inhibitor Resistance

S. M. Stefan^{1,2}, K. Stefan¹, L. Prange¹, T. N. Niehus¹, G. Gopakumar¹, H. Busch³, J. König⁴, V. Namasivayam¹, M. Rafehi⁵

¹University of Lübeck, Medicinal Chemistry and Systems Polypharmacology, Lübeck, Germany

²Medical University of Lublin, Department of Biopharmacy, Lublin, Poland

³University of Lübeck, Medical Systems Biology, Lübeck, Germany

⁴University of Erlangen-Nürnberg, Institute of Experimental and Clinical Pharmacology and Toxicology, Erlangen, Germany

⁵University of Augsburg, Department of Medical Education, Augsburg, Germany

Background & Challenges: The introduction of protein kinase inhibitors (PKIs) represented a milestone in cancer therapy – clinical development is thriving worldwide, and dozens of PKIs have been approved since then. However, two major challenges have not been resolved yet: (i) Selectivity over other kinases; and (ii) specificity over unrelated proteins, particularly PKI resistance-mediating ATP-binding cassette transporters (ABCs). Both observations are rooted in hinge motifs, sterically planar and chemically rather homogenous scaffolds necessary for kinase inhibition. Given the ATP-competitive character of most PKIs and the presence of similar nucleotide-binding domains (NBDs) in ABCs, resistance against PKIs was commonly explained by off-target binding to NBDs of ABCs. This is a false perception for four reasons: (i) Co-localization of imatinib with the membrane-spanning domain (MSD) of ABCG2 in a recent cryo-EM structure; (ii) required MSD (and not NBD) binding for ABCs-mediated resistance; (iii) availability of non-ATP-competitive PKIs; and (iv) demonstrated inhibition of non-NBD-bearing transporters, i.e., solute carriers (SLCs).

Approach & Results: Recently, we hypothesized the existence of common structural motifs ('multitarget binding sites') amongst phylogenetically, structurally, and/or functionally distinct protein families. A systematic search on public databases (e.g., PubMed, PKIDB, KLIFS) yielded 104 structurally diverse PKIs associated to ABCs (single-target: 50%; multi-target: 50%). Functional assessment against ABC-B1, -C1, and -G2 showed a larger polypharmacology of PKIs than documented in the literature (single-target: 20%; multi-target: 65%) – and 14% showed surprisingly no activity. These 15 entirely inactive and 19 most potent multi-target ABCs inhibitors had different pharmacological profiles against OATP1B1, OCT2, OAT1, MATE1, and MATE2K (on average 34% vs 82% activity). Computational analysis provided distinct molecular features that either impeded (e.g., bromine-(substitutions), benzimidazole, azaindole) or promoted (e.g., morpholine, piperazine, quinoline) ABCs- and SLCs-mediated resistance and pharmacokinetic constraints.

Conclusions: Our results not only supported the hypothesis of common structural motifs between kinases, ABCs, and SLCs in line with our hypothesis of 'multitarget binding sites'; we also identified common molecular features amongst PKIs which could resolve both major problems in current kinase research.

Regulatory Toxicology

P103

Proposing a novel modular dermal exposure model (MODEXMO) for non-dietary exposure assessment

F. M. Kluxen¹, K. Wend², C. Wiemann³, E. Felkers⁴

¹BASF SE, Limburgerhof, Germany

²German Federal Institute for Risk Assessment (BfR), Berlin, Germany

³BASF Österreich GmbH, Vienna, Austria

⁴Bayer AG, Crop Science Division, Monheim am Rhein, Germany

A modular non-dietary exposure assessment approach with interacting prediction models is proposed for pesticides / plant protection products (PPPs), which may also apply for other substances. Dermal absorption prediction models (DAPREMOs) could replace relative dermal absorption values (DAVs) by directly predicting internal exposure from external doses with a statistical model. It is well-known that absolute dermal penetration depends primarily on applied dose. Exposure prediction models (EXPREMOs) can predict relatively low area doses, since exposure estimates are averaged over large body surfaces, regardless of the actual residue surface distribution. While this has no consequence in the current assessment approach using DAVs, it ignores the exposure scenario-dependent spatial distributions of residue on skin, e.g., due to individual splash events during mixing and loading operations. Surface distribution prediction models (SUDIPREMOs) can refine EXPREMO-assumed default surface areas to provide DAPREMOs with more accurate inputs for different area doses in multiple exposure sub-streams. As this allows mapping the exposure sub-streams to specific anatomical regions, physiologically-based pharmacokinetic (PBPK) models may incorporate region-specific parameters for more relevant in vitro to in vivo extrapolation (IVIVE) and target tissue exposure estimation.

³BASF SE, German Crop Protection Association, Limburgerhof, Germany
⁴BASF Österreich GmbH, Vienna, Austria

In pesticide risk assessment, ensuring the safety of re-entry workers, residents, and bystanders is essential. Dermal exposure following pesticide application is the primary route of non-dietary exposure for these groups. Consequently, dermal exposure models and methodologies are needed that accurately reflect real-world conditions. A significant improvement would be a method for the experimental determination of dermal absorption rates of dried residues.

Currently, risk assessment within the European Union considers two absorption rates for dermal exposure: one for the concentrated plant protection product and another for the diluted spray solution as applied. However, exposure may also occur through contact with dried pesticide residues on surfaces of previously treated crops. There is currently no international consensus on how dry residues should be consistently applied onto the skin membrane. To close this gap, a dedicated expert workshop was convened, bringing together specialists with extensive experience in dermal exposure and absorption. The workshop aimed to consolidate current scientific knowledge, identify technical requirements for a pragmatic best-practice testing approach, and develop a test protocol aligned with regulatory frameworks, while avoiding overly stringent demands. Fourteen key topics were examined: the nature of the skin source, labelling of test compounds, choice of platform and transfer devices, application volume and distribution of the test material, assessment of residue uniformity, drying conditions, skin preparation prior to application, pressure and rotation applied to skin membranes, occlusion, transfer efficiency measurement, exposure duration, and skin washing procedures.

An existing publicly available in vitro method for assessing dermal absorption of dried pesticide residues provides a solid foundation for best-practice testing. The methodological steps of this approach need to be carefully designed to balance scientific rigor with practical feasibility, thereby meeting regulatory expectations. Nonetheless, additional research is required to fully validate this approach and to support its harmonisation for regulatory use across the European Union.

P108

From In Vivo to In Vitro and Back Again? Uncovering False Positive Results in Skin Sensitisation Testing with PVC Plasticisers

M. Brink¹, N. Engel¹, S. Keup¹, M. Graß¹
¹Evonik Oxeno GmbH & Co. KG, Marl, Germany

As defined by the United Nations Globally Harmonized System of Classification and Labelling of Chemicals (UN GHS) a skin sensitizer refers to a substance that will lead to an allergic response after repeated skin contact. The current knowledge of the underlying mechanisms leading to skin sensitisation are well understood and summarised in an Adverse Outcome Pathway (AOP). [OECD 2014]

In recent years in vitro assays have been developed and validated to cover the initiating and key events of the AOP and to allow the prediction of skin sensitisation hazards for regulatory purposes. [OECD 2025] However, in some cases skin sensitisation testing of some substances, still relies on in vivo methods namely murine Local Lymph Node Assay (LLNA) or guinea pig assays according to Buehler or Magnusson and Kligman, respectively. Especially those substances that are difficult to test in vitro (i.e. low water solubility) or in silico (UVCBs) often lead to inconclusive results according to OECD Guideline no. 497.

Some plasticisers for PVC are UVCBs with a variable composition depending on their starting materials and additionally, they are poorly water soluble. This makes them very hard to test in regulatory accepted in vitro assays due to technical challenges. Here we present findings for different plasticisers tested in various in silico, in vitro and in vivo studies (GLP conditions) over a period of time from 2008 to 2025. Due to low water solubility and limited availability of appropriate and validated solvents, in vitro tests were technically challenging and additionally led to discordant results. In recent years the majority of tested plasticisers led to positive results in the LLNA. In all instances, positive LLNA results were later determined to be false positives through negative follow-up LLNA challenges (according to Vohr et al., 2000 and Gamer et al. 2008) or guinea pig assays, respectively.

References

1. OECD (2014), OECD Series on Testing and Assessment, No. 168., <https://doi.org/10.1787/9789264221444-en>.
2. OECD (2025), *Guideline No. 497*, <https://doi.org/10.1787/b92879a4-en>.
3. Homey, B. et al. (1998): *Toxicology and applied pharmacology* 153 (1), 83–94.
4. Vohr, H.-W. et al. (2000): *Archives of toxicology* 73 (10–11), 501–509.
5. Gamer, A. et al. (2008): *Regulatory toxicology and pharmacology* 52 (3), 290–298.

P109

Formaldehyde releasers: Example of different assessments by the MAK Commission

J. Botterweck¹, S. Michaelsen¹, B. Laube¹, R. Lohmann¹, E. Leibold², A. Hartwig¹
¹Karlsruhe Institute of Technology (KIT), Department of Food Chemistry and Toxicology, Karlsruhe, Germany

²BASF SE, Ludwigshafen, Germany

The Permanent Senate Commission for the Investigation of Health Hazards of Chemical Compounds in the Work Area (MAK Commission) proposes maximum workplace concentrations (MAK values) for chemicals to give scientific policy advice on occupational safety.

Formaldehyde releasers are compounds that release formaldehyde upon hydrolysis. They are used as biocides in e.g. metalworking fluids, adhesives, paints, disinfectants and cosmetics. Formaldehyde can cause irritation as well as acute and chronic toxicity in target tissues such as eyes, respiratory tract, and skin. Additionally, formaldehyde is a local carcinogen in the upper respiratory tract following inhalation exposure. For formaldehyde a non-genotoxic mode of action for the tumor induction can be assumed and therefore a threshold can be derived (Carcinogen Category 4). The determining factor for carcinogenicity of formaldehyde releasers is the rate of formaldehyde release within the respiratory tract. Therefore, the MAK commission considers data on the substance itself and its hydrolysis rate, which is a function of pH, temperature and concentration.

If hydrolysis of the formaldehyde releasers occurs under physiological conditions, or if no data on formaldehyde release are available, it is assumed that formaldehyde is fully released in the tissues. If data allow the derivation of a MAK value (from inhalation studies of the formaldehyde releasers or by analogy to formaldehyde), the substance is classified as Category 4 carcinogen.

If the formaldehyde releaser is present as an aerosol, effects may be more severe because of impaction in the lower respiratory tract such as larynx and lung. Consequently a MAK value cannot be derived by analogy to that of formaldehyde and the formaldehyde releaser is classified as a Category 2 carcinogen (substances that are considered to be carcinogenic for man because sufficient data from long-term animal studies), with the footnote: "Prerequisite for category 4 in principle fulfilled, but insufficient data available for the establishment of a MAK value."

If it can be demonstrated that carcinogenic effects are unlikely to be induced by formaldehyde because of minimal formaldehyde release under physiological conditions (formaldehyde is inactivated in the nose faster than released) these substances are not classified as carcinogen.

P110

What does the BAT-AG do? The DFG working group Assessment Values in Biological Material of the Permanent Senate Commission for the Investigation of Health Hazards of Chemical Compounds in the Work Area

W. Weistenhöfer¹, B. Brinkmann², G. Schriever-Schwemmer², S. Michaelsen², H. Drexler¹, A. Hartwig²
¹Friedrich-Alexander University of Erlangen-Nuremberg, Institute and Outpatient Clinic of Occupational, Social, and Environmental Medicine, Erlangen, Germany
²Karlsruhe Institute of Technology (KIT), Institute of Applied Biosciences, Department of Food Chemistry and Toxicology, Karlsruhe, Germany

The Working Group "Assessment Values in Biological Material" (BAT-AG) of the Permanent Senate Commission for the Investigation of Health Hazards of Chemical Compounds in the Work Area (MAK Commission) evaluates health-based biological tolerance values (BAT values) and biological guidance values (BLW). In addition, biological reference values (BAR) for the adult population not exposed at work and exposure equivalents for carcinogenic substances (EKA) are derived.

BAT values serve as the basis for the Committee on Hazardous Substances to derive biological limit values (BGW) in TRGS 903; values from the EKA are transferred to TRGS 910 as equivalence values for tolerance and acceptance risk, if applicable. The BLW and BAR can be found in Occupational Health Regulation (AMR) 6.2 Biomonitoring, but not in the technical rules.

Detailed documentation is available for each assessment value and is published in open access in the MAK Collection for Occupational Safety and Health in German and English.

To protect unborn children, BAT values are assigned to pregnancy risk groups in collaboration with the "Developmental Toxicity" working group with regard to their teratogenic effects. Pregnant women can work without risk to their unborn child if prenatal toxic effects are unlikely when the MAK value or the BAT value is observed (Group C), or if a correspondingly low concentration can be derived in the biological material (Note regarding prerequisite for Group C).

Conceptual topics are also discussed, including requirements for suitable human biomonitoring parameters with regard to characteristics such as specificity, sensitivity, kinetics, sampling time, preanalytical criteria, and reliable analytical determination. Other topics that have been discussed in the past include human biomonitoring after accident-related events and the significance of sex-specific factors in deriving BAT values.

The work of the BAT-AG, which involves deriving assessment values in biological material, assigning BAT values to pregnancy risk groups, and addressing conceptual topics, serves as the basis for assessing occupational exposure to hazardous substances within the scope of occupational health care.

P112

Introduction of a new pregnancy risk group to clarify the potential teratogenic hazards of a substance Working group Developmental Toxicity of the Permanent Senate Commission for the Investigation of Health Hazards of Chemical Compounds in the Work Area (MAK Commission) of the DFG

G. Schriever-Schwemmer¹, S. Michaelsen¹, W. Weistenhöfer², H. Drexler², A. Hartwig¹

¹Karlsruhe Institute of Technology (KIT), Institute for Applied Biosciences, Food Chemistry and Toxicology, Karlsruhe, Germany

²Friedrich-Alexander University of Erlangen-Nuremberg, Institute and Outpatient Clinic of Occupational, Social, and Environmental Medicine, Erlangen, Germany

The Permanent Senate Commission for the Investigation of Health Hazards of Chemical Compounds in the Work Area (MAK Commission) of the German Research Foundation (DFG) derives limit values for hazardous chemical compounds in air and biological material for the protection of exposed employees at the workplace. In the case of pregnancy, however, compliance with MAK and BAT values does not always mean protection for the unborn child, as this endpoint is not taken into account in the derivation of the limit values. The commission therefore reviews all substances to determine whether they are likely to have a harmful effect on the fetus and assigns the substances with MAK and BAT values to specific pregnancy risk groups. Pregnancy risk groups A, B, and C are risk-based groups, i.e., a statement is made as to whether compliance with the MAK or BAT value can ensure the protection of the unborn child. If there is a lack of data on teratogenic effects, in particular, quantitative data for establishing a risk-based reference, substances with MAK or BAT values are assigned to pregnancy group D. Since the available data indicate at least a potential hazard or suspicion of a teratogenic effect for some substances, group B (suspected) was introduced.

The arguments for and against a suspected developmental (neuro)toxic effect are collected for each substance. An expert judgement must be used to assess whether there is sufficient plausibility for a realistic potential hazard or suspicion for humans at the workplace for an exposure at the level of the MAK value.

Criteria for assignment to group B (suspected) have been compiled on the basis of considerations and discussions.

The xylidine isomers have been classified as Group B (suspected) substances, the first and only substances to date to receive this classification. No data on prenatal developmental toxicity are available. Xylidine isomers are methemoglobin formers, to which the human fetus is significantly more sensitive than adults. The suspicion of a harmful effect on the fetus is based on the fact that there could be a potential risk to the unborn child due to oxygen deficiency.

In the case of substances assigned to pregnancy risk group B (suspected), it is particularly important to check very carefully whether there is an unacceptable risk to women in the workplace in accordance with the Maternity Protection Act.

P113

Practical approach to dermal risk assessment for seven reprotoxic substances contained in epoxy resin systems

K. Heine¹, F. Richter¹, K. Kersting²

¹Forschungs- und Beratungsanstalt Gefahrstoffe GmbH (FoBiG), Freiburg, Germany

²BG BAU - Berufsgenossenschaft der Bauwirtschaft, Referat Gefahrstoffe-Biostoffe, Frankfurt a. M., Germany

This study, commissioned by the Working Group on Epoxy Resin Ingredients ('AK EIS'), evaluates dermal absorption and subsequent systemic health risks of seven substances typically used in epoxy resin systems as reactive diluents, which were recently classified as reproductive toxicants Category 1B under the European CLP regulation. The assessment was conducted in light of recent amendments to the German Hazardous Substances Ordinance (Article 10a GefStoffV), implementing EU Directive 2022/431 that expanded the requirement for inclusion of Category 1A/1B **reprotoxic substances** in the "list of exposures" ("Expositionsverzeichnis") if health risks arise from exposure.

Using the German Research Foundation (DFG) MAK Commission's criteria for a skin notation ("H"), the study assessed whether the dermal absorption of these substances results in a dose exceeding 25% of the systemically tolerable dose.

Dermal penetration rates (Flux) were calculated based on experimental data and mathematical models, which used physicochemical substance properties. The highest resulting Flux, typically from the Fiserova-Bergerova model, was used conservatively, for calculating the total dermal absorption in a defined exposure scenario (1 hour exposure of both hands and forearms, i.e. 2000 cm²). Toxicological reference values were derived from oral repeated dose animal studies (e.g., OECD 408, 443), with the lowest tolerable value covering the critical effect (male fertility).

Comparison of these values showed that for none of the seven substances the estimated dermally absorbed dose exceeded 25% of the derived systemically tolerable dose. The percentage ranged from < 1 to 17.8%.

The assessment therefore concludes that, beyond the known issue of skin sensitisation, there is **no systemic health risk** from skin contact with these seven reprotoxic substances. Nevertheless, due to their skin sensitising properties, gloves must be worn at all times to avoid skin contact. However, our findings indicate that it should not be necessary to include them in the "list of exposures",

thereby reducing the documentation burden for the companies using these substances.

Fig. 1

Stoffname	Abkürzung	CAS-Nr.	EG-Nr.	Einstufungen
1,4-Butandiol-diglycidylether	BOOGE	2425-79-8	219-371-7	H360F, H302, H312, H332, H318, H315, H317, H412
1,6-Bis(2,3-epoxypropyl)hexan	REACH-HDGE	933999-84-9	618-939-5	H360F, H315, H317, H319, H412
1,6-Hexandiol-diglycidylether*	HDGE	16096-31-4	240-260-4	H360F, H315, H319, H317, H412
C12/C14-Monoglycidylether	C12/C14-GE	68609-97-2	271-846-8	H360F, H315, H317
Reaktionsmasse von 1-(2,3-Epoxypropyl)-2,2-bis [(2,3-Epoxypropyl)methyl]butan und 1-(2,3-Epoxypropyl)-2-[(2,3-Epoxypropyl)methyl]-2-hydroxyethylbutan	REACH-TMP-TGE-Polymer	-	701-135-4	H360F, H314, H317, H318, H341, H411
Trimethylolpropane, (chloromethyl)oxirane polymer **	TMP-TGE-Polymer	30499-70-8	608-489-8	H360F, H314, H317, H318, H341, H411
1,1,1-Tris(glycidyl-oxy-methyl)propane **	TMP-TGE	3454-29-3	222-384-0	H360F, H314, H317, H318, H341, H411

* Aktualisierung der Einstufung in Zusammenhang mit Substanz EG-Nr. 618-939-5

** Aktualisierung der Einstufung in Zusammenhang mit Substanz EG-Nr. 701-135-4

P114

Beyond COVID-19: pivotal toxicity studies in rats support platform approach for mRNA vaccines

A. Galeev¹, C. Hessel¹, A. Chaturvedi¹, C. Lindemann¹, J. Diekmann¹

¹BioNTech SE, Non-clinical Safety, Mainz, Germany

Non-clinical safety of BioNTech's modRNA-LNP platform was well-characterized during development of BNT162b2 (Comirnaty®). Several BNT162 vaccine candidates were evaluated in two GLP-compliant repeat-dose toxicity studies in rats (Rohde et al. 2023) and in a GLP-compliant combined DART study (Bowman et al. 2021). No adverse findings were observed in these studies. Non-adverse findings were generally consistent with immune/inflammatory responses to a vaccine.

Accordingly, a modRNA vaccine candidate against tuberculosis, BNT164b1, was well tolerated in a GLP-compliant repeat-dose toxicity study in rats, with no vaccine-related systemic clinical signs or mortalities. BNT164b1 induced transient, dose-dependent inflammatory responses attributed to vaccine-induced activation of the immune system: e.g. increased acute phase reactants, white blood cell counts and body temperature. The control group immunized with non-translatable modRNA-LNP had similar findings, indicating platform-dependent activation of innate immunity, rather than antigen-dependent inflammation (Agrawal et al. 2025).

Collectively, the results of multiple toxicological studies with different mRNA vaccine candidates establish a predictable and favorable safety profile of the underlying modRNA-LNP platform. The platform enables the expedited development and deployment of next-generation mRNA vaccines against emerging pathogens (WHO, 2023). Foundational animal trials remain essential to generating the safety and efficacy data that make such platforms possible in the first place.

References

Agrawal, Neha, et al. "mRNA-based tuberculosis vaccines BNT164a1 and BNT164b1 are immunogenic, well-tolerated and efficacious in rodent models." *bioRxiv* (2025): 2025-09.

Bowman, Christopher J., et al. "Lack of effects on female fertility and prenatal and postnatal offspring development in rats with BNT162b2, a mRNA-based COVID-19 vaccine." *Reproductive Toxicology* 103 (2021): 28-35.

Rohde, Cynthia M., et al. "Toxicological assessments of a pandemic COVID-19 vaccine—demonstrating the suitability of a platform approach for mRNA vaccines." *Vaccines* 11.2 (2023): 417.

WHO. "Evaluation of the quality, safety and efficacy of messenger RNA vaccines for the prevention of infectious diseases: regulatory considerations." Vol annex 3, TRS no 1039. Published 2022.

P115

Assessment of fragrance exposure in young children using human-biomonitoring data from the KiSA-Study NRW Germany (2020/2021)

Y. Chovolou¹, S. Sievering¹, J. Engelmann¹, B. Köllner¹, M. Kraft¹

¹North Rhine Westphalia Office for Nature, Environment and Climate, Environmental Medicine, Toxicology, Epidemiology, NIS, Essen, Germany

Fragrances are widely used in a wide range of everyday products including cosmetics, perfumes, toys, textiles, air fresheners and scented candles and thus have the potential to contribute to human exposure. The aim of this pilot study was therefore to estimate the internal exposure levels of young children in NRW to commonly used fragrances (linalyl acetate, 7-hydroxycitronellal and geraniol). The results shown here are part of the HBM survey of the state of North Rhine-Westphalia, Germany (KiSA-Study NRW) which investigates the exposure of children to pollutants at regular intervals of 3 years.

Lysmeral is a synthetically produced fragrance with sensitising and reproductive toxic properties. The lysmeral metabolites lysmerol (Lys-OH) and tert-butylbenzoic acid (TBBA) were measured above the limits of quantification (LoQ) in almost all urine samples (n=100). The median exposure was 0.7 µg/L (range <0.2 µg/L to 4 µg/L) for Lys-OH and 12 µg/L for TBBA (range 2 µg/L to 109 µg/L). Geraniol is a natural acyclic monoterpene with strong irritant effect on the eyes, skin and mucous membranes. Geraniol is also an allergen with well-documented sensitising properties. The geraniol metabolites 8-carboxygeraniol (8-CG) and Hildebrandt's acid (HS) were measured in all analysed samples. The median exposure was 8 µg/L (range 1 µg/L to 48 µg/L) for 8-CG and 599 µg/L (range 93 µg/L to 11964 µg/L) for HS. 7-hydroxycitronellal is a fragrance and flavouring agent with a known sensitising potential. The specific metabolite 7-hydroxycitronellyl acid (7-HCA) was detected in all urine samples analyzed. The median exposure was 12 µg/L (range 2 µg/L to 72 µg/L). All measured 7-HCA concentrations were well below the health-based guidance value of 9000 µg/L (HBM-I).

To conclude, the results of the KiSA-Study NRW demonstrate a widespread exposure of young children to selected fragrances.

P116

Implementation of CLH report template in IUCLID

A. Zwintscher¹, M. Wehr¹, B. Pieczyk¹, F. Breuer¹, W. Zobl¹, M. Roberts²

¹Fraunhofer Institute for Toxicology and Experimental Medicine (ITEM), Safety Assessment and Toxicology - Regulatory Affairs, Hanover, Germany

²European Chemicals Agency (ECHA), Helsinki, Finland

The classification and labelling of certain hazardous substances is harmonised at EU Level under the Classification, Labelling and Packaging Regulation (CLP Regulation (EC) No 1272/2008) to support the protection of human health and the environment.

The CLP regulation promotes adequate risk management and ensures consistent communication of chemical hazards across the EU, through for example, standardised labels. A CLH report is central to a proposal (or review) for harmonised classification and labelling, and can be submitted by Member States Competent Authorities, ECHA or EFSA.

In the past, data was manually transferred into a report template and submitted as a Harmonised Classification and Labelling (CLH) Report.

To improve this process, the ECHA funded project "Implementation of a Harmonised Classification and Labelling Report template for the IUCLID Report Generator Open procedure" aimed to integrate CLH report templates into IUCLID, enhancing automation and efficiency in data reuse. IUCLID (International Uniform Chemical Information Database) is already used as a database and management system for various chemical substance properties and study data across different regulations. With this implementation, substance data stored in IUCLID can now be automatically utilized for CLH reports.

As part of the project, the individual IUCLID data fields were first mapped to the latest ECHA CLH report document. Based on this mapping, the CLH report template was then integrated into the IUCLID report generator.

Additionally, a user manual was created to facilitate its application.

The project was completed by the multidisciplinary project team at Fraunhofer ITEM, and the results are available on the IUCLID6 server.

The methodology to map the individual IUCLID data fields to the ECHA report template is presented, as well as the process to generate complex CLH reports using the facilities provided by ECHA.

P117

Alcoholic beverages or ethanol: Challenges for classification and human health

O. Licht¹, F. Breuer¹, M. Große Hovest², M. May³, A. Zwintscher¹

¹Fraunhofer Institute for Toxicology and Experimental Medicine (ITEM), Safety assessment and toxicology, Hanover, Germany

²Ecolab Deutschland GmbH, Monheim am Rhein, Germany

³BODE Chemie GmbH, Hamburg, Germany

It is well known that drinking alcoholic beverages can lead to severe impact on human health. Although drinking alcohol is generally accepted in human societies dealing with its negative effects has led to several initiatives to prevent people from drinking, esp. pregnant women or adolescents.

On the other hand, ethanol as a chemical substance is widely used in different industrial sectors e.g. as solvent, from chemical, pharmaceutical or cosmetic industry. Besides that, ethanol is an important biocidal active substance in hand and surface disinfectants.

Currently ethanol is under evaluation by EU member states under BPD/BPR. In this context also classification and labelling play an important role as it has impact on the status of the authorization. Classification as CMR Category 1A or 1B triggers exclusion criteria under BPR. In parallel, an updated dossier for a harmonized classification under CLP is being prepared and according to information on the ECHA website it should be submitted for evaluation by end of

2026. This evaluation will be performed by ECHAs Risk Assessment Committee (RAC).

We will address the different regulatory activities and their potential implications for the use of the substance ethanol, also in perspective to the major health concern (drinking of alcoholic beverages by the general public). Current difficulties with the application of CLP, focusing on substance intrinsic properties without considering substance potency or route specific differentiations and OECD guideline requirements for testing specific endpoints, will be discussed with emphasis on the specific ethanol situation.

P118

Estragole: Low concern in low doses?

O. Kelber^{1,2}, H. Siewers^{3,2}, J. Reichling^{4,2}

¹Phyto & Biotics Tech Platform, Phytomedicines Supply and Development Center, Bayer Consumer Health, Steigerwald Arzneimittelwerk GmbH, Darmstadt, Germany

²Kooperation Phytopharmaka GbR, Working Group Science, Bonn, Germany

³PhytoLab GmbH & Co. KG, Vestenbergsgreuth, Germany

⁴Institute for Pharmacy and Molecular Biotechnology (IPMB), University Heidelberg, Heidelberg, Germany

Question: There are different approaches to assess the safety of trace constituents of natural products. Given the recent regulatory awareness of estragol, a widely spread constituent of medicinal and food plants [1], results from such approaches could have direct regulatory impact.

Methods: To leverage recently generated such data, relevant in vitro and in vivo studies have been retrieved, presented and assessed.

Results: Earlier studies have already been elucidating the dose dependency of potential genotoxic effects of estragole [2, 3]. In vitro data on the formation of E-3'-N2-dG DNA adducts in human liver cell lines after repeated incubation at concentration of 0–50 µM have shown an apparent threshold at 0.5 µM, still significantly above values estimated for normal human dietary intake [3]. Also approaches to set a limit based on a 3-month rat study focusing on the formation of liver cell foci [4–7] suggest that safe dose levels might be higher than previously assumed.

New data support this view. The number of DNA adducts in human hepatic samples was significantly below numbers correlated to mutagenicity in HepG2-CYP1A2 cells in vitro [8–10].

Conclusions: The scientific evidence for a threshold of mutagenic effects of estragole above exposures occurring with the intake of natural products is evolving fast. Accordingly, regulatory measures with potentially detrimental effects on treatment options highly relevant in phytotherapy might need to be reconsidered.

Acknowledgements: Many thanks for fruitful discussions to D. Schrenk and J. Fahrner, RPTU Kaiserslautern-Landau, Germany.

References:

- [1] EMA Committee on Herbal Medicinal Products (HMPC), EMA/HMPC/137212/2005 Rev 1
- [2] Yang S, Wesseling S, Rietjens IMCM. Toxicol Lett 2021., 337, 1–6
- [3] Schulte-Hubbert R, Küpper JH, Thomas AD, Schrenk D et al. Toxicology 2020, 444: 152566
- [4] Miller EC Swanson AB, Phillips DH et al. Cancer Res. 1983, 43: 1124–34
- [5] Bristol DW. Toxicity Report Series 2011, 82: 1–111
- [6] Marsman DS, Popp JA. Carcinogenesis 1994,15:111–117
- [7] Kunz HW, Tennekens HA, Port RE et al. Environ Health Perspect. 1983, 50: 113–22
- [8] Ackermann D, Peil M, Küpper JH et al. Zeitschrift für Phytotherapie, 2023; 44, S 01: S18
- [9] Ackermann G, Peil M, Stegmüller S et al. Lebensmittelchemie 2024, 78, S3
- [10] Ackermann G, Peil M, Quarz C et al. P041, Naunyn-Schmiedeberg's Archives of Pharmacology 2025, <https://doi.org/10.1007/s00210-025-03881-x>

Pharmacoepidemiology and drug safety

P119

Critical analysis of the Anatomical Therapeutic Chemical (ATC) system

L. J. Bindel¹, R. Seifert¹

¹Hannover Medical School (MHH), Institute of Pharmacology, Hanover, Germany

Purpose: The ATC classification is the global standard for drug utilization studies, but its structural and conceptual restrictions remain underexplored. While designed to provide a consistent, hierarchical framework from anatomical to chemical levels, the system increasingly fails to reflect contemporary pharmacotherapy, characterised by multi-indicational use, complex mechanisms and frequent repurposing. This study aims to critically evaluate the ATC classification in terms of consistency, sufficiency and terminology.

Methods: A systematic analysis of all 14 ATC main groups and their sublevels was conducted based on the "ATC/DDD Index 2025" and the official "2025 WHO guidelines". The internal logic of the ATC structure, the completeness of therapeutic areas covered, the treatment of combination products, and the terminology applied were examined. Discrepancies were recorded both within individual groups and across the ATC as a whole.

Results: Major inconsistencies were observed in all main groups. Classification principles (anatomical, therapeutic, pharmacologic, chemical, miscellaneous) were mixed within and across levels, resulting in opacity. Numerous "other/miscellaneous" categories (e.g. A16, B06, N07, V) lacked coherent logic, and drugs with multiple indications were often not represented in all relevant groups, fragmenting therapeutic areas. Overlaps and duplications were frequent, with corticosteroids, antibacterials, and hormones appearing in several groups. Combination products were inconsistently handled, sometimes integrated, sometimes excluded, or placed in separate categories. Terminology further undermined clarity, with vague or outdated terms such as "antidepressants" or "diuretics" obscuring pharmacological rationale and reflecting historical rather than scientific logic. Overall, the ATC is marked by systemic rather than isolated insufficiencies, inconsistencies and nomenclature issues.

Conclusion: The ATC classification is no longer adequate for representing modern pharmacotherapy. Its single-indication logic, reliance on miscellaneous categories, and outdated terminology distort drug consumption analyses and result in misinterpretations. A mechanistically oriented classification and nomenclature, based on pharmacological characteristics and molecular targets, would provide a more precise, consistent and adaptable framework. Such reform would benefit drug utilisation research, clinical practice and education.

P120

Why do healthy volunteers participate? – understanding perception and preferences in clinical trials

E. Krohmer¹, M. König¹, C. Vogt¹, M. Streckbein², S. Baumann³, R. Böhm⁴, F. Müller⁵, V. Wurmbach¹, A. Blank¹

¹Heidelberg University Hospital, Clinical pharmacology and pharmacoepidemiology, Heidelberg, Germany

²CRS, Mannheim, Germany

³CRS, Berlin, Germany

⁴Socratec, Oberursel, Germany

⁵Böhringer-Ingelheim, Biberach an der Riß, Germany

Background: Phase I clinical trials are crucial for drug development and depend on the participation of healthy volunteers (HVs). We explored how HVs perceive these trials and what influences their decisions to join, which is essential for successful recruitment and reliable trial participation.

Objectives: Evaluation of preferences and perception of clinical trials from the perspective of experienced HVs in Germany.

Methods: Based on literature research and semi-structured interviews with prior participants, we developed and piloted a questionnaire which covered the following domains: Recruitment, informed consent (IC), motivation, decision process regarding trial participation, and public perception of trials. The final questionnaire applying 3- to 5-point Likert scales was distributed at four different trial sites (academic and commercial research phase I units) via LimeSurvey from October 2024 to August 2025. Data analysis was performed with RStudio.

Results: In total, 196 questionnaires were fully completed. The population was distributed across age and gender (102 female), the majority participated in two or more studies (73%). Personal contact and internet search were the most prevalent recruitment methods, also rated as most successful. Overall, HVs were satisfied with their IC process. The main trial motivation was the financial compensation (87% important/somewhat important), followed by altruistic reasons for science and access to a free medical examination. Most important aspects for decision making were the total financial compensation (92%), expenditure of time (90%), risk (81%), and organizational aspects (88%). In general, the trials risk profiles still played a dominant role in the decision process. Overall, the majority believed that duration (87% rather/very high) and risk (73%) influences compensation. They would participate in future trials (98%), but only tell selected people about their trial participation (58%).

Conclusion: The responses of 196 HVs confirmed that financial compensation is the primary motivation, but perceived risk and intervention invasiveness also play a major role in decision making. Still, most participants believe that the medical risk is financially compensated, even though it is clearly stated in the Clinical Trials Regulation that compensating risk is unethical. Furthermore, a gap is visible between volunteers' willingness to participate in future trials and the willingness to openly share their involvement.

P121

PRenancy outcomes Intensive Monitoring (PRIM): Leveraging Pharmacovigilance data for post-authorization safety study in pregnancy exposures

B. Rezaallah¹, A. Beckmeyer-Borowko¹, V. Jehl¹

¹Novartis Pharma AG, Patient Safety and Pharmacovigilance, Basel, Switzerland

Introduction: Medication use during pregnancy is common, yet pregnant women are often excluded from clinical trials, resulting in limited safety data for informed decision making when family planning.

Objective: The PRIM (PRenancy outcomes Intensive Monitoring) initiative was pioneered by Novartis, aiming to leverage pharmacovigilance data (PV) to estimate adverse pregnancy outcomes following drug exposure.

Method: PRIM consists of two main components: the PRIM program, which collects pregnancy safety data within a pharmacovigilance system, and PRIM studies, which use these data for structured analysis.

PRIM study is Non-Interventional Study, meeting the criteria Good Pharmacovigilance Practices Module VIII for post-authorization safety study. It is supported by a defined study protocol, Statistical Analysis Plan and reporting. The data include spontaneous reports of pregnancies exposed to medicinal products. PRIM utilizes prospective cases to reduce bias and includes both adverse and normal pregnancy outcomes for prevalence calculations.

Results: The primary objective of the PRIM study is to estimate the prevalence of adverse pregnancy and fetal outcomes such as major and minor congenital anomalies, preterm birth, and spontaneous abortion. Exploratory objectives include characterizing the timing of drug exposures and assessing maternal and neonatal health outcomes.

Conclusion: The PRIM captures a substantial number of global drug exposures during pregnancy in PV, and this allows for faster data collection and analysis compared to a traditional pregnancy registry. The PRIM study has limitations such as underreporting, missing or incomplete information, and the absence of an internal control arm. The inability to establish causality or adjust for confounding factors is also noted. Despite their limitations, the PRIM studies are expected to provide valuable information to patients and healthcare professionals about the risks of drug use during pregnancy in a timelier manner than other study types.

P122

Sex-specific Reports in Publications of Clinical Trials with Newly Approved Drugs in Europe (2017 – 2021)

R. Schulz¹, S. Engeli¹

¹Universitätsmedizin Greifswald, Institut für Pharmakologie, Greifswald, Germany

Question: This work aimed to analyze the relevance of sex- and gender-specific reporting of trial results of newly approved drugs in Europe in the years 2017–2021. By doing so, we wanted to examine to what extent study authors are aware of the importance of conveying sex- and gender-related information.

Methods: Publications of drugs approved between 2017 and 2021 as part of the regulatory approval process were evaluated. These publications were examined for sex-disaggregated reporting of efficacy and adverse effects. Furthermore, sex- and gender specific analyses were checked for the form of statistical presentation and for an indication of the time point at which such analyses were planned.

Results: Sex- and gender related information was available for only 43% of the active substances (n = 59/137) and in only 34% of the studies (n = 91/268). Almost exclusively, sex-specific subgroup analyses for efficacy were available (women vs. men). Reports of adverse effects differentiated for women and men were reported for only 4% of the active substances. The majority of sex-specific efficacy analyses were presented descriptively without statistical significance statements. In 43% of the studies, no time point for the planning of available subgroup analyses was indicated. Additionally, an analysis of the study participants showed a balanced distribution with a female proportion of 49.7%. When comparing the sex ratio of study participants with the ratio of diseased women and men in European populations, 7/28 evaluated indications showed a divergent imbalance. For six of these indications, the female proportion of study participants was 15% lower than the proportion of diseased women. Furthermore, we found that none of the reviewed publications conducted an analysis of the impact of gender. Instead, the terms "sex" and "gender" were frequently used interchangeably.

Conclusions: In summary, sex- and gender-specific subgroup analyses were not regularly reported – a clear divergence to relevant regulatory agency guidelines that call for sex-differentiated data collection and analysis. This could be interpreted as a conscious decision by the study authors to omit this information. Moreover, the format of presentation and the indication of the timing of the available subgroup analyses often allow only a limited interpretation of the results. Finally, better balanced recruitment strategies to reflect disease prevalences in the general population are warranted.

P123

Trends in Polypharmacy and PRISCUS 2.0 Prescriptions in Western Pomerania Between 1997–2021 – a SHIP Analysis

S. Pohlmann¹, T. Ittermann², M. Gollasch³, S. Engeli¹

¹Universitätsmedizin Greifswald, Institut für Pharmakologie, Greifswald, Germany

²Universitätsmedizin Greifswald, Institut für Community Medicine, Greifswald,

Germany
³Universitätsmedizin Greifswald, Innere Medizin D (Geriatric), Greifswald, Germany

Question: Polypharmacy is commonly defined as the taking of at least five drugs simultaneously. Potentially inappropriate medications (PIM) describe risky drugs for the elderly. The German PRISCUS 2.0 list defines a set of medicines that are PIM for patients 65 and older.

Methods: The University Medicine Greifswald initiated a population representative survey with SHIP ("Study of Health in Pomerania"). The data, from the area of Western Pomerania, allows displaying the development of polypharmacy and PIM over the past 20 years. The baseline of SHIP-START-0 (1997–2001) included 4,308 participants, while SHIP-TREND-0 (2008–2012) included 4,420 participants. Each cohort went through follow-ups approximately every 5 years resulting in SHIP-START-1, -2, -3 and -4 as well as SHIP-TREND-1. We applied descriptive statistics, ChiQuadrat tests, linear regressions, and generalized estimating equations to describe and analyse time trends for polypharmacy and PIM 2.0 prescriptions.

Results: Polypharmacy and PIM-prescription both show an increasing prevalence with age progression. This is shown in both, the general analysis of the age groups at all times of survey, as well as in the analysis of individuals, who were re-evaluated at all follow-ups. Although women tend to use more medication than men in early adulthood, elderly men often use more medication than women of the same age. Overall prevalence for woman and men for polypharmacy and PIM is very similar, and therefore not further explored as a factor in this analysis. Analysing the prevalence of polypharmacy and PIM across time through the survey dates did not show the increase we expected. For SHIP-START, as well as for SHIP-TREND, the prevalence even decreases through the survey dates:

Polypharmacy in the age-group 70–74-years-old: SHIP-START-0 40.1%; START-1 50.2%; START-2 47.1%; START-3 35.1%; START-4: 34.6% and

PRISCUS 2.0 in the age-group 70–74-years-old: SHIP-START-0 40.1%; START-1 39.6%; START-2 35.0; START-3 33.7%; START-4: 26.2%

Conclusions: Plotting SHIP-data demonstrates the development of polypharmacy and PIM over time, which might be highly important for clinical practice and the future of medicine. The decrease in polypharmacy and PIM might be caused by rising caution, as both medication problems are increasingly widely known to be associated with secondary health problems in elderly patients.

P124

Drugs in wastewater in Saxony in the course of cannabis legalization 2024

A. Schulze¹, R. Oertel¹, B. Renner¹, M. Geißler²

¹TU Dresden, Institute of Clinical Pharmacology, Dresden, Germany

²TU Dresden, Institute of Medical Microbiology and Virology, Dresden, Germany

Introduction: There are already numerous approaches to using wastewater for epidemiological studies, suggesting that wastewater-based epidemiology (WBE) could become a powerful tool for monitoring public health trends through the analysis of biomarkers such as drugs, chemicals and pathogens. The analysis of illicit drugs in wastewater is an objective and effective tool for monitoring whether, for example, changes in legislation have an impact on consumption behaviour.

Objectives: Our study aimed to determine the influence of the legalization of cannabis on drug consumption in Saxony with WBE in 2024. Using statistical methods, eight different regions were compared. Furthermore, changes in drug consumption over the course of the year were examined. Additional it also offered us the opportunity to evaluate the trend of the other drugs.

Materials and methods: Amphetamine, methamphetamine, MDMA, ketamine, clarithromycin, gabapentin and metoprolol as well as the metabolites of cannabis (THC-COOH), cocaine (benzoylecgonine) and nicotine (cotinine) in the wastewater were measured. The samples came from 8 wastewater treatment plants in urban and small-town areas in Saxony. Three months before the change in the law on 1 April 2024 and nine months after legalization, two 24-hour composite samples of raw wastewater were taken each week. The daily load (mg/day) was calculated from the daily discharge of the wastewater treatment plant inflows, which was standardised to the population equivalents (PE) in the drained catchment areas (in mg/1,000 persons/day).

Results: In comparison to other substances, no clearly increasing consumption or revenue trends could be identified for THC-COOH in 2024, despite its legalization. In contrast, the results for the other substances tested revealed notable temporal and regional differences. Particularly noteworthy are the considerable fluctuations in ketamine occurrence, which arise independently of the trends observed for other substances and represent a significant deviation. Moreover, major cities show the highest consumption rates compared to rural areas.

Conclusion: The legalization of cannabis did not result in any significant changes in consumption patterns so far. A longer observation period would be advisable here. Focusing on other substances and their patterns of use appears to be more promising and will be further monitored.

P125

Multitarget screening of pharmaceuticals in municipal wastewater to evaluate the treatment performance of wastewater treatment plants

M. Koora¹, U. Hofmann¹, J. Zander¹, R. Oertel¹, S. Schubert¹, B. Renner¹

¹TU Dresden, Institut für Klinische Pharmakologie, Dresden, Germany

Introduction: Micropollutants such as pharmaceuticals, personal care products, pesticides, or corrosion inhibitors enter wastewater systems via domestic and industrial wastewater. However, they are often inadequately removed in municipal wastewater treatment plants (WWTPs). The EU Urban Wastewater Treatment Directive (UWWTD) therefore stipulates that such substances, which can contaminate water even in trace concentrations, must be removed by WWTPs with a minimum efficiency of 80%.

Objectives: The aim of this study was therefore to develop a simultaneous method tailored to the target indicator substances of the UWWTD and to include potential substitutes. The analytes are to be detected with high sensitivity and selectivity in the typical concentration ranges of the influent and effluent of municipal WWTPs, using efficient sample preparation and high sample throughput.

Materials and methods: For this study, 24-hour composite samples were taken from the influent and effluent of the WWTPs. The presented method uses solid-phase extraction (SPE) with a low sample volume to enable a high-throughput approach combined with reversed-phase ultra-high-performance liquid chromatography (RP-UHPLC) coupled to an Orbitrap mass spectrometer. The method presented here was designed to detect the following pharmaceuticals: amisulpride, candesartan, carbamazepine, citalopram, clarithromycin, diclofenac, irbesartan, metoprolol, propranolol, tramadol, valsartan and venlafaxine. In addition, isotope-labeled internal standards are used to compensate matrix effects and measurement deviations.

Results: Using the wastewater of a WWTP of more than 640.000 population equivalents in north-east of Germany as an example, it was demonstrated that the developed method could detect all tested pharmaceuticals in the influent and effluent. Most of these pharmaceuticals are only eliminated to a small extent by the conventional WWTP.

Conclusion: The multitarget screening method presented here is suitable for testing raw and treated wastewater to determine whether WWTPs comply with the UWWTD and remove at least 80% of pharmaceuticals.

P126

Age-related effectiveness of clinical pharmacological/pharmaceutical care for patients treated with oral antitumor therapeutics: an analysis of the randomized AMBORA trial

S. Huynh^{1,2,3}, Q. Wu⁴, K. Gessner^{1,3}, P. Dürr^{1,2,3}, C. Staerk^{5,6}, F. Dörje^{2,3,7}, A. Mayr¹, M. F. Fromm^{1,3,7}

¹Friedrich-Alexander University of Erlangen-Nuremberg, Institute of Experimental and Clinical Pharmacology and Toxicology, Erlangen, Germany

²Universitätsklinikum Erlangen and Friedrich-Alexander-Universität Erlangen-Nürnberg, Pharmacy Department, Erlangen, Germany

³Comprehensive Cancer Center Erlangen-EMN, Universitätsklinikum Erlangen, Erlangen, Germany

⁴Institute for Medical Biometry and Statistics, Philipps-University Marburg, Marburg, Germany

⁵Technische Universität Dortmund, Department of Statistics, Dortmund, Germany

⁶Leibniz Research Institute for Environmental Medicine (IUF), Düsseldorf, Germany

⁷Friedrich-Alexander University of Erlangen-Nuremberg, FAU NeW - Research Center New Bioactive Compounds, Erlangen, Germany

Background: Elderly patients are particularly vulnerable due to a progressive decline in organ functions and an increasing number of comedications and comorbidities. These factors place older individuals at a higher risk of side effects and medication errors. The randomized AMBORA trial¹ demonstrated that intensified clinical pharmacological/pharmaceutical care considerably improves medication safety, reduces side effects, and enhances treatment perception compared with routine care in patients treated with a broad spectrum of oral antitumor therapeutics (OAT). This post-hoc analysis explores, whether the effects of the AMBORA intervention differ by age.

Methods: Patients starting therapy with OATs in the AMBORA trial were stratified into two groups: older (> 70 years; n = 76) and younger (≤ 70 years; n = 126). Intervention efficacy was evaluated over a period of 12 weeks by the number of antitumor drug-related problems (DRP, unresolved medication errors and side effects) and patient treatment satisfaction [Treatment Satisfaction Questionnaire for Medication (TSQM), category convenience] with the oral antitumor therapy. Outcomes were compared between intervention and control groups within each age cohort and tested for age-related interaction effects.

Result: The number of DRP per patient related to the OAT was significantly reduced in the intervention groups compared with control among both older (3.43±3.03 vs. 5.66±3.69 [mean], p < 0.05) and younger patients (4.08±2.74 vs. 5.90±3.97, p < 0.01) with no significant age interaction (ANOVA test for age interaction, n.s.). Treatment satisfaction was higher in both older (91.37±11.18 vs. 71.24±14.29 [mean], p < 0.01) and younger intervention groups (91.67±12.05 vs. 76.11±18.03, p < 0.01) compared to the control groups with a significantly higher improvement among older patients (age interaction: p < 0.01).

Discussion: This analysis shows the effectiveness of the AMBORA intervention in reducing medication errors and side effects in elderly and young patients.

Notably, elderly patients experienced a significantly greater improvement in treatment satisfaction.

Conclusion: Oral antitumor therapies are associated with a range of medication errors and side effects. An intensified clinical pharmacological/pharmaceutical care has a positive effect on medication safety and patient treatment perception in older patients.

References:

1. Dürr P et al. J Clin Oncol 39: 1983-1994, 2021

P127

Prescription errors in a psychiatric and substance abuse setting: pharmacological evaluation and drug safety

C. Dokos¹, K. Manaridou², J. Eberlein², O. Konstantakopoulou³, A. Skitsou³, P. Galanis⁴, G. Charalambous³

¹Klinikum Luedenscheid, Department of Acute and Emergency Medicine, Hilden, Germany

²St. Josef Ameos Oberhausen, Oberhausen, Germany

³Frederick University, Department of Nursing, Nicosia, Cyprus

⁴National and Kapodistrian University of Athens, Department of Nursing, Athens, Greece

Question: Prescription errors (PE) is a healthcare quality index. Aim of this study is the pharmacological evaluation of PE in a psychiatric and substance abuse setting, in order to implement a framework of drug safety. **Methods:** A prospective observational study was conducted at St. Josef AMEOS Psychiatric Hospital Oberhausen during 2023 - 2024. PE were defined and classified according to adapted EQUIP methodology. An extensive checking of possible drug interactions in each case of PE was performed. The check was conducted using Drugs.com database. In addition, each PE was assessed in a double blind manner (K.M and C.D), regarding the nature and severity of the PE. Through literature search, we identified any possible effect of the pharmaceutical substance upon the psychopathology of the patient. After evaluation an algorithm of safety procedures in prescribing was developed. The AMEOS ethics committee approved this study (AMEOS-ETH-2023-001). **Results:** Over 6020 paper-based therapeutic plans were evaluated and 150 cases of PE were included in this study. Almost 93.3% were minor PE, 5.0% were major PE, and 1.7% were serious. Writing errors were most common (38%). Errors most frequently involved musculoskeletal medications (36.7%), followed by gastrointestinal (18.7%) and CNS/psychotropics (14.7%). Two cases of allergy were recorded (metamizol, ceftriaxon), although both were identified through patients history. 15% of PE were identified as unnecessary drug administration, four cases (6%) as drug overdose/toxicity (acetylsalicylic acid, ibuprofen, simvastatin, levothyroxin) without any pathological laboratory parameters, a serious drug interaction (lithium and enalapril) with significant elevated serum lithium levels and 12% of the cases involved antibiotics (subtherapeutic dosage, therapeutic duration, wrong description). Three cases of PE were identified (lithium, oxazepam, ironglycinsulfat) were recorded with significant effect on the psychopathology of the patient. **Conclusions:** PE and drug safety studies in mental health care settings, particularly in Germany, remain scarce. Education in taking patient history, possible allergies and pharmacotherapeutic groups (analgesics, antibiotics) is essential. We developed a safety algorithm in order to prevent antibiotic PE.

P128

Human versus artificial intelligence: Physicians outperform ChatGPT in real-world pharmacotherapy counseling

J. Heck¹, B. Krichevsky^{2,3}

¹Hannover Medical School (MHH), Institute for Clinical Pharmacology, Hanover, Germany

²Hannover Medical School (MHH), Institute for General Practice and Palliative Care, Hanover, Germany

³University Hospital Schleswig-Holstein (UKSH), Interdisciplinary Emergency Department, Kiel, Germany

Question: To assess the utility of the artificial intelligence (AI) chatbot ChatGPT (openly available version 3.5) in responding to real-world pharmacotherapeutic queries from healthcare professionals.

Methods: Three independent and blinded evaluators with different levels of medical expertise and professional experience (*beginner*, *advanced*, and *expert*) compared AI chatbot- and physician-generated responses to 70 real-world pharmacotherapeutic queries submitted to the clinical-pharmacological drug information center of Hannover Medical School between June and October 2023 with regard to quality of information, answer preference, answer correctness, and quality of language. Interrater reliability was assessed with Krippendorff's alpha. Two separate investigators not otherwise involved in the conduct or analysis of the study selected the top three clinically relevant errors in chatbot- and physician-generated responses.

Results: All three evaluators rated the quality of information of physician-generated responses higher than the quality of information of AI chatbot-generated responses and, accordingly, thought that the physician-generated responses were better than the chatbot-generated responses (answer preference). All evaluators detected factually wrong information more frequently in chatbot-generated responses than in physician-generated responses. While the *beginner* and *expert* evaluators rated the quality of language of physician-generated responses higher than the quality of language of chatbot-generated responses, there was no significant difference according to the *advanced* evaluator.

Conclusions: ChatGPT's responses to real-world pharmacotherapeutic queries were substantially inferior compared to conventional physician-generated responses with regard to quality of information and factual correctness. Our study suggests that to date it must be strongly cautioned against the use of ChatGPT in pharmacotherapy counseling.

(Krichevsky B et al. Human vs. artificial intelligence: Physicians outperform ChatGPT in real-world pharmacotherapy counselling. Br J Clin Pharmacol. 2025; e70321. doi:10.1002/bcp.70321)

P129

Transition from Cytotec® to Angusta®: Real-World Comparison of Oral Misoprostol Formulations for Labor Induction at a Tertiary Birth Center

C. Le Roux¹, L. Machill², L. Fiengo Tanaka¹, S. Brehm¹, E. Hauenstein³, C. Brucker³, M. Krause³, S. Jäger¹

¹Institute of Clinical Pharmacology, Klinikum Nuremberg and Paracelsus Medical University, Nuremberg, Germany

²Paracelsus Medical University, Nuremberg, Germany

³Klinikum Nuremberg and Paracelsus Medical University, Clinic of Gynecology and Obstetrics, Nuremberg, Germany

Question

Cytotec® (Cy), containing the prostaglandin E1 analog misoprostol, was used off-label for labor induction in Germany until import was stopped due to safety concerns. A 25µg misoprostol tablet (Angusta®, Ang) approved for labor induction became available in 2021. Serious adverse events (e.g. uterine tachysystole, uterine rupture, fetal bradycardia, neonatal asphyxia, death) continue to be reported with Ang. The German regulatory authority (BfArM) recently issued an official warning.¹ This ongoing retrospective study evaluates changes in induction practices and associated changes in safety and efficacy after the introduction of Ang.

Methods

Klinikum Nürnberg's database is being screened for singleton inductions with Cy (50µg followed by 100µg 4-hourly) or Ang (25µg 2-hourly). The final cohort will include 100 patients in each of the following time periods: (1) Pre-transition [2018]: Cy only, (2) Transition from Cy to Ang [2021], and (3) Post-transition [2024]: Ang only. Delivery, maternal and neonatal outcomes will be assessed. Labor induction with castor oil will be analyzed as confounding factor.

Results

From ongoing data acquisition, cleaned and validated data are available for 121 patients (Table1). Both Cy groups required a median of 2 administrations (vs. 4 in Ang, $p < 0.01$), but reached a higher median cumulative dose of 150µg misoprostol (vs. 100µg in Ang, $p < 0.01$). Median time from first dose to vaginal delivery was 16.1h (Ang) vs. 12.2h (Cy2021) and 15.1h (Cy2018), $p=0.24$. Rates of cesarean section were higher with Ang (30% vs. 17% and 21%, $p<0.05$). Tocolysis was required for 18 patients (21%) who received Cy vs. one (2.7%) who received Ang, $p < 0.01$. There were no cases of uterine rupture. Occurrence of postpartum hemorrhage $\geq 500\text{mL}$ ($p=0.68$) and $\geq 1000\text{mL}$ ($p=0.77$) were similar across all groups. No differences were observed in neonatal Apgar scores, umbilical cord blood gas analyses, fetal blood sampling rates, or NICU admissions. There were no cases of neonatal or maternal deaths.

Conclusion

Preliminary data indicate no significant difference in time to delivery and maternal and neonatal safety across all groups, but an increased pill burden and higher rate of cesarean deliveries with Ang. Final analysis will include a larger sample size and incorporate a 2024 cohort.

References

BfArM-Risk information-Angusta (misoprostol for induction of labour): Reports of overdose and contraindicated use with labour already in progress. June 2025.

Fig. 1

Table 1: Patient characteristics

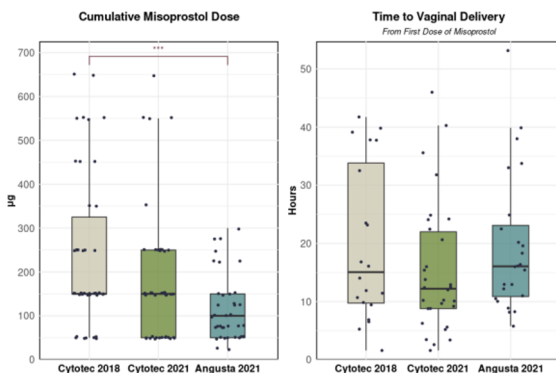
	Angusta 2021, n=37	Cytotec 2021, n=42	Cytotec 2018, n=42	P value ^a
Age in years, median, [IQR]	32 [29, 34]	32 [29, 35]	31 [28, 34]	0.96
BMI at conception (kg/m ²), median, [IQR]	22.9 [20.9, 25.1]	25.5 [21.0, 29.2]	24.6 [22.7, 28.2]	0.08
Smoker, n (%)	5 (13.5)	2 (4.7)	3 (7.1)	0.38
Previous pregnancy loss, n (%)	9 (24.3)	9 (21.4)	9 (21.4)	0.94
Primigravida, n (%)	18 (48.6)	20 (47.6)	26 (42)	0.35
Gestational age at induction of labor in weeks + days, median [IQR]	40+5 [39+2, 41+2]	40+4 [39+4, 41+1]	40+1 [39+0, 41+0]	0.42
Indication for induction of labor, n (%)				
Prelabor rupture of membranes	12 (32.4)	20 (47.6)	13 (31.0)	0.22
Postdate pregnancy ^b	18 (48.6)	13 (31.0)	16 (38.1)	0.27
Maternal ^c	5 (13.5)	5 (11.9)	5 (11.9)	1
Fetal ^d	1 (2.70)	4 (9.5)	8 (19.0)	0.06
Patient request	1 (3)	0 (0)	0 (0)	0.30
Midwife Cocktail prior to misoprostol, n (%)	2 (5)	5 (12)	18 (43)	<0.01

^ap-value: Kruskal-Wallis test, Fisher's exact test, Pearson's chi-squared test. ^bGestational age > 40+0.

^cPregnancy-induced hypertension, chronic hypertension, preeclampsia, gestational diabetes.

^dIntrauterine growth restriction, oligohydramnios, polyhydramnios, macrosomia.

Fig. 2



P130

Comorbidities and comedication in functional gastrointestinal diseases – pharmacoepidemiological data on a herbal medicinal product

S. Göttlich¹, B. Vinson², Q. Kelber¹, E. Raskopf¹, K. Shah¹, K. Nieber³, K. Kraft⁶, R. Mösges^{4,5}

¹Phyto & Biotics Tech Platform, Phytomedicines Supply and Development Center, Bayer Consumer Health, Steigerwald Arzneimittelwerk GmbH, Darmstadt, Germany

²Medical Affairs, Phytomedicines Supply and Development Center, Bayer Consumer Health, Steigerwald Arzneimittelwerk GmbH, Darmstadt, Germany

³ClinNovis GmbH, Cologne, Germany

⁴Institute for Medical Statistics and Bioinformatics, University Clinics Cologne, Cologne, Germany

⁵Institute for Pharmacy, University of Leipzig, Leipzig, Germany

⁶University Medicine Rostock, Center for Internal Medicine, Rostock, Germany

Question: Pharmacoepidemiological studies on Herbal Medicinal products (HMPs) are often lacking [1]. Therefore it is desirable to study comorbidities and comedication in a medicinal product, STW 5 [2,3], which is used in functional gastrointestinal diseases.

Methods: Real world data (RWD) were captured from the PhytoVIS study, where RWD on the usage of HMPs from more than 20,000 patients were collected. The respective data sets were evaluated based on the ATC code.

Results: From the 1515 patients using STW 5, 32.8% reported one or more comorbidities, most frequently hypertension (11.9%), metabolic disorders (9.0%), and back pain (3.6%). 56% reported no comedication, 28.1% taking one and 15.9% taking up to nine additional medicines (Fig. 1). 45.6% of female and 39.9% of male patients, resp. 76.3% of those over 65 years of age reported comedication. The ATC code C (cardiovascular system) accounted for 26.3%, A (alimentary system and metabolism) for 20.0%, H (systemic hormone preparations excluding sex hormones and insulin) for 12.8%, and N (nervous system) for 8.4% of the co-medication, to name the four most common ATC codes. Thyroid hormones (17.9%) and low-dose ASS (4.0%) were among the medicines most frequently mentioned. There was no evidence of interactions between STW 5 and the co-medication. Approximately one-third of the patients had a comorbidity, and almost half were receiving co-medication in addition to treatment with STW 5.

Conclusions: The data thus provide a unique pharmacoepidemiological overview for a large cohort of patients with functional gastrointestinal diseases and show the suitability of the PhytoVIS study for pharmacoepidemiological research.

References:

[1] Wegener T, Nieber K, Kraft K, Siegmund S, Kelber O, Jobst D, Steinhoff B. Versorgungsorschung mit pflanzlichen Arzneimitteln: Die pharmako-epidemiologische Datenbank PhytoVIS. Pharmind 2021, 83, 3, 416 – 423

[2] Malfertheiner P. STW 5 (Iberogast) Therapy in gastrointestinal functional disorders. Dig Dis. 2017, 35 Suppl 1: 25-29

[3] Storr M, Ottlinger B, Allescher H-D, Malfertheiner P. STW 5 (Iberogast) bei funktionellen gastrointestinalen Erkrankungen. Pharmakon 2016, 4: 356-364

[4] Nieber K, Raskopf E; Greinert O, Zadayan G, Schleicher S, Sha-Hosseini K, Wegener T, Kelber O, Singh J, Mösges R. Epidemiological data from 1515 patients with functional GI diseases under an herbal therapy. Der Internist 2019 Suppl. 1: S23, PS032

G-protein coupled receptors

P131

A cell-based platform for profiling GRK inhibitors and kinase specificity

N. K. Blum¹, M. Kiefer¹, A. Decker¹, J. Drube², F. Nage³, C. Hoffmann², S. Schulz^{1,3}

¹Institute of Pharmacology and Toxicology, University Hospital Jena, Jena, Germany

²Institute of Molecular Cell Biology, University Hospital Jena, Jena, Germany

³TTM Antibodies GmbH, Jena, Germany

G protein-coupled receptor (GPCR) signaling is regulated by four ubiquitously expressed GPCR kinase isoforms (GRKs): GRK2, GRK3, GRK5, and GRK6. Their overexpression is linked to diseases such as cancer and heart failure, motivating the search for potent and selective GRK inhibitors. To assess these compounds in a cellular environment, we used HEK293 cell lines co-expressing the β_2 adrenergic receptor (β_2) and one GRK isoform on a quadruple GRK2/3/5/6 knockout (ΔQ) background. With the 7TM phosphorylation assay, we quantified isoproterenol-induced β_2 phosphorylation at the T360/S364 site. Among the inhibitors tested, Compound 8h and Compound 18 showed high potency for GRK2/3 and GRK5/6 inhibition, respectively, and proved effective in additional functional readouts. Furthermore, the assay allowed evaluation of protein kinase A (PKA) and C (PKC) specificity in ΔQ cell lines expressing the vasoactive intestinal peptide receptor 2 (VPAC2) or mu-opioid receptor (MOP). Altogether, this versatile cell-based platform supports medium- to high-throughput screening and mechanistic studies of kinase inhibitors.

P132

Validation of phosphorylated GPR17 receptors as pharmacological target for the treatment of demyelinating diseases

S. Fritzewanker¹, S. Schulz¹, O. Kudina¹, F. Nagai¹

¹Jena University Hospital, Pharmacology and Toxicology, Jena, Germany

Multiple sclerosis (MS) is a neuroinflammatory disorder characterized by immune cell infiltration into the central nervous system (CNS), leading to inflammation, demyelination, and axonal damage. Following demyelination, oligodendrocyte precursor cells (OPCs) become activated, proliferate, and differentiate into oligodendrocytes capable of restoring myelin sheaths—a process known as remyelination. However, remyelination often fails to fully compensate for myelin loss, resulting in chronic demyelination and persistent conduction deficits along axons, which drive progressive disability in MS patients. Current MS therapies mainly target the immune response and show limited efficacy in the chronic progressive phase. The adult CNS retains a limited ability to replace lost myelin through resident OPC proliferation and their maturation into new myelinating oligodendrocytes. Consequently, research has increasingly focused on identifying treatments that preserve oligodendrocytes and enhance remyelination. One promising target is the orphan G protein-coupled receptor GPR17, which is transiently expressed in late-stage OPCs and immature oligodendrocytes, but not in mature myelinating cells. Experimental studies in mice demonstrate that genetic deletion or pharmacological inhibition of GPR17 accelerates developmental myelination and remyelination, whereas its overexpression or activation impairs oligodendrocyte differentiation. These findings indicate that GPR17 antagonists may enhance remyelination in MS and other demyelinating disorders. For GPR17, we identified phosphorylation at serine351 and threonine356 in an agonist- and GRK-dependent manner. During brain development, non-phosphorylated GPR17 is abundantly expressed in white matter regions undergoing active myelination. After postnatal day 20, when myelination nears completion, GPR17 phosphorylation markedly increases. This temporal and spatial shift suggests tight developmental regulation of the endogenous GPR17 ligand. In the adult brain, GPR17 is present in OPCs distributed throughout the CNS, and most receptors appear in a phosphorylated, active state. These findings reveal that GPR17 regulation during oligodendrocyte differentiation is far more intricate than previously assumed. Understanding the mechanisms controlling GPR17 phosphorylation will be essential to determine how this receptor acts as an intrinsic barrier to efficient myelin repair.

P133

Adenosine evokes Ca^{2+} release and Ca^{2+} entry in connective tissue type mast cells via A3 receptors and via Gq-signaling

M. Bukva¹, F. C. Haffelder¹, M. Betz¹, C. Grimm², C. E. Müller³, M. Freichel¹, V. Tsvilovsky¹

¹Heidelberg University, Institute of Pharmacology, Heidelberg, Germany

²Ludwig-Maximilians-University Munich, Walther-Straub-Institute of Pharmacology and Toxicology, Munich, Germany

³University of Bonn, Pharmaceutical Institute, Pharmaceutical & Medicinal Chemistry, Bonn, Germany

Mast cells (MCs) are tissue-resident immune cells that regulate inflammation and allergic responses. They contribute to every phase of acute inflammation, modulating both innate and adaptive immune responses (1). Adenosine, one of the most abundant extracellular signaling mediators, plays a key role in the pathogenesis of asthma and obstructive pulmonary disease through its effects on MCs. The cellular actions of adenosine are mediated by A1, A2a, A2b, and A3 receptors, though their inflammatory roles in mast cells remain controversial (2). An increase in free cytosolic calcium ($[\text{Ca}^{2+}]_i$) is a prerequisite for the activation of MCs (3).

The number of reports studying contribution of individual adenosine receptors in Ca^{2+} -signaling in primary mast cells is very limited. In murine peritoneal mast cells (PMCs) we detected transcripts of A2a, A2b and A3 receptor genes.

Adenosine stimulation in PMCs evoked responses involving both intracellular Ca^{2+} -release and Ca^{2+} -entry. These two phases of $[\text{Ca}^{2+}]_i$ increase were almost entirely abolished by the A3 receptor blocker MRS-1523, Gq blocker YM-254890, or phospholipase C blocker U73122. Furthermore, adenosine and the A3-specific agonist 2-CI-IB-MECA induced $[\text{Ca}^{2+}]_i$ transients with almost identical kinetics and amplitudes. In contrast to the A2a-specific agonist PSB-0777, the A2b-specific agonist Bay-6583 failed to evoke any $[\text{Ca}^{2+}]_i$ elevation. However, $[\text{Ca}^{2+}]_i$ transients induced by PSB-0777 were insensitive to the A2a-specific antagonist preladenant but were antagonized by YM-254890 and U73122.

Thus, we conclude that PSB-0777 can non-specifically activate A3 receptors in PMCs, and that adenosine induces Ca^{2+} release and Ca^{2+} entry in PMCs exclusively through A3 receptors and Gq signaling.

References:

1. Front Cell Dev Biol. 2024;12:1466491.
2. Int J Mol Sci. 2021;22(10):5203.
3. Nat Rev Immunol. 2014;14(7):478-94.

P134

Voltage dependence of the constitutive activity of G protein coupled receptor

Y. M. Tao¹, M. Ulrich¹, S. B. Kirchhofer¹, C. Kurz², M. Bünemann¹

¹Marburg University, Institute of Pharmacology and Clinical Pharmacy, Marburg, Germany

G protein-coupled receptors (GPCRs) are pivotal transmembrane proteins involved in diverse cellular signalling pathways and represent a third of major drug targets.

In the last two decades it became apparent, that many agonist-activated GPCRs are sensitive to the electrical membrane potential. So far it was not clear whether voltage affects intrinsic properties of ligand binding or alters the conformation of receptors independently of ligands. We therefore investigated the voltage dependence of ligand-free GPCRs that exhibit a high constitutive activity.

In this study, we characterize the voltage sensitivity of the constitutively active G protein-coupled receptor 55 (GPR55), which is implicated in physiological processes such as pain perception, inflammatory processes, and cancer. Applying electrophysiology to single cell FRET-microscopy we observe that the constitutive activity of GPR55 is attenuated upon membrane depolarization. This behaviour contrasts with the constitutively active kappa-opioid receptor (KOR), where we observe that depolarization induces receptor activation. Thus, we detected voltage-dependent modulation of the constitutive activity of two different GPCRs, suggesting that the membrane potential modulates receptor activity in the absence of ligands. Furthermore, the directionality of voltage modulation is receptor specific though it certainly influences the equilibrium of conformational states of GPCRs.

In conclusion, voltage sensitivity in constitutively active GPCRs such as GPR55 and KOR represents a novel aspect of receptor pharmacology. Elucidating the underlying mechanisms may enable precise modulation of GPCR voltage dependency, supporting the development of targeted therapies.

P135

The effect of the D130A mutant in the β 2-adrenergic receptor DRY motif on intracellular signalling

M. Neukirch¹, M. Bouvier², H. Schihada¹, F. Heydenreich¹

¹Marburg University, Pharmaceutical Chemistry, Marburg, Germany

²Université de Montréal, Biochemistry, Montreal, Canada

G protein-coupled receptors (GPCRs) are membrane proteins expressed in every human cell. They play a crucial role for cellular response by transducing

extracellular signals across the cell membrane. Consequently, GPCRs represent a main target for pharmaceuticals. The β 2-adrenergic receptor (β 2AR) is a model class A GPCR that couples primarily to Gs. The conserved DRY motif stabilizes the receptor in its inactive conformation and plays an important role in the activation of the receptor. We determined the importance of the aspartate within the DRY motif by analysing the effect of the D1303x49A mutant on intracellular signalling. Optimized BRET-based assays were used to detect constitutive activity, ligand-dependent G protein activation and downstream signalling in living cells. The mutant did not show a significant difference in constitutive activity compared to the wild-type receptor. However, mutating the D1303x49 residue led to a gain of function and novel, previously undetected G protein coupling preferences of the β 2AR. Upon mutation, we observed changes to the G protein activation pattern, either in potency, efficacy or a combination of both. Significant differences in coupling behaviour in all four G protein families suggest a promiscuous coupling of β 2AR D1303x49A. The effect of the mutation on intracellular signalling was further validated by monitoring the downstream signalling effect of the Gq/11 family using a PKC-c1b biosensor. Since no G protein was overexpressed, these findings represent the receptor mutant's capacity to signal through endogenously expressed Gq/11 proteins, validating the physiological importance of the observed gain in Gq coupling.

P136

Development of functional nanobodies targeting GPCRs

S. B. Kirchhofer¹, K. Hinnah¹, J. Fischer¹, K. Johnsson^{1,2}

¹Max Planck Institute for Medical Research, Department of Chemical Biology, Heidelberg, Germany

²École Polytechnique Fédérale de Lausanne, Institute of Chemical Sciences and Engineering, Lausanne, Switzerland

G-Protein-coupled receptors (GPCRs) are one of the most prominent classes of drug targets. As key mediators of intracellular signal transduction, they regulate various physiological and pathophysiological processes, making them highly relevant clinical targets, with more than one third of all FDA-approved drugs acting directly on these receptors. The majority of clinically approved drugs targeting GPCRs are small molecules. However, these compounds often exhibit limited receptor selectivity, which can result in off-target interactions and associated adverse effects. To overcome these limitations, the development of highly specific biologicals, such as antibodies or smaller antibody fragments like nanobodies / VHH (Variable Heavy Domain of Heavy Chain), which are capable of selectively bind and modulate GPCRs has gained increasing interest in the recent years.

Utilizing a phage display-based approach on living cells, we developed a novel strategy to selectively generate highly selective and functional nanobodies directed against GPCRs. The phage display methodology enabled high-throughput screening of a large library of nanobodies, allowing the identification of candidates with desired binding and functional properties. Our approach not only allows the selection of nanobodies that specifically target the GPCR of interest, but also facilitates the identification of functional nanobodies selectively modulating distinct signaling pathways downstream of the receptor.

We further characterized these newly selected nanobodies targeting distinct GPCRs with respect to their functional properties. To this end, we employed different cell-based assays utilizing luminescence or BRET (bioluminescence resonance energy transfer) readouts, as well as microscopy- and flow cytometry-based approaches.

Taken together, we present a novel phage display-based approach for the generation of highly selective and functional nanobodies targeting GPCRs.

P137

Integrated Neurotransmission and Cytoskeletal Pathway Modulation by Tannin-Free Natural Products in *Caenorhabditis elegans* Unveils Promising Anthelmintic Drug Targets

M. Talukder¹, M. Rabbi¹, N. Ahmed¹, M. Zim¹, M. Sajib¹, M. Ahmed¹, B. Roy¹

¹Bangladesh Agricultural University, Department of Parasitology, Mymensingh, Bangladesh

Despite of the Southeast Asia's rich medicinal flora, Bangladesh lags in lead anthelmintic compound discovery. Moreover, target-specific resistance (TSR) and non-target-specific resistance (NTSR) surge have influenced the lead compounds bio-discovery over the past decades. To date, prior research are limited to basic efficacy tests and conventional extraction protocol. Therefore, the study was designed to assess the anthelmintic potency of 19 tannin-free natural products (NPs) induced alterations of neurotransmission in *C. elegans*. The anthelmintic activity was assessed by examining the motility (head thrashes and body bends), mortality, egg hatch inhibition (EHI) and expression of *cat-1*, *ser-1*, *dat-1*, and *tba-1* genes. Eleven (11) plant extracts, *Azadirachta indica* A. Juss., *Cassia alata* L., *Portulaca oleracea* L., *Saraca asoca* (Roxb.) W.J.de Wilde, *Eleusine indica* L. Gaertn., *Persicaria hydropiper* L. Delarbre, *Foeniculum vulgare* Mill., *Clerodendrum infortunatum* L., *Linum usitatissimum* L., *Hibiscus rosa-sinensis* L., and *Vitex negundo* L. revealed a significant neurobehavioral and developmental impairments in *C. elegans*. *Persicaria hydropiper* L. Delarbre @ 1 mg/mL, caused the lowest body bending (31 ± 1.7 , $p < 0.01$), while *Eleusine indica* L. Gaertn. reduced head thrashing (66.3 ± 3.0 , $p < 0.01$). *L. usitatissimum* L. exhibited the highest lethality ($87.3 \pm 1.8\%$, $p < 0.01$) and the LD₅₀ values of *Eleusine indica* L. Gaertn. (0.40 mg/mL) and *Linum usitatissimum* L. (0.411 mg/mL) were the lowest. Interestingly, *C. infortunatum* L. exhibited the strongest EHI ($97.5 \pm 3.0\%$, $p < 0.01$). Gene expression analysis revealed a significant down-regulation of the dopaminergic and serotonergic pathway indicating the metabolic and reproductive disruptions. This pioneering study underscores the anthelmintic potency of native plant extracts, highlighting their neuromodulatory and developmental impact on *C. elegans*. Altogether, these findings suggest that the selected genes may serve as potential drug targets, paving the way for lead compounds identification and development to the advance anthelmintic drug discovery from the NPs.

P138**The protease-activated receptor 2 (PAR2) as a target for blood glucose regulation and atherogenesis**U. Meyer¹, A. Flöβer², J. Friebe³, A. Böhm², U. Rauch-Kröhnert³, B. H. Rauch¹¹Universität Oldenburg, Oldenburg, Germany²Universität Greifswald, Greifswald, Germany³Charité - Universitätsmedizin Berlin, Berlin, Germany**Question**

Atherosclerosis is a major risk factor for cardiovascular disease and can be exacerbated by dyslipidaemia. In addition to the process of blood coagulation, the activation of protease-activated receptor 1 (PAR-1) has been implicated in the pathophysiology of inflammation, leukocyte migration and atherosclerotic plaque formation. Vorapaxar, a PAR 1 antagonist, has been shown to inhibit thrombin-mediated signalling pathways that link coagulation with vascular inflammation and plaque biology, thereby reducing the risk of stroke and heart attack. Recent studies have indicated elevated PAR2 expression levels in atherosclerotic plaques. This finding indicates a substantial role for these G protein-coupled receptors in atherosclerotic processes. The objective of the present study was to investigate the PAR2 axis in atherogenesis and to examine an additional effect of vorapaxar on blood glucose levels.

Methods

ApoE knockout mice, a model organism for atherosclerosis, were fed a Western diet (WD) for four months. The effects of this diet on the subjects' weight, lipid metabolism parameters and plaque formation were examined. To determine the influence of PAR2, ApoExPAR2 double knockout mice were analyzed in comparison. Subsequently, ApoE and ApoExPAR2 KO animals were fed a WD for 4 months, treated with or without vorapaxar, and subjected to an oral glucose tolerance test.

Results

ApoExPAR2-KO mice exhibit a significant increase in hepatic lipid accumulation following WD, a condition known as steatosis, in comparison to ApoE-KO animals. The lower hepatic triglyceride lipase expression observed in the double knockout mice resulted in a significant elevation in triglyceride and LDL cholesterol levels. Furthermore, ApoExPAR2-KO mice exhibit an increase in body weight compared to ApoE animals, despite consuming an equivalent amount of food. Notably, despite the presence of these pro-atherogenic risk factors, ApoExPAR2-KO animals exhibit a reduced prevalence of plaques and atherosclerotic lesions. Furthermore, blood glucose levels in ApoE-KO animals are significantly lower than in ApoExPAR2 mice, suggesting a role of PAR2 in the regulation of blood glucose tolerance. Vorapaxar exerts no additional effect.

Conclusion

The significant reduction in atherogenesis in ApoExPAR2-KO mice demonstrates the crucial role of PAR2 in the development of atherosclerotic lesions. In addition, PAR2 appears to play an important role in the regulation of lipid and glucose metabolism.

P139**Investigating the Role of Mdm2 in Arrestin Cotrafficking with GPCRs**S. Ernst¹, L. M. Jackel¹, M. Bünnemann¹, C. Krasel¹¹Marburg University, Institut für Pharmakologie und klinische Pharmazie, Marburg, Germany

Introduction: Arrestins are important regulatory proteins of GPCRs. They can "arrest" receptor signaling by binding to the phosphorylated C-terminus of GPCRs and sterically block further G protein coupling. Furthermore, they decrease the presence of active GPCRs at the plasma membrane by initiating receptor internalization. Depending on the stability of this complex, arrestin can either dissociate from the receptor (Class A) or it can internalize together with the GPCR into early endosomes (Class B).

Objective: It has been shown that Class B receptors induce strong and long-lasting ubiquitination of arrestin, while stimulation of a Class A receptor results only in transient attachment of ubiquitin to arrestin. The E3 ubiquitin ligase that was shown to bind to arrestin is Mdm2, which is best known for its regulatory role in cell division, particularly through negative regulation of the tumor suppressor protein p53. Here we investigate whether Mdm2 regulates the cotrafficking of arrestin with GPCRs due to its role as ubiquitin ligase.

Materials and Methods: We used Crispr/Cas9 to generate a Mdm2 knockout in HEK293 cells. To analyse the importance of Mdm2 for arrestin trafficking, BRET assays were performed using the Mdm2 knockout cells, in which a Renilla luciferase was fused to arrestin and a GFP to a FYVE domain to investigate the enrichment of arrestin at endosomes. Furthermore we used confocal imaging and western blotting to study arrestin Mdm2 interaction and the effect of Mdm2 depletion on arrestin ubiquitination.

Results & Conclusions: Confocal imaging revealed that arrestin facilitates the translocation of Mdm2, which is predominantly found in the nucleus, into the cytosol, suggesting an interaction between these two proteins in living cells. The generated HEK293 cells contained a 19 bp deletion in exon 2 of the Mdm2 gene

and displayed a marked phenotype. BRET experiments and confocal imaging using this cell line demonstrated that various receptors such as the NTSR1, V2R, AT1R, and PTHR still lead to the colocalization of arrestin with GPCRs at early endosomes. Furthermore the inhibition of the E1 ubiquitin-activating enzyme with a small molecule and so nearly the complete inhibition of cellular ubiquitination, had no effect on arrestin trafficking. These results suggest that the E3 ligase Mdm2 has no effect on arrestin trafficking and, contrary to prevailing opinion, the ubiquitin status of arrestin overall seems not to affect its trafficking.

P140**The Function of Gai2 in Macrophages during Myocardial Infarction and its Role in the Development of myocardial Ischemia/Reperfusion Injury**J. Phierl¹¹Institut für Pharmakologie, Experimentelle Therapie und Toxikologie, Universität Tübingen, Tübingen, Germany

G proteins are a class of ubiquitously expressed proteins that facilitate communication between signaling pathways within and between cells. These proteins are involved in numerous signal transduction pathways within different cell types, including, but not limited to, neutrophils and macrophages. As demonstrated in a previous study conducted by our lab, the knockout of the G α_2 subunit in neutrophils leads to a limited migration pattern of those leukocytes as well as a significant decrease in platelet-neutrophil complexes. This phenomenon has also been observed in G α_2 knockouts in megakaryocytes and in macrophages. Analogous results could be observed utilizing an antibody directed against G α_2 . In an acute murine model simulating myocardial infarction, the absence or inhibition of G α_2 has been shown to result in a reduced area of affected tissue during ischemia-reperfusion processes. [1, 2]

In the course of the present thesis, the objective is to continue this project, with a focus on the identification of the underlying mechanisms through which the G α_2 antibody is leading to a reduction of the myocardial ischemia/reperfusion injury. It is therefore essential to elucidate the mechanism of uptake, the precise mechanism by which the antibody inhibits the G protein, and the resulting effect on cellular functions. In accordance with the conclusions of other recent publications, it is evident that, in addition to neutrophils and thrombocytes, macrophages too are involved in the process of myocardial ischemia/reperfusion injury. The second objective of this study is therefore to evaluate whether a knockout or inhibition of G α_2 in macrophages contributes to the protective effects on the myocardial ischemia/reperfusion injury. Moreover, the present study aims to assess the influence of the antibody on the function of macrophages.

[1] Köhler & Leiss et al. (2024). Targeting Gai2 in neutrophils protects from myocardial ischemia reperfusion injury. *Basic Res Cardiol.*, Vol. 119 (717-732). <https://doi.org/10.1007/s00395-024-01057-x>

[2] Köhler et al. (2014). Gai2- and Gai3-deficient mice display opposite severity of myocardial ischemia reperfusion injury. *PLoS ONE*, Vol. 9, No. 5. <https://doi.org/10.1371/journal.pone.0098325>

P141**Unraveling the roles of GRKs in GPCR phosphorylation through genetic knockouts and phosphosite specific antibodies**D. Freund¹, N. K. Blum¹, A. Decker¹, F. Nagel¹, J. Drube³, R. S. Haider³, C. Hoffmann², S. Schulz^{1,2}¹Jena University Hospital, Institut für Pharmakologie und Toxikologie, Jena, Germany²TM Antibodies GmbH, Jena, Germany³Jena University Hospital, Institut für Molekulare Zellbiologie, Jena, Germany

A crucial step for the G-Protein-coupled receptor (GPCRs) activation/deactivation cycle is the agonist-dependent phosphorylation. Mainly mediated by ubiquitously occurring GPCR kinases GRK2, GRK3, GRK5 or GRK6, the rules and principles that determine GPCR phosphorylation are not yet fully understood.

Combining CRISPR-Cas9-modified GRK knock-out HEK293 cells and phosphosite-specific antibodies we investigated the GRK specificity of a large number of GPCRs. Given the structural similarities between GRK2 and GRK3 and between GRK5 and GRK6 we focused on the GRK2/3 and GRK5/6 double and quadruple GRK2/3/5/6 knock-out cells to establish a preliminary classification of GPCRs.

So far, 20 GPCRs, different in structural and functional aspects, have been investigated. The results of our experiments show that GPCRs can be separated into four groups: The first and largest group is preferentially phosphorylated by GRK2/3 isoforms; the second group is preferentially phosphorylated by GRK5/6 isoforms; the third group can be equally phosphorylated by GRK2/3 or GRK5/6 isoforms; and the fourth group is phosphorylated in a GRK-independent manner. Our data will help to assess the extent to which sequence motifs, receptor structure, G protein coupling or the chemical nature of the ligand determine the specificity and selectivity of GPCR phosphorylation.

P142

Gi-modulating compound reverses acetylcholine and adenosine effects on sarcomere shortening and pro-arrhythmic extra-constrictions in adult rat cardiomyocytes

M. Rosso¹, J. Kockskämper¹, R. Reher², A. Naim², T. Berger²

¹Institute of Pharmacology and Clinical Pharmacy, Marburg, Germany

²Institute of Pharmaceutical Biology and Biotechnology, Marburg, Germany

Introduction Selective small molecule inhibitors of Gi proteins are lacking. Recently, *N*-hydroxyapiosporamide (NHAP), derived from the marine fungus *Apiospora* sp. 589, was identified as a putative selective inhibitor of Gi proteins using native metabolomics. Here, we tested whether NHAP may reverse Gi-mediated effects on sarcomere shortenings in adult rat cardiomyocytes.

Methods Sarcomere shortening was assessed in isolated rat ventricular and atrial myocytes field-stimulated at 1 Hz or 0.5 Hz, respectively, at room temperature. Isoprenaline (Iso, 30 nM) was used to increase shortening via beta-adrenergic receptors coupled to Gs signalling. Acetylcholine (ACh, 1 µM) or adenosine (Ado, 10 µM) were used to activate Gi signalling via M2 or A1 receptors in ventricular or atrial myocytes, respectively.

Results In ventricular myocytes pre-treated with Iso, addition of ACh greatly reduced fractional sarcomere shortening (FS). Further addition of NHAP (30 µM) in the presence of Iso and ACh largely reversed the ACh-induced negative-inotropic effect thus increasing FS by ≈31% (n=11, P<0.001). By contrast, addition of DMSO (solvent) to Iso- and ACh-treated cells did not alter FS (n=11, P=NS). The NHAP-induced increase in FS in the presence of Iso and ACh was concentration-dependent with smaller effects occurring at 10 µM or 3 µM NHAP. In atrial myocytes pre-treated with Iso, Ado greatly reduced FS. Addition of NHAP (30 µM) in the presence of Iso and Ado largely reversed the Ado effect increasing FS by ≈44% (n=11, P<0.01). Iso also induced the occurrence of pro-arrhythmic extra-constrictions (PEC) in the majority of both ventricular (8/11 cells) and atrial (9/11 cells) myocytes. ACh and Ado silenced the Iso-induced PEC. NHAP – but not DMSO – caused the re-occurrence of PEC (in 7/11 ventricular and in 6/11 atrial cells) thus reversing the anti-arrhythmic effects of ACh and Ado.

Conclusion In ventricular and atrial myocytes pre-treated with Iso, NHAP (30 µM) reverses both the negative-inotropic and the anti-arrhythmic effects elicited by ACh (in ventricular myocytes) or Ado (in atrial myocytes). The results are in line with the notion that NHAP inhibits Gi signalling induced by activation of M2 and A1 receptors in adult cardiomyocytes.

P143

Characterization of the interaction between the apelin receptor and arrestin

G. Baquero Cevallos^{1,2}, S. Ernst¹, M. Bünemann¹, C. S. M. Helker², C. Krasel¹

¹Marburg University, Institute of Pharmacology and Clinical Pharmacy, Marburg, Germany

²Marburg University, Institute of Cell Biology, Marburg, Germany

Background: The apelin receptor plays an important role during cardiovascular development as well as pathological angiogenesis. It has been proposed that certain signaling pathways of this receptor are G-protein independent but mediated by arrestins. Therefore, we wanted to characterize the interaction of the apelin receptor with arrestins in response to different ligands. **Methods:** We worked in transiently transfected HEK293T cells and employed resonance energy transfer-based methods (FRET, BRET) and confocal microscopy. **Results:** The three agonists [Pyr1]-apelin13, apelin36 and APELA all caused measurable interaction of luciferase-tagged arrestin3 with YFP-tagged apelin receptor. Apelin36 was more potent in inducing this interaction than the other two ligands with an EC50 of approximately 100 nM whereas [Pyr1]-apelin13 and APELA induced receptor-arrestin interaction with an EC50 of approximately 1 µM, in agreement with the literature. Arrestin recruitment is usually preceded by GRK-mediated phosphorylation of the receptor. We could measure agonist-induced GRK2 interaction with the apelin receptor in the presence of Gs which occurred with similar EC50s. Five phosphorylation sites have been proposed to exist in the apelin receptor: Ser335, Ser339, Ser345, Ser348 and Ser369. Single serine replacement with alanine had no effect on arrestin recruitment, in contrast to previous papers that described critical roles of Ser348 (Chen et al., J Biol Chem 289: 31173–31187 (2014)) or Ser339 (Chen et al., Redox Biol 36: 101629 (2020)) in this process. We also created some larger replacements but neither the replacement of T334S with Ala nor the replacement of S345YSS with AYAA had any measurable effect on arrestin3 recruitment. Furthermore, we could not reproduce reports that apelin36 causes translocation of arrestin3 to endosomes. In our hands, the apelin receptor could only recruit arrestin3 to the plasma membrane, regardless of the ligand used. **Discussion:** We conclude that a more thorough characterization of apelin receptor-arrestin interaction is required to understand the potential arrestin-mediated signaling of this receptor.

P144

Analysis of molecular mechanisms of ligand bias in muscarinic receptors

J. Enaigle¹, B. Bremer¹, A. Flöser¹, K. Klingelhöfer¹, M. Bünemann¹

¹Marburg University, Institut für Pharmakologie und Klinische Pharmazie, Marburg, Germany

G protein-coupled receptors (GPCRs) transmit extracellular signals to the inside of the cell via intracellular effector proteins. Agonist binding causes a conformational change in the receptor, leading to activation of heterotrimeric G-proteins. Subsequently G protein-coupled receptor kinases (GRK) phosphorylate the receptor. Now arrestin is enabled to bind to the activated phosphorylated receptor, inducing receptor desensitization and tolerance. Sometimes the induction of tolerance is the wanted mechanism of drugs such as in the case of gonadorelins, however for many agonists the development of tolerance is detrimental (e.g. opioids). Depending on the relative efficacies of agonists to recruit G proteins, GRKs and arrestins to the receptor a ligand bias towards or

against tolerance can be generated. Here we set out to identify the mechanism of agonist bias for agonists of different muscarinic receptors. We therefore measured the recruitment of each of these proteins in an interference free manner (Flöser et al., 2021). To detect a potential agonist-bias we performed single-cell FRET measurements using six different agonists. We transfected HEK293T cells with a YFP-tagged receptor and a CFP-tagged Gβγ-subunit, G-protein-independent GRK2-CAAX mutants and arrestin3. We observed that pilocarpine exhibits an bias towards arrestin3-binding compared to GRK2 or G protein binding in the case of M3R, whereas in the case of M5R such a ligand bias for pilocarpine was absent. This data indicate a receptor-subtype specific mechanism of generating agonist-bias. In order to assess this further, future experiments will also investigate the impact of positive allosteric modulators (PAM) on a potential ligand bias at the M1 and M2 receptor. In contrast to the investigated ligands who bind to the orthosteric binding pocket, PAM bind to the allosteric binding pocket of the receptor. In presence of orthosteric agonists, application of PAM BQCA on the M1 receptor and LY2119620 on the M2 receptor may shift a potential bias.

P145

Determinants of G-protein coupling specificity in muscarinic acetylcholine receptors

A. Wißmann¹, S. B. Kirchhofer¹, V. Jelinek¹, M. Bünemann¹

¹Marburg University, Institut für Pharmakologie und klinische Pharmazie, Marburg, Germany

The family of muscarinic acetylcholine receptors can be divided into two distinct groups: M1,3&5-receptors all bind predominantly to the Gq-protein, while the M2&4-receptors bind very selectively to the Go-protein. Our group has produced chimeras of the M2/M3 receptor and the Gq/Go subunit to identify structural determinants which are important for G-protein binding and activation.

We transfected the chimeras into HEK293T cells, in which we measured the binding between GPCR and G protein using FRET measurements. We were able to confirm that the structural elements TM 5,6 and the C-terminus are important for G protein coupling. For example the exchange of TM 5&6 in the M3 receptor led to a lower Gq affinity. But if we alter the C-terminus, the Go affinity decreases. Some chimeric receptors showed G-protein binding without subsequent activations determined by BRET assays. These results are in line with a two step mechanism of activation. If we inserted the C-terminus of the M3 receptor into M2, the Go activation was enhanced. However, inserting TM 5&6 from the M3 receptor into the M2, the Go activation was reduced.

Under both measurement conditions, we found that it always depends on a combination of different structural elements that are decisive for coupling specificity. To narrow things down, we are now investigating the receptor chimeras in combination with the G protein chimeras; here we are focusing primarily on a Go chimera in which the bridge between β2 & β3 contains 6 amino acids of the Gq protein. This region was previously identified to be important for G protein binding. By replacing just six amino acids, we were able to re-enable binding between the receptor and the G protein where there was none with the Go wild type. A combination of a chimeric approach on the level of Gq/Go proteins and M2/M3 receptors may provide us with detailed informations on the mechanism of G protein selectivity of muscarinic receptor subtypes.

P146

Velusetrag enhances cardiac Ca²⁺ dynamics via human 5-HT₄ receptors

P. Pauls¹, I. C. Molderings¹, U. Gergs², J. Neumann², J. S. Schulte¹, U. Kirchhefer¹

¹University Medical Centre of Münster, Institut für Pharmakologie und Toxikologie, Münster, Germany

²Martin Luther University Halle-Wittenberg, Institut für Pharmakologie und Toxikologie, Halle (Saale), Germany

Background: Velusetrag is a selective serotonin 5-HT₄ receptor agonist that was originally developed as a gastrointestinal prokinetic agent. Since 5-HT₄ receptors are also expressed in the human heart, with elevated mRNA levels reported in heart failure, we studied the potential cardiac effects of this compound using transgenic (TG) mice overexpressing human 5-HT₄ receptors and wild-type (WT) controls lacking cardiac expression of these receptors.

Methods: Ventricular myocytes were isolated from TG and WT mice. Intracellular Ca²⁺ transients were recorded using Indo-1 fluorescence, and contractility was assessed by recording sarcomere shortening. Whole-cell L-type Ca²⁺ currents (I_{CaL}) were obtained using the patch-clamp technique. Cells were exposed to 10 µM velusetrag and subsequently to 1 µM of the β-adrenergic agonist isoprenaline.

Results: In WT myocytes, velusetrag had no effect on Ca²⁺ transient amplitude, while isoprenaline increased it by 65%. In TG myocytes, velusetrag enhanced Ca²⁺ transient amplitude by 52% (in [r.u.]: TG_{basal}: 0.106 ± 0.006 vs. TG_{velusetrag}: 0.161 ± 0.013, p = 0.0239, n = 10 animals, each with an average of 10 cells, ordinary one-way ANOVA), with no further rise upon isoprenaline application. Consistently, velusetrag did not alter I_{CaL} in WT cells but increased it by 42% in TG cells. Isoprenaline subsequently enhanced I_{CaL} by 52% in WT but produced no additional effect in TG cells. Despite the augmented Ca²⁺ handling, velusetrag did not significantly change sarcomere shortening in either genotype. Isoprenaline increased contractility in WT but not TG myocytes. To explore the basis of this absent inotropic response in TG, we compared both genotypes under basal conditions. The raw data revealed significantly higher peak I_{CaL} (by 22%), higher Ca²⁺ transient amplitude (by 28%), and increased sarcomere shortening (by 61%) in TG compared with WT cardiomyocytes.

Conclusion: Overexpression of human 5-HT₄ receptors enhances Ca²⁺ cycling and contractility in mouse ventricular cardiomyocytes under basal conditions. Velusetrag selectively activates these receptors, further enhancing sarcolemmal

Ca²⁺ influx and intracellular Ca²⁺ transients likely through cAMP-dependent mechanisms. Although velusetrag was developed as a prokinetic agent, its pronounced cardiac effects raise potential safety concerns, particularly under conditions of elevated 5-HT₄ receptor expression such as heart failure.

P147

Modular optimization of cell-free GPCR synthesis for Cryo-EM studies

A. Grimm¹, F. Bernhard¹, Z. Köck¹, P. Dahlhaus^{1,2}, F. Merino^{1,2,3}

¹Goethe University Frankfurt, Institute of Biophysical Chemistry, Frankfurt a. M., Germany

²Marburg University, Institute for Pharmaceutical Chemistry, Marburg, Germany

³Cube Biotech, Monheim am Rhein, Germany

G protein-coupled receptors (GPCRs) are essential pharmacological targets and their fast and reliable synthesis at high-quality is prerequisite for future drug development. We demonstrate a modular cell-free expression pipeline that cotranslationally integrates GPCRs and other complex membrane proteins in selected lipid environments. Followed by a two-step purification protocol, the samples are directly suitable for Cryo-EM studies (1, 2). Key advantages of the cell-free expression strategy are (i) cotranslational stabilization of GPCRs with supplied ligands or interaction partners, (ii) choice of membrane composition and translocon-independent integration, (iii) production of full-length and non-engineered GPCRs.

Our modular process for GPCR expression protocol development systematically optimizes GPCR yield and quality. Cell-free synthesis reduces the complexity of protein synthesis down to the basic translation process. Problems with low or no protein production are thus mainly caused by poor initiation of translation. The newly established NSEC (nanoparticle-based size exclusion) approach is an universal and fast screening method to make a first quality assessment of cell-free synthesized membrane proteins independent of their type, origin or function.

We show representative NSEC quality profiles of numerous GPCRs and other membrane proteins and document the efficiency of our cell-free expression platform by Cryo-EM structures of the human histamine 2 and β 1-adrenergic receptors in complex with heterotrimeric Gs protein. We approach the large but still underexplored class of olfactory GPCRs (oGPCRs) and tune their quality by systematically screening of reaction condition modules. Most powerful tools are interaction partners such as engineered G protein subunits, supplying selective ligands during synthesis and using modified nanoparticle topologies.

Merino, F., Köck, Z., Ermel, U., Dahlhaus, P., Grimm, A., Seybert, A., Kubicek, J., Frangakis, A.S., Dötsch, V., Hilger, D., and Bernhard, F. Cryo-EM structure of a cell-free synthesized full-length human β 1-adrenergic receptor in complex with Gs. Structure

Köck, Z., Schnelle, K., Persechino, M., Umbach, S., Schihada, H., Janulien, D., Parey, K., Pockes, S., Kolb, P., Dötsch, V., Möller, A., Hilger, D., and Bernhard, F. (2024) Cryo-EM structure of a cell-free synthesized human histamine 2 receptor/Gs complex in nanodisc environment. *Nat commun.* **15**, 1831.

P148

Characterisation of carboxy-terminal phosphorylation dynamics of the human β_2 -adrenoceptor

C. T. Luchmann¹, R. Reinscheid¹, S. Schulz¹

¹Jena University Hospital, Institut für Pharmakologie und Toxikologie, Jena, Germany

The human β_2 -adrenoceptor (ADRB1) is a key G protein-coupled receptor (GPCR) in cardiac physiology, and its dysregulation is associated with cardiovascular diseases such as heart failure and hypertension. Although ADRB1 has been the subject of intensive research, the mechanisms controlling the termination of its signalling remain poorly understood. To elucidate these mechanisms, we used phosphosite-specific antibodies and Western blot analysis to characterise the phosphorylation of Ser/Thr residues in the C-terminus. Our data reveal that all investigated residues undergo dynamic changes in phosphorylation upon stimulation with isoprenaline and/or direct activation of PKC. Interestingly, the resulting phosphorylation barcodes differed significantly between these conditions. Moreover, simultaneous activation of both pathways produced a third, intermediate phosphorylation pattern. Finally, we demonstrate that comparable phosphorylation changes can be triggered by activation of Gq-coupled receptors, such as the angiotensin II type 1 receptor and the arginine vasopressin type 1A receptor, which are also expressed in cardiomyocytes. These findings indicate that the phosphorylation profile of ADRB1 can be precisely modulated by distinct signalling inputs. In the long term, these insights may contribute to a deeper understanding of receptor desensitisation mechanisms under pathophysiological conditions.

P149

Selection and characterization of fully synthetic IgG fragments targeting Neurotensin Receptor 1

A. C. Niederer¹, C. Thom², P. Heine², M. Hilge², C. Klenk¹, A. Plückthun²

¹Justus Liebig University Gießen, Rudolf-Buchheim Institute of Pharmacology, Gießen, Germany

²University of Zurich, Department of Biochemistry, Zurich, Switzerland

Neurotensin (NTS) is a 13-amino acid neuropeptide that modulates key physiological processes including nociception, blood pressure regulation, thermoregulation, and dopaminergic signaling. It primarily acts through neurotensin 1 receptor (NTSR1), a class A GPCR, that is implicated in psychiatric and neurodegenerative disorders as well as in the progression of different cancer types, making it an attractive target for therapeutic intervention. However,

traditional small-molecule drug-discovery approaches often struggle with peptide-activated GPCRs due to the receptor's spacious ligand-binding pockets and the difficulty of achieving sufficient selectivity and *in vivo* stability.

To address these limitations, we developed immunoglobulin-derived fragments (Fabs) as protein-based ligands capable of modulating NTSR1. Using a thermostabilized NTSR1 variant as a target, we obtained several synthetic anti-NTSR1 Fabs by phage display of a synthetic Fab library and high-throughput selection. Subsequent cryo-EM structures of Fab:NTSR1 complexes revealed two mechanistic classes of binders: Fabs that stabilize an active-like receptor conformation, and Fabs that occlude the orthosteric pocket, suggesting antagonistic properties.

Here, we characterize the pharmacological properties of the different Fabs. We assessed binding of Fabs and effects on downstream receptor signaling on NTSR1-expressing cells, and we established a workflow to measure kinetics of Fab binding to the isolated receptor. These analyses uncovered distinct Fab subsets with divergent receptor preferences: First, we identified Fabs that were acting as agonists on NTSR1. Second, several non-activating Fabs bound both wild-type and thermostabilized NTSR1 with comparable affinity, while others showed clear selectivity between both variants, which likely results from differences in the interaction surfaces of the two receptors. Fab association and dissociation measurements further revealed large kinetic heterogeneity, indicating unique interaction patterns of Fab:NTSR1 complexes and hinting at the stabilization of diverse receptor conformational states upon Fab binding.

Together, these findings highlight Fabs as versatile modulators of NTSRs. By defining their structural, kinetic, and functional properties, this work expands the pharmacological toolkit for targeting neurotensin signaling and demonstrates the promise of protein-based ligands as alternatives to small molecules in GPCR drug discovery.

P150

Role of non-canonical G protein signaling pathways during polarization of neutrophilic granulocytes

L. Maaß¹, S. Beer-Hammer¹, B. Weigelin²

¹University Hospital Tübingen, Department of Experimental and Clinical Pharmacology and Pharmacogenomics, Division of Pharmacology, Experimental Therapy and Toxicology, Tübingen, Germany

²University Hospital Tübingen, Werner Siemens Imaging Center, Tübingen, Germany

Neutrophils, as first actors of the immune system, contribute significantly to ischemia-reperfusion injury (IRI), which occurs in the context of myocardial infarction or stroke and aggravates clinical outcome. After ischemia, reperfusion takes place, during which – among others – neutrophils exit the bloodstream and migrate directionally into the infarcted area. By releasing reactive oxygen species, proteolytic enzymes and inflammatory mediators neutrophils contribute to this sterile inflammation. It is well described that neutrophil migration into the infarcted area is regulated by G-protein signaling pathways. In particular, the isoforms Gai2 and Gai3 seem to play an important role. Our group has shown that the specific deletion of Gai2 or Gai3 in platelets or in neutrophils and macrophages, significantly reduced the extent of IRI after myocardial infarction, whereas the outcome in cerebral stroke was different.

In contrast, non-canonical G-protein signaling pathways remain poorly understood and their role in neutrophil polarization and migration during ischemia-reperfusion injury following myocardial infarction or stroke is largely unknown. The ischemic phase leads to massive cell death with the release of DAMPs (damage-associated molecular patterns) like HMGB-1 (high-mobility-group-box 1). These and other chemoattractants (e.g. fMLP) bind to surface-receptors of circulating neutrophils, most of which are associated with Gai-proteins. Binding to these GPCRs induces polarization, i.e. the directional orientation of the cell by forming a leading-edge containing F-actin.

In my project, murine neutrophils are isolated and stimulated with chemoattractants to induce polarization. The aim is to compare chemoattractants that bind GPCRs with those that are non- or indirectly G-protein-dependent, such as HMGB-1, to identify potential differences. This may give an insight into non-canonical G-protein signaling pathways. Moreover, it is unclear whether different chemoattractants trigger the two Gai-isoforms differently. Therefore, I plan to compare the polarization of Gnai2-, Gnai3-, and Gnai2/3-deficient neutrophils after stimulating them with different chemoattractants. In addition, the interactions between G-proteins, activators of G-protein signaling (AGS), and other mediators remain unclear. Thus, I aim to investigate these interactions and the role of biomolecular condensates in neutrophil polarization.

P151

Overcoming Structural Barriers to lock Gs in its inactive state

L. Jürgenliemke¹, F. Eryilmaz¹, N. Merten¹, L. Grätz¹, J. H. Voss^{2,3}, M. Dörfler¹, G. M. König¹, M. Crüsemann^{1,4}, C. E. Müller⁵, D. Hilge⁶, E. Kostenis¹

¹University of Bonn, Institute of Pharmaceutical Biology, Bonn, Germany

²Skape Bio, Copenhagen, Denmark

³University of Bonn, Pharmaceutical Institute, Pharmaceutical & Medicinal Chemistry, Bonn, Germany

⁴Goethe University Frankfurt, Institute for Pharmaceutical Biology, Frankfurt a. M., Germany

⁵Marburg University, Department of Pharmaceutical Chemistry, Marburg, Germany

Introduction

Heterotrimeric G proteins (G $\alpha\beta\gamma$) are the principal transducers downstream of G protein-coupled receptors (GPCRs). Pharmacological stabilization of their inactive

state holds significant promise as both research tools and therapeutic agents by enabling precise dissection of GPCR signaling and targeted intervention in G protein-driven diseases. Among the four major G protein families, only Gq can currently be maintained fully signaling-silent by the cyclic peptides FR900359 (FR) and YM-254890 (YM), which act by blocking guanine-nucleotide exchange. Equally selective and potent inhibitors for other G protein families, including Gs and G12/13, are lacking. This represents a critical gap in the toolkit for controlling heterotrimeric G protein signaling.

Objective

To address this gap for experimental inhibition of Gs, we took advantage of FR and engineered synthetic Gas variants with artificial FR-binding sites to confer sensitivity to this inhibitor.

Methods

Using targeted mutagenesis, we generated a panel of engineered Gas variants, including the previously published Gas11, where 11 amino acids responsible for inhibitor binding were replaced with corresponding Gαq residues. These variants were thoroughly characterized through biochemical and BRET-based assays as well as inhibitor-binding studies, to evaluate their functionality and inhibitor sensitivity.

Results

Engineered Gas variants displayed profound "Gq-like" FR binding, confirming successful transfer of the FR-binding site to Gas. Nevertheless, full inhibition of Gs signaling was not achieved, especially under conditions of high receptor expression and strong agonist stimulation. Because the mutations required for FR sensitivity overlap with regions that regulate nucleotide exchange, GTP hydrolysis, and Gβγ binding, incomplete inhibition may result from any of these factors. Our data indicate that impaired Gβγ-binding, which, similarly to FR, restricts GDP dissociation, undermines inhibition efficacy in Gs proteins.

Conclusion

We identify Gβγ binding as a key structural barrier limiting FR-mediated inhibition of Gs. Rational design of constructs that preserve Gβγ regulation while enabling FR engagement will therefore be crucial to develop potent, selective Gs inhibitors. Our insights provide a foundation for future pharmacological strategies targeting Gs signaling pathways.

P152

Development of an in vitro co-culture model of inflammatory bowel disease to examine the effect of histamine H₄ receptor on gastrointestinal inflammatory processes

A. Bahgat¹, B. Schirmer¹, D. Neumann¹, R. Seifert¹

¹Hannover Medical School (MHH), Institute of Pharmacology, Hanover, Germany

Introduction: Histamine, a mediator in immunological processes, reveals its pleiotropic functions upon binding to its receptors, such as the histamine H₄ receptor (H₄R), which is a GPCR mainly expressed in immune cells and in tissues such as the intestine. Studies have described the pro-inflammatory role of H₄R on the pathophysiology of inflammatory bowel disease in model systems such as mice. However, the effect of H₄R on intestinal inflammation on cellular and molecular level is yet to be elaborated [1]. Our aim is the development of an in vitro co-culture model of intestinal inflammation suitable to examine further functions of H₄R.

Methods: As a model, we used Caco-2 cells, THP-1 cells, and inserts with a porous membrane. On the apical side, Caco-2 cells differentiate upon confluency to form a polarized epithelial monolayer. To examine differentiation of Caco-2 cells, the transepithelial electrical resistance (TEER) was measured for 21 days. On the basolateral side, THP-1-derived macrophage-like cells imitate the underlying immune environment. To derive macrophages, we stimulated THP-1 cells with 100 nM PMA for 24 h to differentiate to resting macrophages (M0). M0 cells were differentiated to activated macrophages (M1) through co-stimulation with 20 ng/ml LPS and 20 ng/ml IFN-γ for 48 h. IL-8 release, H₄R expression, and histamine release of THP-1, M0, and M1 cells were observed using ELISA, RT-qPCR, and HPLC-MS, respectively. We transfected Caco-2 cells with a plasmid containing human H₄R gene using two separate methods: electroporation and chemical transfection. H₄R expressions of transfected Caco-2 cells and untreated Caco-2 cells were compared using RT-qPCR.

Results: We demonstrate a maximum TEER of Caco-2 cells after about 12 days. Significant increase of IL-8 release and gradual increase of H₄R expression of THP-1 cells throughout the differentiation to M1 cells can be observed. In contrast, we could not detect quantifiable histamine release of THP-1 cells and its derived macrophages. Transfected Caco-2 cells showed significant increase of H₄R expression compared to untreated Caco-2 cells.

Conclusion: For the co-culture, we were able to introduce H₄R into Caco-2 cells, which will be combined with M1 macrophages after differentiation time of 2 weeks. The functional activity of H₄R in transfected Caco-2 cells should be examined prior to experiments with the co-culture.

[1] Schirmer and Neumann (2021). *Int J Mol Sci*, 22(6116).

Mixture Toxicology

P153

Integrated transcriptomics and proteomics analysis of pesticide mixtures in a rat study

H. Sprenger¹, A. Vogt², O. Poetz², D. Lichtenstein¹, A. Braeuning¹

¹German Federal Institute for Risk Assessment (BfR), Department Chemical and Product Safety, Berlin, Germany

²Signatope GmbH, Reutlingen, Germany

The simultaneous presence of multiple pesticide residues in food is a potential concern, as combined effects on human health remain poorly understood. A key challenge in mixture toxicology is the identification of modes of action (MoA) that drive adverse outcomes. Omics-based approaches provide new opportunities to characterize such MoA and thereby improve the scientific basis for mixture risk assessment.

This study builds on earlier work within the EuroMix project, where the toxicological effects of two pesticides with steatogenic potential were investigated in a 28-day oral gavage study in female Wistar rats [1, 2]. Thiacloprid (THI) and clothianidin (CTD) were applied at five dose levels, alone and in combination. Hepatotoxicity was assessed through pathology and histopathology. The present study expands this analysis to capture dose-dependent molecular responses at the transcriptome and proteome levels.

Liver samples from different dose levels were analyzed using RNA sequencing and proteomics. The proteomics component combines a targeted approach, focusing on xenobiotic-metabolizing enzymes and transport proteins, with an untargeted global proteome analysis.

RNA-Seq showed a dose-dependent rise in differentially expressed genes and enriched GO terms. CTD mainly affected cell division pathways, while THI effects were linked to fatty acid metabolism. The mixture combined single-compound effects but also caused additional down-regulation of genes related to cell adhesion and signal transduction. Targeted proteomics confirmed a dose-dependent induction of Cyp2b2, suggesting a synergistic mixture effect, and untargeted proteomics indicated stronger responses for CTD and the mixture than for THI. Benchmark dose modeling highlighted the most sensitive pathways for mechanistic interpretation.

By integrating transcriptomic and proteomic data with existing histopathology findings, this study provides deeper mechanistic insights into the hepatotoxicity of THI, CTD and their mixtures. The data enhance our understanding of pesticide mixture effects and support more informed risk assessment.

1. Alarcan, J. et al. *Food Chem Toxicol* 140, 111306 (2020). <https://doi.org/10.1016/j.fct.2020.111306>

2. Alarcan, J. et al. *Arch Toxicol* 95, 1039–1053 (2021). <https://doi.org/10.1007/s00204-020-02969-y>

P154

Exploration of the Mixture Toxicity of Bisphenols in Zebrafish Larvae and HepG2 Cells

R. Chen¹, B. Bauer¹, H. Hintzsche¹

¹University of Bonn, Department of Food Safety, Bonn, Germany

Background and Purpose: Bisphenol analogues (BPs), widely used in polycarbonate plastics and epoxy resins, are frequently detected in consumer products and the environment, raising concerns for human and ecological health. Most toxicological studies focus on single compounds, whereas real-life exposure involves complex mixtures, and knowledge of their cumulative toxicity and underlying mechanisms remains limited. This study investigates the toxicological effects and potential interactions of four bisphenol analogues — BPA, BPE, BPF, and BPS — using zebrafish larvae and HepG2 cell models.

Methods: Acute toxicity of four bisphenol analogues was assessed in zebrafish larvae over 48 h, including single compounds and binary, ternary, and quaternary mixtures, with mortality as the endpoint. Cytotoxicity in HepG2 cells was evaluated using the MTT assay after 4 h and 24 h exposures for both single compounds and mixture combinations. Genotoxicity of single compounds was assessed in HepG2 cells using the comet assay after 4 h and 24 h exposures to detect DNA strand breaks.

Results: BPA, BPE, BPF, and BPS exhibited concentration-dependent mortality in zebrafish larvae and cytotoxicity in HepG2 cells, with toxicity ranked as BPA > BPE > BPF > BPS. In zebrafish larvae, mixture exposures produced composition-dependent effects, with some binary and ternary combinations (e.g., BPF + BPS, BPA + BPF + BPS) showing higher mortality, while others were less toxic. In HepG2 cells, prolonged exposure (24 h vs. 4 h) significantly increased cytotoxicity. Mixture experiments also revealed composition-dependent interactions, with BPA-containing combinations generally being more toxic, whereas BPE- or BPS-dominated mixtures tended to be less toxic.

Conclusions: These findings demonstrate distinct differences in potency among bisphenol analogues and reveal the complexity of mixture interactions beyond simple dose–response relationships. Importantly, quaternary mixtures did not produce substantially greater toxicity than ternary mixtures, suggesting non-linear mixture effects. Overall, the results highlight the need to integrate differential potency and mixture interactions into toxicological evaluation and risk assessment of bisphenols, and point to the importance of further mechanistic investigations.

P155**Mixture Toxicity of long-chain PFAS in Larval Zebrafish**D. Wu¹, B. Bauer¹, H. Hintzsche¹¹University of Bonn, Ernährungs- und Lebensmittelwissenschaften, Bonn, Germany

Per- and polyfluoroalkyl substances (PFAS) are highly persistent and bioaccumulative, raising concerns for ecosystems and human health. Long-chain perfluorinated carboxylic acids such as PFDA, PFUnDA, PFDoDA and GenX, merit attention due to their rising occurrence and limited mixture toxicity data. Previous studies have primarily focused on single-compound acute toxicity, whereas evidence regarding combined effects and organ-specific outcomes remains scarce.

Larval zebrafish were exposed for 48 h to PFDA, PFUnDA, PFDoDA, and GenX, both individually and in binary, tertiary, and quaternary combinations. Concentration–response relationships were established to calculate LC50 values, and mixture interactions were characterized using concentration addition and independent action models to distinguish additive, synergistic, or antagonistic effects. In addition, histopathological analysis was conducted to evaluate structural alterations.

At lower concentrations, mortality was absent or minimal, while increasing concentrations resulted in progressively higher lethality. This mortality trend was consistent across replicates for all tested compounds.

The present study characterized the acute toxicity of selected PFAS, and additional PFAS mixtures experiments and histopathology are being conducted to further elucidate mixture effects and strengthen mixture-oriented ecological and human health risk assessments.

P156**Anthropogenically Produced Polymers: Tackling Toxic Conditions**C. Schmidt¹¹University of Tübingen, Medizinische Fakultät, Tübingen, Germany

Question: Anthropogenically produced micro- and nano-polymers ("mAPPs" and "nAPPs") are more accurate terms than micro- and nanoplastic particles [Schmidt ECS. Allergo J 2025, 34:99]. For decades, these were the subject of debates due to their ecotoxicological effects and potential health implications. To explore the relationship between APP exposure and health risks such as acute toxicity and inflammation, a parenteral pilot study was conducted to evaluate physiological responses and preventive measures.

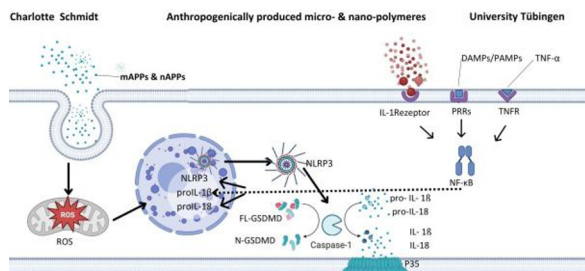
Objectives: My research aims at identifying and classifying polymer-related and polymer-induced factors that contribute to inflammation, ROS generation, and vascular calcification, thereby estimating the potential health risks associated with mAPPs and nAPPs.

Methods: APP exposure was investigated as a possible inducer of ROS depending on particle size, shape, polarity, zeta potential, hydrophobicity, and contamination level. A hydrogenic solution was administered parenterally to bypass hepatic filtration. Blood samples were taken before and after study completion for differential blood counts, quantification of inflammatory mediators such as interleukins, and measurement of polymer particle concentration.

Results: The study demonstrated that the number of plastic particles in the blood decreased moderately after the consumption of infusion solutions; yet, a rise of specific plastic particles in a specific size could be observed. Although these particles are by no means biologically neutral, the study found that micro- and nanoplastic particles did not alter cytokine levels or cause dysregulation of physiological processes.

Conclusion: My findings show the pivotal role of biomarkers, deepening the understanding of toxicokinetics, particularly in relation to the assessment of potential immunological effects associated with mAPPs and nAPPs. Provided that laboratory biomarkers and physiological parameters are closely monitored, future exploratory studies may further elucidate the links between environmental toxicology of mAPPs and nAPPs. No adverse physiological parameters indicative of health effects were observed; nonetheless, the possibility of polymeric contamination cannot be excluded.

Acknowledgements: I sincerely thank Professor Dr. Monika Rieger for her invaluable advice & continuous encouragement, as well as Professor Dr. Florian Lotz for his expert feedback and steadfast support. Funding by the DAAD grant no. 57595573 is acknowledged.

Fig. 1

The author has no competing interests.

P157**Transcriptomic Insights into Liver Toxicity from Mixture Effects: A Case Study of Pesticide and Microcystin Exposure**S. Kießig¹, E. Zini Moreira Silva², I. Suciu¹, D. Morais Leme^{1,2}, P. Marx-Stölting¹¹German Federal Institute for Risk Assessment (BfR), Pesticides Safety, Testing and Assessment Strategies Pesticides, Berlin, Germany²Federal University of Paraná (UFPR), Department of Genetics, Curitiba, Brazil

Hundreds of chemicals, of natural origin or synthetic, are part of our environment. Consequently, humans are exposed to complex mixtures, often less studied compared to individual substances and to well-defined product formulations. Assessing the risks posed by such mixtures remains challenging, as interactions between substances may enhance overall toxicity to humans. To evaluate potential risks more effectively, New Approach Methodologies (NAMs), such as *in vitro* assays combined with transcriptomic analyses, can be applied. Among the many relevant contaminants, pesticides and natural toxins such as microcystins (MCs) play a significant role due to their co-occurrence in food and drinking water. Thus, the present work investigates the mixtures of this class of natural toxin with a hepatotoxic pesticide using a pathway-based gene expression analysis applied to the HepaRG cell line – a well-established human hepatocyte *in vitro* model.

We examined two MCs, MC-LR and MC-LA, and one liver toxic pesticide, propyzamide, as well as their mixtures in non-cytotoxic concentrations in HepaRG cells over 24h. We analysed mRNA expression using qPCR array panels (Molecular Toxicology PathwayFinder 384HT, Qiagen) to screen for liver toxicity markers for individual substances and mixtures. Ingenuity Pathway Analysis was used to investigate disease and molecular pathways effects. Mixture effects were modelled using PROAST (RIVM) based on five differently expressed genes.

Both MCs and propyzamide affected xenobiotic metabolism and oxidative stress. Exposure altered expression of CYP enzymes (*CYP1A1*, *CYP1A2*, *CYP2B6*, *CYP3A4*) and the antioxidant enzyme glutathione peroxidase 2 (*GPX2*). These genes, linked to nuclear receptors (AhR, PXR, CAR, Nrf2), served as markers for mixture evaluation. MCs showed a strong down-regulation in the mentioned markers; their combination resulted in dose addition, suggesting a shared mechanism of action. Propyzamide alone caused up-regulation of the target genes, while mixtures with the MCs resulted in antagonism. A comparative analysis of the array data revealed antagonistic effects and provided insights into the pathways involved.

Our findings demonstrate that mixtures of MCs and the hepatotoxic pesticide propyzamide interact on a transcriptome level, showing additive or antagonistic effects on liver toxicity markers. These results highlight the value of transcriptomic NAMs for characterizing mixture effects and improving chemical risk assessment.

P158**Effect Biomonitoring via Untargeted Metabolomics: A Pilot Study Investigating the Urinary Metabolome of Firefighters**C. Kersch¹, M. P. Boehler¹, B. Rossbach², A. Kaiflie-Pechmann¹, S. Schmitz-Spanke¹¹Friedrich-Alexander University of Erlangen-Nuremberg, Institute and Outpatient Clinic of Occupational, Social, and Environmental Medicine, Erlangen, Germany²Johannes Gutenberg-University, Institute of Occupational, Social and Environmental Medicine, Mainz, Germany**Background**

Firefighters are regularly exposed to a wide variety of stressors ranging from a mixture of toxic compounds found in smoke to physical strain and heat. Previous studies have primarily focused on exposure biomonitoring, looking for specific markers. For example, biomonitoring following live fire training repeatedly showed elevated urinary levels of PAH metabolites, proving exposure despite the use of protective gear. In contrast, there is little data on effect biomonitoring linked to occupational fire fighting activities. This pilot study aims to use an untargeted approach to differentiate between the metabolic responses to fire exposure and physical exertion using urine samples collected from controlled training sessions of firefighters.

Methods

For this study we used samples collected from two individual probands, before and after they went through two training scenarios on different days: One used only respiratory protection training to monitor physical stress without smoke exposure. The other exposes the participants to smoke in a controlled fire setting. The metabolites were extracted from the urine samples using acetonitrile and analyzed using untargeted GC-MS spectrometry. For data analysis we used eRah as well as Metaboanalyst 6.0.

Results

Our study was able to identify 79 human metabolites. Principal Component Analysis (PCA) showed a clear separation between the respiratory protection and fire scenario. A t-test found four significantly regulated metabolites for fire exposure: A decrease in catechol and 3-hydroxyphenylacetic acid and an increase in 5-hydroxy-L-tryptophan and serotonin. According to pathway analyses the tryptophan pathway is primarily impacted. A ROC analysis (Receiver Operating Characteristic) highlights a panel of key metabolites from the shikimic acid pathway and tyrosine metabolism as the best markers for a separation between the two exposure scenarios.

Conclusion

Changes in the tryptophan as well as the catecholamine pathway indicate a major systemic stress caused by fire exposure. While the metabolic changes indicate biological effects, a more comprehensive study is needed for specificity. Additionally, due to the conditions of the study we cannot distinguish between the effect from toxicologic exposure and stressors such as heat. In our opinion, urine offers an easily accessible and non-invasive way for effect biomonitoring of firefighters and promising insights into possible toxicological effects.

P159

Unravelling the potential use of metabolomics for *in vitro* PoD derivation and IVIVE for plant protection product mixture effects

A. Stagos-Georgiadis^{1,2}, P. Marx-Stölting¹, T. Tralau³, D. Bloch¹

¹German Federal Institute for Risk Assessment (BfR), Pesticides Safety Department, Berlin, Germany

²University of Potsdam, Institute of Nutritional Science, Potsdam, Germany

³German Federal Institute for Risk Assessment (BfR), Berlin, Germany

Plant protection products (PPPs) contain one or more active substances (AS) as well as a varying number of co-formulants. AS hazard and risk are extensively evaluated prior to approval for different endpoints whilst PPP evaluation is limited to hazard assessment. As a result, potentially toxic co-formulants and PPPs exhibiting relevant mixture effects are not considered in non-dietary risk assessment. In addition, NAM based approaches have been increasingly recognised to account for early-stage effects. In particular, metabolomics is explored as a promising approach for next-generation risk assessment (NGRA) providing important mechanistic information about biological pathways with the potential to derive thresholds such as point of departures (PoDs). In our case, the use of metabolomics enables a comprehensive assessment of the PPP as a whole mixture moving beyond traditional active substance-based PPP risk assessment, which tends to overlook interactions that might increase toxicity. *In vitro* metabolomics was applied to a PPP, its AS mixture, and its AS mixture with a co-formulant of concern to elucidate hepatotoxicity mechanisms and assess mixture effects. The intracellular metabolome of HepaRG cells was analysed following 24-hour exposure to the different conditions at seven concentration levels. Metabolite profiling was conducted using LC-MS/MS and a total 318 unique analytes were identified, annotated and allocated in 13 ontology classes. Particularly, up-regulation of diacylglycerols and ceramides in combination with carnitine and sphingomyelin depletion was identified as biomarkers related to hepatic steatosis and apoptosis in all test conditions. Concomitantly, a metabolomics-based PoD was derived by principle component analysis (PCA) plots using the whole set of measured metabolites for all test conditions. In particular, a PoD of 4 µM was calculated for PPP whereas a PoD of 11 µM and a PoD of 28 µM were calculated for the mixture of AS with the co-formulant of concern and the mixture of AS, respectively. Subsequently, *in vitro-in vivo* extrapolation (IVIVE) will be conducted on the PPPs *in vitro* PoD in order to calculate an Acceptable Operator Effect Level (AOEL). Then, exposure estimates will be compared to the calculated AOEL to determine if the risk is acceptable for operators. This innovative approach enables the assessment of the PPP as a whole mixture and the transition from *in vivo* to NAM-based approaches.

P160

Toxicokinetics in Mixture Toxicity Assessment: Screening for Potential CYP Inhibitors and Substrates to form Common Kinetic Groups (CKGs)

A. Kadlic^{1,2}, B. Liebnau^{1,3}, A. Braeuning¹, D. Bloch¹, P. Marx-Stölting¹

¹Bundesinstitut für Risikobewertung (BfR), Pesticide Safety, Berlin, Germany

²Technical University of Dortmund, Chemical Biology, Dortmund, Germany

³Potsdam University, Nutritional Science, Potsdam, Germany

Recent interest in mixture toxicity evaluation has intensified discussions on whether current mixture assessment frameworks are sufficient or if they require refinement to better protect public health. Traditionally, the toxicodynamic approach had dominated, employing the dose addition concept and focusing on target organ toxicity and mode of action. However, recent insights advocate for an enhanced strategy integrating toxicokinetic principles into the mixture assessments. Braeuning et al. introduced the concept of Common Kinetic Groups (CKGs) that includes the consideration of toxicokinetic properties, such as absorption, distribution, metabolism, and excretion (ADME) and grouping chemicals according to their potential roles as inhibitors, substrates, or inducers of molecular mechanisms.

Here we present results from *in silico* analysis focusing on most common CYP (Cytochrome P450) enzymes (CYP-1A2, -2C19, -2C9, -2D6, -3A4), pivotal in xenobiotic metabolism, to investigate potential inhibitors and/or substrates within mixtures. We conducted a screening of over 200 pesticide active substances utilizing three open-access and one commercial predictive tools: SuperCYPs Pred, CYPstrate, ADMETLab3.0, and ADMET Pred, respectively. The predictions were tested *in vitro*, and binary mixtures were performed to evaluate concentration/dose addition modeling.

By elucidating the interplay between toxicokinetics and mixture toxicity, our research contributes to the understanding of chemical interactions and their impact on human health. Integrating toxicokinetic principles into mixture toxicity assessment not only enhances regulatory strategies for risk assessment and management but also facilitates informed decision-making in chemical safety. Moreover, combining *in silico* approaches with *in vitro* testing enhances screening efficiency and reduces reliance on traditional *in vivo* studies, emphasizing the role of computational tools in advancing toxicological sciences and promoting alternatives to animal testing.

P161

Evaluation of Mixture Toxicity of Metabolism Disrupting Chemicals in Diet using a GIT-liver Organ-on-a-chip System

Y. C. Fung¹, P. Marx-Stölting¹, D. Bloch¹

¹German Federal Institute for Risk Assessment (BfR), Department Pesticides Safety, Berlin, Germany

Metabolic disrupting chemicals (MDCs) are substances that interfere with metabolism in the human body, increasing the risk of metabolic disorders such as diabetes and fatty liver disease, with liver steatosis being the initial stage of non-alcoholic fatty liver disease progression[1]. Since liver is the first line of defence against dietary exposure of MDCs, it is the principal organ involved in Phase-I detoxification[1]. Nevertheless, major studies on MDCs' liver toxicity were conducted in a 2D *in vitro* system, where experimental concentrations were higher than normal exposure levels[1]. Additionally, those studies were focused primarily on single substances. Yet, we are exposed to a mixture of MDCs in the real world. This project aims to evaluate the hepatic response to a realistic exposure of MDCs mixture using a gastrointestinal tract-liver organ-on-a-chip (GIT-liver OoC) system. The GIT-liver OoC utilises an *in vitro* microphysiological platform to mimic the physiological and functional interactions between the human gut and liver[2]. It allows for cross-talk between organs through interconnected microfluidic chambers and simulates blood flow to provide shear stress[2]. This contribution shall illustrate a project that combines realistic co-exposure scenarios to MDCs and human-based *in vitro* test systems. The human hepatoma HepaRG cell line in combination with human stellate cells will be used as 3D spheroids in the liver chamber of the chip to investigate metabolic properties. Besides, the human colon adenocarcinoma Caco-2 cell line will be used in the gut chamber to reproduce the intestinal barrier property. Mixtures of MDCs in realistic exposure concentrations will be applied to the GIT chamber. Cytotoxicity assays will be performed after 72 hours of treatment in both the gut and liver chambers. Liver function markers and the degree of triglyceride accumulation will be measured in the liver chamber. Additionally, transcriptomic and metabolomic analyses will be conducted in later stages. This project is expected to develop an effective GIT-liver OoC system that provides a more physiologically relevant tool for predicting the effects of mixture exposures through diet. Ultimately, this system could improve risk assessment frameworks and contribute to regulatory strategies for combined exposures to MDCs using new approach methodologies (NAMs).

1. Fritsche K. et al. Int. J. of Mol. Sci. 2023. **24**(3): p. 2686
2. Yang J. et al. Comm. Bio. 2023. **6**(1): p. 310

P162

Realistic exposure scenarios of dietary mixtures: Assessing co-exposure with Organ on a Chip systems

F. Zimmerer¹, D. Bloch¹

¹German Federal Institute for Risk Assessment (BfR), Department Pesticides Safety, Berlin, Germany

Co-exposure is a relevant topic in risk assessment, raising questions about the need for stricter regulations on mixtures. While most single substances are individually regulated within safe concentration ranges, real-life exposure involves several toxicants concurrently. Additive effects, synergies or antagonism may alter the overall toxicity of the mixture, which would lead to the underestimation of risk. Especially in diets, one often is exposed to a high number of co-occurring toxicologically relevant substances, for example contaminants, additives, pesticide or veterinary drug residues. Testing every possible combination using *in vivo* experiments is not justifiable, neither ethically nor economically. Moreover, the 3R principle for animal testing (Reduce, Refine, Replace) and the potential lack of predictivity for humans, heightens the need for alternative methods to assess mixtures and their effects. This project aims to evaluate interactions in dietary mixtures including animal-product related substances, focusing primarily on realistic exposure concentrations and occurrence levels. Using New Approach Methodologies (NAMs), such as Organs on a Chip (OoC), the project contributes to the reduction of animal testing and next generation risk assessment (NGRA). The experiments will be conducted with a two-chamber OoC system, containing liver-spheroids comprised of HepaRG and stellate cells. In later stage, an intestine model will be used in the second chamber, media flow connecting the sides, to assess barrier functions of the gut to foodborne toxicants. Additionally, the impact of complexity of *in vitro* models on baseline toxicity, the non-specific effect of toxicants on membranes, will be determined. The single substances and their combinations will be tested systematically. That allows the comparison of the calculated with the experimentally determined effect, as well as the assessment of the barrier impact and the protective mechanism of cells. The results of this project will contribute to a more thorough comprehension of mixture toxicity of foodborne toxicants in risk assessment, especially at realistic exposure concentrations and in complex *in vitro* test systems. Furthermore, it will lay out

helpful insights for the utilization of OoC systems in regulatory frameworks, along with their advantages and limitations for mixture assessment.

P163

Relative potency factors for PFAS – how well does the concept align with human data?

H. Mielke¹, K. Abraham², R. Hoogenboom³

¹German Federal Institute for Risk Assessment (BfR), Exposure, Berlin, Germany

²German Federal Institute for Risk Assessment (BfR), Department Food and Feed Safety in the Food Chain, Berlin, Germany

³Wageningen University & Research, Wageningen Food Safety Research, Wageningen, Netherlands

The concept of relative potency factors (RPFs) describing the toxic potential of chemicals in a group relative to a pivotal member of the group is appealing as it reduces the complexity of the assessment of mixtures. For per- and polyfluoroalkyl substances (PFAS), several sets of RPFs were suggested. We explore the impact of those RPFs on our data set on vaccination antibodies in one-year-old children (Abraham et al. 2020).

In the absence of specific data, EFSA (2020) assumed equipotency, i.e., RPFs {1–1–1–1} for {PFOA–PFOS–PFHxS–PFNA}, respectively, and derived a TWI for the sum of these four PFAS, the only ones detected consistently in infant blood. Bil et al. (2023) derived internal RPFs from lower thymus weights in rats from studies by NTP. Bil et al. (2023) also derived RPFs for another potentially immunotoxic endpoint, i.e., globulin concentrations in rats. Using these factors, PFOA equivalent doses (PEQ) were computed and the strength of the dose-response relation was evaluated by ANOVA as performed by EFSA (2020). Furthermore, using a differential evolution algorithm (DEA), relative potency ranges which minimize the ANOVA p-value were determined (Table 1). In all cases, the highest PEQ exposure group had the lowest antibody titer.

Table 1: RPFs relative to PFOA (RPF=1) and resulting p-values for the ANOVA on the vaccination antibody data (Abraham et al. 2020). "DEA" refers to optimum for the respective antibody.

	PFOS	PFHxS	PFNA
EFSA 2020	1	1	1
PFOA only	0	0	0
Bil (2023) thymus weight	4	0.5	6
Bil (2023) globulins	0.2	0.03	1
DEA Hib	0.12–0.15	0.47–0.53	0.03–0.74
DEA Tet	0.32–0.34	6.71–6.93	0.18–0.58
DEA Diph	0.08–0.11	0.63–0.77	1.46–2.58

Figure 1: p-values for RPFs from Table 1. "DEA" refers to the RPFs optimized for the respective antibody.

RPFs derived by Bil et al. (2023) using data on organ weights do not perform well on our data. The optimized RPFs show how good the fit may become. They are closest to those derived from effects on globulin levels in blood. Although globulin production may not be specific for lymphocytes only, it could be a better endpoint for human immune data than lower thymus weights observed at high doses which affected also the growth of the rats. As RPFs don't work well for the different vaccine antibodies from the same study, we expect that this works only in special cases.

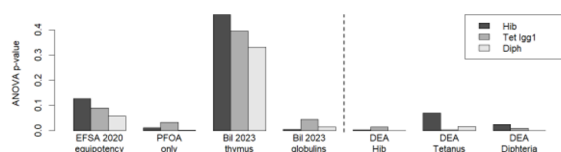
References

Abraham et al. 2020. Arch Toxicol 94:2131–2147.

Bil et al. 2023. Environ Int 171, 107727.

EFSA CONTAM Panel, 2020. EFSA J 18:6223.

Fig. 1



P164

Impact of sodium dodecyl sulfate on activation of dendritic cells of sensitizing chemicals

O. A. Aruna¹, N. Lobes¹, B. Blömeke¹

¹University Of Trier, Environmental Toxicology, Trier, Germany

Irritant- and allergic contact dermatitis (ACD) are common occupational skin diseases caused by low molecular weight chemicals. A key aspect of their pathomechanism is the activation of innate immune cells. Both groups produce danger signals leading to inflammation and, in ACD, to sensitization and differentiation of naïve T cells into chemical-specific T cells. Thus, exposure to a mixture of sensitizers and an irritant (e.g., sodium dodecyl sulfate, SDS) may enhance the load of danger signals and potentially the sensitizing potential and potency. However, it remains unclear how components within a mixture interact to activate dendritic cells (DC), a decisive step in sensitization. By testing sensitizers alone and in combination with SDS, we aimed to address this topic in vitro and provide insights for risk assessment.

Methods: Several sensitizers with varying potencies and/or reaction mechanisms were selected to assess co-exposure effects on DC activation using THP-1 monocytes as surrogates. THP-1 cells are commonly used to study DC activation by chemicals through evaluation of co-stimulatory molecule CD86 and adhesion molecule CD54. Expression levels were determined by flow cytometry as mean fluorescence intensity (MFI).

Results: SDS (200 µM) in mixtures with sensitizers (2,4-dinitrochlorobenzene, cinnamaldehyde, farnesol, cumene hydroperoxide, benzyl alcohol) produced chemical- and concentration-dependent modulation of DC activation (CD86 and CD54), using THP-1 monocytes as DC surrogates. For 2,4-dinitrochlorobenzene, SDS increased CD86 and CD54 at lower (µM) concentrations compared to the sensitizer alone. With farnesol, SDS enhanced CD86, while CD54 was only elevated at low farnesol concentrations. Mixtures with benzyl alcohol or cinnamaldehyde had little effect on CD86 but decreased CD54 levels. For cumene hydroperoxide, SDS enhanced CD86 at high but inhibited it at intermediate concentrations; CD54 was unaffected.

Conclusion: SDS modulates DC activation in substance- and concentration-specific manner. While the magnitude is restricted, the overall impact is significant, highlighting the need to evaluate mixture effects to strengthen the scientific basis for their risk assessment.

P165

Interaction of sulfur mustard, Lewisite and other irritant agents with the human TRPA1 channel

F. Frielingsdorf^{1,2}, F. Erdmann², S. Rothmiller¹, D. Steinritz^{1,3}, K. Lutterberg¹

¹Bundeswehr Institute of Pharmacology and Toxicology, Munich, Germany

²Martin Luther University Halle-Wittenberg, Institute of Pharmacy, Halle (Saale), Germany

³Ludwig Maximilian University of Munich, Munich, Germany

The Transient Receptor Potential Ankyrin 1 (TRPA1) channel is a non-selective cation channel known as a sensor for noxious, electrophilic, and irritant chemicals and plays a major role in pain sensation and inflammation. This ion channel is also a target for the chemical warfare agent sulfur mustard (SM), an alkylating vesicant which causes blistering and inflammation upon exposure. Since it is sensitive to SM, this work aims to determine if TRPA1 is also affected by other chemical warfare agents and riot control agents.

We investigated the effects on TRPA1 using HEK 293 cells stably overexpressing TRPA1. To monitor the calcium influx, we transfected the HEK 293 cells with the calcium indicator Aequorin. After cultivating the transfected cells for two days, we measured change in luminescence as indicator for calcium influx for 60 s after the injection of SM, Levinstein mustard, the unpurified product of the SM synthesis, Lewisite, Phosgene oxime (CX), tert-Butanethiol and Butanethiol. The results were analysed by determining the increase in luminescence normalized to the signal of an injection 100 µM Allyl-Isothiocyanate (AITC) injection, a specific TRPA1 agonist.

The injection of 100 µM tert-Butanethiol and 10 µM Butanethiol showed an increase in luminescence similar to AITC. The luminescence signal of 0.1 µM CX was 1.3 times higher than the AITC signal. The measured calcium influx of 10 µM purified SM injection showed only about 0.6 times the level of the AITC signal, while the 100 µM purified SM injection signal was comparable to AITC. Compared to AITC, the calcium influx of 1 µM Levinstein mustard injection was more than 40 times higher. The analysed concentrations of Lewisite (0.1 µM and 1.0 µM) both showed a higher effect of around 30 to 35 times on the calcium influx compared to AITC.

These results indicate that activation of the TRPA1 channel is likely involved in the nociceptive mechanisms triggered by irritating substances. The significantly elevated calcium influx and thus higher TRPA1 activation observed with Lewisite, which induces rapid pain response upon skin exposure, point towards a possible involvement of TRPA1 in this process. The comparison of the calcium influx signal of unpurified to the purified SM also indicate this involvement of TRPA1 in the pain-inducing mechanism with chemical irritants. Therefore, targeting TRPA1 could be beneficial after exposure to reactive chemical agents.

Pharmacogenomics and personalized medicine

P166

The more data the better? – Comparison of long read sequencing and a commercial pharmacogenetic testing method

A. Glässer¹, M. Steffens¹, P. Darm², M. Hahn², C. Scholl¹

¹Federal Institute for Drugs and Medical Devices, Bonn, Germany

²University Hospital Frankfurt, Frankfurt a. M., Germany

Background/Aims: Commercial pharmacogenetic tests primarily use polymerase chain reaction (PCR) or microarray technologies. These tests focus on genetic variants of certain genes that significantly impact the clinical phenotype of a patient. In contrast, exome or whole-genome sequencing (WGS) are gaining importance in pharmacogenetic research providing a complete insight into all relevant pharmacogenes. In this context, long read sequencing by Oxford Nanopore Technologies or Pacific Biosciences are commonly used. In this study, we compared the results of different pharmacogenetic testing methods and their impact on the actual detected phenotype.

Methods: Depressive patients (n=20) hospitalized for affective disorders were included in this study. DNA samples were isolated from blood or swabs and were analyzed by a commercial genetic testing company (Humatrix AG (Stratipharma)) or by long read sequencing (Oxford Nanopore Technologies) in an experimental approach. For target gene enrichment, adaptive sampling or the PGx panel provided by Twist Bioscience were used. For star allele calling and phenotype prediction of long read sequencing data, the bioinformatic tools *Stargazer* and *Aldy* were used.

Results: Interestingly, we found small differences in the overall number of detected single nucleotide polymorphisms (SNP) depending on the enrichment method (adaptive sampling vs. Twist) using the same DNA sample. A comparison of DNA obtained from swab or blood sample of the same patient also resulted in slightly different numbers of detected SNP in some patients/genes.

The star allele and phenotype prediction of the most common pharmacogenes (CYP2B6, CYP2C19, CYP2C9, CYP2D6) analyzed by the commercial genetic testing company compared to long read sequencing revealed differences in some patients and was also dependent on the bioinformatic tools used for long read data (cf. table 1). Notably, the observed differences mainly apply to the non-extensive (= normal) phenotypes indicating that more genetic details allowing another phenotype prediction.

Conclusion: More data allows for another phenotype prediction especially in non-normal phenotypes. However, no gold standard is currently established regarding bioinformatic analyses or quality requirements of long read data making bioinformatic analysis of this data much more challenging. The usage of different bioinformatic software tools can impact the phenotype prediction in a significant manner.

Fig. 1

	Stratipharma vs. Long read (Aldy) identical phenotype/number of all patients	Stratipharma vs. Long read (Stargazer) identical phenotype/number of all patients
CYP2B6	8/11	4/11
CYP2D6	10/11	8/11
CYP2C9	11/11	9/11
CYP2C19	11/11	8/11

P167

From Whole-Genome Sequencing to Pharmacogenetic Counseling in Rare Diseases

T. Krüger¹, J. Krause², H. Kirpal¹, M. Elbrach², K. S. Just¹

¹Uniklinik RWTH Aachen, Institute of Clinical Pharmacology, Aachen, Germany

²Uniklinik RWTH Aachen, Center for Human Genetics and Genomic Medicine, Aachen, Germany

Question: Adverse drug reactions (ADRs) pose a major burden on healthcare and economic systems, with ADR-related mortality rising in Europe and worldwide (1). Pharmacogenetic testing can reduce ADRs by up to 30 % and is increasingly recognized as a key tool for personalized therapy (2). However, its implementation remains limited due to costs not covered by health insurance and the lack of widely available diagnostic tools. Whole genome sequencing (WGS) provides a comprehensive approach, capturing known and novel pharmacogenetic variants, including rare and structural variants that may be missed by targeted panels. This study explored the feasibility and acceptance of pharmacogenetic analysis and counseling based on WGS data obtained for rare disease diagnostics.

Methods: As part of the German model project on genome sequencing in rare disease patients a collaboration between the Center for Human Genetics and Genomic Medicine and the Institute for Clinical Pharmacology at Uniklinik RWTH Aachen performed an additional pharmacogenetic analysis of 15 genes with published guideline recommendations or drug label annotations. The cohort included 66 patients (32 % male, 68 % female; 39 % < 18 years, 61 % ≥ 18 years). Patients carrying actionable variants were invited for video or in-person counseling, followed by a standardized follow-up survey.

Results: At least one actionable variant was identified in 64 patients (97 %). To date, nine patients (14 %) have received pharmacogenetic counseling, and seven completed the follow-up survey. Among respondents, five (71 %) reported feeling

more confident in managing their medication, while two (29 %) reported no change. All respondents (100 %) considered the offer of pharmacogenetic testing and counseling useful.

Conclusion: These findings demonstrate that WGS performed for diagnostic purposes can simultaneously provide valuable pharmacogenetic insights. There is clear patient interest in pharmacogenetic counseling. Effective collaboration between human genetics and clinical pharmacology is essential to ensure meaningful interpretation and communication of pharmacogenetic results. Further analyses and counseling sessions are planned to refine this interdisciplinary approach and identify additional patient needs.

References

1. Koyama T et al. *Drug Saf.* 2024;47(3):237–249.
2. Swen JJ et al. *Lancet.* 2023;401(10374):347–356.

Nuclear receptors, enzymes and other targets

P168

Cancer-associated mutations in the GC-2 isoform of soluble guanylyl cyclase disrupt subcellular localisation and protein interactions

S. Stomberg¹, S. Behrends¹

¹TU Braunschweig, Institut für Pharmakologie, Toxikologie und klinische Pharmazie, Brunswick, Germany

Background: A unique paediatric case revealed a new potential link between soluble guanylyl cyclase (sGC), the physiological receptor for nitric oxide (NO), and tumorigenesis. A 10-year-old girl was diagnosed with brain metastases from pulmonary adenocarcinoma, a presentation rarely seen at this age [1]. Next-generation sequencing identified five non-targetable mutations, including one in *GUCY1A2*, the gene encoding the α_2 subunit of GC-2, a lesser-studied sGC isoform. *GUCY1A2* was first proposed as a candidate cancer gene in 2006 [2], yet its role in cancer remains uncertain. In this patient, the mutation affected the highly conserved C-terminal motif that normally anchors GC-2 at cell–cell contacts, thereby shaping cGMP microdomains at the cell membrane. Screening of the COSMIC database revealed a tenfold higher mutation density in the α_2 C-terminus compared to other sGC subunits, suggesting a potential cancer-associated hotspot [3]. In this study, we aimed to investigate the functional consequences of these C-terminal mutations in GC-2.

Methods: All experiments were carried out in transiently transfected HEK 293 cells. The C-terminal variants were assessed for enzymatic activity using a NO-stimulated cGMP assay, interactions with known binding partners using co-immunoprecipitation, and subcellular localisation using fluorescently tagged constructs and confocal laser scanning microscopy.

Results: All variants retained normal NO-stimulated cGMP synthesis. However, several mutations disrupted GC-2 localisation at cell–cell contacts and impaired interactions with key polarity and scaffolding proteins, including scribble, Lin7a, and Shank2.

Conclusions: C-terminal mutations in *GUCY1A2* uncouple GC-2's enzymatic activity from its microdomains at the cell membrane, potentially reprogramming intracellular cGMP signalling. These findings reveal a novel mechanism by which somatic *GUCY1A2* mutations may contribute to tumorigenesis.

References

- [1] De Martino L., Errico M.E., Ruotolo S. et al. (2018). Pediatric lung adenocarcinoma presenting with brain metastasis: a case report. *Journal of Medical Case Reports*, 12(1), 243
- [2] Sjöblom, T., Jones, S., Wood, L.D. et al. (2006). The Consensus Coding Sequences of Human Breast and Colorectal Cancers. *Science* 314, 268–274
- [3] Sondka, Z., Dhir, N.B., Carvalho-Silva, D. et al. (2024). Cosmic: A curated database of somatic variants and clinical data for cancer. *Nucleic Acids Research*, 52(D1), D1210–D1217

P169

Acute mitochondrial dysfunction after exposure to blistering agents in keratinocytes

T. Demel¹, E. Liesenfeld¹, D. Steinritz¹, S. Rothmiller¹

¹Bundeswehr Institute of Pharmacology and Toxicology, Molecular Toxicology, Munich, Germany

Question

Blister agents such as Lewisite (LEW) and sulfur mustard (SM) both cause severe chemical burns, primarily affecting the skin, eyes, and lungs. There is a distinct difference with regard to the onset of symptoms. LEW typically causes more immediate effects, while those of SM tend to develop delayed. This study investigates whether differences in mitochondrial function contribute to the distinct

pathophysiological profiles of LEW and SM. Specifically, we investigated whether exposure to LEW or SM acutely impair mitochondrial activity in human keratinocytes.

Methods

Human keratinocyte (HaCaT) cells were exposed to either LEW or SM. Mitochondrial membrane potential was assessed using the JC-10 fluorescent probe. Mitochondrial oxygen consumption rates (OCR) and responses to mitochondrial inhibitors and the uncoupler FCCP were measured using the Agilent Seahorse XF Pro Analyzer in permeabilized cells with different metabolic substrates (pyruvate, glutamate, succinate) to dissect site-specific mitochondrial impairments.

Results

LEW induced rapid and significant mitochondrial dysfunction, shown by a pronounced drop in mitochondrial membrane potential and severe alterations in oxygen consumption rate (OCR). Substrate-specific testing revealed that LEW disrupts ATP production primarily by interfering with enzymes involved in the early stages of the mitochondrial energy-generating cascade, particularly the pyruvate dehydrogenase complex, which is essential for substrate supply to NADH-coenzyme Q oxidoreductase (complex I). Although these upstream steps of the mitochondrial respiratory chain are most severely impacted, subsequent complexes of oxidative phosphorylation and citric acid cycle are still affected, but to a lesser extent. In contrast, SM did not produce similar acute effects on mitochondrial function up to 1.5 hours after exposure.

Conclusion

These findings suggest that LEW, but not SM, induces acute mitochondrial dysfunction, likely contributing to its faster onset of symptoms. The mitochondrial impairment, particularly at the early stages of the mitochondrial energy-generating cascade, may represent a key mechanism underlying the rapid cellular damage observed after LEW exposure. This highlights that two substances from the same class of chemical warfare agents (vesicants), despite causing similar clinical symptoms, can exhibit fundamentally different molecular mechanisms of toxicity.

P170

Differential Effects of AOC3 and MAO Inhibition on H₂O₂ Homeostasis and Apoptosis in Mouse Islets

L. Naundorf¹, M. Düfer¹

¹University of Münster, Institute of Pharmaceutical and Medicinal Chemistry, Department of Pharmacology, Münster, Germany

Amine oxidase copper containing 3 (AOC3) is a protein with both enzymatic activity, deaminating primary amines, and adhesive properties, playing a role in leukocyte adhesion and transmigration. Previous studies have shown both an upregulation of AOC3 in diabetic patients and an insulin-like effect on adipocytes¹. Therefore, we further investigated the role of AOC3 in islets of Langerhans and how its effects differ from those of other enzymes with similar substrates, namely monoamine oxidases (MAO).

AOC3- and MAO-inhibitors alone or in combination were tested on pancreatic islets or islet cells from C57BL/6N mice. Apoptotic cell death (TUNEL assay), insulin secretion and H₂O₂-status (BES-H₂O₂ fluorescence) were monitored at different time points. A novel covalently-binding compound (PT010) was used to inhibit AOC3, pargyline was used as an unspecific MAO blocker.

The inhibition of AOC3 by 5 µM PT010 significantly decreased the rate of apoptosis induced by glucolipotoxicity (0.5 mM palmitate, 33 mM glucose, 7 days). MAO inhibition by pargyline (10 µM) however did not alter the rate of glucolipotoxicity-induced apoptosis, showcasing a difference in effect between the two enzymes. The combined inhibition of the two enzymes did not have an additive beneficial effect vs. AOC3 inhibition. As H₂O₂ is a product of both enzymes, the H₂O₂-status was monitored. After 48 h of glucolipotoxicity (0.1 mM palmitate, 25 mM glucose) the H₂O₂-status was significantly decreased compared to control. This decrease could be partially prevented by the combination of PT010 and pargyline, but not by either inhibitor alone. Contrary, after 2 h of glucolipotoxicity the H₂O₂-levels were increased and while pargyline did not have any effect on the H₂O₂-status, PT010 alone and the combination partially prevented the increase. The reduction in glucose-stimulated (15 mM glucose) insulin secretion resulting from 48-hour culture in glucolipotoxic medium was not influenced by PT010, but a significant protective effect was observed for insulin release normalized to the insulin content.

Our data show that various changes resulting from a glucolipotoxic environment are counterbalanced either by reducing the activity of AOC3 alone or in combination with MAO inhibition. Overall, the protective effect of AOC3-inhibition on cell mass is most promising when considering AOC3 modulating compounds as a therapeutic option for islet cell preservation in type 2 diabetes mellitus.

¹ Stolen et al (2004)

P171

The ICER-XIAP interaction decreases ICER protein levels

D. Hofmann¹, D. Koppenhöfer¹, L. Anh Ngoc¹, H. Kremer¹, K. Grimm¹, U. Kirchhefer¹, F. U. Müller¹, M. D. Seidl¹

¹Institut für Pharmakologie und Toxikologie, Münster, Germany

Introduction: ICER (inducible cAMP early repressor) is a short inhibitory transcription factor with pro-apoptotic properties that counteracts cAMP signaling. We have previously shown that ICER interacts specifically with the X-linked inhibitor of apoptosis (XIAP) in the cytoplasm of human but not rodent cells. XIAP

exerts anti-apoptotic functions by binding and inhibiting active caspases, and its RING domain confers E3 ubiquitin ligase activity.

Objectives: We aimed to determine whether the ICER–XIAP interaction affects the protein levels and stability of ICER and to understand the role of XIAP's RING domain in this process.

Methods: HEK293T cells were transfected with various combinations of plasmids encoding HA-tagged ICER and myc-tagged XIAP variants. Protein levels were analyzed by Western blotting and normalized to total protein. Additional experiments included MG-132 treatment to evaluate proteasome dependency.

Results: Co-overexpression of ICER-HA and myc-XIAP resulted in lower ICER-HA protein levels compared to ICERdelA-HA, a truncated ICER variant unable to interact with XIAP. Treatment with the proteasome inhibitor MG-132 led to an overall increase in protein levels, but did not alter these differences in protein levels. To clarify whether the E3 ubiquitin-ligase activity of XIAP is primarily responsible for the ICER destabilization, we co-overexpressed ICER with a XIAP variant lacking the RING domain. In presence of myc-XIAPdelRING we also observed lower ICER-HA protein levels compared to the non-interacting ICERdelA-HA.

Conclusion: Our data demonstrate that XIAP lowers ICER protein levels via a mechanism that is independent of its RING domain. However, the interaction between XIAP and ICER contributes to the increased degradation of ICER and may represent a mechanism that regulates ICER turnover in human cells.

P172

FXR antagonism as a potential approach in renal cancer pharmacotherapy

E. Ristl¹, T. Carlucci¹, S. Winter², E. Schäffeler², M. Schwab^{2,3}, O. Burk¹

¹Dr. Margarete Fischer-Bosch Institute of Clinical Pharmacology and University of Tübingen, Transport and Nuclear Receptors, Stuttgart, Germany

²Dr. Margarete Fischer-Bosch Institute of Clinical Pharmacology and University of Tübingen, Stuttgart, Germany

³University of Tübingen, Departments of Clinical Pharmacology, and of Pharmacy and Biochemistry, Stuttgart, Germany

The farnesoid X receptor (FXR, *NR1H4*) is highly expressed in normal kidney and renal cell carcinoma (RCC), which ranks among the ten most prevalent malignancies worldwide and remains therapeutically challenging due to its pronounced capacity to develop treatment resistance. Given FXR's role in the regulation of apoptotic processes, this study aims at investigating whether it may be a suitable therapeutic target in renal cancer pharmacotherapy.

TCGA data sets of clear cell (cc), papillary (p), and chromophobe (ch) RCC were analyzed for FXR gene expression. Immortalized human renal proximal tubular cells (RPTEC/TERT1) and renal tumor cell lines (A498, A704, 786-O, ACHN) were analyzed for FXR protein by Western blot and for mRNA expression of FXR and selected renal target genes by quantitative RT-PCR. Caspase 3/7 activities were determined in FXR ligand-activated cells. Cell proliferation was analyzed by quantifying viable cells by ATP measurements. Cell migration was studied by wound healing assay. Transcriptomic analyses were performed by RNA sequencing.

ccRCC and pRCC demonstrated increased expression of FXR, as compared to paired adjacent non-tumor tissue. In contrast, FXR expression was reduced in chRCC. As ccRCC is derived from the proximal tubule epithelium, we quantified FXR-regulated genes, identified in ligand-activated RPTEC/TERT1, in the ccRCC model cell line A498, which expresses high levels of FXR protein. Selected target genes, amongst others anti-apoptotic BCL2 and TNFAIP8, were also upregulated in A498, which had been treated with the FXR agonist trofexor, thereby demonstrating functional FXR activity. In RPTEC/TERT1, the FXR-induced expression of anti-apoptotic genes resulted in protection from apoptosis. Altogether, these data suggest that in ccRCC FXR may be pro-tumorigenic. Thus, inhibiting the receptor may suppress renal tumor cell growth. In agreement with this hypothesis, siRNA-mediated FXR knock-down and treatment with five different FXR antagonists all consistently inhibited A498 proliferation, while FXR agonists did not. Additionally, FXR antagonists slowed down cell migration. Transcriptomic analysis of antagonist-treated cells elucidated the respective molecular mechanisms. Validation in patient-derived renal tissue models is required and ongoing. In conclusion, FXR antagonists may represent a novel therapeutic option to reduce the proliferative capacity and migration of renal tumor cells.

P173

Fingolimod (FTY720) modulates β-adrenergic atrial response depending on PP2A-B56α expression

J. Kaller¹, C. Hermes¹, U. Kirchhefer¹, M. D. Seidl¹

¹Institute of Pharmacology and Toxicology, University Hospital Münster, Münster, Germany, Münster, Germany

Protein phosphatase 2A (PP2A) is a heterotrimeric enzyme that regulates cardiac contractility by dephosphorylating myocardial proteins. The enzymatic activity of PP2A can be enhanced by small molecule activators of PP2A (SMAPs) and previous studies have already discussed a contribution of PP2A regulatory B-subunits, such as B56α, to this activation.

Here, we investigated whether stimulation with the SMAP fingolimod (FTY720) modulates atrial contractility and whether loss of PP2A-B56α alters this response.

Methods

Force of contraction (FOC) was recorded in isolated left atria from B56 α -deficient mice (B56 α -KO) and wild-type littermates (WT). The atria were preincubated with 5 μ M FTY720 in the presence or absence of 3 nM okadaic acid (OA, a potent PP2A inhibitor), or DMSO as control, followed by stimulation with increasing concentrations of isoproterenol (ISO). Data is presented as mean \pm standard deviation (SD) and nonparametric tests were used for statistical analysis.

Results

Under basal conditions, both genotypes showed a comparable response to FTY720 stimulation, leading to a reduced FOC. However, this effect was not statistically significant and did not differ between WT atria and B56 α -KO atria.

Under ISO stimulation, FTY720 treatment did not alter the ISO-induced maximal FOC in WT atria ($n = 12$ – 13), but induced a rightward shift in EC50 compared to control (FTY720: 0.29 ± 0.15 μ M vs. DMSO: 0.15 ± 0.09 μ M, $p = 0.023$). Additional treatment with OA did not influence these effects.

The loss of PP2A-B56 α leads to an altered cardiac contractile phenotype. This is demonstrated by a reduced ISO-induced increase in FOC in B56 α -KO atria ($n = 10$ – 12), which showed a $26 \pm 13\%$ increase from baseline compared with a $60 \pm 31\%$ increase observed in WT atria ($p = 0.002$). Notably, at baseline a comparable FOC was detected in B56 α -KO and WT atria (KO: 2.3 ± 1.0 mN vs. WT: 2.2 ± 1.0 mN). B56 α -KO atria also showed a rightward shift of the EC50 under ISO stimulation (KO: 0.39 ± 0.28 μ M vs. WT: 0.15 ± 0.09 μ M, $p = 0.012$). Preincubation with FTY720 enhanced the ISO-induced increase in FOC in B56 α -KO atria to $50 \pm 19\%$ increase from baseline ($p = 0.004$ vs. control) while no further right shift of the EC50 could be detected. These effects were also not affected by OA.

Conclusion

Overall, our data demonstrate that loss of PP2A-B56 α modulates atrial response to FTY720, which was only detectable under β -adrenergic stimulation and independent of PP2A activity.

P174

The B"-regulatory subunit G5PR of PP2A modulates cardiac contractility in mouse ventricular cardiomyocytes

A. Johann¹, J. S. Schulte¹, U. Kirchhefer¹

¹Institut für Pharmakologie und Toxikologie UKM, Münster, Germany

Introduction Protein Phosphatase 2A (PP2A) is a major serine/threonine phosphatase that regulates diverse cellular processes by dephosphorylation of key target proteins. The activity, localization and substrate specificity of PP2A are determined by the composition of its holoenzyme, which consists of a scaffolding A, a catalytic C, and a variable B-regulatory subunit. Altered mRNA expression of the B"-regulatory subunit G5PR (PPP2R3C) has been reported in an animal model of heart failure, suggesting a role in the pathogenesis or progression of cardiac disease. In this study, we elucidated the impact of G5PR expression on cardiac function.

Materials & Methods To examine the role of G5PR, mouse models with cardiac-specific overexpression (TG) or heterozygote knockdown (HZ) were analyzed in comparison to corresponding wild-type littermates (WT). Cardiomyocyte contractility and Ca²⁺ handling were assessed under basal conditions and β -adrenergic stimulation with 1 μ M isoprenaline. The effect of recombinant G5PR on PP2A activity was tested *in vitro*.

Results Sarcomere length shortening was enhanced by 32% in TG cardiomyocytes vs. WT ($n=6$ – 7 , $P<0.05$). The time of 50% relengthening was prolonged by 15% in TG vs. WT ($P<0.05$). Moreover, the peak amplitude of Ca²⁺ transients was reduced by 18% in TG ($P<0.05$), suggesting an increased myofilament Ca²⁺ sensitivity. In contrast, HZ cardiomyocytes exhibited decreased sarcomere shortening by 18% vs. WT ($n=5$ – 6 , $P<0.05$) and increased peak amplitude of Ca²⁺ transients by 27% ($P<0.05$). Under isoprenaline, sarcomere shortening and time of 50% relengthening was comparable between TG and WT as well as HZ and WT. Of note, the peak amplitude of Ca²⁺ transients was unchanged between TG and WT, but enhanced by 40% in HZ vs. WT ($P<0.05$). To test whether higher expression of G5PR alters PP2A activity, we used recombinant G5PR in a phosphatase activity assay. Basal PP2A activity was increased by 119% ($P<0.05$, $n=3$) after application of 10 nM G5PR.

Conclusions In summary, heart-directed overexpression of G5PR was associated with higher myocellular contraction, prolonged relaxation and reduced Ca²⁺ transient amplitudes. Cardiomyocyte contraction and Ca²⁺ transients were reversed in HZ cardiomyocytes indicating for the first time a functional role of this PP2A B"subunit in regulating cardiac contractility and Ca²⁺ cycling. Our experiments also suggest that these effects are due to a direct change in PP2A activity.

P175

Crystallographic analysis complements the structural and kinetic profile of human FTase β -subunit isoforms

D. C. Rittmann¹, M. C. Kehrenberg¹, A. Hagemann¹, H. S. Bachmann¹

¹Witten/Herdecke University, Witten, Germany

Introduction: Farnesylation is a posttranslational modification essential for protein functionality and the progression of different diseases like cancer, progeria and hepatitis D. Different FTase inhibitors (FTIs) are under clinical investigation showing discrepant results. FTase is a heterodimer composed of an α - (FT α) and a β -subunit (FT β). We identified new transcriptional variants of FT β interacting with FT α , called F1, F2, F3, CF1, CF2. Four of the five variants form an active isoenzyme performing FTase activity (F1, F2, CF1 and CF2) but differ in their catalytic properties. Crystallizing these isoenzymes could reveal their structural and functional differences, potentially improving FTIs.

Objective: Our aim is the determination of the structures of the FTase isoenzymes and its impact on the pharmacological role of the FTIs and their future design.

Methods: First, FT β variants were co-expressed heterologously in *Escherichia coli*. Michaelis constant (Km) as well as inhibition constants (Ki) of four FTIs were determined by a continuous fluorescence assay. Afterwards, molecular dynamics (MD) modelling of F1, F2 and F3 and FT α has been performed. The consistency between the catalytic data and the structural models indicate that crystallization of the isoenzymes will enable direct structural analysis. Therefore a purification protocol to achieve high-grade purity has been established.

Results: Significant differences in the kinetic parameters could be observed for the isoenzymes between their affinities to the tested substrates as well as a different inhibitability by the four FTIs. Additionally, the MD modelling confirmed this discrepancy. So, purification and crystallization of the isoenzymes is needed. A sequential purification protocol combining manual and automated chromatography has been established.

Conclusion: The results demonstrate a need for further investigations based on the proteins structural data. The essential role of FTase in various diseases underlines the importance to uncover structural features causing significant catalytic differences. Resolving structural differences of the isoenzymes can be used as a basis for the development of putative new FTIs and therapeutic approaches.

P176

Role of hypo-/ hyperthyroid tanyocytes in the regulation of metabolism and fertility

A. Chandrasekar¹, P. M. Schmidtlein¹, L. Kleindienst¹, S. Abele¹, F. Spiecker¹, M. Schwaninger¹, H. Müller-Fielitz¹

¹Institute of experimental and clinical pharmacology and toxicology, Lübeck, Germany

Thyroid hormones regulate brain function, energy metabolism and modulate fertility. In order to mediate these effects in the brain, thyroid hormones are actively transported through the blood-brain barrier from the periphery to the brain and vice-versa. Tanyocytes, radial glial cells lining the wall and the floor of the third ventricle, play an important role in the transport and mediating the functions of thyroid hormones. They express important thyroid hormone related genes including the transporters (*Slco1c1*, *Slc16a2*), deiodinases (*Dio2*, *Dio3*) and receptors of thyroid hormones (*Thra*, *Thrb*, *Tshr*). Our previous data suggested that thyroid hormones modulate tanyocytic functions and morphology, however, the precise mechanism is unclear. We identified that tanyocytes alter their gene and intracellular calcium response in global hypo- and hyperthyroid animals. In this project we use genetic tools to manipulate thyroid hormone receptors (THR) specifically in tanyocytes in order to create hypo- and hyperthyroid tanyocytes in adult euthyroid animals. Hypothyroid tanyocytes were created by using a mouse model floxed for the dominant negative *Thra1L400R* and *Thrb*. Injection of the adeno-associated virus (AAV) AAV-*Dio2*-Cre-GFP in the lateral ventricle allowed the expression of the dominant negative *Thra1L400R* and a knockout of the *Thrb* specifically in tanyocytes. Hyperthyroid tanyocytes, on the other hand, were created by injecting an AAV expressing the constitutive active form of the *Thra1* (*ThraVP16*) in the lateral ventricle to limit the expression to tanyocytes. We used qPCR and RNAscope to investigate the changes in gene expression mediated by hypo- or hyperthyroid tanyocytes. Further, we identified metabolic changes in these mice using indirect calorimetry. In hypothyroid tanyocytes, we identified a change in glucose metabolism as indicated by an increase in glucose tolerance. Mice in which tanyocytes were hyperthyroid showed a metabolic phenotype characterised by a reduction in body weight, increase in food intake and higher fat mass. The metabolic changes were supported by an increase in the mRNA of *Dio3* followed by a decrease in the mRNA of *Dio2* in the tanyocytes as seen using both RNAscope and qPCR. Overall, we hypothesize that the modulation of *Thra1* activity specifically in tanyocytes influences the hypothalamic regulation of physiological functions and diseases.

P177

Modulation of tropomyosin-related kinase (Trk) signaling by *Ballota nigra* L. *Crataegus oxyacantha* L., *Pasiflora incarnata* L. and *Valeriana officinalis* L. and their combination *in vitro*

G. Ulrich-Merzenich¹, A. Shcherbakova¹, H. Aziz-Kalbhenn², O. Kelber³

¹University Hospital Bonn (UKB), Medical Clinic III, AG Synergy Research, Bonn, Germany

²Medical Affairs, Phytomedicines Supply and Development Center, Bayer Consumer Health, Steigerwald Arzneimittelwerk GmbH, Darmstadt, Germany

³Phyto & Biotics Tech Platform, Phytomedicines Supply and Development Center, Bayer Consumer Health, Steigerwald Arzneimittelwerk GmbH, Darmstadt, Germany

Question: Used to improve nervous stress and promote sleep, extracts of *Ballota nigra* L., *Crataegus oxyacantha* L., *Passiflora incarnata* L., and *Valeriana officinalis* L. modulate neurotrophic activity, alone and in combination [1]. This was demonstrated by *in vitro* studies on the human neuroblastoma cell line SH-SY5Y, which was treated with the plant extracts and lorazepam (LZ) as a reference drug. Neither the individual plant extracts nor their combination (Calmalaif®) or LZ reduced the viability of the cells or stimulated the release of TNF- α and IL-1 β . They induced the release of GABA and melatonin and increased the gene expression (GE) of brain-derived neurotrophic factor (BDNF). Recently, positive allosteric modulation of neurotrophin/Trk receptors has been proposed as a potential new therapeutic concept to influence mood disorders [2].

Neurotrophin/Trk signaling by the four extracts alone and in combination and by LZ as a reference drug should therefore be investigated.

Methods: Based on deep sequencing data from our previous study [1], the GEs involved in the neurotrophin/Trk pathway (Log2FC, mean expression, p-value) were analyzed for the individual extracts and their combination in three different concentrations (2.5, 5, 25 μ g/ml) and LZ. RT-PCR was performed for selected genes involved in neurogenesis/neuroprotection.

Results: At the high concentrations, all four plant extracts, LZ and the plant combination significantly modulated components of the neurotrophin/Trk signaling pathway, each with individual profiles, with NTRK2 (TrkB) being the most strongly regulated. The GE of superoxide dismutase (SOD) was increased by the four plant extracts, LZ and by the combination in a concentration-dependent manner.

Conclusions: Based on GE, all four plant extracts and their combination activate the neurotrophin/Trk pathway involved in modulating mood swings while reducing oxidative stress.

References:

[1] Ulrich-Merzenich G, Shcherbakova A, Kelber O, Kolb C. Neurotrophic activity of *Ballota nigra* L., *Crataegus oxyacantha* L., *Passiflora incarnata* L., *Valeriana officinalis* L. *in vitro* and *in vivo*. *Planta Med* 2022; 88: 1425-1426

[2] Madjid N, Lidell V, Nordvall V, Lindsog M, Ögren SO, Forsell P, Sandin J. Antidepressant effects of novel positive allosteric modulators of Trk receptor mediating signaling - a potential therapeutic concept. *Psychopharmacology* 2023; 240: 1789-1804.

General Toxicology

P178

Storing food in beeswax wraps results in consumer exposure to chlorinated paraffins (CP)

O. Kappenstein¹, A. Aha², T. Tietz¹, W. Vetter², A. Luch¹, S. Zellmer¹

¹German Federal Institute for Risk Assessment (BfR), Berlin, Germany

²Universität Hohenheim, Stuttgart, Germany

Question: Short- (SCCP) and medium chain (MCCP) chlorinated paraffins with a chlorine content > 45 % were identified as persistent organic pollutants (POP) by the Stockholm Convention. SCCP are classified as Carc. 2 (Reg (EG) No. 1272/2008). Target organs are liver, kidney and thyroid. It was studied, whether beeswax wraps, used as food contact materials, are a source of chlorinated paraffins (CP).

Methods: New and used beeswax wraps (n=32) were analyzed for the presence of CP. A combination of open-vessel microwave-assisted extraction and countercurrent chromatography in co-current mode allowed the separation of CP from beeswax and other lipophilic contaminants. CPs were quantified using GC/ECNI-Orbitrap-HRMS.

Results: All beeswax wraps contained SCCP and MCCP in the range of 0.13 to 20 μ g/dm². In general, the CP content was higher in used beeswax wraps. One highly contaminated wrap, which was stored for 3 years below a kitchen stove, contained of 260 μ g/dm² (170 μ g/g wax). Kitchen stoves are a source of CP (Gallistl et al. 2018), which are used as flame retardants. Transfer of CP in food/simulants has been reported by Wang and co-workers (2019). Assuming migration behaviour comparable to transition of wax from packaging into lipophilic food like salami slices (Grob et al. 1991), the median CP content in the beeswax wraps would result in a daily exposure of 6.7 ng/kg bw. Using the highly contaminated beeswax wrap for packaging of salami slices and assuming that this stack is eaten each day, a daily exposure of 490 ng/kg bw can be estimated. This is more than double of the average consumption for adults and elderly, according to a recent market basket study (Krätschmer et al. 2021).

Conclusion: New and used beeswax wraps were found to contain chlorinated paraffins, that can be transferred into food. Depending on the storage or use conditions of the wraps and the food coming into contact, comparably high CP exposure even above the average of German consumers may result.

Acknowledgments: The project was funded by the German Federal Institute for Risk Assessment Grant Agreement Number 60-0102-02.P628.

References:

Gallistl C, Sprengel J, Vetter W (2018) *Sci Total Environ* 615:1019-1027

Grob K, Biedermann M, Artho A, Egli J (1991) *Z Lebensm Unters Forsch* 193(3):213-9

Krätschmer K, Schächtele A, Vetter W (2021) *Environ Pollut* 272 (2021) 116019

Wang C, Gao W, Liang Y, et al. (2019) *Chemosphere* 225:557-564

P179

Direct Interactions of Micro-/Nanoplastics with Proteins – A Key to Mechanistic Understanding?

H. Siegl¹, J. Heilscher², F. Ott², A. Thünemann³, S. Drusch⁴, A. Braeuning⁵, S. Rohn¹, H. Kieserling²

¹German Federal Institute for Risk Assessment (BfR), Department of Food and Feed Safety in the Food Chain, Berlin, Germany

²Technische Universität Berlin, Department of Food Chemistry and Analysis, Berlin, Germany

³Federal Institute for Materials Research and Testing (BAM), Department of Synthesis and Scattering Methods of Nanostructured Materials, Berlin, Germany

⁴Technische Universität Berlin, Department of Food Technology and Material Science, Berlin, Germany

⁵German Federal Institute for Risk Assessment (BfR), Department of Chemical and Product Safety, Berlin, Germany

Micro-/Nanoplastics (MNP) have gained widespread scientific and public attention within the last two decades. While knowledge about measuring techniques, occurrence and exposure was improved substantially, questions on toxicological impact of MNP remained unclear. A major reason for that are the continued remaining knowledge gaps with regard to mechanistic understanding of MNP effects. Our work aimed at investigating MNP properties, protein interactions, and cellular effects in combination. Therefore, we characterized MNP-protein-adsorption, changes in protein structure, cellular uptake and cellular modes of action.

In a first study, we studied the molecular interactions of β -lactoglobulin, a serum and storage protein, with different MNP materials¹. We identified structural changes, depending on physicochemical MNP properties, using FTIR- and fluorescence spectroscopy. Furthermore, we investigated cellular uptake of MNP individually and as a complex with β -lactoglobulin and studied the effects on cell growth and viability, using colorimetric MTT testing, flow cytometry, and cell impedance measurements. MNP material properties, especially hydrophobicity, had an impact on protein folding and consequently also on cellular interactions. In a second study, we applied α -amylase, an extracellular digestive protein with enzymatic activity. Here, in addition, we investigated the influence of MNP binding on enzyme activity, using a colorimetric starch degradation assay. We observed for the most MNP, that adsorption processes resulted in a decrease of enzyme activity. Furthermore, we used Alexa633 staining to visualize MNP uptake with and without the presence of α -amylase.

Taken together, this work aims to close data gaps regarding mechanistic effects of MNP on cells by investigating direct MNP-protein-interactions. Mechanistic knowledge is crucial for understanding toxicological effects of MNP, and therefore, also for the risk assessment of possible hazards on human health.

¹Kieserling, H.; Siegl, H.; Heilscher, J.; Drusch, S.; Braeuning, A.; Thünemann, A. F.; Rohn, S. Towards understanding particle-protein complexes: Physicochemical, structural, and cellbiological characterization of β -lactoglobulin interactions with silica, polylactic acid, and polyethylene terephthalate nanoparticles. *Colloids and Surfaces B: Biointerfaces* 2025, 253, 114702. DOI: <https://doi.org/10.1016/j.colsurfb.2025.114702>.

P180

The impact of vitamin variants on sulfur mustard-induced cellular senescence in human mesenchymal stem cells

A. Neu^{1,2}, D. Steinritz^{1,3}, A. Schmidt², S. Rothmiller¹

¹Institute of Pharmacology and Toxicology, Munich, Germany

²University of the Bundeswehr Munich, Institute of Sports Sciences, Munich, Germany

³Ludwig Maximilian University of Munich, Walter-Straub-Institute, Munich, Germany

Question

Sulfur mustard (SM) is a bifunctional alkylating blister agent frequently connected to chronic wound healing disorders (WHD). Human mesenchymal stem cells (hMSC) play a crucial role in the wound healing process by releasing cytokines and chemokines as well as differentiation into new tissue cells. However, chronic senescence in hMSC has been described following SM exposure, impairing their function in wound healing. The hallmarks of chronic senescent hMSC include diminished migration and cytokinesis, accompanied by a pro-inflammatory microenvironment. A new approach in targeting SM-induced WHD is the reduction of chronic senescence.

The present study examined the potential of the drug candidates niacin (vitamin B3) and nicotinamide riboside (NR) to prevent senescence.

Methods

The hMSC were treated with the drug candidates 23 hours prior (\pm prophylaxis) or one hour after (\pm therapy) a 40 μ M SM exposure. Senescence-associated β -galactosidase staining was used to identify senescent cells. In order to assess alterations in gene expression occurring at day one, 12, and 21 after SM exposure, a series of PCR arrays for NAD⁺ and DNA damage reaction (DDR) pathways were utilized. Furthermore, concentration determination studies for both

drug candidates were performed using NAD⁺/NADH assays in conjunction with assays of toxicity, apoptosis and necrosis.

Results

Both niacin and NR were able to reduce SM-induced senescence as prophylaxis in hMSC. Concentration were optimized to induced highest increase of NAD⁺ levels without causing cytotoxicity (15 µM Niacin, 500 µM NR). SM exposed hMSC revealed a time-dependent increase in the apoptosis marker annexin V, while no influence of niacin was detected. A number of genes associated with cell cycle control or DDR exhibited substantial alterations in expression. The analysis revealed the upregulation of DDR genes, including APEX1 and ATRIP, while FANCD2 and BRCA1 demonstrated diminished expression in untreated SM exposed cells. No changes in the mentioned genes were observed in hMSC with niacin prophylaxis.

Conclusion

In conclusion, the results demonstrate a reduction in senescence after prophylactic administration of niacin and NR. Further studies are required to elucidate the molecular mechanism of action of the tested drug candidates in the context of SM-induced senescence in hMSC. Their potential as a prophylactic measure for WHD following SM exposure, is a promising avenue for future research.

P181

First drug candidates aiming to improve wound healing after sulfur mustard-induced senescence

S. Rothmiller¹, A. Neu^{1,2}, L. Pettersson^{1,3}, D. Steinritz^{1,4}

¹Bundeswehr Institute of Pharmacology and Toxicology, Munich, Germany

²University of the Bundeswehr Munich, Department of Human Sciences, Institute of Sport Sciences, Neubiberg, Germany

³Ludwig Maximilian University of Munich, Faculty of Medicine, Munich, Germany

⁴Ludwig-Maximilians-University Munich, Walther-Straub-Institute of Pharmacology and Toxicology, Ludwig-Maximilians-University, Munich, Germany

Question

Exposure to sulfur mustard (SM), an alkylating chemical warfare agent, induces skin blisters and results in prolonged wound healing disorders. Senescence in wound healing associated cells like mesenchymal stem cells and fibroblasts was recently identified as a novel pathomechanism since senescent cells show reduced migratory ability and promote a pro-inflammatory microenvironment. Targeted therapy following SM exposure can take new forms, such as preventing senescence induction, preventing negative effects, or even eliminating senescent cells.

Methods

Sulfur mustard was applied to human mesenchymal stem cells and primary dermal fibroblasts for 21 days in order to induce chronic senescence, whereas solvent was used as a non-senescent control. Senescent cells were identified by SA-β-gal staining, NAD⁺ and ATP levels via quantitation assays, gene regulation by qRT-PCR, scratch assay by IncuCyte scratch wound assay and viability via Alamar Blue. Cells were treated with TargetMol anti-aging compound library. Hits were defined by a viability of non-senescent cells at least 20% higher than those of senescent cells and a strictly standardized mean difference of at least three.

Results

Prophylactic treatment with vitamin B3 derivatives (niacin and nicotinamide riboside) significantly reduced senescence and increased intracellular NAD⁺ and ATP levels. These may improve DNA damage repair mechanisms after SM exposure and thus reduce senescence due to unresolved DNA damage. Thus, both are interesting drug candidates. Prophylactic treatment with the growth factor FGF-2 was also able to reduce senescence and showed an upregulation of TIMP1 and downregulation of FGF-5. Moreover, in healthy mesenchymal stem cells, addition of FGF-2 significantly improved wound closure times in a scratch assay model. More research is needed, as reducing senescence and increasing migration with a single drug candidate appears promising. Targeted removal of senescent cells can be achieved by senolytics. By testing an anti-aging substance library, we could already identify over 30 hits. Saracatinib (AZD0530), a dual kinase inhibitor, has emerged as the most promising molecule thus far.

Conclusions

To summarize, SM-induced senescence following SM exposure is still a novel research area, and we provide the first pharmacological candidates targeting this pathomechanism. Further research may lead to novel treatment options for long-lasting wounds caused by SM poisoning.

P182

Enzyme inhibition as the basis for a rapid test device for sulfur mustard

D. Barre¹, D. Steinritz^{1,2}, S. Rothmiller¹

¹Bundeswehr Institute of Pharmacology and Toxicology, Munich, Germany

²Ludwig Maximilian University of Munich, Walther Straub Institute of Pharmacology and Toxicology, Munich, Germany

Question:

Sulfur mustard (SM) is a chemical warfare agent that, despite being prohibited under the Chemical Weapons Convention, has been used in several instances in recent years. Exposure to SM leads to early symptoms such as erythema and eye irritation, followed by the characteristic formation of skin blisters. The resulting slow-healing wounds can only be treated symptomatically. Early identification and appropriate decontamination are therefore crucial to minimize tissue damage. Current established methods for SM detection are often time-consuming and require high sample concentrations to produce reliable results. Consequently, there is a pressing need for a faster, more sensitive, and field-deployable detection method.

Methods:

The objective of the study was to develop a test system based on SM-induced enzyme inhibition. The reduction in enzyme activity should result in a color change visible to the naked eye in the respective enzymatic test used. To achieve this, a screening of enzymes for their interaction with SM was conducted. The selected enzymes were known to interact with alkylating agents or to contain sulphureous amino acids in their active site.

Results:

In the screening process, colorimetric assays were performed to evaluate the interaction between SM and the enzymes. By optimizing parameters such the buffer composition and appropriate controls, a robust general test setup was established. The results demonstrated a dose-dependent inhibition of several enzymes by SM, with glycerol-3-phosphate dehydrogenase emerging as the most promising candidate.

Conclusion:

SM-induced inhibition of enzyme activity could form the basis for a diagnostic rapid test. Further improvements in robustness and sensitivity are required to achieve a field-ready testing device. Nevertheless, this prototype represents a promising first step toward a rapid detection method that could enable timely initiation of targeted treatment and decontamination measures.

P183

Toxicological assessment of the genotoxic and cytotoxic potential of ring-shaped monochlorinated hydrocarbons produced from lindane waste

E. Liesenfeld¹, S. Stegmüller¹, E. Richling¹

¹University of Kaiserslautern-Landau (RPTU), Lebensmittelchemie & Toxikologie, Kaiserslautern, Germany

The project Halocycles (PN: P2021-10-007) funded by the Carl-Zeiss foundation mainly focuses on the recycling and upcycling of persistent polyhalogenated hydrocarbons, such as lindane. These compounds pose a major environmental hazard and were stored in landfills for decades. Due to their high persistence and difficult disposal a new electrochemical process was developed to degrade these substances without wasting the halogens or carbon skeletons. The up to 20 uncharacterized products resulting from this process are subjected to toxicological testing to ensure their safety for e.g. further large-scale synthesis in the future. In this presentation we will focus on four structurally similar cyclic monochlorinated compounds (monochlorinated five-, six-, seven- and eight-membered rings) to give an overview about the used test battery which is established in our research group. Up to now, various cytotoxicity tests were carried out in HepG2 cells to determine the cytotoxic potential of the substances and to obtain initial indications of their mechanism of action (MoA). Subsequently, their mutagenic potential was investigated using Ames fluctuation assay, in which the *Salmonella* thyphimurium strains TA98 (frameshift mutations) and TA100 (base pair exchange mutations) were tested with and without metabolic activation by rat liver S9-mix. In addition, to identify DNA double-strand breaks and to examine oxidative stress, a modified comet assay with and without formamidopyrimidin-glycosylase (FPG) was performed. Cytotoxicity tests revealed that after a treatment period of 2 hours only slight reductions in cell viability were demonstrated, with the neutral red assay proving to be the most sensitive test method. After a treatment period of 24 hours, reductions in cell viability of less than 10% were observed for the monochlorinated five-, six- and seven-membered rings. The eight-membered ring showed only a reduction in cell viability of approximately 50% compared to the control. Again, the neutral red test was most sensitive for a treatment period of 24 hours. The results of the Ames fluctuation assay showed that the test substances had no mutagenic effects in TA98 bacteria, while in TA100 bacteria, the six-ring and eight-membered ring compounds showed significant mutagenic effects. Overall, various toxicological effects can be observed, which vary depending on the substance. Further experiments in the course of the project will now investigate the exact MoA.

P185

In vitro toxicity testing of new battery materials

F. Neuendorf¹, K. Sowa², M. Grünebaum², M. Esselen¹

¹University of Münster, Institute for Food Chemistry, Münster, Germany

²Helmholtz Institute Münster, Münster, Germany

The demand for batteries is rising continuously due to the expansion of the renewable energy and e-mobility sectors¹. The present focus of research endeavors is on the development of batteries that exhibit enhanced efficiency and elevated capacities, with the objective of utilizing them in small handheld electronics and electric vehicles. Moreover, stationary energy storage solutions

such as redox-flow-batteries could be a promising way to stabilize the power grid during fluctuations in renewable energy production.

Using batteries in handheld devices and toys, as well as the disassembly process during recycling, poses a risk of human exposure to battery materials. Furthermore, a substantial amount of the battery waste is not collected and recycled properly, which may result in the release of battery materials into the environment¹.

So far, research has primarily focused on the improvement of battery materials and the toxicity of the materials has not been deeply investigated. However, several toxic effects have already been shown for a number of battery materials^{2,3}. Consequently, a comparison of novel battery materials in *in-vitro* acute cytotoxicity tests as well as genotoxicity and mutagenicity assays could provide an assessment of the toxicological concerns during the development of new batteries.

Literature

¹ Cornelis P. Baldé, Ruediger Kuehr, Tales Yamamoto, Rosie McDonald, Elena D'Angelo, Shahana Althaf, Garam Bel, Otmar Deubzer, Elena Fernandez-Cubillo, Vanessa Forti, Vanessa Gray, Sunil Herat, Shunichi Honda, Giulia Iattoni, Deepali S., Khetriwal, Vittoria Luda di Cortemiglia, Yuliya Lobuntsova, Innocent Nnorom, Noémie Pralat, Michelle Wagner. The Global E-Waste Monitor 2024; Gent/Bonn, 2024.

² Qiao, Y.; Wang, S.; Gao, F.; Li, X.; Fan, M.; Yang, R. Toxicity analysis of second use lithium-ion battery separator and electrolyte. *Polymer Testing* **2020**, *81*, doi: 10.1016/j.polymeresting.2019.106175.

³ Kubot, M.; Frankenstein, L.; Muschiol, E.; Klein, S.; Esselen, M.; Winter, M.; Nowak, S.; Kasnatscheew, J. Lithium Difluorophosphate: A Boon for High Voltage Li Ion Batteries and a Bane for High Thermal Stability/Low Toxicity: Towards Synergistic Dual Additives to Circumvent this Dilemma. *ChemSusChem* **2023**, *16*, doi: 10.1002/cssc.202202189.

P186

Impact of arsenite and cadmium on the cysteine oxidation of proteins in human epithelial lung cells

M. Link¹, J. Kuhn¹, M. Parsdorfer¹, A. Hartwig¹

¹Karlsruhe Institute of Technology (KIT), Karlsruhe, Germany

The cellular redox regulation is important for maintaining signaling pathways and genomic stability. It is known that human carcinogens such as arsenite and cadmium can interact with cysteine residues in proteins and other sulfur-containing cellular molecules. Regarding the mechanisms of metal toxicity, it has not yet been described which specific redox-regulated proteins are affected.

To answer this research question, the effects of NaAsO₂ and CdCl₂ were investigated in human bronchial epithelial cells (BEAS-2B). The global reversible iodoacetyl probe (BIAM) followed by LC-MS/MS measurement and protein identification.

To study the reversible cysteine oxidation, an incubation time of 4 h for the metal compounds was used, respectively. A 10-minute incubation with H₂O₂ was used to stimulate protein oxidation. The BIAM-Switch analysis revealed a decrease in the reversible cysteine oxidation of specific proteins upon exposure to concentrations as low as 0.1 µM arsenite, while 0.1 µM CdCl₂ also showed increased protein oxidation in specific proteins compared to control samples. For instance, 0.1 µM arsenite significantly reduced the reversible cysteine oxidation of CTBP2, which is involved in chromatin remodeling.

In contrast to the comparatively weak effects observed upon metal exposure, oxidative stimulation with H₂O₂ resulted in the oxidation of multiple cellular proteins, particularly those involved in the oxidative stress response and mitotic processes. A 4-hour preincubation with NaAsO₂ or CdCl₂ prior to the H₂O₂ exposure resulted in an enhancement of the H₂O₂-stimulated reversible cysteine oxidation, even at low metal concentrations. At higher concentrations, cysteines of proteins with DNA-, RNA-, protein-, or metal-binding sites were mostly affected. For example, an increase in reversible cysteine oxidation was observed in proteins such as BAG family molecular chaperone regulator 2, peroxiredoxin-2, and DnaJ homolog subfamily C member 9. Interestingly, other members of the same protein families were unaffected.

In conclusion, the present study indicates that even low concentrations of NaAsO₂ or CdCl₂ result in specific alterations of redox-sensitive proteins. This could help to further understand the toxic and carcinogenic mechanisms of these metal compounds.

P187

Oxidative DNA Damage induced by the natural substance Annonacin found in Sour sop (*Annona muricata*)

N. S. A. Hadi^{1,2}, A. Breuninger¹, N. Aivodji³, H. Stopper¹

¹Julius Maximilian University of Würzburg, Institute of Pharmacology and Toxicology, Würzburg, Germany

²Pwani University, School of Health and Human Sciences, Kilifi, Kenya

³University of Abomey-Calavi, School of Life and Earth Sciences, Cotonou, Benin

Question: Acetogenins are a class of bioactive polyketides primarily found in the Annonaceae family, recognized for their potent cytotoxic, antiproliferative, and anti-tumor properties. Annonacin, the major acetogenin in *Annona muricata*, has demonstrated notable anticancer potential but has also raised safety concerns due to reported neurotoxic and possible genotoxic effects. However, the underlying mechanisms remain poorly understood. This study aimed to elucidate the genotoxic potential of annonacin in human cell models and to determine whether metabolic activation contributes to its effects.

Methods: Human promyelocytic leukemia (HL-60) and hepatocellular carcinoma (HepG2) cells were exposed to increasing concentrations of annonacin. Genotoxicity was evaluated using the cytokinesis-block micronucleus (CBMN) assay, with the cytokinesis-block proliferation index (CBPI) calculated to assess cytostatic effects. DNA strand breaks and oxidative lesions were quantified via formamidopyrimidine DNA glycosylase (FPG)-modified comet assay. Intracellular reactive oxygen species (ROS) production was measured by dihydroethidium (DHE) fluorescence, while mitochondrial membrane potential (ΔΨ_m) was assessed using tetramethylrhodamine ethyl ester (TMRE). The inclusion of HepG2 cells allowed investigation of potential metabolic activation.

Results: No statistically significant increase in micronucleus frequency was detected in either HL-60 or HepG2 cells. However, annonacin treatment significantly reduced CBPI values in both cell lines, suggesting cytostatic or cell cycle-impaired effects. The FPG-modified comet assay revealed elevated levels of oxidized DNA bases, indicating oxidative DNA damage. Concomitantly, annonacin markedly increased ROS generation in HL-60 cells, and caused a pronounced decline in mitochondrial membrane potential, confirming mitochondrial dysfunction.

Conclusions: Our findings indicate that annonacin induces indirect DNA-damage through mitochondrial complex I inhibition and subsequent ROS generation rather than direct DNA interaction. These results enhance the mechanistic understanding of acetogenin-induced DNA-damage and highlight the need to assess mitochondrial toxicity in natural product safety evaluation. Our next experiments are planned to examine dose-response thresholds and compare pure annonacin with the whole *Annona muricata* extract.

Keywords: Annonacin; Acetogenins; *Annona muricata*; Genotoxicity; Oxidative DNA damage; Reactive oxygen species.

P188

Quantitative analysis of DNA repair capacity in a modified Comet Assay using DNA repair inhibitors

K. Krotz¹, H. Stopper¹

¹Institute of Pharmacology and Toxicology, Würzburg, Germany

The relationship between DNA damage and DNA repair plays a central role in cell biology and genetics. While DNA damage can result from various endogenous as well as exogenous influences, DNA repair ensures that this damage is repaired to prevent mutations and associated diseases, thereby preserving genomic integrity.

The most important types of DNA damage are base damage, single-strand breaks, double-strand breaks, mismatches and crosslinks. Some of the damage is repaired specifically by different DNA repair pathways. The most important repair mechanisms include base excision repair (BER), nucleotide excision repair (NER), mismatch repair (MMR) and the repair of double-strand breaks using non-homologous end-joining (NHEJ) and homologous recombination (HR).

The present work uses the comet assay, modified by the application of various DNA repair inhibitors. DNA-damaging substances are applied to generate types of DNA damage which require certain repair pathways. Then, inhibitors aiming at these DNA repair pathways are used. Olaparib is applied, a poly(ADP-ribose)-polymerase (PARP) inhibitor that disturbs the BER pathway. Aphidicolin inhibits the DNA polymerases α, δ and ε and consequently NER. SCR7 inhibits DNA ligase IV, thereby disrupting NHEJ.

We were able to show that the intensity of DNA damage increases after treatment with the inhibitors in human HL-60 cells, HeLa cells, M059K cells, TK6 cells and peripheral blood mononuclear cells in a manner that is specific for the induces lesions and required DNA pathways. Differences between cell types were identified and correlate with sensitivities for cell death induction by the DNA damaging substances.

This modified Comet Assay is currently used to investigate differences in DNA repair capacity in normal weight versus obese individuals (BMI>35).

P189

Interaction of Neonicotinoid Insecticides with Nicotinic Acetylcholine Receptors – a direct cholinergic interaction?

F. Springer¹, S. Muschik¹, T. Seeger¹, D. Steinritz¹, K. V. Niessen¹

¹Bundeswehr Institute of Pharmacology and Toxicology, Munich, Germany

Question

Neonicotinoids (NNIs) are neuroactive insecticides chemically similar to nicotine. The dual use of NNIs as chemical agents has to be considered due to their high availability and depiction in literature. NNI intoxication results in a hyperstimulation of the cholinergic system, triggering a cholinergic crisis. This is caused via NNIs agonistic binding to nicotinic acetylcholine receptors (nAChRs) and consequently

depolarisation of the postsynaptic membrane. Elevated NNI concentrations result in nAChR desensitization. If not treated, this dysfunctional state is fatal due to central and peripheral respiratory failure.

Methods

To determine affinity and binding state of selected NNIs towards the binding sites of the endogenous ligand acetylcholine (orthosteric binding sites) of the nAChR a scintillation-proximity assay (SPA) was used. [³H]epibatidine and [³H]nicotine served as a reporter ligand for these binding sites in separate assays. The SPA was performed on a custom-designed automated pipetting platform, enabling testing under controlled conditions. Due to being highly genetically conserved, membrane fragments containing 2αδγ-nAChRs from the electric organ (electroplax) of *Tetronarce californica* were used.

Results

For all substances tested, the inhibitory constant (pK_i) was calculated and compared to the agonists (±)epibatidine and nicotine. In order to demonstrate additional modulating effects, binding behaviour was compared to the bispyridinium compound MB327 (pK_i [³H]epibatidine = 4.5 ± 0.1). MB327 has been shown to have a biphasic effect (modulation and inhibition) and being able to restore the functional activity of dysfunctional nAChRs.

Conclusions

Compared to epibatidine, the affinity of the evaluated NNIs to the nAChR is relatively weak. For some substances, such as thiaplopid or imidaclopid, an apparent increase in affinity of [³H]epibatidine is observed at the orthosteric [³H]epibatidine binding site. Binding at the [³H]nicotine binding site shows similar effects. Biphasic binding effects might be related to an allosteric effect as being described for MB327. These affinity data are essential for the assessment of human toxicity.

P190

Testing Immunotoxicity *in vitro* – the Impact of Bisphenol A, F and S on Human T Helper Cells

P. Krohn^{1,2}, N. Regehr¹, K. Siewert¹, C. Curato¹

¹German Federal Institute for Risk Assessment (BfR), Chemical and Product Safety, Berlin, Germany

²Technische Universität Berlin, Berlin, Germany

Human health risks due to chemicals, particularly on the immune system, are not well understood. Prominent examples are bisphenols, such as Bisphenol A, F or S (BPA, BPF, BPS), petroleum-based industrial chemicals, which may be released from food contact materials in small amounts. In 2024, the EU completely banned the use of BPA for food contact materials based on increased levels of a T cell subset, Th17 cells, in mice upon BPA exposure.

Here, we assessed toxic and T cell subset effects of BPA, alternative bisphenols and arylhydrocarbon receptor (AhR) agonists on human memory T cells. PBMCs were isolated from buffy coats and cultured for five days under CD3/CD28 stimulation with different concentrations of BPA, BPF, BPS (0 – 800 µM) and AhR agonists b-naphthoflavone (bNF; 0 – 3.1 µM) and 6-Formylindolo(3,2-b)carbazole (FICZ; 0 – 0.2 µM). Live cell numbers, frequencies of apoptotic cells, ATP and supernatant cytokine levels and frequencies of Th1, Th2 and Th17 cells, determined by surface chemokine receptor staining, were chosen as readouts.

In a series of independent experiments (n = 4–6), memory CD4+ T cell viability and ATP levels? started to decline from 12.5 µM for all bisphenols, partially accompanied by an increase in apoptotic cells[FDKS1]. At lower, non-toxic concentrations, we did not observe changes in IL-17A expression nor Th17 cell frequencies [FDKS2] for all bisphenols. AhR agonists bNF and FICZ [FDKS3] showed dose-dependent trends for reduced IL-17A/F cytokine levels and CCR4+CCR6+CXCR3- Th17 cell frequencies, while CCR4-CCR6-CXCR3+ Th1 cell percentages increased. Here, FICZ exhibited stronger effects than bNF.

In conclusion, our results indicate immune effects for AhR agonists on human T cells. Compared to mice studies, we did not observe memory T cell plasticity directed towards a Th17 phenotype for bisphenols, while effects on human naïve T cell differentiation have to be investigated next. Our results emphasize the need for human focused *in vitro* immunotoxicity assays to assess possible adverse effects in the target species[FDKS4].

P191

Nuclear but not cytosolic RAC1 is a prerequisite for a full-blown etoposide-triggered DNA damage response in human endothelial cells

V. Thalayasingam¹, G. Fritz¹, C. Henninger¹

¹University Hospital Düsseldorf, Heinrich Heine University Düsseldorf, Institute of Toxicology, Düsseldorf, Germany

Introduction: The small Rho GTPase RAC1 is a key regulator of actin cytoskeleton dynamics, cell migration, adhesion, proliferation, and intracellular signaling. Beyond these well-established functions, RAC1 is hypothesised to play a role in the early DNA damage response (DDR) following exposure to topoisomerase II inhibitors such as doxorubicin and etoposide. These agents induce cytotoxic DNA double-strand breaks (DSB), and endothelial cells are among the first tissues to encounter them after intravenous drug administration.

Objectives: Here, we investigated whether cytosolic RAC1 signaling contributes to the etoposide-induced DNA damage response (DDR) or if nuclear RAC1 plays a more prominent role in this context, using human endothelial cells as a model system.

Material & methods: Human endothelial EA.hy926 cells were transfected with different RAC1 variants (wild-type (WT), dominant-negative (T17N), constitutively active (Q61L)), fused to eGFP and modified with either a nuclear localization sequence (NLS) or a nuclear export sequence (NES). Transfections were performed using polyethylenimine. Additionally, cells were treated with the RAC1 inhibitor EHT1864, followed by a one-hour exposure to etoposide. Cellular responses were assessed by measuring cell viability (resazurin reduction assay), DSB formation (immunofluorescent detection of γH2AX and pATM foci), and levels of phosphorylated H2AX (Western blot analysis).

Results: Pharmacological inhibition of RAC1 with EHT1864 significantly reduced the formation of etoposide-induced γH2AX foci (DSB), as well as overall γH2AX protein levels. Consistently, transfection with nuclear dominant-negative RAC1 led to a marked decrease in foci formation following etoposide exposure, whereas cytosolic dominant-negative RAC1 had no such effect. The inhibitory effect of EHT1864 was attenuated in cells transfected with constitutively active RAC1 variants. In addition, RAC1 inhibition was associated with a modest improvement in cell viability after etoposide treatment.

Conclusion: Blocking nuclear, but not cytosolic RAC1 prevents etoposide-induced DSB formation in human endothelial cells. Hence, the presence of active nuclear RAC1 is a prerequisite for the full activation of the etoposide-induced DDR. Pharmacological inhibition of RAC1 may therefore represent a strategy to protect normal tissue from the genotoxic effects of topoisomerase II inhibitors.

P192

Protective Effects of Delphinidin and Maqui Berry Delphinidin Glycosides Against Oxidative Stress and DNA Damage

G. Martelli¹, C. Lörcher¹, N. S. Aboud Hadi¹, E. E. Bankoglu¹, D. Schmück², N. Roewer³, H. Stopper¹

¹Institute of Pharmacology and Toxicology - Julius-Maximilians-University of Würzburg, Würzburg, Germany

²SAPIOTEC GmbH, Würzburg, Germany

³University Hospital Würzburg, Würzburg, Germany

Anthocyanins are well-known antioxidants of the flavonoid group. They are present in various widely consumed foods and supplements, where they mainly occur as glycosides of anthocyanidins (aglycons). So far, most studies have focused on whole-plant extracts and aglycons. However, the influence of the sugar moiety on their antioxidant activity remains unclear. Therefore, this project aimed to compare the antioxidant effects of four major Maqui Berry (MB) anthocyanins to those of their aglycon, delphinidin. We tested whether the compounds and MB extract reduced oxidative stress in the human cell line Caco-2 using the fluorogenic probe 2',7'-dichlorodihydrofluorescein diacetate (DCFH2-DA). The FPG (formamido pyrimidine glycosylase) comet assay was applied to investigate the protective effect against H2O2-mediated DNA damage. In the DCFH2-DA assay, all tested compounds and MB extract similarly decreased oxidative stress produced by H2O2. This effect was preserved when the medium was replaced with anthocyanin-free medium before hydrogen peroxide treatment. In the FPG comet assay, delphinidin glycosides and MB extract exhibited comparable effects to those of delphinidin. Our results suggested that delphinidin and its MB glycosides have similar antioxidative effects. A micronucleus assay was also performed to explore whether delphinidin and its glycosides exert a genoprotective effect by inhibiting CYP450-mediated intracellular activation of the pyrrolizidine alkaloid riddelline, using HepG2 cells. The micronucleus assay showed that delphinidin and its glycosides similarly inhibit riddelline activation. Further analyses are needed to investigate the role of membrane transporters in Caco-2 and HepG2 cells.

P193

Glyphosate: Effects on the embryonic development of the South African clawed frog *Xenopus laevis* – A comparison between the active ingredient and commercial formulations

H. Flach¹, P. Dietmann¹, S. Pfeffer¹, M. Kühl¹, M. Liess^{2,3}, S. Kühl¹

¹Ulm University, Institute of Biochemistry and Molecular Biology, Ulm, Germany

²Leipzig University, Department System-Ecotoxicology, Helmholtz Centre for Environmental Research, Leipzig, Germany

³RWTH Aachen University, Institute for Environmental Research (Biology V), Aachen, Germany

Background:

Human-induced environmental changes, including land use, climate change, and pollution, increasingly threaten global biodiversity and ecosystem functioning. Among widely used agrochemicals, the herbicide glyphosate has gained attention due to its harmful effects on non-target organisms including insects, fish, and amphibians. Amphibians are the most threatened vertebrate group, making their sensitivity to environmental contaminants especially relevant. As glyphosate is commonly applied in formulations containing adjuvants that can modify its toxicity, their effects must be considered. This presentation aimed to investigate the specific effects of pure glyphosate during embryogenesis in *Xenopus laevis* (South African clawed frog) and to compare these with the effects of four commercial glyphosate formulations.

Method:

Embryos at 2-cell stage were exposed to glyphosate concentrations between 0.01 to 243 mg/L. After up to 14 days of incubation at 14 °C, when the embryos reached NF-stage 44/45, morphological and functional analyses were conducted.

Results:

Pure glyphosate caused significant alterations in multiple developmental endpoints, including reduced body length, head area, and smaller eyes in *X. laevis* tadpoles. Additionally, impaired mobility and developmental disturbances of neural and cardiac structures were observed after 14 days of incubation. Detailed analyses revealed structural changes in cranial nerves and the heart, indicating disrupted cardiomyocyte differentiation. Commercial glyphosate formulations led to significantly higher toxicity depending on the formulation: mortality increased by up to 200-fold compared to glyphosate alone, while the prevalence and type of sub-lethal malformations were similar between treatments.

Conclusion:

Both pure glyphosate and its formulations exert significant negative effects on multiple endpoints of early embryonic development in *X. laevis*, at concentrations reflecting realistic environmental levels and worst-case scenarios. These findings highlight the necessity of assessing active ingredients and co-formulants both individually and in combination during pesticide risk assessments and regulatory approval processes. Considering the global decline of amphibian populations, partly linked to herbicide use, stringent environmental monitoring and more comprehensive evaluation of agrochemical formulations are essential to improve ecological risk assessment and biodiversity protection.

P194**Does Bisphenol A content in canned food pose a health risk?**

T. Tietz¹, C. Jung¹, C. Lorenz¹, M. Wollenberg¹

¹German Federal Institute for Risk Assessment (BfR), Exposure, Berlin, Germany

Introduction:

Bisphenol A (BPA) is a chemical compound used as a raw material in the production of polycarbonate plastics and epoxy resins. It is present in numerous consumer products such as smartphones, drinking bottles, plastic tableware, paints, adhesives and food can coatings. In 2023, the BfR performed a hazard assessment on BPA resulting in a tolerable daily intake value (TDI) of 200 ng/kg bw/d [1]. Due to missing data on BPA content in food, no risk assessment could be performed at that time.

Objectives:

Data on BPA in canned food and comparable differently packaged food were generated. An exposure estimation was conducted alongside with a respective risk assessment for different population groups in Germany.

Results:

BPA content of 243 canned food samples and comparable non-canned foods was measured, applying a method with a very low limit of quantification of (for some foods) 10 ng/kg food. Emphasis was placed on the choice of the foods as to cover all relevant food groups, for which canned foods are available (e.g. vegetables, fruits, oils, meat, fish, drinks and grain-based foods). BPA exposure of consumers was estimated applying different consumption scenarios for canned foods. The exposure distributions were combined with the probabilistic hazard assessment performed earlier [1, 2], resulting in a probabilistic risk assessment.

Conclusion:

Even for very conservative consumption scenarios, BPA exposure was well below the TDI of 200 ng/kg bw/d. Probabilistic risk assessment resulted in no concern for increased health risks for BPA exposure from canned foods in the German population.

[1] <https://www.bfr.bund.de/cm/349/bisphenol-a-bfr-proposes-health-based-guidance-value-current-exposure-data-are-needed-for-a-full-risk-assessment.pdf>

[2] <https://www.who.int/publications-detail-redirect/9789241513548>

P195**The nephrotoxins cyclosporin A and acetaminophen affect the DNA repair capacity of renal proximal tubular cells**

A. Dimitriadis¹, N. Schupp¹

¹University of Düsseldorf, Institute of Toxicology, Medical Faculty, Düsseldorf, Germany

Introduction: Proximal tubular epithelial cells (PTEC) are constantly exposed to possibly toxic metabolites and oxidants, which can also cause DNA damage. The kidney has a regenerative potential for the replacement of damaged PTEC but it is known that renal function declines, suggesting that the deteriorated cells are not replaced by fully functional cells.

Objectives: To understand the possible causes of this loss of kidney cell function, we tried to understand the role of toxins during the regeneration process after genotoxic insults. Therefore, we tested whether the contact with nephrotoxins impaired the DNA repair of the renal proximal tubular cell line HK-2.

Materials & Methods: Concentrations of cyclosporin A (CycA), acetaminophen (APAP), bleomycin, etoposide and cisplatin suitable for a 24 h treatment of HK-2

cells were determined in the MTT assay. HK-2 cells were then pre-treated for 24 h with non-genotoxic concentrations of the nephrotoxins CycA (20 µM) and APAP (10 mM) before the genotoxic compounds bleomycin, etoposide and cisplatin were added for further 24 h. DNA damage and repair was evaluated with the alkaline Comet Assay.

Results: Without pre-treatment, HK-2 cells were able to reduce DNA damage caused by bleomycin (lesions needing mainly base excision repair, BER), etoposide (causing DNA double strand breaks, needing homologous recombination, HR, or non-homologous end joining, NHEJ) and cisplatin (lesions needing mainly nucleotide excision repair, NER) significantly within 4 h. Repair of bleomycin-induced DNA lesions was not hindered by CycA but was inhibited by APAP, which was reported to interfere with dNTP synthesis needed for efficient BER. The repair of DNA damage caused by etoposide, mainly conducted by HR or NHEJ, was not impaired by either substance. No significant repair of cisplatin-induced DNA lesions was detected after pre-treatment with either substance, since CycA was reported to inhibit enzymes of the NER and the supposed reduction of dNTPs by APAP also had an impact here.

Conclusion: A distinct influence of CycA and APAP on the different DNA lesions caused by the three genotoxic substances was detected, further strengthening earlier reports on CycA and APAP inhibiting DNA repair pathways. At least for CycA, which was used in concentrations that can be achieved in the kidney, this means inhibition of renal DNA repair even under *in vivo* conditions, which may result in regenerated PTEC being less healthy.

P196**The insecticide Flupyradifurone negatively affects the insect *Adalia bipunctata* (two-spotted ladybird) and the amphibian *Xenopus laevis* (African clawed frog)**

M. Wiedenmann¹, J. Schneider¹, P. Dietmann¹, S. Pfeffer¹, S. Kühl¹, H. Flach¹

¹Ulm University, Institute of Biochemistry & Molecular Biology, Ulm, Germany

Introduction: Globally, approximately 19% of all insect species are currently threatened with extinction, while amphibians face an even higher risk, with about 41% affected. One key driver contributing to the decline of these species is the environmental contamination by pesticides. In particular, spray applications of pesticides can exert an influence on non-target insects, such as the two-spotted ladybird (*Adalia bipunctata*). Pesticides can furthermore accumulate in sediments and surface waters, potentially impairing aquatic organisms such as the African clawed frog (*Xenopus laevis*). One of these pesticides is Flupyradifurone, a novel insecticide. With a degradation time exceeding 450 days in soil and 150 days in aquatic systems, Flupyradifurone shows a high probability of potential negative effects on *Adalia bipunctata* and *Xenopus laevis*. This study investigates these potential effects of Flupyradifurone on both insect and amphibian representatives to evaluate its broader ecological impact.

Methods: Adult *A. bipunctata* were exposed orally to concentrations between 0.1–2.0 mg/mg bw over ten days, followed by morphological and functional assessment, including analyses of the untreated F1 generation. *X. laevis* embryos were exposed to concentrations between 0.01–100 mg/L from the 2-cell stage to NF-stage 44/45 (after up to 14 days) at 14 °C, after which morphological and functional parameters were examined.

Results: Results indicate a concentration-dependent increase in mortality and a decline in motor function in *A. bipunctata*, along with reduced reproductive capacity and altered elytral coloration in the F1 generation. In *X. laevis* embryos, exposure led to developmental delays and morphological deformities, including reduction in body size, eye surface area, head surface area and width, and cartilage. Additional analyses revealed that processes involved in eye differentiation were adversely affected at a molecular level. Furthermore, a dose-dependent impairment of mobility as well as an increase in heart rate was detected.

Conclusion: Flupyradifurone has significant harmful effects on morphological and functional levels of both non-target insects (*A. bipunctata*), and amphibians (*X. laevis*). The findings of the present study demonstrate that the ecological consequences of this insecticide extend far beyond the target organisms of pest insects. Consequently, its approval and utilization should be contingent on a more comprehensive evaluation of these risks.

P197**Alterations of Membrane and Functional Properties in T and B Cells Induced by Per- and Polyfluoroalkyl Substances (PFAS)**

A. Meißner¹, C. Esser¹

¹Leibniz Research Institute for Environmental Medicine (IUF), Düsseldorf, Germany

PFAS are widely used synthetic chemicals with water- and oil-repellent properties. They are amphiphilic and, depending on chain length, are highly persistent in biological systems. Epidemiological studies linked PFAS exposure to reduced antibody responses following vaccination. Immunosuppression is recognized as of high concern. These findings form the basis for risk assessment of selected PFAS such as PFOA, PFOS, PFNA and PFHxS, though the molecular mechanisms remain largely unknown.

T-cell membrane fluidity is crucial for membrane protein functions, cell interactions, and signal transduction. Importantly, it also governs the formation and stability of lipid rafts, microdomains coordinating T cell receptor-mediated signaling. Cholesterol in membranes is a major factor in regulating membrane fluidity. We hypothesized that PFAS can integrate into cell membranes due to their chemical structures and thereby induce alterations in membrane fluidity,

including displacement of cholesterol. To test this, we exposed Jurkat cells, a human T cell line, to perfluorooctanoic acid (PFOA). Toxicity correlated with exposure duration. In Jurkat cells, PFOA (1.5 nM–150 µM, non-toxic doses) decreased membrane fluidity as measured by a fluorescence-based excimer assay. Cholesterol staining indicated reduced cholesterol in Jurkat cells, consistent with PFAS-induced changes in lipid organization associated with lower membrane fluidity. Quantification of the lipid raft marker GM1 revealed that PFOA treatment (25–150 µM) combined with antigen receptor stimulation (anti-CD3/anti-CD28) increased GM1 levels by more than two thirds. Moreover, PFOA exposure significantly enhanced CD69 expression, an early activation marker, and was associated with increased internalization of the TCR complex. Next, we used TCR-stimulated mouse primary T cells. Unexpectedly, PFOA reduced GM1 expression in these cells to control levels. Extending the results to primary murine B cells, we tested if PFOA modulated markers of cell activation. We found that it reversed the LPS-induced upregulation of CD86 and MHC II and downregulation of CD184 (CXCR4).

These results indicate that PFOA modulates membrane-associated processes and immune cell activation. Future studies will address PFOA-mediated impairment of downstream signaling of the T cell receptor, and further functional parameters. PFAS-induced membrane alterations in immune cells may be a key mechanism in their immunotoxic effects.

P198

RAC1 deficiency confers agent-specific protection against anticancer drug-induced normal tissue injury in detoxifying organs

S. Gatzmanga¹, C. Heinrich¹, A. Vijayendran¹, G. Fritz¹

¹University Hospital Düsseldorf, Heinrich Heine University Düsseldorf, Institute of Toxicology, Düsseldorf, Germany

Introduction: The small GTPase RAC1 is involved in the regulation of multiple cellular stress responses and influences normal tissue injury following anticancer drug treatment. Doxorubicin (DOX), an anthracycline derivative commonly used in anticancer therapy, and cisplatin (CIS), a platinum-based cytostatic agent, cause severe adverse effects that impair the patients quality of life. While pharmacological inhibition of RAC1 has shown cytoprotective potential, genetic evidence regarding its impact on organ- and agent-specific toxicity remains limited.

Objective: Using a poly(I:C)-inducible *Rac1*^{fllox/Mx1-Cre} mouse model, we investigated the contribution of RAC1 to DOX- and CIS-induced tissue injury in the detoxifying organs liver and kidney.

Results: Loss of *Rac1* markedly reduced DOX-induced DNA double-strand break (DSB) formation and apoptotic cell death in both liver and kidney. In contrast, after CIS exposure, DNA damage was only slightly reduced in the liver of *Rac1* knockout animals and the number of apoptotic cells remained unaffected in both organs. Transcriptomic profiling revealed that the DOX-induced expression of DNA damage response (DDR), inflammation-, fibrosis-, and apoptosis-related genes was significantly attenuated in RAC1-deficient mice as compared to the wild-type animals, whereas transcriptional changes induced by CIS treatment remained largely unaltered in the absence of *Rac1*.

Conclusion: These findings provide first genetic evidence that RAC1 critically mediates organ-specific sensitivity to DOX-, but not CIS-induced normal tissue toxicity. RAC1 deficiency attenuates DOX-induced DSB formation and apoptosis, modulating the DDR in an organ-specific manner. Targeting RAC1 may thus be useful to reduce normal tissue toxicity evoked by anthracycline-based anticancer therapy.

P199

Larvicidal and Repellent Efficacy of *Citrus sinensis* peel and *Cymbopogon citratus* Extracts Against Mosquitoes and Assessment of Their Environmental Safety

O. Salako¹, K. Salako¹, K. Lamidi¹, J. Nwuzor¹

¹University of Lagos, Pharmacology, Therapeutics and Toxicology, Idi-Araba, Lagos, Nigeria

Mosquito-borne diseases, such as malaria, remain a major global health concern, with sub-Saharan Africa bearing the greatest burden. There is also an increasing resistance of *Anopheles* mosquitoes to conventional insecticides which has reduced the efficacy of long lasting insecticidal nets (LLINs) and indoor residual spraying (IRS), highlighting the need for a more effective but safer and eco-friendly control measure. The aim of the study was to evaluate the larvicidal and repellent efficacy of *Citrus sinensis* (orange) peel and *Cymbopogon citratus* (lemon grass) extracts against mosquitoes alongside the assessment of their environmental safety using tadpoles as non-target organisms.

Hydro-ethanolic extracts of the plants were prepared by maceration at room temperature in 20% ethanol solution for 72 hours. Phytochemical screening, larvicidal bioassay, repellency assay using cotton wool damped with extract placed in a position within the test chamber, and environmental safety assessment were performed in the study.

Phytochemical screening shows the presence of phenolic compounds, tannins, flavonoids, saponins and glycosides with *Citrus sinensis* having the higher flavonoid (48.94 ± 0.29 mg/g) and phenolic (84.17 ± 0.39 mg/g) contents. Larvicidal bioassay were carried out at concentrations ranging from 25 – 1000 µg/ml. *C. sinensis* exhibited a concentration dependent mortality with LC₅₀ of 504.7 µg/ml. *C. citratus* showed 46.67% mortality at 1000 µg/ml while *C. sinensis* showed 93.3% mortality at the same concentration. Repellency assay revealed that both extracts showed avoidance behavior within 30 – 60 minutes and caused

100% mortality within 12 hours of exposure. Environmental safety assessment showed that *C. sinensis* caused 100% tadpole mortality at 100 µg/ml while *C. citratus* exhibited a lower mortality of 30% at the same concentration, thereby indicating lower negative environmental impact.

In conclusion, *C. sinensis* showed greater larvicidal activity, while *C. citratus* exhibited moderate larvicidal activity but greater environmental safety. The dual larvicidal and repellent effects of these extracts suggest strong potential for their integration in sustainable plant-based mosquito control strategies. Their accessibility, affordability and biodegradability further support their use as eco-friendly alternatives to synthetic insecticides, promoting environmental and public safety.

P200

Kinetics of 15 PFAS in humans: Results of a pilot investigation and of a study in humans

H. Mertens¹, B. H. Monien¹, L. Richter¹, H. Mielke¹, K. Abraham¹

¹Bundesinstitut für Risikobewertung (BfR), Lebens- und Futtermittelsicherheit in der Nahrungskette, Berlin, Germany

Per- and polyfluoroalkyl substances (PFAS) are ubiquitous environmental contaminants. The half-lives of the long-chain compounds in humans are in the range of years, leading to accumulation and plasma levels in the µg/L range. In contrast, short-chain and "alternative" PFAS have lower levels or are not detectable in humans in case of background exposure. This may be the result of lower external exposure, but also of shorter half-lives compared to long-chain compounds.

To get better data on kinetics, a healthy volunteer orally ingested a mixture of 15 predominantly ¹³C-labeled PFAS ("MPFAS") in a pilot investigation (MPFBA, MPFPeA, MPFHxA, MPFHpA, MPFOA, MPFNA, MPFDA, MPFUdA, MPFDoA, PFBS, MPFHxS, MPFOS, DONA, HFPO-DA, 6:2FTS). Concentrations were measured over 450 days in plasma and during the first days in urine and feces, using UHPLC-MS/MS analysis after extraction.

Absorption was quick and almost complete. Volumes of distribution were calculated to be between 110 and 177 mL/kg bw for most compounds, but higher in case of MPFDA, MPFUdA and MPFDoA (maximum of 354 mL/kg bw). Half-lives were found to vary extremely: from 0.5 days (MPFPeA) and 1.5 days (MPFHxA) to 51 days (PFBS) and 152 days (MPFHpA) in case of the short-chain and "alternative" compounds. In case of long-chain compounds, half-lives of several years were confirmed for MPFOA, MPFNA, MPFHxS and MPFOS; with even higher chain-lengths of the carboxylic acids (PFCA), half-lives were found to decrease (shortest half-life for MPFDoA: 295 days). Urinary losses explained the excretion in case of the short-chain and "alternative" PFAS. Fecal losses of the long-chain PFCA explained about half of their total excretion. Overall, differences in elimination kinetics appear to be determined by several different renal and gastrointestinal factors (fraction unbound in plasma, binding affinity to organic anion transporters, fecal loss).

Variability of the kinetic data in case of the short-chain and "alternative" PFAS was investigated in a follow-up study with 12 volunteers (6 men and women each, age 23–52 years) over 105 days. Results in general confirmed those of the pilot investigation. Details will be presented during the conference.

P201

Internal Exposure of Vegans, Omnivores and Strict Raw Food Eaters to Furfuryl Alcohol by Urinary Excretion of a Specific Mercapturic Acid

C. Goerdeler¹, T. Henning¹, C. Weikert¹, K. Abraham¹, B. H. Monien¹

¹German Federal Institute for Risk Assessment (BfR), Food and Feed Safety in the Food Chain, Berlin, Germany

Introduction: Furfuryl alcohol (FFA) is a heat-induced food contaminant formed by degradation of sugars, occurring in many different foods with highest levels in coffee. Based on the increased incidence of renal tubular neoplasms in male mice and increased nasal neoplasms in male rats in 2-year inhalation studies, the International Agency for Research on Cancer (IARC) has classified FFA as possibly carcinogenic to humans. As data on FFA contents in foods are scarce and insufficient for estimating external exposure, we developed a method for the quantification of a mercapturic acid (*N*-acetyl-S-[2-methylfuran]-L-Cys, FFAMA) in urine samples as a biomarker to assess FFA internal exposure.

Objectives: Urinary FFAMA excretion was determined in participants of the Risks and Benefits of a Vegan Diet (RBVD) study and in raw food eaters to examine (1) the influence of diet (omnivore, vegan, raw-food) on internal exposure, and (2) temporal changes in exposure between 2017 and 2021 in vegan and omnivore study participants.

Methods: 24 h urine samples were collected from non-smoking adults (29 omnivores, 31 vegans, 14 raw-food eaters) and smoking adults (7 omnivores, 5 vegans). Urinary FFAMA levels were quantified by liquid chromatography-tandem mass spectrometry (LC-MS/MS).

Results: The FFAMA excretion of non-smoking omnivores (median 13.5, IQR: 7.40 – 23.5 µg/d) was significantly higher compared to those of non-smoking vegans (5.7, IQR: 2.12 – 16.6 µg/d; *p* = 0.032) and of strict raw-food eaters (median 1.42, IQR: 0.85 – 2.09 µg/d; *p* < 0.001). The FFAMA excretion of smoking omnivores (4.74, IQR: 4.64 – 16.4 µg/d) and vegans (11.9, IQR: 6.39 – 55.4 µg/d) did not differ significantly from their non-smoking counterparts. There was no difference observed between the urinary FFAMA excretion in 2017 and in 2021.

Conclusions: The nearly 90% lower median FFA exposure of raw-food eaters compared with omnivores indicated that diet containing heat-treated foodstuffs is the major exposure source. Additional background exposure may originate from inhalation (house dust, industrial emissions). Slightly higher exposure levels in omnivores compared with vegans suggest a yet unidentified dietary factor influencing FFA intake. The comparison of the time points indicated no change in FFA exposure during the study period.

P202

Antibodies raised against fentanyl as antidotes against Carfentanil

A. Breit¹, F. Endt¹, D. Steinritz², N. Amend², T. Gudermann^{1,2}

¹Ludwig-Maximilians-University Munich, Walther-Straub-Institute of Pharmacology and Toxicology, Munich, Germany

²Bundeswehr Institute of Pharmacology and Toxicology, Munich, Germany

The ultra-potent synthetic opioid carfentanil (CAR) acts lethally by potently activating μ opioid receptors (μ OR). Treatment based on competitive antagonists is of limited use due to the ultra-high affinity of the CAR/ μ OR complex. Thus, preventing formation of this complex by CAR neutralizing antibodies might be a promising alternative strategy. We tested nine antibodies raised against fentanyl (ab-FEN) in receptor-ligand binding and receptor activation assays using μ OR expressing HEK293 cells in the presence of FEN or CAR. When high antibody concentrations were pre-incubated with opioids, seven ab-FEN significantly inhibited FEN binding to the μ OR completely and four CAR binding up to 90 %. None of the tested antibodies affected remifentanyl, morphine or endomorphine-1. Concentration-response curves revealed IC50-values of ab-FEN between 25 and 74 nM against FEN and between 121 and 900 nM against CAR. Of note, hill-slopes against FEN were way above one (2.7 to 6.0), indicating extremely high positive cooperativity of ab-FEN, which was not observed against CAR. Furthermore, low antibody concentrations (1.0 nM) enhanced FEN- and to a lesser extent CAR-induced μ OR activation, indicating bi-functional actions of ab-FEN. Moreover, when lethal CAR concentrations were first added to cells, ab-FEN also disrupted the μ OR/CAR complex with CAR still being present. Overall, ab-FEN could prevent and reverse CAR intoxications *in vivo* and opioid efficacy enhancing effects at low ab-FEN concentrations point to a new application of these antibodies as enhancer of an opioid-based pain therapy. Our data might pave the way for future antibody development and refinement.

P203

Influence of oxidants and uremic toxins on viability, DNA integrity, and epithelial function of proximal renal tubule cells

M. Eichhorn¹

¹Heinrich Heine University Düsseldorf, Institute of Toxicology, Düsseldorf, Germany

Question: Accumulation of uremic toxins and the accompanying oxidative stress within the kidney is often associated with acute kidney injury, which can further progress to chronic kidney disease. Proximal tubule cells are particularly vulnerable to such stressors due to their high transport activity and, thus, their high exposure to harmful substances. The aim of this study was to conduct *in vitro*-investigations of the cytotoxic, genotoxic and barrier effects of four selected substances - methylglyoxal (MGO), indoxyl sulfate (IS), tert-butylhydroquinone (tBHQ) and menadione - in human (HK-2) and porcine (LLC-PK1) proximal tubule cells.

Methods: HK-2 and LLC-PK1 cells were exposed for up to 24 h to the above-mentioned substances. Viability was determined using the MTT assay after 4 h and 24 h. Based on cell viability data, concentration ranges for further experiments were determined. Genotoxicity was examined using the alkaline comet assay. Trans epithelial electrical resistance (TEER) as an indicator of epithelial integrity of LLC-PK1 cell monolayers was measured for every 24 h up to 72 h after treatment.

Results: HK2 and LLC-PK1 showed different sensitivities to the tested compounds. In the MTT assay, three of the four substances demonstrated clear concentration-dependent effects, with HK-2 cells exhibiting higher susceptibility. While tBHQ and menadione showed an induction of DNA damage in the comet assay in both cell lines, in LLC-PK1 cells MGO was genotoxic after 24 h. No genotoxic effects were detected for IS in either cell line. tBHQ, MGO and menadione led to an increase of TEER values in lower concentrations, while loss of epithelial integrity occurred in higher concentrations and longer exposure duration.

Conclusion: This study provides data for the toxicological evaluation of selected oxidative and uremic substances in two *in vitro* proximal tubule models. Menadione emerged as the most potent inducer of cytotoxicity and DNA damage, while other compounds mainly caused sub-lethal oxidative stress. TEER data complemented viability- and DNA damage-related endpoints by reflecting functional impairment exerted by the substances. The observed differences between HK-2 and LLC-PK1 indicate cell line and species-specific variations in metabolic capacity or uptake mechanisms.

P204

Genotoxicity testing of 2-chloroethanol and chloroacetaldehyde

B. Bauer¹, S. Wang¹, K. Klai¹, Z. Albrecht¹, H. Hintzsche¹

¹University of Bonn, Bonn, Germany

In recent years, the European Union has experienced an increasing number of food recalls linked to ethylene oxide residues found in sesame seeds, spices or food additives. In some non-EU countries, ethylene oxide is employed as a fumigant to enhance food hygiene. Ethylene oxide, classified as a carcinogen without a threshold limit, rapidly degrades to 2-chloroethanol, which is primarily detectable in treated food. Subsequently, 2-chloroethanol is metabolised into

chloroacetaldehyde. Most existing genotoxicity data for both compounds are derived from studies using outdated methods, therefore complicating risk assessment.

This study aims to address the knowledge gap regarding the genotoxic potential of 2-chloroethanol and its metabolite chloroacetaldehyde. Human cell lines HeLa and HepG2 were exposed to these substances for 4 and 24 h. The MTT test determined non-cytotoxic concentrations for further genotoxicity testing. The potential for aneugenic and clastogenic effects, as well as induction of DNA strand breaks, was evaluated using the micronucleus test and the comet assay, respectively.

2-Chloroethanol exhibited cytotoxicity only at extremely high concentrations (≥ 80 mM). Signs of genotoxicity, indicated by a concentration-dependent increase in micronuclei and DNA strand breaks, were only observed at a concentration of 100 mM. Conversely, chloroacetaldehyde demonstrated comparable cytotoxicity at approximately 1000-fold lower concentrations compared to 2-chloroethanol. Results concerning the genotoxicity of chloroacetaldehyde, along with mutagenicity assessment via the Ames test for both substances, will also be discussed. Based on these *in vitro* genotoxicity findings, there is no evidence to classify 2-chloroethanol as genotoxic in terms of DNA strand breaks or chromosome damage.

P205

Investigation of Endothelial Stress Response to Anthracyclines and Selected Pharmacological Inhibitors

K. K. Calisan¹, L. Meßling¹, G. Fritz¹

¹Heinrich Heine University Düsseldorf, Institute of Toxicology, Düsseldorf, Germany

Recent advances in cancer therapy have markedly improved patient survival, yet the incidence and severeness of treatment-related acute and chronic adverse effects (AE) remains a major clinical problem. Anthracycline-induced cardiotoxicity is a clinically highly relevant AE, which limits the applicable dose of doxorubicin (DOX) in the treatment of solid tumors (e.g. breast cancer), leukemias, and lymphomas. Due to their barrier function endothelial cells are exposed to the highest concentration of *i.v.* applied substances. Hence, we hypothesize that these cells play an important role in the pathophysiology of DOX-induced cardiac damage. Possible strategies to mitigate endothelial toxicity include the use of protective agents that counteract distinct modes of action of DOX, notably dextrazoxane (DEZ) and ICRF-193. Moreover, modulators that might influence the endothelial response, such as olaparib (OLA) and entinostat (EST), were investigated additionally.

To analyze these approaches, human umbilical vein endothelial cells (HUVEC) were treated with DOX alone or in combination with the mentioned pharmacological modulators. Cellular viability was quantified using the Alamar Blue Assay. Cell-cycle effects were assessed by flow cytometry and measuring EdU incorporation. DNA damage formation and DNA damage response (DDR) were evaluated by immunofluorescence staining of nuclear γ H2AX and 53BP1 foci and by Western blot analysis, respectively.

DOX induced a concentration- and time-dependent cytotoxicity as anticipated. Even at low (*i.e.* sublethal) concentrations, DOX triggered S/G2-phase arrest and caused the formation of γ H2AX/53BP1 foci, along with increased expression of DDR-related markers. In contrast, DEZ, ICRF-193 and OLA exhibited low toxicity at the concentrations used, whereas EST caused concentration-dependent cytotoxic effects, including G1 arrest and DDR marker induction. Combination treatments showed that DEZ and ICRF-193 exerted significant cytoprotective effects as reflected by a reduction of DOX-induced loss of viability, DDR activation, and DNA damage formation. Conversely, DOX+OLA showed additive toxicity, while EST enhanced DOX-induced toxicity synergistically across all assays.

These findings highlight DEZ and ICRF-193 as promising drug candidates for mitigating endothelial injury and cardiac damage during DOX-based anticancer therapy, while OLA and EST may exacerbate DOX-induced cardiotoxicity.

P206

Methylmercury and the Placenta: Targeting Copper and Iron Transfer and Redox Balance

M. Jelinek¹, D. Pellowski^{2,3}, M. Maeres^{2,3}, J. Bornhorst^{1,3}, V. Michaelis¹

¹University of Wuppertal, Food Chemistry with the Focus on Toxicology, Wuppertal, Germany

²University of Potsdam, Department of Food Chemistry, Potsdam, Germany

³Trace Age DFG Research Unit 2558, Interactions of Essential Trace Elements in Healthy and Diseased Elderly, Potsdam-Berlin-Jena-Wuppertal, Germany

Mercury (Hg) enters the environment through natural and anthropogenic sources and accumulates in the aquatic habitat as methyl mercury (MeHg) due to sulfate-reducing bacteria. This leads to biomagnification and bioaccumulation in the food chain making MeHg exposure a present scenario for humans. Especially pregnant women and their developing fetus are at risk as it has been established that MeHg can cross placental membranes leading to impaired fetal (neuro)development. However comprehensive mechanisms regarding MeHg-induced toxicity and its impact on essential copper (Cu) and iron (Fe) homeostasis in placental trophoblasts – the critical cell type responsible for mediating nutrient transfer from mother to child, has hardly been elucidated.

To investigate MeHg-induced changes in Cu and Fe transfer across the trophoblast layer of the placental barrier the BeWo 30 *in vitro* Transwell model was utilized. MeHg chloride was applied 1 h after Cu or Fe treatment,

respectively. Samples were taken after 6 and 24 h from both compartments and transferred metal amounts quantified using ICP-MS/MS. Furthermore, redox balance-associated endpoints like the formation of reactive oxygen and nitrogen species (RONS) and glutathione levels (GSH) were assessed using *in vitro* dye assays or liquid chromatography coupled to tandem mass spectrometry.

First data indicates a slight impact of Cu on Hg transfer, while physiological MeHg concentrations were resulting in decreased Cu and Fe transfer to the fetal side of the barrier model. Combining MeHg with either Cu or Fe lead to RONS formation 2 h after treatment, partly supported by altered reduced and oxidized GSH levels. Interestingly, MeHg alone only decreased GSH/GSSG ratio without further evidence of RONS formation.

This study clearly demonstrated MeHg's impact on Cu and Fe transfer across the trophoblast layer potentially driven by oxidative stress mechanisms. As fetal development can already be impaired by MeHg concentrations that cause no symptoms in the pregnant women, a mechanistic understanding of MeHg-induced toxicity at the placental barrier, including its interference with essential trace element homeostasis is essential to refine Hg risk characterization during pregnancy.

P208

Cobalt- and Nickel-induced toxicity in neuronal cells

E. Gerisch¹, C. Büsse¹, A. Thiel¹, B. Witt¹, T. Schwerdtle^{3,4}, J. Bornhorst^{1,4}

¹University of Wuppertal, Food Chemistry with focus on Toxicology, Wuppertal, Germany

²University of Kaiserslautern-Landau (RPTU), Food Chemistry and Toxicology, Kaiserslautern, Germany

³Max Rubner-Institut (MRI), Karlsruhe, Germany

⁴Trace Age DFG Research Unit 2558, Interactions of Essential Trace Elements in Healthy and Diseased Elderly, Potsdam-Berlin-Jena-Wuppertal, Germany

Cobalt (Co) and nickel (Ni) are transition metals used in industrial applications including battery production, metal alloys, and catalysts. Due to the ongoing technological development and growing demand for electric mobility, the environmental concentrations of Co and Ni are rising. This accumulation leads to elevated concentrations of Ni and Co in soil, food, and drinking water resulting in a higher human exposure. Both metals are known to cause adverse effects after chronic exposure at higher doses, and there is growing evidence suggesting that they may also exert neurotoxic properties as they may cross the blood-brain-barrier. Since Ni and Co often occur together in industrial applications and thus in the environment, simultaneous exposure is a realistic scenario. However, there is currently little knowledge about the combined toxic effect of both metals on the neuronal system.

To study these neurotoxic effects, the human cell line LUHMES (Lund Human Mesencephalic) is used. LUHMES cells acquire the ability to proliferate but can be differentiated to dopaminergic-like neurons with a developed neuronal network, providing a valuable *in-vitro* model for investigating neurotoxicity.

The incubation of LUHMES cells was performed with Co(II) and Ni(II) individually and in combination for 24 h as well as for 48 h. After 24 h of incubation, a reduced metabolic activity and cell structure indicated a neurotoxic potential of single and combined metal exposure. These effects will be further investigated after 48 h applying various cytotoxicity assays like Hoechst, Resazurin, Calcein-AM and CellTiter-Glo. The bioavailability of the metals in LUHMES cells after individual and combined Co(II) and Ni(II) exposure will be quantified using Inductively Coupled Plasma Mass Spectrometry (ICP-MS). Also, initial findings using the Calcein-AM assay suggest a potential disruption of neurite integrity in LUHMES cells following Co(II) and Ni(II) exposure. To further investigate these findings, β III-tubulin immunostaining is used to assess neurite structure and integrity.

P209

Gadolinium in the brain: A close look at cellular toxicity

L. Pusch¹, V. Michaelis¹, A. Jeibmann^{2,3}, U. Karst⁴, H. Richter², J. Bornhorst¹

¹University of Wuppertal, Food Chemistry with Focus on Toxicology, Wuppertal, Germany

²Vetsuisse Faculty, University of Zurich, Diagnostic Imaging Research Unit (DIRU), Clinic for Diagnostic Imaging, Zurich, Switzerland

³University of Münster, Clinic of Radiology, Münster, Germany

⁴University of Münster, Institute of Inorganic and Analytical Chemistry, Münster, Germany

Gadolinium (Gd) is a lanthanide used in clinics for magnetic resonance imaging (MRI) as a contrast agent, because of its paramagnetic characteristics. There are two different types of Gadolinium-based contrast agents (GBCAs), which have been applied so far: linear GBCAs and macrocyclic GBCAs. Due to their chemical structure, it is known that linear GBCAs release more Gd³⁺ in the body, because of their lower stability than macrocyclic GBCAs. Since GBCAs are eliminated by the kidneys in the human body, the kidneys are a target of Gd³⁺-induced toxicity. Furthermore, studies have shown an association between the administration of linear GBCA and the onset of nephrogenic systemic fibrosis (NSF), particularly in patients suffering from kidney failure. Because of that, the approval of most linear GBCAs is suspended nowadays. In addition to the kidneys, Gd accumulation was also observed in the brain, after multiple injections of GBCA. However, it is still unknown how GBCAs enter the brain and what effects they exert on its cellular structures.

To investigate the cytotoxicity of GBCAs in the brain, the astrocytoma cell line CCF-STTG1 was utilized, since they are the most abundant cell type in the brain and part of the blood-brain-barrier. CCF-STTG1 cells will be incubated for 24 h with concentrations ranging from 0–1000 μ M and 10 mM of three linear and three macrocyclic GBCAs covering physiological and accumulation scenarios.

Cytotoxicity will be investigated by using the cytotoxicity assays Hoechst and Resazurin, which determine indirect cell count and the cellular viability by means of metabolic activity.

P210

Fluoride intake in Europe: Estimation of total daily intake and correlation to equivalent doses in epidemiological studies

S. Scheffler¹, F. Partosch², A. Zwintscher¹, A. Bitsch¹

¹Fraunhofer Institute for Toxicology and Experimental Medicine (ITEM), Hanover, Germany

²Ramboll Deutschland GmbH, Hamburg, Germany

Fluoride exposure and its potential health effects remain a topic of ongoing scientific debates. Recent reports from Health Canada and the National Toxicology Program conclude with moderate confidence that fluoride exposure at drinking water concentrations above 1.5 mg/L is associated with lower IQ in children. In European countries, drinking water levels are generally below 0.3-mg/L fluoride but populations are still chronically exposed through other sources, including fluoridated salt (voluntary or regulated), fluoridated toothpaste, and fluoride-rich foods such as fish and black tea. Consequently, total daily intake in Europe may approach or exceed exposure levels associated with adverse effects in recent reports. However, epidemiological data concerning fluoride-related health effects in Europe are limited. Therefore, it would be beneficial to consider existing studies from non-EU countries to transfer observed effects to the exposure situation in Europe. Additionally, animal data could also deliver supporting information, if equivalent doses could be calculated. In this work, we present a methodology to estimate daily fluoride intake and excretion in Europe as well as correlated exposure levels in animal and epidemiological studies.

P211

From field to cup: risk assessment regarding the presence of *Convolvulus arvensis* L. in herbal teas and food supplements

A. C. Manolica¹, G. I. Badea², A. Trifan³, M. O. Popa¹

¹National Institute of Research and Development for Biological Sciences,

"Stejarul" Research Centre for Biological Sciences Piatra Neamt subsidiary, Bucharest, Romania

²National Institute of Research and Development for Biological Sciences, Centre of Bioanalysis, Bucharest, Romania

³Grigore T. Popa University of Medicine and Pharmacy, Department of Pharmacognosy-Phytotherapy, Iasi, Romania

Question: *Convolvulus arvensis* L. (field bindweed) has a history of traditional medicinal use, but it is also a problematic contaminant in crops that can end up in food and feed products. Products containing *C. arvensis* are sold in Europe, claiming to support various health issues. Conversely, earlier studies identified *C. arvensis* as a common undeclared contaminant in marketed herbal teas and food supplements. Nonetheless, concerns about its safe use remain, as *C. arvensis* contains tropane alkaloids (TAs), toxic natural compounds that may pose health risks even at low levels.

Methods: In our study, we evaluate, based on available published data, the possible health risks associated with the consumption of herbal teas and food supplements containing *C. arvensis* as an intended ingredient or as a natural contaminant.

Results: The available toxicological data from observational and animal studies indicate that some *C. arvensis* bioactives (e.g., tropane alkaloids, resin, saponins) may cause acute, sub-chronic, genotoxic, and reproductive toxicities. Observational and experimental *in vivo* studies report that ingestion of *C. arvensis* by rodents or livestock can lead to gastrointestinal irritation, progressive weakness, and, in severe cases, death. Controlled feeding studies in mice showed a dose-dependent increase in illness. Post-mortem examinations revealed intestinal fibrosis and vascular sclerosis of the small intestine in horses exposed to long-term ingestion of *C. arvensis*.

Conclusions: Significant uncertainties still exist regarding the human risk linked to consuming products containing *C. arvensis*, due to the current lack of data on the occurrence and concentrations of toxic tropane alkaloids in its derived preparations. Furthermore, the absence of controlled human toxicological studies emphasizes the need for caution when using *C. arvensis* for therapeutic or supplement purposes. *In vivo* and clinical research are essential to establish its safety levels and to clarify dose-response relationships relevant to human health.

Acknowledgment. This work is performed through the Core Program within the National Research, Development, and Innovation Plan 2022–2027, carried out with the support of MRID, project no. 23020301, and contract no. 7N/2023. This work was supported by a grant of the Ministry of Research, Innovation and Digitization, CNCS-UEFISCDI, project number 21TE/03.02.2025, within PNCDI IV.

P212

Ecotoxicity of selected β -Lactam Antibiotics on *C. elegans*

O. Krings¹, F. Glahn¹

¹Martin Luther University Halle-Wittenberg, Institute of Environmental Toxicology, Halle (Saale), Germany

Antibiotics are a class of pharmaceuticals used in large amounts in human medicine all over the world. Many antibiotics (AB) leave the body still in a biologically active form. Thus, hospitals emit considerable amounts of AB into the wastewater systems. Classic "three-stage" wastewater treatment plants fail to remove many AB, thus leading to residues in surface- and groundwater. Unfortunately, such traces of AB lead to development of multi-resistant bacteria

and can also affect non-target organisms. As some β -lactam antibiotics, like Ampicillin (AMP) and Piperacillin (PIP) are often applied together with beta-lactamase-inhibitors (Sulbactam (SUL) and Tazobactam (TAZ), respectively) to increase their efficiency we conducted toxicity tests with these substances as single agents or in combination on the model organism *C. elegans*.

For acute toxicity testing *C. elegans* was cultured in Nematode Growth Medium (NGM) with different concentrations of AMP, PIP, SUL and TAZ and *E. coli* inactivated by Paraformaldehyde.

Treatment of *C. elegans* with SUL (0.05 to 1 mM) for 24 h or 0.05 to 0.5 mM for 48 h did not have toxic effects on the worms. Also, AMP and SUL in combination (1 mM and 0.5 mM) were not toxic after up to 48 h. TAZ (0.05 to 1 mM) for 24 h or 0.05 to 0.5 mM for 48 h did not exert toxicity on *C. elegans*, as well. We also treated *C. elegans* with PIP (0.05 to 1 mM) for up to 48 h, alone or in combination with TAZ (0.00625 to 0.125 mM), but we could not find toxic effects in these experiments as well.

The investigated AB and beta-lactamase-inhibitors did not have acute toxic effects on *C. elegans* in concentration much higher than those present in the environment. Nevertheless, we will look further into possible long-term effects of the compounds investigated and other commonly used AB on *C. elegans* and other model organisms. Moreover, we will analyze the eco-toxicological effects of degradation products occurring during treatment of aqueous solutions of AB in experimental settings simulating a fourth purification stage of wastewater treatment.

Pharmacokinetics and PK/PD modelling

P213

Implementing Therapeutic Drug Monitoring for Venetoclax: Analytical Validation and Clinical Feasibility

A. Dreber¹, T. Hube¹, S. Twarock¹

¹Institut für Translationale Pharmakologie, Düsseldorf, Germany

Venetoclax, a selective BCL-2 inhibitor, has emerged as an important therapeutic option in hematologic malignancies, including acute myeloid leukemia (AML) and chronic lymphocytic leukemia (CLL). Despite its broad clinical use, considerable interpatient variability in pharmacokinetics has been observed. Contributing factors include drug–drug interactions, plasma protein binding, and dietary influences such as high-fat meals prior to administration. In clinical practice, however, these aspects have not been systematically examined or consistently controlled. Consequently, the clinical implications of venetoclax variability remain insufficiently defined, particularly in the context of allogeneic stem cell transplantation, where altered pharmacokinetics could directly affect treatment efficacy and patient safety.

To address this gap, we analyzed venetoclax plasma levels in samples from hematologic patients under routine clinical care to characterize pharmacokinetic variability and assess the practical feasibility of therapeutic drug monitoring (TDM) implementation. Using high-performance liquid chromatography with diode-array detection (HPLC-DAD), we were able to reliably measure venetoclax plasma levels, supporting its suitability for routine venetoclax TDM.

Moreover, we observed pronounced interpatient variability, highlighting the potential benefits of systematic exposure assessment. Building on these findings, we plan to evaluate whether pharmacokinetic differences are associated with clinical endpoints, including the effectiveness of engraftment and overall survival in transplant recipients.

With our study we aim to further clarify the clinical relevance of venetoclax exposure and support the rationale for implementing TDM in future practice to improve patient safety and ensure effective antineoplastic therapy.

P214

Population Pharmacokinetic Analysis of Ampicillin in Automated Peritoneal Dialysis

H. Huang¹, M. Taubert¹, Z. Chen¹, M. Bilal¹, P. Pichler², W. Poeppel³, H. Burgmann⁴, M. Zeitlinger⁵, G. Reznicek⁶, U. Fuhr⁷, M. Wiesholzer^{2,7,8}, D. Tüchler^{2,7,8,9}

¹University of Cologne, Department I of Pharmacology, Cologne, Germany

²UK St. Pölten, Department of Internal Medicine 1, St. Pölten, Austria

³Austrian Armed Forces, Department of Dermatology and Tropical Medicine, Vienna, Austria

⁴Medical University of Vienna, Internal Medicine I, Vienna, Austria

⁵Medical University of Vienna, Department of Clinical Pharmacology, Vienna, Austria

⁶University of Vienna, Department of Pharmaceutical Sciences, Vienna, Austria

⁷Karl Landsteiner Institute for Nephrology and Hematooncology, St. Pölten, Austria

⁸Karl Landsteiner University of Health Sciences, Krems an der Donau, Austria

⁹Medical University of Vienna, Center for Pathophysiology, Vienna, Austria

Question: Automated peritoneal dialysis (APD) is a home therapy option for patients with end-stage kidney disease. Bacterial peritonitis is a common and serious complication of APD, requiring antibacterial treatment. Ampicillin is considered the first-line treatment for peritonitis caused by *Listeria monocytogenes*, and is appropriate for targeted treatment after susceptibility testing. However, data on pharmacokinetics (PK) of ampicillin in APD patients are

scarce. Therefore, such data is urgently needed for pharmacokinetics-based drug therapy and dosage recommendations.

Methods: A cross-over PK study with dense sampling was conducted in six APD patients without peritonitis. Single doses of ampicillin were administered intraperitoneally (IP) or intravenously (IV) at the start of the long dwell (15 h, lodextrin), followed by a 9-hour APD treatment consisting of 6 short cycles (Glucose).

Population PK analysis was performed using nonlinear mixed-effects modeling (NONMEM, version 7.5.1), followed by Monte Carlo simulations to assess the probability of achieving ampicillin concentrations above minimum inhibitory concentrations (MICs) of 2 and 8 mg/L for at least 50% of the dosing interval (fT-MIC $\geq 50\%$). A fixed protein binding of 28% for ampicillin in plasma was applied. Separate simulations were performed for patients with peritonitis assuming arbitrarily 3-fold and 10-fold increase in transfer rates between plasma and peritoneal fluid.

Results: A total of 371 ampicillin concentrations (plasma, dialysate fluid, and urine) were available for population PK model development. A two-compartment model for plasma concentrations and a one-compartment model for dialysate concentrations with transit compartments for mutual transfer described the data best. Parameter estimates of the final model, along with 95% confidence intervals from bootstrap results, are given in Table 1. The accumulation of ampicillin was less than 1.2-fold in plasma and peritoneal dialysate fluid. Based on simulations, daily doses of 500 mg (1.5 g) IV or 250 mg (1 g) IP were predicted to achieve a target MIC of 2 mg/L (8 mg/L) in both plasma and dialysate, irrespective of the presence of peritonitis (Figure 1).

Conclusions: Our results provide the pharmacokinetic/pharmacodynamic rationale for ampicillin dosing in APD patients, suggesting that an IV dose of 1.5 g or an IP dose of 1 g daily is sufficient to treat peritoneal dialysis-related peritonitis with an MIC of up to 8 mg/L.

Fig. 1

Table 1 Ampicillin parameter estimates of the final model

Parameter description	Parameter abbreviation and unit	Estimates	RSE (%)	Bootstrap (n=100)	Median	95% CI
Clearance	CL (L/h)	1.80	5.80	1.50	1.50 (1.37)	
Central volume of distribution (plasma)	V _c (L)	4.88	30.1	4.88	2.44 (2.46)	
Inter-compartmental clearance	Q (L/h)	9.13	28.6	8.98	5.14 (5.12)	
Peripheral volume of distribution (plasma)	V _p (L)	12.3	16.7	12.0	8.16 (8.15)	
Fraction of IP dose absorbed	Fraction	0.786	2.86	0.779	0.743 (0.69)	
Initial residual volume of dialysis compartment	V _{DI} (L)	0.111	16.7	0.105	0.102 (0.79)	
Inter-compartmental clearance from plasma to dialysate fluid through blood compartment	CL _{pl} (L/h)	0.357	9.06	0.358	0.360 (0.362)	
Volume of blood compartment from plasma to dialysate fluid	V _b (L)	0.282	16.4	0.177	0.186 (0.285)	
Renal clearance	CL _R (L/h)	0.244	17.9	0.237	0.177 (0.285)	
Fraction of released dialysate that contributes to the volume of dialysate	SHARC (dwell)	0.543	7.25	0.533	0.438 (0.628)	
Inter-compartmental clearance from dialysate back to plasma through blood compartment	CL _{pl} (L/h)	0.380	9.04	0.381	0.314 (0.448)	
Volume of blood compartment from dialysate back to plasma	V _b (L)	0.341	16.4	0.196	0.203 (0.401)	
Inter-individual variability (CV, %)						
CL		11.2	17.0 (8)	12.0	7.86 (5.6)	
V _c		62.9	40.5 (30)	35.0	4.75 (46.7)	
Q		72.9	31.2 (20)	71.6	38.6 (35.5)	
V _p		38.8	30.0 (20)	37.6	23.1 (45.4)	
V _{DI}		36.9	36.4 (25)	35.3	12.0 (44.2)	
CL _{pl}		36.6	34.7 (19)	36.7	15.5 (31.4)	
CL _R		16.8	21.6 (8)	16.4	6.62 (26.4)	
Q _{pl}		21	35.5 (2)	20.6	6.66 (23.9)	
V _b		34.3	40.0 (25)	27.1	7.16 (32.2)	
Residual variability (SD)						
Proportional error (plasma)		0.125	6.34	0.115	0.0881 (0.143)	
Proportional error (dialysate)		0.122	6.36	0.108	0.101 (0.146)	
Additive error (dialysate)		0.86	15.4	1.03	0.913 (1.33)	
Proportional error (urine)		0.262	26.3	0.201	0.0901 (0.444)	

* RSE is reported as CV%. RSE: relative standard error; CI: confidence interval; BV: inter-individual variability; SD: standard deviation; SHARC: Shrinkage.

Fig. 2

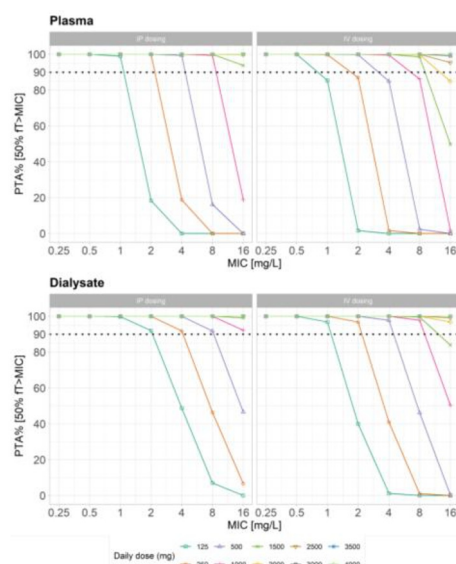


Figure 1 Probability of target attainment (PTA) in plasma (top) and dialysate (bottom) after intraperitoneal (left) and intravenous (right) infusion of ampicillin in patients without peritonitis on day 8 (following multiple once daily doses) for different doses and minimum inhibitory concentrations (MICs)

P215

Pharmacokinetics of herbal medicinal products: casticin-3'-glucuronide in healthy volunteers after oral administration of *Vitex agnus-castus* BNO 1095
A. Neumann¹, D. Fitz¹, B. Nausch², M. Soeberdt², C. Abels²

¹Bionorica research GmbH, Bioanalytics, Innsbruck, Austria

²Bionorica SE, Research & Development, Neumarkt i.d.OPf., Germany

Vitex agnus-castus L. (VAC), *fructus* is a well-known drug with traditional and well-established use registration for the treatment of premenstrual syndrome, irregular menstruation and mastodynia [1], but its pharmacokinetics have not been studied in humans so far, and animal data are scarce. Using a high-resolution LC-ToF-MS screening, we detected casticin-3'-glucuronide in rat plasma after oral administration of *Vitex agnus-castus* BNO 1095 (dry extract of VAC *fructus*). Because it was one of the most intense signals, this phase II metabolite of casticin – a flavone, which is a major constituent of VAC [2] – was selected as marker to study pharmacokinetics of VAC in human subjects. In a single center, open-label phase I clinical trial (EudraCT number 2022-003480-20), healthy volunteers (n = 36; average age 31.4 years, 24 female/12 male) received 80, 40 or 20 mg VAC BNO 1095 on 8 consecutive days. For measurement of plasma concentrations of casticin-3'-glucuronide, we used HPLC-MS/MS following protein precipitation and further sample clean-up using OstroTM plates (Waters). The quantitation method was fully validated according to the ICH M10 guideline. Its result were accurate and precise, and the lower level of quantification (LLOQ) was 0.1 ng/ml. Based on the determined AUC and C_{max} values, casticin-3'-glucuronide exposure is dose proportional, because AUC and C_{max} increased with increasing dose. Beyond reporting the first data regarding pharmacokinetics of VAC in humans, this study also confirmed safety and tolerability of VAC doses even 4x higher than the recommended daily dose of the marketed product Agnucaston® 20 mg.

Conflicts of interest: All authors are employees of Bionorica research GmbH and Bionorica SE, respectively. Bionorica SE is manufacturer of Agnucaston® and Agnucaston® 20 mg.

[1] European Medicines Agency. Assessment report on *Vitex agnus-castus* L., *fructus*. 2018; EMA/HPMC/606741/2018

[2] Hoberg E, Meier B, Sticher O. Quantitative High Performance Liquid Chromatographic Analysis of Casticin in the Fruits of *Vitex agnus-castus*. *Pharmaceut Biol* 2001; 39: 1, 57–61

P216

Pharmacokinetics impossible: characterization of herbal medicinal products by means of pharmacodynamic fingerprints

P. Peterburs¹, B. Nausch¹, M. Soeberdt¹, C. Abels¹

¹Bionorica SE, Research & Development, Neumarkt i.d.OPf., Germany

Herbal medicines have been used for centuries, and medicinal herbs were used as "compound libraries" to identify single, active chemicals. Prominent examples are digoxin/digitoxin from foxglove (*Digitalis lanata/purpurea*), aspirin and its precursor salicin from willow bark (*Salix* spp.), and atropine from deadly nightshade (*Atropa belladonna*). Pharmacology, i.e. pharmacodynamics, toxicity, and pharmacokinetics, of these individual compounds can be characterized quite easily, because, at least somewhat simplified, it is one single substance with one specific target and mechanism of action. In contrast, herbal medicinal plants are multi-substance mixtures ("Vielstoffgemisch"), i.e., they contain several active and inactive compounds, and thus targeting more than one target. In addition, many herbal medicinal products contain even a mixture of several medicinal plants,

further complicating their pharmacology. However, novel techniques offer the possibility to elucidate the complex pharmacology of herbal medicinal products.

Here, we used the BioMAP® Diversity PLUS Platform (Eurofins DiscoverX, MO, USA) to establish a pharmacological fingerprint of several extracts from medicinal plants. The BioMap® Diversity PLUS panel utilizes several primary human cell cultures and coculture systems that were designed to mimic various aspects of the human body to generate a fingerprint of the pharmacological behavior of the test items, based on measurement of 148 clinically relevant biomarkers. Subsequently, this fingerprint can be compared to a library of the fingerprints of over 4500 well-known and already characterized drugs, leading to information about a possible pharmacological "mode of action" of a mixture of multiple components.

Using this method, we identified similarity in the behavior of two of our plant extracts with drugs acting on the endocannabinoid system respectively on retinoic acid receptor-related orphan receptor γ (ROR γ) with possible modulatory effects on Th-cells.

This technique allows for characterizing herbal medicines by means of a pharmacological fingerprint and for elucidating yet unknown mechanisms of action.

Conflicts of interest: All authors are employees of Bionorica SE.

P217

PBPK-WebSim: Open & FAIR Web-Based PBPK Modeling framework from Annotated SBML

V. Kumar^{1,2}, S. Kumar^{1,2}, S. Sharma², D. Deepika^{1,2}

¹German Federal Institute for Risk Assessment (BfR), Pesticide Safety, Berlin, Germany

²Pere Virgili Health Research Institute (IISPV), Tarragona, Spain

Physiologically based pharmacokinetic (PBPK) models are critical for drug development and chemical safety assessment, yet their accessibility and reproducibility remain limited by siloed, platform dependent-implementations. PBPK-WebSim introduces a transformative solution for the field: SBML encoded PBPK models—richly annotated with the Physiologically Based Pharmacokinetics Ontology (PBPKO)—can now be compiled into browser-native WebAssembly (WASM) executables, boosting transparency and democratizing access. Powered by the high-performance Rust library "diffsol," which implements Backward Differentiation Formula (BDF) and Singly Diagonally Implicit Runge-Kutta (SDIRK) methods ideal for stiff ODE systems, PBPK-WebSim achieves simulation speed near that of native code, all without external dependencies.

Enriching SBML files with PBPKO makes model metadata machine-readable, advancing interoperability, validation, and comparative analysis. End users enjoy interactive parameter controls and real-time visualizations, hosted as GitHub pages for broad availability. By fusing SBML standardization, semantic annotation, and portable WebAssembly technology, this framework delivers a fully FAIR (Findable, Accessible, Interoperable, Reusable) modeling environment. PBPK-WebSim thereby streamlines collaborative research, education, and regulatory science, facilitating reproducible pharmacokinetics analytics and accelerating model translation into real-world applications

P218

Isolated Perfused Porcine Kidney as a Tool to Study Renal Elimination of Highly Protein Bound Drugs

Z. Jiang¹, P. J. Ottens², T. Heinen¹, D. J. Touw³, L. Beljaars^{2,4}, J. Stevens³, R. Posma², M. Taubert¹, H. G. D. Leuvenink², U. Fuhr¹

¹University of Cologne, Institute of Pharmacology, Cologne, Germany

²University of Groningen, Department of Surgery - Organ Donation and Transplantation, Groningen, Netherlands

³University of Groningen, Department of Clinical Pharmacy and Pharmacology, Groningen, Netherlands

⁴Reno-NL, Groningen, Netherlands

⁵University Medical Center Groningen, Department of Critical Care, Groningen, Netherlands

Background

Renal clearance of highly protein bound drugs may exceed plasma flow when calculated from the fraction unbound, suggesting that part of the bound drug is eliminated during kidney passage. Understanding the respective mechanisms is critical to assess and predict drug elimination¹. So far a good model to assess these mechanisms is lacking.

Aims

To assess isolated perfused porcine kidney as a tool to quantify and selectively modify the pharmacokinetic processes including protein binding involved in renal elimination of drugs.

Method

Fresh porcine slaughterhouse kidneys were perfused ex-vivo with artificial plasma containing real erythrocytes at 37 °C as described², using constant flow (target mean arterial pressure 75 mmHg). Beyond standard components including

albumin (39.2 g/L) and creatinine (679 μ M), the perfusate contained the GFR markers iohexol (250 mg/L) and iohalamate (45 μ g/L). Flucloxacillin, an antibiotic with high plasma protein binding and extensive renal clearance also by active secretion in humans was used as a model drug. After 1.5 hours of perfusion with urine recirculation, flucloxacillin (150 mg/L [kidney F257], 75 mg/L [F653, F654]) was added to the perfusate, re-circulation was stopped and for 1 hour at 10 min intervals, concentrations of renally eliminated substances were measured in arterial and venous plasma (flucloxacillin: free and total concentrations) and in urine.

Renal clearance for an interval was calculated as the amount of drug recovered in urine over the effective intrarenal plasma concentration, i.e. the geometric mean of arterial and venous concentrations at start and end of the interval. Mean and SD for renal clearance were calculated for intervals with relatively stable conditions at perfusion end ($n=2-4$).

Results

The porcine kidneys were functional to eliminate all marker substances (Fig. 1). Flucloxacillin clearance calculated from total plasma concentrations was up to 3-fold higher than GFR markers, indicating active secretion also in porcine kidney, while flucloxacillin clearance calculated from free concentrations exceeded renal plasma flow 1.5- to 3-fold, implying elimination of bound drug (Table 1).

Conclusion

Isolated perfused porcine kidneys handle marker substances similar to humans and enable quantitative assessment of renal drug elimination under controlled conditions.

References

1. Al-Qassabi J et al. J Pharm Sci, 2024. **113**: 1664-1673.
2. Pool MBF et al. J Surg Res, 2024. **301**: 248-258.

Fig. 1

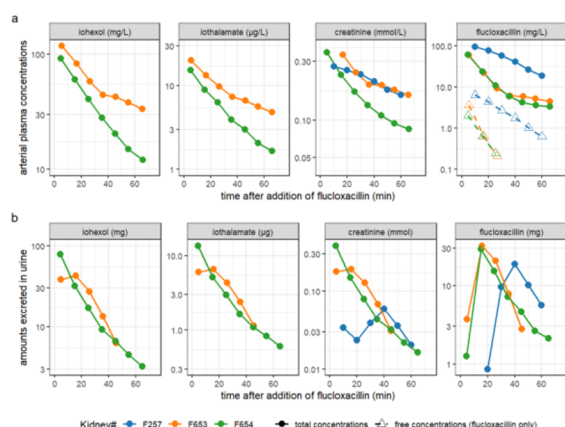


Figure 1. Pharmacokinetic profiles of substances in plasma (a) and urine (b); for urine, points in time reflect the end of respective collection intervals.

Fig. 2

kidn. ID	plasma flow (L/h)	clearance (L/h), mean \pm SD				
		iohexol	iothalamate	creatinine	fluc. (total)	fluc. (free)
F257	23.0 \pm 2.3	not avail.	n.a	1.12 \pm 0.39	1.64 \pm 0.62	39.2 \pm 15.7
F653	48.6 \pm 0.2	1.23 \pm 0.49	1.36 \pm 0.46	1.43 \pm 0.64	4.38 \pm 2.33	177 \pm 94*
F654	66.9 \pm 0.4	1.56 \pm 0.11	1.93 \pm 0.04	1.44 \pm 0.29	4.34 \pm 1.12	176 \pm 46*

Table 1. Calculated renal clearances of each substance. Total or free: calculated based on total or on individually measured / (*) average free plasma concentrations.

P219

Enteric-coated Solid Dosage Forms with Sodium Bicarbonate: Impact of pH Value and Mechanical Stress on Drug Release into the Stomach

S. Schmidt¹, M. Werthschulte², M. Piepenstock², K. Zupanets², J. Breikreutz¹

¹Heinrich Heine University Düsseldorf, Institute of Pharmaceutics and Biopharmaceutics, Düsseldorf, Germany

²Medice Arzneimittel Pütter GmbH & Co. KG, Iserlohn, Germany

INTRODUCTION

Oral sodium bicarbonate (also called sodium hydrogen carbonate) preparations are being used as pH-regulators in metabolic acidosis, which is associated with accelerated progression of chronic kidney disease [1]. As the film-coating composition of Nephrotrans® has been changed in the meantime, the dissolution

testings should be repeated from a previous study [2] and additionally, a recently proposed dissolution setup (Physiolution® Advanced Modular Platform, PL-Wroclaw) should be applied to simulate the mechanical stress on the dosage forms during the GI passage [3].

RESULTS

AND

DISCUSSION

When using the Physiolution apparatus applying mechanical stress by periodic vertical movements of the basket and inflating a balloon inside, both products remained intact and did not show any sodium bicarbonate release (Fig. 1). However, Bicanorm® fully released sodium bicarbonate at pH 4.5 (Fig. 2).

CONCLUSION

Elevated pH values in the stomach have a strong impact on the undesired early sodium bicarbonate release. Whereas Nephrotrans® maintained its resilience against the acidic dissolution media, the enteric coating of Bicanorm® lost its functionality at pH 4.5. The applied mechanical stress shows only minor impact on the dissolution profiles of the two investigated medicinal products.

REFERENCES

1. Di Iorio, B.R., Bellasi A., Raphael K.L. et al., Treatment of metabolic acidosis with sodium bicarbonate delays progression of chronic kidney disease: the UBI Study. J Nephrol, 2019. **32**(6): p. 989-1001.
2. Breikreutz, J., Gan T.G., Schneider B., Kalisch P., Enteric-coated solid dosage forms containing sodium bicarbonate as a drug substance: an exception from the rule? J Pharm Pharmacol, 2007. **59**(1): p. 59-65.
3. Garbacz, G., et al., Bio-relevant dissolution testing of hard capsules prepared from different shell materials using the dynamic open flow through test apparatus. Eur J Pharm Sci, 2014. **57**: p. 264-72.

Figure

Captions

Fig. 1: Drug dissolution of Bicanorm® tablets (closed circles) and Nephrotrans® (open squares) soft capsules using Physiolution® at pH 1.1; $n=6$, mean \pm s, 37 \pm 0.5 °C, closed star: vertical movement, open star: balloon inflation. Fig. 2: Drug dissolution of Bicanorm® tablets (closed circles) and Nephrotrans® (open squares) soft capsules using Physiolution® at pH 4.5; $n=6$, mean \pm s, 37 \pm 0.5 °C, closed star: vertical movement, open star: balloon inflation.

Fig. 1

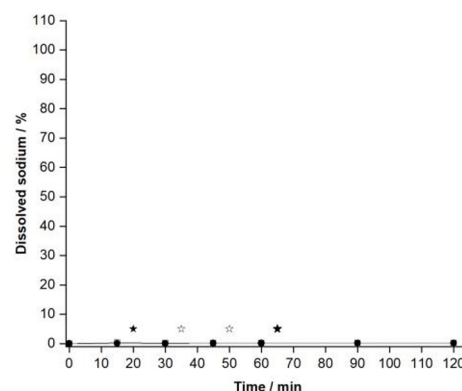
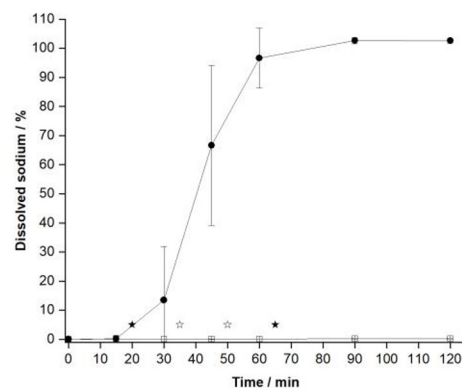


Fig. 2



P221

Leveraging Dynamic Time-Kill In-vitro Modeling and Genomic Approaches to Characterize the Pharmacokinetic/ Pharmacodynamics and Resistance Potential of Cystobactamid

K. Khalid¹, D. Kohnhäuser¹, M. Brönstrup¹, K. Rox¹

¹Helmholtz Center for Infection research, PK/PD, Brunswick, Germany

The long-standing prediction of "10 million deaths by 2050" due to antimicrobial resistance (AMR) highlights its global threat; however, a recent estimate of "three deaths per minute from 2025 to 2050" further underscores its urgency¹. A 2.3-fold rise in deaths attributed to methicillin-resistant *Staphylococcus aureus* (MRSA) over the past three decades exemplifies the urgent need for new antibacterials¹. The para-aminobenzoic acid-based novel drug class cystobactamid, discovered from *Cystobacter velatus* Cbv34 in 2014, exhibits broad-spectrum activity. Through extensive optimization, it has advanced to the lead stage², positioning it as a promising next-generation antibiotic. With proof of concept established³, the next step involves elucidating pharmacokinetic/pharmacodynamic (PK/PD) relationships and assessing resistance potential. Determining the relevant PK/PD index⁴ is critical for optimizing dosing, minimizing resistance, and improving clinical success rates⁵.

A one-compartment in vitro dynamic time-kill model simulating in vivo PK was developed to assess the pharmacodynamic effects of cystobactamid at varying concentrations (0.5–16× MIC) against MRSA ATCC 33591. Bacterial counts (log₁₀ CFU/mL) were plotted over time to derive kill kinetics and enable PK/PD modeling. Initial results at several-fold MIC (q24h) demonstrated effective suppression of bacterial regrowth. Follow-up studies will explore fractionated dosing to identify which PK driver best correlates with the PD effect.

In parallel, adaptive laboratory evolution under static conditions generated resistant mutants to compare with those from dynamic assays. Under static exposure, MICs increased 16-fold. Genomic DNA was sequenced (Illumina), revealing 35 mutated genes, 22 shared across all lineages, indicating strong genetic convergence. Notably, a mutation in *parE*, encoding DNA topoisomerase IV subunit B, was detected along with non-synonymous mutations in genes linked to DNA metabolism and transport.

In summary, this study establishes foundational PK/PD insights for cystobactamids using a dynamic kill model and provides a comparative genomic view of resistance evolution under static versus dynamic conditions.

References

1. Naghavi M. *et al. Lancet* 2024, 404, 1199–1226. 2. Kohnhäuser D. *et al. J. Med. Chem.* 2024, 67, 3. Testolin G. *et al. Chem. Sci.* 2020, 11, 1316–1334. 4. Ambrose P. G. *et al. Clin. Infect. Dis.* 2007, 44, 79–86. 5. Bissanz C. *et al. Antibiotics* 2024, 13.

Pharmacological education

P222

Prescription talks in medical school from the perspective of 5th year medical students in Cologne

R. Göhler¹, J. Matthes²

¹University of Cologne, Medical Faculty, Cologne, Germany

²University of Cologne, Centre of Pharmacology and Student Dean's Office of the Medical Faculty, Cologne, Germany

Objective: In about every second doctor-patient contact, a drug prescription is made. Patient counselling and participation can make a significant contribution to the decision for optimal therapy and its adequate implementation. In addition to (general) pharmacological training, it is thus reasonable to prepare medical students for conducting prescription talks. We are doing so with a simulation-based module. As part of an ongoing study, we are surveying participating students about prescription talks in their medical studies and investigating the learning effects in the simulation module.

Methods: Fifth-year medical students in Cologne can attend a module in small groups in which one student conducts an unprepared prescription talk with an actor. This is observed by fellow students and a teacher and discussed immediately afterwards regarding content and process (15–20 min). Reference is made to a conversation guide, among other things. In a second round, the same student conducts the conversation again as if it were for the first time. The conversations are videotaped and analyzed in terms of content and process using a guideline-based checklist. All students in a semester, including those who do not participate in the module, are invited to answer questions online about the prescription talk per se and in their studies within 4–5 days after the module. When they enter their final practical year, the students will be invited again to answer questions and simulate prescription talks.

Results: From summer 2024 to summer 2025, 335 students took part in the survey, 192 (57%) of whom had participated in the simulation module, including 29 (9%) who had conducted the prescription talks themselves. 108 out of 329 (33%) respondents stated that the topic had already been addressed in other courses. 229 out of 324 (71%) believed that preparation for conducting prescription talks should be intensified in medical studies. 151 out of 155 (97%) stated that this should take place during the clinical study phase at the earliest. However, 36 (23%) could already imagine this happening in the first half of the third year of study, i.e. before completing the course on Basic Pharmacology.

Summary & conclusion: Most of 5th-year medical students in Cologne stated that teaching should be intensified with regard to prescription talks. Only one-third stated that the topic had already been covered during their studies. There is thus a need for the corresponding courses like ours.

Inhalation Toxicology

P223

The inhalation toxicity of 1,3,4,6,7,9,9b-Heptaazaphenylene-2,5,8-triamine (Melem)

M. Negru¹, H. Bauer², M. Lee¹, Q. Li¹, F. A. Grimm¹

¹Clariant Produkte (Deutschland) GmbH, Toxicology, Frankfurt a. M., Germany

²Clariant Plastics and Coatings (Deutschland) GmbH, Frankfurt a. M., Germany

Nitrogen-based flame retardants enhance safety through gas release, heat absorption, and char formation, but require toxicological assessment to ensure safe application. Based on comprehensive high-tier toxicological studies (OECD 408, OECD 422, and OECD 414), Melem demonstrated a No Observed Adverse Effect Level (NOEL) of 1000 mg/kg bw for systemic toxicity, reproductive/developmental toxicity, maternal toxicity, fetal developmental toxicity, and teratogenicity. Despite sharing an aromatic structure like melamine, Melem's physicochemical properties—notably its low water solubility (0.93 mg/L) and partition coefficient (−0.2) contribute to its favorable toxicological profile. These properties establish Melem as a flame retardant with a low order of toxicity. This distinction is particularly significant considering melamine's documented effects on the urinary bladder, where it causes bladder stone formation associated with urinary bladder tumors at doses of 750 mg. Melem, though manufactured as a respirable powder (below 10 µm), becomes immobilized in final products, eliminating consumer inhalation exposure risk. To assess the inhalation toxicity of Melem, we conducted an acute inhalation toxicity study according to OECD test guideline 403 in rats. The study revealed no toxicologically relevant observations at the limit dose of 5.33 mg/L. A subsequent 14-day range-finding study (OECD 412) in Sprague Dawley (n=10/sex) across multiple concentration groups (0.5, 1, and 2 mg/L; 6-hour daily nose-only exposure) demonstrated absence of clinical manifestations, weight alterations, pathological findings, or mortality. Minor pulmonary responses were observed, including non-statistically significant lung weight increases, elevated reactive alveolar macrophage populations in bronchoalveolar lavage (BAL) fluid, and increased lactate dehydrogenase (LDH) levels. A 28-day nose-only inhalation study (6 hours daily at 0.5, 1, and 2 mg/L) showed no treatment-related effects on blood parameters or eye structures in both sexes. After 60 days recovery, pulmonary effects decreased by 60% with fewer reactive macrophages. However, elevated LDH levels and inflammatory responses remained particle concentration-dependent in the alveolar region. Melem's partially reversible pulmonary effects after exposure cessation suggest it's a promising flame retardant with a favorable toxicity profile.

P224

Inflammatory effects of Saharan dust in co-cultures: the role of microbial constituents

L. Boßmann¹, G. Bredeck^{1,2}, A. A. M. Kämpfer¹, I. Masson¹, M. Frentrup³, U. Nübel³, T. Wahle¹, R. P. F. Schins^{1,4}

¹Leibniz Research Institute for Environmental Medicine (IUF), Düsseldorf, Germany

²Centro de Investigaciones Biológicas Margarita Salas (CIB-CSIC), Madrid, Spain

³Leibniz Institute DSMZ - German Collection of Microorganisms and Cell Cultures, Microbial Genome Research, Brunswick, Germany

⁴Maastricht University, Department of Pharmacology and Toxicology, Maastricht, Netherlands

The exposure to Saharan dust (SD) is anticipated to rise with climate change and is associated with increased respiratory morbidity and mortality. In previous studies we found the inflammatory properties of SD on macrophages to be mediated by the NLRP3 inflammasome pathway and downstream secretion of interleukin (IL)-1β. Heat-inactivation resulted in a strong reduction of its proinflammatory activity, suggesting that microbial constituents contribute to the inflammatory properties of SD. In the present study, we further explored the role of microbial components in the inflammatory potency of SD. Based on an in-depth analysis of the microbial composition of SD during dust events, microbial mixtures composed of Gram-positive bacteria, Gram-negative bacteria, or fungi as well as a microbial cocktail containing all three mixtures, were prepared and gamma-irradiated before use. Co-cultures of A549 human lung epithelial cells and THP-1 macrophages were exposed to SD in the presence and the absence of microbial mixtures in quasi-air-liquid interface (qALI) conditions.

In the qALI co-cultures, heat-inactivation of SD at 220°C abrogated the increased secretion of IL-1β. Furthermore, the cytokine-inducing effects of pristine SD could be restored upon addition of microbial mixtures to the heat-inactivated SD. A clear dose dependency of IL-1β secretion was observed in qALI co-cultures with both bacterial mixtures but not with the fungi mixture. When compared at equal total microbial loads, exposure to either Gram-positive or Gram-negative bacterial mixtures alone elicited stronger cytokine responses than exposure to the cocktail of bacteria and fungi.

The results of this work support the importance of microbial constituents, especially from bacteria, in the inflammatory effect of SD. Future experiments will focus on the investigation of Toll-like receptor signalling in SD exposed macrophages.

This work has received funding from the Leibniz Association in the framework of the Leibniz Collaborative Excellence Programme project DUSTRISK under grant agreement number K225/2019.

P225**Ambient and Indoor Fine Particulate Matter from Düsseldorf and Prague Induce Divergent Oxidative and Inflammatory Responses**G. Bredeck^{1,2}, J. Vossen², T. Spannbrücker², T. Wahle², V. Silvonen³, L. Salo³, T. Rönkkö⁴, J. Topinka⁴, S. Saarikoski⁴, R. P. F. Schins^{2,6}¹Centro de Investigaciones Biológicas Margarita Salas (CIB-CSIC), Biomedicine, Madrid, Spain²Leibniz Research Institute for Environmental Medicine (IUF), Düsseldorf, Germany³Tampere University, Aerosol Physics Laboratory, Faculty of Engineering and Natural Sciences, Tampere, Finland⁴Institute of Experimental Medicine of the CAS, Prague, Czech Republic⁵Finnish Meteorological Institute, Helsinki, Finland⁶Maastricht University, Department of Pharmacology and Toxicology, Maastricht, Netherlands

Ambient particulate matter has been linked to respiratory morbidity and mortality, causing about 6.7 million premature deaths annually. Several studies revealed region-specificities in the composition and health effects of fine particulate matter (PM_{2.5}). Nevertheless, region-specific mechanisms of toxicity and the differences in toxicity between ambient and indoor air remain insufficiently understood.

We compared the oxidative and inflammatory potency of PM_{2.5} from two European cities, including ambient and indoor PM_{2.5}, to determine whether city and indoor-specific exposures elicit similar mechanisms of toxicity. Ambient PM_{2.5} was collected in Düsseldorf and both ambient and indoor PM_{2.5} in Prague in spring 2022. Hydroxyl radical (•OH) generation was measured by electron paramagnetic resonance spectroscopy, and alveolar epithelial A549 cells and THP-1 macrophages were exposed to non-cytotoxic concentrations (4, 20, 100 µg/cm²) for 24 h.

During the sampling campaign, mean PM_{2.5} concentrations were higher in Düsseldorf ambient air (12.7 µg/m³) than in Prague ambient air (10.8 µg/m³) and lowest in Prague indoor air (6.9 µg/m³). Electrical Low-Pressure Impactor (ELPI+) measurements indicated that particles smaller than 70 nm accounted for approximately 6% in Düsseldorf ambient PM_{2.5} and 10% in Prague ambient and indoor PM_{2.5}. Prague ambient PM_{2.5} exhibited about 50% higher •OH-forming capacity than Düsseldorf ambient and Prague indoor PM_{2.5}. Consistent with the •OH-forming capacity, all PM_{2.5} samples upregulated the oxidative stress marker *heme oxygenase 1* in A549 cells in a concentration-dependent manner, though the magnitude was similar across all samples and reached significance only for Prague ambient and indoor PM_{2.5}. None of the samples altered *interleukin 8* (*IL8*) gene expression, yet Düsseldorf and Prague ambient PM_{2.5} increased *IL-8* release concentration-dependently. In THP-1 macrophages, only Düsseldorf ambient PM_{2.5} induced *IL-8* and *IL-1β* release.

These results emphasise the hazardous nature of urban indoor PM_{2.5} and ambient PM_{2.5} across cities. Disentangling why •OH formation, oxidative stress, and inflammatory effects diverge will help identify the components driving toxicity. Because indoor PM_{2.5} partly mirrors ambient PM_{2.5} in composition and oxidative potency, yet differs in inflammatory activity, source-directed strategies will be essential to understand the role of PM_{2.5} composition and mitigate the health burden of air pollution.

P226**Establishment of the hOGG1-modified in vivo comet assay for detection of DNA damage in rat lungs tissue after instillation of particles**H. Angelov¹, H. Brockmeyer¹, G. Bruer², M. A. Djuari¹, M. Engelke¹, C. Müller¹, J. Wabra¹, M. L. Winkler¹, C. Ziemann¹¹Fraunhofer Institute for Toxicology and Experimental Medicine (ITEM), Mechanistic Toxicology, Hanover, Germany²Fraunhofer Institute for Toxicology and Experimental Medicine (ITEM), Inhalation Toxicology, Hanover, Germany

The in vivo alkaline comet assay according to OECD 489 can detect both DNA-strand breaks and oxidatively damaged DNA upon enzyme modification and is currently an integral part of regulatory genotoxicity testing strategies. While the liver is the primary organ examined for chemicals and pharmaceuticals, the assay is also valuable for genotoxicity testing of particles in the lung after instillation.

This study aimed to establish a robust protocol for particle testing in lung tissue. Key challenges included identification of an efficient and reliable cell isolation method that minimizes basal DNA damage, finding appropriate technical positive controls for better adhering to the 3R principles, and implementing an effective enzyme incubation step for detection of oxidatively damaged DNA, relevant for particle-exposed lungs.

Initially, we addressed cell isolation from lung tissue by comparing various buffers and mechanical devices (e.g., douncer, scissors, pistils). Optimal tissue dissociation was finally achieved using tissue punches and a grinding step with disposable pistils in tissue buffer-filled reaction cups. Vehicle controls showed low baseline tail intensities (TI) of less than 4% increasing to 9–12% in animals treated with ethyl methanesulfonate (EMS, 300 mg/kg, 3h). But for 3R reasons, also technical in vitro positive controls were established. EMS-treated L-929 cells (4.85 mM, 1h), cryopreserved in large batches, served to show appropriate electrophoresis. Both freshly treated and thawed cells (stored up to 11 months) showed consistent TI values of 12–16%. For sensitive detection of oxidatively-damaged DNA, an incubation step ± human 8-oxoguanine DNA glycosylase 1 (hOGG1) enzyme was chosen. Potassium bromate (KBrO₃)-incubated L5178Y/TK⁺ cells served as technical positive control to ensure hOGG1-functionality. A respective incubation protocol with optimized KBrO₃ (5 mM KBrO₃) and hOGG1 concentration (100 µl of a 2.5 µg/ml solution of hOGG1 in enzyme buffer) and incubation times (1 h and 15 min, respectively) was finally

developed to allow for clear distinction between buffer- and hOGG1-treated KBrO₃ samples.

In conclusion, the optimized in vivo comet assay protocol enables reliable detection of both DNA strand breaks and oxidative DNA damage in rat lung tissue following particle exposure. Future work will focus on enhancing oxidative damage detection by combining hOGG1 with endonuclease IV, which removes AP sites that can inhibit hOGG1 activity.

Immunopharmacology / inflammation / anti-infectives**P227****Adipose–Tendon Cross-Talk as a Missing Link in Fluoroquinolone-Induced Tendinopathy**M. Rollmann¹, T. Hube¹, S. Twarock¹¹Institut für Translationale Pharmakologie, Düsseldorf, Germany

Fluoroquinolone (FQ) antibiotics are widely prescribed for bacterial infections but are increasingly associated with severe and sometimes irreversible adverse events. Among these, tendinopathy represents one of the most prominent and clinically debilitating complications. Although mitochondrial toxicity, oxidative stress, and matrix degradation have been proposed, these mechanisms do not sufficiently explain why tendons are particularly vulnerable, why only a subset of patients develops long-lasting complications, or why such complications can emerge months to years after drug exposure. We hypothesize that adipose depots adjacent to tendons may act as primary targets of FQ toxicity. Drug-induced adipose dysfunction and inflammation could generate a pro-inflammatory, matrix-altering microenvironment that secondarily contributes to tendon damage.

As a first proof of concept, differentiated 3T3-L1 adipocytes and tendon cells were treated with ciprofloxacin, ofloxacin, levofloxacin, or moxifloxacin, and inflammatory gene expression was analyzed. After 24 hours, tendon cells showed no significant induction of Interleukin-1β, Interleukin-6, TNFα, or MCP-1, whereas adipocytes responded in a dose-dependent manner to three out of four compounds with marked upregulation of these inflammatory markers. These preliminary findings support the idea that adipose tissue, rather than tendon cells themselves, may represent the initial target of FQ-induced toxicity.

In the next phase, we will employ ex vivo cultures of adipose and tendon explants from human body donors, complemented by biopsies from patients with Achilles tendon rupture, to further investigate adipose–tendon cross-talk under FQ exposure. The results are expected to provide mechanistic insight into FQ-associated tendinopathy and support the development of future preventive strategies.

P228**PERK inhibition rewires translational and CMGC protein kinase networks into an antiviral state**M. S. Shaban¹, H. Schuele Weiser¹, A. Weber¹, J. Meier-Söldch¹, F. Dort¹, C. Mayr-Buro¹, N. Karl¹, J. Wilhelm¹, J. Ziebuhr¹, U. Linne², M. Kracht¹¹Justus Liebig University Gießen, Rudolf Buchheim Institute of Pharmacology, Gießen, Germany²Marburg University, Mass Spectrometry Facility of the Department of Chemistry, Marburg, Germany

Despite the success of protein kinase inhibitors in oncology, fewer than 5% of human kinases are targeted therapeutically, and no kinase inhibitors have been approved for treating infectious diseases, including RNA virus infections. A significant challenge in developing kinase inhibitor-based antivirals lies in understanding the complex, dynamic interactions between kinases and their substrates during cellular perturbation.

In this study, we explored how inhibiting a single protein kinase can globally alter the cellular state of virus-infected cells. By targeting PERK, a key sensor of coronavirus-induced ER stress, we demonstrate how pharmacological PERK inhibition reshapes host translational and kinase signaling networks toward an antiviral phenotype.

Specifically, we integrated transcriptomic, translational, proteomic, and phospho-proteomic analyses from Huh7 liver cells infected with human coronavirus 229E (HCoV-229E) under conditions of PERK inhibition. Deep bioinformatic analyses of these datasets revealed a previously unrecognized link between PERK and the Rho GTPase-PAK signaling axis. We show that inhibiting PAK kinases has potent antiviral effects, highlighting the therapeutic potential of targeting kinase network rewiring.

A novel aspect of our study is the application of the human kinome motif atlas, which includes 89,000 phosphorylation sites and 303 serine / threonine kinase motifs, to assess the effects of PERK inhibition. This analysis revealed that coronavirus infection co-regulates entire kinase families, not just isolated enzymes, offering a systems-level perspective of the reorganization of the kinome and downstream signaling responses.

Further bioinformatic analysis of HCoV-229E-infected cells, supported by re-analysis of SARS-CoV and SARS-CoV-2 datasets, identified a core CMGC kinase module and over 140 substrates activated by various coronaviruses, which were suppressed by PERK inhibition. Comparing pharmacological and genetic perturbations allowed us to distinguish on- from off-target effects, revealing the polypharmacology of PERK inhibitors.

P229

Dynamics of a pro-inflammatory BAF complex in the IL-1-triggered NF- κ B signaling pathway

J. Meier-Sölch¹, L. Deuster¹, L. Leib¹, J. Juli¹, A. Weber¹, U. Linne², M. Kracht¹
¹Justus Liebig University Gießen, Rudolf-Buchheim-Institute of Pharmacology, Gießen, Germany

²Marburg University, Mass spectrometry facility of the Department of Chemistry, Marburg, Germany

Interleukin-1 (IL-1) is a potent proinflammatory cytokine centrally involved in innate immune responses and the pathogenesis of autoimmune and autoinflammatory diseases. IL-1 rapidly activates multiple target genes via the transcription factor (TF) NF- κ B in a coordinated manner. However, the transient interactions between NF- κ B, other TFs, chromatin modifiers, and the transcriptional machinery remain incompletely understood. To elucidate nuclear NF- κ B interactions, we determined the protein interactome of the NF- κ B subunit p65 using a proximity-based biotinylation LC-MS/MS approach. We found multiple TFs and epigenetic regulatory complexes, notably 11 components of the BRG1/BRM-associated factor (BAF) complex, a member of the mSWI/SNF chromatin-remodeling complex subfamily. We therefore set up experiments to investigate the composition, dynamics, and functional significance of a pro-inflammatory BAF complex in IL-1-triggered NF- κ B responses.

HeLa cells expressing doxycycline-inducible fusion proteins of p65 and the miniTurbo (mTb) biotin ligase (p65-HA-mTb) were used to establish a biotin-streptavidin-based pulldown assay combined with Western blotting to study cytokine-regulated changes of a pro-inflammatory, multi-subunit BAF complex consisting of known (e.g. p50/p105, I κ B α , cJUN) and newly identified (e.g. SMARCA4, SMARCC1, SMARCE1) p65 interactors. Using p65 mutants, we found that p65 interaction with SMARCA4 occurs independently of p65 DNA binding or dimerization. Inhibition of SMARCA4/2 ATPase activity with FHD-286 did not affect p65:BAF interactions but showed dose- and time-dependent effects on IL-1-responsive genes, with strong inhibition of *IL8* and *IL6*, moderate reduction of *cJUN*, *TNFAIP3*, and *NFKBIA*, and unchanged induction of *BIRC3*. Treatment of SMARCA4-deficient cells resulted in additive transcriptional effects, demonstrating that both catalytic activity and further domains of SMARCA4 contribute to the regulation of the inflammatory response. These effects were corroborated at the genome-wide level by RNA-Seq experiments.

We have identified a dynamically regulated BAF complex as a key downstream regulator in the IL-1-NF- κ B pathway. The data show that pharmacological modulation of p65:BAF complex activity results in the selective modulation of cytokine-inducible inflammatory genes, potentially advancing targeted anti-inflammatory therapies for chronic inflammatory diseases.

P230

Caenorhabditis elegans as an infection model for the repurposing of farnesyltransferase inhibitors as antibiotics

L. Scholleck¹, H. S. Bachmann¹, A. Hagemann¹

¹Witten/Herdecke University, Department für Humanmedizin, Witten, Germany

Question

Antibiotic resistance is a major global health concern, highlighting the urgent need for the discovery of new antimicrobial agents. Drug repurposing is a promising and cost-effective alternative to conventional drug development by identifying new applications for existing compounds. Farnesyltransferase inhibitors (FTIs) were originally developed as anticancer drugs and have recently shown indications of antimicrobial activity. We aimed to investigate whether FTIs can improve host survival and reduce bacterial burden in *Caenorhabditis elegans* (*C. elegans*) infected with *Staphylococcus aureus* (*S. aureus*).

Methods

C. elegans were infected with *S. aureus* and subsequently treated with FTIs. Lifespan assays were performed to assess survival outcomes. Reactive oxygen species (ROS) production and bacterial colonization in *C. elegans* are quantified using biochemical assays and fluorescence microscopy, enabling visualization of oxidative stress and infection dynamics *in vivo*.

Results

S. aureus infected worms showed a reduced lifespan. Initial experiments indicate that FTI treatment tends to prolong survival, consistent with previous findings that inhibitors of the mevalonate pathway can extend the lifespan of *C. elegans*. Additionally, preliminary data suggest a reduction of bacterial colonization, and a decrease in oxidative stress in infected worms.

Conclusions

Our findings suggest a dual role of FTIs by promoting host defense and reducing bacterial infection, supporting their repurposing as anti-infective agents. Future work will focus on *C. elegans* knockout strains defective in key stress-response pathways such as MAPK and SKN-1 signaling. This study highlights the potential of FTIs as candidates for antimicrobial drug repurposing and demonstrates the value of *C. elegans* as a translational infection model in pharmacological research.

P231

Viral phosphodiesterases circumvent bacterial phage defense – A characterization of the cyclic nucleotide-cleaving PDE Apyc1

L. Schütte¹, L. J. Bindel¹, H. Bähre², B. Schirmer¹, R. Seifert^{1,2}

¹Hannover Medical School (MHH), Institute of Pharmacology, Hannover, Germany

²Hannover Medical School (MHH), Research Core Unit Metabolomics, Hannover, Germany

Bacteriophages are viruses that infect bacteria and use the bacterial host cell for replication. As they exist ubiquitously in the environment, phages are a persistent threat to bacterial populations. In response, bacteria have developed anti-phage defense systems against phage infection. One defense system relies on the activation of host-immunity by formation of cyclic nucleotides. Specifically, 3",5"-cyclic cytidine monophosphate (cCMP) and 3",5"-cyclic uridine monophosphate (cUMP) are involved in the pyrimidine cyclase system for anti-phage resistance (Pycsar). In this system, certain effectors are activated by cCMP and cUMP, which leads to bacterial cell death and thus prevents phage propagation [1].

Due to this evolutionary pressure, phages have developed mechanisms to circumvent bacterial immunity. Phage phosphodiesterases (PDEs) with a broad cyclic nucleotide specificity play a central role in disrupting the host-immunity of bacteria. As these PDEs prevent activation of Pycsar by cleaving cUMP and cCMP, they are referred to as anti-Pycsar 1 enzymes (Apyc1) [2].

The characterization of Apyc1 homologs is an important step in further understanding their role in circumventing anti-phage defense systems. Furthermore, viral PDEs or their inhibitors may constitute a novel class of antibacterial or antiviral drugs, respectively, which are urgently needed in light of the growing threat of multi-drug-resistant pathogens [3].

The Apyc1 gene from *Bacillus* phage SBSPhiJ was cloned into a pET expression vector containing an N-terminal His-tag. Following the transformation of the vector, the protein was expressed in *E. coli* and purified by affinity and size exclusion chromatography. The purified enzyme was then analyzed in enzyme assays containing 3",5"-cNMPs and 2",3"-cNMPs as substrates. The products of these reactions were unequivocally identified via LC-IMS-QTOF. Apyc1-SBSPhiJ converted 3",5"-cNMPs to the corresponding 5"-NMPs and 2",3"-cNMPs to the corresponding 3"-NMPs. In addition, quantitative analyses (LC-QQQ) showed a faster conversion of purine 3",5"- and 2",3"-cNMPs (cAMP, cGMP) than of the pyrimidine equivalents (cCMP, cUMP). Ongoing experiments include the optimization of reaction conditions and identification of kinetic parameters (v_{max} , K_m) and enzyme inhibitors.

[1] Tal et al. (2021). *Cell*, 184(23), 5728–5739.e16.

[2] Hobbs et al. (2022). *Nature*, 605(7910), 522–526.

[3] Seifert and Bugert (2023). *Trends Biochem Sci*, 48(10), 835–838.

P232

Changing the frame in atopic dermatitis: novel therapy with Lebrikizumab

A. Roșu¹, M. C. Roșu², A. D. Ruța¹, S. N. Ruscă¹, B. N. Ruța¹

¹George Emil Palade University of Medicine, Pharmacy, Science, and Technology of Târgu Mureș, Târgu Mureș, Romania

²CMI Dr. Roșu Maria Cristina, Sighetu Marmației, Romania

Lebrikizumab is a monoclonal antibody (lab-engineered protein) designed to block IL-13, which plays a significant role in type 2 allergic reactions. Its primary use is for moderate-to-severe atopic dermatitis. Based on robust Phase 3 results from the ADVocate 1 and ADVocate 2 trials—where nearly 80% of patients receiving lebrikizumab as monotherapy or with topical corticosteroids achieved skin clearance and symptom relief by week 16—the FDA granted approval for lebrikizumab on September 13, 2024. Interleukin-13 has been identified as a central mediator in the pathophysiology of atopic dermatitis (AD), contributing to pruritus, skin thickening, increased transepidermal water loss, and susceptibility to secondary infection.

A comprehensive literature search was performed on PubMed using the keywords "Lebrikizumab," "Atopic Dermatitis," "IL-13," and related synonyms. The search strategy targeted the most recent publications from the past five years, with a specific focus on clinical trials and other studies that elucidate the pharmacological characteristics and mechanistic profile of this monoclonal antibody.

In clinical studies, lebrikizumab treatment was associated with reductions in serum levels of periostin, total immunoglobulin E (IgE), and several type 2-associated chemokines, including CCL17 [thymus and activation-regulated chemokine (TARC)], CCL18 [pulmonary and activation-regulated chemokine (PARC)], and CCL13 [monocyte chemoattractant protein-4 (MCP-4)]. Lebrikizumab is a humanized IgG4 monoclonal antibody that binds interleukin-13 (IL-13) with high affinity, selectively inhibiting IL-13 signaling via the IL-4 receptor α (IL-4R α) and IL-13 receptor α 1 (IL-13R α 1) heterodimer complex. Inhibition of IL-13 signaling is expected to provide therapeutic benefit in disorders where IL-13 is a key driver of pathogenesis. Notably, lebrikizumab does not disrupt IL-13 binding to the IL-13 receptor α 2 (IL-13R α 2, the decoy receptor), thereby preserving the physiological internalization and clearance of IL-13.

Lebrikizumab demonstrates a novel and targeted pharmacological approach in the management of moderate-to-severe atopic dermatitis, acting through high-affinity inhibition of IL-13 signaling. Its mechanism directly addresses the

immunological dysregulation and barrier impairment characteristic of atopic dermatitis, resulting in clinically meaningful improvements in skin inflammation, pruritus, and overall disease severity.

P233

Impact of farnesyltransferase inhibitors on ROS development in bacteria

M. Klose¹, H. S. Bachmann¹, L. Weber¹

¹Witten/Herdecke University, Institute of Pharmacology and Toxicology, Witten, Germany

Question

Antimicrobial resistance is rising globally, undermining existing therapies. Drug repurposing – systematically evaluating already established compounds for antimicrobial use – offers a pragmatic route to novel options. Farnesyltransferase inhibitors (FTIs), primarily developed for oncology, show antimicrobial activity against gram-positive [1] and gram-negative pathogens [2]. However, the antibacterial mechanisms of FTIs remain unresolved. Reactive oxygen species (ROS) are implicated in antibiotic action and can influence resistance development [3]. Therefore, we quantified ROS dynamics during FTI exposure to elucidate the role of ROS in antibacterial effects.

Methods

Bacterial models included methicillin-susceptible and -resistant *Staphylococcus aureus* (*S. aureus*). Antimicrobial susceptibility testing followed CLSI guidelines. Intracellular ROS were quantified using 2',7'-dichlorofluorescein diacetate (DCFH-DA) and CellROX Deep Red. Expression of ROS-associated genes (e.g., *sodA*) was measured by qPCR. The role of ROS was evaluated by co-incubation with the ROS scavenger N-acetylcysteine (NAC) to assess its influence on antimicrobial effects. Membrane potential and envelope stress were monitored using DiOC2(3) assays and NPN/SYTOX Green uptake, respectively.

Results

Our data indicate compound-specific ROS responses in methicillin-susceptible and -resistant *S. aureus* strains. In DCFH-DA assays, tipifarnib yields higher ROS readouts than lonafarnib. Consistent with a ROS contribution, co-incubation with NAC attenuates the antimicrobial effects of tipifarnib more than those seen with lonafarnib. Parallel measurements with CellROX Deep Red corroborated these DCFH-DA trends in matched endpoint and short-kinetic assays.

Conclusion

Taken together, our data indicate compound-specific ROS responses: tipifarnib generates higher ROS signals and is more completely reversed by NAC than lonafarnib. This aligns with our proteomic observations of stronger induction of stress-response proteins under tipifarnib, while both inhibitors exhibit signatures consistent with cell-envelope involvement. These differences are highly relevant for resistance considerations, given prior reports that antibiotic-induced ROS can influence resistance development [4]. However, dedicated experiments are required before inferring any compound-specific impact on resistance.

[1] PMID: 34917041

[2] PMID: 40911556

[3] PMID: 19647477

[4] PMID: 32041713

P234

Multicentre, double-blind, randomised, placebo-controlled study to investigate the efficacy of nasal spray and mouthwash containing hypochlorous acid in viral infections of the upper respiratory tract

A. Lippert¹, A. Hoffmann¹, M. Winter², L. Zyka³, N. Attia³, C. A. Mueller³, B. Renner¹

¹TU Dresden University of Technology, Institute of Clinical Pharmacology, Faculty of Medicine, Dresden, Germany

²Team Winter Kompetenzzentrum, Vienna, Austria

³Medical University of Vienna, Department of Otorhinolaryngology, Vienna, Austria

Respiratory viruses such as SARS-CoV2 cause a large number of days of absence from work, burden of symptoms and, in a small proportion of patients, severe courses of disease. Causal treatment options are limited. This applies particularly to patients without risk factors who are looking for an easy-to-use, low-risk treatment to shorten their course of disease and/or alleviate symptoms. Several ideas have been proposed, including local treatment with disinfectant agents or potentially antimicrobial plant preparations. Clinical data in this field are scarce.

In this ongoing international study, we are investigating the effect of reducing the viral load on the mucous membranes of the nose and mouth-throat area using 2 medical devices containing sodium hypochlorite on the course of disease. The study hypothesis is that the frequent (five times daily) inactivation of viruses on

the mucosa surface slows the virus replication and causes a shorter and milder disease. There are the two study centres in Dresden and Vienna. Both aim for 30 adult participants.

Upon enrolment in the study, participants are tested for SARS-CoV2. Samples are collected from positive participants at two time points by gargling with physiological sodium chloride solution for determination of the viral load via qPCR. All participants are treated at home. They report symptoms in a structured journal. Primary outcome is the development of a sum parameter describing symptom abundance and severity. Secondary outcome is the decline of viral load and time to negative lateral flow antigen test (AG-testing) in the subset of SARS-CoV2 positive participants.

Up to now (as of October 2025) 27 participants have been included over both study sites. The study is still blinded, as recruitment is ongoing. Group 1 provided a faster recovery from SARS-CoV2 indicated by AG-testing and patients' reports. In conclusion first treatment differences between groups have become apparent in this study.

P235

Canonical and unconventional functions of the protein kinases CDK12 and CDK13 in inflammation and the tumor microenvironment

F. C. Schmidt¹, J. Priester¹, M. Kracht¹

¹Justus Liebig University Gießen, Rudolf Buchheim Institute of Pharmacology, Gießen, Germany

Cyclin-dependent kinases 12 and 13 (CDK12/13) phosphorylate serine 2 and 5 in the CTD of RNA polymerase II, an essential step of transcriptional elongation. In addition to this canonical function, CDK12/13 have roles in maintaining genome stability, regulation of translation and RNA processing. However, the role(s) of CDK12/13 in inducible gene expression programs have not been defined. In this study, we characterized functional and molecular links between CDK12/13 and the inflammatory IL-1-NF-κB signalling pathway.

We treated HCT116 epithelial colon carcinoma cells with CDK12/13 inhibitors in the context of IL-1-induced inflammation. The inhibitors showed consistent differential effects on NF-κB-mediated gene expression and protein secretion, that were gene length dependent. Next, we assessed whether these effects were related to the canonical function of CDK12/13 by analysing transcriptional elongation for genes of varying lengths using a modified RT-qPCR assay. Treatment with the CDK12/13 inhibitor THZ531 showed a block of elongation and accumulation of short pre-mRNA products for long genes (*BIRC3*, *SAMD4A*), while a shorter gene (*IL8*) revealed elevated expression. This led to the conclusion that CDK12/13's canonical functions are relevant for a small group of long inflammatory genes only.

Additionally, we evaluated a novel CDK12/13 degrader, PROTAC BSJ-4-116, which efficiently depletes CDK12/13 but also demonstrates off-target suppression of the entire IL-1-NF-κB pathway. We sought to exploit this polypharmacology in a coculture system of epithelial tumor cells with human macrophages derived from peripheral blood monocytes. After coculture, the cell types were separated and PROTAC effects on IL-1 target gene expression were assessed by RT-qPCR. Additionally, we analysed the PROTAC effect on cell death and proliferation via microscopy. Our results indicated cell type specific effects of the PROTAC, which suppressed IL-1 target gene expression in HCT116 or HeLa cells but had differential effects on macrophages. Furthermore, single-cell data quantification showed that the PROTAC induced apoptosis in HeLa and macrophages, but reduced proliferation specifically in HeLa cells.

Overall, our results show that CDK12/13 inhibition is a novel mode of modulating the inflammatory IL-1-NF-κB pathway in a gene and cell type specific manner, which, in the long-term, may be exploited for improved kinase inhibitor-based targeted therapies in autoimmunity and cancer.

P236

Angiotensin II as an Adjunct Vasopressor in Septic Shock: A Concise Review

D. Schmidbauer¹, E. G. Bán¹

¹George Emil Palade University of Medicine, Pharmacy, Science, and Technology of Târgu Mureș, Department of Pharmacology, Campus Hamburg, Târgu Mureș, Romania

Introduction: Septic shock remains characterized by vasodilatory shock and high mortality despite source control, timely antimicrobials, and organ support. Many patients exhibit catecholamine hyporesponsiveness, consistent with dysregulation of the renin-angiotensin-aldosterone system (RAAS), supporting angiotensin II (AT-II) as a non-adrenergic vasopressor.

Objectives: To evaluate the efficacy, safety, and clinical role of AT-II as an adjunct vasopressor in adults with septic shock.

Methods: We conducted a narrative review of clinical studies on AT-II in adults with septic/distributive shock (2014–2025). Sources included PubMed and ClinicalTrials.gov; contemporary sepsis guidelines and EU/US label documents were hand-searched. Inclusion required adjunct use of AT-II and reporting of ≥1 predefined hemodynamic or safety outcome; mortality was noted when reported. We excluded animal/in vitro studies, paediatric cohorts, single-patient case reports, and non-peer-reviewed preprints. Evidence was synthesized qualitatively.

Results: Across randomized and observational data, AT-II rapidly attains target mean arterial pressure (MAP) and reduces vasopressor exposure within hours in catecholamine-refractory vasodilatory shock. Exploratory phenotyping suggests stronger hemodynamic responses with RAAS dysregulation e.g., elevated renin or a high Ang I:II ratio. Earlier initiation at lower noradrenaline doses yields clearer MAP responses. A prespecified ATHOS-3 analysis indicates that early down-titration to ≤ 5 ng/kg/min at 30 min marks AT-II hyper-responsiveness. Renal findings are mixed; in severe AKI/renal replacement therapy (RRT) subsets, post hoc analyses reported faster liberation from RRT. In ARDS subsets, PaO₂/FiO₂ improved within 48 h independent of ventilator settings, with outcomes data limited. A survival benefit remains unproven; safety appears acceptable, with infrequent but clinically relevant ischemic/thrombotic events. Guidelines position AT-II as an adjunct for refractory vasodilatory shock.

Conclusion: AT-II, used as an adjunct vasopressor in catecholamine-refractory septic shock, reliably raises MAP and reduces catecholamine exposure. Exploratory signals in selected phenotypes (high-renin, earlier initiation) highlight a key research gap: mortality-powered, biomarker-guided trials are needed to clarify survival effects. Evidence is largely centred around ATHOS-3; broader multicentre RCTs and registries are needed to confirm generalizability.

3R Practice / Alternative Methods

P237

A bioartificial human skin equivalent that serves as a novel approach to investigate the decontamination process of the highly toxic nerve agent VX
A. Schwab¹, D. Steinritz^{1,2}, F. Worek¹, N. Amend^{1,2}

¹Bundeswehr Institute of Pharmacology and Toxicology, Munich, Germany

²Ludwig-Maximilians-University Munich, Walther-Straub-Institute of Pharmacology and Toxicology, Munich, Germany

Introduction:

Nerve agent poisoning remains an ongoing threat despite the ratification of the Chemical Weapon Convention by 193 states. The convention, bans the **development, production, stockpiling and use of chemical weapons**. Due to limited therapeutic options for nerve agent poisoning, a rapid and effective decontamination procedure is essential to prevent systemic effects and facilitate survival.

Objectives:

We investigated penetration- and diffusion processes of the nerve agent VX, studying different decontamination solutions by using a three-dimensional bioartificial human skin equivalent (Full-Thickness skin model).

Materials & Methods:

The well-established Franz diffusion cell was used as model to investigate the effectiveness of different decontamination agents (Reactive skin decontamination lotion (RSDL), potassium salt of the acetohydroxamic acid (AHAK), Sodium hypochlorite (NaOCl) and water). The amount of penetrated VX in the acceptor chamber was assessed by a well-established acetylcholinesterase inhibition assay (Ellman assay). The decontamination process was initiated five- or thirty-minutes post exposure (VX 10 % (v/v) solution in isopropanol), and the experiment lasted 300 minutes.

Results:

A substantial decontamination efficacy was observed for the FDA approved RSDL and for AHAK. The amount of VX in the acceptor chamber was reduced by 99.97 % (AHAK) and 97.16 % (RSDL) (decontamination five minutes post exposure). In addition, AHAK was tested as prophylaxis and showed significant protective effects, which leads to future perspectives for preventive decontamination. In contrast, the hydrophilic agents (water and NaOCl) were less effective considering decontamination, particularly when applied 30 min after exposure.

Conclusion:

In conclusion, the Full-Thickness skin model represents an innovative technology for elucidating decontamination processes in VX poisoning, aligning with the principles of the 3R concept (Replacement, Reduction and Refinement).

P238

Developmental- and Species-Specific Dynamics of DNA Repair in Neural Progenitors

L. Czernik¹, M. Pahl¹, L. Dittmann¹, E. R. de Caro¹, L. M. Stark¹, J. Tigges¹, K. Koch^{1,2}, E. Fritsche^{2,3,4}

¹Leibniz Research Institute for Environmental Medicine (IUF), Environmental Toxicants and the Brain, Düsseldorf, Germany

²DNTOX GmbH, Düsseldorf, Germany

³Swiss Centre for Applied Human Toxicology (SCAHT), Basel, Switzerland

⁴University of Basel, Department of Pharmaceutical Sciences, Basel, Switzerland

Human brain development is highly sensitive to genotoxic agents due to its complexity, rapid growth, and the longevity of neural cells, making prenatal exposure a risk for lasting impairments. The cellular DNA damage response,

shaped by a genotoxin's mode of action (MoA), may vary across developmental stages as DNA repair capacities shift. Yet, most data rely on costly, time-intensive rodent models with limited human relevance. This study applies the OECD-endorsed developmental neurotoxicity testing battery (DNT IVB) Neurosphere Assay, a New Approach Methodology to assess chemical effects on seven key neurodevelopmental processes (KNDPs) in neural progenitor cell (NPC) neurospheres. Using primary human NPCs (hNPCs), we assessed the impact of four model genotoxins with distinct MoAs on the KNDPs NPC proliferation, migration, neurite outgrowth, and differentiation into neurons and oligodendrocytes: *N*-ethyl-*N*-nitrosourea (ENU; DNA alkylation), etoposide (ETOP; topoisomerase II inhibitor), hydroxyurea (HU; ribonucleotide reductase inhibitor), and 5-azacytidine (5-AZA; DNA methyltransferase inhibitor). Comparative testing in age-matched rodent NPCs (rNPCs) delineated species-specific responses. Developmental stages were modelled by exposure during proliferation, pre-, early, or late differentiation. We observed MoA-, cell type-, and developmental stage-specific sensitivities of hNPCs to genotoxins. ENU selectively impaired oligodendrocyte differentiation, 5-AZA most strongly affected neuronal differentiation, and ETOP caused broad effects on proliferating and differentiating hNPCs. Resistance increased with maturation, as confirmed by comparing primary to matured human iPSC-derived oligodendrocytes overexpressing SOX10. Strikingly, rodent oligodendrocytes were more resilient than their highly sensitive human counterparts. Underlying molecular mechanisms were explored using transcriptomics (bulk and single-cell RNA sequencing) of proliferating and differentiating hNPCs exposed to genotoxins, revealing pronounced effects of epigenetic modulator 5-AZA across all modelled developmental stages. These findings provide new insights into species-specific impacts of genotoxins on distinct neural cell types and developmental stages, emphasising the value of human-based models. Future work will further elucidate the cell type-specific mechanisms underlying prenatal genotoxin exposure and refine the applicability domain of the Neurosphere Assay for testing genotoxic MoAs.

P239

A First Step Towards a Human-Relevant In Vitro Test Battery for Developmental Immunotoxicity

C. Spruck¹, A. Bartel¹, G. Brockerhoff¹, S. Fayyaz², Q. L.², F. A. Grimm², K. Koch^{1,3}, E. Fritsche^{3,4,5}, J. Tigges¹

¹Leibniz Research Institute for Environmental Medicine (IUF), Düsseldorf, Germany

²Clariant Produkte (Deutschland) GmbH, Frankfurt a. M., Germany

³DNTOX GmbH, Düsseldorf, Germany

⁴Swiss Centre for Applied Human Toxicology (SCAHT), Basel, Switzerland

⁵University of Basel, Pharmaceutical Sciences, Basel, Switzerland

The mammalian immune system is a complex cellular network coordinating innate and adaptive immune responses. Compared to adults, neonates are potentially more susceptible to chemical disruption, meaning immunotoxic effects during early development may be missed in studies restricted to adult animals. Under regulatory frameworks such as the EU REACH Regulation, the need for developmental immunotoxicity (DIT) testing - for example by including the DIT cohort in the OECD Test Guideline 443 - is determined through a weight-of-evidence assessment from complementary studies. However, DIT studies are resource-intensive, require many animals, and are complicated by species-specific developmental differences that limit the transferability of rodent data to humans.

In line with the European Green Deal and international initiatives to reduce animal testing, this project aims to innovate DIT assessment by taking a first step towards developing a human cell-based *in vitro* test battery (IVB). As a fundamental resource, we created the Human Immune System Development Map (HiDmap), a curated, literature-based representation of prenatal immune development integrating immune cell types, migration, signaling, and niche-specific maturation. The HiDmap provides a structured scientific framework for the development of New Approach Methods (NAMs) for DIT testing.

Within this project, we modeled human primitive hematopoiesis by differentiating human induced pluripotent stem cells (hiPSCs) into induced hematopoietic stem cells (iHSCs) using a commercial kit (StemCellITM Technologies). On day 12, iHSCs were analyzed by flow cytometry for the expression of the HSC markers CD34 and CD43, while cytotoxicity and proliferation were assessed in parallel. Results demonstrated robust and reproducible hiPSCs differentiation into iHSCs within 12 days. We also established essential assay components for regulatory method development, including an endpoint-specific negative control for differentiation and positive controls for cytotoxicity, proliferation, and CD34⁺CD43⁺ iHSCs differentiation.

This work represents a first step towards a human-relevant *in vitro* DIT IVB focusing on primitive hematopoiesis. In the next phase, the method will be evaluated with a training set of DIT-positive and -negative compounds and expanded by an additional endpoint assessing iHSC migration to further enhance predictive power and regulatory applicability.

P240

A human iPSC-derived oligodendrocyte model for developmental neurotoxicity assessment across early and late stages of oligodendrogenesis

L. M. Stark¹, M. A. Wolter¹, A. Dönmez^{1,2}, E. Fritsche^{1,2,3,4}, K. Koch^{1,2}

¹Leibniz Research Institute for Environmental Medicine (IUF), Düsseldorf, Germany

²DNTOX GmbH, Düsseldorf, Germany

³University of Basel, Department of Pharmaceutical Sciences, Basel, Switzerland

⁴Swiss Centre for Applied Human Toxicology (SCAHT), Basel, Switzerland

Oligodendrogenesis depends on tightly orchestrated mechanisms such as differentiation, lipid synthesis, and oxidative stress regulation, rendering oligodendrocytes highly susceptible to various exogenous noxae. Since

oligodendrocytes are essential for myelination and rapid saltatory conduction, disturbances in their development contribute to developmental neurotoxicity (DNT) which plays an important role in the emergence of neurodevelopmental disorders. Currently, regulatory DNT assessment is not mandatory for chemical registration and relies exclusively on rodent *in vivo* studies with limited human relevance. To address this, human-based New Approach Methods (NAMs) modelling key neurodevelopmental processes (KNDPs) have been compiled into a DNT *in vitro* testing battery (DNT-IVB). Therein, oligodendrocyte differentiation of primary human neural progenitor cells (NPCs) has emerged as one of the most sensitive KNDPs towards chemical exposure. Incorporating a more mature oligodendrocyte model into this framework could improve the detection of chemicals interfering with both early and late stages of oligodendrogenesis.

To establish a biologically relevant and easily quality controlled model for chemical assessment, we used genetically engineered human induced pluripotent stem cells (hiPSCs) overexpressing the oligodendrocyte transcription factor *SOX10*. After neural induction, oligodendrocyte lineage conversion was evaluated based on morphology and developmental stage-specific marker expression over 10 days of differentiation. To identify differences in the sensitivity of critical windows of oligodendrogenesis to chemical exposure, we investigate environmental chemical effects on early and late stages of oligodendrogenesis by exposing cells during differentiation (days 0–6) and maturation (days 4–10), respectively. To define the applicability domain, we currently test modulators of neurodevelopmentally relevant signaling pathways and known *in vitro* DNT positive and negative compounds. Consistent with previous DNT-IVB findings, oligodendrocyte differentiation is regulated by BMPs, PLC, GSK-3, and Wnt signaling, as well as nuclear receptors (LXR, PPARs).

By addressing limitations of primary cell-based models and incorporating later-stage KNDPs, our work contributes to the refinement of the DNT-IVB. Given the rising incidence of DNT-related disorders, well-characterized and predictive human-relevant NAMs are crucial to improve chemical safety assessment.

P241

Expanding the biological coverage of developmental neurotoxicity *in vitro* battery (DNT-IVB): Integrating human glial-cell related endpoints

A. S. Cheruvil Lilikumar¹, E. Zühr¹, R. Guzzo¹, E. Fritsche^{2,3,4}, K. Koch^{1,4}

¹Leibniz Research Institute for Environmental Medicine (IUF), Environmental Toxicants and the Brain, Düsseldorf, Germany

²Swiss Centre for Applied Human Toxicology (SCAHT), Basel, Switzerland

³University of Basel, Department of Pharmaceutical Sciences, Basel, Switzerland

⁴DNTOX GmbH, Düsseldorf, Germany

The rising prevalence of neurodevelopmental disorders highlights the need for predictive, mechanistically informative methods to assess chemical effects beyond resource-intensive *in vivo* developmental neurotoxicity (DNT) studies. To address these limitations, an *in vitro* DNT battery (DNT-IVB) covering eight key neurodevelopmental processes has been developed, though glia-related endpoints remain limited. This study expands the DNT-IVB with assays for early neural progenitor cell (NPC) migration, astrocyte (AC) maturation, refined through inclusion of human-induced pluripotent stem cell (hiPSC)-derived microglia (iMGs), which are expected to enhance the physiological relevance of the battery.

NPCs like radial glia (RG) provide scaffolds for neuronal migration and differentiate into neurons and glia. A human NPC migration assay was established using hiPSC-derived NPC (hiNPC) neurospheres differentiated for 5 days and migration distances measured on days 3 and 5. Effects of 18 DNT-relevant pesticides spanning 7 chemical classes and 3 *in vivo* negatives are being tested. Results will be compared with the primary NPC-based migration assay of more mature RG that is assessed in the DNT-IVB.

Mature ACs are generated from primary NPCs or hiNPCs within 5 days in presence of BMP2 and CNTF. Astrocytic identity was verified by immunocytochemistry (GFAP, AQP4, S100b) and functionality demonstrated via TNF α -induced inflammatory activation (ICAM1 upregulation) and glutamate uptake. Within the human astrocyte maturation (hAM) assay, we investigate effects on AC maturation, migration and morphology using a compound training set containing known human DNT positives and negatives as well as DNT-IVB false negatives. Manganese chloride (100 μ M) induced cell body shrinkage and morphological alterations, whereas chlorpyrifos, 5,5-diphenylhydantoin, penicillin G, and D-mannitol caused no effects.

iMGs expressing IBA1, P2RY12, and TMEM119 were generated from SP11/CEBPA-overexpressing hiPSCs within 8 days and successfully integrated into the hAM assay, supporting astrocyte-microglia interaction. Selected pesticides will be evaluated in presence and absence of iMGs to elucidate microglial contribution in DNT.

In conclusion, by comparing the performance of the new glia-related assays to the historical DNT-IVB data, especially focusing on false negatives, we will evaluate whether these assays not only increase the biological relevance but also the predictive capacity of the DNT-IVB.

P242

Characterisation and applicability of an *in vitro* liver model coculturing four different cell types in 3D

N. Wewer¹, L. Rogalski¹, J. Böhme¹, M. Paul¹, D. Lichtenstein¹

¹German Federal Institute for Risk Assessment (BfR), Berlin, Germany

Question: Traditional 2D monocultures lack cell-cell and cell-matrix interactions and have been shown to exhibit less physiologically relevant behavior. Many toxicological responses in the liver depend on the interplay between various liver

cell types, which cannot be fully replicated in monocultures. To improve the predictability of human toxicity, we developed a 3D liver model by coculturing four different cell types as a spheroid, providing a more accurate *in vitro* representation of human liver physiology.

Methods + Results: Various cell lines, different cell numbers per spheroid, and suitable coculture media were evaluated to determine optimal culture conditions. The final model comprises hepatocytes (HepaRG), macrophages (THP-1), endothelial cells (HMEC-1) and hepatic stellate cells (HStEC), with 4,000 cells per spheroid in total to ensure cultivation without the formation of a necrotic core. The spheroids were maintained for six days with cell-type ratios resembling those found *in vivo* in human liver tissue. The model was functionally characterized by morphological assessment, fluorescence imaging of cell-specific markers, mRNA expression analysis, and quantification of liver-specific secretion markers, specific CYP-enzymes and transporters. Results of the 3D coculture model were compared with those from a 3D monoculture of HepaRG cells after three and six days to investigate the effects of a more physiological environment on hepatic function. To demonstrate the model's applicability, mono- and coculture spheroids were treated with different reference compounds known to target liver-related endpoints, such as steatosis, phospholipidosis, inflammation, fibrosis, and xenobiotic metabolism. The system exhibited endpoint-specific responses on various molecular levels confirming its suitability for studying multicellular interactions *in vitro*.

Conclusion: In conclusion, this 3D liver model is a promising *in vitro* system displaying relevant human liver physiology and enables the investigation of drug-induced disease mechanisms.

P243

Automated high-throughput screening of Engineered Human Cardiac tissues using myrPlate technology

M. Nazari-Jelani¹, C. McNulty^{2,1}, T. Meyer¹

¹Universitätsmedizin Göttingen, Pharmacology and Toxicology, Göttingen, Germany

²University College Dublin, School of Biomolecular and Biomedical Science, Dublin, Ireland

Advancing predictive, animal-free assays is essential for detecting cardioactive and cardiotoxic effects during early drug discovery. This study presents methodological advances in the application of engineered human myocardium models for quantitative, high-throughput screening in line with the 3R principles (Replacement, Reduction, Refinement).

Two human-derived 3D cardiac tissue models were evaluated: Engineered Human Myocardium (EHM) and Bioengineered Heart Muscle (BHM). Both were cultivated in a 48-well myrPlate system (myriamed GmbH), which features flexible poles of defined stiffness, enabling measurement of tissue contractility under physiologically relevant load. Human iPSC-derived cardiomyocytes were cast into fibrin hydrogels, and ten novel cardioactive compounds were tested. Quantitative analysis of the **force of contraction (FOC)** demonstrated both positive and negative inotropic responses, with several compounds showing concentration-dependent and time-dependent effects on EC₅₀ and Emax values. By adjusting pole stiffness, hypertensive loading conditions were simulated, supporting its use as a functional hypertension model.

To enhance scalability, the BHM model was optimised through the addition of human stromal cells, which accelerated tissue condensation and spontaneous beating, suggesting fibroblast-mediated mechanical and biochemical cues facilitate iPSC differentiation and 3D tissue formation. Data acquisition and analysis were automated using a Python-based analysis script linked to a MySQL database, enabling extraction of treatment timelines and generation of dose-response and time-course curves from high-throughput image data.

Together, these results demonstrate that engineered human myocardium models integrated with the myrPlate platform and automated analysis provide robust, quantifiable endpoints for phenotypic screening. This approach offers a scalable, reproducible, and human-relevant alternative to animal testing in cardiovascular pharmacology and toxicology research.

P244

From Microscopy to Metrics: Statistical Insights from the VICT3R Project

T. Tug¹, W. Dammann², J. Rahnenführer², F. Bringezu¹, R. Kellner¹, N. Simetska¹, J. Irwan¹, S. Fischer¹, S. E. Escher¹

¹Fraunhofer Institute for Toxicology and Experimental Medicine (ITEM), Division Safety Assessment and Toxicology, Hanover, Germany

²Technische Universität Dortmund, Department of Statistics, Dortmund, Germany

³Merck Healthcare KGaA, Chemical and Preclinical Safety, Darmstadt, Germany

The VICT3R project has been initiated to advance toxicology research by developing Virtual Control Groups (VCGs) aimed at significantly reducing the use of animals in such studies. The VICT3R database builds on previous work from the eTRANSafe initiative, utilizing extensive historical control data from animal toxicity studies to create VCGs that can serve as substitutes for concurrent control groups. To ensure regulatory acceptance, a comprehensive database of high-quality control data is being established, supported by advanced statistical and artificial intelligence methodologies.

One major focus area is the microscopic domain, encompassing histopathological findings represented in the SEND format (Standard for the Exchange of Nonclinical Data). This standardized structure ensures consistent data transfer from pharmaceutical companies to the U.S. Food and Drug Administration (FDA) and facilitates the integration of datasets from multiple institutions. The

microscopic data provide detailed descriptions of cell types, tissue alterations, and pathological lesions, serving as a rich source of information to characterize toxicological outcomes.

Data curation constitutes a critical foundation of the VICT3R framework. Each dataset undergoes systematic harmonization, involving ontology mapping, standardization of terminology, and rigorous quality control steps to ensure consistency across studies. Automated and manual validation processes detect inconsistencies, missing values, and format deviations, thereby enhancing data integrity and analytical reproducibility. The curated database thus provides a robust and transparent resource for subsequent statistical modeling and machine learning applications. By ensuring high-quality, standardized input data, the curation pipeline directly supports the generation of reliable, regulatory-compliant virtual control groups—contributing to the overarching goal of improving toxicological prediction while minimizing animal use in preclinical research.

Statistical analysis applies diverse methods to explore, evaluate, and interpret microscopic findings. Techniques such as modeling, variance decomposition, and clustering are used to detect associations and uncover patterns within the histopathological landscape. By assessing within- and between-study variability, these analyses help evaluate the reliability and transferability of virtual control groups and improve understanding of lesion frequencies and study heterogeneity.

P245

From urine to hepatocytes: An induced pluripotent stem cell (iPSC) based workflow for toxicity tests

N. Graffmann¹, C. Loerch¹, D. Herebian², C. Kordes¹, J. Adjaye^{1,3}

¹University Hospital Düsseldorf, Heinrich Heine University Düsseldorf, Institute for Stem Cell Research and Regenerative Medicine, Düsseldorf, Germany

²University Hospital Düsseldorf, Heinrich Heine University Düsseldorf, Department of General Pediatrics, Neonatology and Pediatric Cardiology, Düsseldorf, Germany

³University College London, EGA Institute for Women's Health- Zayed Center for Research Into Rare Diseases in Children (ZCR), London, United Kingdom

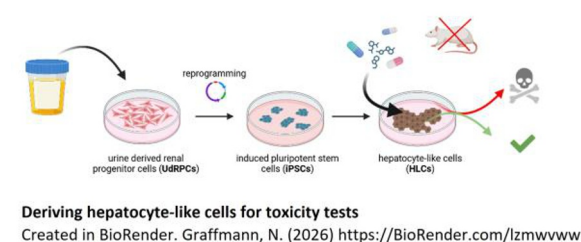
The current gold standards for assessing drug and toxin metabolism and to test novel drugs for hepatic diseases are animal models or isolated human primary hepatocytes (PHH). Both systems are not only associated with significant ethical concerns but are limited in their ability to predict toxicity and drug activity either because of species differences or because of culture-induced dedifferentiation. To overcome these limitations, hepatocyte-like cells (HLCs) generated *in vitro* from human induced pluripotent stem cells (iPSCs) are a promising novel tool.

Using urine derived renal progenitor cells (UdRPCs) as a source for generating iPSCs, we can collect material from patients of all ages and diseases. This allows us to cover various cytochrome P450 (CYP) 2D6 genotypes as well as common and rare diseases in our iPSC bank. By differentiating the iPSCs towards hepatocyte like cells (HLCs), we generate a robust tool for disease modelling and drug testing. Our improved HLC differentiation protocol enhances expression of the essential hepatic transcription factor farnesoid X receptor (FXR) by employing forskolin in the final differentiation step (Loerch et al., 2024). Basal CYP3A4 activity is increased by 5-fold and can be induced 1.5-fold further with rifampicin. Similarly, the addition of forskolin increases CYP2D6 activity up to 6-fold. HLCs derived with this novel protocol are able to fully metabolize tamoxifen and caffeine via distinct CYP450 pathways.

Thus, we propose iPSC-derived HLCs as a promising tool for future toxicity assessments and patient-specific drug tests.

Loerch, C., Szepanowski, L.-P., Reiss, J., Adjaye, J., and Graffmann, N. (2024). Forskolin induces FXR expression and enhances maturation of iPSC-derived hepatocyte-like cells. *Frontiers in Cell and Developmental Biology* 12.

Fig. 1



P246

From neural progenitor cell proliferation to neural network formation: refining human DNT assays for higher predictive power

R. Guzzo¹, A. S. Cheruvil Lilikumar¹, I. Scharkin¹, K. Bartmann², O. Myhre³, E. Zühr¹, E. Fritsche^{4,5}, K. Koch^{1,2}

¹Leibniz Research Institute for Environmental Medicine (IUF), JRG Koch, Düsseldorf, Germany

²DNTOX GmbH, Düsseldorf, Germany

³Norwegian Institute of Public Health (NIPH), Oslo, Norway

⁴Swiss Centre for Applied Human Toxicology (SCAHT), Basel, Switzerland

⁵University of Basel, Department of Pharmaceutical Sciences, Basel, Switzerland

Brain development relies on a complex interplay of key neurodevelopmental processes (KNDPs), such as neural progenitor cell (NPC) proliferation and neural network formation (NNF). Their disruption caused developmental neurotoxicity (DNT) which is associated with neurodevelopmental disorders. Given the limitations of current *in vivo* DNT guideline studies, an *in vitro* DNT testing battery (DNT-IVB) has been established covering eight KNDPs. To address uncertainties related to developmental timing and species differences, the fetal NPC-based proliferation assay and the rat neural network formation (rNNF) assay within the DNT-IVB were refined.

As a complementary model to the fetal NPC proliferation assay, hiPSC-derived NPC (hiNPC) neurospheres were generated using dual SMAD inhibition to model early embryonic NPC proliferation. After three days of compound exposure, proliferative capacity was quantified by BrdU incorporation. An initial screening of DNT-relevant pesticides from various chemical classes yielded results consistent with the fetal NPC assay. Ongoing testing of DNT-IVB positive and negative pesticides, along with compounds known to interfere with cell cycle regulation and mitotic spindle function, aims to further delineate developmental stage-specific sensitivities of proliferative processes.

To overcome species-related limitations of the rNNF assay, a human neural network formation (hNNF) assay was established to improve human relevance of network activity assessment. Neural activity is recorded on microelectrode arrays (MEAs) using co-cultures of hiPSC-derived excitatory and inhibitory neurons with primary astrocytes. To further enhance physiological relevance through greater glial diversity, human microglia-like cells (iMGs) were generated from genome-edited hiPSCs overexpressing CEBPA and SPI1. After eight days of differentiation, iMGs (IBA1+/TMEM119+/P2RY12+) were integrated into neuron-astrocyte networks. Protocols for neuron and astrocyte generation are currently being optimized, and the impact of iMG on network activity and chemical sensitivity will be systematically evaluated. The refined hNNF assay will subsequently be used to assess the DNT potential of selected pesticides.

Comparative evaluation of the refined assays will determine how integration of hiPSC-derived models and iMG involvement enhances the DNT-IVB's predictive power and human relevance, thereby increasing confidence in DNT-IVB data and supporting regulatory acceptance.

P247

An integrative workflow for internal dose-based classification of systemic toxicity using *in vitro* concentrations of bioactivity and PBK modeling

J. Brandt¹, P. Demuth¹, A. Weyrich¹, E. Fabian¹, S. Kolle¹, C. Gomes¹, K. Wiench¹, R. Landsiedel^{2,1}

¹BASF SE, Ludwigshafen, Germany

²Free University of Berlin, Pharmazie, Pharmakologie, Toxikologie, Ludwigshafen, Germany

1. Introduction

Non-animal data plays an increasingly important role in chemical safety assessment. However, for specific target organ toxicity after repeated exposure (STOT RE), robust approaches integrating toxicokinetics and toxicodynamics are lacking. The following workflow addresses this gap by translating external dose limits into substance-specific internal dose thresholds using physiology based kinetic (PBK) models and integrating transcriptomics as a new approach methodology (NAM) for bioactivity quantification.

2. Objectives

The project aim was to establish and evaluate a workflow for STOT RE classification using high-throughput transcriptomics to generate benchmark concentrations (BMC) for chemical compounds. Using PBK modeling, GHS guidance values on STOT RE for oral rat studies were converted to compound-specific internal concentrations, which were used to classify the compound based on the *in vitro* BMC.

3. Materials & methods

Initially, read-across is used to identify nearest neighbors with sufficient data, guiding the selection of test concentrations. The PBK model htk was parameterized with substance-specific physicochemical and kinetic data and applied to define internal dose limits based on GHS STOT RE class boundaries. In parallel, toxicodynamics were addressed by *in vitro* transcriptomics (RNA-Seq) in HepaRG cells to derive a transcriptomic point of departure (tPOD) via multiple statistical approaches (25th gene, 5th percentile, 1st mode) to realize a GHS classification.

4. Results

The NAM-based classification workflow was applied to N-Vinylpyrrolidone (NVP, CAS-Nr.: 88-12-0). RNA-seq analysis resulted in tPODs ranging from 66.2 - 300.0 µM. Substance-specific translation of the STOT RE classification limits of 10 and 100 mg/kg bw/day yielded internal dose limits of 32.4 and 323.9 µM. Using the most sensitive tPOD as a protective estimate results in a potential hazard classification of Category 2 for STOT RE, which matches the current classification of NVP.

5. Conclusion

The NAM-based classification workflow, integrating high-throughput transcriptomics and PBK modeling, offers a promising approach that may support hazard assessment for STOT RE. When applied to NVP, the method yielded a hazard classification aligning with existing GHS classifications derived from *in vivo* data, which supports the potential regulatory applicability of the approach. Further testing and validation is planned to confirm its robustness and reliability.

P248

Hazard assessment of micro- and nanoplastics: An integrated workflow of test material generation and *in vitro* assessment of uptake and bioactivity to support the OECD-CBC project

P. Demuth¹, H. Mangold², P. Schmidt³, S. Kolle¹, W. Wohleben⁴

¹BASF SE, Experimental Toxicology and Ecology, Ludwigshafen, Germany

²BASF SE, Polymer Recycling, Ludwigshafen, Germany

³BASF SE, Microplastics and Nanoplastics, Ludwigshafen, Germany

⁴BaA, Division Hazardous substances and biological agents, Berlin, Germany

Inhalation of air-borne micro- and nanoplastics (MNPs) can potentially be associated with adverse effects. New approach methods (NAMs) could help to extend the understanding of underlying mechanisms and identify critical properties of MNPs, including particle size, aging and fragmentation, which determine bioactivity. The Chemicals and Biotechnology Committee (CBC) at OECD recently initiated a project, led by South Korea, on the Safety Testing of Nanoplastics.

In support of the first and second phase of the OECD project –consisting of the test material generation, aging and fragmentation– the present study established a workflow to generate and characterize MNPs which mimic those found in the environment. We generated particles of PET, PBAT and three versions of PA, representing textile fragments, biodegradable agroplastics and degraded fishing gear, respectively. The workflow includes controls for aging-induced effects, specifically the isolation of aged MNP particles from the mixture with UV-degradation-generated oligomers. In support of the third phase of the OECD project –consisting of toxicity testing– the present study addressed the potential lung toxicity and the alveolar uptake of respirable MNP particles by applying two low-tier *in vitro* methods. A549 cells, cultivated at the air-liquid interface on permeable membranes were applied to analytically quantify the uptake of MNPs across a biological barrier by pyGCMS. Metabolic activity as well as release of lactate dehydrogenase and cytokines (IL-6, IL-8) were assessed to detect an impaired barrier integrity. In the Alveolar Macrophage Assay (AMA), which was developed to identify harmful particles posing a risk to human health, rat alveolar macrophages (NR8383) were exposed to MNP dispersions to assess activation, inflammation and cytotoxicity.

In total, 8 different MNPs were synthesized via several approaches and subsequently characterized regarding descriptors of molecular identity and of physical structure. Application of the A549 barrier model showed that none of the tested MNPs impaired barrier integrity in the *in vitro* system, thus allowing for quantification of MNP uptake.

This approach will help to provide fit-for-purpose reference MNPs, applicable for toxicological assessments. In parallel, the adaptation of low-tier *in vitro* assays to MNP testing depicts a crucial step towards a better understanding of how the diverse particle properties determine potential adversity.

P249

Integrating Primary Human Hepatocytes and TK6 Cells in 3D Co-Culture Systems for Enhanced Genotoxicity Evaluation

S. Stojanovic¹, S. Batti¹, L. Keuter¹, M. Niehues¹, M. Raschke¹, V. Ziegler¹

¹Bayer AG, Berlin, Germany

Genotoxicity testing is a crucial part of drug development, traditionally performed using *in vitro* assays and animal models to assess chromosomal damage, such as micronuclei (MN) formation. However, these conventional methods often produce inconsistent or *in vivo*-irrelevant results, partly due to differences in metabolic capacities.

To overcome these limitations, we aim to develop a human-relevant 3D co-culture microphysiological system (MPS). This system integrates primary human hepatocyte (PHH) liver spheroids, which provide metabolic competence, with human TK6 cells for MN assessment. The liver spheroid model not only provides drug metabolism, but it also allows additional readouts e.g. inclusion of the Comet Assay.

We utilized the HUMIMIC Chip2 microfluidic platform from TissUse GmbH. Primary human hepatocytes (PHHs) were seeded into multicavity membrane inserts, where they self-assembled into liver spheroids. We monitored the viability and functionality of these spheroids over 12 days by measuring LDH activity and urea release. Additionally, metabolic activity was assessed by treating the spheroids with a cocktail of reference drugs serving as substrates for phase I and phase II enzymes, with metabolite formation analyzed by LC-MS.

Separately, TK6 cells were seeded into the HUMIMIC Chip2 and cultured in the same medium used for the liver spheroids. Their growth rate and baseline MN frequencies were measured by flow cytometry and compared to results from standard static cultures. Initial tests with genotoxic agents like Mitomycin C and Vinblastine showed a clear increase in MN formation in TK6 cells in circulation, demonstrating functionality of the assay system.

Afterwards, TK6 cells were introduced into the HUMIMIC Chip2 liver chip to establish a microfluidic co-culture system. Basic characterization of this combined model produced results comparable to the individual cultures, supporting further development. The next step will involve testing reference drugs to assess the assay's proficiency.

Ultimately, we aim to develop a model incorporating all relevant components to perform physiologically relevant *in vivo*-like MN test.

P250

Assessment of the effects of chemicals on selected *in vitro* models for addressing metabolic syndrome in the liver for the ENVESOME project

V. Kremepe¹, R. Puts¹, D. Deepika¹, V. Kumar¹, D. Morais Leme^{1,2}, P. Marx-Stötinger¹

¹German Federal Institute for Risk Assessment (BfR), Department Pesticides Safety, Berlin, Germany

²Federal University of Paraná (UFPR), Department of Genetics, Curitiba, Brazil

The ENVESOME consortium uses a science-based exposome framework that integrates systems biology, human biomonitoring and *in vitro* data. This approach strengthens our understanding of how chemical and environmental stressors, including air pollution, light and noise, contribute to disease. The exposome encompasses all environmental exposures experienced by an individual throughout their life, providing a comprehensive approach to linking exposure to health outcomes. The project aims to address major data gaps by updating limit values for chemicals and possible persistent contaminants by integrating other environmental stressors than chemicals. This will be achieved through new approach methodologies (NAMs), as well as quantitative adverse outcome pathways (qAOPs) and networks (AONs), which focus on cardiovascular, respiratory, metabolic, neurodegenerative and immune-related disorders.

Within this framework, our work focuses on metabolic disruption associated with the exposome. Specifically, we explore the mechanisms that lead to liver steatosis, which is a key event in metabolic-associated steatotic liver disease (MASLD). We use a set of *in vitro* liver models to study the effects of metabolism-disrupting chemicals (MDCs), progressing from 2D cell lines to more complex 3D and multicellular systems. Here, we present the first results from assays conducted in HepaRG and HepG2 cells of selected chemicals, including polychlorinated biphenyls (PCBs), pesticides, plasticisers, toxic metals and perfluoroalkyl substances (PFAS), which have been identified as potential steatotic agents.

By combining *in vitro* data with exposome profiling, ENVESOME will help elucidating molecular mechanisms linking chemical exposure and other environmental stressors to steatosis and metabolic disease. The identified chemicals of concern will undergo further assessment in advanced liver models and omics-based analyses. This will support ENVESOME's goal of improving the prediction and mitigation of metabolic health risks posed by environmental pollutants.

P251

A primary hepatocyte model to assess species-specific CAR activation and hepatocarcinogenic risk of compounds

A. Scheffschick^{1,2}, O. S. Talkhan^{1,2}, G. Schicht^{1,2}, V. P. Brandt^{1,2}, M. Vogler^{1,2}, M. Goettel³, A. Dör⁴, E. Fabian⁵, D. Seehofer⁶, R. Landsiedel^{6,5}, G. Damm^{1,2}

¹Universität Leipzig, Leipzig, Germany

²University of Leipzig Medical Center, Department of Hepatobiliary and Transplantation Surgery, Leipzig, Germany

³BASF SE, Global Toxicology Agricultural Solutions, Limburgerhof, Germany

⁴BASF Agricultural Solutions US LLC, Regulatory Toxicology Crop Protection, Research Triangle Park, NC, United States

⁵BASF SE, Experimental Toxicology and Ecology, Ludwigshafen, Germany

⁶Free University of Berlin, Pharmazie, Pharmakologie und Toxikologie, Berlin, Germany

The constitutive androstane receptor (CAR) regulates hepatic xenobiotic metabolism by inducing cytochrome P450 (CYP) enzymes and mediates non-genotoxic hepatocarcinogenesis in rodents by promoting hepatocyte proliferation. Phenobarbital (PB), an indirect CAR activator, induces liver tumors in rodents but not in humans, indicating species-specific response on CAR activation. Since uncontrolled proliferation is a hallmark of tumor formation, *in vitro* systems that capture proliferation are valuable for assessing carcinogenic potential of test substances. Here, we aimed to establish a primary hepatocyte model enabling simultaneous assessment of hepatocyte proliferation and CYP activity to investigate species-dependent CAR responses.

Primary mouse hepatocytes (PMH; male and female) and human hepatocytes (PHH; male) were treated with PB (200 and 1000 µM) or with epidermal and hepatocyte growth factors (EGF, HGF; 50 ng/ml each) as positive controls w/o steatotic conditions. Cell viability was monitored by AlamarBlue™ and BCA assays, morphology by microscopy, and proliferation by Ki67 and BrdU staining. CYP activities and mRNA expression were analyzed by AROD assays and qPCR. Obtained data were compared to results from strain-matched male C57BL/6J mice, which received 500 ppm PB.

EGF/HGF stimulated proliferation in all groups, validating the cells' ability to undergo proliferation. Steatotic and non-steatotic PMH proliferated, while steatosis suppressed proliferation in PHH. PB significantly induced proliferation in male PMH (5-fold) but not in PHH. Female PMH showed proliferation after 48 hours (20-fold), however not significantly, and proliferation was repressed after 72 hours. In earlier performed studies *in vivo*, PB increased proliferation up to ~10-fold. CYP activities and mRNA levels declined over time *in vitro*, suggesting dedifferentiation, with higher PB-induced CYP RNA expression observed after 48

hours than 72 hours (up to 10-fold RNA induction). In vivo, PB produced stronger CYP activities and RNA induction (up to ~50-fold).

Overall, our in vitro data demonstrate species-differences in PB-mediated proliferation consistent with known in vivo tumorigenic outcomes: PMH showed strong CAR-associated proliferation, whereas PHH were resistant, indicating divergent regulatory mechanisms. This primary hepatocyte model provides a useful tool to assess hepatocarcinogenic risk, although optimization—e.g., 3D or sandwich cultures—is needed to improve robustness.

P252

Leveraging Historical Control Data to Identify Covariates in 28-Day Repeated Dose Toxicity Studies

N. Becker¹, M. Dammann¹, K. Becker¹, F. M. Kluxen², J. L. Cairns¹, D. Funk-Weyer¹, C. Gomes¹, R. Buesen¹, M. Dilger¹

¹BASF SE, Experimental Toxicology and Ecology, Ludwigshafen, Germany

²BASF SE, Agricultural Solutions, Limburgerhof, Germany

In conventional vertebrate toxicology studies, control groups are essential for establishing a reference against which treatment effects are compared. Historical Control Data (HCD) aggregates control group data across multiple studies and provides a powerful framework for validating control responses [1, 2]. It plays a critical role in the identification of treatment-related effects by identifying cases where control groups rather than treated groups deviate from the biological baseline. Additionally, HCD enables systematic investigation of external factors that may influence control responses, such as environmental conditions and study design variables.

The current study presents a comprehensive analysis of HCD derived from 185 28-day repeated dose toxicity studies conducted at BASF between 2009 and 2023. Using a combination of regression analysis, significance testing, principal component analysis (PCA), and effect size estimation, we systematically identified covariates that impact the HCD distribution. Variables such as study date, season, sex, starting age, and vehicle exhibited consistent and meaningful influence on control data. In contrast, factors including the presence of additional blood samples, number of animals per cage, cage enrichment, and the inclusion of urinalysis were found to have no or negligible effects on the assessed HCD.

These findings strengthen the scientific foundation when integrating HCD in toxicological assessments by identifying filter criteria for more targeted and biologically meaningful HCD. They also challenge the current paradigm of limiting HCD usage to a five-year window in lieu of applying evidence-based applicability timespans. Additionally, our results provide a basis to reduce animal use in mandatory in vivo studies by constructing Virtual Control Groups (VCGs), which could serve as substitutes for concurrent controls in selected study designs [3].

References:

1. Kluxen, F. M. et al., Using Historical Control Data in Bioassays for Regulatory Toxicology. *Regul. Toxicol. Pharmacol.* 125, 105024 (2021).
2. Kluxen, F. M. et al., Historical control data of rare events: Issues, chronological patterns and their relevance for toxicological evaluations. *Regul. Toxicol. Pharmacol.* 151, 105673 (2024).
3. Steger-Hartmann, T. et al., Introducing the concept of virtual control groups into preclinical toxicology animal testing. *ALTEX* 37(3), 343–349 (2020).

P253

Performance of Different Approaches to Generate Virtual Control Groups

N. Becker¹, M. Dammann¹, K. Becker¹, F. M. Kluxen², J. L. Cairns¹, D. Funk-Weyer¹, C. Gomes¹, R. Buesen¹, M. Dilger¹

¹BASF SE, Experimental Toxicology and Ecology, Ludwigshafen, Germany

²BASF SE, Agricultural Solutions, Limburgerhof, Germany

Virtual Control Groups (VCGs) could be a potential 3R approach in toxicological study design as an ethically favorable alternative to traditional Concurrent Control Groups (CCGs). By stringent filtering of control animal data from previously conducted studies (Historical Control Data, HCD), VCGs can be generated and used instead of CCGs to determine treatment relation, if statistical integrity or biological relevance assessments are not compromised. This study investigates the development, validation, and application of VCGs in 28-day oral toxicity studies in rats.

Using a HCD database of 185 studies performed at BASF between 2009 and 2023, four distinct approaches for generating VCGs were explored: individual animal sampling, whole-study sampling, domain-wise sampling, and simulation-based modeling (Figure 1). Each method was applied to twelve 28-day legacy studies, and the resulting statistical results for the various endpoints in each study were compared to those derived from conventional CCGs. VCGs were generated using a multi-iteration approach to enhance statistical robustness.

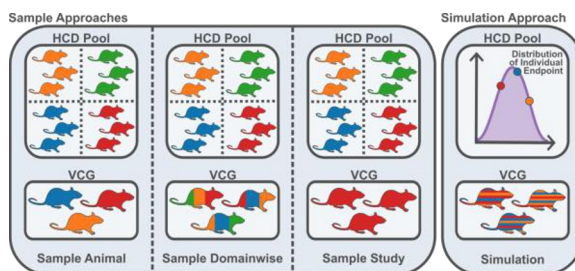
Among the evaluated methods, simulation-based VCGs demonstrated superior performance in terms of flexibility, predictive accuracy, and reproducibility. However, the analysis also highlighted challenges in modeling endpoints with high intrinsic intra- and interstudy variability, like elements of the Functional Observational Battery (FOB).

A reanalysis of three studies, each involving blinded analysis by subject matter experts for the investigated endpoints, found that multi-iteration VCGs generally accurately captured population characteristics. The VCG generation procedure provided a stable baseline across most endpoints, potentially making the VCGs more robust than traditional CCGs.

In conclusion, the results support further investigation of the VCG concept, identification of mitigation strategies for endpoints where modeling is still challenging, and exploration of the path toward regulatory acceptance.

Figure 1: Overview of VCG generation methods. Approaches include sampling individual animals, entire control groups, or domain-specific data from filtered HCD. The simulation method uses endpoint distributions to probabilistically generate virtual control animals.

Fig. 1



P254

Closing the Regulatory Gap in Developmental Immunotoxicity: Human-Relevant Approaches for Next-Generation Chemical Safety Assessment

J. Tigges¹, C. Spruck¹, K. Koch^{1,2}, F. A. Grimm³, E. Fritsche^{2,4,5}

¹Leibniz Research Institute for Environmental Medicine (IUF), Düsseldorf, Germany

²DNTOX GmbH, Düsseldorf, Germany

³Clariant Produkte (Deutschland) GmbH, Frankfurt a. M., Germany

⁴Swiss Centre for Applied Human Toxicology (SCAHT), Basel, Switzerland

⁵University of Basel, Department of Pharmaceutical Sciences, Basel, Switzerland

The developing immune system is a highly sensitive target for chemical exposure during prenatal and early postnatal life. Epidemiological evidence links early-life environmental exposures to immune-mediated outcomes such as allergies, reduced vaccine responses, and autoimmune diseases, highlighting the public health relevance of developmental immunotoxicity (DIT). Despite these concerns, current regulatory frameworks rarely include dedicated DIT assessments. Under the EU REACH Regulation, DIT testing—such as inclusion of the DIT cohort in OECD TG 443—is only triggered through weight-of-evidence evaluations. As emphasized in the ECHA's *Key Areas of Regulatory Challenge* document, this approach can overlook critical developmental windows and early immune effects.

The European Green Deal and 3R policies drive the shift toward human-relevant, animal-free safety assessment. DIT testing currently relies on in vivo rodent studies which, beyond ethics, show limited predictivity for human immune development due to species-specific differences in ontogeny, creating a scientific and regulatory gap.

To address this, **new approach methodologies (NAMs)** that mechanistically reflect key processes of immune development – e.g. differentiation, migration, and proliferation – are urgently needed. This paradigm shift is reflected in ongoing initiatives including the European Partnership for the Assessment of Risks from Chemicals (PARC) and the international DIT working group lead by the Johns Hopkins Center for Alternative to Animal Testing, which promote DIT NAM development. Proof-of-concept systems, such as **human stem cell-based assays modeling hematopoietic stem cell differentiation and the CD34 assay developed by Khan et al. (2023)** demonstrate the feasibility of assessing chemical impacts on immune differentiation in vitro. However, no validated or regulatory-accepted assays currently exist. The same holds for **adverse outcome pathways** for DIT, which are essential to mechanistically anchor such assays and identify critical key events for NAM development and regulatory assessment.

Embedding NAMs within **Integrated Approaches to Testing and Assessment and Defined Approaches**, combined with **physiologically based pharmacokinetic modeling**, will link mechanistic in vitro data to realistic human exposure. **Mirroring the developmental neurotoxicity-IVB roadmap**, this strategy could accelerate the transition toward a human-relevant, transparent, and sustainable DIT testing framework.

P255

The in vitro transgenic rodent assay in primary MutaMouse hepatocytes compared to the mammalian cell gene mutation assay using the HPRT gene

A. Goepfert¹, K. M. Ronnenberg¹, C. Ruelker¹, S. Spang¹, N. Honarvar¹, R. Landsiedel^{1,2}

¹BASF SE, Experimental Toxicology and Ecology, Ludwigshafen, Germany

²Free University of Berlin, Pharmazie und Toxikologie, Berlin, Germany

Gene mutations can be detected in mammalian cells *in vitro* using indicator genes such as the hypoxanthine-guanine-phosphoribosyltransferase (HPRT) gene. These assays have been adopted as OECD test guidelines (TG, e.g. OECD TG no. 476) and are used for regulatory purposes. The *in vitro* transgenic rodent assay (TGRA) in primary MutaMouse hepatocytes is a novel approach for the detection and quantification of gene mutations. Its methodology follows the same principles as the *in vivo* TGRA, an *in vivo* gene mutation assay with regulatory adoption (OECD TG no. 488). Although the potential of the *in vitro* TGRA to

identify mutagens has been reported, its performance compared to an established *in vitro* gene mutation assay has not been reported.

This study compared the *in vitro* TGRA with the HPRT assay using ten known *in vivo* mutagens. The *in vitro* TGRA correctly identified all ten mutagens, whereas the HPRT assay identified only nine. Benchmark concentration (BMC) modelling for the nine substances detected by both assays revealed overlapping confidence intervals for six compounds, indicating comparable sensitivity. For three mutagens, the HPRT assay yielded lower BMC intervals.

Additionally, eight substances known to be non-mutagenic *in vivo* tested negative in the *in vitro* TGRA. While increased cytotoxicity did not induce increased mutant frequencies, it reduced DNA yield, thereby impairing mutagenicity assessment.

The results of this study contribute to the understanding of the sensitivity and robustness of the *in vitro* TGRA and provide essential information for the validation of the assay.

P256

Alternative Vertebrate and Invertebrate Model Organisms Show Similar Sensitivity as Rodents to a Diverse Set of Chemicals

G. Hayot¹, C. Cramer von Clausbruch¹, C. Weiss¹, T. Dickmeis¹

¹Karlsruhe Institute of Technology (KIT), IBCS-BIP, Eggenstein – Leopoldshafen, Germany

Regulatory bodies aim at phasing out the use of protected animals for toxicity testing, without impairing the protection of human health and the environment from chemical risks. New approach methodologies intend to replace test systems employing animals, notably mammals, in toxicology research and regulation, while increasing the throughput of toxicity testing. The PrecisionTox consortium (www.precisiontox.org) aims at OMICS based toxicity prediction for humans using non-sentient organisms (NSOs) across the tree of life.

In this context, we systematically produced toxicity data from five distantly related alternative nonmammalian model organisms and a human cell line. We observed that *Daphnia magna* and *Danio rerio* embryos were susceptible to more chemicals than *Xenopus laevis* embryos, *Drosophila melanogaster* and *Caenorhabditis elegans*.

Clustering of the EC50 values showed that the toxicity of compounds across the model organisms revealed groups enriched for features of chemical class and mode of action. We observed that the toxicity of chemicals was highly correlated across the model organisms, and we showed that the average toxicity values for the model organisms closely matched published values for rodents. Our findings suggest broad conservation of chemical toxicity under standardized experimental conditions across a phylogenetically diverse set of model organisms, providing a conservative estimate of mammalian toxicity. To further explore the conservation of molecular mechanisms underlying the conserved toxicity, we then focused on a subset of structurally related chemicals and used an OMICS-based approach, combining RNA sequencing and untargeted metabolome analysis in *Danio rerio* embryos and a human cell line. In this way, we aimed to define molecular signatures of toxicity and to test their correlation with the structure of the chemicals. The molecular pathways altered after chemical exposure overlapped across the compounds and the species, hinting at common modes of action for this subset of chemicals.

P257

LC-MS/MS-coupled cell-based assays for identification of potential endocrine disruptors of thyroid peroxidase activity

D. Hilgefort¹, S. Arnold², F. Schumacher¹, L. Dahmen², N. Hambruch², R. Landsiedel^{1,3}, K. Renko², B. Kleuser¹

¹Free University of Berlin, Institute of Pharmacy, Berlin, Germany

²German Federal Institute for Risk Assessment (BfR), German Centre for the Protection of Laboratory Animals (Bf3R), Berlin, Germany

³BASF SE, Experimental Toxicology and Ecology, Ludwigshafen, Germany

Thyroid peroxidase (TPO) is a key enzyme in thyroid hormone synthesis, catalyzing the iodination of tyrosine residues in thyroglobulin and the coupling of iodotyrosines to form bound triiodothyronine (T3) and thyroxine (T4). Interference with TPO activity disrupts thyroid function and leads to adversities, as demonstrated *in vitro* and *in vivo* and documented in respective AOPs (e.g. AOP 42, 363, 365). Given the increasing concern about endocrine-disrupting chemicals (EDCs) in the environment and the fact that regulatory accepted test methods are still animal-based, robust and mechanistically relevant *in vitro* assays to identify TPO inhibitors are urgently needed. The development of such methods aligns with the goals of New Approach Methodologies (NAMs), which aim to provide human-relevant, ethical, and mechanistically driven alternatives to animal testing.

In this study, we are developing LC-MS/MS-coupled cell-based assay systems expressing functional TPO to evaluate the enzyme's disruption by potential thyroid hormone system disruptors. These cell-based systems are compared directly to their lysate-based counterparts and current protocols, focused on fluorometric detection of peroxidase activity. While allowing a simple and flexible application, lysate-based assays lack physiological complexity of intact cells and do not allow the measurement of general cell toxicity as important confounder. In contrast, cell-based assays have the advantage of maintaining enzyme localization, endogen cofactor availability, and potential metabolic interactions. Moreover, they allow the simultaneous assessment of cell viability, providing an additional layer of information that can distinguish between specific enzyme inhibition and general cytotoxicity. Also, the simultaneous detection of iodotyrosines and coupled reaction products might enable to distinguish effects of test substances on different catalytic activities of TPO enzyme.

LC-MS/MS-based quantification of the reaction products moniodotyrosine (MIT), diiodotyrosine (DIT) and thyroxine (T4) enables direct measurement of TPO activity. Unlike current fluorimetric protocols, which assess only general peroxidase activity and rely on surrogate substrates, LC-MS/MS detection captures the actual biochemical conversion catalyzed by TPO. This approach increases analytical specificity and might provide deeper mechanistic insight into possible mode of actions (MoAs) of environmental contaminants.

P258

Conversion of DNA repair pathways during PTELC differentiation as a possible reason for susceptibility to nephrotoxins

S. Hartmann¹, I. M. Mboni Johnston¹, N. Schupp¹

¹Uniklinik Düsseldorf, Toxikologie, Düsseldorf, Germany

Introduction

The kidney is constantly exposed to nephrotoxins and oxidative stress. Proximal tubular epithelial cells (PTECs), responsible for most resorption processes are highly vulnerable to injury. To maintain tissue integrity, PTECs must repair DNA damage or undergo apoptosis when damage is irreparable. After apoptosis, surviving cells may repair, or dedifferentiate, proliferate, and restore the tubular epithelium, supported by a small local stem-like cell population. However, regenerated cells *in vivo* often show reduced function, contributing to progressive renal impairment and potentially chronic kidney disease.

Objective

This study evaluated whether human proximal tubular epithelial-like cells (PTELCs) derived from human induced pluripotent stem cells (hiPSCs) provide a physiologically relevant model for nephrotoxicity testing. We examined how differentiation influences oxidative stress responses, toxin induced susceptibility, and DNA damage dynamics.

Methods

PTELCs were generated from hiPSCs using a one-step protocol. Gene expression changes in DNA repair and redox pathways were analysed by RT-qPCR. Functional maturation was assessed through evaluation of transport function using flow cytometry and microscopy, and epithelial integrity was evaluated by transepithelial electrical resistance measurement. DNA damage after exposure to cisplatin and other nephrotoxins at defined differentiation stages was quantified with the alkaline comet assay.

Results

Transporter activity and intact epithelial resistance confirmed successful PTELC maturation. During differentiation, cells showed downregulation of stem cell-associated DNA repair pathways induced by double-strand breaks, such as homologous recombination (HR) and upregulation of repair mechanisms typical of mature epithelia. Cisplatin exposure revealed a substantial differentiation-dependent variation in DNA damage formation, along with altered levels of mature PTELC markers and transporters.

Conclusion

hiPSC-derived PTELCs reproduced essential features of proximal tubular cell biology and changes in DNA repair capacity and susceptibility to the nephrotoxin cisplatin during differentiation. These findings support their use as a meaningful *in vitro* model for renal toxicity testing.

P259

Metals meet the Worm: Bioavailability of Nickel and Cobalt in *Caenorhabditis elegans*

M. F. Schröder¹, T. Dohmann¹, A. Thiel¹, T. Schwerdtle², V. Michaelis¹, J. Bornhorst¹

¹Bergische Universität Wuppertal, Food Chemistry with Focus on Toxicology, Wuppertal, Germany

²Max Rubner-Institut (MRI), Karlsruhe, Germany

Nickel (Ni) and Cobalt (Co) naturally occur in the Earth's crust and are ubiquitously present, mainly in the oxidation state +II. Due to their important roles in lithium-ion batteries, the metals' use in modern technologies continues to increase. As their presence in everyday products rises, the risk of improper disposal increases as well, leading to a higher entry of these toxic metals into the environment. Because of that, Co and Ni no longer pose risks only through respiratory exposure (factories, mines) or dermal contact (jewelry), but also through exposure via the food chain. The effects of oral uptake of these metals are still insufficiently understood, especially with regard to combined exposure, which represents the most realistic scenario at this point.

To investigate the cellular uptake of these metals upon oral exposure, we used the multicellular nematode *Caenorhabditis elegans* (*C. elegans*) as a model organism. We showed that Co(II) and Ni(II) uptake in *C. elegans* is not only influenced by their individual concentrations, but also by the presence of the respective other metal, with combined exposure resulting in decreased levels of both metals compared to their single exposure. Since specific transporters for Co(II) and Ni(II) uptake are not yet known, we hypothesize that their uptake is actively regulated by non-specific transporters for divalent metal cations, namely

Divalent Metal Transporter 1 (DMT-1) and Transient Receptor Potential Cation Channel Subfamily M Member 7 (TRPM-7), and that competition between Co(II) and Ni(II) for these transporters occurs. *C. elegans* features orthologues for both of these human transporter-encoding genes.

We used loss-of-function mutants of DMT-1 orthologue *smf-3*, as well as of TRPM-7 orthologues *glt-1* and *gon-2*, to assess the impact of each transport protein on the uptake of Co(II) and Ni(II) compared to the wild type (N2). To this end, worms were exposed to different concentrations of the metals, comparing single and combined exposures, selected ratios representing their relative abundance in lithium-ion batteries, and two exposure times (1 h and 24 h). The transporters' impact was then evaluated via worm survival rate and via the bioavailability of Co(II) and Ni(II). These data will improve the understanding of their uptake mechanisms and bioavailability in order to identify potential detoxification strategies.

P260

Impact of doxorubicin and DNA repair/DDR inhibitors on cardiovascular differentiation and function of hiPSC

L. Meßling¹, G. Fritz¹

¹Institute of Toxicology, Düsseldorf, Germany

Introduction: Anthracyclines, such as doxorubicin (Dox), are chemotherapeutic agents widely used to treat various cancers, including breast cancer, leukemia, and lymphoma. However, their use is limited by dose-dependent irreversible cardiotoxicity. Endothelial cells (EC) play a key role in vascular homeostasis and act as a barrier against drugs like Dox. Understanding EC stress responses to Dox and modulators of DNA repair and damage response (DDR) (Olaparib, Entinostat, Dexamethasone, ICRF193) is essential for alleviating cardiotoxic effects of anticancer therapeutics. **Objectives:** The primary objective was to evaluate the impact of Dox and selected modulators on cardiovascular cells at different differentiation stages, focusing on hiPSC-derived ECs, as a 3R-compliant experimental approach. **Materials and Methods:** Human induced pluripotent stem cells (hiPSCs) were differentiated into ECs. Progenitor ECs were harvested on day 4 and fully differentiated EC on day 6. Differentiation and cellular responses were assessed by analysis of mRNA expression, cytotoxicity (Alamar blue), cell proliferation (EdU), drug transport (FACS), and DNA damage, replication stress, and barrier function via immunofluorescence. **Results:** Differentiation into ECs was confirmed by detecting downregulated expression of stem cell markers and upregulated endothelial markers, comparable to those in primary human umbilical vein endothelial cells (HUVEC). Progenitor EC exhibited higher sensitivity to the tested compounds than undifferentiated hiPSC and fully differentiated EC. A marked decrease in cell proliferation was observed during differentiation. Barrier function analysis revealed that Dox severely compromised the integrity of the endothelial monolayer and downregulated junction genes. Dox induced DNA damage and activated replicative stress responses in a dose-dependent manner. The impact of pharmacological modulators on replicative stress response remains under investigation. Additionally, drug transport analysis showed stable Dox import/export capacity across all cell stages. **Conclusion:** Dox and the tested modulators exhibit significant differentiation stage-specific toxicity, particularly in progenitor EC, and affect differentiation accuracy. Using a hiPSC-based cardiovascular differentiation model is considered a useful, human-relevant 3R approach to understand the mechanisms of anthracycline-induced cardiotoxicity and to develop cardioprotective strategies in cancer therapy.

P261

Comparison of ToxCast derived effect levels with EchA based classification thresholds applying in vitro to in vivo extrapolation (IVIVE) strategies

P. Demuth¹, E. Fabian¹, J. L. Cairns¹, V. Gir², L. Simeon³, D. Funk-Weyer¹, R. Landsiedel^{1,4}

¹BASF SE, Experimental Toxicology and Ecology, Ludwigshafen, Germany

²BASF SE, Digitalization, Ludwigshafen, Germany

³BASF SE, Computational Biology, Ludwigshafen, Germany

⁴Free University of Berlin, Pharmazie, Pharmakologie und Toxikologie, Berlin, Germany

New approach methods (NAMs) can help to assess the effects that chemical compounds have on biological systems without the use of animal data. While in vivo studies apply predefined upper dose limits (e.g., 1,000 mg/kg), test concentrations of in vitro methods are often not predefined and use very high concentrations, e.g. up to the solubility limit. This is bearing the risk of generating irrelevant and false positive results. In vitro to in vivo extrapolation (IVIVE) is enabling translation of in vitro test concentrations to in vivo exposure doses. This is not only central to Next Generation Risk Assessment (NGRA) but can also be applied to better understand the in vivo relevance of in vitro results (<https://doi.org/10.1089/aivt.2023.0018>).

Within this project we evaluated how STOT-RE hazard classifications (which are largely based on in vivo data) correlate with respective classifications derived from results of in vitro studies. For this we used publicly available databases (ToxCast and harmonized CLP classification databases, respectively) and IVIVE models.

CLP classifies substances according to their hazard and assigns hazard statements (H-phrases). The classification criteria are i.a. based on in vivo studies with distinct doses limiting for each category within a hazard class. These were compared to the effect concentrations extracted from the ToxCast database that were translated to corresponding in vivo doses by IVIVE applying physiologically based pharmacokinetic (PBPK) modeling. Model specific input parameters were either derived from the ToxCast database or QSAR-generated and included hepatic clearance (Cl_{int}), fraction unbound to plasma (F_{ub}) and the apparent permeability coefficient (P_{app}). Where experimental intrinsic clearance data was unavailable, a worst-case assumption was applied by setting Cl_{int} to zero.

Across the 2755 compounds analyzed, 2019 have hazard classifications associated with systemic toxicity, while 736 are not classified in this regard. IVIVE-derived doses were compared to the substances with and w/o classification to evaluate the correlation between in vivo-derived and in vitro-derived doses and the corresponding hazard classification and categorization.

This demonstrates that integrating PBPK modeling with curated in vitro effect data can be used to assign hazard classes and categories. And this can be used to assess the correlation of in vitro- and in vivo derived classifications.

P262

Impact of Genotoxic Stress on developmental processes of *Caenorhabditis elegans*

E. Inan¹, B. Jeyakumar¹, J. Krautstrunk¹, G. Fritz¹

¹Heinrich Heine University Düsseldorf, Institute of Toxicology, Düsseldorf, Germany

Background

DNA damage response (DDR) pathways are essential for maintaining genomic integrity and enabling normal development. Disruptions in these mechanisms can cause developmental defects, infertility, or lethality, particularly under genotoxic stress. This study aimed to investigate the impact of mutation in distinct DDR components on developmental and reproductive outcomes in the 3R compliant model organism *Caenorhabditis elegans* following exposure to the DNA-crosslinking anticancer drug cisplatin (CisPt).

Method

C. elegans strains carrying mutations in key DDR-related genes were exposed to CisPt in order to assess their sensitivity to CisPt-induced genotoxic stress. Developmental and reproductive endpoints were evaluated, including brood size, hatching rate, and early larval development arrest (L1 arrest). These parameters were measured both under control conditions and after CisPt exposure to distinguish between the influence of DDR genes on developmental processes under basal situation and following genotoxic insult.

Result

DDR mutants exhibited distinct response patterns. Several mutants, particularly those defective in DNA damage sensing (*atm-1*, *atf-1* and *cep-1*), as well as base excision repair (BER) involving *parp-1* and *nth-1*, already showed reduced fertility under untreated conditions, indicating that these genes are required for normal germline and embryonic development. Despite their overall lower brood sizes, these strains displayed no pronounced response to CisPt treatment and no significant differences in hatching rate compared to wild type. In contrast, the *ercc-1* mutant defective in nucleotide excision repair (NER) showed the strongest sensitivity to CisPt, characterized by severe reductions in fertility, markedly decreased hatching rate, and a high proportion of L1 larval arrest upon CisPt treatment. These findings suggest that especially defects in NER lead to pronounced developmental sensitivity to DNA crosslinking agents.

Conclusion

Our results demonstrate that DDR pathways contribute to developmental stability and resistance against endogenous DNA damage and following genotoxic stress. While DNA damage sensors and BER components appear essential for maintaining basal fertility, the NER gene *ercc-1* plays a particularly critical role in protecting both reproductive and embryonic development from CisPt-induced DNA damage. These findings emphasize the importance of intact DNA repair systems for resilience during early life stages.

P263

Establishing a zebrafish neurosphere assay as in vitro culture for DNT testing

J. Brakus¹, B. Kühne¹, N. Ohnesorge¹, M. Barenys¹

¹German Federal Institute for Risk Assessment (BfR), German Centre for the Protection of Laboratory Animals (Bf3R), Berlin, Germany

The OECD/EFSA developmental neurotoxicity in vitro battery (DNT-IVB) has been developed to assess the potential impacts of substances on neurodevelopment. However, it currently lacks new approach methods (NAMs) to evaluate behavioral changes. To address this aspect, the OECD expert group on Developmental Neurotoxicity (Project 4.124: New Guidance Document on Developmental Neurotoxicity (DNT) in vitro assays) is focusing on identifying key aspects for behavioral assessment in zebrafish and creating standardized protocols. We propose that adding a zebrafish neurosphere assay to the battery could enhance the interpretation of behavioral results, improving the assessment of their relevance to humans using a parallelogram approach.

Our aim is to develop an *in vitro* culture for DNT toxicity testing in zebrafish neurospheres, mimicking specific assays of the already existing human-based DNT-IVB and assessing the endpoints of proliferation, migration and differentiation. We have successfully generated zebrafish neurospheres by isolation and dissociation of 48 hour post-fertilization (hpf) zebrafish brains. We have established a serum-free proliferation medium with growth factors, which enables these neurospheres to proliferate for ca. 14 days in suspension. Following mechanical passaging, neurospheres are plated on an extracellular matrix containing PDL-Laminin to evaluate neural progenitor cell migration,

revealing preliminary findings of radial migration and neuronal differentiation assessed by immunostaining of the migrating area. Further optimization of the protocols to immunostain astrocytes and oligodendrocytes is needed for the establishment of the method.

In the next phase, we will evaluate a set of well-established positive and negative compounds and compare the results with the ones of the human neurosphere assay and zebrafish behavioral assays. Our novel approach aims to enhance chemical hazard assessment for DNT risk in humans by combining human cell-based assays with zebrafish whole organism testing, while also considering other methods within the OECD's IVB framework.

P264

Exploring toxic histopathology in the larval zebrafish model

B. Bauer¹, S. Jenabi¹, H. Hintzsche¹

¹University of Bonn, Food Safety, Bonn, Germany

The need for alternative in vivo models has become increasingly urgent to reduce reliance on traditional mammalian testing, improve compliance with the 3R principle of humane experimental technique, and enhance throughput in toxicity screening. As small vertebrates, larval zebrafish offer a promising model due to their genetic and physiological similarities to humans, rapid development, and ease of genetic manipulation for generating transgenic reporter lines. This study investigates histopathological alterations in a larval zebrafish model to elucidate the spectrum of toxic effects induced by known hepatotoxins and cardiotoxins. Using Hematoxylin and Eosin (H&E)-stained sections, we characterized tissue-specific lesions and morphological changes following exposure to selected toxicants. Our findings reveal distinct hepatic and cardiac tissue alterations, including hepatocyte degeneration, vacuolization, and cardiomyocyte disarray, which may serve as biomarkers for toxicological assessment. Misinterpretation of histopathological findings in fish species has generally been subject to criticism in the past. Therefore, the generated images will serve as an input for training a deep-learning algorithm for differentiating true effects from artefacts in the future.

P265

The Botanical Safety Consortium - advancing botanical safety through collaborative innovations

O. Kelter^{1,2}, C. A. Mitchell^{1,2}

¹Phyto & Biotics Tech Platform, Phytomedicines Supply and Development Center, Bayer Consumer Health, Steigerwald Arzneimittelwerk GmbH, Darmstadt, Germany

²Botanical Safety Consortium (BSC), Washington, D.C., United States

³Health and Environmental Sciences Institute, Washington, D.C., United States

Question: Botanical ingredients — derived from plants, algae, and fungi — are widely used in foods, supplements, cosmetics, and herbal medicinal products. Despite their popularity, evaluating the safety of these complex mixtures poses a significant challenge [1]. Traditional toxicity testing methods, developed for single, well-defined chemical entities, are often ill-suited to capture the multifaceted nature of botanicals, which can contain hundreds of constituents that vary by source, preparation, and use. As a result, there is an urgent need for innovative approaches that can more accurately assess potential risks while supporting the continued development and safe use of botanical products.

Methods: To meet this need, ongoing efforts have focused on developing and applying New Approach Methodologies (NAMs) to evaluate key toxicity endpoints relevant to botanical safety, such as liver toxicity [2], genotoxicity [3], and developmental and reproductive toxicity (DART), among others.

Results: Progress includes establishing systematic frameworks for literature review, authenticating botanical test materials, and integrating advanced chemical analyses and ADME modeling [4] to improve interpretation of in vitro data. Select case studies using botanicals known for safety concerns, like aristolochia and kava, have helped stress-test these methods and refine assay approaches.

Conclusions: Looking ahead, the focus is on expanding the relevance and predictive power of these tools across a broader range of botanicals and real-world exposure scenarios. This includes improved integration of in vitro and in silico data, closing key gaps in predictive modeling, and ensuring that scientific advances translate into regulatory practice. Training, transparent data sharing, and global engagement remain central to these efforts.

References:

- [1] Patel D, Sorkin C, Mitchell CA. et al. *Reg Toxicol Pharmacol* 2023; 144: 105471
- [2] Roe, AL, Krzykwa J, Calderón AI et al. *J Dietary Suppl* 2025; 22: 162–192
- [3] Witt KL, van Benthem J, Kobets T et al. *Food Chem Toxicol.* 2025;197:115277
- [4] Liu Y, Lawless M, Li M. *J Appl Toxicol.* 2024; 44:1236–1245

Signal transduction and second messengers

P266

The MRP4/5-inhibitor probenecid enhances anti-proliferative effects of cNMPs in human gynecological cancer cell lines

S. Walter¹, L. A. Giller¹, R. Seifert¹

¹Hannover Medical School (MHH), Institute of Pharmacology, Hanover, Germany

Question. Gynecological tumors, including tumors of the female breast and genital organs, pose a significant health burden worldwide, and the development of new therapies is necessary. Cyclic nucleotides (cNMPs) are second messengers with apoptosis-inducing effects in various human cancer cell lines. Multidrug resistance transporters (MRPs) 4 and 5 are expressed in many tumor cells and play an important role in the export of cNMPs, thereby terminating their actions. In this study, we used the breast cell lines MCF-7 and ZR-756-1, and the TNBC cell line MDA-MB-231. In addition, the ovarian cell lines CAOV3, PA-1, SK-OV-3, and SW626, as well as endometrial cancer cell lines (HEC-1-B), were used. We analyzed the cell lines for their cNMP pattern, the expression of MRPs, and investigated their response to cNMPs using membrane-permeable acetoxymethyl ester analogues (cNMP-AMs).

Methods. cNMP-levels were quantified with HPLC-MS/MS analysis. The expression of MRP4 and 5 was examined by western blot analysis. Effects of cNMP-AMs on proliferation were analyzed using AlamarBlue assays. Induction of apoptosis were investigated by flow cytometry. Degradation of cNMPs was inhibited by IBMX and efflux by probenecid, an inhibitor of MRP4 and 5.

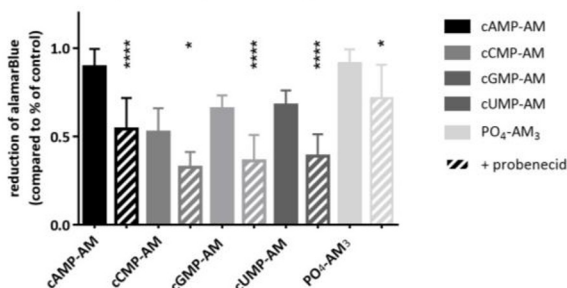
Results. This study revealed significant differences between the cell lines. MRP5 is highly expressed in CAOV-3 and MCF-7, and both in SK-OV-3 and HEC-1 B cells. Anti-proliferative effects of all cNMP-AMs were observed in PA-1, HEC-1 B, MCF-7, MDA-MB-231, and ZR-75-1, while SW626 cells were resistant to cNMP-AM treatment. IBMX showed no significant effect, whereas inhibition of efflux by probenecid enhanced the anti-proliferative effects in the CAOV3, SW626, ZR-75-1, and partially SK-OV-3 cells.

Conclusions. The anti-apoptotic effect of cNMP-AM treatment can be significantly enhanced by inhibiting MRP4 and 5 in almost all cell types used. In initially cNMP-resistant cell lines, pre-incubation with probenecid demonstrated an apoptotic effect. Inhibition of MRPs 4 and 5 is, therefore, a promising pharmacological strategy to enhance the apoptosis-inducing effects of cNMPs in otherwise treatment-resistant gynecological tumors.

1: Seifert R. cCMP and cUMP Across the Tree of Life: From cCMP and cUMP Generators to cCMP- and cUMP-Regulated Cell Functions. *Handb Exp Pharmacol.* 2017;238:3-23. doi: 10.1007/164_2016_5005

Fig. 1

Inhibition of proliferation by cNMP-AMs and probenecid in ZR-75-1 cells



P267

Adenosine-specific transcriptional programs in mast cells

Q. Liang¹, V. Tsvilovsky¹, A. Belkacemi¹, C. Richter¹, N. Ludwig², A. Keller², M. Freichel¹

¹Heidelberg University, Institute of Pharmacology, Heidelberg, Germany

²Saarland University, Chair for Clinical Bioinformatics, Saarbrücken, Germany

Mast cells were shown to play a key role in innate and adaptive immune responses. However, their uncontrolled activation can lead to the untimely release of proinflammatory mediators resulting in pathological reactions such as allergies. Understanding mast cell activation mechanisms is crucial for optimizing beneficial effects and mitigating harm.

Our studies in mouse peritoneal mast cells (PMCs) demonstrate that stimulation with adenosine (ADO), Compound 48/80 (C48/80), or antigens, e.g., Dinitrophenol (DNP), triggers Ca²⁺ release from intracellular stores, followed by Ca²⁺ influx, leading to mast cell activation. While antigen-evoked degranulation can be enhanced by co-stimulation with ADO (1 or 5 µM), ADO alone does not induce degranulation. Nevertheless, ADO can induce the synthesis of cytokines, such as IL8.

To define the ADO-specific transcriptional program and its impact on de novo synthesized mediators in PMCs, we performed bulk RNA sequencing. By

comparing responses to ADO stimulation with those to C48/80 and DNP, we identified 393 genes uniquely regulated by ADO. To characterize these ADO-specific responses, we conducted a series of downstream analyses including transcription factor activity inference, protein classification, functional analysis, protein-protein interaction network construction, and topology analysis. The results revealed that ADO-specific response involved phosphoinositide signaling, glycolysis and mitochondrial activity, as well as a reduction in core nuclear functions.

To further dissect responses dependent specifically on Ca^{2+} influx, we utilized an *Orai1/2*-double-knockout model and compared it with wild-type cells. This approach enables the identification of transcriptional programs specifically engaged by calcium influx. Moreover, we stimulated PMCs with two additional ADO receptor agonists N6-methyladenosine (m6A) and the more stable ADO analogue Cl-IB-MECA to determine whether a longer lasting stimulation of A3 receptors could be achieved. To correlate changes in genes expression with changes in chromatin accessibility and miRNA expression, we performed ATAC and miRNA sequencing on the same batch of samples and constructed a TF-miRNA-gene regulatory network.

Taken together, by applying transcriptomic analysis on PMCs with controlled Ca^{2+} entry pathways, this study seeks to explain relationships between specific calcium signals, chromatin opening, gene expression and release of inflammatory mediators.

P268

Exploring Overlapping and Distinct Interaction Partners of $\text{G}\alpha_2$ and $\text{G}\alpha_3$ in the Inner Ear

J. R. Tischler^{1,2}, G. Bauer^{1,2}, B. Nürnberg¹, E. Reisinger²

¹University of Tübingen, Department of Pharmacology, Experimental Therapy and Toxicology, Tübingen, Germany

²University of Tübingen Medical Center, Gene Therapy for Hearing Impairment Group, Department of Otolaryngology - Head & Neck Surgery, Tübingen, Germany

The closely related G-protein alpha subunits $\text{G}\alpha_2$ and $\text{G}\alpha_3$ play pivotal roles in the development of the organ of Corti, the auditory sensory epithelium responsible for sound transduction in the inner ear. They are particularly involved in establishing the planar cell polarity of hair bundles and the elongation of the row 1 stereocilia. However, the extent of their functional redundancy versus specificity remains largely unresolved. Beyond their classical role as inhibitors of adenylyl cyclase, increasing evidence suggests that $\text{G}\alpha$ isoforms may engage in distinct non-canonical signaling mechanisms mediated by unique interaction partners.

To dissect these isoform-specific interaction networks, we are currently characterizing the activation state-dependent interactomes of $\text{G}\alpha_2$ and $\text{G}\alpha_3$. HEK293 cells were transiently transfected with EE-tagged $\text{G}\alpha_2$ or $\text{G}\alpha_3$ constructs. The respective cell lysates were co-incubated with lysate from the UB-OC2 cell line - an immortalized progenitor sensory hair cell model and pulled down with an anti-EE-Sepharose under defined conditions (GTP-bound active vs. GDP-bound inactive forms). The eluted complexes were analyzed by mass spectrometry. To optimize recovery of membrane-associated interaction partners, various lysis buffers and modified composition were used to improve membrane protein solubilization.

Preliminary proteomic analyses have identified several novel candidate interactors for both $\text{G}\alpha_2$ and $\text{G}\alpha_3$, including both shared and isoform-specific proteins. Among the identified candidates were several cytoskeleton-associated proteins, including F-actin capping protein, F-actin uncapping protein, Myosin-9, Myosin-10 and unconventional Myosin-1. The identification of these proteins expands our understanding of $\text{G}\alpha$ -coupled signaling beyond classical GPCR pathways and may suggest isoform-specific and activation state-dependent roles in inner ear development.

Our results indicate that $\text{G}\alpha$ might directly regulate cytoskeleton formation, which is in agreement with its localization at the tips of the stereocilia.

P269

Characterization of exosomes from organ of Corti explants of adult mice and their therapeutic potential against ototoxicity

R. Arora^{1,2}, B. Nürnberg¹, E. Reisinger²

¹University of Tübingen, Department of Pharmacology, Experimental Therapy and Toxicology, Tübingen, Germany

²University of Tübingen Medical Center, Gene Therapy for Hearing Impairment Group, Department of Otolaryngology - Head & Neck Surgery, Tübingen, Germany

G_i and related proteins have been suggested to be potentially involved in controlling pathogenic mechanisms after different forms of cochlear injury, i.e., noise trauma, ototoxicity, or sudden sensorineural hearing loss. Common to these is hypoxia, followed by reperfusion injury associated with the generation of reactive oxygen species. Isolated exosomes from mature heat-stressed inner ear tissues, particularly vestibular organs, have been shown as mediators of protection against ototoxicity (Breglio *et al.*, 2020). Here, we hypothesized that hypoxia induces the release of exosomes from inner ear tissues to counteract oxidative stress, and we expect non-canonical exosomal-mediated G protein signaling to be involved in this process.

Apical tips of the organ of Corti from adult mice (>P21) were cultured as explants. Following a hypoxic or heat shock treatment, the conditioned medium was used to quantify and characterize the released exosomes. Along with the standard detection protocols of sequential ultracentrifugation and Western blotting, we used

the cutting-edge immune capture-based technology of Leprechaun device (Unchained Labs) to determine vesicle concentration, size profile, and cargo content of these exosomes.

After adapting this technique to mouse inner ear explants, we, for the first time, found exosomes to be released from mouse organ of Corti explants. We analyzed the size- and tetraspanin-based distribution of exosomes derived from inner ear explants from mice of age groups of pre- and post-onset of hearing. Further, we determined the temporal release profile of exosomes derived from these explants after heat shock. In parallel, we explored the potential of extracellular vesicles derived from control and *Gnai3*-knock-out platelets to attenuate stress-mediated apoptosis of neomycin-treated inner ear tissue explants. Our results increase our understanding of endogenous protective pathways in the inner ear, thereby offering translational potential for targeted pharmacological modulation in hearing preservation and ototoxicity prevention.

P270

Correlation between label-free impedance analysis and Ca^{2+} fluorescence *in vitro* imaging

P. A. Schwenk¹, J. Erl², A. K. Grimm², J. Wegener², J. Schlossmann¹

¹University of Regensburg, Pharmacology and Toxicology, Regensburg, Germany

²University of Regensburg, Analytical Chemistry, Chemo- and Biosensors, Regensburg, Germany

Several approaches are available for investigating and unraveling GPCR-dependent signaling pathways using cell-based assays. One of the more modern label-based fluorescence indicators is the popular and frequently used genetically encoded calcium indicator GCaMP, which can be utilized to measure intracellular Ca^{2+} levels. Since Ca^{2+} is a crucial second messenger involved in various cellular mechanisms and signaling pathways, the GCaMP sensor can be applied to investigate GPCR-dependent signaling cascades. In addition to label-based methods, label-free, non-invasive measurement methods can also be used to detect possible GPCR activation, such as by measuring impedance, also known as ECIS (electric cell-substrate impedance sensing). In the ECIS assay, any change in cell shape results in a change in the measured impedance. Since GPCR activation can lead to a remodeling of the actin cytoskeleton, this label-free measurement method is also well-suited for investigating GPCR pharmacology. Although these two measurement methods (GCaMP and ECIS) are often used independently, there are no scientific studies yet that utilize both assay approaches to investigate how and to what extent the results of these two methods correlate. If a strong correlation exists, combining Ca^{2+} fluorescence imaging with label-free impedance analysis has great potential for analyzing and deciphering GPCR signaling pathways more holistically, considering multiple perspectives.

To investigate a possible correlation, HEK293T cells were first transiently transfected with a plasmid of the Ca^{2+} sensor pN1-GCaMP6m-XC and an empty vector, then incubated for 40–48 hours. The cells were subsequently preincubated with various inhibitors or chelators (FR900359 [Gq inhibitor], thapsigargin [SERCA inhibitor], BAPTA-AM [Ca^{2+} chelator], and Y-27632 [Rho kinase inhibitor]) at different concentrations before being stimulated with ATP to activate the GPCR signaling pathway.

In both label-based Ca^{2+} fluorescence imaging and label-free impedance analysis, the various inhibition approaches of the GPCR signaling pathway and changes in intracellular Ca^{2+} concentration after ATP stimulation are similarly well recognizable, making the results obtained highly consistent and reproducible. The combined use of Ca^{2+} fluorescence imaging and label-free impedance analysis thus offers enormous potential for analyzing and deciphering various GPCR signaling pathways more holistically, considering multiple perspectives.

P271

Validation of potential G-protein interaction partners in auditory hair cells of mice

L. Ordling^{1,2}, G. Bauer^{1,2}, B. Nürnberg¹, E. Reisinger²

¹University of Tübingen, Department of Pharmacology, Experimental Therapy and Toxicology, Institute of Experimental and Clinical Pharmacology and Pharmacogenomics, and ICePhA Mouse Clinic, Tübingen, Germany

²University of Tübingen Medical Center, Gene Therapy for Hearing Impairment Group, Department of Otolaryngology - Head & Neck Surgery, Tübingen, Germany

Heterotrimeric G-proteins of the $\text{G}\alpha_i$ family play a critical role in the development and maintenance of auditory hair-cell stereocilia through non-canonical signaling pathways beyond classical GPCR activation. Genetic ablation of $\text{G}\alpha_3$ causes high-frequency hearing loss, whereas combined loss of $\text{G}\alpha_2$ and $\text{G}\alpha_3$ leads to profound deafness in mice. The isoform-specific roles and molecular interaction networks of these $\text{G}\alpha$ proteins, however, are still poorly defined.

Using pulldown assays followed by mass spectrometry, we identified several cytoskeleton-associated proteins—Moesin, Myosin-9, Myosin-15, and the actin-capping protein CAPZB—as potential $\text{G}\alpha_2$ - and $\text{G}\alpha_3$ -interacting partners. To validate these interactions, we focused on $\text{G}\alpha_3$ and examined expression patterns and spatial proximity of the respective proteins in organs of Corti from wild-type mice (P3–P21) by immunohistochemistry and in situ proximity ligation assays (PLA).

Our results reveal dynamic and cell-type-specific interactions of $\text{G}\alpha_3$ with these cytoskeletal regulators, consistent with a developmental shift from actin polymerization (Myosin-15, CAPZB) to cytoskeletal stabilization (Moesin, Myosin-9). These findings support a model in which $\text{G}\alpha_3$ functions as a molecular scaffold linking non-canonical G-protein signaling to cytoskeletal homeostasis in sensory hair cells.

Understanding these mechanisms may have pharmacological relevance, as disturbances in G-protein-mediated cytoskeletal control could underlie susceptibility to ototoxic drug effects or age-related hearing loss. The identified pathways may therefore represent promising targets for pharmacological or gene-based interventions to preserve hair-cell integrity and hearing function.

P272

Development of tools for a better understanding of 3',5'-cUMP function in cells

B. Schirmer¹, R. Kromke¹, A. Hussein¹, H. Bähre², A. Bosse¹, T. Dolgner¹, R. Seifert^{1,2}

¹Hannover Medical School (MHH), Institut für Pharmakologie, Hannover, Germany

²Hannover Medical School (MHH), Zentrale Forschungseinrichtung Metabolomics, Hannover, Germany

Introduction: The presence of 3',5'-cyclic uridine monophosphate (cUMP) in cells has already been shown by sensitive and specific mass spectrometric methods. However, the generators and effectors of these nucleotide species and thus their biological functions are not sufficiently researched. A first indication for a dedicated function of cUMP in bacteria was provided by the discovery of the central role of cUMP in one of the bacterial anti-phage defense systems, which has been termed *pyrimidine cyclase system for antiphage resistance* (Pycsar). Our hypothesis is that the identified Pycsar proteins can be used as tools for further research on cellular effects of cUMP.

Methods: The Pycsar cUMP generator *PaPycC* of *Pseudomonas aeruginosa* was cloned into eukaryotic expression vectors allowing transient and inducible expression of either native or His-tagged protein. Enzymatic activity and substrate selectivity were tested using highly sensitive mass spectrometry (MS). The Pycsar cUMP effector *PaPycTIR* was cloned into a eukaryotic expression vector allowing expression of the protein within a FRET frame (mTurquoise2/mVenus). Starting from the core cyclic nucleotide binding domain, truncated forms of the enzyme were generated by targeted mutagenesis with the aim of yielding a biosensor for cUMP. FRET intensity was measured in cellular lysates using a microplate reader. AlphaFold3-based structure prediction was used to complement experimental data. Non-targeted MS-based metabolomics were used to uncover possible effectors of cUMP in eukaryotic cells.

Results: *PaPycC* shows substrate selectivity for UTP also in the eukaryotic context; one of the *PaPycTIR* mutants generated so far shows a FRET signal dependent on the concentration of cyclic nucleotides. The FRET signal change is highest for different cGMP concentrations followed by cUMP. Structural prediction of the mutants identified additional possible candidates for establishment of cUMP binding selectivity. A non-targeted metabolomic analysis uncovered first hits for cUMP-regulated metabolites in eukaryotic cells.

Conclusion: The Pycsar cUMP generator *PaPycC* and the corresponding effector *PaPycTIR* are promising candidates for further optimization to turn them into tools for selective analysis of cUMP effects in living eukaryotic cells. Exchanging the mTq2 fluorophore for a nanoluciferase module in an optimized biosensor will then possibly yield a useful real-time live cell sensor for cUMP.

P273

ALIsens®-Based Hazard Assessment of Methyl Methacrylate: No Evidence for Respiratory Sensitization Potential

Gutleb, A.C.¹, Blumbach, K.², Burla, S.¹, Faulhammer, F.³, Sommer, T.M.², Wiench, K.³

¹INVITROLIZE, 25 rue de Remich, L-5471 Wellenstein, Luxembourg

²Evonik Operations GmbH, Product Stewardship, Germany

³BASF SE, Global Toxicology and Ecotoxicology, Germany

The potential of methyl methacrylate (MMA) to induce respiratory sensitization was assessed using ALIsens®, a three-dimensional (3D) human-relevant alveolar model cultured at the air-liquid interface (ALI). The system addresses Key Events 2 and 3 (KE2 and KE3) of the proposed Adverse Outcome Pathway (AOP #39) for respiratory sensitization.

To confirm model responsiveness, ALIsens® was exposed to lipopolysaccharide (LPS) and thymic stromal lymphopoietin (TSLP), with chloramine T (Ch-T) as a reference respiratory sensitizer, lactic acid (LA) as a non-sensitizer, and 2-mercaptobenzothiazole (2-MBT) as a skin-sensitizer control. Following dose-range finding experiments for MMA it was not possible to determine a CV75, and therefore the highest achievable concentration of 500 µg/cm² and half that concentration (250 µg/cm²) were chosen as exposure doses.

Two mechanistic endpoints were evaluated: (1) surface marker expression on dendritic-like THP-1 cells (KE3) and (2) cytokine and chemokine release profiles (KE2). Classification of respiratory sensitizers in ALIsens® model is based on the increased expression of the thymic stromal lymphopoietin receptor (TSLPr) to a value equal or higher than 150%.

MMA did not trigger key biological responses associated with respiratory sensitization in the ALIsens® model and expression of TSLPr was not increased above the proposed threshold of 150% compared to vehicle controls. Across all mechanistic endpoints – either previously published or obtained in this study including protein binding (KE1), cytokine/chemokine secretion (KE2), and dendritic-cell activation (KE3) – MMA consistently produced negative results, supporting the conclusion that MMA lacks respiratory sensitization potential.

P274

Evaluating the effects of seeding cell number, cultivation method, intentional damage and extraction timepoint on the transcription of 12 cytochrome P450 genes in HepaRG cells

K. Jochum¹, V. Städele¹, P. Marx-Stöting¹

¹German Federal Institute for Risk Assessment (BfR), Department of Pesticides Safety, Berlin, Germany

The HepaRG cell line represents a widely used model for in vitro hepatotoxicity testing. Among other things, the expression of various cytochrome P450 (CYP) enzymes makes these cells particularly useful in toxicity assessments, as variation in expression resulting from CYP interactions of substances may pose risks to human health. Thus, for regulatory risk assessments, reproducible and stable basal expression despite possible influencing factors is crucial.

To identify factors influencing basal expression, the impact of changes in four cultivation parameters, i.e., cell number, cultivation method, timepoint, and damage, on the transcription of 12 CYP genes in HepaRG cells was investigated with RT-qPCR. To this end, cells were cultivated according to two different methods and seeded at five densities per cultivation method. Extracts from undamaged and intentionally damaged cells were compared and mRNA was extracted at two timepoints after completion of differentiation.

Timepoint and cell number were shown to have the largest impact on transcription. Very high and very low cell numbers decreased transcription over recommended numbers. Transcription increased after two additional weeks in culture. This effect was strongly modulated by cell number with transcription after two weeks increasing most strongly for very high and very low cell numbers. Deliberately damaging the cell monolayer affected transcription only marginally, and no evidence was found for an effect of cultivation method.

In conclusion, before initiating a CYP expression experiment with HepaRG cells, cell number and extraction timepoint are the key parameters to be considered.

INDEX

A

- Abdelwahed, A. - P003
 Abele, S. - P176
 Abels, C. - P215, P216
 Abraham, K. - P163, P200, P201
 Abuzed, K. A. - 37
 Adjaye, J. - 62, P245
 Aha, A. - P178
 Aherrahrou, R. - 34
 Aherrahrou, Z. - 34
 Ahlf, P. - P015
 Ahmed, M. - P137
 Ahmed, N. - P137
 Aivodji, N. - P187
 Aközbeke, C. - P068, P069
 Albrecht, W. - 31
 Albrecht, Z. - P204
 Aljohmani, A. - 45, P003
 Allakonda, L. - P041
 Alt, P. - 40
 Amend, N. - P202, P237
 Angelov, H. - P226
 Anh Ngoc, L. - P171
 Antonmel, A. - P106
 Apicella, C. - 08
 Arias-Loza, P. - P053
 Arndt, L. - P073
 Arnold, C. - 23
 Arnold, S. - 56, P099, P101, P257
 Arora, R. - P269
 Artursson, P. - 01
 Arun, S. - P051
 Aruna, O. A. - P164
 Aßmann, A.-S. - 28
 Attia, N. - P234
 Ayllon Gavilan, M. - 50
 Aziz-Kalbhenh, H. - P177
- B**
 Bach, N. - 12
 Bachmann, H. S. - P175, P230, P233
 Badea, G.-I. - P211
 Bafti, S. - P249
 Bahgat, A. - P152
 Bähre, H. - P231, P272
 Baier, M. - P029
 Bajraktari-Stylejmani, G. - P091
 Balan, M. - P048
 Balazki, P. - P100
 Bals, R. - 45
 Bán, E.-G. - P236
 Bankoglu, E. E. - P192
 Baquero Cevallos, G. - P143
 Bär, C. - P078
 Barenys, M. - P263
 Barre, D. - P182
 Barro, C. - 41
 Bartel, A. - P239
 Bartels, N. - P076
 Barth, H. - 23, 49, P008, P011
 Bartmann, K. - 44, P246
 Bassan, A. - P084
 Batke, M. - P104
 Bauer, B. - 27, P154, P155, P204, P264
 Bauer, G. - P268, P271
 Bauer, H. - P223
 Bauer, R. - 15
 Baumann, R. - P064, P065
 Baumann, S. - P120
 Baume, C. - P017
 Bay, C. - P077, P088, P091
 Beck, A. - P021, P025
 Becker, K. - P252, P253
 Becker, N. - P252, P253
 Beckmann, M. W. - 47
 Beckmann, M. - P059
 Beckmann, R. - 12
 Beckmeyer-Borowko, A. - P121
 Bedke, J. - P071
 Beer-Hammer, S. - 46, P005, P150
 Behrends, S. - P168
 Beljaars, L. - P218
 Belkacemi, A. - P025, P267
 Belov, V. N. - 13
 Bendt, F. - 44
 Benndorf, R. A. - 05, P013
 Beranek, J. - P075
 Berečić, B. - P033, P046
 Berens, V. - 27
 Bergamino, M. - P077
 Berger, J. - P021
 Berger, T. - P142
 Bergmann, O. - P046
 Bergmann, T. - P014
 Berking, C. - 47
 Bernhard, F. - P147
 Bert, B. - P004
 Betz, M. - P133
 Beuke, L. - P023
 Beydemir, Ş. - P096
 Beyerle, P. - P006, P020
- Bharti, K. - 14
 Bialas, N. - 39
 Bilal, M. - P214
 Bindel, L. J. - P119, P231
 Binder, E. - 36
 Birkenfeld, A. - 36
 Bischof, H. - 36
 Bisha, M. - P069
 Bitsch, A. - P078, P210
 Blank, A. - P077, P120
 Bloch, D. - 28, P159, P160, P161, P162
 Blömeke, B. - P164
 Blum, N. K. - P131, P141
 Bocklitz, T. - P053
 Bode, H. B. - 12
 Boehler, M.-P. - P158
 Boekhoff, I. - P006, P020, P021
 Bofinger, L. - 27
 Böhm, A. - P138
 Böhm, R. - P016, P120
 Böhme, J. - P242
 Bollheimer, L. C. - 13
 Bolz, S. - 36
 Bonn Garcia, S. J. - 07
 Borho, J. - 49
 Bornhorst, J. - 43, P206, P208, P209, P259
 Boßmann, L. - P224
 Bosse, A. - P272
 Böttcher, M. - 02
 Bottermann, K. - 09, P028, P030, P031, P039, P048
 Botterweck, J. - P109
 Boulassel, S. - P006, P020, P021
 Bouvier, M. - P135
 Braeuning, A. - 26, P007, P055, P153, P160, P179
 Brakus, I. - P263
 Brandt, J. - P247
 Brandt, V. P. - P251
 Bredeck, G. - P224, P225
 Brehm, S. - P129
 Breit, A. - P021, P202
 Breitkreutz, J. - P219
 Bremer, B. - P144
 Breuer, F. - P116, P117
 Breuninger, A. - P187
 Bridgwood, K. - P054
 Brik, A. - 39
 Bringezu, F. - P244
 Brink, M. - P108
 Brinkmann, B. - P110
 Brizi, V. - P063
 Brockerhoff, G. - P239
 Brockmann, E. - P053
 Brockmeyer, H. - P226
 Brönstrup, M. - P221
 Brucker, C. - P129
 Bruckmüller, H. - 37
 Bruer, G. - P226
 Brüggemeier, U. - P063
 Brüning, T. - 39
 Bruns, F. - P043
 Buchholz, J. - 33
 Buesen, R. - P252, P253
 Buhrmann, A. - P094
 Bukva, M. - P133
 Bulk, E. - P023
 Bünemann, M. - 06, P134, P139, P143, P144, P145
 Burger, C. - 33
 Burgmann, H. - P214
 Burhenne, J. - P077, P088, P091
 Burk, O. - P172
 Burnet, M. - P058
 Busch, H. - P102
 Buschmann, K. - P027
 Büsse, C. - P208
 Butzke, D. - P004
- C**
 Cachorro, E. - P038
 Cairns, J. L. - P252, P253, P261
 Callisan, K. K. - P205
 Callegaro, G. - P055
 Camacho-Londoño, J. E. - P024
 Can, Ö. D. - P095
 Canesi, S. - 44
 Carlucci, T. - P172
 Carta, G. - 54
 Cascorbi, I. - 58, P015, P018
 Cebrian Serrano, A. - P006
 Chakkor, Y. - 34
 Chalvatzis, D. - 11
 Chandrasekar, A. - 17, P176
 Charalambous, G. - P127
 Chatterjee, S. - P078
 Chaturvedi, A. - P114
 Chen, R. - P154
 Chen, Z. - P214
 Cheruvil Lili Kumar, A. S. - 42, P241, P246
 Choi, H. - P021
 Chovolou, Y. - P115
 Chowdhury, R. R. - 55
 Christmann, M. - 52, P079, P083, P085
 Chu, J. - P091
 Chubarov, V. - 11
- Ciftci, B. - P096
 Constantinescu, A. - 17
 Cramer von Clausbruch, C. - P256
 Cronin, M. - P054
 Cross, K. - P084
 Crudo, F. - 53
 Crüsemann, M. - P151
 Cuba, L. - 47, P014
 Curato, C. - P190
 Cylan, M. - 01
 Czernik, L. - P238
 Czock, D. - P077
- D**
 Dahlhaus, P. - P147
 Dahmen, L. - 56, P101, P257
 Damm, G. - P104, P251
 Dammann, M. - P252, P253
 Dammann, W. - P244
 Darakchieva, V. - P048, P049
 Darm, P. - P166
 de Caro, E. R. - P238
 Dechend, R. - 34
 Decker, A. - P131, P141
 Deepika, D. - 14, 28, P056, P217, P250
 Dekant, R. - 33
 Del Favero, G. - 24, 53
 Demel, T. - P169
 Demir Özkay, Ü. - P095
 Demuth, P. - 57, P247, P248, P261
 Dengler, M. - P058
 Denk, T. - 12
 Denker, N. - P018
 Dethlefs, M. - 35
 Deuster, L. - P229
 Dharamvir Singh, A. - P041
 Diaba-Nuhoho, P. - 10
 Dickhut, S. - P016
 Dickmeis, T. - P256
 Diehm, J. - 49
 Diekmann, J. - P114
 Dierks, J. - P053
 Diesel, B. - 19
 Dietmann, P. - P193, P196
 Dietrich, A. - 40, P022
 Dilger, A. M. - 25
 Dilger, M. - P252, P253
 Dimitriadis, A. - P195
 DiSpirito, A. - 64
 Dittmann, L. - 03, P238
 Dittrich, G. M. - P033, P044
 Djuari, M. A. - P078, P086, P226
 Dobner, J. - 44
 Dobrev, D. - P043
 Dohmann, T. - P259
 Doi, A. - P251
 Dokos, C. - P127
 Dolgner, T. - P272
 Domschikowski, J. - P016
 Dönmez, A. - 29, 44, P240
 Donovan, S. - 24
 Dörfler, M. - P151
 Döring, M. - P062
 Dörje, F. - 47, P014, P126
 Dort, F. - P228
 Dreber, A. - P213
 Dressler, J. - P005
 Drenniok, C. - P059
 Drexler, H. - P110, P112
 Dreyer, R. - P075
 Drube, J. - P131, P141
 Drusch, S. - P179
 Düfer, M. - P023, P170
 Dunst, J. - P016
 Duque Escobar, J. - 35
 Duraj, M. - P021
 Dürr, P. - 47, P014, P126
 Dürschmied, D. - P024
- E**
 Eberhagen, C. - 64
 Eberlein, J. - P127
 Ebmeier, J. - 02
 Ehrich, P. - P094
 Eichenlaub, M. - 57
 Eichhorn, M. - P203
 Eisel, K. - P058
 El Shafie, R. - P016
 El-Armouche, A. - 10, P038, P059
 Elbracht, M. - P167
 Ende, N. - 32
 Endt, F. - P202
 Engel, F. - P066
 Engel, N. - P108
 Engel, P. - 16
 Engelhardt, S. - 64
 Engeli, S. - P122, P123
 Engelke, J. - P144
 Engelke, M. - P078, P086, P226
 Engemann, J. - P115
 Engler, J. - 64
 Enoch, S. - P054
 Epple, M. - 39

- Erdmann, F. - P165
 Erl, J. - P270
 Ernst, S. - P139, P143
 Eryilmaz, F. - P151
 Escher, S. E. - P084, P244
 Esselen, M. - P185
 Esser, C. - P001, P197
 Eteve-Pitsaer, C. - P050
- F**
 Fabian, E. - 57, P100, P247, P251, P261
 Fahimi, E. - P069
 Fassnacht, M. - P076
 Faupel, T. C. - P094
 Fayyaz, S. - P239
 Felkers, E. - P103
 Fellendorf, J. - 23
 Fender, A. - P043
 Fester, K. - P059
 Fetz, V. - 28
 Fiengo Tanaka, L. - P129
 Fietkau, R. - 47
 Fikenzer, S. - P064
 Fischer, D. - P061, P070
 Fischer, F. - 51
 Fischer, J. W. - 09, P028, P030, P031, P032, P039, P048, P062, P106
 Fischer, J. - P136
 Fischer, S. - P244
 Fitz, D. - P215
 Flach, H. - P193, P196
 Flockerzi, V. - P025
 Flögel, U. - P062
 Flores Espinoza, F. - P092
 Flößer, A. - P138
 Flößer, A. - P144
 Foth, H. - P104
 Franz, M. J. - 11
 Freichel, M. - P024, P050, P133, P267
 Frentrup, M. - P224
 Frericks, M. - 29, P054
 Freund, D. - P141
 Frey, N. - 18
 Freyberger, A. - P104
 Frick, M. - 49
 Fricker, G. - P018
 Friebe, J. - P138
 Friellingsdorf, F. - P165
 Fritsche, E. - 03, 42, 44, 55, P238, P239, P240, P241, P246, P254
 Fritz, G. - 43, P191, P198, P205, P260, P262
 Fritzwanker, S. - P132
 Fröhling, S. - 48
 Fromknecht, S. - 36
 Fromm, M. F. - 47, 59, P014, P076, P087, P126
 Fuhr, U. - P072, P214, P218
 Fung, Y. C. - P161
 Funk, F. - P037, P040, P042, P066
 Funk-Weyer, D. - P099, P252, P253, P261
 Fürst, R. - 12, 18, 20
- G**
 Galanis, P. - P127
 Galeev, A. - P114
 Gamm, O. - P051
 Gasthaus, D. - 29
 Gatzmanga, S. - P198
 Gaul, C. - P098
 Gaul, S. - P064, P065
 Gebel, J. - P070
 Gebert, L. - P028
 Geisenfelder, L. - 33
 Geisler, L. - P075
 Geißler, M. - P124
 Gergs, U. - P034, P035, P036, P146
 Gerhard, R. - P009, P010
 Gerisch, E. - P208
 Gerner, C. - 53
 Gessner, A. - 59, P076, P087
 Gessner, K. - 47, P014, P126
 Gieske, M. - 08
 Giller, L. A. - P266
 Giri, V. - P261
 Glahn, F. - P212
 Glässner, A. - P166
 Glimm, H. - 48
 Gobrecht, P. - P061, P070
 Goel, R. K. - P093
 Goepfert, A. - P255
 Goerdeler, C. - P201
 Goettel, M. - P251
 Gohla, P. - P042
 Göhrler, R. - P222
 Gollasch, M. - P123
 Gomes, C. - P247, P252, P253
 Gómez Ochoa, S. A. - P050
 Gopakumar, G. - P102
 Gorantla, S. P. - 58, P015
 Gorreßen, S. - 09, P028, P030, P039, P040, P048, P066
 Gorski, D. J. - P028, P030
 Gottal, J. - 64
 Gotthard, J. - P058
- Göttlich, S. - P130
 Graber, S. - P029
 Grafakou, M. E. - 15
 Graffmann, N. - 62, P245
 Grandoch, M. - P062
 Graß, M. - P108
 Grätz, L. - P151
 Greco, S. - P084
 Grell, S. - 10
 Grether-Beck, S. - 63
 Grimm, A. - P147
 Grimm, A. K. - P270
 Grimm, C. - 60, P024, P133
 Grimm, F. A. - P223, P239, P254
 Grimm, K. - P171
 Gröner, M. - P038
 Große Hovest, M. - P117
 Gröttrup, H. - P012
 Gründler, L. - 31
 Grünebaum, M. - P185
 Grünschlager, F. - 57
 Guan, K. - P051
 Gudermann, T. - 11, 38, 40, P006, P020, P021, P022, P022
 Gulich, K. - P004
 Gundert-Remy, U. - P104
 Gunesch, S. - 51
 Guzzo, R. - P241, P246
 Gynther, M. - 58
- H**
 Haake, V. - P105
 Haarmann-Stemmann, T. - 63
 Haase, A. - 05
 Hadi, N. S. A. - P187, P192
 Hadova, K. - P036
 Haefeli, W. E. - P077
 Haffelder, F. C. - P133
 Hagelaar, R. - 50
 Hagemann, A. - P175, P230
 Hahn, M. - P166
 Haider, R. S. - P141
 Hambrich, N. - P099, P257
 Hamburg, K. - P088
 Hamm, A. F. - P016
 Hammar, R. - 01
 Hammer Wagner, H. S. - 01
 Hammerl, I. - 20
 Han, L. - 41
 Hansen, F. K. - P069
 Hapuarachchi, S. - P090
 Harms, M. - 05
 Hartmann, A. - P016
 Hartmann, L. - P027
 Hartmann, S. - P258
 Hartung, F. - 63
 Hartwig, A. - 51, P109, P110, P112, P186
 Hasarova, Z. - P054
 Hasoumi, M. - 13
 Hasse, M. - P051
 Hauenstein, E. - P129
 Hayot, G. - P256
 Hebar, P. - P039
 Heber, S. - P011
 Hechler, L. - P061
 Heck, J. - P128
 Hedtstück, M. - P052
 Heiles, S. - P053
 Heilscher, J. - P179
 Heine, K. - P113
 Heine, P. - P149
 Heinen, T. - P218
 Heinrich, C. - P198
 Heinrich, H. - P071
 Heinrich, M. - 11
 Helker, C. S. M. - P143
 Heller, K. - P062
 Hellmann, L. - P038
 Hengstler, J. G. - 31, P104
 Henning, T. - P201
 Henninger, C. - P191
 Herdegen, T. - P016
 Herebian, D. - P245
 Hermes, C. - P173
 Hernandez Torres, L. - 34
 Herzog, N. - 25
 Heß, N. - P050
 Hessel, C. - P114
 Hessel-Pras, S. - P007
 Heuberger, J. - P075
 Heydenreich, F. - P135
 Heymann, F. - P075
 Hilge, M. - P149
 Hilgefort, D. - 56, P099, P101, P257
 Hilger, D. - 07, P151
 Hille, H. - 34
 Hinkal, G. - P105
 Hinnah, K. - P136
 Hintzsche, H. - 27, P154, P155, P204, P264
 Hoene, M. - 36
 Hofacker, L. - P073
 Hoffmann, A. - P234
 Hoffmann, A. - 27
- Hoffmann, C. - P131, P141
 Hofmann, B. - P034, P035
 Hofmann, D. - P171
 Hofmann, T. - 22
 Hofmann, U. - P125
 Honarvar, N. - P255
 Hoogenboom, R. - P163
 Huang, H. - P214
 Hube, T. - P028, P048, P213, P227
 Hübenthal, U. - 44
 Hübschmann, D. - 48
 Hundertmark, N. - 23
 Hunszinger, V. - 23
 Hussein, A. - P272
 Huynh, S. - P126
 Huzain, O. - 41
- I**
 Inan, E. - P262
 Irwan, J. - P084, P244
 Ittermann, T. - P123
- J**
 Jablinski, J. - 26
 Jäckel, L. M. - P139
 Jacob, K. - P021
 Jäger, S. - P129
 Janssen, S. - P001
 Jaslan, D. - P024
 Jauch, A. T. - 64
 Jehl, V. - P121
 Jeibmann, A. - P209
 Jelinek, M. - P206
 Jelinek, V. - P145
 Jenabi, S. - 27, P264
 Jeyakumar, B. - P262
 Jiang, Z. - P218
 Jobst, M. - 24, 53
 Jochum, K. - P274
 Johann, A. - P174
 Johnen, G. - 39
 Johnsson, K. - P136
 Juli, J. - P229
 Jülicher, S. M. - P032, P106
 Jung, C. - P194
 Jürgenliemke, L. - P151
 Jurida, L. - P045
 Just, H. - 30
 Just, K. S. - 13, P026, P167
- K**
 Kabagema-Bilan, C. - 36
 Kadic, A. - P055, P160
 Kaehler, M. - 58, P015, P018
 Kaiffo-Pechmann, A. - P158
 Kaiser, N. - P038
 Kaller, J. - P173
 Kalwa, H. - P064, P065
 Kämmerer, S. - P038
 Kamp, H. - P105
 Kämpfer, A. A. M. - P224
 Kandemir, Ü. - P095
 Kanzler, S. - P060
 Kappenstein, O. - P178
 Karl, N. - P228
 Karst, U. - P209
 Kasten, A. - 58, P018
 Kästing, M. - P091
 Kastner, N. - P027
 Kaub, L. - 64
 Kaur, A. - P093
 Kehrenberg, M. C. - P175
 Kelber, O. - 15, P074, P118, P130, P177, P265
 Keller, A. - P267
 Kellner, R. - P244
 Kerler, Y. - P089
 Kern, M. - P019
 Kersch, C. - P158
 Kersting, K. - P113
 Keup, S. - P108
 Keuter, L. - P249
 Khajavi, N. - P006, P020, P021
 Khalid, K. - P221
 Kick, C. - P023
 Kiefer, M. - P131
 Kiefmann, M. - 40, P022
 Kiemer, A. K. - 19
 Kieserling, H. - P179
 Kießig, S. - P055, P157
 Kirchhefer, U. - P146, P171, P173, P174
 Kirchhofer, S. B. - P134, P136, P145
 Kirpal, H. - P167
 Kistermann, S. - P011
 Klai, K. - P204
 Klapproth, E. - 10, P059
 Kleindienst, L. - 17, P176
 Klenk, C. - P149
 Kleuser, B. - 56, P099, P257
 Klimas, J. - P036
 Klingelhöfer, K. - P144
 Klose, M. - P233
 Kluxen, F. M. - P103, P107, P252, P253
 Knolle, P. - 64

- Kocabas, N. - P105
 Koch, K. - 03, 29, 42, 44, 55, P238, P239, P240, P241, P246, P254
 Köck, Z. - P147
 Kockskämper, J. - P142
 Koczera, P. - P026
 Koehler, L. - P059
 Kogel, A. - P064, P065
 Kohlmann, E. - 59
 Kohnhäuser, D. - P221
 Köhrer, K. - P028
 Kojda, G. - P068, P069
 Kollatz, J. - 24
 Kolle, S. - P247, P248
 Köllner, B. - P115
 Kölz, C. - P005
 König, G. M. - P151
 König, I. - 23
 König, J. - 59, P087, P102
 König, M. - P120
 Konstantakopoulou, O. - P127
 Koora, M. - P125
 Koppenhöfer, D. - P171
 Kordes, C. - P245
 Korn, E. - P029
 Korus, J. - 29
 Kostenis, E. - P151
 Köster, K.-A. - 35
 Kostka, K. - 39
 Kowalczyk, J. - 30
 Krabbe, J. - 39
 Kracht, M. - P045, P067, P228, P229, P235
 Kraft, K. - P130
 Kraft, M. - P115
 Kraft, N. - 29
 Krammer, T. - P029
 Krasel, C. - P139, P143
 Krauel, K. - P024
 Krause, D. S. - 32
 Krause, J. - P167
 Krause, M. - P129
 Krautstrunk, J. - 43, P262
 Kremer, H. - P171
 Krempe, V. - P250
 Kretschmer, R. - P031
 Krey, S. - P099
 Krichevsky, B. - P128
 Krings, O. - P212
 Krohmer, E. - P120
 Krohn, P. - P190
 Kroiss, M. - P076
 Kromke, R. - P272
 Krotov, M. - P040
 Krotz, K. - P188
 Krüger, M. - P037, P040, P066
 Krüger, T. - P167
 Krutmann, J. - 63
 Kucherak, M. - P063
 Kudina, O. - P132
 Kuehnl, J. - 02
 Kühl, M. - P193
 Kühl, S. - P193, P196
 Kuhn, J. - P186
 Kühne, B. - P263
 Kulaeva, L. - 50
 Kulartz, J. - 58, P018
 Kumar, S. - 14, P056, P217
 Kumar, V. - 14, 28, P056, P217, P250
 Kunz, S. - P075
 Küpper, J.-H. - 25, 61
 Kurlbaum, M. - P076
 Kurz, C. - P134
 Kurz, M. - 06
 Kurz, T. - P069
 Kushwaha, R. - 46
- L**
 Laemmerhofer, M. - 36
 Lahu, L. - P062
 Lajine, M. H. E. - 56
 Lam, C. - 12
 Lamidi, K. - P199
 Lampe, J. - P094
 Landsiedel, R. - 57, P099, P100, P247, P251, P255, P257, P261
 Lange, D. - 02
 Langejürgen, A. - P010
 Langen, C. B. - P013
 Langolf, A. - 07
 Lara Neves, M. - P004
 Laube, B. - P109
 Laufs, U. - P064, P065
 Laurentius, T. - 13
 Lautwein, T. - P028, P030
 Le Roux, C. - P129
 Lebek, S. - P029
 Lee, J. - P027
 Lee, M. - P223
 Lehnert, F. - P035
 Lehr, S. - 09, P039
 Lei, Q. - 41
 Leib, L. - P229
 Leibinger, M. - P061
- Leibold, E. - P109
 Leiss, V. - 36
 Lensker, P. - 47
 Lerch, S. - 30
 Lesage, R. - P100
 Letsch, A. - P016
 Leuvenink, H. G. D. - P218
 Levinson, R. T. - P050
 Levkau, B. - P062
 Li, H. - P027
 Li, Q. - P223, P239
 Li, W. - P051
 Liang, Q. - P267
 Licht, O. - P117
 Lichtenstein, D. - 26, P055, P153, P242
 Liebnau, B. - P160
 Liesenfeld, E. - P169, P183
 Liess, M. - P193
 Lietz, S. - P008
 Lindemann, C. - P114
 Lindner, K. - P008
 Link, M. - P186
 Linne, U. - P228, P229
 Lippert, A. - P059, P234
 Liu, L. - P075
 Liu, S. - 28
 Lobes, N. - P164
 Lochschmidt, L. - 11
 Loeffler-Kapezov, J. T. - 58
 Loerch, C. - P245
 Lofrano, A. - 62
 Lohmann, R. - P109
 Lohse, S. - P071
 Lölsberg, P. - 32
 Londenberg, A. - P084
 Lopes, A. C. C. - 01
 Lörch, C. - P192
 Lorenz, C. - P194
 Lorenz, K. - 10, P047, P052, P053
 Loza, K. - 39
 Lu, R. - 16
 Luch, A. - P178
 Luchmann, C. T. - P148
 Ludwig, N. - P267
 Lukas, D. - P029
 Lukowski, R. - 36
 Lumpp, T. - 51
 Lundquist, P. - 01
 Luo, X. - P051
 Lutterberg, K. - P019, P165
 Lutz, S. - P033
- M**
 Maares, M. - P206
 Maaß, L. - P150
 Machill, L. - P129
 Mackensen, A. - 47
 Mäder, C. - P064, P065
 Mähli, G. - 56
 Mahmoud, A. B. - 19
 Maier, L. S. - P029
 Mally, A. - 33
 Manaridou, K. - P127
 Mangerich, A. - 25, 32, P104
 Mangold, H. - P248
 Mann, C. - P043
 Mannebach Götz, S. - P025
 Manolica, A.-C. - P211
 Marko, D. - 53
 Marks, J. - 10
 Märte, H. - P043
 Martelli, G. - P192
 Martin, S. - P107
 Martorelli, M. - P058
 Maruyama, E. - P031
 Marx-Stölting, P. - 28, P055, P157, P159, P160, P161, P250, P274
 Masson, I. - P224
 Mateju, D. - P063
 Matsch, J. - P071
 Matt, L. - 36
 Matthes, J. - P222
 May, M. - P117
 May, T. - P099
 Mayr, A. - P126
 Mayr-Buro, C. - P228
 Mboni Johnston, I. M. - P258
 McNulty, C. - P243
 Mecklenburg, L. - P060
 Meid, A. - P077
 Meier-Sölch, J. - P067, P228, P229
 Meißner, A. - P197
 Meiching-Kollmuss, S. - P100
 Melyshi, A. M. - P021
 Menger, M. - P089
 Merino, F. - P147
 Merten, N. - P151
 Mertens, H. - P200
 Meßling, L. - P205, P260
 Messerschmidt, J. - P059
 Metten, H. - 58
 Meyer, J. - P019
 Meyer, M. - 27
- Meyer, T. - P046, P243
 Meyer, U. - P017, P138
 Michaelis, V. - P206, P209, P259
 Michaelsen, S. - P109, P110, P112
 Mielke, H. - P104, P163, P200
 Miller, B. - 13
 Mitchell, C. A. - P265
 Moenning, J.-L. - 30
 Moissl-Eichinger, C. - 15
 Molderings, I. C. - P146
 Monien, B. H. - P200, P201
 Morais Leme, D. - P157, P250
 Mösges, R. - P130
 Moskaliov, I. - P061
 Muehe, L. - P018
 Muehlich, S. - 11
 Mueller, C. A. - P234
 Mühlberg, E. - P091
 Müller, C. - P226
 Müller, C. E. - P133, P151
 Müller, F. - P087, P120
 Müller, F. U. - 08, P171
 Müller, I. - 40
 Müller, J. P. - 13, P026
 Müller, M.-C. - P017
 Müller, M. - P066
 Müller, O. - 34
 Müller, R. - 18, 19
 Müller, T. - P073
 Müller, T. D. - P006, P020
 Müller-Fielitz, H. - 17, P176
 Münch, J. - 05
 Muschik, S. - P189
 Musengi, Y. - 28
 Mustroph, J. - P029
 Myhre, O. - P246
- N**
 Nagai, F. - P132
 Nagel, F. - P131, P141
 Nagel, G. - P085
 Nagel, T. - P059
 Naimi, A. - P142
 Najjar, A. - 02
 Namasivayam, V. - P102
 Napieczynska, H. - 34
 Naundorf, L. - P170
 Nausch, B. - P215, P216
 Nazari Jeirani, M. - P243
 Nedunchezian, A. - P046
 Neef, S. - P029
 Neef, S. K. - 58
 Negru, M. - P223
 Nenoff, W. - P034
 Neu, A. - P180, P181
 Neu, L. A. - 42
 Neuefeind, L. - P029
 Neuendorff, F. - P185
 Neukirch, M. - P135
 Neumann, A. - P215
 Neumann, D. - P152
 Neumann, J. - P034, P035, P036, P146
 Neurath, M. F. - 47
 Nicolai, M. M. - 32
 Nieber, K. - P130
 Niederer, A. C. - P149
 Niedermeyer, T. - 24
 Niehues, M. - P249
 Niehus, T.-N. - P102
 Niemann, V. - P062
 Nies, A. T. - P005
 Niessen, K. V. - P189
 Noble, M. - P063
 Nordbeck, P. - P053
 North, E. - P076
 Nössner, E. - P071
 Nübel, U. - P224
 Numata, J. - 30
 Nürnberg, B. - P268, P269, P271
 Nwuzor, J. - P199
- O**
 Oelgeschläger, M. - 28, 56, P075
 Oertel, R. - P124, P125
 Oetjen, E. - 35
 Ohnesorge, N. - P263
 Ording, L. - P271
 Osmaniye, D. - P097
 Oswald, S. - 58
 Ott, F. - P179
 Otten, M. - P043
 Ottenheim, R. - P024
 Ottens, P. J. - P218
 Oyson, E. - P010
 Özorhan, Ü. - 34, P094
- P**
 Pahl, M. - P238
 Papatheodorou, P. - 23
 Papenheim, D. - P045
 Parsdorfer, M. - P186
 Partosch, F. - P104, P210
 Paul, M. - P242

- Pauls, P. - P146
 Pavel, M. - 47, P014
 Peddinghaus, C. - P052
 Pellowski, D. - P206
 Peter, A. - 36
 Peterburs, P. - P216
 Petersilie, L. - 42
 Petralla, S. - P018
 Pettersson, L. - P181
 Petz, A. - P028, P030
 Pfeffer, S. - P193, P196
 Pfeifle, H. - P028
 Pferschy-Wenzig, E.-M. - 15
 Phielier, I. - P140
 Pichler, P. - P214
 Picurová, J. - P087
 Pieczyk, B. - P116
 Piepenstock, M. - P219
 Pieper, R. - 30
 Pierchala, N. - 44
 irmann, S. - 48
 Piroth, M. - P028
 Plückthun, A. - P149
 Poepl, W. - P214
 Poetz, O. - 01, P153
 Pohlmann, S. - P123
 Popa, M. O. - P211
 Posma, R. - P218
 Potnuri, A. G. - P041
 Prange, L. - P102
 Priesmeier, L. - P046
 Priester, J. - P235
 Prince, C. - 10
 Przygoda, L. - 30
 Puris, E. - 58
 Pusch, L. - P209
 Puts, R. - P055, P250
- Q**
 Qasem, S. - P033
 Quanz, M. - P063
- R**
 Raasch, W. - 34
 Rabbi, M. - P137
 Rafehi, M. - P102
 Rahat, I. - P097
 Rahmenführer, J. - P244
 Ramm, F. - P089, P092
 Rao, S. - P054
 Raolji, V. - P055
 Raschke, M. - P249
 Rasenberger, B. - 52, P079
 Raskopf, E. - P130
 Rauch, B. H. - P017, P138
 Rauch-Kröhnert, U. - P138
 Rausch, S. - P071
 Rebhahn, V. - 24
 Recordati, C. - 44
 Regehr, N. - P190
 Reher, R. - P142
 Reichert, A. - P062
 Reichert, D. - P001
 Reichling, J. - P118
 Reifenberg, G. - P027
 Reinach, P. - P021
 Reinhardt, J. P. - 08
 Reinscheid, R. - P148
 Reisinger, E. - P268, P269, P271
 Renko, K. - 56, P099, P101, P257
 Renner, B. - P124, P125, P234
 Rennert, R. - 24
 Rezaallah, B. - P121
 Reznicek, G. - P214
 Richling, E. - 61, P183
 Richter, C. - P025, P267
 Richter, F. - P113
 Richter, H. - P209
 Richter, L. - P200
 Richter, S. - P012
 Riede, M. - 57
 Riffle, B. - P100
 Ristl, E. - P172
 Rittmann, D. C. - P175
 Roberts, M. - P116
 Roever, M. - P107
 Roever, N. - P192
 Rogalski, L. - P242
 Rohn, S. - P179
 Rollmann, M. - P227
 Rönkkö, T. - P225
 Ronnenberg, K. K. M. - P255
 Rose, C. - 42
 Rose, K. - P038
 Rosenkranz, N. - 39
 Rossbach, B. - P158
 Rossi, A. - 44, 63, P001
 Rossol, M. - P142
 Rostock, M. - P016
 Roşu, A. - P232
 Roşu, M.-C. - P232
 Rothmiller, S. - P019, P165, P169, P180, P181, P182
- Rox, K. - P221
 Roy, B. - P137
 Ruelker, C. - P255
 Ruiz, R. - 24
 Rupperecht, L. - 11
 Ruscă, S.-N. - P232
 Ruța, A.-D. - P232
 Ruța, B.-N. - P232
- S**
 Saarikoski, S. - P225
 Sadallah, J. - 37
 Saftig, P. - 10
 Sailer, J. - 64
 Sajib, M. - P137
 Salah, H. - P025
 Salako, K. - P199
 Salako, O. - P199
 Sallbach, J. - 52, P079
 Salo, L. - P225
 Samson, S. - P032, P106
 Sane, R. - P101
 Sängler, M. - 25
 Saoud, M. - 24
 Sauter, K. - P058
 Sauter, M. - P077, P091
 Schaefer, M. - P064, P065
 Schäffeler, E. - 48, P071, P172
 Schaller, S. - P100
 Schanbacher, C. - P047, P052
 Schanbacher, F. - 24
 Scharkin, I. - 44, 55, P246
 Scheffler, S. - P210
 Scheffschick, A. - P251
 Schepky, A. - 02
 Scherer, B. - 50
 Schermer, Y. - 61
 Schicht, G. - P251
 Schihada, H. - 07, P135
 Schildt, S. - P029
 Schiller, H. - 41
 Schilling, O. - 45
 Schins, R. P. F. - P224, P225
 Schirmer, B. - P152, P231, P272
 Schlawis, C. - P107
 Schlossmann, J. - P270
 Schmalz, C. - P016
 Schmid, N. - 59
 Schmidbauer, D. - P236
 Schmidt, A. - P180
 Schmidt, A. - P083
 Schmidt, C. - P156
 Schmidt, F. C. - P235
 Schmidt, G. - P012, P073
 Schmidt, H. - 23
 Schmidt, P. - P248
 Schmidt, S. - P219
 Schmidtko, A. - 16
 Schmidtlein, P. M. - P176
 Schmitt, J. - P037, P040, P042, P066, P106
 Schmitz, F. - P025
 Schmitz-Spanke, S. - P158
 Schmück, D. - P192
 Schneckmann, R. - P048
 Schneider, G. - P067
 Schneider, J. - P196
 Scholl, C. - P166
 Scholleck, L. - P230
 Schomburg, L. - P099
 Schredelseker, J. - 38
 Schreier, P. C. F. - P006, P020, P021
 Schriever-Schwemmer, G. - P110, P112
 Schröder, M. F. - P259
 Schröder, S. - 35
 Schröder, S. - P128
 Schubert, M. - P051
 Schubert, S. - P125
 Schuele Weiser, H. - P228
 Schulte, J. S. - 08, P146, P174
 Schulte, U. - P024
 Schulz, R. - P122
 Schulz, S. - P131, P132, P141, P148
 Schulze, A. - P124
 Schulze, M.-G. - P089
 Schulze Westhoff, M. - P128
 Schumacher, F. - 56, P257
 Schumacher, P. - 51
 Schupp, N. - P195, P258
 Schupp, T. - P104
 Schütte, L. - P231
 Schwab, A. - P023
 Schwab, A. - P237
 Schwab, M. - 48, 58, P005, P071, P172
 Schwaninger, M. - 17, 34, P094, P176
 Schwarz, R. - P036
 Schwarzenbach, C. - 52
 Schwegmann, S. - 46
 Schwenk, P. A. - P270
 Schwerdtle, T. - P208, P259
 Schwingen, M. - P030
 Seeger, T. - P189
 Seehofer, D. - P251
 Seher, T. - P062
- Seibel, J. - P074
 Seidl, M. D. - 08, P171, P173
 Seidler, P. - P075
 Seifert, R. - P119, P152, P231, P266, P272
 Sellin, M. E. - 01
 Semmler, D. - 09, P039, P106
 Serafimov, K. - 36
 Shaban, M. S. - P228
 Shah, K. - P130
 Sharma, S. - 14, P056, P217
 Shcherbakova, A. - P177
 Sieber, S. A. - 12
 Sieg, H. - P179
 Sievering, S. - P115
 Siewers, H. - P118
 Siewert, K. - P190
 Sigal, M. - P075
 Sikandar, A. - P046
 Silvonen, V. - P225
 Simeon, L. - P261
 Simetska, N. - P244
 Simon, M. - P014
 Skitsou, A. - P127
 Smieja, D. - P060
 Soeberdt, M. - P215, P216
 Sonnenburg, A. - P104
 Sonntag, A. - 24
 Sowa, K. - P185
 Spaehn, D. - 36
 Spang, S. - P255
 Spannbrucker, T. - P225
 Sparrer, K. - 23
 Spellerberg, B. - P008
 Spiecker, F. - 34, P176
 Sponfeldner, M. I. - 47
 Sprengel, R. - 24
 Sprenger, H. - 26, P007, P055, P153
 Springer, F. - P189
 Spruck, C. - P239, P254
 Stadler, M. - 38
 Städele, V. - P 274
 Staerk, C. - P126
 Stagkos-Georgiadis, A. - P159
 Stahnke, J. - P089, P092
 Stark, L. M. - 03, P238, P240
 Stefan, K. - P102
 Stefan, S. M. - P102
 Stefanidis, K. - P099
 Steffens, M. - P166
 Stegmüller, S. - 61, P183
 Steinbach, A. - 12
 Steinhoff, O. - P062
 Steinmann, D. - P016
 Steinritz, D. - P019, P165, P169, P180, P181, P182, P189, P202, P237
 Stevens, J. - P218
 Stinchcombe, S. - P100
 Stingl, J. C. - 13
 Stoeger, T. - 41
 Stojanovic, S. - P249
 Stoll, M. - 08
 Stölting, I. - 34
 Stomberg, S. - P168
 Stopper, H. - P187, P188, P192
 Stößer, S. - 51
 Strano, A. - P051
 Strasburger, R. - P094
 Streckebain, M. - P120
 Struß, N. - P077
 Suci, I. - 28, P055, P157
 Suleimen, B. - P021
 Suvorova, T. - P032, P069, P106
 Svendsen, K. - 37
 Synhaeve, N. - P105
 Szafranski, K. - 39
- T**
 Talkhan, O. S. - P251
 Talukder, M. - P137
 Tao, Y. M. - P134
 Tardio, L. B. - 08
 Tatge, H. - P009
 Taubert, M. - P072, P214, P218
 te Vrugt, J. - P037
 Thalayasingam, V. - P191
 Thao-Vi Dao, V. - P069
 Theile, D. - P088
 Theisen, L. - P063
 Thiel, A. - P208, P259
 Thieme, S. - 20
 Thom, C. - P149
 Throm, V. - P024
 Thünemann, A. - P179
 Tiedemann, L. - P015
 Tietz, T. - P178, P194
 Tigges, J. - 03, 29, P238, P239, P254
 Tischlarik, J. R. - P268
 Tolstik, E. - P053
 Tomicic, M. T. - 52, P079, P083
 Topinka, J. - P225
 Touw, D. J. - P218
 Tralau, T. - 28, P159
 Tran, B. T. T. - 16

Treede, H. - P027
 Tremmel, R. - 48
 Trescher, S. - 38
 Trifan, A. - P211
 Tsau, I. - P071
 Tsvilovskyy, V. - P133, P267
 Tüchler, D. - P214
 Tug, T. - P244
 Tupiec, J. - 13
 Turan Yücel, N. - P097
 Twarock, S. - P213, P227
 Ueffing, M. - 36

U

Uhl, P. - P077, P091
 Ullah, I. - P046
 Ulrich, M. - 06, P134
 Ulrich-Merzenich, G. - P177

V

van Alst, C. - P043
 van Boxtel, R. - 50
 van de Water, B. - P055
 van Roosmalen, M. - 50
 Vater, I. - 58
 Vetter, W. - P178
 Vijayendran, A. - P198
 Vinogradov, M. - P021
 Vinson, B. - P130
 Vogel, C. F. A. - 63
 Vogel, V. - P008
 Vogler, M. - P251
 Vogt, A. - P153
 Vogt, C. - P120
 Vogt, L. - P071
 Völkl, M. - 18
 vom Brocke, J. - P104
 von Bubnoff, N. - 58, P015
 von Törne, C. - 64
 Voss, C. - 41
 Voss, J. H. - P151
 Voss, S. - 02
 Vossen, J. - P225
 Vujčić Spasić, M. - 64

W

Wabra, J. - P226
 Wagmann, L. - 27
 Wahle, T. - P224, P225
 Wang, J. - P046
 Wang, L. - 09
 Wang, S. - P204
 Wardas, B. - P025
 Weber, A. - P228, P229
 Weber, D. G. - 39
 Weber, I. E. - 19
 Weber, L. - P233
 Wedler, M. - 28
 Wegener, J. - P270
 Wehr, M. - P116
 Weigelin, B. - 46, P150
 Weigert, C. - 36
 Weikert, C. - P201
 Weiß, J. - P088, P091
 Weiser, T. - P098
 Weishaupt, A.-K. - 43
 Weiss, C. - P256
 Weistenhöfer, W. - P110, P112
 Wend, K. - P103, P107
 Wensch, P. - 11
 Werthschulte, M. - P219
 Weser, N. - P059
 Westerink, E. - 50
 Westphal, G. - 39
 Wewer, N. - 26, P242
 Weyrich, A. - P247
 Wiedenmann, M. - P196
 Wiemann, C. - P103, P107
 Wiench, K. - P247
 Wiesholzer, M. - P214
 Wiest, J. - 56
 Wight, T. N. - P028
 Wilhelm, J. - P228
 Willi, L. - 33
 Wilmes, A. - 54
 Winkler, M. L. - P078, P086, P226
 Winter, A. - 39
 Winter, M. - P234
 Winter, S. - P071, P172
 Winterhalter, M. - 24
 Wirth, S. - P045
 Wißmann, A. - P145
 Witt, B. - P208
 Witzennath, M. - 45
 Wohlenberg, A.-S. - 32
 Wohlleben, W. - P248
 Wojnowski, L. - P027
 Wölbern, A. M. - P092
 Wolf, S. - 04
 Wollenberg, M. - P194
 Wollin, K.-M. - P104
 Wolter, M. A. - P240
 Wolter, S. - P266

Woods, M. - 52, P079
 Worek, F. - P237
 Wozniak, J. - 13
 Wruck, W. - 62
 Wu, D. - P155
 Wu, Q. - P126
 Wu, Y. - P009
 Wuerger, L. T. D. - P007
 Wullich, B. - 47
 Wunder, F. - P063
 Wunsch, B. - P023
 Wurmbach, V. - P120

X

Xia, N. - P027

Y

Yamoune, S. - 13
 Yang, W. - P072
 Yazici, C. - P095
 Yildiz, D. - 45, P002, P003

Z

Zabri, H. - 09, P039
 Zahler, S. - 12
 Zander, J. - P125
 Zardkouhi, A. - P048
 Zech, T. - 20
 Zeitlinger, M. - P214
 Zellmer, S. - P178
 Zhao, C. - P025
 Zhou, F. - 16
 Zickgraf, F. M. - P105
 Ziebuhr, J. - P228
 Ziegler, V. - P249
 Ziemann, C. - P078, P086, P226
 Zierler, S. - P021
 Zim, M. - P137
 Zimmerer, F. - P162
 Zimmermann, W.-H. - P044, P046
 Zini Moreira Silva, E. - P157
 Zischka, H. - 64
 Zobl, W. - P116
 Zühr, E. - 42, P241, P246
 Zupanets, K. - P219
 Zwintscher, A. - P116, P117, P210
 Zykaj, L. - P234